

Signal Processing of Discrete-time Signals

Andrew C. Singer and David C. Munson Jr.

March 25, 2013

Chapter 1

Overview of Discrete-time Signal Processing

- 1 DSP overview
- 2 Continuous-time signals
- 3 Discrete-time signals

GOALS

- | |
|--|
| <ol style="list-style-type: none">1. Overview of discrete-times signal processing2. Introduction to discrete-time and continuous time signals |
|--|

□

1.1 DSP overview:

This is a textbook covering the topic of discrete-time signal processing. The tremendous advances in integrated circuit technologies over the last few decades have enabled a remarkable revolution in the way in which we measure and process information. The types of information, or the “signals” as we call them, that we have interest in processing can range widely from measurements of our environment, such as temperature, rainfall, geophysical or seismic data, to signals governing man-made machines of interest, such as the velocity of a moving vehicle, or the controller modulating signals to the fuel injectors within our cars, to purely man-made sources of information, such as radio or television signals, or the MP3 encoding of recorded music.

The abstract concept of a signal is that of a measurement of a quantity of interest that is indexed by an associated reference axis. Most often, we will refer to this reference axis as the “time” axis for the signal and refer to these as signals that vary as a function of time. For example, within an analog circuit, we may measure the voltage across a given resistor within the circuit fabric and label this “signal” $v_r(t)$ to denote that this is the voltage v of a particular resistor r taken at a particular point in time t . As time varies, the voltage may be plotted against the independent variable t to produce a voltage vs. time plot, where we typically assume that negative time is to the left, and positive time to the right. For most signals of interest, there is a common notion of a reference time, $t = 0$, such that signals may be plotted with this reference time in the center, so long as the reference time is known to those interpreting the graph.

Another example of a signal may be the sequence of closing prices of the Dow Jones Industrial Averages (DJIA) as reported daily from the New York Stock Exchange. Unlike the resistor voltage example, the sequence of prices will be indexed by an integer reference axis indicating the specific day in a sequence of days at which the index closed at a particular value. We may write $p[n]$, to denote the closing price of the DJIA on the n^{th} day of trading, referenced to some common day $n = 0$. Note that while the resistor voltage $v_r(t)$ could be referenced to any time t taking on any real value, the price $p[n]$ can only be referenced to n taken as an integer. We refer to signals whose index t can take on any real value as continuous-time signals, since the “time” signal is assumed to be available over a continuum of values t . We refer to signals whose index n can only take on values from the integers, i.e. only discrete values, as discrete-time signals. While this text is largely about discrete-time signal processing, that is the processing and analysis of discrete-time signals, we will also be interested in understanding how similar properties of continuous-time signals relate to discrete-time signals, when the discrete-time signals themselves are related in a direct way to a continuous-time signal. A common means for this to occur is through the notion of sampling.

When you play a song through your MP3 player, you are processing a discrete-time recording of music, which is stored as samples of the music signal in the memory on your player. Your player then converts this set of samples into a continuous-time electrical signal which is then transduced into an acoustic signal that you hear through your headphones. This is the process of converting a discrete-time signal into a continuous-time signal, which is done because our auditory processing system (our ears) want continuous-time signals. However the microprocessors and digital circuitry on your MP3 player work best with discrete-time samples of the music that can be stored sequentially in the memory on your device. Similarly, when the MP3 file was created, a continuous-time version of the music (either from a magnetic tape recording, or a live studio performance) was processed such that it could be sampled in time and stored digitally to be used by your MP3 player. This process of conversion from a continuous-time signal to a discrete-time signal is called sampling, and in its simplest form we could take the signal $v_r(t)$ and create a discrete-time signal from it by simply recording the values at a periodic rate $f_s = 1/T$, called the sampling rate to produce the discrete-time signal $v_r[n] = v_r(nT)$, which is precisely what is done on modern digital sampling oscilloscopes. If the sampling rate is sufficiently fast, then when plotted on the oscilloscope, the signal $v[n]$ with a properly normalized time axis will be virtually indistinguishable from the continuous-time signal $v_r(t)$. Of course the notion of “sufficiently fast” will depend heavily on the content of the signal $v_r(t)$, but we are getting ahead of ourselves, and will return to this notion again shortly, and then again more carefully when we revisit sampling in later chapters.

This enables us to define or adopt some notation that will be convenient to use throughout this text. We will denote a continuous-time signal using the round braces notation we just employed for the resistor voltage, namely, $x_c(t)$, for a continuous-time signal x . Note that the term “analog” is often used synonymously to the term “continuous time,” however there is an important difference between the two. A continuous-time

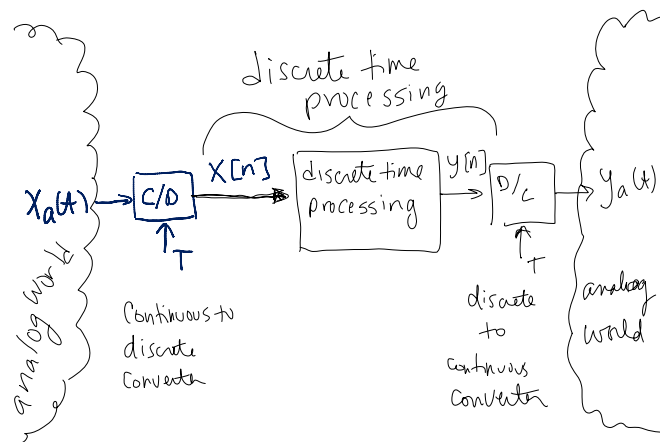


Figure 1.1: Discrete-time signal processing in an analog world. Note that in the “analog world” both the independent “time” variable is continuous as are the possible values of the signal $x_a(t)$. In the “discrete-time” world, after the C/D converter, the independent time variable n is now discrete, however the amplitudes $x[n]$ may still take on real-valued quantities. If the discrete-time processing takes place on a digital signal processor or standard microprocessor, then the discrete-time signal would need to also be a digital signal, i.e. its amplitude must also be quantized to a finite precision using a finite-precision analog-to-digital (A/D) converter.

signal is one for which the independent variable (t in the case of $x_c(t)$) takes on any value in a continuum, i.e. any real number. An analog signal is one for which the *values* of the signal can take on any level within a continuum, i.e. $x_c(t) \in \mathbb{R}$. Note that a continuous-time signal could be an analog signal, if both t and $x_c(t)$ can take on values from the reals. However a discrete-time signal $x[n]$ could also be an analog signal, if its values can be arbitrary real numbers. The term “digital” refers to signals that have been quantized such that their values must lie within a finite set, as could be represented in digital form, using a binary representation. Most of the signals we will be interested in for this text will be discrete-time analog signals, since we will not consider effects of numerical quantization, that is the effects of forcing the signals $x[n]$ to only take on values that can be represented using a binary representation with a finite number of bits. For simplicity, we will simply refer to these as discrete-time signals.

Discrete-time signals will be denoted using the square braces notation used for the DJIA prices, namely, discrete-time signal x will be denoted $x[n]$. In both the discrete-time and continuous-time cases we will refer to the independent variables t and n as the “time axis” though in some cases this may be something different such as the position of a vehicle along a track, or of the reading head along a magnetic tape, or the index labeling of the n^{th} sheep to be sheared at a wool processing plant. While many examples of such discrete-time signals exist in which the independent axis is not simply a time variable, a vast majority of discrete-time signal processing is undertaken for the case when a continuous-time signal or measurement is sampled, and then processed digitally by a special purpose piece of hardware, to produce a new set of discrete-time output signals and these new output signals are then converted to continuous-time signals for use in our “continuous-time, analog world”, as indicated in Figure 1.1.

In the figure, we note that many signals of interest in our “analog world” (where both time and amplitude can be taken from the real numbers) are indeed continuous in nature, our notion of time itself is indeed continuous and many such signals are indexed with respect to time. However, for a variety of reasons, it is more practical to build processors for these signals out of digital electronics, and therefore, we need discrete-time representations of signals. Much of this course will take you through the steps necessary to fully understand (and hopefully to build!) systems of the sort depicted in Figure 1.1. In the figure, note that the signals of interest begin within the analog world to the left, with the signal of interest $x(t)$. This signal is then processed using a “continuous-to-discrete” converter or “C/D” converter for short. In simple terms, the C/D converter simply samples the signal $x(t)$ at equally spaced samples, spaced T seconds apart in time to produce the discrete-time signal $x[n] = x(nT)$. We mentioned earlier that the necessary sampling rate $f_s = 1/T$ at which the C/D converter must operate was dependent upon the makeup of the signal $x(t)$.

$$x(t) \longrightarrow \boxed{\text{CT Filter}} \longrightarrow y(t)$$

Figure 1.2: A continuous time (CT) filter processing the continuous-time signal $x(t)$ to produce the continuous-time output $y(t)$.

We will elaborate on this a bit here, and in more detail later. You may recall from a course on continuous signals and systems the concept of the frequency content of continuous-time signals, as developed by Fourier through what we now call the Fourier series representation of periodic signals and the Fourier transform for aperiodic signals. For a large class of signals $x(t)$, we can define the following two expressions, which together make up what is referred to as the continuous-time Fourier transform (CTFT) representation for aperiodic signals,

$$\begin{aligned} x(t) &= \frac{1}{2\pi} \int_{-\infty}^{\infty} X(\omega) e^{j\omega t} d\omega \\ X(\omega) &= \int_{-\infty}^{\infty} x(t) e^{-j\omega t} dt. \end{aligned}$$

We refer to the signal $X(\omega)$ as the Fourier transform of the signal $x(t)$. The first relation above is called the Fourier transform synthesis equation, as it depicts the “recipe” or formula for synthesizing the signal $x(t)$ out of the class of periodic complex exponential sequences $e^{j\omega t} = \cos(\omega t) + j \sin(\omega t)$, where $j = \sqrt{-1}$. When the signal $X(\omega)$ satisfies $|X(\omega)| = 0$ for $|\omega| > B$, then we say that the signal $x(t)$ is “band limited” to $F = B/2\pi$ Hz, since there is no energy in the signal outside of the range from $-B < \omega < B$. We refer to twice the highest frequency in $x(t)$ as the Nyquist frequency, i.e. $2F$, which is also equal to the total width of the frequency band (or band width) of the signal, when you include the negative and the positive frequencies. When the C/D converter used in Figure 1.1 satisfies $(1/T) > 2F$, then it is possible to exactly recover the signal $x(t)$ from its samples. Namely, we can directly compute

$$x(t) = \sum_{n=-\infty}^{\infty} x[n] \text{sinc}\left(\frac{\pi}{T}(t - nT)\right), \quad (1.1)$$

where the “sinc” function is defined as

$$\text{sinc}(t) = \begin{cases} \frac{\sin(t)}{t}, & t \neq 0 \\ 1 & t = 0. \end{cases}$$

In practice, we sample slightly faster than $2F$, i.e. smaller values of T , to ensure that we can capture all of the information in the signal $x(t)$. The equation given in (1.1) is precisely the process that is undertaken in an ideal D/C, or discrete-to-continuous converter, as depicted in figure (1.1), in order to construct the signal $y(t)$ from the discrete-time signal $y[n]$, just prior to the signal $y(t)$ being sent back out into the analog world. Note that we could process the signals directly within the analog world. This is precisely what analog electronics is for and this is a huge industry. However, as the processing that is desired becomes more complex, the capacitors, inductors, and resistors, and transistors, and diodes, and other circuit components depicted in Figure (1.2) become increasingly difficult to design and manufacture and become more expensive.

The alternative to processing such signals while leaving them within the analog world, is to sample them, and process them in discrete-time, as depicted in Figure (1.3). The discrete-time (DT) filter shown in the figure depicts the process of mathematically manipulating the samples in $x[n]$, which essentially comprises multiplication, addition and movement through storage registers.

As we will see in later chapters, often such discrete-time operations can be described by what are known as difference equations operating on the signals $x[n]$ and $y[n]$, much like the governing equations for continuous-time filters can often be described in terms of differential equations. An example of such a difference equation might be

$$y[n] = b_0 x[n] + b_1 x[n-1] + \cdots + b_N x[n-N],$$



Figure 1.3: Discrete-time filtering alternative to the continuous-time filtering of a continuous-time signal.

where, since the output $y[n]$ can be computed directly from samples of the input, the difference equation is called “non recursive”. This is in contrast to a recursive implementation that might take the form

$$y[n] = a_1 y[n-1] + a_2 y[n-2] + \cdots + a_N y[n-N] + b_0 x[n] + b_1 x[n-1] + \cdots + b_M x[n-M],$$

where the coefficients b_k and a_k are selected to produce the desired relationship between the input $x[n]$ and output $y[n]$.

The term DSP is often used to describe “digital signal processing” which describes not only discrete-time signal processing, but also the additional step of quantizing the output of the ideal C/D converter to create a “digital signal” which is not only a discrete-time signal, but one that is also capable of being represented by a fixed number of bits. The additional step of quantization that takes place within the C/D converter is something that we will explore in more detail in later chapters. However for now, we will choose to ignore these bits of detail. Some more sophisticated forms of DSP that have impacted the technology you use regularly, include telecommunications, in which the modulation, coding, echo cancellation and line equalization is done nearly completely in discrete-time in modern systems. Speech processing uses analysis and synthesis methods for low bit-rate speech transmission over cellular and other communications links, speech recognition systems are sophisticated digital algorithms that process sampled and digitized speech. Image processing that takes place for HD video and other digital image and multimedia applications, ranging from coding for video conferencing, digitization and compression in digital cameras and camcorders (such as those on the mobile telephone in your pocket), fax transmission, HDTV, digital video recorders (DVRs), and image archiving; noise removal; deblurring; and object recognition. DSP has a massive footprint in consumer electronics from CD/DVD players, to Digital Satellite TVs, HD-DVRs, cellular phones, MP3/MP4 players. It’s nearly impossible to find consumer electronics to do not contain DSP these days. Modern medical imaging is largely based on discrete-time signal processing technology, including the pervasive computed tomography (CT) and magnetic resonance imaging (MRI) - even X-ray technology uses an array of detectors to construct a digital representation of the received radiation, so X-ray films are as much a part of the past as film-based cameras, 8 track tapes, film-based movie cameras and more.

Digital representation and processing is often preferred over direct analog/continuous-time processing for three (or more) main reasons. First, discrete-time systems are more versatile – sophisticated processing, time varying and adaptive filtering, nonlinear processing, multidimensional signals (especially image processing) can all be captured with relative ease in such systems. Second, the guaranteed accuracy, as determined by the register lengths (number of bits) used to perform the computations, and not by the non-ideal integrated circuit components, including resistors capacitors, inductors, operational amplifiers, and other components whose performance is not only not ideal, but will vary over time and with temperature. Finally digital implementations are often smaller, cheaper, lower power, thanks in large part to the incredible scaling of integrated microelectronics through the process known as “Moore’s Law”, whereby such integration densities nearly double every 18 months. Due to speed limitation of analog-to-digital converters and computers, digital signal processing was initially employed (during 1960s) in application areas having low-bandwidth signals, such as telephone quality speech (approximately 3 KHz bandwidth). The practical frequency range for digital processing has increased vastly over the years and continues to climb. As an example, digital signal processing is now commonly employed in radar, where sampling rates may be tens or even hundreds of megahertz. Optical communications links are starting to use digital signal processing with sampling rates in excess of $50GHz$! Note that here we use the units of Hz to represent samples-per-second, in addition to its more common meaning of cycles-per-second. This slight abuse of notation is common in the discrete-time signal processing industry and one with which we all must live.

1.2 Continuous-time (CT) signals

While the class we will refer to as continuous-time signals is defined by properties of the independent time axis, t , we can further break down this class of signals into subclasses that will be useful in various contexts. For example, we refer to finite-length continuous-time signals, as signals $x(t)$ for which the independent time axis is only defined over a finite interval, i.e., $x(t), t \in [0, 1]$, as might be convenient for measurements taken within a specific time interval, or for which the signals are not present outside of the interval of interest. For example, $x(t)$ might correspond to the temperature of the water column in the ocean from the surface, $t = 0$ to the ocean bottom at, say, $t = 25$ meters, for a shallow water environment. It does not make sense to consider the temperature as existing outside of this region, since there is no ocean outside this region at this location in the ocean.

Having defined finite-length signals, we can similarly define infinite-length signals as those for which the time axis of interest, or over which the signals of interest are defined is indeed infinite, i.e. $x(t), t \in \mathbb{R}$. Finally, we can also define continuous-time periodic signals as infinite-length signals for which the following relationship holds $x(t) = x(t + P)$ for some value of $P \in \mathbb{R}$. We refer to the minimum value of $P > 0$ for which this relationship holds as the “fundamental period” or just the “period” of the periodic signal.

1.3 Discrete-time (DT) signals

We can repeat this exercise for discrete-time signals as well. While the class we will refer to as discrete-time signals is defined by properties of the independent time axis, n , we can further break down this class of signals into subclasses. Once again, we refer to finite-length discrete-time signals, as signals $x[n]$ for which the independent time axis is only defined over a finite interval, i.e. $x[n], n \in [0, N]$, as might be convenient for a finite set of measurements, or for which the signals are not present outside of the interval of interest. Once again, $x[n]$ might correspond to the number of words on the n^{th} page of a specific book that only has N pages. It does not make sense to consider pages that do not exist!

Having defined finite-length signals, we can similarly define infinite-length discrete-time signals as those for which the time axis of interest, or over which the signals of interest are defined is indeed infinite, i.e. $x[n], n \in \mathbb{Z}$, where \mathbb{Z} refers to the set of integers. Finally, we can also define discrete-time periodic signals as infinite-length signals for which the following relationship holds $x[n] = x[n + P]$ for some value of $P \in \mathbb{Z}$. We refer to the minimum value of $P > 0$ for which this relationship holds as the “fundamental period” or just the “period” of the periodic signal. We will return to the concept of discrete-time and continuous-time periodic signals in Chapter 2.

Chapter 2

CT and DT Signal Representations

- 1 Fourier Series
- 2 Fourier Transform
- 3 Discrete Fourier Series
- 4 Discrete-Time Fourier Transform
- 5 Discrete Fourier Transform
- 6 Applications

GOALS

1. Development of representations of CT and DT signals in the frequency domain.
2. Familiarization with Fourier Series and transform representations for CT and DT signals.

□

Since the signals we encounter in engineering, science, and everyday life are as varied as the applications in which we engage them, it is often helpful to first study these applications in the presence of simplified versions of these signals. Much like a child learning to play an instrument for the first time, it is easier to start by attempting to play a single note before an entire musical score. Then, after learning many notes, the child becomes a musician and can synthesize a much broader class of music, building up from many notes. This approach of building-up our understanding of complex concepts by first understanding their basic building blocks is a fundamental precept of engineering and one that we will use frequently throughout this book.

In this chapter, we will explore signals in both continuous time and discrete time, together with a number of ways in which these signals can be built-up from simpler signals. Simplicity is in the eye of the beholder and what makes a signal appear simple in one context may not shed much light in another context. Many of the concepts we will develop throughout this text arise from studying large classes of signals, one building block at a time, and extrapolating system (or application) level behavior by considering the whole as a sum of its parts. In this chapter, we will focus specifically on sinusoidal signals as our basic building blocks as we consider both periodic and aperiodic signals in continuous and discrete time. Along this path, we will encounter the Fourier series representations of periodic signals as well as Fourier transform representations of aperiodic, infinite-length signals. In later chapters, we will find that so-called “time-domain” representations of signals sometimes prove more fruitful, and for discrete-time signals there is a natural way to construct signals one sample at a time.

2.1 Fourier Series representation of finite-length and periodic CT signals

In many applications in science and engineering, we often work with signals that are periodic in time. That is, the signal repeats itself over and over again with a given period of repetition. Examples of periodic signals might include the acoustic signal that emanates from a musical instrument, such as a trumpet when a single sustained note is played, or the vertical displacement of a mass in a frictionless spring-mass oscillator set into motion, or the horizontal displacement of a pendulum swaying to and fro in the absence of friction.

Mathematically, we represent a periodic signal, $x(t)$, as one whose value repeats at a fixed interval of time from the present. This interval, denoted T below, is called the “period” of the signal, and we express this relationship

$$x(t) = x(t + T), \text{ for all } t. \quad (2.1)$$

Equation (2.1) will, in general, be satisfied for a countably infinite number of possible values of T when $x(t)$ is periodic. The smallest, positive value of T for which Eq. (2.1) is satisfied, is called the “fundamental period” of the signal $x(t)$. For sinusoidal signals, such as

$$x(t) = \sin(\omega_0 t + \phi), \quad (2.2)$$

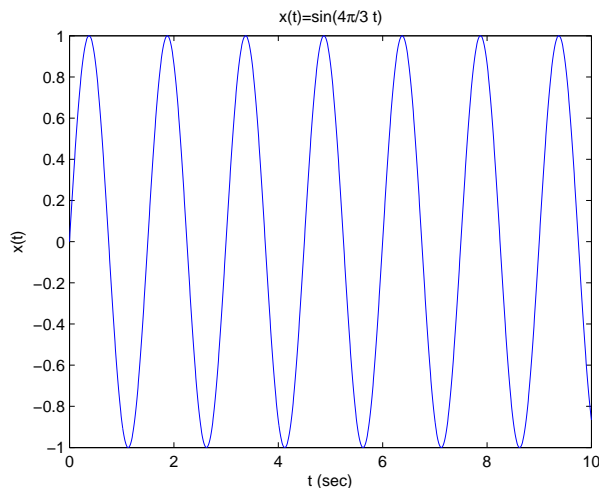
we can relate the angular frequency of oscillation, ω_0 to the fundamental period, T . This can be computed by noting that sinusoidal functions are equal when their arguments are either equal or differ only through a multiple of 2π , i.e.

$$\begin{aligned} x(t) &= x(t + T) \\ \sin(\omega_0 t + \phi) &= \sin(\omega_0(t + T) + \phi) \\ \sin(\omega_0 t + \phi + 2k\pi) &= \sin(\omega_0(t + T) + \phi) \\ \sin(\omega_0(t + 2k\pi/\omega_0) + \phi) &= \sin(\omega_0(t + T) + \phi) \end{aligned} \quad (2.3)$$

which, for $k = 1$, yields the relationship

$$T = 2\pi/\omega_0, \quad (2.4)$$

between the fundamental period, T , and the “fundamental angular frequency” ω_0 . By analogy to sinusoidal signals, we refer to the value of $\omega_0 = 2\pi/T$ as the fundamental angular frequency of any signal that is periodic with a fundamental period T .

Figure 2.1: The periodic sinusoidal signal $x(t) = \sin((4\pi/3)t)$.

Here, we will provide a number of examples of periodic signals in continuous-time, including sinusoidal, square wave, triangular wave and complex exponential signals. By noting that any two periodic signals, $x(t)$ and $y(t)$ with the same period T can be added together to produce a new periodic signal of the same period, i.e.,

$$\begin{aligned} s(t) &= x(t) + y(t) \\ s(t+T) &= x(t+T) + y(t+T) = s(t+T), \end{aligned}$$

in 1807 Jean Baptiste Fourier (1807) considered the notion of building a large set of periodic signals from sinusoidal signals sharing the same period. Ignoring the phase, ϕ , for now, note that from (2.4), sinusoidal signals that share the same period must have fundamental angular frequencies given by $k\omega_0 = 2k\pi/T$ for different values of k . If two sinusoidal signals shared the same fundamental frequency, then they would be the same sinusoidal signal (recall that, for now, we are neglecting the phase, ϕ). We call such sinusoidal signals whose fundamental frequencies $k\omega_0$ are integer multiples of one fundamental frequency, harmonically-related sinusoids. Such harmonically-related sinusoids could indeed share the period, $2\pi/\omega_0$ while they would have different fundamental frequencies and hence different “fundamental periods.”

We now consider how we might build-up a larger class of periodic signals from the basic building blocks of harmonically-related sinusoids. To extend our discussion to include complex-valued signals, we will employ Euler’s relation to construct complex exponential signals of the form

$$\begin{aligned} x(t) &= e^{j(\omega_0 t + \phi)} \\ &= \cos(\omega_0 t + \phi) + j \sin(\omega_0 t + \phi) \end{aligned} \tag{2.5}$$

and in doing so, we can push the phase out of the picture so that it can be absorbed in a complex scalar constant out front, i.e.

$$x(t) = c e^{j\omega_0 t},$$

where, $c = e^{j\phi}$ is simply a complex constant whose effects on the sinusoidal nature of the signal have been conveniently parked outside the discussion. Complex-exponential signals of the form (2.5) are periodic with fundamental angular frequency $\omega_0 = 2\pi/T$ since they are simply constructed by pairing the real-valued periodic signal $\cos(\omega_0 t)$ with the purely imaginary signal $j \sin(\omega_0 t)$.

By simply adding together harmonically-related sinusoidal signals, we can construct a large class of periodic waveforms of amazing variety. For example, in Figure 2.2, note how by taking odd-valued harmonics (sinusoids with harmonically-related fundamental frequencies that are odd multiples of a single frequency, $\omega_0 = 2\pi$), we obtain an increasingly improving approximation to a square wave with unit period.

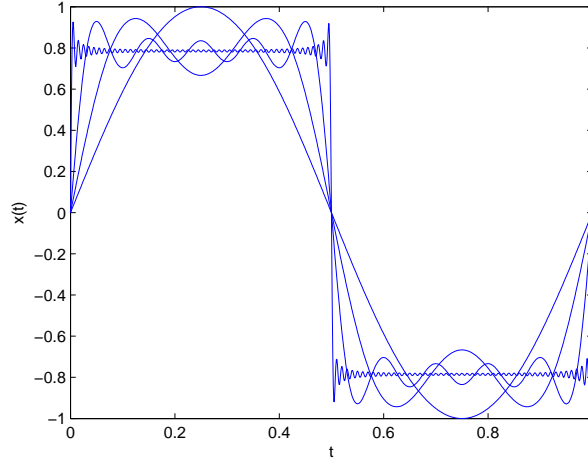


Figure 2.2: The periodic sinusoidal signal $x(t) = \sum_{k=1}^N \frac{1}{k} \sin(2k\pi t)$, for $k = 1, 3, 9$ and 99 .

Generalizing this idea, we can explore the class of signals that can be constructed by such harmonically-related complex exponentials of the form

$$x(t) = \sum_{k=-\infty}^{\infty} X[k] e^{jk\omega_0 t}. \quad (2.6)$$

To bring the period of the periodic signal $x(t)$ into the equation, (2.6) is often written

$$x(t) = \sum_{k=-\infty}^{\infty} X[k] e^{j2\pi kt/T}, \quad (2.7)$$

where $T = 2\pi/\omega_0$ is the fundamental period and ω_0 is the fundamental frequency of the periodic signal $x(t)$. The construction in (2.7) is referred to as the continuous-time Fourier series (CTFS) representation of $x(t)$ and (2.7) is often called the continuous-time Fourier series synthesis equation.

The Fourier series coefficients $X[k]$ can be obtained by multiplying (2.7) by $e^{-j2\pi kt/T}$ and integrating over a period of duration T to obtain

$$\begin{aligned} \int_0^T x(t) e^{-j2\pi kt/T} dt \\ = \int_0^T \left(\sum_{m=-\infty}^{\infty} X[m] e^{j2\pi(m-k)t/T} \right) dt, \end{aligned}$$

where the limits of integration indicate that we have chosen to evaluate the integral over the period $0 \leq t \leq T$. Note the use of the dummy variable m in the summation for the CTFS, since the variable k was already in use. To use k again would invite disaster into our derivation. Interchanging the order of integration and summation (which can be done under suitable conditions on the summation), we obtain,

$$\begin{aligned} \int_0^T x(t) e^{-j2\pi kt/T} dt \\ = \sum_{m=-\infty}^{\infty} \int_0^T X[m] e^{j2\pi(m-k)t/T} dt. \end{aligned} \quad (2.8)$$

To proceed, we need to evaluate the integral

$$\begin{aligned}\int_0^T e^{j2\pi(m-k)t/T} dt &= \frac{T}{j2\pi(m-k)} e^{j2\pi(m-k)t/T} \Big|_0^T \\ &= \frac{T}{j2\pi(m-k)} [e^{j2\pi(m-k)} - 1] \\ &= T\delta[m-k],\end{aligned}$$

where the second line arises from simple integration of an exponential function. The second line is readily seen to be equal to zero when $m \neq k$ and though one might be tempted to evaluate this line for $m = k$ (using a formula bearing the name of a famous 17th-century French mathematician), our efforts will be better spent setting $m = k$ into the integrand on the left hand side of the first line, from which we obtain

$$\int_0^T 1 dt = T.$$

An interpretation of this result is that integration of a periodic complex exponential over an integer multiple, $(m-k)$, of its fundamental period, in this case $T/2\pi(m-k)$, is zero. The only periodic complex exponential that survives integration over the period T is the DC, i.e. $m = k$, term.

We can now return to (2.8) and apply this result, to obtain

$$\begin{aligned}\int_0^T x(t) e^{-j2\pi kt/T} dt &= \sum_{m=-\infty}^{\infty} X[m] T\delta[m-k] \\ &= TX[k],\end{aligned}\tag{2.9}$$

by the sifting property of the Kronocker delta function. We can now turn (2.9) around to obtain the continuous-time Fourier series analysis equation,

$$X[k] = \frac{1}{T} \int_0^T x(t) e^{-j2\pi kt/T} dt.\tag{2.10}$$

Putting the synthesis and analysis equations together, we have the continuous-time Fourier series representation of a periodic signal $x(t)$ as

CT Fourier Series Representation of a Periodic Signal

$$X[k] = \frac{1}{T} \int_0^T x(t) e^{-j\frac{2\pi kt}{T}} dt\tag{2.11}$$

$$x(t) = \sum_{k=-\infty}^{\infty} X[k] e^{j\frac{2\pi kt}{T}}\tag{2.12}$$

Example: CTFS of a Square Wave

Let us return to the square wave signal that we visited in Figure 2.2. In the figure, we appeared to have a method for constructing the periodic signal that, in the interval $[0, 1]$, satisfies

$$x(t) = \begin{cases} 1, & 0 \leq t \leq 0.5 \\ -1 & \text{else.} \end{cases}\tag{2.13}$$

Using (2.10), we obtain,

$$\begin{aligned}
X[k] &= \int_0^1 x(t) e^{-j2\pi kt} dt \\
&= \int_0^{0.5} e^{-j2\pi kt} dt - \int_{0.5}^1 e^{-j2\pi kt} dt \\
&= \frac{-1}{j2\pi k} ([e^{-j\pi k} - 1] - [1 - e^{-j\pi k}]) \\
&= \frac{-1}{j2\pi k} 2[(-1)^k - 1] \\
&= \begin{cases} 0, & k \text{ even} \\ \frac{2}{j\pi k} & k \text{ odd.} \end{cases}
\end{aligned} \tag{2.14}$$

Note that the $k = 0$ case can be readily evaluated by considering the integral in (2.14) for which the integral can be easily seen to vanish by the antisymmetry of $x(t)$ over the unit interval.

2.1.1 CT Fourier Series Properties

We have now been properly introduced to a method for building-up continuous-time periodic signals from a class of simple sinusoidal signals in (2.11) and a method for analysing the make-up of such periodic signals in terms of their constituent sinusoidal components in (2.12). Now that introductions are out of the way, we can explore some of the many useful properties of the CTFS representation. As we shall see, it is often helpful to consider the properties of a whole signal by virtue of the properties of its parts, and the relations we develop next will often prove useful in this process.

2.1.1.1 Linearity

The CTFS can be viewed as a linear operation, in the following manner. When two signals $x(t)$ and $y(t)$ are each constructed from their constituent sinusoidal signals according to the CTFS synthesis equation (2.12), the linear combination of these signals, $z(t) = ax(t) + by(t)$, for a, b real-valued constants, can be readily obtained by combining the constituent sinusoidal signals through the same linear combination. More specifically, when $x(t)$ is a periodic signal with CTFS coefficients $X[k]$ and $y(t)$ is a periodic signal with CTFS coefficients $Y[k]$ then the signal $z(t) = ax(t) + by(t)$ has CTFS coefficients given by $Z[k] = aX[k] + bY[k]$. The linearity property of the CTFS can be compactly represented as follows

$$x(t) \xleftrightarrow{\text{CTFS}} X[k], y(t) \xleftrightarrow{\text{CTFS}} Y[k] \implies z(t) = ax(t) + by(t) \xleftrightarrow{\text{CTFS}} aX[k] + bY[k].$$

This result can be readily shown by substituting $z(t) = ax(t) + by(t)$ into the integral in (2.11) and expanding the integral into the two separate terms, one for $X[k]$ and one for $Y[k]$.

2.1.1.2 Time Shift

When a sinusoidal signal $x(t) = \sin(\omega_0 t)$ is shifted in time, the resulting signal $x(t - t_0)$ can be represented in terms of a simple phase shift of the original sinusoidal signal, i.e. $x(t - t_0) = \sin(\omega_0(t - t_0)) = \sin(\omega_0 t - \phi)$, where $\phi = \omega_0 t_0 = 2\pi t_0/T$. Periodic signals that can be represented using the CTFS contain many, possibly infinitely many, sinusoidal (or complex exponential) signals. When such periodic signals are delayed in time, each of the constituent sinusoidal components of the signal are delayed by the same amount, however this translates into a different phase shift for each component. This can be readily seen from the CTFS analysis equation (2.11), as follows. For the signal $y(t) = x(t - t_0)$, we have

$$\begin{aligned}
Y[k] &= \frac{1}{T} \int_{t=0}^T x(t-t_0) e^{-j \frac{2\pi k}{T} t} dt \\
&= \frac{1}{T} \int_{s=-t_0}^{T-t_0} x(s) e^{-j \frac{2\pi k}{T} (s+t_0)} ds \\
&= \frac{1}{T} \int_{s=-t_0}^0 x(s) e^{-j \frac{2\pi k}{T} (s+t_0)} ds + \frac{1}{T} \int_{s=0}^{T-t_0} x(s) e^{-j \frac{2\pi k}{T} (s+t_0)} ds \\
&= \frac{1}{T} \int_{s=-t_0}^0 x(s+T) e^{-j \frac{2\pi k}{T} (s+T+t_0)} ds + \frac{1}{T} \int_{s=0}^{T-t_0} x(s) e^{-j \frac{2\pi k}{T} (s+t_0)} ds \\
&= \frac{1}{T} \int_{\tau=T-t_0}^T x(\tau) e^{-j \frac{2\pi k}{T} (\tau+t_0)} d\tau + \frac{1}{T} \int_{s=0}^{T-t_0} x(s) e^{-j \frac{2\pi k}{T} (s+t_0)} ds \\
&= \frac{1}{T} \int_{t=0}^T x(t) e^{-j \frac{2\pi k t_0}{T}} e^{-j \frac{2\pi k}{T} t} dt \\
&= X[k] e^{-j \frac{2\pi k t_0}{T}},
\end{aligned}$$

where, the second line follows from the change of variable, $s = t - t_0$, the fourth line follows from the periodicity of both the signal $x(t)$ and the signal $e^{-j2\pi kt/T}$ with period T , the fifth line follows from the change of variable $\tau = s + T$, and the last line follows from the definition of $X[k]$ after factoring the linear phase term $e^{-j2\pi kt_0/T}$ out of the integral. The time shift property of the CTFS can be compactly represented as follows

$$x(t) \xleftrightarrow{CTFS} X[k] \implies y(t) = x(t - t_0) \xleftrightarrow{CTFS} X[k] e^{-j \frac{2\pi k}{T} t_0}.$$

We see that a shift in time of a periodic signal corresponds to a modulation in frequency by a phase term that is linear with frequency with a slope that is proportional to the delay. This can be made easier if we adopt the convenient, but conceptually more challenging concept of integration over a period for the definition of the CTFS.

2.1.1.3 Frequency Shift

When a periodic signal $x(t)$ has a CTFS representation given by $X[k]$, a natural question that might arise is the what happens when the shifting that was discussed in section 2.1.1.2 is applied to the CTFS representation, $X[k]$. Specifically, if a periodic signal $y(t)$ were known to have a CTFS representation given by $Y[k] = X[k - k_0]$, it is interesting to understand the relationship in the time-domain between $y(t)$ and $x(t)$. This can be readily seen through examination of the CTFS analysis equation,

$$\begin{aligned}
Y[k] &= X[k - k_0] \\
&= \frac{1}{T} \int_{t=0}^T x(t) e^{-j \frac{2\pi}{T} (k-k_0)t} dt \\
&= \frac{1}{T} \int_{t=0}^T x(t) e^{j \left(\frac{2\pi k_0}{T}\right)t} e^{-j \frac{2\pi}{T} kt} dt \\
&= \frac{1}{T} \int_{t=0}^T \left(x(t) e^{j \left(\frac{2\pi k_0}{T}\right)t} \right) e^{-j \frac{2\pi}{T} kt} dt,
\end{aligned}$$

which leads to the relation

$$x(t) \xleftrightarrow{CTFS} X[k] \implies y(t) = x(t) e^{j k_0 \omega_0 t} \xleftrightarrow{CTFS} X[k - k_0],$$

where $\omega_0 = \frac{2\pi}{T}$. We observe that a shift in the continuous time Fourier series coefficients by an integer amount k_0 corresponds to a modulation in the time domain signal $x(t)$ by a term whose frequency is proportional to the shift amount.

2.1.1.4 Time Reversal

When a periodic signal $x(t) = e^{j2\pi t/T}$ is time-reversed, i.e. $y(t) = x(-t)$, the effect on its CTFS representation can be simply observed

$$\begin{aligned} X[k] &= \frac{1}{T} \int_{t=0}^T e^{j\frac{2\pi}{T}t} e^{-j\frac{2\pi k}{T}t} dt \\ &= \begin{cases} 1, & \text{for } k = 1 \\ 0 & \text{otherwise} \end{cases} \end{aligned}$$

and

$$\begin{aligned} Y[k] &= \frac{1}{T} \int_{t=0}^T e^{-j\frac{2\pi}{T}t} e^{-j\frac{2\pi k}{T}t} dt \\ &= \begin{cases} 1, & \text{for } k = -1 \\ 0 & \text{otherwise.} \end{cases} \end{aligned}$$

More generally, from the CTFS synthesis equation,

$$x(t) = \sum_{k=-\infty}^{\infty} X[k] e^{j\frac{2\pi k}{T}t},$$

we see that by simply changing the sign of the time variable t , we obtain the general relation

$$\begin{aligned} y(t) &= x(-t) = \sum_{k=-\infty}^{\infty} X[k] e^{-j\frac{2\pi k}{T}t} \\ &= \sum_{k=-\infty}^{\infty} X[k] e^{j\frac{2\pi(-k)}{T}t} \\ &= \sum_{m=-\infty}^{\infty} X[-m] e^{j\frac{2\pi k}{T}t}, \end{aligned}$$

yielding the relation

$$x(t) \xleftrightarrow{CTFS} X[k] \implies y(t) = x(-t) \xleftrightarrow{CTFS} X[-k],$$

i.e., changing the sign of the time axis corresponds to changing the sign of the CTFS frequency index.

2.1.1.5 Time Scaling

When a periodic signal undergoes a time-scale change, such as one that compresses the time axes, $y(t) = x(at)$, where $a > 1$ is a real-valued constant, the resulting signal $y(t)$ would remain periodic, however the period would change correspondingly, such that $y(t + T_y) = y(t)$ would be satisfied for a different period T_y . This can be easily seen by substituting in for $x(t)$ in the relation, $y(t) = x(at) = y(t + T_y) = x(a(t + T_y))$ and noting that $x(at) = x(at + T)$, due to the periodicity of $x(t)$ with period T . This leads to the relation $x(a(t + T_y)) = x(at + T)$ or $T_y = T/a$. This makes intuitive sense, since the time-axis in the signal $y(t)$ has been compressed by a factor of a , therefore the time at which it will repeat must also have compressed by the same factor. Now, even though the period of the signal $y(t)$ has changed, we also are interested in the full CTFS representation of $y(t)$. This is given by

$$\begin{aligned}
y(t) &= \sum_{k=-\infty}^{\infty} X[k] e^{j \frac{2\pi k}{T} at} \\
&= \sum_{k=-\infty}^{\infty} X[k] e^{j \frac{2\pi k}{T_y} t},
\end{aligned}$$

where the second line follows from the definition of T_y . Note that although we have that

$$x(t) \xleftrightarrow{CTFS} X[k] \implies y(t) = x(at) \xleftrightarrow{CTFS} X[k],$$

that is the sequence of CTFS coefficients $Y[k]$ is identical to $X[k]$, the CTFS representation for $x(t)$ and $y(t)$ differ substantially, since they are defined for completely different periods, $T \neq T_y$. As a result, the fundamental frequency for the periodic signal $x(t)$ is $2\pi/T$, which is different from that of $y(t)$, which is $2\pi a/T$. Hence, the frequency content of the signals differ substantially.

2.1.1.6 Conjugate Symmetry

The effect of conjugating a complex-valued signal on its CTFS representation can be seen by simply conjugating the CTFS synthesis relation,

$$\begin{aligned}
x(t) &= \sum_{k=-\infty}^{\infty} X[k] e^{j \frac{2\pi k}{T} t} \\
x^*(t) &= \left(\sum_{k=-\infty}^{\infty} X[k] e^{j \frac{2\pi k}{T} t} \right)^* \\
&= \sum_{k=-\infty}^{\infty} X^*[k] e^{-j \frac{2\pi k}{T} t} \\
&= \sum_{k=-\infty}^{\infty} X^*[k] e^{j \frac{2\pi(-k)}{T} t} \\
&= \sum_{m=-\infty}^{\infty} X^*[-m] e^{j \frac{2\pi m}{T} t}
\end{aligned}$$

yielding that

$$x(t) \xleftrightarrow{CTFS} X[k] \implies x^*(t) \xleftrightarrow{CTFS} X^*[-k].$$

When the periodic signal $x(t)$ is real valued, i.e. $x(t)$ only takes on values that are real numbers, then the CTFS exhibits a symmetry property. This arises directly from the definition of the CTFS, and that real numbers equal their conjugates, i.e. $x(t) = x^*(t)$, such that

$$x(t) = x^*(t) \xleftrightarrow{CTFS} X[k] \implies X[k] = X^*[-k].$$

Note that when the signal is real-valued and is an even function of time, such that $x(t) = x(-t)$, then its CTFS is also real-valued and even, i.e. $X[k] = X^*[k] = X[-k]$. It can be shown by similar reasoning that when the signal is periodic, real-valued, and an odd function of time, that the CTFS coefficients are purely imaginary and odd, i.e. $X[k] = -X^*[k] = -X[-k]$.

2.1.1.7 Products of Signals

When two periodic signals of the same period are multiplied in time, such that $z(t) = x(t)y(t)$, the resulting signal remains periodic with the same period, such that $z(t) = x(t)y(t) = x(t+T)y(t+T) = z(t+T)$. Hence,

each of the three signals admit CTFS representations using the same set of harmonically related signals. We can observe the effect on the resulting CTFS representation through the analysis equation,

$$\begin{aligned}
 Z[k] &= \frac{1}{T} \int_{t=0}^T (x(t)y(t))e^{-j\frac{2\pi k}{T}t} dt \\
 &= \frac{1}{T} \int_{t=0}^T (y(t) \left(\sum_{m=-\infty}^{\infty} X[m]e^{j\frac{2\pi m}{T}t} \right))e^{-j\frac{2\pi k}{T}t} dt \\
 &= \sum_{m=-\infty}^{\infty} X[m] \frac{1}{T} \int_{t=0}^T y(t)e^{-j\frac{2\pi(k-m)}{T}t} dt \\
 &= \sum_{m=-\infty}^{\infty} X[m]Y[k-m].
 \end{aligned}$$

The relationship between the CTFS coefficients for $z(t)$ and those of $x(t)$ and $y(t)$ is called a discrete convolution between the two sequences $X[k]$ and $Y[k]$,

$$x(t) \xleftrightarrow{CTFS} X[k], y(t) \xleftrightarrow{CTFS} Y[k] \implies z(t) = x(t)y(t) \xleftrightarrow{CTFS} \sum_{m=-\infty}^{\infty} X[m]Y[k-m].$$

2.1.1.8 Convolution

A dual relationship to that of multiplication in time, is multiplication of CTFS coefficients. Specifically, when the two signals $x(t)$ and $y(t)$ are each periodic with period T , the periodic signal $z(t)$ of period T , whose CTFS representation is given by $Z[k] = X[k]Y[k]$ corresponds to a periodic convolution of the signals $x(t)$ and $y(t)$. This can be seen as follows,

$$\begin{aligned}
 z(t) &= \sum_{k=-\infty}^{\infty} (X[k]Y[k]) e^{j\frac{2\pi k}{T}t} \\
 &= \sum_{k=-\infty}^{\infty} \left(\frac{1}{T} \int_{\tau=0}^T x(\tau)e^{-j\frac{2\pi k}{T}\tau} d\tau \right) Y[k]e^{j\frac{2\pi k}{T}t} \\
 &= \frac{1}{T} \int_{\tau=0}^T x(\tau) \left(\sum_{k=-\infty}^{\infty} Y[k]e^{j\frac{2\pi k}{T}(t-\tau)} \right) d\tau \\
 &= \frac{1}{T} \int_{\tau=0}^T x(\tau)y(t-\tau)d\tau
 \end{aligned}$$

where the integral relationship in the last line is called periodic convolution. This leads to the following property of the CTFS,

$$x(t) \xleftrightarrow{CTFS} X[k], y(t) \xleftrightarrow{CTFS} Y[k] \implies z(t) = \frac{1}{T} \int_{\tau=0}^T x(\tau)y(t-\tau)d\tau \xleftrightarrow{CTFS} Z[k] = X[k]Y[k].$$

2.1.1.9 Integration

When the signal $y(t)$ and $x(t)$ are related through a running integral, i.e. $y(t) = \int_{\tau=0}^t x(\tau)d\tau$, we can relate their CTFS as follows,

$$\begin{aligned}
x(t) = \frac{d}{dt} \int_{\tau=0}^t x(\tau) d\tau &= \frac{d}{dt} \int_{\tau=0}^t \left(\sum_{k=-\infty, k \neq 0}^{\infty} X[k] e^{j \frac{2\pi k}{T} \tau} + X[0] \right) d\tau \\
&= \frac{d}{dt} \left(\sum_{k=-\infty, k \neq 0}^{\infty} X[k] \int_{\tau=0}^t e^{j \frac{2\pi k}{T} \tau} d\tau + X[0] t \right) \\
&= \frac{d}{dt} \sum_{k=-\infty, k \neq 0}^{\infty} X[k] \left[\frac{T}{j2\pi k} e^{j \frac{2\pi k}{T} \tau} \right]_{\tau=0}^t + X[0] \\
&= \frac{d}{dt} \sum_{k=-\infty, k \neq 0}^{\infty} X[k] \left[\frac{T}{j2\pi k} \left(e^{j \frac{2\pi k}{T} t} - 1 \right) \right] + X[0] \\
&= \frac{d}{dt} \sum_{k=-\infty, k \neq 0}^{\infty} X[k] \frac{T}{j2\pi k} e^{j \frac{2\pi k}{T} t} - \frac{d}{dt} \sum_{k=-\infty, k \neq 0}^{\infty} X[k] \frac{T}{j2\pi k} + X[0] \\
&= \frac{d}{dt} \sum_{k=-\infty, k \neq 0}^{\infty} \left(X[k] \frac{T}{j2\pi k} \right) e^{j \frac{2\pi k}{T} t} + X[0] \\
&= \frac{d}{dt} \left(\sum_{k=-\infty, k \neq 0}^{\infty} Y[k] e^{j \frac{2\pi k}{T} t} + X[0] t \right)
\end{aligned}$$

From this, if we let $y(t) = \sum_{k=-\infty, k \neq 0}^{\infty} \left(X[k] \frac{T}{j2\pi k} \right) e^{j \frac{2\pi k}{T} t} + X[0] t$

$$\begin{aligned}
\frac{d}{dt} y(t) &= \sum_{k=-\infty, k \neq 0}^{\infty} X[k] e^{j \frac{2\pi k}{T} t} + X[0] \\
&= x(t).
\end{aligned}$$

This yields the property,

$$x(t) \xleftrightarrow{CTFS} X[k] \implies y(t) = \int_{\tau=0}^t x(\tau) d\tau \xleftrightarrow{CTFS} \begin{cases} \frac{T}{j2\pi k} X[k] & k \neq 0 \\ 0 & k = 0 \end{cases},$$

where we must only consider $x(t)$ such that $X[0] = 0$, or else $y(t)$ would not be periodic.

2.1.1.10 Differentiation

Similarly, we can consider the relationship between $y(t) = \frac{d}{dt} x(t)$ and their corresponding CTFT representations. From the definition of the CTFS, we have

$$\begin{aligned}
y(t) &= \frac{d}{dt} x(t) \\
&= \frac{d}{dt} \sum_{k=-\infty}^{\infty} X[k] e^{j \frac{2\pi k}{T} t} \\
&= \sum_{k=-\infty}^{\infty} X[k] \frac{d}{dt} e^{j \frac{2\pi k}{T} t} \\
&= \sum_{k=-\infty}^{\infty} \left(X[k] \frac{j2\pi k}{T} \right) e^{j \frac{2\pi k}{T} t}
\end{aligned}$$

from which we obtain the relation

$$x(t) \xleftrightarrow{\text{CTFS}} X[k] \implies y(t) = \frac{d}{dt} x(t) \xleftrightarrow{\text{CTFS}} \left(\frac{j2\pi k}{T} \right) X[k].$$

2.1.1.11 Parseval's relation

The energy contained within a period of a periodic signal can also be computed in terms of its CTFS representation using Parseval's relation,

$$x(t) \xleftrightarrow{\text{CTFS}} X[k] \implies \frac{1}{T} \int_{t=0}^T |x(t)|^2 dt = \sum_{k=-\infty}^{\infty} |X[k]|^2.$$

This relation can be derived using the definition of the CTFS as follows,

$$\begin{aligned} \frac{1}{T} \int_{t=0}^T |x(t)|^2 dt &= \frac{1}{T} \int_{t=0}^T x(t) x^*(t) dt \\ &= \frac{1}{T} \int_{t=0}^T x(t) \left(\sum_{k=-\infty}^{\infty} X^*[-k] e^{j \frac{2\pi k}{T} t} \right) dt \\ &= \sum_{k=-\infty}^{\infty} X^*[-k] \left(\frac{1}{T} \int_{t=0}^T x(t) e^{j \frac{2\pi k}{T} t} dt \right) \\ &= \sum_{k=-\infty}^{\infty} X^*[-k] \left(\frac{1}{T} \int_{t=0}^T x(t) e^{-j \frac{2\pi(-k)}{T} t} dt \right) \\ &= \sum_{k=-\infty}^{\infty} X^*[-k] X[-k] \\ &= \sum_{m=-\infty}^{\infty} |X[m]|^2. \end{aligned}$$

Parseval's relation shows that the energy in a period of a periodic signal is equal to the sum of the energies contained within each of the harmonic components that make up the signal through the CTFS representation.

2.2 Fourier transform representation of CT signals

Now that we have seen how we may build-up a large class of continuous-time periodic signals from the set of simpler complex exponential periodic signals, we return to apply this line of thinking to the more general class of continuous-time aperiodic (not periodic) signals. Just as was the case for periodic signals, a remarkably rich class of aperiodic signals can also be constructed from linear combinations of complex exponentials. In the case of periodic continuous-time signals, since the signals of interest were periodic, the CTFS was restricted to construct such signals through combinations of harmonically related exponentials. However for more general aperiodic signals, we may consider building an even larger class of signals by removing this restriction on the ingredients used to makeup a given signal. Since harmonically related complex exponentials can be enumerated, the CTFS took the form of a summation over the countably infinite set of all harmonically related exponentials of a given fundamental frequency. However, removing the restriction to only using harmonically related terms, the class of all possible complex exponentials arises from a continuum of possible frequency components and the form used with which to construct linear combinations will take the form of an integral, rather than an infinite summation. Just as with the continuous-time Fourier series, where the CTFS analysis equation provided a method for calculating the frequency components that makeup a given periodic signal, the continuous-time Fourier transform provides a method for calculating the spectrum of frequency components that makeup an aperiodic signal from this class. The resulting integral used to construct this large class of signals using this specific spectrum of frequency components is called the Fourier integral, or the continuous-time Fourier synthesis equation.

One method for introducing the continuous-time Fourier transform is through the CTFS. By considering continuous-time aperiodic signals as the result of taking continuous-time periodic signals to the limit of an infinite period, we may observe how the CTFS transitions from a countable sum of harmonically-related complex exponentials, into a continuous integral over the continuum of possible frequencies. Let us return to the square wave signal that we visited in Figure 2.2. In this case, however, we will alter the signal to take the form

$$x(t) = \begin{cases} 1, & 0 \leq t \leq 1 \\ 0 & \text{else} \end{cases}$$

over the unit interval, $t \in [0, 1]$. Using (2.10), we once again obtain its CTFS representation, however this time, we consider the period of repetition of the “on” period of the square wave to be given by the variable T , i.e. we have

$$x(t) = \begin{cases} 1, & 0 \leq t \leq 1 \\ 0 & \text{else} \end{cases}$$

for $t \in [0, T]$, and then repeating every T seconds. This yields the following CTFS representation

$$\begin{aligned} X[k] &= \int_0^T x(t) e^{-j \frac{2\pi k}{T} t} dt \\ &= \int_0^1 e^{-j \frac{2\pi k}{T} t} dt \\ &= \frac{-T}{j2\pi k} \left(e^{-j \frac{2\pi k}{T}} - 1 \right) \\ &= \frac{-T}{j2\pi k} e^{-j \frac{\pi k}{T}} \left(e^{-j \frac{\pi k}{T}} - e^{j \frac{\pi k}{T}} \right) \\ &= \frac{T}{j2\pi k} e^{-j \frac{\pi k}{T}} 2j \sin \left(\frac{\pi k}{T} \right) \\ &= \begin{cases} \frac{\sin \left(\frac{\pi k}{T} \right)}{\frac{\pi k}{T}} e^{-j \frac{\pi k}{T}} & k \neq 0 \\ 1 & k = 0, \end{cases} \end{aligned} \quad (2.15)$$

where the $k = 0$ term is once again determined by closer examination of the first line of the derivation, rather than attempting further analysis on the expression containing vanishing terms in the numerator and denominator. We consider the expression in (2.15) for various values of T in Figure 2.3. By plotting the magnitude of the CTFS coefficients $|X[k]|$ versus the harmonically related frequency components $\frac{2\pi k}{T}$ for various values of T , ranging from $T = 4$, up to $T = 32$, we see that the envelope containing the CTFS coefficients remains constant, while the CTFS coefficients move closer and closer to one another in absolute frequency.

The envelope that is observed in the figure, can be viewed as the value that the CTFS representation would take on as the period of the signal is made larger and larger. Recognizing this process, Fourier defined this envelope as

$$X(\omega) = \int_{t=-\infty}^{\infty} x(t) e^{-j\omega t} dt, \quad (2.16)$$

where the angular frequency variable ω (measured in radians) takes on all values on the real line, and for which (2.16) is known as the continuous-time Fourier transform (CTFT).

For our example, the continuous-time Fourier transform would evaluate to

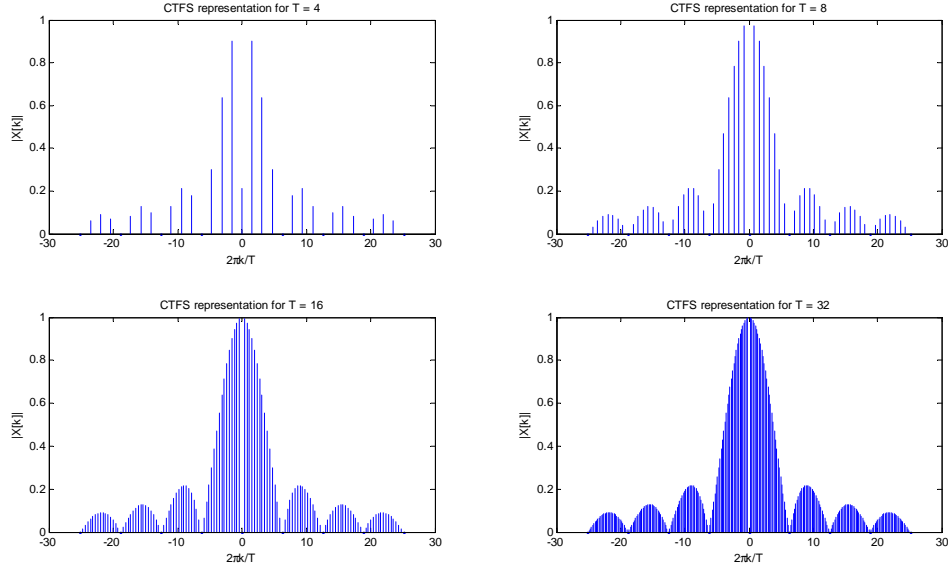


Figure 2.3: CTFS representation of the periodic signal in 2.17 for $T = 4, 8, 16, 32$.

$$\begin{aligned}
 X(\omega) &= \int_{-\infty}^{\infty} x(t)e^{-j\omega t} dt \\
 &= \int_0^1 e^{-j\omega t} dt \\
 &= \frac{-1}{j\omega} (e^{-j\omega} - 1) \\
 &= \frac{-1}{j\omega} e^{-j\omega/2} (e^{-j\omega/2} - e^{j\omega/2}) \\
 &= \frac{1}{j\omega} e^{-j\omega/2} 2j \sin(\omega/2) \\
 &= \begin{cases} \frac{\sin(\frac{\omega}{2})}{\frac{\omega}{2}} e^{-j\frac{\omega}{2}} & \omega \neq 0 \\ 1 & \omega = 0. \end{cases} \tag{2.17}
 \end{aligned}$$

While the CTFT analysis equation (2.16) provides the composition of any of a large class of signals through a linear superposition of complex exponential signals of the form $e^{j\omega t}$, the CTFT synthesis equation provides the recipe for constructing such signals from their constituent set, as

$$x(t) = \frac{1}{2\pi} \int_{\omega=-\infty}^{\infty} X(\omega) e^{j\omega t} d\omega.$$

Because a complex exponential $e^{j\omega t}$ is periodic with period $T = 2\pi/\omega$, we refer to $f = 1/T = 2\pi/\omega$ as (regular) frequency, measured in Hz, or cycles per second.

Together, the two expressions make up the CTFT representation for aperiodic signals,

$$\begin{aligned}
 x(t) &= \frac{1}{2\pi} \int_{\omega=-\infty}^{\infty} X(\omega) e^{j\omega t} d\omega \\
 X(\omega) &= \int_{t=-\infty}^{\infty} x(t) e^{-j\omega t} dt
 \end{aligned}$$

CT Fourier Transform Representation of Aperiodic Signals

$$x(t) = \frac{1}{2\pi} \int_{\omega=-\infty}^{\infty} X(\omega) e^{j\omega t} d\omega \quad (2.18)$$

$$X(\omega) = \int_{t=-\infty}^{\infty} x(t) e^{-j\omega t} dt \quad (2.19)$$

2.2.1 CT Fourier Transform Properties

We have now been properly introduced to a method for building-up continuous-time aperiodic signals from a class of complex exponential signals in (2.18) and a method for analysing the make-up of such periodic signals in terms of their constituent sinusoidal components in (2.19). Once again, now that introductions are out of the way, we can explore some of the many useful properties of the CTFT representation. Many of the properties of the CTFT follow directly, or along similar lines, of those of the CTFS.

2.2.1.1 Linearity

The CTFT can be viewed as a linear operation, in the following manner. When two signals $x(t)$ and $y(t)$ are each constructed from their constituent complex exponential signals according to the CTFT synthesis equation, the linear combination of these signals, $z(t) = ax(t) + by(t)$, for a, b real-valued constants, can be readily obtained by combining the constituent complex exponential signals through the same linear combination. More specifically, when $x(t)$ is an aperiodic signal with CTFT coefficients $X(\omega)$ and $y(t)$ is an aperiodic signal with CTFT $Y(\omega)$ then the signal $z(t) = ax(t) + by(t)$ has a CTFT representation given by $Z(\omega) = aX(\omega) + bY(\omega)$. The linearity property of the CTFT can be compactly represented as follows

$$x(t) \xleftrightarrow{\text{CTFT}} X(\omega), y(t) \xleftrightarrow{\text{CTFT}} Y(\omega) \implies z(t) = ax(t) + by(t) \xleftrightarrow{\text{CTFT}} aX(\omega) + bY(\omega).$$

2.2.1.2 Time Shift

For the signal $y(t) = x(t - t_0)$, we have

$$\begin{aligned} Y(\omega) &= \int_{t=-\infty}^{\infty} x(t - t_0) e^{-j\omega t} dt \\ &= \int_{s=-\infty}^{\infty} x(s) e^{-j\omega(s+t_0)} ds \\ &= \int_{s=-\infty}^{\infty} x(s) e^{-j\omega t_0} e^{-j\omega s} ds \\ &= X(\omega) e^{-j\omega t_0}, \end{aligned}$$

where, the second line follows from the change of variable, $s = t - t_0$. The time shift property of the CTFT can be compactly represented as follows

$$x(t) \xleftrightarrow{\text{CTFT}} X(\omega) \implies y(t) = x(t - t_0) \xleftrightarrow{\text{CTFT}} X(\omega) e^{-j\omega t_0}.$$

We see that a shift in time of an aperiodic signal corresponds to a modulation in frequency by a phase term that is linear with frequency with a slope that is proportional to the delay.

2.2.1.3 Frequency Shift

When a signal $x(t)$ has a CTFT representation given by $X(\omega)$, a natural question that might arise is the what happens when the shifting that was discussed in section 2.2.1.2 is applied to the CTFT representation, $X(\omega)$. Specifically, if a signal $y(t)$ were known to have a CTFT representation given by $Y(\omega) = X(\omega - \omega_0)$, it

is interesting to understand the relationship in the time-domain between $y(t)$ and $x(t)$. This can be readily seen through examination of the CTFT analysis equation,

$$\begin{aligned} Y(\omega) &= X(\omega - \omega_0) \\ &= \int_{t=-\infty}^{\infty} x(t) e^{-j(\omega - \omega_0)t} dt \\ &= \int_{t=-\infty}^{\infty} (x(t) e^{j\omega_0 t}) e^{-j\omega t} dt, \end{aligned}$$

which leads to the relation

$$x(t) \xleftrightarrow{CTFT} X(\omega) \implies y(t) = x(t) e^{j\omega_0 t} \xleftrightarrow{CTFT} X(\omega - \omega_0).$$

We observe that a shift in the frequency of the continuous time Fourier transform by an amount ω_0 corresponds to a modulation in the time domain signal $x(t)$ by a term whose frequency is proportional to the shift amount.

2.2.1.4 Time Reversal

Analogous to the result for the CTFS, we have from the CTFT synthesis equation,

$$x(t) = \frac{1}{2\pi} \int_{\omega=-\infty}^{\infty} X(\omega) e^{j\omega t} d\omega,$$

we see that by simply changing the sign of the time variable t , we obtain the general relation

$$\begin{aligned} y(t) &= x(-t) = \frac{1}{2\pi} \int_{\omega=-\infty}^{\infty} X(\omega) e^{-j\omega t} d\omega \\ &= \frac{1}{2\pi} \int_{\omega=-\infty}^{\infty} X(\omega) e^{j(-\omega)t} d\omega \\ &= \frac{1}{2\pi} \int_{\omega=-\infty}^{\infty} X(-\omega) e^{j\omega t} d\omega, \end{aligned}$$

yielding the relation

$$x(t) \xleftrightarrow{CTFT} X(\omega) \implies y(t) = x(-t) \xleftrightarrow{CTFT} X(-\omega),$$

i.e., changing the sign of the time axis corresponds to changing the sign of the CTFT frequency index.

2.2.1.5 Time Scaling

When signal undergoes a time-scale change, such as one that compresses the time axes, $y(t) = x(at)$, where $a > 1$ is a real-valued constant, the resulting signal $y(t)$ is given by

$$\begin{aligned} y(t) &= \int_{\omega=-\infty}^{\infty} X(\omega) e^{j\omega at} d\omega \\ &= \int_{\nu=-\infty}^{\infty} \frac{1}{|a|} X(\nu/a) e^{j\nu t} d\nu, \end{aligned}$$

where the second line follows from the substitution $\nu = a\omega$. This yields the following relation for $y(t) = x(at)$,

$$x(t) \xleftrightarrow{CTFT} X(\omega) \implies y(t) = x(at) \xleftrightarrow{CTFT} \frac{1}{|a|} X(\omega/a).$$

2.2.1.6 Conjugate Symmetry

The effect of conjugating a complex-valued signal on its CTFT representation can be seen by simply conjugating the CTFT synthesis relation,

$$\begin{aligned}
 x(t) &= \frac{1}{2\pi} \int_{-\infty}^{\infty} X(\omega) e^{j\omega t} d\omega \\
 x^*(t) &= \left(\frac{1}{2\pi} \int_{-\infty}^{\infty} X(\omega) e^{j\omega t} d\omega \right)^* \\
 &= \frac{1}{2\pi} \int_{-\infty}^{\infty} X^*(\omega) e^{-j\omega t} d\omega \\
 &= \frac{1}{2\pi} \int_{-\infty}^{\infty} X^*(\omega) e^{j(-\omega)t} d\omega \\
 &= \frac{1}{2\pi} \int_{-\infty}^{\infty} X^*(-\omega) e^{j\omega t} d\omega
 \end{aligned}$$

yielding that

$$x(t) \xleftrightarrow{CTFT} X(\omega) \implies x^*(t) \xleftrightarrow{CTFT} X^*(-\omega).$$

When the signal $x(t)$ is real valued, then the CTFT exhibits a symmetry property. This arises directly from the definition of the CTFT, and that real numbers equal their conjugates, i.e. $x(t) = x^*(t)$, such that

$$x(t) = x^*(t) \xleftrightarrow{CTFT} X(\omega) \implies X(\omega) = X^*(-\omega).$$

Note that when the signal is real-valued and is an even function of time, such that $x(t) = x(-t)$, then its CTFT is also real-valued and even, i.e. $X(\omega) = X^*(\omega) = X(-\omega)$. It can be shown by similar reasoning that when the signal real-valued, and an odd function of time, that the CTFT is purely imaginary and odd, i.e. $X(\omega) = -X^*(\omega) = -X(-\omega)$.

2.2.1.7 Products of Signals

When signals are multiplied in time, such that $z(t) = x(t)y(t)$, the resulting signal has a CTFS representation that can be obtained through the analysis equation,

$$\begin{aligned}
 Z(\omega) &= \int_{-\infty}^{\infty} (x(t)y(t)) e^{-j\omega t} dt \\
 &= \int_{-\infty}^{\infty} (y(t) \left(\frac{1}{2\pi} \int_{-\infty}^{\infty} X(\nu) e^{j\nu t} d\nu \right)) e^{-j\omega t} dt \\
 &= \frac{1}{2\pi} \int_{-\infty}^{\infty} X(\nu) \left(\int_{-\infty}^{\infty} y(t) e^{-j(\omega-\nu)t} dt \right) d\nu \\
 &= \frac{1}{2\pi} \int_{-\infty}^{\infty} X(\nu) Y(\omega - \nu) d\nu.
 \end{aligned}$$

The relationship between the CTFT representation for $z(t)$ and those of $x(t)$ and $y(t)$ is seen to be a convolution between the two CTFTs $X(\omega)$ and $Y(\omega)$,

$$x(t) \xleftrightarrow{CTFT} X(\omega), y(t) \xleftrightarrow{CTFT} Y(\omega) \implies z(t) = x(t)y(t) \xleftrightarrow{CTFT} \frac{1}{2\pi} \int_{-\infty}^{\infty} X(\nu) Y(\omega - \nu) d\nu.$$

2.2.1.8 Convolution

A dual relationship to that of multiplication in time, is multiplication of CTFT representations. Specifically, the signal whose CTFT representation is given by $Z(\omega) = X(\omega)Y(\omega)$ corresponds to a convolution of the signals $x(t)$ and $y(t)$. This can be seen as follows,

$$\begin{aligned}
z(t) &= \frac{1}{2\pi} \int_{\omega=-\infty}^{\infty} (X(\omega)Y(\omega)) e^{j\omega t} d\omega \\
&= \frac{1}{2\pi} \int_{\omega=-\infty}^{\infty} \left(\int_{\tau=-\infty}^{\infty} x(\tau) e^{-j\omega\tau} d\tau \right) Y(\omega) e^{j\omega t} d\omega \\
&= \int_{\tau=-\infty}^{\infty} x(\tau) \left(\frac{1}{2\pi} \int_{\omega=-\infty}^{\infty} Y(\omega) e^{j\omega(t-\tau)} d\omega \right) d\tau \\
&= \int_{\tau=-\infty}^{\infty} x(\tau) y(t-\tau) d\tau
\end{aligned}$$

where the integral relationship in the last line is recognized as a convolution. This leads to the following property of the CTFT,

$$x(t) \xleftrightarrow{CTFT} X(\omega), y(t) \xleftrightarrow{CTFT} Y(\omega) \implies z(t) = \int_{\tau=-\infty}^{\infty} x(\tau) y(t-\tau) d\tau \xleftrightarrow{CTFT} Z(\omega) = X(\omega)Y(\omega).$$

2.2.1.9 Integration

When the signal $y(t)$ and $x(t)$ are related through a running integral, i.e. $y(t) = \int_{\tau=-\infty}^t x(\tau) d\tau$, we can relate their CTFTs as follows,

$$x(t) \xleftrightarrow{CTFT} X(\omega) \implies y(t) = \int_{\tau=-\infty}^t x(\tau) d\tau \xleftrightarrow{CTFT} \frac{1}{j\omega} X(\omega) + \pi X(0)\delta(\omega),$$

where the relation is easiest shown using the differentiation property derived next together with the following observation. When $\omega = 0$, $Y(\omega)$ is unbounded if $X(0)$ is nonzero.

2.2.1.10 Differentiation

Similarly, we can consider the relationship between $y(t) = \frac{d}{dt}x(t)$ and their corresponding CTFT representations. From the definition of the CTFT, we have

$$\begin{aligned}
y(t) &= \frac{d}{dt}x(t) \\
&= \frac{d}{dt} \frac{1}{2\pi} \int_{\omega=-\infty}^{\infty} X(\omega) e^{j\omega t} d\omega \\
&= \frac{1}{2\pi} \int_{\omega=-\infty}^{\infty} X(\omega) \frac{d}{dt} e^{j\omega t} d\omega \\
&= \frac{1}{2\pi} \int_{\omega=-\infty}^{\infty} (j\omega X(\omega)) e^{j\omega t} d\omega
\end{aligned}$$

from which we obtain the relation

$$x(t) \xleftrightarrow{CTFT} X(\omega) \implies y(t) = \frac{d}{dt}x(t) \xleftrightarrow{CTFT} j\omega X(\omega).$$

2.2.1.11 Parseval's relation

The energy contained in a finite-energy signal (note that the CTFT exists in the case of finite energy signals, i.e. signals that can be square integrated) can also be computed in terms of its CTFT representation using Parseval's relation,

$$x(t) \xleftrightarrow{CTFT} X(\omega) \implies \int_{t=-\infty}^{\infty} |x(t)|^2 dt = \frac{1}{2\pi} \int_{\omega=-\infty}^{\infty} |X(\omega)|^2 d\omega.$$

Section	CTFT Property	Continuous Time Signal	Continuous Time Fourier Transform
	Definition	$x(t)$	$X(\omega) = \int_{t=-\infty}^{\infty} x(t)e^{-j\omega t} dt$
2.2.1.1	Linearity	$z(t) = ax(t) + by(t)$	$Z(\omega) = aX(\omega) + bY(\omega)$
2.2.1.2	Time Shift	$y(t) = x(t - T)$	$Y(\omega) = X(\omega)e^{-j\omega T}$
2.2.1.3	Modulation	$y(t) = x(t)e^{j\omega_0 t}$	$Y(\omega) = X(\omega - \omega_0)$
2.2.1.4	Time Reversal	$y(t) = x(-t)$	$Y(\omega) = X(-\omega)$
2.2.1.5	Time Scaling	$y(t) = x(at)$	$Y(\omega) = \frac{1}{ a } X(\omega/a)$
2.2.1.6	Conjugate Symmetry	$x(t) = x^*(t)$	$X(\omega) = X^*(-\omega)$
2.2.1.7	Products of Signals	$z(t) = x(t)y(t)$	$Z(\omega) = \frac{1}{2\pi} \int_{\nu=-\infty}^{\infty} X(\nu)Y(\omega - \nu) d\nu$
2.2.1.8	Convolution	$z(t) = \int_{\tau=-\infty}^{\infty} x(\tau)y(t - \tau) d\tau$	$Z(\omega) = X(\omega)Y(\omega)$
2.2.1.9	Integration	$y(t) = \int_{\tau=-\infty}^t x(\tau) d\tau$	$Y(\omega) = \frac{1}{j\omega} X(\omega) + \pi X(0)\delta(\omega)$
2.2.1.10	Differentiation	$y(t) = \frac{d}{dt} x(t)$	$Y(\omega) = j\omega X(\omega)$
2.2.1.11	Parseval's Relation	$x(t)$	$\int_{t=-\infty}^{\infty} x(t) ^2 dt = \frac{1}{2\pi} \int_{-\infty}^{\infty} X(\omega) ^2 d\omega$
	Other properties?	tx(t), even part, odd part	
		conjsym part, conjasym part	

Table 2.1: Properties of the Continuous Time Fourier Transform

This relation can be derived using the definition of the CTFS as follows,

$$\begin{aligned}
\int_{t=-\infty}^{\infty} |x(t)|^2 dt &= \int_{t=-\infty}^{\infty} x(t)x^*(t) dt \\
&= \int_{t=-\infty}^{\infty} x(t) \left(\frac{1}{2\pi} \int_{\omega=-\infty}^{\infty} X^*(\omega)e^{-j\omega t} d\omega \right) dt \\
&= \frac{1}{2\pi} \int_{\omega=-\infty}^{\infty} X^*(\omega) \left(\int_{t=-\infty}^{\infty} x(t)e^{-j\omega t} dt \right) d\omega \\
&= \frac{1}{2\pi} \int_{\omega=-\infty}^{\infty} X^*(\omega) (X(\omega)) d\omega \\
&= \frac{1}{2\pi} \int_{\omega=-\infty}^{\infty} X^*(\omega) X(\omega) d\omega \\
&= \frac{1}{2\pi} \int_{\omega=-\infty}^{\infty} |X(\omega)|^2 d\omega.
\end{aligned}$$

Parseval's relation shows that the energy measured in the time-domain of a finite-energy signal is equal to the energy measured in the frequency domain through its CTFT representation.

2.2.2 CTFT Examples

Derivations of some of the signals in the Table 2.2.

2.3 Discrete-Fourier Series representation of DT periodic signals

In Section 2.1 we discussed the Fourier series representation as a means of building a large class of continuous time periodic signals from a set of simpler, harmonically related complex exponential signals. In this section, we consider the analogous notion of building a large class of periodic signals in discrete time from a set of simpler, harmonically related complex exponential discrete time signals. An important difference between the continuous time Fourier series and what we will develop in this section as the discrete time Fourier series (DTFS), is that while the series used to construct periodic signals in continuous time is infinite, the series used to construct discrete time periodic signals is in fact a finite sum. This difference simplifies a number

Continuous Time Signal	Continuous Time Fourier Transform
$x(t)$	$X(\omega) = \int_{t=-\infty}^{\infty} x(t)e^{-j\omega t} dt$
$e^{-at}u(t), \text{Real}\{a\} > 0$	$\frac{1}{j\omega + a}$
$te^{-at}u(t), \text{Real}\{a\} > 0$	$\frac{1}{(j\omega + a)^2}$
$e^{j\omega_0 t}$	$2\pi\delta(\omega - \omega_0)$
1	$2\pi\delta(\omega)$
$\delta(t - T_0)$	$e^{-j\omega T_0}$
$\cos(\omega_0 t)$	$\pi[\delta(\omega - \omega_0) + \delta(\omega + \omega_0)]$
$\sin(\omega_0 t)$	$-j\pi[\delta(\omega - \omega_0) - \delta(\omega + \omega_0)]$
$\frac{W}{\pi} \text{sinc}\left(\frac{Wt}{\pi}\right) = \begin{cases} \frac{\sin(Wt)}{\pi t} & t \neq 0 \\ \frac{W}{\pi} & t = 0 \end{cases}$	$\begin{cases} 1, & \omega < W \\ 0, & \omega > W \end{cases}$
$\begin{cases} 1, & t < T \\ 0, & t > T \end{cases}$	$2T \text{sinc}\left(\frac{\omega T}{\pi}\right) = \begin{cases} \frac{2\sin(\omega T)}{\omega} & \omega \neq 0 \\ 2T & \omega = 0 \end{cases}$
more	more
more	more
more	more
more	more
more	more

Table 2.2: Continuous Time Fourier Transform Pairs

of issues that were delicate in the continuous case, such as notions of convergence, and existence of certain limits.

Mathematically, we represent a periodic discrete time signal, $x[n]$, as a signal whose value repeats at a fixed number of samples from the present. This interval, denoted N below, is called the “period” of the signal, and we express this relationship

$$x[n] = x[n + N], \text{ for all } n. \quad (2.20)$$

Equation (2.20) will, in general, be satisfied for a countably infinite number of possible values of N . The smallest, positive value of N for which Eq. (2.20) is satisfied, is called the “fundamental period” of the signal $x[n]$. Discrete time sinusoidal signals, such as

$$x[n] = \sin(\omega_0 n + \phi), \quad (2.21)$$

often enable us to relate the frequency of oscillation, ω_0 to a fundamental period, N . While analogous to their continuous time cousins, discrete time sinusoids need not always be periodic. While this may require a more careful notion of what is meant by discrete time “frequency,” we will place this issue aside for the moment and consider how the period of a periodic sinusoid relates to the arguments of the sinusoidal function. This can again be computed by noting that sinusoidal functions are equal when their arguments are either equal or differ only through a multiple of 2π , i.e.

$$\begin{aligned} x[n] &= x[n + N] \\ \sin(\omega_0 n + \phi) &= \sin(\omega_0(n + N) + \phi) \\ \sin(\omega_0 n + \phi + 2k\pi) &= \sin(\omega_0(n + N) + \phi) \\ \sin(\omega_0(n + 2k\pi/\omega_0) + \phi) &= \sin(\omega_0(n + N) + \phi) \end{aligned} \quad (2.22)$$

which yields the relationship

$$N = 2\pi k/\omega_0. \quad (2.23)$$

Depending on the value of ω_0 , (2.23) may not provide an integer solution for N for any value of k . Note that only if ω_0/π is rational, will there be an integral solution to (2.23), for which the smallest integer value of N is the fundamental period associated with the discrete time frequency ω_0 . In Figure (2.4), the two

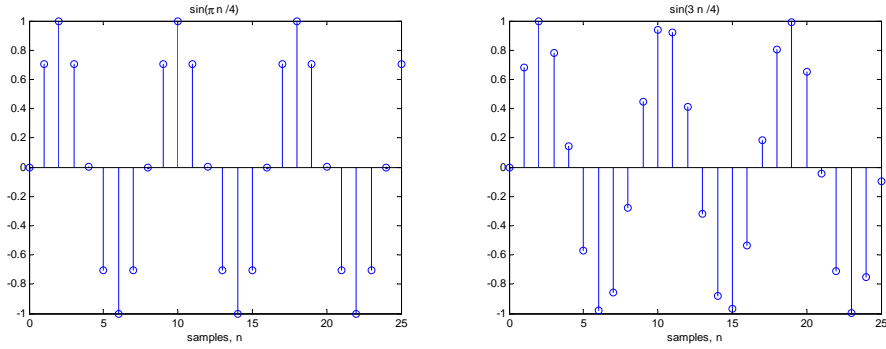


Figure 2.4: Examples of periodic and aperiodic sinusoidal signals $x[n] = \sin(\pi n/4)$ and $x[n] = \sin(3n/4)$.

sinusoidal signals $x[n] = \sin(\pi n/4)$ and $x[n] = \sin(3n/4)$ are shown. Note that the fundamental period of $N = 2\pi/(\pi/4) = 8$ can be readily seen from figure for the periodic signal $x[n] = \sin(\pi n/4)$. However, the aperiodic signal $x[n] = \sin(3n/4)$ does not exhibit periodicity for any value of n seen in the figure, and since the frequency argument of the sinusoid is not a rational multiple of π , we are guaranteed that no such integer period exists.

As in continuous time, any two periodic signals, $x[n]$ and $y[n]$ with the same period N can be added together to produce a new periodic signal of the same period, i.e.,

$$\begin{aligned} s[n] &= x[n] + y[n] \\ s[n + N] &= x[n + N] + y[n + N] = s[n + N]. \end{aligned}$$

We again consider how we might build-up a larger class of periodic signals from the basic building blocks of harmonically-related discrete time sinusoids. To extend our discussion to include complex-valued signals, we again employ Euler's relation to construct complex exponential signals of the form

$$\begin{aligned} x[n] &= e^{j(\omega_0 n + \phi)} \\ &= \cos(\omega_0 n + \phi) + j \sin(\omega_0 n + \phi) \end{aligned} \quad (2.24)$$

enabling us to write

$$x[n] = ce^{j\omega_0 n},$$

where, $c = e^{j\phi}$ is simply a complex constant whose effects on the sinusoidal nature of the signal have again been conveniently parked in front of the discussion. Complex-exponential signals of the form (2.24) may be periodic or aperiodic depending on whether or not ω_0/π is rational.

Analogous to the CTFS, we can explore the class of signals that can be constructed by such harmonically-related complex exponentials of the form

$$x[n] = \frac{1}{N} \sum_{k=0}^{N-1} X[k] e^{jk\omega_0 n}, \quad (2.25)$$

where $\omega_0 = 2\pi k/N$. Note that the summation in (2.25) only covers N terms, rather than the infinite sum in (2.6) for the CTFS. This is due to the finite number of harmonically related complex exponentials that can be constructed with period N . Note that since the independent (time) variable in discrete time signals only takes on integer values, complex exponentials of frequency ω_0 are indistinguishable from those with frequency $\omega_0 + k2\pi$ for any k , i.e.

$$e^{j\omega_0 n} = e^{j(\omega_0 + k2\pi)n}.$$

This result together with the fundamental period of N yields,

$$e^{j\frac{2\pi k}{N}n} = e^{j\frac{2\pi(k+N)}{N}n}.$$

As a result, there are only N distinct complex exponential signals of period N . The resulting DTFS synthesis equation, written in terms of the fundamental period of the signal set becomes

$$x[n] = \frac{1}{N} \sum_{k=0}^{N-1} X[k] e^{j2\pi kn/N}, \quad (2.26)$$

where $\omega_0 = 2\pi/N$ is the fundamental frequency of the periodic signal $x[n]$. The construction in (2.26) is referred to as the discrete-time Fourier series (DTFS) representation of $x[n]$ and (2.26) is often called the discrete-time Fourier series synthesis equation.

The Fourier series coefficients $X[k]$ can be obtained by multiplying (2.26) by $e^{-j2\pi kn/N}$ and summing over a period of duration N to obtain

$$\begin{aligned} \sum_{n=0}^{N-1} x[n] e^{-j2\pi kn/N} &= \sum_{n=0}^{N-1} \left(\frac{1}{N} \sum_{m=0}^{N-1} X[m] e^{j2\pi(m-k)n/N} \right) \\ \sum_{n=0}^{N-1} x[n] e^{-j2\pi kn/N} &= \frac{1}{N} \sum_{m=0}^{N-1} X[m] \left(\sum_{n=0}^{N-1} e^{j2\pi(m-k)n/N} \right). \end{aligned}$$

To proceed, we need to evaluate the sum

$$\begin{aligned} \sum_{n=0}^{N-1} e^{j2\pi(m-k)n/N} &= \begin{cases} \frac{1-e^{j2\pi(m-k)N/N}}{1-e^{j2\pi(m-k)/N}} & m \neq k \\ N & m = k \end{cases} \\ &= \begin{cases} \frac{1-e^{j2\pi(m-k)}}{1-e^{j2\pi(m-k)/N}} & m \neq k \\ N & m = k \end{cases} \\ &= \begin{cases} 0 & m \neq k \\ N & m = k, \end{cases} \end{aligned}$$

which leads to the result

$$\begin{aligned} \sum_{n=0}^{N-1} x[n] e^{-j2\pi kn/N} &= \frac{1}{N} \sum_{m=0}^{N-1} X[m] N \delta[m-k], \\ &= X[k], \end{aligned}$$

by the sifting property of the Kronocker delta function. We can now return obtain the discrete-time Fourier series analysis equation,

$$X[k] = \sum_{n=0}^{N-1} x[n] e^{-j2\pi kn/N}. \quad (2.27)$$

Putting the synthesis and analysis equations together, we have the discrete-time Fourier series representation of a periodic signal $x[n]$ as

DT Fourier Series Representation of a Periodic Signal

$$X[k] = \sum_{n=0}^{N-1} x[n] e^{-j\frac{2\pi kn}{N}}, \text{ all } k \quad (2.28)$$

$$x[n] = \frac{1}{N} \sum_{k=0}^{N-1} X[k] e^{j\frac{2\pi kn}{N}}, \text{ all } n, \quad (2.29)$$

note that by convention, we define the signal $X[k]$ over all values of k , noting that due to the periodicity of the sequence $x[n]$ and of the signals $e^{j2\pi kn/N}$, the sequence $X[k]$ will also be periodic with period N . In this derivation we used the following useful result for summation of a finite-length geometric series, which holds for any $r \neq 1$,

$$\sum_{k=m}^n r^k = \frac{r^m - r^{n+1}}{1-r}.$$

Example: DTFS of a Square Wave

Consider the periodic discrete time sequence of period $N = 8$ that satisfies

$$x[n] = \begin{cases} 1, & 0 \leq n < 4 \\ 0 & 4 \leq n < 8 \end{cases} \quad (2.30)$$

Using (2.27), we obtain,

$$\begin{aligned} X[k] &= \sum_{n=0}^7 x[n] e^{-j2\pi kn/8} \\ &= \sum_{n=0}^3 e^{-j2\pi kn/8} \\ &= \begin{cases} \frac{1-e^{-j2\pi k4/8}}{1-e^{-j2\pi k/8}}, & k \neq 0 \\ 4, & k = 0 \end{cases} \\ &= \begin{cases} \frac{1-e^{-j\pi k}}{1-e^{-j\pi k/4}}, & k \neq 0 \\ 4, & k = 0 \end{cases} \\ &= \begin{cases} \frac{e^{-j\pi k/2}(e^{j\pi k/2}-e^{-j\pi k/2})}{e^{-j\pi k/8}(e^{j\pi k/8}-e^{-j\pi k/8})}, & k \neq 0 \\ 4, & k = 0 \end{cases} \\ &= \begin{cases} e^{-j3\pi k/8} \frac{\sin(\pi k/2)}{\sin(\pi k/8)}, & k \neq 0 \\ 4, & k = 0. \end{cases} \end{aligned}$$

2.3.1 DT Fourier Series Properties

We have now been properly introduced to a method for building-up discrete-time periodic signals from a class of simple sinusoidal signals in (2.38) and a method for analysing the make-up of such periodic signals in terms of their constituent sinusoidal components in (2.37). Now that introductions are once again out of the way, we can explore some of the many useful properties of the DTFS representation.

2.3.1.1 Linearity

The DTFS can be viewed as a linear operation, in the following manner. When two signals $x[n]$ and $y[n]$ are each constructed from their constituent sinusoidal signals according to the DTFS synthesis equation (2.38), the linear combination of these signals, $z[n] = ax[n] + by[n]$, for a, b real-valued constants, can be readily obtained by combining the constituent sinusoidal signals through the same linear combination. More specifically, when $x[n]$ is a periodic signal with DTFS coefficients $X[k]$ and $y[n]$ is a periodic signal with DTFS coefficients $Y[k]$ then the signal $z[n] = ax[n] + by[n]$ has DTFS coefficients given by $Z[k] = aX[k] + bY[k]$. The linearity property of the DTFS can be compactly represented as follows

$$x[n] \xleftrightarrow{DTFS} X[k], y[n] \xleftrightarrow{DTFS} Y[k] \implies z[n] = ax[n] + by[n] \xleftrightarrow{DTFS} aX[k] + bY[k].$$

This result can be readily shown by substituting $z[n] = ax[n] + by[n]$ into the summation in (2.37) and expanding the summation into the two separate terms, one for $X[k]$ and one for $Y[k]$.

2.3.1.2 Time Shift

When a sinusoidal signal $x[n] = \sin[\omega_0 n]$ is shifted in time, the resulting signal $x[n - n_0]$ can be represented in terms of a simple phase shift of the original sinusoidal signal, i.e. $x[n - n_0] = \sin(\omega_0(n - n_0)) = \sin(\omega_0 n + \phi)$, where $\phi = -\omega_0 n_0$. Periodic signals that can be represented using the DTFS contain many sinusoidal (or complex exponential) signals. When such periodic signals are delayed in time, each of the

constituent sinusoidal components of the signal are delayed by the same amount, however this translates into a different phase shift for each component. This can be readily seen from the DTFS analysis equation 2.37, as follows. For the signal $y[n] = x[n - n_0]$, we have

$$\begin{aligned}
 Y[k] &= \sum_{n=0}^{N-1} x[n - n_0] e^{-j \frac{2\pi k}{N} n} \\
 &= \sum_{m=N-n_0}^{N-1} x[m] e^{-j \frac{2\pi k}{N} (m+n_0)} + \sum_{m=0}^{N-1-n_0} x[m] e^{-j \frac{2\pi k}{N} (m+n_0)} \\
 &= \sum_{m=0}^{N-1} x[m] e^{-j \frac{2\pi k}{N} (m+n_0)} \\
 &= \sum_{m=0}^{N-1} x[n] e^{-j \frac{2\pi k}{N} n_0} e^{-j \frac{2\pi k}{N} m} \\
 &= X[k] e^{-j \frac{2\pi k}{N} n_0},
 \end{aligned}$$

where, the second line follows from the change of variable, $m = n - n_0$, noting that any values of m that would then become negative can be made positive by the periodicity of $x[m]$, i.e., $x[-k] = x[N - k]$, and we have collected these terms in the first summation of the second line, and the second sum contains the remaining terms; the third line follows from the periodicity of both the signal $x[n]$ and the signal $e^{-j 2\pi k n / N}$ with period N , and the last line follows from the definition of $X[k]$ after factoring the linear phase term $e^{-j 2\pi k n_0 / N}$ out of the sum. The time shift property of the DTFS can be compactly represented as follows

$$x[n] \xleftrightarrow{DTFS} X[k] \implies y[n] = x[n - n_0] \xleftrightarrow{DTFS} X[k] e^{-j \frac{2\pi k}{N} n_0}.$$

We see that a shift in time of a periodic signal corresponds to a modulation in frequency by a phase term that is linear with frequency with a slope that is proportional to the delay.

2.3.1.3 Frequency Shift

When a periodic signal $x[n]$ has a DTFS representation given by $X[k]$, a natural question that might arise is the what happens when the shifting that was discussed in section 2.3.1.2 is applied to the DTFS representation, $X[k]$. Specifically, if a periodic signal $y[n]$ were known to have a DTFS representation given by $Y[k] = X[k - k_0]$, it is interesting to understand the relationship in the time-domain between $y[n]$ and $x[n]$. This can be readily seen through examination of the CTFS analysis equation,

$$\begin{aligned}
 Y[k] &= X[k - k_0] \\
 &= \sum_{n=0}^{N-1} x[n] e^{-j \frac{2\pi}{N} (k - k_0) n} \\
 &= \sum_{n=0}^{N-1} (x[n] e^{j \frac{2\pi}{N} k_0 n}) e^{-j \frac{2\pi}{N} k n}
 \end{aligned}$$

which leads to the relation

$$x[n] \xleftrightarrow{DTFS} X[k] \implies y[n] = x[n] e^{j k_0 \omega_0 n} \xleftrightarrow{DTFS} X[k - k_0],$$

where $\omega_0 = \frac{2\pi}{N}$. We observe that a shift in the discrete time Fourier series coefficients by an integer amount k_0 corresponds to a modulation in the time domain signal $x[n]$ by a term whose frequency is proportional to the shift amount.

2.3.1.4 Time Reversal

From the DTFS synthesis equation,

$$x[n] = \frac{1}{N} \sum_{k=0}^{N-1} X[k] e^{j \frac{2\pi k}{N} n},$$

we see that by simply changing the sign of the time variable n , we obtain the relation

$$\begin{aligned} y[n] &= x[-n] = \frac{1}{N} \sum_{k=0}^{N-1} X[k] e^{j \frac{2\pi k}{N} (-n)} \\ &= \frac{1}{N} \sum_{k=0}^{N-1} X[k] e^{j \frac{2\pi (-k)}{N} n} \\ &= \frac{1}{N} \sum_{k=0}^{N-1} X[k] e^{j \frac{2\pi (N-k)}{N} n} \\ &= \frac{1}{N} \sum_{m=0}^{N-1} X[N-m] e^{j \frac{2\pi m}{N} n}, \end{aligned}$$

yielding the relation

$$x[n] \xleftrightarrow{DTFS} X[k] \implies y[n] = x[-n] \xleftrightarrow{DTFS} X[N-k],$$

i.e., changing the sign of the time axis corresponds to changing the sign of the DTFS frequency index, where, to keep the terms within the range from 0 to N , we add N to the index, which has no impact on their values, owing to the periodicity of the DTFS coefficients $X[k]$ with period N as a function of k .

2.3.1.5 Conjugate Symmetry

The effect of conjugating a complex-valued signal on its DTFS representation can be seen by simply conjugating the DTFS synthesis relation,

$$\begin{aligned} x[n] &= \frac{1}{N} \sum_{k=0}^{N-1} X[k] e^{j \frac{2\pi k}{N} n} \\ x^*[n] &= \frac{1}{N} \left(\sum_{k=0}^{N-1} X[k] e^{j \frac{2\pi k}{N} n} \right)^* \\ &= \frac{1}{N} \sum_{k=0}^{N-1} X^*[k] e^{-j \frac{2\pi k}{N} n} \\ &= \frac{1}{N} \sum_{k=0}^{N-1} X^*[k] e^{j \frac{2\pi (-k)}{N} n} \\ &= \frac{1}{N} \sum_{k=0}^{N-1} X^*[k] e^{j \frac{2\pi (N-k)}{N} n} \\ &= \frac{1}{N} \sum_{m=0}^{N-1} X^*[N-m] e^{j \frac{2\pi m}{N} n} \end{aligned}$$

yielding that

$$x[n] \xleftrightarrow{DTFS} X[k] \implies x^*[n] \xleftrightarrow{DTFS} X^*[N-k].$$

When the periodic signal $x[n]$ is real valued, i.e. $x[n]$ only takes on values that are real numbers, then the DTFS exhibits a symmetry property. This arises directly from the definition of the DTFS, and that real numbers equal their conjugates, i.e. $x[n] = x^*[n]$, such that

$$x[n] = x^*[n] \xleftrightarrow{DTFS} X[k] \implies X[k] = X^*[N - k].$$

Note that when the signal is real-valued and is an even function of time, such that $x[n] = x[-n]$, then its DTFS is also real-valued and even, i.e. $X[k] = X^*[k] = X[-k] = X[N - k]$. It can be shown by similar reasoning that when the signal is periodic, real-valued, and an odd function of time, that the DTFS coefficients are purely imaginary and odd, i.e. $X[k] = -X^*[k] = -X[-k] = -X[N - k]$.

2.3.1.6 Products of Signals

When two periodic signals of the same period are multiplied in time, such that $z[n] = x[n]y[n]$, the resulting signal remains periodic with the same period, such that $z[n] = x[n]y[n] = x[n + N]y[n + N] = z[n + N]$. Hence, each of the three signals admit DTFS representations using the same set of harmonically related signals. We can observe the effect on the resulting DTFS representation through the analysis equation,

$$\begin{aligned} Z[k] &= \sum_{n=0}^{N-1} (x[n]y[n])e^{-j\frac{2\pi k}{N}n} \\ &= \sum_{n=0}^{N-1} \left(\frac{1}{N} \sum_{m=0}^{N-1} X[m]e^{j\frac{2\pi m}{N}n} \right) y[n]e^{-j\frac{2\pi k}{N}n} \\ &= \frac{1}{N} \sum_{m=0}^{N-1} X[m] \left(\sum_{n=0}^{N-1} y[n]e^{-j\frac{2\pi(k-m)}{N}n} \right) \\ &= \frac{1}{N} \sum_{m=0}^{N-1} X[m]Y[k - m], \end{aligned}$$

where the periodicity of $Y[k]$ is used to determine values of $Y[k - m]$ for terms $k - m$ that fall outside the range of 0 to $N - 1$. The relationship between the DTFS coefficients for $z[n]$ and those of $x[n]$ and $y[n]$ is seen to be a form of discrete convolution, called a periodic convolution, between the two sequences $X[k]$ and $Y[k]$,

$$x[n] \xleftrightarrow{DTFS} X[k], y[n] \xleftrightarrow{DTFS} Y[k] \implies z[n] = x[n]y[n] \xleftrightarrow{DTFS} \frac{1}{N} \sum_{m=0}^{N-1} X[m]Y[k - m].$$

2.3.1.7 Convolution

A dual relationship to that of multiplication in time, is multiplication of DTFS coefficients. Specifically, when the two signals $x[n]$ and $y[n]$ are each periodic with period N , the periodic signal $z[n]$ of period N , whose DTFS representation is given by $Z[k] = X[k]Y[k]$ corresponds to a periodic convolution of the signals $x[n]$ and $y[n]$. This can be seen as follows,

$$\begin{aligned}
z[n] &= \frac{1}{N} \sum_{k=0}^{N-1} (X[k]Y[k]) e^{j\frac{2\pi k}{N}n} \\
&= \frac{1}{N} \sum_{k=0}^{N-1} \left(\sum_{m=0}^{N-1} x[m] e^{-j\frac{2\pi k}{N}m} \right) Y[k] e^{j\frac{2\pi k}{N}n} \\
&= \sum_{m=0}^{N-1} x[m] \left(\frac{1}{N} \sum_{k=0}^{N-1} Y[k] e^{j\frac{2\pi k}{N}(n-m)} \right) \\
&= \sum_{m=0}^{N-1} x[m] y[n-m]
\end{aligned}$$

where the summation in the last line is called periodic convolution. This leads to the following property of the DTFS,

$$x[n] \xleftrightarrow{DTFS} X[k], y[n] \xleftrightarrow{DTFS} Y[k] \implies z[n] = \sum_{m=0}^{N-1} x[m] y[n-m] \xleftrightarrow{DTFS} Z[k] = X[k] Y[k].$$

2.3.1.8 Parseval's relation

The energy contained within a period of a periodic signal can also be computed in terms of its CTFS representation using Parseval's relation,

$$x[n] \xleftrightarrow{DTFS} X[k] \implies \sum_{n=0}^{N-1} |x[n]|^2 = \frac{1}{N} \sum_{k=0}^{N-1} |X[k]|^2.$$

This relation can be derived using the definition of the DTFS as follows,

$$\begin{aligned}
\sum_{n=0}^{N-1} |x[n]|^2 &= \sum_{n=0}^{N-1} x[n] x^*[n] \\
&= \sum_{n=0}^{N-1} x[n] \left(\frac{1}{N} \sum_{k=0}^{N-1} X^*[N-k] e^{j\frac{2\pi k}{N}n} \right) \\
&= \frac{1}{N} \sum_{k=0}^{N-1} X^*[N-k] \left(\sum_{n=0}^{N-1} x[n] e^{j\frac{2\pi k}{N}n} \right) \\
&= \frac{1}{N} \sum_{k=0}^{N-1} X^*[N-k] \left(\sum_{n=0}^{N-1} x[n] e^{-j\frac{2\pi(N-k)}{N}n} \right) \\
&= \frac{1}{N} \sum_{k=0}^{N-1} X^*[N-k] X[N-k] \\
&= \frac{1}{N} \sum_{m=0}^{N-1} |X[m]|^2.
\end{aligned}$$

Parseval's relation shows that the energy in a period of a periodic signal is equal to the sum of the energies contained within each of the harmonic components that make up the signal through the DTFS representation.

2.4 Discrete-time Fourier transform representation of DT signals

As with continuous-time signals, it is often convenient to represent discrete-time signals as a linear combination of simpler signals, or "basis signals". From continuous-time system theory, we know that complex

exponential signals of the form e^{st} are a special class of signals called, “eigensignals” in that when placed as the input to a linear, time-invariant system, the output of the system will be of the form e^{st} scaled by a complex constant. As a result, such signals played an important role in the development of signal analysis and synthesis methods through the CT Fourier transform and Laplace transform. For discrete-time systems, we have that eigensignals of discrete-time linear-shift invariant systems include all signals that can be written in the form of a discrete-time complex exponential sequence, or z^n for all n and for any, possibly complex, z . By restricting the class of such signals to have unity magnitude, we arrive at the class of complex exponentials of the form $e^{j\omega n}$ for all n and for real-valued ω . These signals play a particularly important role in the analysis of discrete-time systems due to this eigenfunction property, which implies that the response of a linear shift-invariant system to a complex exponential input will be a complex exponential output of the same frequency with amplitude and phase determined by the system. For real-valued systems, i.e. systems with real-valued impulse responses, when the input is sinusoidal of a given frequency, the output will remain sinusoidal of the same frequency, again with amplitude and phase determined by the system. This important property of linear shift invariant systems makes the representation of signals in terms of complex exponentials extremely useful for studying linear system theory.

The discrete-time Fourier transform enables the construction of a wide class of signals from a superposition of complex exponentials. Through the eigenfunction property, the response of a linear shift invariant system to any signal in this class, i.e. any signal with a discrete-time Fourier transform, can be constructed by adding up the responses to each of the eigenfunctions that make up the original signal. By linearity of the system, the response of the system to a linear combination of complex exponentials will be given by the same linear combination of the responses to the complex exponentials. The eigenfunction property of LSI systems enables us to express very simply the response of the system to each of these complex exponentials.

The discrete-time Fourier transform, or DTFT, enables the representation of discrete-time sequences by a superposition of complex exponentials. Many sequences of interest can be represented by the following Fourier integral

$$x[n] = \frac{1}{2\pi} \int_{-\pi}^{\pi} X_d(\omega) e^{j\omega n} d\omega, \quad (2.31)$$

where,

$$X_d(\omega) = \sum_{n=-\infty}^{\infty} x[n] e^{-j\omega n} \quad (2.32)$$

is the discrete-time Fourier transform of the sequence $x[n]$. These two expressions comprise the Fourier representation of the sequence $x[n]$. Note that the DTFT, $X_d(\omega)$, is a complex-valued function of the real-valued variable ω , when the sum (2.32) exists. The integral corresponds to the inverse DTFT and represents the synthesis of the signal $x[n]$ from a superposition of signals of the form

$$\frac{1}{2\pi} X_d(\omega) e^{j\omega n} d\omega,$$

where we interpret the integral as the limit of a Riemann sum, i.e.

$$\frac{1}{2\pi} \int_{-\pi}^{\pi} X_d(\omega) e^{j\omega n} d\omega = \lim_{\Delta\omega \rightarrow 0} \sum_{k=0}^{2\pi/\Delta\omega} X_d(-\pi + k\Delta\omega) e^{j\omega n} \Delta\omega.$$

The value of the DTFT, $X_d(\omega)$, determines the relative amount of each of the complex exponentials $e^{j\omega n}$ that is required to construct $x[n]$. The DTFT is referred to as Fourier analysis, as we analyze the composition of the signal in terms of the complex exponentials that make it up. The inverse DTFT is referred to as Fourier synthesis, as it can be viewed as synthesizing the signal from these basic components that make it up.

There is a strong similarity between the discrete-time Fourier transform and the z-transform for discrete-time signals that we will study in Chapter 4. This relationship is similar to that between the continuous-time Fourier transform and the Laplace transform for continuous-time signals. The more general Laplace transform of a continuous-time signal can be written

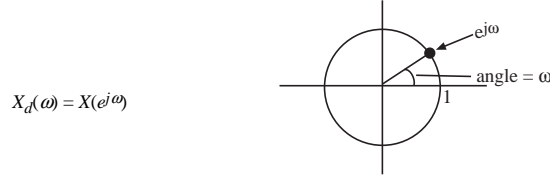


Figure 2.5: The DTFT viewed as evaluating the z-transform along the unit circle $z = e^{j\omega}$ in the z -plane.

$$X_L(s) = \int_{t=-\infty}^{\infty} x(t)e^{-st} dt, \quad (2.33)$$

when the integral exists. Substituting $s = j\omega$ into (2.33), yields the CTFT. So, for signals for which the CTFT exists, we can view the CTFT as a slice of the Laplace transform through the complex s -plane, along the imaginary axis. Just as the Fourier transform for continuous-time signals can be viewed as evaluating the Laplace transform along a specific curve, namely the imaginary axis in the s -plane, the DTFT can be viewed as evaluating the more general z -transform along a specific curve in the complex z -plane. The z -transform of a discrete-time sequence, given by,

$$X(z) = \sum_{n=-\infty}^{\infty} x[n]z^{-n}, \quad (2.34)$$

is the same as the DTFT for values of z evaluated for a particular slice of the complex z -plane. Specifically, the DTFT can be seen to be the same as the z -transform evaluated along a curve in the z -plane corresponding to the unit-circle, i.e.,

The DTFT exists as a regular function if and only if the region of convergence of the z -transform, the values of z for which the summation in (2.34) converges, includes the unit circle, i.e. $|z| = 1$. For the case of sinusoidal sequences, where $X(z)$ contains poles on the unit circle, $X_d(\omega)$ can be defined in terms of impulse distributions.

While for continuous-time signals, the notion of frequency is relatively well-defined, for discrete-time signals, we also refer to the variable ω in $X_d(\omega)$ as the digital angular frequency. Frequency in continuous-time is measured in Hz (cycles per second), and angular frequency in or radians/sec. For discrete-time, frequency is measured in cycles per sample, and angular frequency in radians per sample. In some textbooks the variable ω is used to represent analog frequency in the continuous-time Fourier transform. Here, we will use the variable ω to denote both continuous-time angular frequency and discrete-time angular frequency and the specific meaning will be clear by the context. For example, we will always refer to discrete-time Fourier transforms using the subscript “d” as in $X_d(\omega)$. Of course, we could use any variable for the DTFT and the continuous-time Fourier transform. When necessary, as in an expression relating a continuous-time frequency variable to an equivalent discrete-time frequency variable through sampling, we may use Ω to represent analog angular frequency and ω to represent digital angular frequency. This enables us to maintain clarity in our discussion and consistency with a number of other texts on the topic.

It is important to recall that while continuous-time sinusoids have a fixed relationship between their frequency of oscillation and the period of the periodic time-domain waveform, discrete-time sinusoids may not be periodic at all. Recall that a signal of the form

$$x[n] = e^{j\omega n}$$

is only periodic if the following relation holds for all n for some integer P

$$x[n] = x[n + P].$$

Specifically, we must have that

$$e^{j(\omega_0 n + k2\pi)} = e^{j(\omega_0(n+P))}$$

which corresponds to requiring that

$$\omega_0 = \frac{2k}{P}\pi,$$

i.e., the digital angular frequency must be a rational multiple of π . This relationship will certainly only hold for a subset of all possible digital angular frequencies. Since the rational numbers are countable, and the real numbers are uncountable, this relationship fails to hold almost everywhere in ω . That is, for practical purposes, almost any digital frequency you come up with, say by spinning a wheel and selecting the angle of the resulting position with respect to its starting position, will correspond to a complex exponential sequence that is *not* periodic. As a result, we rarely discuss the period of discrete-time complex exponentials and refer only to their digital frequency instead.

It is natural to ask why we refer to the variable ω in the DTFT $X_d(\omega)$ as a frequency. This is somewhat more of a conceptual hurdle than would be the case for a continuous-time notion of frequency, since all continuous-time sinusoids are periodic in time, while for discrete-time, we have seen that discrete-time sinusoids (and complex exponentials) are periodic only when the frequency variable is a rational multiple of π . If we consider the discrete-time signal $x[n] = \cos(\omega_0 n)$, as a function of ω_0 , we can see, as illustrated in Figure 2.6 that for small ω_0 , i.e. $\omega_0 = \frac{\pi}{30}$, the signal $x[n]$ varies slowly with time, in the sense that $|x[n] - x[n+1]|$ is small. For larger values of ω_0 , such as $\omega_0 = \frac{\pi}{2}$, we see that $x[n]$ varies more rapidly in time, i.e. $|x[n] - x[n+1]| = 1$. Note that when $\omega_0 = \pi$, the highest discrete-time frequency, we have that $|x[n] - x[n+1]|$ takes on its maximal value of 2.

Indeed, the lowest discrete-time frequency is given by $\omega_0 = 0$, for which $x[n] = \cos(0n) = 1$, i.e. $x[n]$ is a constant, unchanging value. The highest discrete-time frequency is given by $\omega_0 = \pi$ for which $x[n] = \cos(\pi n) = (-1)^n$, alternating sign with every sample. In Figure 2.7, we show the two signals $x[n] = \cos(\frac{5\pi}{4}n)$ and $x[n] = \cos(-\frac{3\pi}{4}n)$, which can be seen to be identical. This is a fundamental difference between the concept of frequency in discrete-time and that in continuous-time. Specifically, we have seen previously that discrete-time angular frequencies are only unique over an interval of length 2π , and outside of this range, the frequencies repeat. As such, since $\omega_0 = \frac{5\pi}{4} = 2\pi - \frac{3\pi}{4}$, then the signals $x[n] = \cos(\frac{5\pi}{4}n)$ and $x[n] = \cos(-\frac{3\pi}{4}n)$ must be identical.

We will see shortly that discrete-time Fourier transforms are in fact periodic with period 2π , i.e. $X_d(\omega) = X_d(\omega + 2\pi)$, which is consistent with these observations.

To demonstrate that the Fourier transform synthesis equation, or inverse DTFT, in fact inverts the DTFT, we can simply plug the definition of the DTFT into the synthesis equation as follows. From the DTFT synthesis equation, we have

$$\begin{aligned} x[n] &= \frac{1}{2\pi} \int_{-\pi}^{\pi} X_d(\omega) e^{j\omega n} d\omega \\ &= \frac{1}{2\pi} \int_{-\pi}^{\pi} \left(\sum_{m=-\infty}^{\infty} x[m] e^{-j\omega m} \right) e^{j\omega n} d\omega \\ &= \sum_{m=-\infty}^{\infty} x[m] \left(\frac{1}{2\pi} \int_{-\pi}^{\pi} e^{j\omega(n-m)} d\omega \right) \\ &= \sum_{m=-\infty}^{\infty} x[m] \delta[n-m] \\ &= x[n], \end{aligned}$$

where we have used that

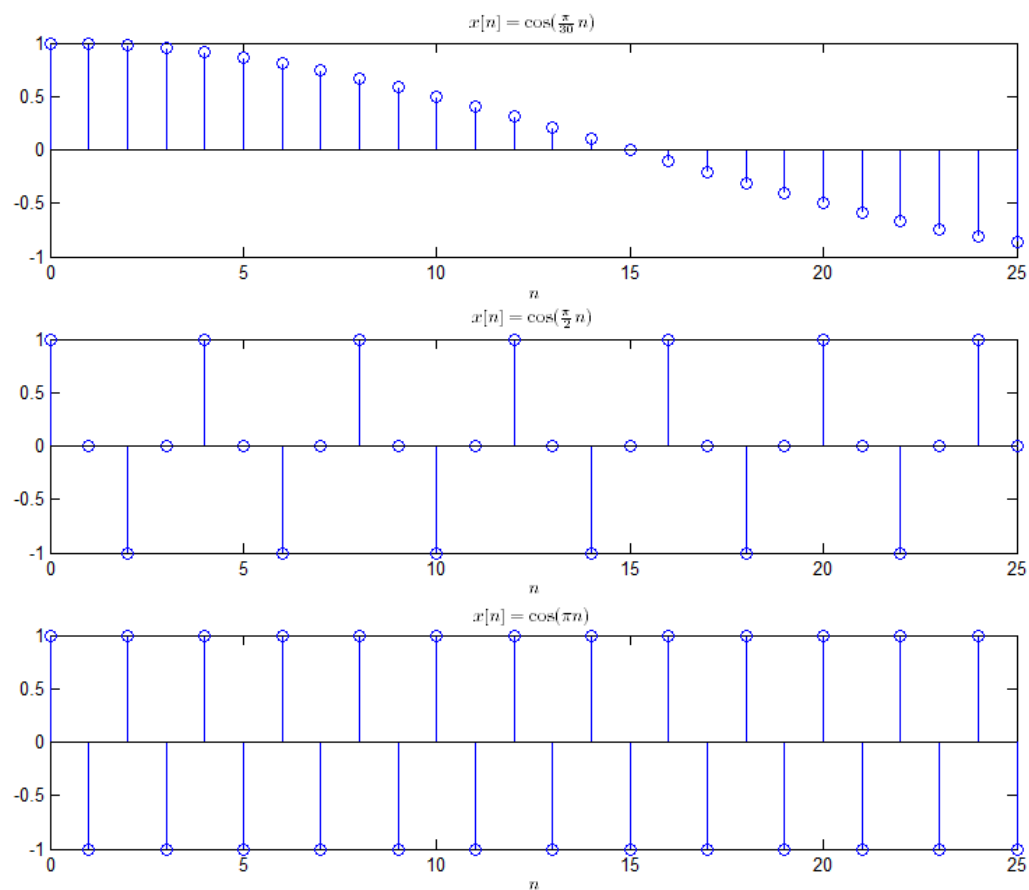


Figure 2.6: Discrete-time sinusoidal signals $\cos(\omega_0 n)$ shown for $\omega_0 = \frac{\pi}{30}$, $\frac{\pi}{2}$, and π .

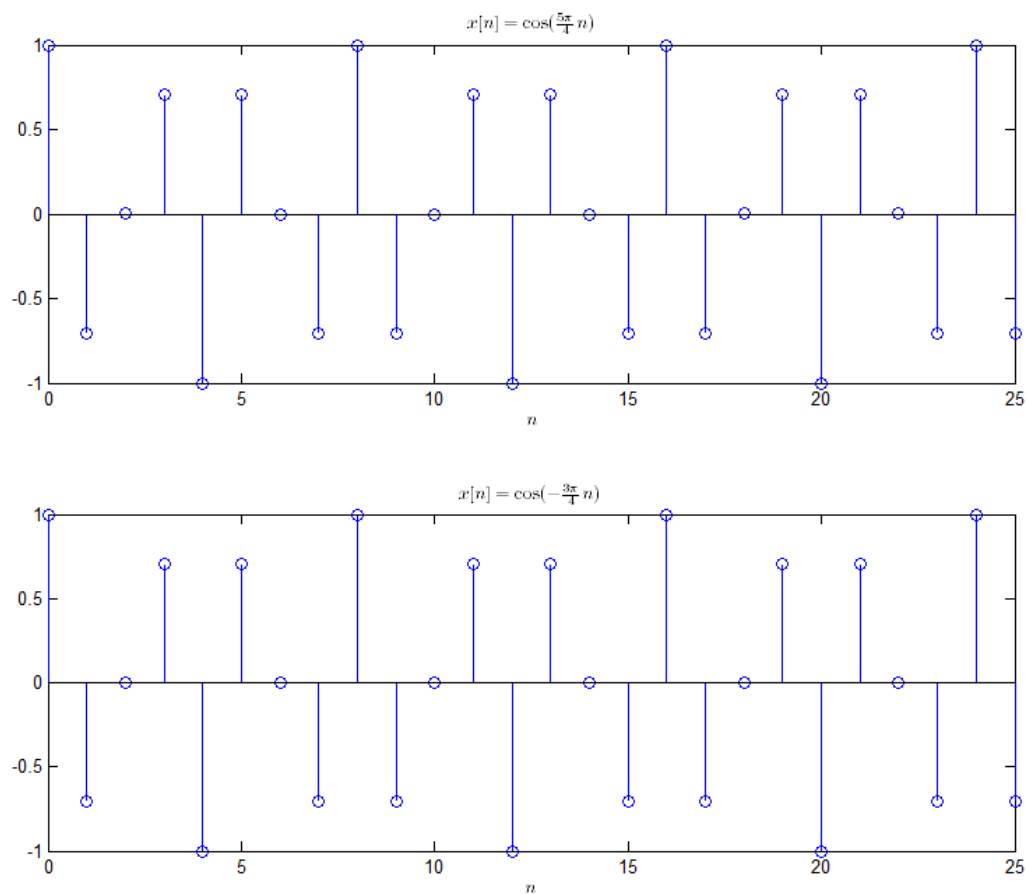


Figure 2.7: Discrete-time sinusoidal signals $\cos(\omega_0 n)$ shown for $\omega_0 = \frac{5\pi}{4}$ and $-\frac{3\pi}{4}$.

$$\begin{aligned}
\frac{1}{2\pi} \int_{-\pi}^{\pi} e^{j\omega(n-m)} d\omega &= \begin{cases} 1, & n = m \\ \frac{e^{j\pi(n-m)} - e^{-j\pi(n-m)}}{2\pi j(n-m)}, & n \neq m, \end{cases} \\
&= \begin{cases} 1, & n = m \\ \frac{(-1) - (-1)}{2\pi j(n-m)}, & n \neq m \end{cases} \\
&= \begin{cases} 1, & n = m \\ 0, & n \neq m \end{cases} \\
&= \delta[n - m].
\end{aligned}$$

2.4.1 Properties of the DTFT

A number of important properties of the DTFT can be derived in a manner similar to those for the DTFS. These are summarized at the end of this section in Table (2.5). Table (2.4) includes a number of DTFT pairs.

2.4.1.1 Linearity

The DTFT can be viewed as a linear operation, in the following manner. When two signals $x[n]$ and $y[n]$ satisfy

$$x[n] \xleftrightarrow{DTFT} X_d(\omega)$$

and

$$y[n] \xleftrightarrow{DTFT} Y_d(\omega),$$

the linear combination of these signals, $z[n] = ax[n] + by[n]$, for a, b real-valued constants, can be readily obtained by combining the constituent complex exponential signals through the same linear combination. This is easily shown from the definition of the DTFT as follows

$$\begin{aligned}
Z_d(\omega) &= \sum_{n=-\infty}^{\infty} (ax[n] + by[n])e^{-j\omega n} \\
&= a \sum_{n=-\infty}^{\infty} x[n]e^{-j\omega n} + b \sum_{n=-\infty}^{\infty} y[n]e^{-j\omega n} \\
&= aX_d(\omega) + bY_d(\omega).
\end{aligned}$$

The linearity property of the DTFT can be compactly represented as follows

$$x[n] \xleftrightarrow{DTFT} X_d(\omega), y[n] \xleftrightarrow{DTFT} Y_d(\omega) \implies z[n] = ax[n] + by[n] \xleftrightarrow{DTFT} aX_d(\omega) + bY_d(\omega).$$

2.4.1.2 Periodicity

The DTFT of every sequence is always periodic in that the following relation holds

$$X_d(\omega) = X_d(\omega + k2\pi),$$

for all integers k . The proof of this property lies in the periodicity of the complex exponential sequences $e^{j\omega n}$ that are used to construct each sequence with a DTFT as follows,

$$\begin{aligned}
X_d(\omega) &= \sum_{n=-\infty}^{\infty} x[n]e^{-j\omega n} \\
&= \sum_{n=-\infty}^{\infty} x[n]e^{-j(\omega+k2\pi)n} \\
&= X_d(\omega + k2\pi).
\end{aligned}$$

This is different from the continuous-time Fourier transform, where we were interested in frequencies spanning an infinite range of real values. In contrast, in discrete-time, all digital frequencies can be captured in a single interval of length 2π . The reason for this periodicity stems directly from the observation that complex exponentials of the form $e^{j\omega n}$ are only unique over an interval of this range. That is the sequence $e^{j\omega n}$ is identical to the sequence $e^{j(\omega+2\pi)n}$. Since these two sequences have identical values, for all n , then the composition of $x[n]$ in terms of these sequences, i.e. the DTFT, must only require a single interval containing them. Since the DTFT is periodic with period 2π , the DTFT only needs to be specified over an interval of that length. It is often convenient to use the interval $-\pi \leq \omega \leq \pi$ so that the low frequencies are centered around $\omega = 0$. Note that since all frequencies that are multiples of 2π are indistinguishable, the low frequencies are also those centered around any multiple of 2π . Similarly, the highest digital frequency corresponds to $\omega = \pi$ as well as all odd multiples of π . We will return to this issue again when we discuss the discrete-time frequency response of linear shift-invariant systems.

2.4.1.3 Real and Imaginary Part Symmetries

For real-valued sequences $x[n]$, we have that the real-part of the DTFT is even, and the imaginary part is odd, i.e.,

The proof follows from trigonometric properties of the real and imaginary parts. Specifically, for real valued $x[n]$, we have

$$\begin{aligned}
\Re\{X_d(\omega)\} &= \Re\left\{\sum_{n=-\infty}^{\infty} x[n]e^{-j\omega n}\right\} \\
&= \Re\left\{\sum_{n=-\infty}^{\infty} x[n](\cos(\omega n) + j\sin(\omega n))\right\} \\
&= \Re\left\{\sum_{n=-\infty}^{\infty} x[n](\cos(\omega n) + j\sin(\omega n))\right\} \\
&= \sum_{n=-\infty}^{\infty} x[n]\cos(\omega n) \\
&= \sum_{n=-\infty}^{\infty} x[n]\cos(-\omega n) \\
&= \Re\{X_d(-\omega)\}.
\end{aligned}$$

That the imaginary part of the DTFT is an odd function of ω , similarly follows from the antisymmetry of the sine function.

2.4.2 Magnitude and Phase Symmetries

For real-valued sequences $x[n]$, we have that the magnitude of the DTFT is an even function and the phase of the DTFT is an odd function, i.e.,

$$\begin{aligned}
|X(\omega)| &= |X_d(-\omega)| \\
\angle X(\omega) &= -\angle X_d(-\omega).
\end{aligned}$$

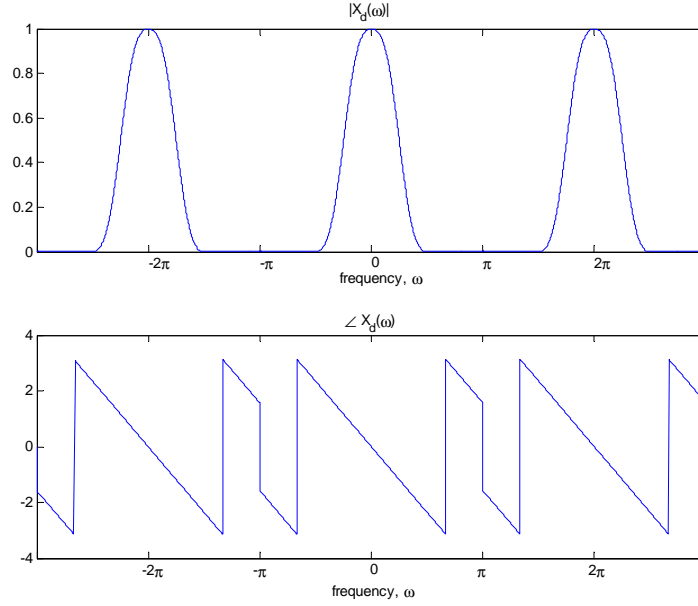


Figure 2.8: Magnitude and phase of an example DTFT.

For example, $|X_d(\omega)|$ and $\angle X_d(\omega)$ might look as shown in Figure (2.8)

The proof of the magnitude and phase symmetries follows from the definition of the DTFT as below. From the definition of the DTFT we have

$$\begin{aligned}
 |X_d(\omega)| &= \left[\left(\sum_{n=-\infty}^{\infty} x[n] \cos(\omega n) \right)^2 + \left(- \sum_{n=-\infty}^{\infty} x[n] \sin(\omega n) \right)^2 \right]^{1/2} \\
 &= \left[\left(\sum_{n=-\infty}^{\infty} x[n] \cos(\omega n) \right)^2 + \left(\sum_{n=-\infty}^{\infty} x[n] \sin(\omega n) \right)^2 \right]^{1/2} \\
 &= \left[\left(\sum_{n=-\infty}^{\infty} x[n] \cos(-\omega n) \right)^2 + \left(- \sum_{n=-\infty}^{\infty} x[n] \sin(-\omega n) \right)^2 \right]^{1/2} \\
 &= |X_d(-\omega)|,
 \end{aligned}$$

and for the phase of the DTFT we have that

$$\begin{aligned}
 \angle X_d(\omega) &= \arctan \frac{-\sum_{n=-\infty}^{\infty} x[n] \sin(\omega n)}{\sum_{n=-\infty}^{\infty} x[n] \cos(\omega n)} \\
 &= \arctan \frac{\sum_{n=-\infty}^{\infty} x[n] \sin(-\omega n)}{\sum_{n=-\infty}^{\infty} x[n] \cos(-\omega n)} \\
 &= -\arctan \frac{-\sum_{n=-\infty}^{\infty} x[n] \sin(-\omega n)}{\sum_{n=-\infty}^{\infty} x[n] \cos(-\omega n)} \\
 &= -\angle X_d(\omega),
 \end{aligned}$$

as desired. The last line above follows since arctan is an odd function of its argument.

2.4.2.1 Time Shift

As we have seen for both continuous-time and discrete-time periodic signals, when a sinusoidal signal is shifted in time, the resulting signal can be represented in terms of a simple phase shift of the original sinusoidal signal. A discrete-time signal $x[n]$ that can be represented using the DTFT as a superposition of possibly infinitely many complex exponential signals of the form $e^{j\omega n}$, would necessarily have each of these constituent complex exponential signals delayed by the same fixed amount, which would correspond to each of the complex exponential signals undergoing a different shift in the phase of their exponent. The resulting change in the DTFT of a discrete time signal $x[n]$ that is delayed by a fixed amount, i.e. $y[n] = x[n - n_0]$ can be derived as follows

$$\begin{aligned} Y_d(\omega) &= \sum_{n=-\infty}^{\infty} x[n - n_0] e^{-j\omega n} \\ &= \sum_{n=-\infty}^{\infty} x[m] e^{-j\omega(m+n_0)} \\ &= \sum_{m=-\infty}^{\infty} x[m] e^{-j\omega n_0} e^{-j\omega m} \\ &= X_d(\omega) e^{-j\omega n_0}, \end{aligned}$$

where, the second line follows from the change of variable, $m = n - n_0$. The time shift property of the DTFT can be compactly represented as follows

$$x[n] \xleftrightarrow{DTFT} X_d(\omega) \implies y[n] = x[n - n_0] \xleftrightarrow{DTFT} X_d(\omega) e^{-j\omega n_0}.$$

We see that a shift in time corresponds to a delay of each of the complex exponential components that make up the signal and that this delay, in turn corresponds to a shift in the phase of each of the frequency components by an amount that is linear with frequency with a slope that is proportional to the delay.

2.4.2.2 Modulation

When a signal $x[n]$ has a DTFT representation given by $X_d(\omega)$, we again are interested in how a shift in frequency would manifest itself in the time domain representation of the original signal. Specifically, if a signal $y[n]$ were known to have a DTFT representation given by $Y_d(\omega) = X_d(\omega - \omega_0)$, it is interesting to understand the relationship in the time-domain between $y[n]$ and $x[n]$. This can be readily seen through examination of the DTFT analysis equation,

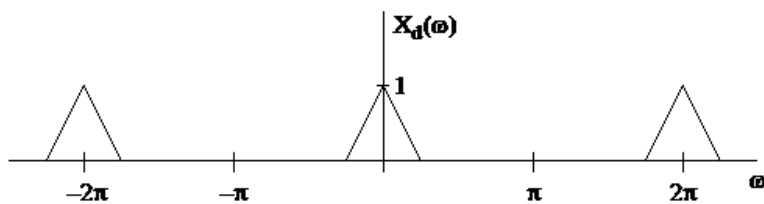
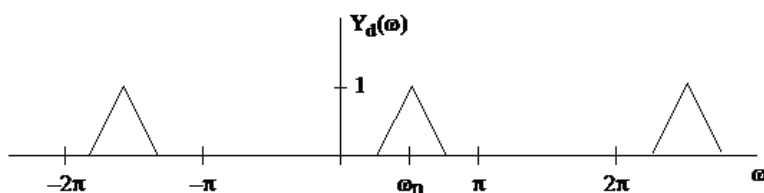
$$\begin{aligned} Y_d(\omega) &= X_d(\omega - \omega_0) \\ &= \sum_{n=-\infty}^{\infty} x[n] e^{-j(\omega - \omega_0)n} \\ &= \sum_{n=-\infty}^{\infty} (x[n] e^{j\omega_0 n}) e^{-j\omega n} \end{aligned}$$

which leads to the relation

$$x[n] \xleftrightarrow{DTFT} X_d(\omega) \implies y[n] = x[n] e^{j\omega_0 n} \xleftrightarrow{DTFT} X_d(\omega - \omega_0).$$

We observe that a shift in the discrete time Fourier transform by an amount ω_0 corresponds to a modulation in the time domain signal $x[n]$ by a term whose frequency is proportional to the shift amount. This property can be used together with linearity to determine the effect of modulation of a signal by a sinusoidal signal,

$$y[n] = \cos(\omega_0 n) x[n] = \frac{1}{2} \left(e^{j\omega_0 n} + e^{-j\omega_0 n} \right) x[n]$$

Figure 2.9: Sample DTFT $X_d(\omega)$ for the signal $x[n]$.Figure 2.10: Resulting DTFT of $y[n] = e^{j\omega_0 n} x[n]$.

resulting in

$$x[n] \xleftrightarrow{DTFT} X_d(\omega) \implies y[n] = x[n] \cos(\omega_0 n) \xleftrightarrow{DTFT} \left[\frac{1}{2} X_d(\omega - \omega_0) + \frac{1}{2} X_d(\omega + \omega_0) \right].$$

Example:

If $x[n]$ has a DTFT as shown in Figure (2.9)

then $y[n] = e^{j\omega_0 n} x[n]$ would have the DTFT as shown in Figure (2.10).

Example

If $X_d(\omega)$ has the form shown in Figure (2.11),

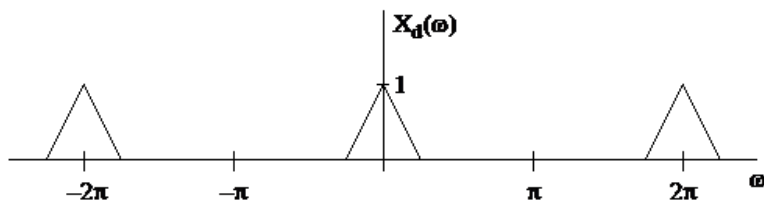
then $Y_d(\omega)$, the DTFT of $y[n] = \cos(\omega_0 n) x[n]$ has the form shown in Figure (2.12)

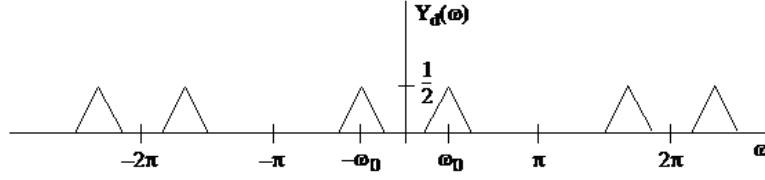
2.4.2.3 Time Reversal

From the DTFT synthesis equation,

$$x[n] = \frac{1}{2\pi} \int_{-\pi}^{\pi} X_d(\omega) e^{j\omega n} d\omega,$$

we see that by simply changing the sign of the time variable n , we obtain the relation

Figure 2.11: Example DTFT for $x[n]$.

Figure 2.12: Resulting DTFT for $y[n]$.

$$\begin{aligned}
 y[n] &= x[-n] = \frac{1}{2\pi} \int_{-\pi}^{\pi} X_d(\omega) e^{j\omega(-n)} d\omega \\
 &= \frac{1}{2\pi} \int_{-\pi}^{\pi} X_d(\omega) e^{j(-\omega)n} d\omega \\
 &= \frac{1}{2\pi} \int_{-\pi}^{\pi} X_d(-\omega) e^{j\omega n} d\omega,
 \end{aligned}$$

yielding the relation

$$x[n] \xleftrightarrow{DTFT} X_d(\omega) \implies y[n] = x[-n] \xleftrightarrow{DTFT} X_d(-\omega),$$

i.e., changing the sign of the time axis corresponds to changing the sign of the DTFT frequency index, ω .

2.4.2.4 Conjugate Symmetry

The effect of conjugating a complex-valued signal on its DTFT representation can be seen by simply conjugating the DTFT synthesis relation,

$$\begin{aligned}
 x[n] &= \int_{\omega=-\pi}^{\pi} X_d(\omega) e^{j\omega n} d\omega \\
 x^*[n] &= \left(\int_{\omega=-\pi}^{\pi} X_d(\omega) e^{j\omega n} d\omega \right)^* \\
 &= \int_{\omega=-\pi}^{\pi} X_d^*(\omega) e^{-j\omega n} d\omega \\
 &= \int_{\omega=-\pi}^{\pi} X_d^*(\omega) e^{j(-\omega)n} d\omega \\
 &= \int_{\omega=-\pi}^{\pi} X_d^*(-\omega) e^{j\omega n} d\omega
 \end{aligned}$$

yielding that

$$x[n] \xleftrightarrow{DTFT} X_d(\omega) \implies x^*[n] \xleftrightarrow{DTFT} X_d^*(-\omega).$$

When the periodic signal $x[n]$ is real valued, i.e. $x[n]$ only takes on values that are real numbers, then the DTFT exhibits additional symmetry. This arises directly from the definition of the DTFT, and that real numbers equal their conjugates, i.e. $x[n] = x^*[n]$, such that

$$x[n] = x^*[n] \xleftrightarrow{DTFT} X_d(\omega) \implies X_d(\omega) = X_d^*(-\omega).$$

Note that when the signal is real-valued and is an even function of time, such that $x[n] = x[-n]$, then its DTFT is also real-valued and even, i.e. $X_d(\omega) = X_d^*(-\omega) = X_d^*(\omega) = X_d(-\omega)$. It can be shown by similar reasoning that when the signal is real-valued and an odd function of time, that the DTFT is purely imaginary and odd, i.e. $X_d(\omega) = X_d^*(-\omega) = -X_d^*(\omega) = -X_d(-\omega)$.

2.4.2.5 Products of Signals

When two discrete-time signals that can each be represented by a DTFT are multiplied in time, such that $z[n] = x[n]y[n]$, the resulting signal also has a DTFT representation. We can observe the effect on the resulting DTFT representation through the analysis equation,

$$\begin{aligned}
 Z_d(\omega) &= \sum_{n=-\infty}^{\infty} (x[n]y[n])e^{-j\omega n} \\
 &= \sum_{n=-\infty}^{\infty} \left(\frac{1}{2\pi} \int_{-\pi}^{\pi} X_d(\nu) e^{j\nu n} d\nu \right) y[n] e^{-j\omega n} \\
 &= \frac{1}{2\pi} \int_{-\pi}^{\pi} X_d(\nu) \left(\sum_{n=-\infty}^{\infty} y[n] e^{-j(\omega-\nu)n} \right) d\nu \\
 &= \frac{1}{2\pi} \int_{-\pi}^{\pi} X_d(\nu) Y_d(\omega - \nu) d\nu,
 \end{aligned}$$

where the periodicity of $Y_d(\omega)$ is used to determine values of $Y_d(\omega - \nu)$ for terms $\omega - \nu$ outside the range of $[-\pi, \pi]$. The relationship between the DTFTs of $z[n]$ and of $x[n]$ and $y[n]$ is seen to be a form of convolution, called a periodic convolution, between the two functions $X_d(\omega)$ and $Y_d(\omega)$,

$$x[n] \xleftrightarrow{DTFT} X_d(\omega), y[n] \xleftrightarrow{DTFT} Y_d(\omega) \implies z[n] = x[n]y[n] \xleftrightarrow{DTFT} \frac{1}{2\pi} \int_{-\pi}^{\pi} X_d(\nu) Y_d(\omega - \nu) d\nu.$$

2.4.2.6 Convolution

A dual relationship to that of multiplication of discrete-time signals in time, is the multiplication of their DTFT representations. Specifically, when two signals $x[n]$ and $y[n]$ have corresponding DTFT representations $X_d(\omega)$ and $Y_d(\omega)$, the signal that corresponds to the DTFT $Z_d(\omega) = X_d(\omega)Y_d(\omega)$ corresponds to a discrete-time convolution of the signals $x[n]$ and $y[n]$. This can be seen as follows,

$$\begin{aligned}
 z[n] &= \frac{1}{2\pi} \int_{-\pi}^{\pi} (X_d(\omega)Y_d(\omega)) e^{j\omega n} d\omega \\
 &= \frac{1}{2\pi} \int_{-\pi}^{\pi} \left(\sum_{m=-\infty}^{\infty} x[m] e^{-j\omega m} \right) Y_d(\omega) e^{j\omega n} d\omega \\
 &= \sum_{m=-\infty}^{\infty} x[m] \left(\frac{1}{2\pi} \int_{-\pi}^{\pi} Y_d(\omega) e^{j\omega(n-m)} d\omega \right) \\
 &= \sum_{m=-\infty}^{\infty} x[m] y[n - m].
 \end{aligned}$$

This leads to the following property of the DTFT,

$$x[n] \xleftrightarrow{DTFT} X_d(\omega), y[n] \xleftrightarrow{DTFT} Y_d(\omega) \implies z[n] = \sum_{m=-\infty}^{\infty} x[m] y[n - m] \xleftrightarrow{DTFT} Z_d(\omega) = X_d(\omega)Y_d(\omega).$$

2.4.2.7 Parseval's relation

A particularly useful relationship between the energy of a sequence in the time-domain and the energy contained in its Fourier transform is captured by Parseval's relation. Since sequences with convergent DTFTs are square summable, they have finite energy and we have that

$$x[n] \xleftrightarrow{DTFT} X_d(\omega) \implies \sum_{n=-\infty}^{\infty} |x[n]|^2 = \frac{1}{2\pi} \int_{-\pi}^{\pi} |X_d(\omega)|^2 d\omega.$$

This relation can be derived using the definition of the DTFT as follows,

$$\begin{aligned} \sum_{n=-\infty}^{\infty} |x[n]|^2 &= \sum_{n=-\infty}^{\infty} x[n] x^*[n] \\ &= \sum_{n=-\infty}^{\infty} x[n] \left(\frac{1}{2\pi} \int_{-\pi}^{\pi} X_d(\omega) e^{j\omega n} d\omega \right)^* \\ &= \sum_{n=-\infty}^{\infty} x[n] \frac{1}{2\pi} \int_{-\pi}^{\pi} X_d^*(\omega) e^{-j\omega n} d\omega \\ &= \frac{1}{2\pi} \int_{-\pi}^{\pi} X_d^*(\omega) \left(\sum_{n=-\infty}^{\infty} x[n] e^{-j\omega n} \right) d\omega \\ &= \frac{1}{2\pi} \int_{-\pi}^{\pi} X_d^*(\omega) X_d(\omega) d\omega \\ &= \frac{1}{2\pi} \int_{-\pi}^{\pi} |X_d(\omega)|^2 d\omega. \end{aligned}$$

Example:

Parseval's relation can be used to compute the energy of a signal in the time domain or the frequency domain. As a result, one of these is often simpler than the other. For example, consider the sequence $x[n] = u[n] - u[n - 10]$. A rather complicated integral can be reduced to a simple sum by noting the transform pair

$$u[n] - u[n - 10] \xleftrightarrow{DTFT} \frac{\sin(5\omega/2)}{\sin(\omega/2)}$$

and using Parseval's relation as follows:

$$\begin{aligned} \frac{1}{2\pi} \int_{-\pi}^{\pi} \left| \frac{\sin(5\omega/2)}{\sin(\omega/2)} \right|^2 d\omega &= \sum_{n=0}^9 (1)^2 \\ &= 10 \end{aligned}$$

Examples of DTFT

We continue our discussion of the discrete-time Fourier transform by considering a few simple examples.

Example

Consider the following sequence containing two non-zero samples,

$$x[n] = \delta[n] + \delta[n - 1].$$

The discrete-time Fourier transform of this sequence can be computed directly from the definition of the DTFT as

$$X_d(\omega) = 1 + e^{-j\omega}.$$

The magnitude of the discrete-time Fourier transform can be easily computed as

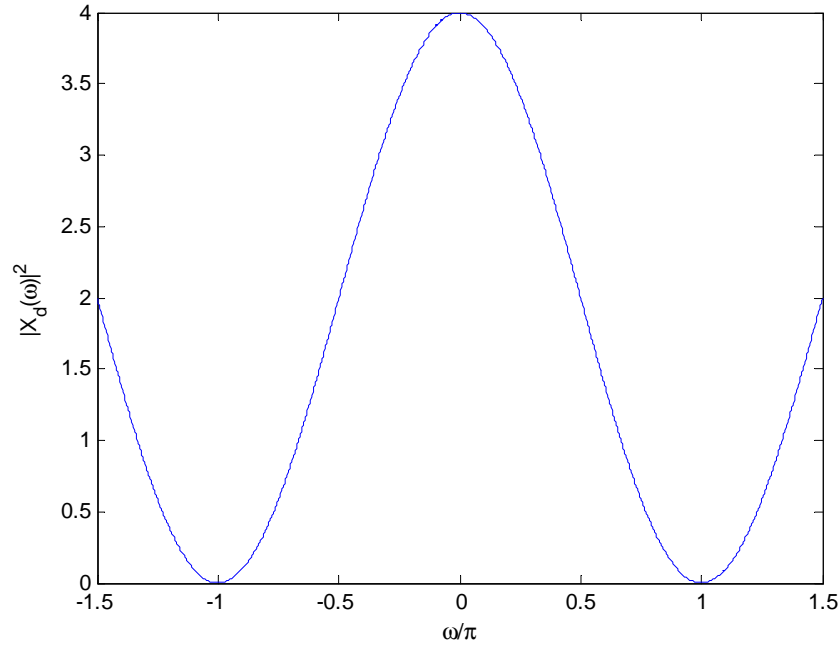


Figure 2.13: Discrete-time Fourier transform magnitude squared, $|X_d(\omega)|^2 = 2 + 2 \cos(\omega)$.

$$\begin{aligned}
 |X_d(\omega)|^2 &= |1 + e^{-j\omega}|^2 \\
 &= |1 + \cos(\omega) - j \sin(\omega)|^2 \\
 &= |1 + \cos(\omega)|^2 + |\sin(\omega)|^2 \\
 &= 1 + 2 \cos(\omega) + \cos^2(\omega) + \sin^2(\omega) \\
 &= 2 + 2 \cos(\omega).
 \end{aligned}$$

This result could also have been obtained by noting that when two exponential terms (or one exponential term and one constant term) have the same magnitude, by factoring out a common phase factor, a sinusoid can be constructed as follows,

$$\begin{aligned}
 |X_d(\omega)|^2 &= |1 + e^{-j\omega}|^2 \\
 &= |e^{-j\omega/2}(e^{j\omega/2} + e^{-j\omega/2})|^2 \\
 &= |e^{-j\omega/2}|^2 |e^{j\omega/2} + e^{-j\omega/2}|^2 \\
 &= |e^{j\omega/2} + e^{-j\omega/2}|^2 \\
 &= |2 \cos(\omega/2)|^2 \\
 &= 4 \cos^2(\omega/2) \\
 &= 2 + 2 \cos(\omega),
 \end{aligned}$$

where, in the last line, the trigonometric identity that $\cos^2(x) = (1 + \cos(2x))/2$. The magnitude squared of the discrete-time Fourier transform is shown in Figure (2.13).

Since $|X_d(\omega)|^2$ is both periodic with period 2π and symmetric around the origin, $|X_d(\omega)|^2$ is completely determined by its values on the interval $0 \leq \omega \leq \pi$. This is similarly true for $\angle X_d(\omega)$.

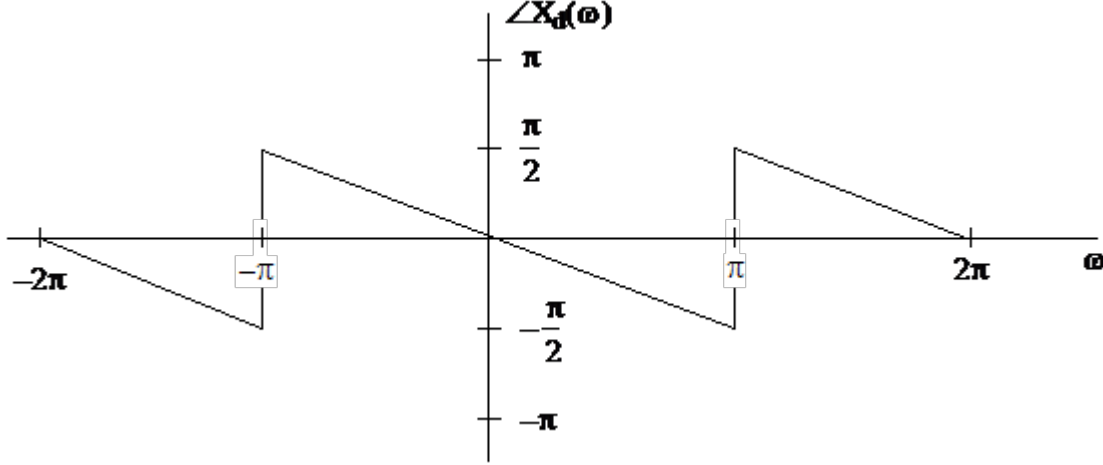


Figure 2.14: Example DTFT phase for $x[n] = \delta[n] + \delta[n - 1]$.

Because of this, when $x[n]$ is real (so that $|X_d(\omega)|$ and $\angle X_d(\omega)$ have even and odd symmetry, respectively) we will often plot them on just the interval $0 \leq \omega \leq \pi$.

To find $\angle X_d(\omega)$ in this example, we write

$$\begin{aligned}
 X_d(\omega) &= 1 + e^{-j\omega} \\
 &= e^{-j\omega/2}(e^{j\omega/2} + e^{-j\omega/2}) \\
 &= e^{-j\omega/2}2\cos(\omega/2),
 \end{aligned} \tag{2.35}$$

Now, since $\cos(\omega/2) \geq 0$ for $-\pi < \omega < \pi$, (2.35) expresses $X_d(\omega)$ in polar form, so that $\angle X_d(\omega) = -\omega/2$, $-\pi < \omega < \pi$. The phase is plotted in Figure (2.14).

Notice that the phase of $X_d(\omega)$ is an odd function. Also note that for $\omega > \pi$, the expression $\angle X_d(\omega) = -\omega/2$ is not valid, however we simply use our knowledge that the DTFT is periodic with period 2π . While it is clear from this example that the discrete-time Fourier transform is periodic in the variable ω with period 2π , the DTFT is, in fact, always periodic with period 2π , as shown in Section 2.4.1.2.

Example

Consider the sequence $x[n] = \delta[n - 1] - \delta[n + 1]$. For this sequence, we will plot the magnitude $|X_d(\omega)|$ and phase $\angle X_d(\omega)$. For the magnitude, we have

$$\begin{aligned}
 |X_d(\omega)| &= |e^{-j\omega} - e^{j\omega}| \\
 &= |-2j \sin(\omega)| \\
 &= |2 \sin(\omega)|,
 \end{aligned}$$

which can be plotted as shown in Figure (2.15)

Note that $|X_d(\omega)|$ is again an even function of ω , and its appearance is completely specified by on just the interval $0 \leq \omega \leq \pi$. The phase of $X_d(\omega)$ is found by noting

$$\begin{aligned}
 X_d(\omega) &= \begin{cases} -2j \sin(\omega), & \{\omega : \sin(\omega) > 0\} \\ 2j \sin(\omega), & \{\omega : \sin(\omega) < 0\} \end{cases} \\
 &= \begin{cases} e^{-j\pi/2}2\sin(\omega), & 0 < \omega < \pi \\ e^{j\pi/2}|2\sin(\omega)|, & -\pi < \omega < 0. \end{cases}
 \end{aligned}$$

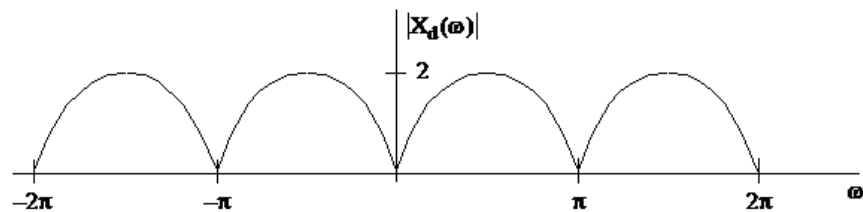
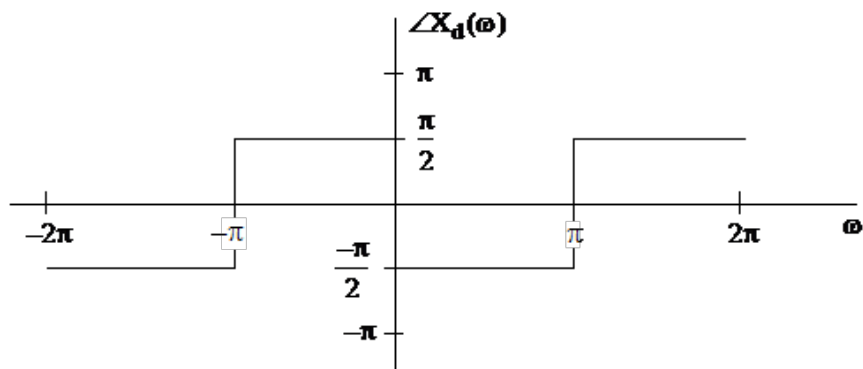
Figure 2.15: Magnitude of the DTFT for $x[n] = \delta[n - 1] - \delta[n + 1]$.

Figure 2.16: DTFT phase example.

Both the top and bottom lines within the bracket are written in polar form, since $\sin(\omega) > 0$ for $0 < \omega < \pi$, and $|\sin(\omega)| > 0$. Thus,

$$\angle X_d(\omega) = \begin{cases} -\frac{\pi}{2}, & 0 < \omega < \pi \\ \frac{\pi}{2}, & -\pi < \omega < 0 \end{cases}$$

which can be plotted as in Figure (2.16).

Notice that $\angle X_d(\omega)$ is an odd function of the variable ω . This is again due to the symmetry properties of the DTFT for real-valued $x[n]$. It is important to recall that these symmetry properties of $\angle X_d(\omega)$ hold only for real-valued sequences $x[n]$. If $x[n]$ were not real-valued, then this symmetry will not be present, as shown in the next example.

Example

Consider the sequence $x[n] = \delta[n] + j\delta[n - 1]$. For this sequence, we have the following discrete-time Fourier transform,

$$X_d(\omega) = 1 + je^{-j\omega},$$

which has a corresponding DTFT magnitude squared

$$\begin{aligned} |X_d(\omega)|^2 &= (1 + je^{-j\omega})(1 - je^{j\omega}) \\ &= 1 - je^{j\omega} + je^{-j\omega} + 1 \\ &= 2 + 2\sin(\omega). \end{aligned}$$

The DTFT magnitude squared is shown in Figure (2.17).

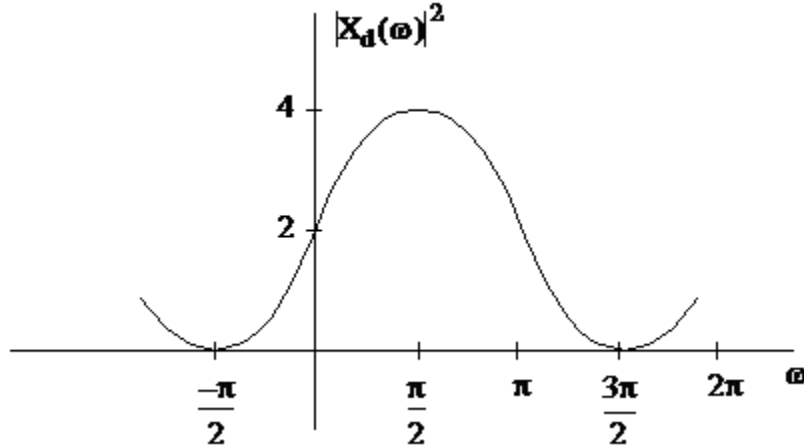


Figure 2.17: DTFT magnitude squared for the sequence $x[n] = \delta[n] + j\delta[n-1]$.

Here, we see that $|X_d(\omega)| = |X_d(-\omega)|$ does not hold.

Example

Consider the following sequence $x[n] = a^n u[n]$, with a real-valued and $|a| < 1$. For this signal, we have

$$\begin{aligned} X_d(\omega) &= \sum_{n=-\infty}^{\infty} a^n e^{-j\omega n} \\ &= \sum_{n=-\infty}^{\infty} (ae^{-j\omega})^n \\ &= \frac{1}{1 - ae^{-j\omega}} \end{aligned}$$

The DTFT magnitude squared is given by

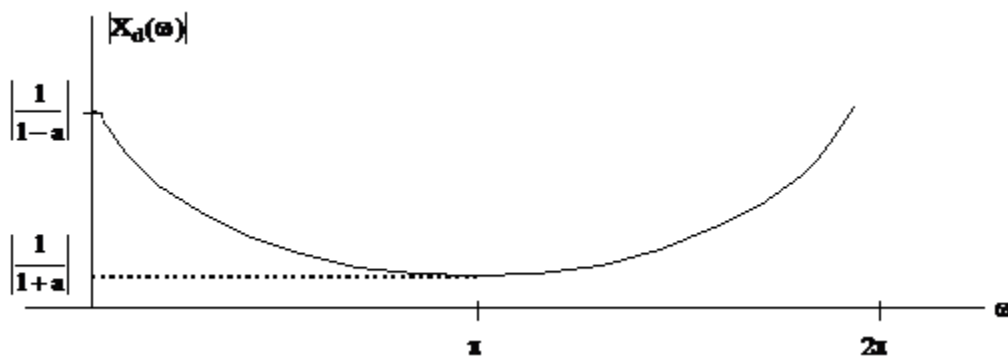
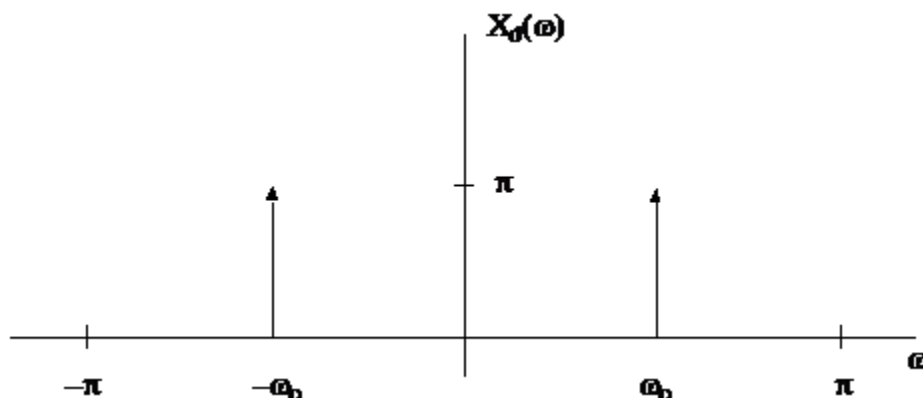
$$\begin{aligned} |X_d(\omega)| &= \frac{1}{(1 - ae^{-j\omega})(1 - ae^{j\omega})} \\ &= \frac{1}{1 + a^2 - 2a \cos(\omega)} \end{aligned}$$

which for $0 < a < 1$, the magnitude squared would appear as depicted in Figure (2.18).

Example

We next consider a sinusoidal input, $x[n] = \cos(\omega_0 n)$ for all n . As we will see in Chapter 4, the z-transform for this sequence is undefined for all z , including z on the unit circle, where it coincides with the discrete-time Fourier transform. However, we are willing to extend the notion of existence of the discrete-time Fourier transform to include such signals with the aid of impulse distributions. Similar to their continuous-time counterparts, we can define the DTFT of discrete-time sinusoidal signals in terms of impulses. As such, we can define the DTFT of such a signal to satisfy

$$\begin{aligned} X_d(\omega) &= \sum_{n=-\infty}^{\infty} \cos(\omega_0 n) e^{-j\omega n} \\ &= \pi(\delta(\omega - \omega_0) + \delta(\omega + \omega_0)), \quad |\omega| < \pi, \end{aligned}$$

Figure 2.18: DTFT Magnitude Squared for $x[n] = a^n u[n]$.Figure 2.19: Depiction of the impulse distribution for the DTFT of $x[n] = \cos(\omega_0 n)$.

in the sense that the inverse discrete-time Fourier transform of this distribution would yield the original signal $x[n]$. Here, $X_d(\omega)$ is a distribution, not a function, so the DTFT does not really exist in the normal sense, and the summation defining the DTFT does not converge in any meaningful sense to any function. However, if we use this distribution as the operational DTFT of the sequence, then taking its inverse DTFT would yield

$$\begin{aligned} \frac{1}{2\pi} \int_{-\pi}^{\pi} X_d(\omega) e^{j\omega n} d\omega &= \frac{\pi}{2\pi} \int_{-\pi}^{\pi} (\delta(\omega - \omega_0) + \delta(\omega + \omega_0)) e^{j\omega n} d\omega \\ &= \frac{1}{2} (e^{j\omega_0 n} + e^{-j\omega_0 n}) \\ &= \cos(\omega_0 n). \end{aligned}$$

If we graphically depict the distribution $X_d(\omega)$, using our notation for representing impulse distributions, we would obtain the sketch in Figure (2.19).

While an impulse distribution cannot be considered a function, nor can it be considered a proper limit of a sequence of functions, we could approximate the above figure using tall, narrow rectangles around the frequencies of interest, i.e. in place of $\delta(\omega - \omega_0)$ and $\delta(\omega + \omega_0)$. This would correspond to the discrete-time Fourier transform of an approximation to $\cos(\omega_0 n)$. Additionally, the quality of the approximation improves as the rectangles get narrower and taller. This is explored further in the next Example.

Example

Consider the finite-length sequence $x[n]$ described below,

$$x[n] = \begin{cases} \cos(\omega_0 n), & 0 \leq n \leq N-1 \\ 0 & \text{otherwise.} \end{cases}$$

The sequence is finite-length, in that it has a finite number, N , of non-zero samples. This sequence can be constructed as a windowed version of the original infinite-length sequence $\cos(\omega_0 n)$. The DTFT of the sequence can be written,

$$\begin{aligned} X_d(\omega) &= \sum_{n=-\infty}^{\infty} x[n]e^{-j\omega n} \\ &= \sum_{n=0}^{N-1} \cos(\omega_0 n)e^{-j\omega n} \\ &= \sum_{n=0}^{N-1} \frac{1}{2} [e^{j\omega_0 n} + e^{-j\omega_0 n}] e^{-j\omega n} \\ &= \sum_{n=0}^{N-1} \frac{1}{2} e^{j\omega_0 n} e^{-j\omega n} + \sum_{n=0}^{N-1} \frac{1}{2} e^{-j\omega_0 n} e^{-j\omega n} \\ &= \frac{1}{2} \frac{1 - e^{-j(\omega - \omega_0)N}}{1 - e^{-j(\omega - \omega_0)}} + \frac{1}{2} \frac{1 - e^{-j(\omega + \omega_0)N}}{1 - e^{-j(\omega + \omega_0)}} \\ &= \frac{1}{2} \frac{e^{-j(\omega - \omega_0)N/2} (e^{j(\omega - \omega_0)N/2} - e^{-j(\omega - \omega_0)N/2})}{e^{-j(\omega - \omega_0)/2} (e^{j(\omega - \omega_0)/2} - e^{-j(\omega - \omega_0)/2})} + \frac{1}{2} \frac{e^{-j(\omega + \omega_0)N/2} (e^{j(\omega + \omega_0)N/2} - e^{-j(\omega + \omega_0)N/2})}{e^{-j(\omega + \omega_0)/2} (e^{j(\omega + \omega_0)/2} - e^{-j(\omega + \omega_0)/2})} \\ &= \frac{1}{2} e^{-j(\omega - \omega_0)(N-1)/2} \underbrace{\frac{\sin(N(\omega - \omega_0)/2)}{\sin((\omega - \omega_0)/2)}}_{\text{periodic sinc centered at } \omega = \omega_0} + \frac{1}{2} e^{-j(\omega + \omega_0)(N-1)/2} \underbrace{\frac{\sin(N(\omega + \omega_0)/2)}{\sin((\omega + \omega_0)/2)}}_{\text{periodic sinc centered at } \omega = -\omega_0} \end{aligned}$$

Note that this expression contains two terms; one term corresponding to a ratio of sin expressions, multiplied by a linear phase term, and another corresponding to a similar ratio of sin expressions and a similar linear phase term. Each of these terms, corresponds to a periodic sinc function, centered at the corresponding positive and negative frequencies of the original cosine expression. The periodic sinc function is simply the DTFT of a length- N sequence of one's, and is depicted in Figure (2.20).

For large N , the main lobe in the periodic sinc becomes narrow and large in amplitude so that the two terms in the DTFT of the windowed cosine sequence do not overlap much and we have that

$$|X_d(\omega)| \approx \frac{1}{2} \left| \frac{\sin(N(\omega - \omega_0)/2)}{\sin((\omega - \omega_0)/2)} \right| + \frac{1}{2} \left| \frac{\sin(N(\omega + \omega_0)/2)}{\sin((\omega + \omega_0)/2)} \right|$$

This relation is expressed in Figure (2.21), again for the case of $N = 25$.

Now, as N becomes large, this figure begins to resemble, in some sense, the figure containing two impulses. Similarly, as N becomes large, the windowed (truncated) cosine sequence becomes a better approximation of the infinite-length cosine sequence.

2.5 Discrete Fourier Transform representation of finite-length DT signals

In Section 2.3 we discussed the discrete Fourier series representation as a means of building a large class of discrete-time periodic signals from a set of simpler, harmonically related discrete-time complex exponential

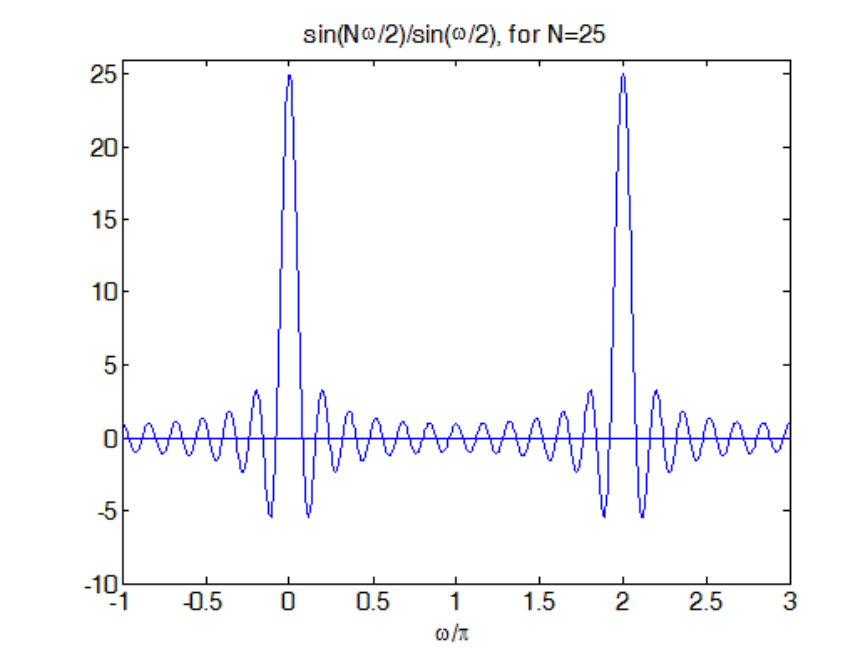


Figure 2.20: Periodic sinc function, $\frac{\sin(N\omega/2)}{\sin(\omega/2)}$ for $N = 25$. Note that the first zero-crossing occurs at $\omega = 2\pi/N$.

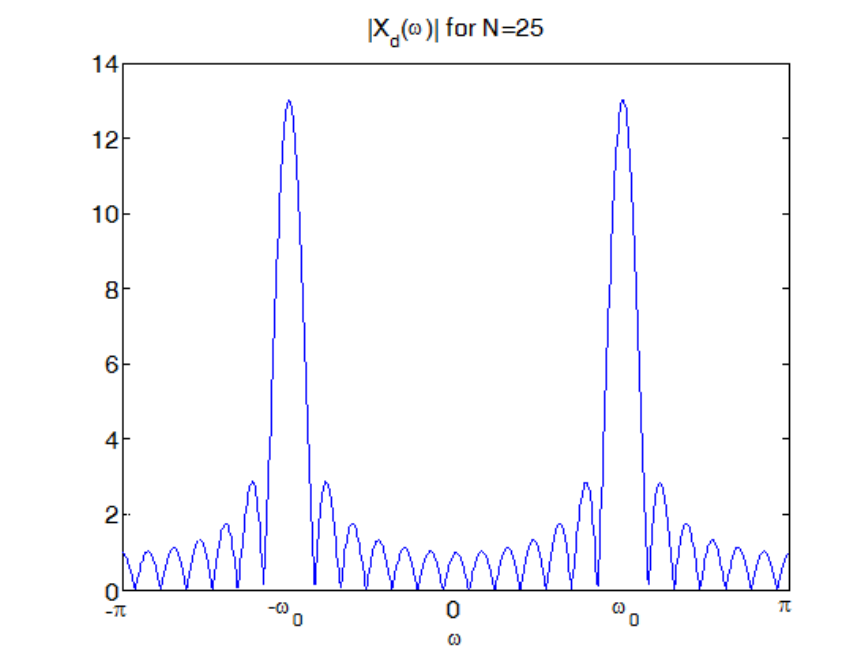


Figure 2.21: The magnitude of the DTFT of the sequence $x[n] = \cos(\omega_0 n)$, for $0 \leq n \leq 24$ and $x[n] = 0$, elsewhere.

Section	DTFT Property	Discrete Time Signal	Discrete Time Fourier Transform
	Definition	$x[n]$	$X_d(\omega) = \sum_{n=-\infty}^{\infty} x[n]e^{-j\omega n}$
2.2.1.1	Linearity	$z[n] = ax[n] + by[n]$	$Z_d(\omega) = aX_d(\omega) + bY_d(\omega)$
2.4.1.2	Periodicity	$x[n]$	$X_d(\omega) = X_d(\omega + k2\pi)$
2.4.1.3, 2.4.2	Real Part Symmetry	$x[n]$ real valued	$\Re\{X_d(\omega)\} = \Re\{X_d(-\omega)\}$
2.4.1.3, 2.4.2	Imaginary Part Symmetry	$x[n]$ real valued	$\Im\{X_d(\omega)\} = -\Im\{X_d(-\omega)\}$
2.4.1.3, 2.4.2	Magnitude Symmetry	$x[n]$ real valued	$ X_d(\omega) = X_d(-\omega) $
2.4.1.3, 2.4.2	Phase Symmetry	$x[n]$ real valued	$\angle X_d(\omega) = -\angle X_d(-\omega)$
2.4.1.3, 2.4.2	Conjugate Symmetry	$x[n]$ real valued	$X_d(\omega) = X_d^*(-\omega)$
2.4.2.1	Time Shift	$y[n] = x[n - d]$	$Y_d(\omega) = X_d(\omega)e^{-j\omega d}$
2.4.2.2	Modulation	$y[n] = x[n]e^{j\omega_0 n}$	$Y_d(\omega) = X_d(\omega - \omega_0)$
2.4.2.3	Time-Reversal	$y[n] = x[-n]$	$Y_d(\omega) = X_d(-\omega)$
2.4.2.4	Conjugation	$y[n] = x^*[n]$	$Y_d(\omega) = X_d^*(-\omega)$
2.4.2.5	Product of Signals	$z[n] = x[n]y[n]$	$Z_d(\omega) = \frac{1}{2\pi} \int_{-\pi}^{\pi} X_d(\nu)Y_d(\omega - \nu)d\nu$
2.4.2.6	Convolution	$z[n] = \sum_{m=-\infty}^{\infty} x[m]y[n - m]$	$Z_d(\omega) = X_d(\omega)Y_d(\omega)$
2.4.2.7	Parseval's Relation	$x[n]$	$\sum_{n=-\infty}^{\infty} x[n] ^2 = \frac{1}{2\pi} \int_{-\pi}^{\pi} X_d(\omega) ^2 d\omega$

Table 2.3: Properties of the Discrete Time Fourier Transform

Discrete Time Signal	Discrete Time Fourier Transform
$x[n]$	$X_d(\omega) = \sum_{n=-\infty}^{\infty} x[n]e^{-j\omega n}$
$a^n u[n], a < 1$	$\frac{1}{1 - ae^{-j\omega}}$
$na^n u[n], a < 1$	$\frac{ae^{-j\omega}}{(1 - ae^{-j\omega})^2}$
$e^{j\omega_0 n}$	$\sum_{k=-\infty}^{\infty} 2\pi\delta(\omega - \omega_0 + 2k\pi)$
1	$\sum_{k=-\infty}^{\infty} 2\pi\delta(\omega + 2k\pi)$
$\delta[n]$	1
$\cos(\omega_0 n)$	$\sum_{k=-\infty}^{\infty} \pi[\delta(\omega - \omega_0 + 2k\pi) + \delta(\omega + \omega_0 + 2k\pi)]$
$\sin(\omega_0 n)$	$-j\pi \sum_{k=-\infty}^{\infty} [\delta(\omega - \omega_0 + 2k\pi) - \delta(\omega + \omega_0 + 2k\pi)]$
$\frac{\omega_0}{\pi} \text{sinc}(\omega_0 n) = \begin{cases} \frac{\sin(\omega_0 n)}{\pi n} & n \neq 0 \\ \frac{\omega_0}{\pi} & n = 0 \end{cases}$	$\begin{cases} 1, & \omega \leq \omega_0 \\ 0, & \omega_0 < \omega \leq \pi \end{cases}$
$\begin{cases} 1, & 0 \leq n < N \\ 0, & \text{otherwise} \end{cases}$	$\begin{cases} \frac{\sin(N\omega/2)}{\sin(\omega/2)} e^{-j\omega(N-1)/2}, & \omega \neq 0 \\ N, & \omega = 0 \end{cases}$

Table 2.4: Discrete Time Fourier Transform Pairs

signals. In this section, we introduce the discrete Fourier transform (DFT) as an analogous notion of building a large class of finite-length signals from a set of simpler, harmonically related finite-length complex exponential discrete time signals. An important difference between the discrete-time Fourier series and what we will develop in this section as the discrete Fourier transform, is that while the periodic signals and the complex exponential signals used to construct them in the case of the DTFS were defined for all n , the signals for which we consider a DFT representation are finite in length and are therefore only defined for a finite interval of the time axis, n . Since this is a subtle difference, we are able to capitalize on all of the development of the DTFS. By considering a finite-length signal defined only on the interval $0 \leq n \leq N-1$, as one period of an infinite-length periodic signal defined for all n , we can directly map the DTFS into the DFT for our purposes. Mathematically, if a signal $x[n]$ is defined only on the interval $0 \leq n \leq N-1$, then by considering the periodic signal $\tilde{x}[n]$, defined as follows

$$\tilde{x}[n] = \sum_{k=-\infty}^{\infty} x[n + rN], \quad (2.36)$$

then over the interval from $0 \leq n \leq N-1$, we have that $x[n] = \tilde{x}[n]$.

The Fourier series coefficients $\tilde{X}[k]$ for this periodic signal can be obtained by

$$\tilde{X}[k] = \sum_{n=0}^{N-1} \tilde{x}[n] e^{-j2\pi kn/N}.$$

While this expression is valid for all k , we only require one period of $\tilde{X}[k]$, i.e. $0 \leq k \leq N-1$, for the inverse DTFS relation to reconstruct $\tilde{x}[n]$. Putting the synthesis and analysis equations together, we have the discrete-time Fourier series representation of a periodic signal $x[n]$ as

$$\tilde{x}[n] = \frac{1}{N} \sum_{k=0}^{N-1} \tilde{X}[k] e^{j\frac{2\pi kn}{N}},$$

which is again valid for all n , since the signal $\tilde{x}[n]$ is periodic and defined for all n . However, if we are only interested in finite-length signals, then viewing them as a single period of an infinite-length periodic signal as in (2.36), we can use the DTFS to both analyze and reconstruct finite-length signals from the first period of the underlying infinite-length periodic signals $\tilde{x}[n]$ and $\tilde{X}[k]$. Specifically, we can define the discrete Fourier transform of a finite-length signal, defined only over an interval of length N samples as

Discrete Fourier Transform Representation of a Finite-Length Signal

$$X[k] = \sum_{n=0}^{N-1} x[n] e^{-j\frac{2\pi kn}{N}}, 0 \leq k \leq N-1, \quad (2.37)$$

$$x[n] = \frac{1}{N} \sum_{k=0}^{N-1} X[k] e^{j\frac{2\pi kn}{N}}, 0 \leq n \leq N-1. \quad (2.38)$$

2.5.1 Discrete Fourier Transform Properties

We can now explore some of the many useful properties of the DFT representation, noting that these follow directly from the properties of the DTFS.

2.5.1.1 Sampling Property

While DFT is related to the DTFS of the periodic signal $\tilde{x}[n] = \sum_{k=-\infty}^{\infty} x[n + kN]$, it can also be shown to be related to the DTFT of the infinite length signal $x_{zp}[n] = x[n]$, $0 \leq n \leq N-1$, and $x_{zp}[n] = 0$, outside this region. The subscript “zp” stands for “zero-padding”, where the infinite length signal $x_{zp}[n]$, can be viewed as padding the finite length signal $x[n]$ with zeros outside the interval $0 \leq n \leq N-1$, over which it is defined. By observing the similarity between the DTFT and DFT representations,

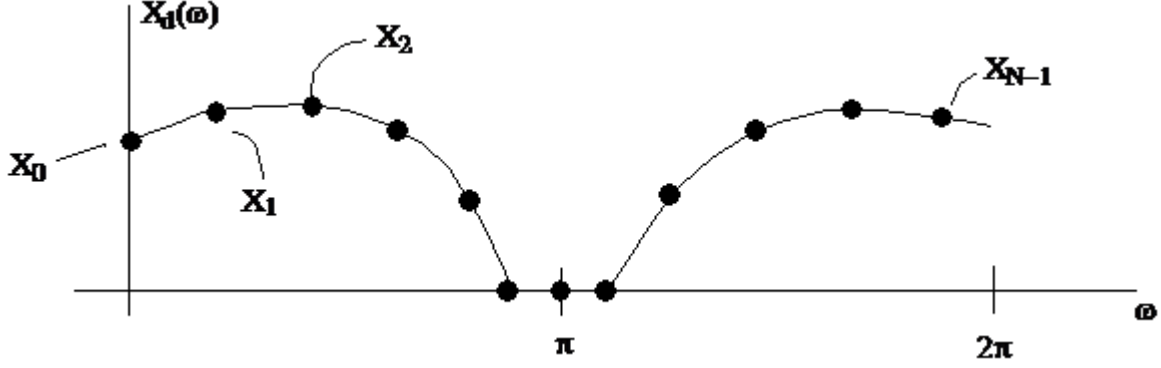


Figure 2.22: The DFT as samples of the DTFT, i.e. $X[k] = X_d(\frac{2\pi k}{N})$.

$$X[k] = \sum_{n=0}^{N-1} x[n]e^{-j\frac{2\pi k}{N}n} = \sum_{n=-\infty}^{\infty} x_{zp}[n]e^{-j\omega n} \Big|_{\omega=\frac{2\pi k}{N}} = X_d(\omega) \Big|_{\omega=\frac{2\pi k}{N}},$$

where $X_d(\omega)$ here refers to the DTFT of the infinite-length sequence $x_{zp}[n]$. We see that the DFT of the finite-length signal $x[n]$ can be viewed as a set of N evenly-spaced samples of the DTFT of the zero-padded infinite-length signal $x_{zp}[n]$ taken at samples $\omega_k = 2\pi k/N$, for $0 \leq k \leq N-1$. This can be seen pictorially in Figure (2.22).

Note that the last DFT sample, $X[N-1]$ does not correspond to a sample taken at $\omega = 2\pi$, but rather to the left of 2π , at $\omega = 2\pi(N-1)/N$.

2.5.1.2 Linearity

The DFT can be viewed as a linear operation as follows

$$x[n] \xleftrightarrow{DFT} X[k], y[n] \xleftrightarrow{DFT} Y[k] \implies z[n] = ax[n] + by[n] \xleftrightarrow{DFT} aX[k] + bY[k].$$

This result can be readily shown by substituting $z[n] = ax[n] + by[n]$ into the summation in (2.37) and expanding the summation into the two separate terms, one for $X[k]$ and one for $Y[k]$.

2.5.1.3 Circular Time Shift

When a periodic signal $\tilde{x}[n] = \sum_{k=-\infty}^{\infty} x[n + kN]$ is shifted in time, the effect on the DTFS of the resulting periodic signal $\tilde{x}[n - n_0]$ can be viewed as applying a linear phase term $e^{-j2\pi kn_0/N}$ to the original DTFS coefficients. For a finite-length signal $x[n]$, we cannot define a time-shift in the same manner, by simply shifting the time index, as this would require evaluating the signal $x[n]$ outside the range over which it is defined, namely $0 \leq n \leq N-1$. However, we can use the time shift property of the DTFS to relate a slightly different notion for finite length signals. By considering a time shift of n_0 samples of the underlying infinite-length periodic signal $\tilde{x}[n - n_0]$ as a “circular shift” of the finite-length sequence $x[n]$, we can study apply the time-shifting property of the DTFS to finite-length signals. To this end, we define a circular shift of a finite-length sequence, $x[n]$ as follows. First, we define the modulo operator, $\ll k \gg_N = k \bmod N$, as,

$$\ll k \gg_N = r, \text{ where } k = \ell N + r,$$

for any integer ℓ . For example $\ll 4 \gg_7 = 4$, $\ll 7 \gg_4 = 3$, $\ll 4 \gg_4 = 0$, $\ll -5 \gg_4 = 3$, $\ll -2 \gg_4 = 2$. Note that it is sometimes helpful to use $\ll -k \gg_N = N - \ll k \gg_N$. Now we can define the finite-length signal $y[n]$ as a circular shift of the finite-length sequence $x[n]$ as

$$y[n] = \tilde{x}[n - n_0] = x[\ll n - n_0 \gg_N],$$

i.e. a circular shift of the finite-length signal $x[n]$ by n_0 samples, is written $x[\ll n - n_0 \gg_N]$ but can be viewed as the result of taking a single period of the periodic signal $\tilde{x}[n - n_0]$, over the range $0 \leq n \leq N - 1$. The corresponding effect on the DFT of the sequence can be compactly represented as follows

$$x[n] \xleftrightarrow{DFT} X[k] \implies y[n] = x[\ll n - n_0 \gg_N] \xleftrightarrow{DFT} X[k] e^{-j \frac{2\pi k}{N} n_0}.$$

We see that a circular shift in time of a finite length signal corresponds to a modulation in frequency by a phase term that is linear with frequency with a slope that is proportional to the delay. Note that the resulting DFT is exactly the same as that which we would have obtained by first periodically extending the sequence $x[n]$ to the signal $\tilde{x}[n]$, and taking the DTFS representation of the resulting time-shifted signal $\tilde{x}[n - n_0]$.

2.5.1.4 Frequency Shift

From the analogous property of the DTFS, we can obtain the relation

$$x[n] \xleftrightarrow{DFT} X[k] \implies y[n] = x[n] e^{jk_0 \omega_0 n} \xleftrightarrow{DFT} X[\ll k - k_0 \gg_N],$$

where $\omega_0 = \frac{2\pi}{N}$, and where we have used the modulo notation to enable the resulting DFT to remain finite-length.

2.5.1.5 Time Reversal

From the DTFS time-reversal property, we obtain,

$$x[n] \xleftrightarrow{DFT} X[k] \implies y[n] = x[\ll -n \gg_N] = x[\ll N - n \gg_N] \xleftrightarrow{DFT} X[\ll -k \gg_N] = X[\ll N - k \gg_N],$$

where the modulo operator in $\ll N - n \gg_N$ and $\ll N - k \gg_N$ only comes into use for $n = 0$ and $k = 0$ since for all other values, the terms within the modulo operator are within the range of $0, \dots, N - 1$. This corresponds in the DFT representation to changing the sign of the DFT frequency index, where, to keep the terms within the range from 0 to N , we add N to the index, and take the result modulo N , which results in a reversal of the order of the DFT coefficients $X[\ll N - k \gg_N] = X[N - \ll k \gg_N]$.

2.5.1.6 Conjugate Symmetry

The effect of conjugating a complex-valued signal on its DFT representation can be seen from the DTFS property as

$$x[n] \xleftrightarrow{DFT} X[k] \implies x^*[n] \xleftrightarrow{DFT} X^*[\ll N - k \gg_N].$$

When the periodic signal $x[n]$ is real valued, i.e. $x[n]$ only takes on values that are real numbers, then the DFT exhibits a symmetry property. This arises directly from the definition of the DFT, and that real numbers equal their conjugates, i.e. $x[n] = x^*[n]$, such that

$$x[n] = x^*[n] \xleftrightarrow{DFT} X[k] \implies X[k] = X^*[\ll N - k \gg_N].$$

2.5.1.7 Products of Signals

When two finite-length signals of the same length are multiplied in time, such that $z[n] = x[n]y[n]$, the resulting signal remains finite length with the same length by definition. Hence, each of the three signals admit DFT representations using the same set of harmonically related signals. We can observe the effect on the resulting DFT from the analogous DTFS property,

$$x[n] \xleftrightarrow{DFT} X[k], y[n] \xleftrightarrow{DFT} Y[k] \implies z[n] = x[n]y[n] \xleftrightarrow{DFT} \frac{1}{N} \sum_{m=0}^{N-1} X[m]Y[\ll k - m \gg_N].$$

Length- N Discrete Time Signal	Discrete Fourier Transform
$x[n], 0 \leq n \leq N-1$	$X[k] = \sum_{n=0}^{N-1} x[n]e^{-j2\pi kn/N}, 0 \leq k \leq N-1$
$ax[n] + by[n]$	$aX[k] + bY[k]$
$x[\ll n - d \gg_N]$	$X[k]e^{-j2\pi kd/N}$
$x[n]e^{j2\pi \ell n/N}$	$X[\ll k - \ell \gg_N]$
$x[\ll -n \gg_N]$	$X[\ll N - k \gg_N]$
$x^*[n]$	$X^*[\ll N - k \gg_N]$
$x[n]y[n]$	$\frac{1}{N} \sum_{m=0}^{N-1} X[m]Y[\ll k - m \gg_N]$
$\sum_{m=0}^{N-1} x[m]y[\ll n - m \gg_N]$	$X[k]Y[k]$
Parseval's relation: $\sum_{n=0}^{N-1} x[n] ^2 = \frac{1}{N} \sum_{k=0}^{N-1} X[k] ^2$.	
$x[n]$ real-valued	$X[k] = X^*[\ll N - k \gg_N]$
$x[n]$ real-valued	$\Re\{X[k]\} = \Re\{X[\ll N - k \gg_N]\}$
$x[n]$ real-valued	$\Im\{X[k]\} = -\Im\{X[\ll N - k \gg_N]\}$
$x[n]$ real-valued	$ X[k] = X[\ll N - k \gg_N] $
$x[n]$ real-valued	$\angle X[k] = -\angle X[\ll N - k \gg_N]$

Table 2.5: Discrete Fourier Transform Properties

2.5.1.8 Circular Convolution

A dual relationship to that of multiplication in time, is multiplication of DFT coefficients. Specifically, when the two signals $x[n]$ and $y[n]$ are each of finite length N , the finite length signal $z[n]$ of length N , whose DFT representation is given by $Z[k] = X[k]Y[k]$ corresponds to a circular convolution of the signals $x[n]$ and $y[n]$. This leads to the following property of the DFT,

$$x[n] \xleftrightarrow{DFT} X[k], y[n] \xleftrightarrow{DFT} Y[k] \implies z[n] = \sum_{m=0}^{N-1} x[m]y[\ll n - m \gg_N] \xleftrightarrow{DFT} Z[k] = X[k]Y[k].$$

2.5.1.9 Parseval's relation

The energy contained within the finite duration of a finite length signal can also be computed in terms of its DFT representation using Parseval's relation,

$$x[n] \xleftrightarrow{DFT} X[k] \implies \sum_{n=0}^{N-1} |x[n]|^2 = \frac{1}{N} \sum_{k=0}^{N-1} |X[k]|^2.$$

The properties of the DFT discussed in this section are summarized in Table (2.5).

2.6 Applications of spectral representations and signal analysis, DFT spectral analysis

In Section 2.5 the DFT was introduced as a method for representing finite-length signals using a linear combination of simpler, finite-length segments of complex exponential signals, in a manner analogous to the construction of periodic signals from the periodic extensions of the same complex exponential family of signals. In Chapter 8 we will explore a number of fast algorithms for explicitly computing the DFT. One of the primary drivers of tremendous growth in the application and use of digital signal processing was, in fact, this discovery. There are two important aspects of the DFT that make its use in digital signal processing systems so pervasive. First, because the DFT is represented by a finite-length sum over quantities that are available, namely the signal $x[n]$, whose DFT is desired, and complex numbers of the form $e^{j2\pi kn/N}$, which can be easily represented using a pair of real numbers in the digital signal processor, one for the real part and the other for the imaginary part, the DFT can be exactly computed. This is in contrast to the CTFT

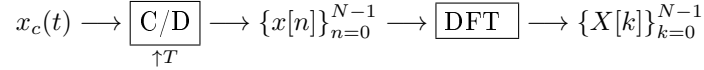


Figure 2.23: System for computing approximate samples of the CTFT of the continuous-time signal $x_c(t)$.

and the DTFT which contain either infinite-length integrals or infinite-length summations that cannot be exactly computed. In addition, even if they could be computed exactly, for example, in the case where the signals of interest have only a finite region of support, the CTFT, $X(\Omega)$, and the DTFT, $X_d(\omega)$, are each functions of a real-valued variable. However, they can only be evaluated for a finite number of values, but there remain an uncountably infinite set of other frequencies that remain unexplored. Second, and perhaps more importantly, as we will see in Chapter 8, the DFT can be computed so efficiently that we can make use of many of the DFT properties developed in this and later chapters for performing a wide variety of operations on the signals of interest to our application. For example, we will see how linear filtering can be very efficiently accomplished in the frequency domain through the multiplication of the DFT representation of signals. We will also explore how this can be accomplished for infinite-length signals by stitching together the outputs generated through the use of the finite-length representations that are each processed using the DFT.

Another equally desirable application that can be well-handled using the DFT is the process of spectral analysis. In many applications, including radio communications, image restoration, video compression, and even analog circuit analysis, it is important to have a direct measure of the frequency content of signals of interest. This can be accomplished in the laboratory using equipment known as a spectrum analyzer, in which the signal of interest is decomposed into its Fourier components, in real-time, and an image of the frequency composition of the signal is displayed on a screen or an oscilloscope. Such measures are extremely useful and require real-time processing of analog signals in order to provide an accurate picture of the frequency composition of a signal as either the signal itself or its environment is changing. While for continuous-time signals, it is the continuous-time Fourier transform that provides information about the frequency content of the signal, as we will explore in more detail in Chapter 5, many of the frequency-domain properties of signals and systems can accurately be measured by discrete-time processing of sampled versions of analog signals. Additionally, many discrete-time signals, such as the music stored on your MP3 player, can be efficiently compressed for storage using methods that exploit their frequency-domain representations.

To make the process more concrete, suppose that we are interested in the frequency content of a continuous-time signal $x_c(t)$, that is known to be approximately bandlimited to B Hz. That is, suppose that we know that

$$x_c(t) \xleftrightarrow{\text{CTFT}} X_c(\Omega) \approx 0, \quad |\Omega| > 2\pi B$$

i.e., that the CTFT of the signal $x_c(t)$, given by $X_c(\Omega)$ is known to be approximately zero outside of the frequency range $|\Omega| < 2\pi B$. However, we don't know the precise frequency composition of $x_c(t)$, and would like to obtain a real-time measurement of $X_c(\Omega)$ based on processing $x_c(t)$. One way to accomplish this is using DFT. Recall that the DFT of a finite-length signal $x[n]$ enables us to compute samples of the DTFT of the infinite-length zero-padded signal $x_{zf}[n]$. We also know from Section 2.5.1 and will explore in greater detail in Chapter 5, how the CTFT of a continuous-time signal $x_c(t)$ is related to the DTFT of a sampled-version of that signal, $x[n] = x_c(nT)$. We will now explore how these notions can be put together to provide a means for constructing a real-time spectrum analyzer using the DFT.

We will approach this problem as follows. Given access to the continuous-time signal $x_c(t)$, we want to compute approximate samples of $X_c(\Omega)$. Here is the proposed method for accomplishing this task. We will assume that the signal of interest $x_c(t)$ has finite support on the interval $[0, (N-1)T]$ and is nearly bandlimited as described above. That is, we are interested in the signal $x_c(t)$ in the range $t \in [0, (N-1)T]$, where T is a parameter of our sampling process that we will be able to control. The signal $x_c(t)$ is to be processed by the processor depicted in Figure 2.23. The signal is sampled at a rate of one sample every T seconds producing the discrete-time signal, $x[n] = x_c(nT)$.

Given the duration of interest, we obtain N samples, which we compactly represent as $\{x[n]\}_{n=0}^{N-1}$. These samples are then processed with the DFT analysis equation (2.37) producing the values $\{X[k]\}_{k=0}^{N-1}$. In the

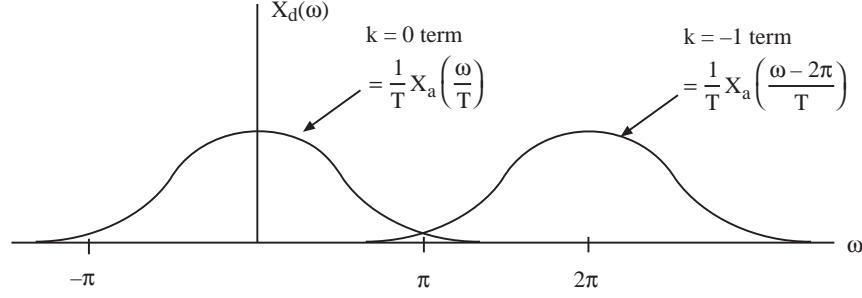


Figure 2.24: Spectrum of $x_c(t)$ scaled in amplitude and frequency and replicated on the digital frequency axis according to the relation $X_d(\omega) = \frac{1}{T} \sum_{k=-\infty}^{\infty} X_c\left(\frac{\omega + 2k\pi}{T}\right)$.

frequency domain, we know that the following relationship between the continuous-time Fourier transform (CTFT) of $x_c(t)$ and the discrete-time Fourier transform (DTFT) of $x[n]$ holds,

$$X_d(\omega) = \frac{1}{T} \sum_{k=-\infty}^{\infty} X_c\left(\frac{\omega + 2k\pi}{T}\right).$$

That is, if $x_c(t)$ is nearly bandlimited and T is sufficiently small, then there is little detrimental aliasing so that then $X_d(\omega)$ will contain copies of $X_c(\Omega)$ scaled to fit within the digital frequency range $|\omega| < \pi$ and scaled in amplitude by a factor of $1/T$. This is depicted in Figure (2.24).

The DFT, $\{X[k]\}_{k=0}^{N-1}$ is a set of samples of $X_d(\omega)$ on the interval $[0, 2\pi]$ such that $X[k] = X_d(\frac{2\pi k}{N})$, $0 \leq k \leq N-1$. Thus, we have (for N odd):

$$X[k] \approx \begin{cases} \frac{1}{T} X_c\left(\frac{2\pi k}{NT}\right), & 0 \leq k \leq \frac{N-1}{2} \\ \frac{1}{T} X_c\left(\frac{2\pi(k-N)}{NT}\right), & \frac{N-1}{2} < k \leq N-1. \end{cases}$$

So, we have that $\{X[k]\}_{k=0}^{N-1}$ actually contains approximate, scaled samples of $X_c(\Omega)$. It is important to note that the first half of the DFT samples provide samples of $X_c(\Omega)$ for $\Omega > 0$, while the second half of the DFT gives samples of $X_c(\Omega)$ for $\Omega < 0$. This peculiarity arises due to the definition of the DFT, where $\{X[k]\}_{k=0}^{N-1}$ is the set of samples of $X_d(\omega)$ on the interval $\omega \in [0, 2\pi]$ rather than on the symmetric interval $\omega \in [-\pi, \pi]$.

2.6.1 DFT Spectral Analysis of Sinusoids

Suppose that we wish to determine the frequency content of a continuous time signal that contains a number of sinusoidal components, of the form

$$x_c(t) = \sum_{i=1}^M A_i \cos(\Omega_i t),$$

and we have available only the following samples of the signal, $x[n] = x_c(nT)$, for $0 \leq n \leq N-1$. From this set of samples, $\{x[n]\}_{n=0}^{N-1}$, we wish to determine as much information about $x_c(t)$ as possible. Namely, we would like to determine the values of M , $\{\Omega\}_{i=1}^M$ and $\{A_i\}_{i=1}^M$.

One approach to this problem is to use DFT spectral analysis as depicted in Figure 2.23. Variations on this type of problem arise in numerous applications, including such wide-ranging topics as digital communications, radio astronomy, and even applications involving rotating machinery. For example, an acoustic transducer coupled to a piece of rotating machinery will output a periodic signal (a sum of sinusoids) plus, perhaps, a smaller nonperiodic component. A frequency (i.e., DFT) analysis of this signal might indicate whether the machinery requires maintenance or replacement. Similarly, in an underwater setting, ships can be identified through DFT analysis of the acoustic signals they emit, which are collected by hydrophones (underwater microphones).

Consider a single sinusoidal component, captured within $x[n]$ as

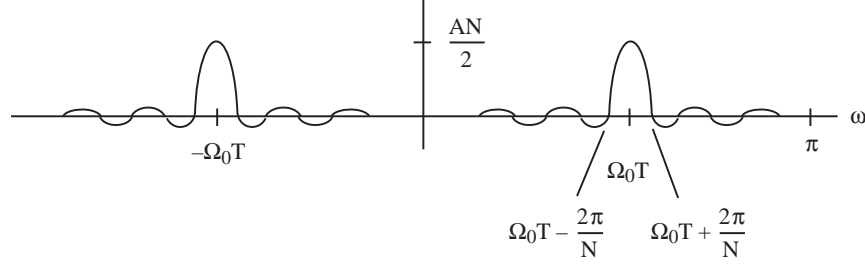


Figure 2.25: Schematic depiction of two periodic sinc functions centered at $\omega = \pm\Omega_0 T$ (without the linear phase term that appears in (2.40)).

$$x[n] = A \cos(\Omega_0 n T),$$

for $0 \leq n \leq N-1$. The DFT of $x[n]$ is a set of samples of the DTFT $X_d(\omega_k)$, for $\omega_k = 2\pi k/N$, $0 \leq k < N$:

$$\begin{aligned} X_d(\omega) &= \sum_{n=0}^{N-1} A \cos(\Omega_0 n T) e^{-j\omega n}, \\ &= \sum_{n=0}^{N-1} \frac{A}{2} \left(e^{-j(\omega - \Omega_0 T)n} + e^{-j(\omega + \Omega_0 T)n} \right) \\ &= \frac{A}{2} \frac{1 - e^{-j(\omega - \Omega_0 T)N}}{1 - e^{-j(\omega - \Omega_0 T)}} + \frac{A}{2} \frac{1 - e^{-j(\omega + \Omega_0 T)N}}{1 - e^{-j(\omega + \Omega_0 T)}} \end{aligned} \quad (2.39)$$

$$= e^{-j(\omega - \Omega_0 T)\frac{N-1}{2}} \underbrace{\frac{\frac{A}{2} \sin\left((\omega - \Omega_0 T)\frac{N}{2}\right)}{\sin\left((\omega - \Omega_0 T)\frac{1}{2}\right)}}_{T_1(\omega)} + e^{-j(\omega + \Omega_0 T)\frac{N-1}{2}} \underbrace{\frac{\frac{A}{2} \sin\left((\omega + \Omega_0 T)\frac{N}{2}\right)}{\sin\left((\omega + \Omega_0 T)\frac{1}{2}\right)}}_{T_2(\omega)}. \quad (2.40)$$

The two periodic sinc functions $T_1(\omega)$ and $T_2(\omega)$ above have peaks at $\omega = \pm\Omega_0 T$ and give rise to a DTFT that appears as in Figure 2.25.

The width of each main lobe is $\frac{4\pi}{N}$ based on the zero crossings of the periodic sinc function. If N is large enough, the main contributions from these pulses do not substantially overlap in frequency and we obtain that

$$\begin{aligned} |X_d(\omega)| &= |T_1(\omega) + T_2(\omega)| \\ &\approx |T_1(\omega)| + |T_2(\omega)| \\ &= \frac{A}{2} \left| \frac{\sin\left((\omega - \Omega_0 T)\frac{N}{2}\right)}{\sin\left((\omega - \Omega_0 T)\frac{1}{2}\right)} \right| + \frac{A}{2} \left| \frac{\sin\left((\omega + \Omega_0 T)\frac{N}{2}\right)}{\sin\left((\omega + \Omega_0 T)\frac{1}{2}\right)} \right|. \end{aligned}$$

Therefore, $\{X[k]\}_{k=0}^{N-1}$ will provide approximate samples of the magnitude of the above plot,

$$\begin{aligned} |X[k]| &= \left| X_d\left(\frac{2\pi k}{N}\right) \right|, \quad 0 \leq k < N \\ &\approx \frac{A}{2} \left| \frac{\sin\left(\left(\frac{2\pi k}{N} - \Omega_0 T\right)\frac{N}{2}\right)}{\sin\left(\left(\frac{2\pi k}{N} - \Omega_0 T\right)\frac{1}{2}\right)} \right| + \frac{A}{2} \left| \frac{\sin\left(\left(\frac{2\pi k}{N} + \Omega_0 T\right)\frac{N}{2}\right)}{\sin\left(\left(\frac{2\pi k}{N} + \Omega_0 T\right)\frac{1}{2}\right)} \right|, \quad \leq k < N, \end{aligned}$$

from which we can estimate Ω_0 and A . If $x[n]$ is obtained from samples of a signal containing a sum of several sinusoids, we will have multiple peaks and we can estimate each of the parameters M , Ω_i , and A_i using one

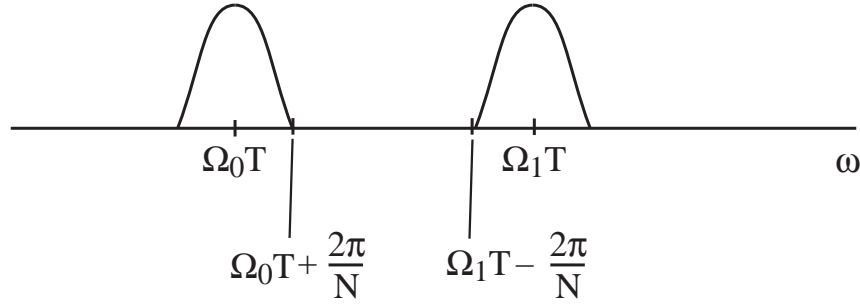


Figure 2.26: Two closely-spaced peaks in the spectral analysis of a signal containing sinusoidal components.

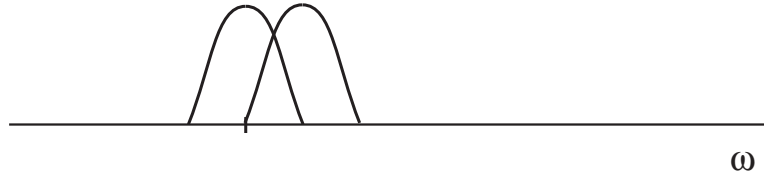


Figure 2.27: Two closely spaced peaks that overlap by 50% of their maximum amplitude.

of a number of possible methods, depending on what other information we have about the environment in which the signals have been obtained. For example, we might use the following algorithm:

$$\begin{aligned} M &= \text{Number of peaks detected on the interval } [0, \pi] \\ \Omega_i T &= \text{Location of the } i^{\text{th}} \text{ peak} \\ \frac{NA_i}{2} &= \text{Amplitude of the } i^{\text{th}} \text{ peak} \end{aligned}$$

Actually, sinusoidal spectral analysis, via the DFT, is not usually this straightforward. Some of the problems that frequently arise include:

1. Two frequencies Ω_i, Ω_k that are so close together that the two peaks add together into a single peak, or do not easily resolve into two distinct peaks. One possible solution is to use a larger value of N , i.e., collect data over a longer observation interval so that peaks will be narrower and therefore will not overlap. Suppose that the signal contains the two frequencies Ω_0 and Ω_1 . Then the main lobes of the periodic sines may look like that shown in Figure 2.26. To clearly distinguish the two peaks, we might require that the main lobes not overlap, i.e.,

$$\begin{aligned} \Omega_1 T - \frac{2\pi}{N} &> \Omega_0 T + \frac{2\pi}{N} \\ (\Omega_1 - \Omega_0) T &> \frac{4\pi}{N} \\ NT &> \frac{4\pi}{(\Omega_1 - \Omega_0)}. \end{aligned}$$

Therefore, the necessary observation interval NT increases as the frequency separation $(\Omega_1 - \Omega_0)$ decreases. So, the closer two sinusoidal components are to one another, the longer you will need to wait, in order to collect sufficient data to resolve the two peaks. In practice the above condition on NT is often too conservative, since we can still discern two peaks even if there is some overlap. If we instead require that there be no more than 50% overlap as shown in Figure 2.27, then the required condition becomes

$$\begin{aligned}\Omega_1 T - \frac{2\pi}{N} &> \Omega_0 T \\ NT &> \frac{2\pi}{(\Omega_1 - \Omega_0)}.\end{aligned}$$

2. In the previous analysis, we ignored the effect of the amplitude of the two frequency components, A_0 and A_1 . If two of the frequencies, Ω_i are fairly close together and one of the amplitudes, A_i , is much smaller than the other, this may cause the small peak to be buried in the sidelobes of the larger peak. One possible solution to this problem is to consider applying a window to the data prior to computing the DFT, to reduce the resulting sidelobes. Since the DTFT of the signal $x[n] = w[n]x_c(nT)$ implicitly contains the window function $w[n]$ multiplying the signal $x_c(nT)$, then the effect of the window $w[n]$ on the resulting DTFT, and therefore the resulting DFT, must be considered. In the analysis so far, we have assumed that a rectangular window, $w[n] = 1$, for $0 \leq n \leq N - 1$, was used. By selecting a window $w[n]$ that has lower side-lobe behavior than the rectangular window, which has a periodic sinc function as its DTFT, we may be able to avoid some of the side lobe issues. This is a matter that is discussed in more detail in chapter 6. Unfortunately, however, this is not a complete solution to the problem. While windowing reduces the size of the resulting side lobes near the peak, it also has the effect of widening the main lobe so that closely spaced sinusoids will be harder to distinguish.
3. The most important difficulty in spectral analysis is the presence of noise in the signal acquisition environment and in the signal itself. There are a host of methods that could be used for sinusoidal spectral analysis that would work perfectly (i.e. perfect estimation of all parameters) if there were no noise. Properly handling the spectral estimation problem in the presence of noise is a topic of great interest in the digital spectral analysis field and a number of methods exist, whose particular implementation and efficacy depends strongly on the type of noise that is present and on the signal-to-noise ratio (SNR), i.e. the relative strength of the signal components A_i and the noise power in the frequency range of interest. The achievable resolution in spectral analysis ultimately depends on properties of the noise, and on NT , the length of observation interval of $x_c(t)$.

2.6.2 Zero-Padding in DFT Spectral Analysis

Consider a spectral estimation problem as described in the previous section, in which we have obtained a set of samples $\{x[n]\}_{n=0}^{N-1}$, from a continuous-time signal, such that $x[n] = x_c(nT)$, for $0 \leq n \leq N - 1$. Let $x_{zp}[n]$ be the infinite length signal obtained by letting $x_{zp}[n] = x[n]$, for $0 \leq n \leq N - 1$, and set to zero outside of this interval. We then have that the DFT of $x[n]$ is related to the DTFT of $x_{zp}[n]$ through

$$X[k] = X_d\left(\frac{2\pi k}{N}\right), \quad 0 \leq k \leq N - 1.$$

We now consider another finite-length signal $x_2[n]$, of length $N + M$, such that

$$x_2[n] = \begin{cases} x[n], & 0 \leq n \leq N - 1 \\ 0 & N \leq n \leq N + M - 1, \end{cases}$$

so that the resulting finite-length signal contains both the original set of samples $x[n] = x_c(nT)$, as well as the additional M zero values from $x_{zp}[n]$ that follow these samples in the signal $x_{zp}[n]$. Let us consider how the length $N + M$ DFT of the signal $x_2[n]$ relates to the DTFT of the signal $x_{zp}[n]$. From the definition of

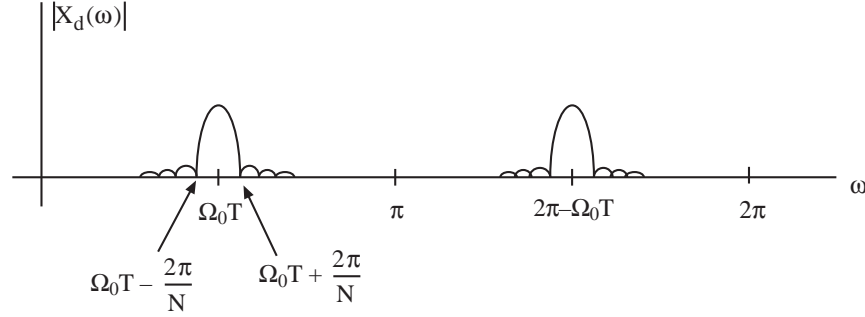


Figure 2.28: DTFT Magnitude for the sequence $x[n] = \cos(\Omega_0 nT)$.

the DFT, we have

$$\begin{aligned}
 X_2[k] &= \sum_{n=0}^{N+M-1} x_2[n] e^{-j \frac{2\pi k}{N+M} n} \\
 &= \sum_{n=0}^{N-1} x_{zp}[n] e^{-j \frac{2\pi k}{N+M} n} \\
 &= \sum_{n=0}^{N-1} x_{zp}[n] e^{-j \omega n} \Big|_{\omega = \frac{2\pi k}{N+M}} \\
 &= X_d\left(\frac{2\pi k}{N+M}\right),
 \end{aligned}$$

i.e., $X_2[k]$ provides a set of $N+M$ samples of the DTFT of $x_{zp}[n]$ equally spaced over the interval $\omega \in [0, 2\pi]$. That is, zero padding of the signal prior to taking the DFT provides a more densely spaced set of samples of precisely the same DTFT as the original, non-zero padded length N signal, $x[n]$. One reason that zero-padding is often used in DFT spectral analysis is the desire for a more densely spaced set of samples of $X_d(\omega)$, for example, to make a visual plot of the samples as an approximation to the true $X_d(\omega)$, which is a function of the continuous variable, ω . A second, and often more compelling reason for zero padding, arises when the sequence length, N , is not a length for which a fast DFT implementation is available. For example, we will explore a number of efficient implementations of the DFT, known collectively as the fast Fourier transform, or FFT, algorithms in chapter 8, for which N must be a power of two, i.e., $N = 2^\nu$. As a result, it may be desirable to pad the length of the sequence out to the nearest length for which an FFT implementation is available. This is a consideration of particular importance if N is large, or if many length- N DFTs are needed. Fast Fourier transform algorithms also exist for non power-of-two sequence lengths, such as when N is a highly-composite number (a product of a small number of prime numbers each raised to a large power, such as $N = 2^v 3^w 5^k$), however these FFT algorithms are a bit more involved than the power-of-two case.

Example: DFT Spectral Analysis of Sinusoids

If $x_c(t) = \cos(\Omega_0 t)$, and we have available the set of samples, $\{x[n]\}_{n=0}^{N-1}$, where $x[n] = \cos(\Omega_0 nT)$, then the magnitude of the DTFT of this sequence looks as shown in Figure 2.28.

Computing the DFT of the sequence $\{x[n]\}_{n=0}^{N-1}$ provides samples of $X_d(\omega)$. Depending on the length, N , of the DFT and the value of $\Omega_0 T$, there may or may not be samples of the DFT at or near the peaks of the mainlobes and sidelobes of the DTFT. Zero-padding prior to the DFT will yield a denser collection of samples of $X_d(\omega)$ and will therefore provide a better representation of $X_d(\omega)$, especially when plotted graphically.

The use of one of a variety of suitably designed windows, $\{w[n]\}_{n=0}^{N-1}$, can aid in DFT spectral analysis when the window is applied to the data prior to taking the DFT, i.e. $Y[k] = \sum_{n=0}^{N-1} w[n] x[n] e^{-j 2\pi k n / N}$. Note the sequence $\{x[n]\}_{n=0}^{N-1}$, already implicitly contains a rectangular window, $w[n] = 1$, $0 \leq n \leq N-1$. A different window could be applied by simply computing

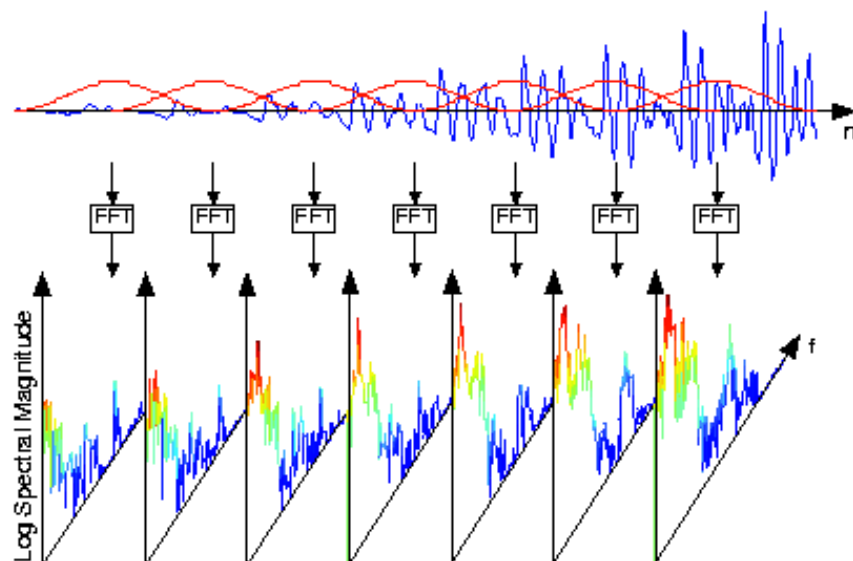


Figure 2.29: Graphical depiction of the process of computing the short-time Fourier transform of a long signal by applying a sequence of overlapping windows. These windowed segments of the longer signal are then processed using the fast Fourier transform (FFT) algorithm for computing the DFT, whose magnitude is then shown as a function of time on a logarithmic scale.

$Y[k] = \sum_{n=0}^{N-1} w[n]x[n]e^{-j2\pi kn/N}$, for a suitable window sequence, such as Hamming window, $w_h[n] = 0.54 - 0.46 \cos(2\pi n/(N-1))$, prior to computing the DFT. This will widen main lobe (by a factor of two) but will also greatly reduce the sidelobe behavior.

Short Time Fourier Transform (or Windowed Fourier Transform)

In practice, for signals of a long duration, such as speech or music recordings or radio transmissions, it is informative to examine the frequency content of the signal as it changes over time. To enable this, we can parse the signal into shorter blocks of time, which are often overlapped with one-another, and compute the DFT of each of these blocks. This process is often termed the short-time Fourier transform (STFT), and a graphical display of the magnitude of the STFT is called the spectrogram of the signal. Figure 2.29 illustrates the process in computing the STFT.

When the signal of interest is a speech signal, as shown in Figure 2.30, the STFT of the signal is often shown as an image, as it appears to the right in the figure.

```

% LOAD DATA
load speech_sig;
x = speech_sig;      % x holds the speech signal
figure(1), clf
plot(0:4000,x)
xlabel('n')
ylabel('x(n)')
% SET PARAMETERS
R = 256;              % R: block length
window = hamming(R); % window function of length R
N = 512;              % N: frequency discretization
L = 35;               % L: time lapse between blocks
fs = 7418;            % fs: sampling frequency
overlap = R - L;
% COMPUTE SPECTROGRAM
[B,f,t] = specgram(x,N,fs>window,overlap);
% MAKE PLOT
figure(2), clf
imagesc(t,f,log10(abs(B)));
colormap('jet')
axis xy
xlabel('time')
ylabel('frequency')
title('SPECTROGRAM, R = 256')

```

The command

```
[B,f,t] = specgram(x,N,fs>window,overlap);
```

computes the short time Fourier transform of a signal using a sliding window. The description of its input and output are as follows.

Input:

x - a vector that holds the input signal

N - specifies the FFT (or DFT) length that specgram uses

fs - a scalar that specifies the sampling frequency

window - specifies a windowing function

overlap - number of samples by which the sections overlap

Output:

B - matrix contains the spectrogram which is the magnitude of the STFT of the input signal

f - a column vector contains the frequencies at which specgram computes the discrete-time Fourier transform. The length of f is equal to the number of rows of B.

t - a column vector of scaled times, with length equal to the number of columns of B. t(j) is the earliest time at which the j-th window intersects x. t(1) is always equal to 0.

Table 2.6: M-file code used to generate the spectrogram shown in Figure 2.30.

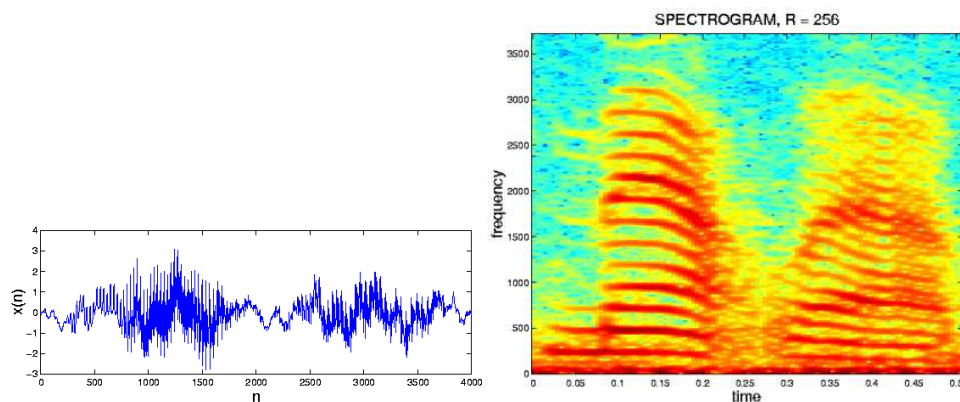


Figure 2.30: A segment of a signal generated from samples of a speech signal and its spectrogram computed using the code shown in table 2.6.

Chapter 3

CT and DT Systems

3.1 Systems as a mapping

In Chapter 1, we explored the mathematical representation of a variety of waveforms of interest, including sensor outputs, recorded data measurements or other information-bearing signals as either continuous-time or discrete-time signals. In this chapter, we develop the notion of a “system” as a means for transforming one signal into another signal. Specifically, a discrete-time system can be viewed as a transformation, or mapping, from one set of sequence values, called the input to the system, to another set of sequence values, called the output of the system.

For the discrete-time system shown in Figure 3.1, we can view the operation of the system as one that takes as input, the signal $x[n]$ and produces as output the signal $y[n]$. From this notation, the system enclosed within the box may appear to be simply mapping each value of the input signal $x[n]$ into a corresponding output value $y[n]$, however this point of view would not capture systems that contain memory. For example, suppose that the system simply delayed the input signal by two samples by using simple delay elements, such that $y[n] = x[n - 2]$. Rather than this sample-at-a-time thought process, we therefore must consider the system in the box as one that is capable of stepping outside the limitations of the time-index, and is capable of viewing the entire signal $x[n]$, from $n = -\infty$ to $n = \infty$, and then producing a new signal $y[n]$ which is also defined over the time index $n = -\infty$ to $n = \infty$. This notion of a system as a general mapping from one signal spanning the entire time horizon onto another entire signal spanning the same time horizon will enable us to consider a wide variety of practical systems in general, and properties of a number of specific systems of interest in practice.

This general notion or definition of a system as a mapping from one signal into another can be used to describe transformations of both continuous-time as well as discrete-time signals, as shown in figure 3.2.

Now that we have a general viewpoint of a system as a mapping from one into another signal, we can more formally define a system by wrapping some mathematical language around this framework. Specifically, we define a system as follows

A **discrete-time system** is a mapping, or a transformation, T , that maps one discrete-time signal, called the input signal, $x[n]$, into another discrete-time signal, called the output signal, $y[n]$, such that $y[n] = T\{x[n]\}$. We will sometimes use this formal system notation, i.e. $y[n] = T\{x[n]\}$, and, when convenient, we may adopt the shorthand $x[n] \rightarrow y[n]$, which carries the same meaning. That is, both should be read, “When the input to the system is $x[n]$, the output of the system is $y[n]$.”

A **continuous-time system** is a mapping, or a transformation, T , that maps one continuous-

$$x[n] \longrightarrow \boxed{\text{DT System}} \longrightarrow y[n]$$

Figure 3.1: A discrete-time system as a mapping from the input signal $x[n]$, to the output signal $y[n]$.

$$x(t) \longrightarrow \boxed{\text{CT System}} \longrightarrow y(t)$$

Figure 3.2: A continuous-time system as a mapping from the input signal $x(t)$, to the output signal $y(t)$.

$$x(t) \longrightarrow \boxed{\text{A/D}} \longrightarrow x[n]$$

$\uparrow T$

Figure 3.3: An A/D converter taking samples $x[n] = x(nT)$.

time signal, called the input signal, $x(t)$, into another continuous-time signal, called the output signal, $y(t)$, such that $y(t) = T\{x(t)\}$.

With these definitions of discrete-time and continuous-time systems, we can begin to explore some of the many properties of systems that process signals in discrete and continuous-time. However before we do, we will consider one more example of a system, but this system does not satisfy either of the definitions given above. Since one way in which discrete-time signals are created is through the process of sampling continuous-time signals with periodic sampling, we will briefly consider the ideal-sampling system as one that takes a continuous-time signal as its input and produces a discrete-time signal as its output. Later, when we consider analog-to-digital converters and digital-to-analog converters, we will explore these concepts more carefully, and will also consider a system that takes a discrete-time signal as its input and produces a continuous-time signal as its output.

3.2 Introduction to Sampling

One example of a *mixed-signal* system is an ideal analog-to-digital converter, or A/D converter in shorthand. While it is mathematically simple to describe the operation of an ideal A/D converter, as we will see when we discuss such systems in more detail, the design and operation of a practical A/D converter can be a complicated process. However, for our purposes here, we will stick with the simple, ideal case. In this case, we consider a system that takes an analog, continuous-time signal $x(t)$ as input and produces a discrete-time signal $x[n]$ as output, as shown in figure 3.3.

Mathematically, the discrete-time output $x[n]$ is related to the continuous-time input signal $x(t)$ through the relation $x[n] = x(nT)$, where the parameter T is called the *sampling period* of the A/D converter and has the sample units as the time index t of the input. While the relationship between the input and outputs of the ideal A/D converter can be succinctly stated, as we will see in later chapters of this text, under certain conditions the original continuous-time signal $x(t)$ may be completely recovered from its samples $x[n]$. As you might imagine, this will place some restrictions on the class of signals $x(t)$, however we will see that this can be accomplished in a way that permits a wide range of possible input signals of interest to be sampled, stored, and completely recovered from its samples. One simple example of a set of signals that can be recovered easily from periodic samples is the class of polynomial signals, i.e. $x(t) = a_0 + a_1t + a_2t^2 + \dots + a_Nt^N$, which can be completely recovered from only $N + 1$ samples. When the number of samples taken becomes large and even infinite, the class of signals that can be perfectly reconstructed from its periodic samples becomes rather large. However, as the class of signals becomes large and complex, more sophisticated means must be used to reconstruct the original continuous-time signal.

For the system in Figure 3.3, we recall that when the input signal $x(t)$ is bandlimited, such that its Fourier transform magnitude satisfies $|X(\omega)| = 0$, for $|\omega| > 2\pi B$, then so long as the sampling rate is sufficiently high enough, i.e. $\frac{1}{T} > 2B$, then the signal $x(t)$ can be completely reconstructed from its samples, $x[n] = x(nT)$, as follows

$$x(t) = \sum_{n=-\infty}^{\infty} x[n] \text{sinc}\left(\frac{\pi}{T}(t - nT)\right). \quad (3.1)$$

This relationship enables us to reconstruct $x(t)$ from the samples $x[n] = x(nT)$, for bandlimited signals.

While this relationship is tremendously powerful, it will be equally important for us to see how the Fourier representations of the signals $x(t)$ and $x[n]$ are also related. We will show that the relationship between $X(\Omega)$, the CTFT of $x(t)$, and $X_d(\omega)$, the DTFT of $x[n]$ is given by

$$X_d(\omega) = \frac{1}{T} \sum_{k=-\infty}^{\infty} X\left(\frac{\omega + 2\pi k}{T}\right), \quad (3.2)$$

which provides the following relationships between a continuous-time signal $x(t)$ and the sequence of samples $x[n] = x(nT)$,

$x(t)$	$\longrightarrow \boxed{\text{A/D}} \longrightarrow$ $\uparrow T$	$x[n]$
$x(t) = \sum_{n=-\infty}^{\infty} x[n] \text{sinc}\left(\frac{\pi}{T}(t - nT)\right)$	time domain	$x[n] = x(nT)$
$X(\Omega) = \begin{cases} TX_d(\Omega T), & \Omega < \frac{\pi}{T} \\ 0 & \text{else} \end{cases}$	frequency domain	$X_d(\omega) = \frac{1}{T} \sum_{k=-\infty}^{\infty} X\left(\frac{\omega + 2\pi k}{T}\right)$

We will show how these relationships can be derived, beginning in the lower right and working our way counterclockwise through the chart.

We begin with a continuous-time signal $x(t)$ that has a well-defined CTFT given by $X(\Omega)$. By taking periodic samples of the signal $x[n] = x(nT)$, we also assume that the signal $x(t)$ is well-defined at the sampling instants $t = nT$. Taking a closer look at the CTFT synthesis equation, and using the sampling instants and the link, we have

$$\begin{aligned}
x[n] &= x(nT) \\
&= \frac{1}{2\pi} \int_{-\infty}^{\infty} X(\Omega) e^{j\Omega(nT)} d\Omega \\
&= \frac{1}{2\pi} \int_{-\infty}^{\infty} X\left(\frac{\omega}{T}\right) e^{j\frac{\omega}{T}(nT)} d\frac{\omega}{T} \\
&= \frac{1}{2\pi T} \int_{-\infty}^{\infty} X\left(\frac{\omega}{T}\right) e^{j\omega n} d\omega \\
&= \frac{1}{2\pi T} \sum_{k=-\infty}^{\infty} \int_0^{2\pi} X\left(\frac{\omega + 2\pi k}{T}\right) e^{j\omega n} d\omega \\
&= \frac{1}{2\pi} \int_0^{2\pi} \underbrace{\left[\frac{1}{T} \sum_{k=-\infty}^{\infty} X\left(\frac{\omega + 2\pi k}{T}\right) \right]}_{X_d(\omega)} e^{j\omega n} d\omega \\
&= \frac{1}{2\pi} \int_0^{2\pi} [X_d(\omega)] e^{j\omega n} d\omega,
\end{aligned}$$

which yields the relationship of (3.2) by the uniqueness property of the DTFT and the last line above. The first line above arises from setting $t = nT$ in the CTFT synthesis equation; the second line comes from setting $\omega = \Omega T$, the fourth line comes from breaking the infinite integral into a sum of integrals of length 2π each. It is helpful to consider what (3.2) represents graphically. We see three components of interest. First, the DTFT is represented by a scaled-frequency axis version of the original CTFT, that is $X(\omega/T)$; next we see that this scaled version is also scaled in amplitude by the factor $\frac{1}{T}$; and finally that copies if

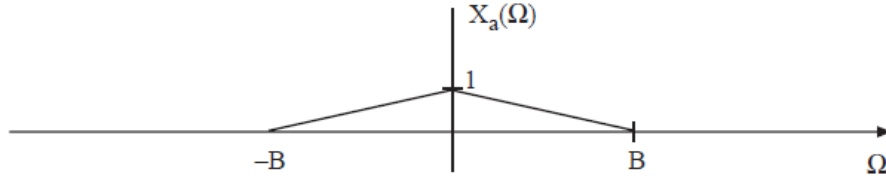


Figure 3.4: An example of a bandlimited CTFT of a signal $x_a(t)$.

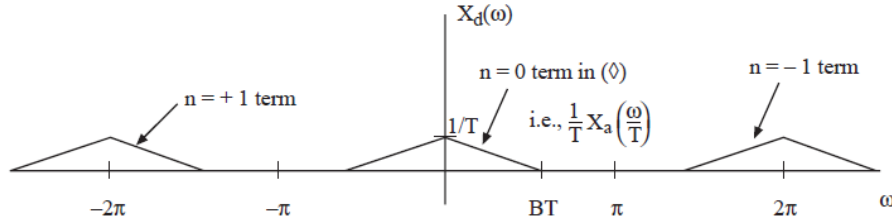


Figure 3.5: Graphical depiction of three of the terms in (3.2) for the bandlimited CTFT signal $x_a(t)$ shown in (3.4).

this amplitude and frequency scaled version of $X(\Omega)$ are placed at equally-spaced intervals on the ω axis. Note that if the original spectrum, $X(\Omega)$ is zero for $|\Omega| > B$, then this periodic replication simply provides the necessary 2π periodicity of the DTFT and within the interval $|\omega| < \pi$, we have the simpler relation

$$X_d(\omega) = \frac{1}{T} X\left(\frac{\omega}{T}\right), \quad |\omega| < \pi,$$

and is 2π periodic elsewhere. However, if the original spectrum $X(\Omega)$ is not bandlimited in this manner, then the summation of shifted replicas of the scaled spectrum $X(\frac{\omega+2\pi k}{T})$ each may have overlap into the interval $|\omega| < \pi$, and each of the terms in the summation must be taken carefully into account. We will consider several examples to illustrate this point.

As an example, let us consider a signal $x_a(t)$ that has a bandlimited spectrum as depicted in Figure 3.4.

When the sampling interval is such that $\frac{\pi}{T} > B$, the terms in the summation (3.2) do not overlap, and we have no detrimental “aliasing” of frequency components, which is what we the effect of copies of the CTFT that are centered outside the region from $-\pi$ to π in discrete frequency, i.e. the region occupied primarily by the $k = 0$ term from (3.2). When frequencies overlap, and masquerade in a band to which they do not belong, we are no longer able to determine those frequency components from the original continuous-time signal from those hiding behind an alias, owing to the periodic replication of the CTFT.

Note that since we assumed that $\frac{\pi}{T} > B$, and since the CTFT $X_a(\Omega)$ is zero for $|\Omega| > B$, then when we substitute $\frac{\omega}{T}$ for Ω in $X_a(\Omega)$, we have that $X_a(\frac{\omega}{T}) = 0$ for $|\omega| > BT$. As a result, the $k = 0$ term is confined to the region $-\pi < \omega < \pi$, and the $k = 1$ term is confined to the region $\pi < \omega < 3\pi$ and more generally, the k^{th} term is confined to the region $-\pi < \omega + k2\pi < \pi$, or $-\pi - k2\pi < \omega < \pi - k2\pi$. Note that when $BT > \pi$, the contribution from the $k = 0$ term and the $k = -1$ term will overlap. This is called “aliasing” and eliminates our ability to completely recover the continuous-time signal $x_a(t)$ from its samples. The condition $BT < \pi$ is equivalent to the Nyquist condition stated previously, since we have $BT < \pi \implies T < \frac{\pi}{B} \implies \frac{1}{T} > \frac{B}{\pi} \implies \frac{1}{T} > 2\left(\frac{B}{2\pi}\right)$, where $\frac{1}{T}$ is the sampling frequency in samples per second, and $\frac{B}{2\pi}$ is the bandwidth of $x_a(t)$ in Hz.

In a second example, we consider the case when $BT = \frac{5\pi}{3}$, or $T = \frac{5\pi}{3B}$, which indeed will give rise to aliasing. In this case we no longer have the simple relationship $X_d(\omega) = \frac{1}{T} X\left(\frac{\omega}{T}\right)$, $|\omega| < \pi$, but rather need to use the more complicated expression (3.2), which contains the infinite sum of copies of $X(\Omega)$, scaled in amplitude, scaled in frequency, and shifted in frequency, $\frac{1}{T} X\left(\frac{\omega-2\pi k}{T}\right)$. For this situation, with $BT = \frac{5\pi}{3}$, we can readily see (either graphically, or through simple calculation) that we need to account for the $k = -1, 0, 1$ terms in the summation. This can be graphically depicted as in Fig. 3.6.

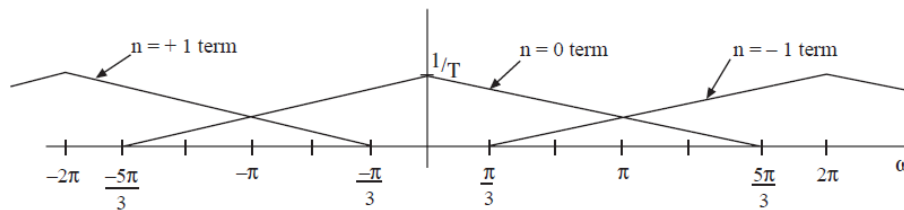


Figure 3.6: A graphical depiction of the various terms that contribute to the DTFT $X_d(\omega)$ is shown when the signal $x_a(t)$ with CTFT in 3.4 is sampled producing $x[n] = x_a(nT)$, for $BT = \frac{5\pi}{3}$. As seen graphically, the induced aliasing requires that three terms in the summation of (3.2).

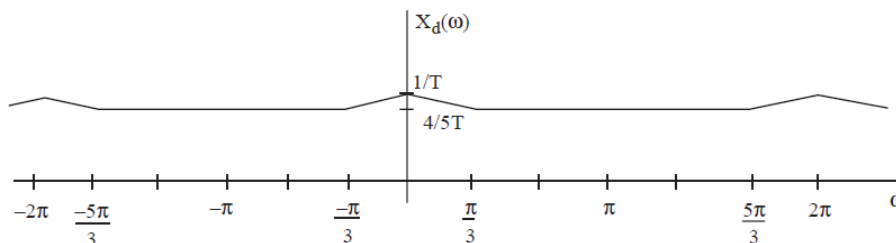


Figure 3.7: The DTFT $X_d(\omega)$ is shown when the signal $x_a(t)$ with CTFT in 3.4 is sampled producing $x[n] = x_a(nT)$, for $BT = \frac{5\pi}{3}$.

The three terms that comprise the scaled, shifted spectrum, $\frac{1}{T}X_a(\frac{\omega+2\pi}{T}) + \frac{1}{T}X_a(\frac{\omega}{T}) + \frac{1}{T}X_a(\frac{\omega-2\pi}{T})$, when added together create the complete DTFT $X_d(\omega)$ shown in Figure 3.7.

The resulting spectrum $X_d(\omega)$, no longer appears as a periodic replication of a scaled in amplitude and in frequency version of $X_a(\Omega)$, but rather a distorted version of this. This is because some of the higher frequencies from the copy of $X_a(\frac{\omega}{T})$ extend outside the range $|\omega| < \pi$ and similarly, some of the higher frequencies from the copy $X_a(\frac{\omega-2\pi}{T})$ extend into this frequency range from the right, and masquerade as lower frequencies. The same is true from the copy $X_a(\frac{\omega+2\pi}{T})$ from the left. This is the reason we use the term “aliasing” to describe this phenomenon.

If we were to select an even slower rate of sampling, i.e. a larger value of the sampling period T , then additional terms beyond these three would also need to be incorporated. For simplicity, we can exploit the periodicity of DTFTs and only concentrate on the terms $X_a(\frac{\omega-2\pi k}{T})$ that fall into the range $-\pi < \omega < \pi$, and then periodically replicate this resulting spectrum with periodicity 2π in ω . The net result will be the same as if we considered all of the terms in the infinite summation making up $X_d(\omega)$.

When there is no aliasing in the resulting spectrum and we have that $X_d(\omega) = \frac{1}{T}X_a(\frac{\omega}{T})$ in the range $-\pi < \omega < \pi$, then we can, at least conceptually, derive a reconstruction formula for recovering $x_a(t)$ perfectly from the samples $x[n] = x_a(nT)$. The “algorithm” for doing so would follow along these lines:

$$x_a(t) = \text{CTFT}^{-1} \left[\begin{cases} T \times \text{DTFT} x[n]|_{\omega=\Omega T} & |\Omega| < \frac{\pi}{T} \\ 0 & \text{otherwise} \end{cases} \right].$$

We can follow through this conceptual algorithm, mathematically, to produce the ideal reconstruction formula

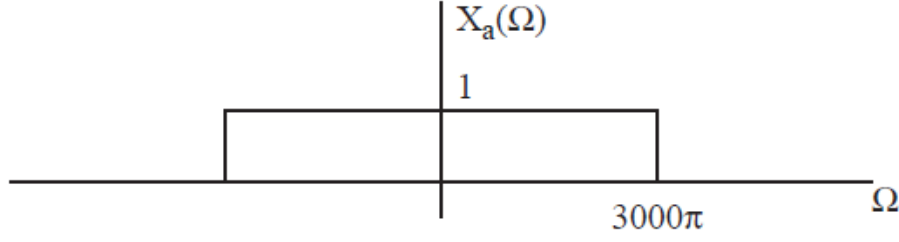


Figure 3.8: A bandlimited signal $x_a(t)$ with spectrum $X_a(\Omega)$ bandlimited to 3000π .

as follows.

$$\begin{aligned}
 x_a(t) &= \frac{1}{2\pi} \int_{-\infty}^{\infty} \left[\begin{cases} T \times \text{DTFT } x[n]|_{\omega=\Omega T} & |\Omega| < \frac{\pi}{T} \\ 0 & \text{otherwise} \end{cases} \right] e^{j\Omega t} d\Omega \\
 &= \frac{T}{2\pi} \int_{-\frac{\pi}{T}}^{\frac{\pi}{T}} \sum_{n=-\infty}^{\infty} x[n] e^{-j(\Omega T)n} e^{j\Omega t} d\Omega \\
 &= \frac{T}{2\pi} \sum_{n=-\infty}^{\infty} x[n] \int_{-\frac{\pi}{T}}^{\frac{\pi}{T}} e^{j\Omega(t-nT)} d\Omega \\
 &= \sum_{n=-\infty}^{\infty} x[n] \left[\frac{e^{j\pi(t-nT)/T} - e^{-j\pi(t-nT)/T}}{2\pi j(t-nT)/T} \right] \\
 &= \sum_{n=-\infty}^{\infty} x[n] \frac{2j \sin(\pi(t-nT)/T)}{2\pi j(t-nT)/T} \\
 &= \sum_{n=-\infty}^{\infty} x[n] \text{sinc}\left(\frac{\pi}{T}(t-nT)\right), \tag{3.3}
 \end{aligned}$$

where in the last three lines of the derivation, we exclude the case $t = nT$, and consider that case separately. When $t = nT$, we have in the integral in the second line of the derivation, an integral of 1 over the interval of length $2\pi/T$. This, together with the scale factor $T/2\pi$ outside the integral tells us that the integral evaluates to one for $t = nT$, which is why we use the sinc function in the last line of the derivation, which then is valid for all values of t .

We consider another example in which we sample a continuous time signal to produce a discrete-time signal and observe how the frequency content of the signal as depicted in the CTFT is mapped to discrete time. Specifically, for the continuous time signal $x_a(t)$ with CTFT given by $X_a(\Omega) = 1$, for $|\Omega| < 3000\pi$, and zero elsewhere, i.e. as shown in Figure 3.8.

We consider sampling the signal $x_a(t)$ at sampling rates of $4kHz$, $6kHz$, and $12kHz$, i.e. $x[n] = x_a(nT)$ for $T = 1/4,000$, $T = 1/6,000$ and $T = 1/12,000$. As shown in Figure 3.9, we see that as the sampling rate increases (i.e. when T decreases) the spectrum $X_a(\Omega)$ is mapped to a smaller and smaller set of frequencies in discrete-time.

The ideal reconstruction formula given in 3.3 can be viewed as a mathematical description of the operation of an ideal digital-to-analog (D/A) converter, which we have referred to as an ideal discrete-to-continuous (D/C) converter. The process of ideal continuous-to-discrete conversion, depicted as

$$x[n] \longrightarrow \boxed{\text{D/C}} \longrightarrow x(t)$$

$\uparrow T$

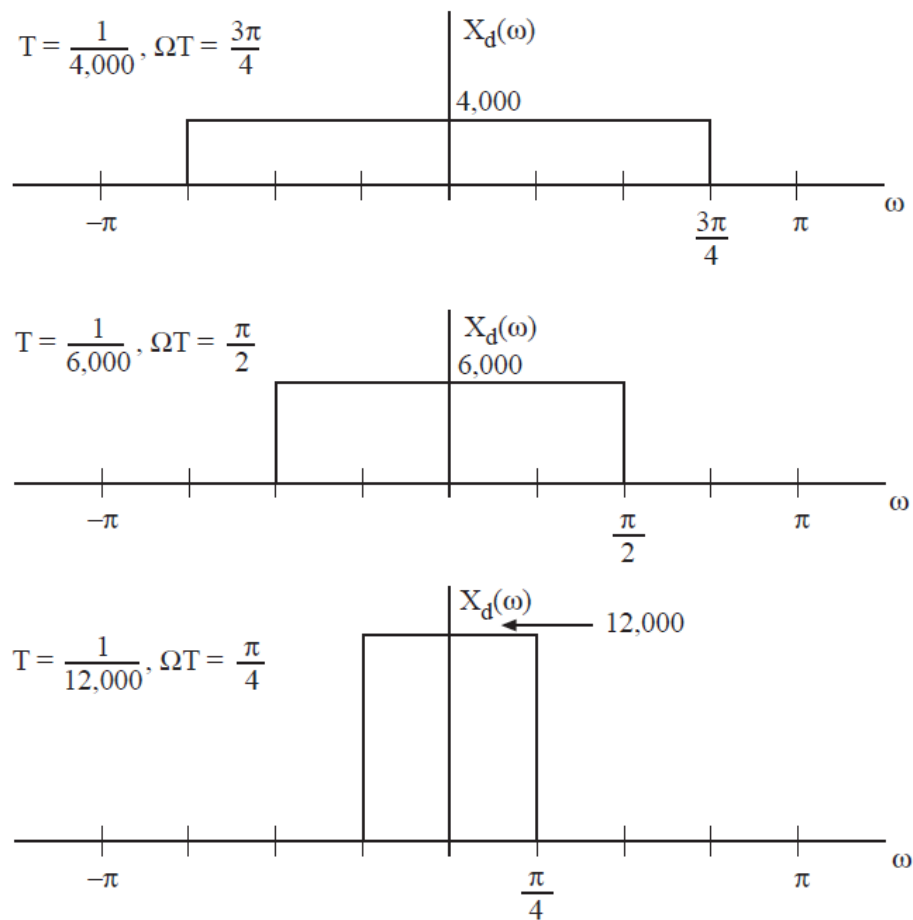


Figure 3.9: Three different DTFTs are generated when $x[n] = x_a(nT)$ for $T = 1/4,000$, $T = 1/6,000$ and $T = 1/12,000$.

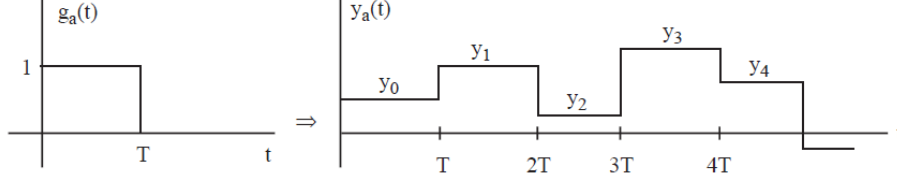


Figure 3.10: The reconstruction of $y_a(t) = \sum_{n=-\infty}^{\infty} x[n]g(t-nT)$, for $g(t)$ given by a rectangular pulse. This is called zero-order-hold (ZOH) reconstruction.

can be thought of as a process of clocking out a specific pulse shape (a sinc function) at integer multiples of the sampling period T scaled by the samples $x[n]$. Mathematically, we can view the process as follows,

$$y(t) = \sum_{n=-\infty}^{\infty} x[n]g(t-nT),$$

where we consider an arbitrary reconstruction pulse $g(t)$ to be used in the C/D converter, and in this case we call the output $y(t)$ to indicate the possibility that $y(t)$ may differ from $x_a(t)$ from which the samples were taken to produce $x[n]$. When $g(t) = \text{sinc}(\pi(t-nT)/T)$, we have perfect reconstruction and $y(t) = x_a(t)$. However, more generally, we may want to consider how $y(t)$ relates to the original signal $x_a(t)$ and the discrete-time signal $x[n]$. For example, later in the text, we will consider the case when $g(t)$ is a rectangular pulse as shown in Figure 3.10.

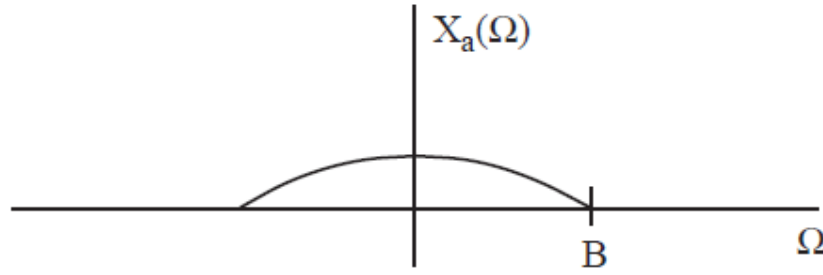
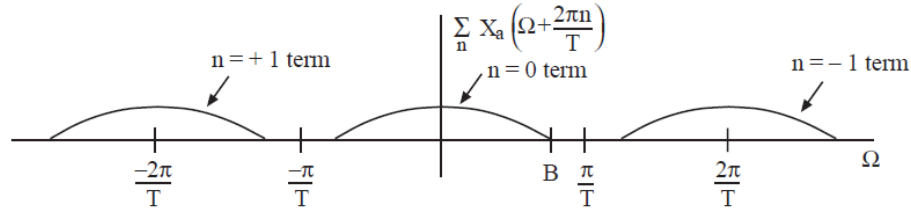
Mathematically, we can explore the spectrum $Y_a(\Omega)$ from this reconstruction in general. We have

$$\begin{aligned} y_a(t) &= \sum_{n=-\infty}^{\infty} x[n]g(t-nT) \\ Y_a(\Omega) &= \int_{-\infty}^{\infty} y_a(t)e^{-j\Omega t}dt \\ &= \int_{-\infty}^{\infty} \sum_{n=-\infty}^{\infty} x[n]g(t-nT)e^{-j\Omega t}dt \\ &= \sum_{n=-\infty}^{\infty} x[n] \int_{-\infty}^{\infty} g(t-nT)e^{-j\Omega t}dt \\ &= \sum_{n=-\infty}^{\infty} x[n]G(\Omega)e^{-j\Omega(nT)} \\ &= G(\Omega) \sum_{n=-\infty}^{\infty} x[n]e^{-j(\Omega T)n} \\ &= G(\Omega)X_d(\Omega T), \end{aligned}$$

where in the fifth line, we used the delay property of CTFTs, for the CTFT of $g(t-nT)$, and in the sixth line we observe the expression for the DTFT of $x[n]$ with the frequency variable ΩT . We note that the resulting expression

$$Y_a(\Omega) = G(\Omega)X_d(\Omega T)$$

is valid for all $-\infty < \Omega < \infty$. When $G(\Omega)$ is an ideal lowpass filter with cutoff frequency $\frac{\pi}{T}$, then only a single period of the periodic spectrum $X_d(\Omega T)$ remains. However for general $G(\Omega)$, we may observe not only the period that is centered at $\Omega = 0$, but also those centered at integer multiples of $\frac{2\pi}{T}$, filtered by $G(\Omega)$. When the signal $x[n]$ arises from sampling $x_a(t)$, we can substitute our expression for $X_d(\omega)$ in terms of

Figure 3.11: Bandlimited spectrum $X_a(\Omega)$.Figure 3.12: The discrete-time spectrum that results from sampling $x_a(t)$ at rate $1/T$.

$X_a(\Omega)$ and obtain

$$Y_a(\Omega) = G(\Omega) \frac{1}{T} \sum_{k=-\infty}^{\infty} X_a\left(\frac{\omega + 2\pi k}{T}\right).$$

If the signal $x_a(t)$ were bandlimited to $B < \pi/T$, then we may have a spectrum as depicted in Figure 3.11.

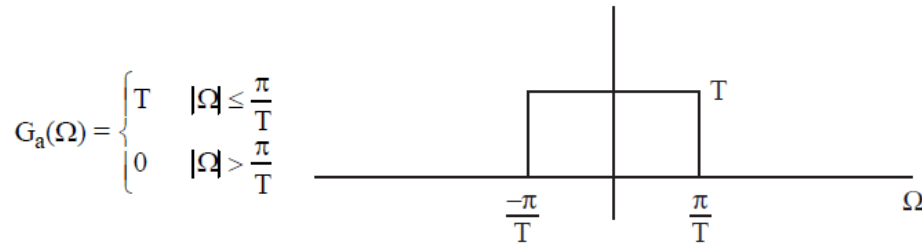
Since $B < \pi/T$, there is no aliasing so the resulting $X_a(\Omega T)$ appears as shown in Fig. 3.12.

Since there is no aliasing, we have that $\sum_{k=-\infty}^{\infty} X_a(\frac{\Omega T + 2\pi k}{T}) = X_a(\Omega)$ in the range $-\frac{\pi}{T} < \Omega < \frac{\pi}{T}$. For an ideal D/C converter, i.e., for $g(t) = \text{sinc}(\pi(t - nT)/T)$, we have that $G(\Omega) = T$ in the range $-\frac{\pi}{T} < \Omega < \frac{\pi}{T}$, and is zero elsewhere, i.e. $G(\Omega)$ is as shown in Figure 3.13.

We can now graphically observe the effect of using this reconstruction filter in the D/C converter. As shown in Figure 3.14, the ideal reconstruction filter passes through only the term centered at $\Omega = 0$, and rejects all other periodic replications of $X_a(\Omega)$.

As a result, we have for the CTFT of the output,

$$\begin{aligned} Y_a(\Omega) &= G(\Omega) \frac{1}{T} \sum_{k=-\infty}^{\infty} X_a\left(\Omega + \frac{2\pi k}{T}\right) \\ &= \begin{cases} X_a(\Omega), & |\Omega| < \frac{\pi}{T} \\ 0 & \text{otherwise.} \end{cases} \end{aligned}$$

Figure 3.13: The CTFT of the ideal reconstruction filter $G(\Omega)$ in an ideal D/C converter.

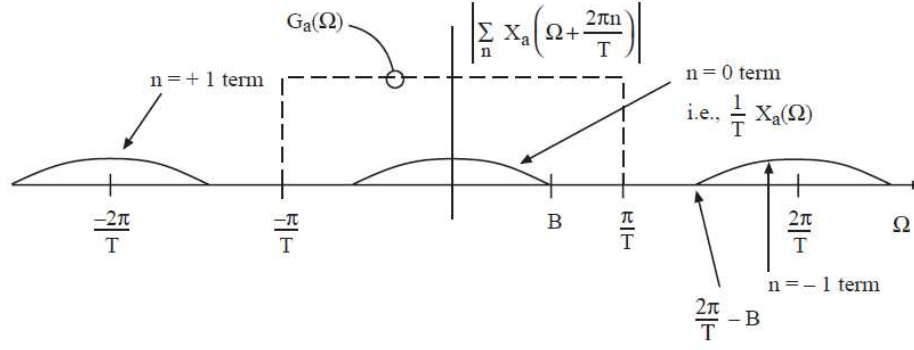


Figure 3.14: Graphical depiction of the operation of an ideal reconstruction filter in an ideal D/C converter.

Therefore, if $X_a(\Omega)$ is bandlimited to $\frac{\pi}{T}$, then we have that $Y_a(\Omega) = X_a(\Omega)$, and $y_a(t) = x_a(t)$, i.e. we have perfect reconstruction of the original continuous-time signal from its samples.

3.3 Some Examples of Discrete-time Systems

Before we investigate some of the properties of discrete-time systems, we begin by exploring some simple systems through their input-output relationships. Along the way, we will introduce a few important concepts. For example, a system with input $x[n]$ and output $y[n]$ is referred to as memoryless if the output at time n is only a function of the input $x[n]$ at the same value of n . For example, consider the following memoryless systems.

System 3.1 One example of a memoryless system is a simple amplification system, i.e. one for which the input-output relationship is given by

$$y[n] = ax[n],$$

where a is a real-valued constant.

System 3.2 Another example of a memoryless system might be as follows

$$y[n] = |x[n]|,$$

where once again, the output at time n is completely determined by the input at time n .

Systems for which the output at time n depend on more information than the current value of the input are said to have memory. We call the minimal set of information in addition to the values of the input $x[n]$, $n \geq m$ required to uniquely determine the output $y[n]$ for all time $n \geq m$ the **state** of the system. For example, in the following system, the state of the system consists of $y[n-1]$.

System 3.3 A system that has memory requires storage of the state of the system in order to compute its output. In this system, the state is one single previous value of the output.

$$y[n] = x[n] + ay[n-1].$$

System 3.4 Another example of a system with state is a simple delay.

$$y[n] = x[n - n_0].$$

here, the state of the system is the previous values of the input, $x[n-1], x[n-2], \dots, x[n-n_0]$. Storing only the single value $x[n-n_0]$ would enable us to compute only one value of $y[n]$, but if $n_0 > 1$, we would be unable to proceed further. As a result, we need to store all intervening values of $x[n]$ in order to uniquely determine $y[n]$, given only future values of the input.

3.4 Linear Systems

While there are a myriad of properties of systems that are of importance to study, perhaps the property of primary importance is ability to distinguish between linear and nonlinear systems. This is largely because some of the mathematical tools we will develop apply only to linear systems. The series of definitions below culminates in the definition of linearity.

A system satisfies the **decomposition property** if its output $y[n]$ can be written as follows

$$y[n] = y_x[n] + y_s[n],$$

where $y_x[n]$ is the response of the system due only to the input $x[n]$, while the initial conditions of the system are set to zero, i.e., all state in the system (if there is any) is set to have zero values in each position, and $y_s[n]$ is the response of the system due only to the state of the system with the input set to zero.

When the output of the system can be decomposed into these two responses, we call $y_x[n]$ the zero state response (ZSR) of the system and $y_s[n]$ the zero input response (ZIR) of the system. We first consider a property called **zero-state linearity**, which considers the input-output functionality of the system when the initial conditions, or state, of the system has been initially set to zero.

A system is **zero-state linear**, if, when the initial conditions of the system are set to zero before the input is applied, it satisfies both homogeneity and additivity, defined as follows.

A system with input $x[n]$ and output $y[n]$ satisfies **homogeneity** if for every input $x[n]$ and for every positive constant a , the following holds,

$$\text{if } x[n] \rightarrow y[n], \text{ then } ax[n] \rightarrow ay[n].$$

This is also sometimes referred to as the scaling property of systems.

A system with input $x[n]$ and output $y[n]$ satisfies **additivity**, if for every pair of inputs $x_1[n]$ and $x_2[n]$, and their corresponding outputs, $y_1[n] = T\{x_1[n]\}$ and $y_2[n] = T\{x_2[n]\}$, the following holds

$$\text{if } x_1[n] \rightarrow y_1[n] \text{ and } x_2[n] \rightarrow y_2[n], \text{ then } x_1[n] + x_2[n] \rightarrow y_1[n] + y_2[n].$$

When the two properties of homogeneity and additivity are combined into a single form, we obtain a more compact relation known as the **superposition** property of linear systems. This is summarized as follows,

A system with input $x[n]$ and output $y[n]$ satisfies **superposition** if for every pair of inputs $x_1[n]$ and $x_2[n]$, and their corresponding outputs, $y_1[n] = T\{x_1[n]\}$ and $y_2[n] = T\{x_2[n]\}$, the following holds

$$\text{if } x_1[n] \rightarrow y_1[n] \text{ and } x_2[n] \rightarrow y_2[n], \text{ then } ax_1[n] + bx_2[n] \rightarrow ay_1[n] + by_2[n],$$

for all real-valued constants a and b .

For systems that satisfy the decomposition property, we are able to set aside the response of the system to any initial conditions (or initial state of the system) and study the input-output behavior of the system due solely to the input. When the system is also **zero-input linear**, then we can extend the notions of linearity to the initial conditions of the system and the responses to these initial conditions.

A system satisfying the decomposition property with a set of N initial conditions $\{y_k[n_k] = c_k\}_{k=0}^N$ and the corresponding zero input response to these initial conditions $y_{s,1}[n]$ and a second set of N initial conditions $\{y_m[n_m] = d_m\}_{m=0}^N$ and the

corresponding zero input response to these initial conditions $y_{s,2}[n]$ is **zero-input linear** if the following holds,

if $\{y_k[n_k] = c_k\}_{k=0}^N \rightarrow y_{s,1}[n]$ and $\{y_m[n_m] = d_m\}_{m=0}^N \rightarrow y_{s,2}[n]$ then

$$\{y_k[n_k] = ac_k + bd_k\}_{k=0}^N \rightarrow ay_{s,1}[n] + by_{s,2}[n],$$

for all real-valued constants a and b .

We can now more formally define a linear system as follows.

A discrete-time system is **linear** if it satisfies the decomposition property and it is both zero-state linear and zero-input linear.

In this section we focus primarily on zero-state linearity, since the decomposition property enables us to park issues of initial conditions outside our immediate focus and return to treat them later as necessary. As we will later see, when systems are not only linear, but also stable, the steady state behavior (long term behavior) will depend little on the effects of the initial conditions, and it is precisely the input-output zero-state behavior that is often of primary interest. We continue our exploration of linear systems by considering a few examples.

Example 1 Determine whether the system described by $y[n] = |x[n]|$ is linear or nonlinear. This system satisfies neither homogeneity nor additivity and is therefore nonlinear. To prove the failure of homogeneity note that $x_1[n] = 1, \forall n$ and $x_2[n] = -1, \forall n$ produce the same output and yet $x_2[n] = -x_1[n]$. Similarly additivity fails because $x_1[n] + x_2[n]$ does not produce the sum of the outputs due to $x_1[n]$ and $x_2[n]$ acting individually.

Example 2 Consider a system described by $y[n] = [x[n-4]]^2/x[n]$. Is this system linear or nonlinear? Check homogeneity: $ax[n] \rightarrow [ax[n-4]]^2/[ax[n]] = ax[n-4]^2/x[n] = ay[n]$. So the system satisfies homogeneity. But, it looks like additivity will fail. Therefore, we must conclude that the system is not linear. Let us find an $x_1[n]$ and $x_2[n]$ to demonstrate this. Let $x_1[n] = 1, \forall n$. Then we have that

$$y_1[n] = \frac{1^2}{1} = 1, \forall n.$$

Now let $x_2[n] = (\frac{1}{2})^n, \forall n$, which gives rise to

$$y_2[n] = \frac{[(\frac{1}{2})^{n-4}]^2}{(\frac{1}{2})^n} = \frac{(\frac{1}{2})^{2n-8}}{(\frac{1}{2})^n} = 2^8(\frac{1}{2})^n, \forall n.$$

For the input $x_1[n] + x_2[n] = 1 + (\frac{1}{2})^n, \forall n$, we have

$$y[n] = \frac{[1 + (\frac{1}{2})^{n-4}]^2}{[1 + (\frac{1}{2})^n]} \neq y_1[n] + y_2[n] = 1 + 2^8(\frac{1}{2})^n, \forall n,$$

since, for $n = 4$, we have

$$y[4] = \frac{[1 + 1]^2}{[1 + (\frac{1}{2})^4]} = \frac{4}{1 + \frac{1}{16}} \neq y_1[4] + y_2[4] = 1 + 2^8(\frac{1}{2})^4 = 1 + 2^4.$$

Example 3 For the following averaging filter, we have $y[n] = \frac{1}{3}[x[n-1] + x[n] + x[n+1]]$. This is a simple example of a low-pass digital filter that could be used to smooth signals and reduce noise by replacing each sample in the output by the average of three adjacent values of the input signal. Is this system linear or nonlinear? We can seek the answer

to this by checking superposition, i.e. by checking homogeneity and additivity all at once. We have that

$$x_1[n] \rightarrow y_1[n] = \frac{1}{3}[x_1[n-1] + x_1[n] + x_1[n+1]],$$

and

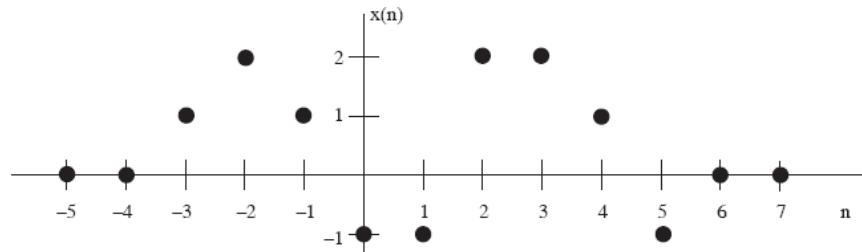
$$x_2[n] \rightarrow y_2[n] = \frac{1}{3}[x_2[n-1] + x_2[n] + x_2[n+1]].$$

Now for an input that is a linear combination, we have

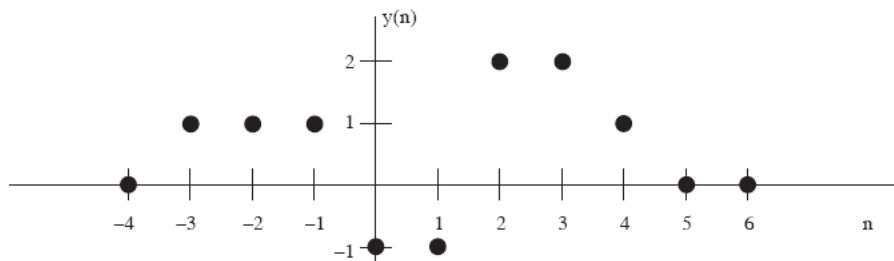
$$\begin{aligned} ax_1[n] + bx_2[n] &\rightarrow y[n] = \frac{1}{3}[(ax_1[n-1] + bx_2[n-1]) + (ax_1[n] + bx_2[n]) + (ax_1[n+1] + bx_2[n+1])] \\ &\rightarrow y[n] = a\frac{1}{3}[x_1[n-1] + x_1[n] + x_1[n+1]] + b\frac{1}{3}[x_2[n-1] + x_2[n] + x_2[n+1]] \\ &\rightarrow y[n] = ay_1[n] + by_2[n] \checkmark. \end{aligned}$$

So we have shown that the system is indeed linear, since the inputs $x_1[n]$ and $x_2[n]$ and coefficients a and b are arbitrary.

Example 4 A median filter is often used in data analysis when there may be outliers in the data, i.e. spurious samples that might be erroneous or artificially large or small, such that a local average of the data would be dominated by their magnitude. For example, we might employ the median filter $y[n] = \text{med} \{x[n-1], x[n], x[n+1]\}$. This operation would amount to looking at each value of the input sequence, and replacing each value by the middle value, in numerical order, of the current, most recent, and next, value of the input. Thus, for example, the input sequence



would produce the median filter output



Notice that for any value of n , the median filter output is always equal to one of the elements of the input sequence $\{x[n]\}_{n=-\infty}^{\infty}$. It is easy to visualize the output $\{y[n]\}_{n=-\infty}^{\infty}$ by mentally sliding a length-three window over the input sequence and then simply taking the output to be the middle element (in algebraic value) among those three input elements falling within the window. So, for example shown, $y[-2] =$

$\text{med}\{x[-3], x[-2], x[-1]\} = \text{med}\{1, 2, 1\} = 1$, and $y[1] = \text{med}\{x[0], x[1], x[2]\} = \text{med}\{-1, -1, 2\} = -1$. Is the median filter in this example linear? Owing to properties of the median, homogeneity would be satisfied, since scaling the samples in an ordered set maintains the ordering with the possibility of reversing the elements if the sign of the scale factor is negative, however this would leave the median of the scaled values equal to the scaled median of the original values. What about additivity? Perhaps we can find a simple set of two input sequences for which we can demonstrate a violation of additivity. Consider for example

$$x_1[n] = \delta[n] \text{ and } x_2[n] = \delta[n - 1],$$

for which the output of our three point local median filter would be

$$y_1[n] = 0, \forall n, \text{ and } y_2[n] = 0 \forall n,$$

however, for the sum of these two inputs, we have that

$$y[n] = T\{\delta[n] + \delta[n - 1]\} = \delta[n] + \delta[n - 1] \neq y_1[n] + y_2[n] = 0 \forall n,$$

and hence the system is not linear. Median filters are often useful in image processing, because unlike linear averaging filters, median filters can remove noise while preserving edge structure. Linear filters tend to blur edges, which is often objectionable in image processing. In the 1-D case, it is easy to see that median filters preserve edges. Consider the edge signal $x[n] = u[n]$. For this signal, the output of the median filter would be $y[n] = u[n]$, thus preserving the edge. However, consider the output of the three-point local averaging filter from example 3 above, for which the output would be $y[n] = \frac{1}{3}\delta[n + 1] + \frac{2}{3}\delta[n] + u[n - 1]$, which is a blurred version of the original edge.

Example 5 For a modulator of the form $y[n] = \cos(\omega_0 n)x[n]$, we may again check linearity directly using the superposition property. For the pair of inputs

$$x_1[n] \rightarrow y_1[n] = \cos(\omega_0 n)x_1[n] \text{ and } x_2[n] \rightarrow y_2[n] = \cos(\omega_0 n)x_2[n],$$

we have that

$$\begin{aligned} ax_1[n] + bx_2[n] &\rightarrow y[n] = \cos(\omega_0 n)(ax_1[n] + bx_2[n]) \\ &\rightarrow y[n] = a \cos(\omega_0 n)x_1[n] + b \cos(\omega_0 n)x_2[n] \\ &\rightarrow y[n] = ay_1[n] + by_2[n] \checkmark. \end{aligned}$$

So the modulator system is indeed linear.

Example 6 A linear constant-coefficient difference equation (LCCDE) is given by the following input-output relation

$$y[n] + a_1 y[n - 1] + \dots + a_N y[n - N] = b_0 x[n] + \dots + b_M x[n - M],$$

which can be more compactly written

$$y[n] + \sum_{k=1}^N a_k y[n - k] = \sum_{k=0}^M b_k x[n - k]. \quad (3.4)$$

This can be shown to be linear more easily when we have considered z-transforms later in this text, however we can show linearity with some facility with such relations. Consider the input-output pair $x_1[n] \rightarrow y_1[n]$ and the input-output pair $x_2[n] \rightarrow y_2[n]$. We have that each satisfy the LCCDE individually, i.e.

$$y_1[n] + \sum_{k=1}^N a_k y_1[n - k] = \sum_{k=0}^M b_k x_1[n - k], \text{ and } y_2[n] + \sum_{k=1}^N a_k y_2[n - k] = \sum_{k=0}^M b_k x_2[n - k].$$

Now by considering the input $x_3[n] = cx_1[n] + dx_2[n]$, we also know that the system must satisfy, by the definition of the system,

$$y_3[n] + \sum_{k=1}^N a_k y_3[n-k] = \sum_{k=0}^M b_k (cx_1[n-k] + dx_2[n-k]).$$

From the definition of the system, if we take a linear combination of the left hand side of the relations for $y_1[n]$ and $y_2[n]$, we obtain

$$\begin{aligned} c \left(y_1[n] + \sum_{k=1}^N a_k y_1[n-k] \right) + d \left(y_2[n] + \sum_{k=1}^N a_k y_2[n-k] \right) &= c \sum_{k=0}^M b_k x_1[n-k] + d \sum_{k=0}^M b_k x_2[n-k] \\ (cy_1[n] + dy_2[n]) + \sum_{k=1}^N a_k (cy_1[n-k] + dy_2[n-k]) &= \sum_{k=0}^M b_k (cx_1[n-k] + dx_2[n-k]) \\ y_3[n] + \sum_{k=1}^N a_k y_3[n-k] &= \sum_{k=0}^M b_k (cx_1[n-k] + dx_2[n-k]), \end{aligned}$$

where the last line follows from the definition of $y_3[n]$ as the response of the system to the input $x_3[n]$ and the LCCDE for the system definition. Putting these together, we have from the second and third lines above that the corresponding output $y_3[n]$ satisfies $y_3[n] = cy_1[n] + dy_2[n]$, which indeed demonstrates linearity of the LCCDE.

3.5 Shift-invariant systems

Another property that will prove immensely powerful in the analysis of discrete-time systems is that of shift-invariance. The ability to characterize the input-output behavior of discrete-time systems would be rather difficult if it were necessary to completely recharacterize the properties of the system depending on the precise time at which a given input was presented. For example, imagine how complicated it would be if every time a driver were to consider driving an automobile, that the driver would need to consult the time of day and make changes appropriately. Suppose that the steering wheel was on the left side of the car during odd-valued hours of the day, but on the right hand side of the car on even-valued hours of the day. Additionally, perhaps the gas pedal would be to the right during the first quarter hour and then in the middle during the second quarter hour, and then on the left for the remainder of the hour. The brake and clutch pedals similarly moving about might cause no end to the confusion and difficulty in vehicle operation. Needless to say, the invariance of the input-output properties of the car, i.e. the driving behavior of the car, is one of the properties of a car that enable a driver to not only operate their vehicle routinely without too much distraction, but also to enable any driver of a car to drive any other car.

A system is **shift invariant** if a shift in the input always leads to a corresponding shift in the output, i.e., the system satisfies

$$\text{if } x[n] \rightarrow y[n], \text{ then } x[n-n_0] \rightarrow y[n-n_0], \forall n_0 \text{ and } \forall x[n].$$

The systems in Examples 1, 2, 3 and 5 are shift-invariant. The system in Example 4 is shiftvarying. Proving that a discrete-time system is indeed shift-invariant or that it is shift varying can be a challenge the first time around, however if you follow the steps taken in the following example, you will come to fewer stumbling blocks. Let us first revisit Example 3.

Example 3 (revisited) For the system defined by the output relation $y[n] = \frac{1}{3}[x[n-1] + x[n] + x[n+1]]$, we consider a shifted version of the input, say, $x_0[n] = x[n-n_0]$. For this input, we can

find the corresponding output as follows

$$\begin{aligned}
 x_0[n] &\rightarrow y_0[n] = \frac{1}{3}[x_0[n-1] + x_0[n] + x_0[n+1]] \\
 &\rightarrow y_0[n] = \frac{1}{3}[x[(n-n_0)-1] + x[(n-n_0)] + x[(n-n_0)+1]] \\
 &\rightarrow y_0[n] = y[n-n_0] \checkmark
 \end{aligned}$$

where the last equality follows from the system definition. Therefore the system is shift-invariant.

Example 5 (revisited) We revisit the modulation example given by

$$y[n] = \cos(\omega_0 n)x[n]$$

and consider whether it is shift invariant or not. Let us once again let $x_0[n] = x[n-n_0]$ and consider the system response to this input, we have

$$\begin{aligned}
 y_0[n] &= \cos(\omega_0 n)x_0[n] \\
 &= \cos(\omega_0 n)x[n-n_0] \\
 &\neq y[n-n_0] = \cos(\omega_0(n-n_0))x[n-n_0],
 \end{aligned}$$

so the system is not shift invariant. Note that while the result may hold for certain values of n_0 , for example, if $\omega_0 = 2\pi/3$, then for $n_0 = 3$, the output would be equivalent to a shifted-by-three version of the input. However, for shift invariance to hold, the output must be a shifted version of the input for all possible (integer) values of n_0 . In this case, shifting the input does not shift the cosine modulation, and as a result the system is shift-varying.

3.6 Causal Systems

A system is **causal** if for every n , $y[n]$ depends only on $x[m]$, $m \leq n$. Thus, for causal systems, current outputs do not depend on future inputs. Systems that are not causal are called noncausal. For systems for which the independent variable n is indeed a time variable, noncausal systems are not physically realizable if the output $y[n]$ must be computed immediately upon acquiring $x[n]$. However, in many DSP systems, data $x[n]$ is acquired and stored before processing (e.g., stored as an image $\{x[n, m]\}$ prior to processing, as in a digital camera). These systems can be noncausal without violating any physical laws of nature. The systems in Examples 1 and 2 are causal. The systems in Examples 3 and 4 are noncausal, since they require $x[n+1]$ in order to compute the three-sample average or median, respectively. The system in Example 6 can be either causal or noncausal, depending on the “direction” in which the equation is iterated. For example, rewriting (3.4) so that $y[n-kN]$ is computed from $x[n]$ and $y[n], y[n-1], \dots, y[n-N+1]$, suggests a noncausal realization, i.e.

$$y[n-N] = \frac{1}{a_N} \left[-y[n] - \sum_{k=1}^{N-1} a_k y[n-k] + \sum_{k=0}^M b_k x[n-k] \right].$$

So an LCCDE describing the relationship between the sequences $y[n]$ and $x[n]$ can be either causal or noncausal, depending on the specific implementation of the LCCDE. Unless specified otherwise, we will typically assume that such an LCCDE corresponds to the causal implementation, i.e. the implementation for which the output $y[n]$ is computed in terms of the present and past values of the input and past values of the output, i.e. using an algorithm in the form of (3.4).

Example 7 For the following system, described by

$$y[n] = \frac{x[n]}{x[5]},$$

the system is nonlinear, shift-varying, and noncausal.

Example 8 The system described by the relation,

$$y[n] = x[-n],$$

corresponds to a time-reversal of the input. This system is linear, shift-varying, and noncausal.

Example 9 The system whose input-output relation is

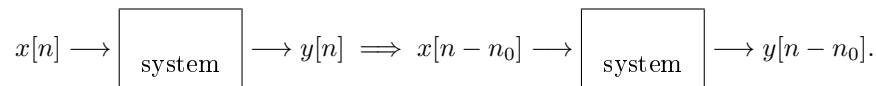
$$y[n] = x[|n|],$$

is linear, shift-varying, and noncausal.

3.7 LSI systems and convolution

We have seen that systems that are linear satisfy superposition, that is, they satisfy homogeneity (scaling) and additivity. We have also seen that systems that are shift-invariant will generate a shifted version of their output when their input is shifted accordingly. Together, these two properties make up an important class of systems that we will explore, namely, linear shift-invariant systems, or LSI systems. In many contexts, the independent variable of a sequence is referred to as time, and the term linear time invariant (LTI) is also used to describe such systems. For discrete-time sequences, we may refer to the time index of a sequence, but realize that the properties of discrete-time signals and systems hold more generally for sequences indexed on a wide variety of non-time based indexes, such as computer memory storage location, trading day in the stock market, individuals in a line of people, units of a product on an assembly line, pixels of a digital image stored in an array, antenna elements in a phased-array, and many, many more examples.

Let us return to the problem of identifying the response of a discrete-time LSI system to an arbitrary input by recalling the notion of shift-invariance in discrete-time systems. Linear, constant coefficient difference equations describe shift-invariant systems, and as such, we are particularly interested in the properties of systems that can be expressed in terms of such difference equations. Recall that when zero initial conditions are applied, i.e. when a system is initially at rest, that a system is *shift-invariant*, if the response to an input sequence $\{x[n]\}_{n=-\infty}^{\infty}$ produces the output sequence $\{y[n]\}_{n=-\infty}^{\infty}$ and for any n_0 , the response to the same input, delayed by n_0 , $\{x[n - n_0]\}_{n=-\infty}^{\infty}$ produces the same output sequence, delayed by n_0 , $\{y[n - n_0]\}_{n=-\infty}^{\infty}$. Graphically this is depicted as



These two properties, when taken together, yield the powerful relationship between the input and the output of an LSI system known as the convolution sum. In the general case, the relationship between the input and output in an LSI system is given by the convolution sum,

$$y[n] = \sum_{k=-\infty}^{\infty} x[k]h[n - k], \quad (3.5)$$

where the sequence $h[n]$ is the response of the system to the unit sample function, or discrete time impulse, $\delta[n]$. As a result, $h[n]$ is often referred to as the impulse response, or unit sample response, of the discrete-time LSI system. By making the change of variable, $m = n - k$, we obtain an equivalent form of the convolution sum,

$$y[n] = \sum_{m=-\infty}^{\infty} h[m]x[n - m] = \sum_{m=-\infty}^{\infty} x[m]h[n - m].$$

which we will write in short-hand notation as $y[n] = x[n] * h[n]$, where $h[n]$ is system unit pulse response (or impulse response) of the LSI system. This notation is somewhat an “abuse of notation”, in that the output at time n appears to depend only on the input and impulse response at time n . As shown in Equation (3.5), the output at time n actually depends on the entire input sequence and the entire impulse response

sequence. Alternative notation that would, perhaps be more explicit in showing this relationship could be $\{y[n]\}_{n=-\infty}^{\infty} = \{x[n]\}_{n=-\infty}^{\infty} * \{h[n]\}_{n=-\infty}^{\infty}$, however we will often drop this explicit sequence notation and assume that in general when we write $y[n]$, we are referring to the entire sequence, and not just the value at a given time n , unless we make this explicit from the context. A perhaps even more correct notation would note that the convolution operation in Equation (3.5) actually produces one sequence, and if we would like to refer to a given time instance of that sequence, we might write $y[n] = (x * h)[n]$, for simplicity, we will stick with the more standard, $y[n] = x[n] * h[n]$.

The convolution sum, Equation (3.5), can be shown as a consequence of the properties of linearity and shift invariance, and as a result, we could even define an LSI system as one whose input and output satisfy the convolution sum. That is,

$$y[n] = \sum_{m=-\infty}^{\infty} h[m]x[n-m] \Leftrightarrow \text{The system is LSI.}$$

The way to show this involves writing the input $x[n]$ in terms of impulses and applying both linearity and shift invariance to the resulting output. Specifically, we write the input as

$$\begin{aligned} x[n] &= \cdots + x[-1]\delta[n+1] + x[0]\delta[n] + x[1]\delta[n-1] + x[2]\delta[n-2] + \cdots \\ &= \sum_{k=-\infty}^{\infty} x[k]\delta[n-k], \end{aligned}$$

which can be viewed as a superposition of delayed and scaled discrete-time impulses, where the amplitude of each discrete-time impulse is scaled by the value of $x[n]$ at that time. In this manner, we can view the entire sequence $x[n]$ as a linear superposition of simpler sequences, where each of these simpler sequences has only one non-zero sample. The weighting in the linear superposition is simply the corresponding value of the sequence $x[n]$. We can now use linearity to write the output of an LSI system in response to the input $x[n]$ as a sum of the responses to each of the delayed and scaled impulses. Specifically, for a linear system, if we know the response to an impulse at time $n = k$, is, say $h_k[n]$, then we also know the response of the system to the input $x[k]\delta[n-k]$. By applying the homogeneity property of linear systems, we know that

$$\delta[n-k] \rightarrow h_k[n] \implies x[k]\delta[n-k] \rightarrow x[k]h_k[n].$$

Now by the additivity property of linear systems, we also can construct the response to the entire input $x[n]$, by adding up the responses to each of the simpler signals that make up the input, that is,

$$\delta[n-k] \rightarrow h_k[n] \implies \sum_{k=-\infty}^{\infty} x[k]\delta[n-k] \rightarrow \sum_{k=-\infty}^{\infty} x[k]h_k[n],$$

which corresponds to

$$x[n] \rightarrow \sum_{k=-\infty}^{\infty} x[k]h_k[n],$$

where $h_k[n]$ is the response of the linear system to a discrete-time impulse at time $n = k$. Now in order to construct the output due to an arbitrary input, we would need to know $h_k[n]$ for all possible values of k , for which the input is non-zero. This would indeed be too much information to keep track of. However, if a system is also shift-invariant, in addition to being linear, then we know that the response of the system due to an impulse at time k is just a delayed version of the response of the system due to an impulse at time 0. That is,

$$\delta[n-k] \rightarrow h_0[n-k] \triangleq h[n-k],$$

where we drop the subscript, since through shift-invariance, we have that $h_k[n] = h[n-k]$. By adding homogeneity, we have that

$$x[k]\delta[n-k] \rightarrow x[k]h[n-k],$$

for each value of k , and more generally, using superposition and the representation of $x[n]$ as a superposition of delayed and scaled discrete time impulses, that

$$x[n] = \sum_{k=-\infty}^{\infty} x[k]\delta[n-k] \rightarrow y[n] = \sum_{k=-\infty}^{\infty} x[k]h[n-k],$$

which proves the convolution sum representation of the input-output relationship for LSI systems.

3.8 Properties of DT LSI Systems

Given that we can completely express the nature of LSI systems through the convolution sum, we can now go back and see how properties of LSI systems affect the resulting convolution sum representation. As a result, we will see that we will be able to deduce properties of LSI systems directly by observing the impulse response as it appears in the convolution sum. We begin by considering the property of causality in LSI systems and consider how the convolution sum representation of a causal system may differ from that of a non-causal system.

Recall that a system is causal if for any n_0 , $y[n_0]$ depends only on $x[n]$, $n \leq n_0$. We can now relate the notion of causality to the impulse response of a LSI system by using the convolution sum representation. Starting with the convolution sum representation of $y[n_0]$,

$$y[n_0] = \sum_{k=-\infty}^{\infty} x[k]h[n_0-k],$$

we see that $y[n_0]$ depends, in general on all values of $x[n]$ such that $h[n_0-k]$ is non-zero. For the corresponding LSI system to be causal, we would require that $h[n_0-k] = 0$ for $k > n_0$. This is equivalent to requiring that $h[n] = 0$, for $n < 0$. This leads to the following property of LSI systems:

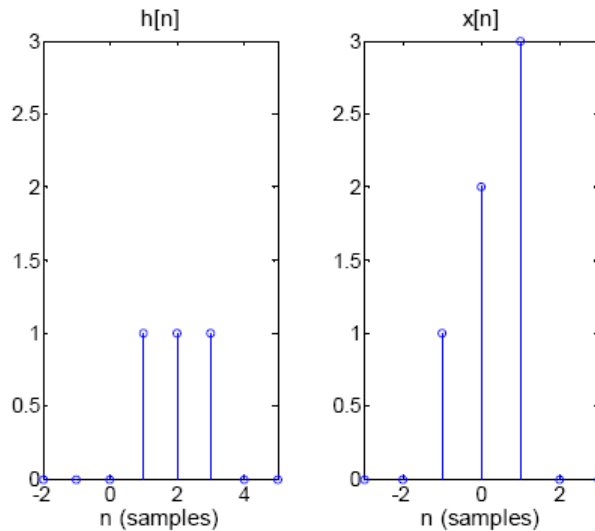
A discrete-time LSI system is causal, if and only if the impulse response satisfies $h[n] = 0$, for $n < 0$.

In this case, the convolution sum reduces to

$$y[n] = \sum_{k=0}^{\infty} h[k]x[n-k] = \sum_{k=-\infty}^n x[k]h[n-k]$$

for causal LSI systems.

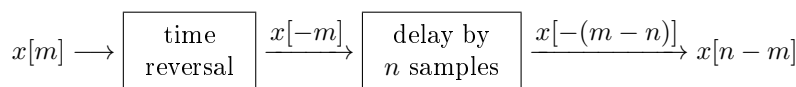
Example: Graphical View of Convolution Given the two sequences $x[n]$ and $h[n]$ shown below,



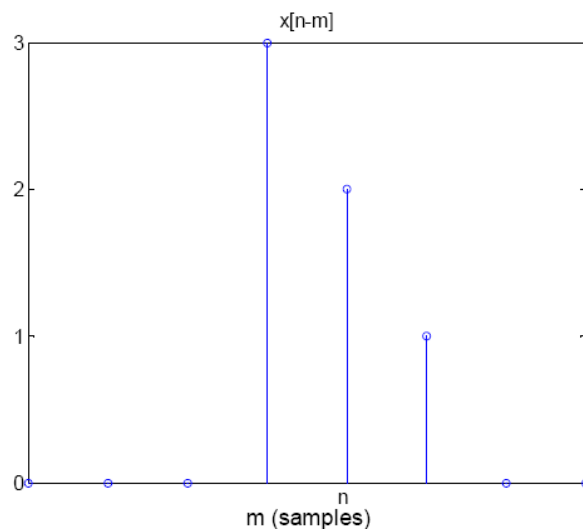
determine $x[n] * h[n]$, i.e. find

$$y[n] = \sum_{m=-\infty}^{\infty} x[m]h[n-m].$$

To do this, we will find the output one term at a time, by plotting $x[n-m]$ versus m , and then summing up the product of $h[m]$ and $x[n-m]$ over m . In order to plot $x[n-m]$ versus m , we want to view this as a sequence over m , where, here, n plays the role of a fixed shift of the sequence. So, to proceed, we first consider the sequence $x[-m]$, which is simply a time-reversed version of $x[m]$. We then desire $x[n-m] = x[-(m-n)]$, which is a shift of the sequence $x[-m]$ to the right by n samples (i.e. a delay of n samples of the time-reversed sequence $x[-m]$). In steps, this corresponds to



which for this example yields the following result,

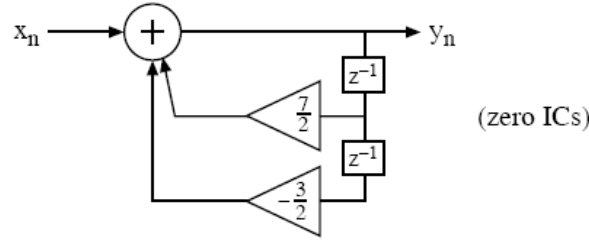


from the figure, we can see that, term by term, the output $y[n]$ can be computed as follows

$$y[n] = \begin{cases} 0, & n < 0, \\ 1 \times 1 = 1, & n = 0, \\ 2 \times 1 + 1 \times 1 = 3, & n = 1, \\ 3 \times 1 + 2 \times 1 + 1 \times 1 = 6, & n = 2, \\ 3 \times 1 + 2 \times 1 = 5, & n = 3, \\ 3 \times 1 = 3, & n = 4, \\ 0, & n > 4. \end{cases}$$

Noting from the figure that $h[n] = 0$ for $n < 0$, we expect that the output $y[n]$ will not depend on the input $x[k]$, for $k > n$, and we see that graphically, only past values of $x[n]$ contribute to the output.

Example Given the discrete-time sequence $x[n] = (1/4)^n u[n]$, determine the output of the causal discrete-time LSI system shown in the figure below.



The system in the figure is described by the following difference equation

$$y[n] = \frac{7}{2}y[n-1] - \frac{3}{2}y[n-2] + x[n]$$

or

$$y[n] - \frac{7}{2}y[n-1] + \frac{3}{2}y[n-2] = \left(\frac{1}{4}\right)^n, n \geq 0, y[-1] = y[-2] = 0.$$

We could solve this using a classical solution method for LCCDEs. However, this time, we will use the convolution formula, since this difference equation describes a LSI system, that can be characterized by its response to a discrete-time impulse, i.e., we can write

$$y[n] = \sum_{m=-\infty}^{\infty} h[m]x[n-m].$$

How do we obtain the impulse response from the given information? One way is to find $h[n]$ directly by solving an appropriate difference equation. As such, from definition of the system and that of the discrete-time impulse response, we have that $h[n]$ is defined to be the solution to the system equations when the input is a discrete-time impulse, i.e.,

$$h[n] - \frac{7}{2}h[n-1] + \frac{3}{2}h[n-2] = \delta[n], n \geq 0, h[-1] = h[-2] = 0.$$

How do we solve this difference equation? The input term has a form that changes with n . We could employ classical methods that require the selection of a particular solution, but we can sidestep this issue by noting that

$$h[n] - \frac{7}{2}h[n-1] + \frac{3}{2}h[n-2] = 0, n > 0.$$

However, now for initial conditions, we would require $h[0]$ and $h[-1]$. To find $h[0]$, we can simply use just use the system definition,

$$\begin{aligned} h[0] - \frac{7}{2}h[-1] + \frac{3}{2}h[-2] &= 1 \\ h[0] &= 1. \end{aligned}$$

Now to find $h[n]$ for $n \geq 1$, we solve

$$h[n] - \frac{7}{2}h[n-1] + \frac{3}{2}h[n-2] = 0, n \geq 1, h[0] = 1, h[-1] = 0.$$

In order to solve this equation, we use the knowledge that a homogenous LCCDE, i.e. one for which the right hand side is zero, have solutions of the form $y[n] = cz^n$, for complex numbers z . Plugging in a general solution of this form, provides

$$\begin{aligned} z^n - \frac{7}{2}z^{n-1} + \frac{3}{2}z^{n-2} &= 0 \\ z^2 - \frac{7}{2}z + \frac{3}{2} &= 0 \end{aligned}$$

where the last line is known as the characteristic equation for the homogeneous LCCDE. The roots of the characteristic equation are given by

$$z = \frac{1}{2}, z = 3.$$

This implies that the impulse response takes the form

$$h[n] = c_1 \left(\frac{1}{2}\right)^n + c_2 3^n.$$

By applying the initial conditions, we can solve for the unknown constants c_1 and c_2 . This yields,

$$\begin{aligned} h[0] &= 1 = c_1 + c_2 \\ h[-1] &= 0 = 2c_1 + \frac{1}{3}c_2 \end{aligned}$$

which we can solve to obtain

$$c_1 = -\frac{1}{5}, \text{ and } c_2 = \frac{6}{5}.$$

This implies that $h[n]$ is given by

$$h[n] = -\frac{1}{5} \left(\frac{1}{2}\right)^n + \frac{6}{5}(3)^n, n \geq 0.$$

We know that $h[n] = 0$ for $n < 0$ from the initial conditions, so we have

$$h[n] = \left[-\frac{1}{5} \left(\frac{1}{2}\right)^n + \frac{6}{5}(3)^n \right] u[n].$$

Now, for the convolution sum, we have

$$\begin{aligned} y[n] &= \sum_{k=-\infty}^{\infty} h[k]x[n-k] \\ &= \sum_{k=-\infty}^{\infty} \left[-\frac{1}{5} \left(\frac{1}{2}\right)^k + \frac{6}{5}(3)^k \right] u[k] \left(\frac{1}{4}\right)^{n-k} u[n-k]. \end{aligned}$$

Since the term $u[k]$ is inside the summation, we can replace the lower limit in the sum to obtain,

$$y[n] = \sum_{k=0}^{\infty} \left[-\frac{1}{5} \left(\frac{1}{2}\right)^k + \frac{6}{5}(3)^k \right] \left(\frac{1}{4}\right)^{n-k} u[n-k].$$

Note that the term $u[n-k]$ is zero for $k > n$, which leads to

$$y[n] = \sum_{k=0}^n \left[-\frac{1}{5} \left(\frac{1}{2}\right)^k + \frac{6}{5}(3)^k \right] u[k] \left(\frac{1}{4}\right)^{n-k}.$$

Now, we can also note that the summation index is k , and that the term $(1/4)^n$ inside the sum does not need to be there, so we can invite it out front, to leave only terms depending on k inside the summation, leading to

$$y[n] = \left(\frac{1}{4}\right)^n \sum_{k=0}^n \left[-\frac{1}{5} \left(\frac{1}{2}\right)^k + \frac{6}{5}(3)^k \right] \left(\frac{1}{4}\right)^{-k}.$$

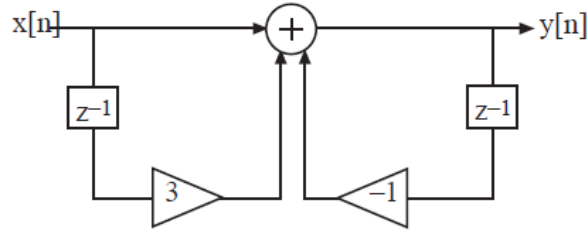


Figure 3.15: Example discrete-time linear, shift invariant (LSI) system. The elements labeled with z^{-1} correspond to delay elements.

We can now take each of the remaining finite-length geometric sums one at a time,

$$\begin{aligned}
 y[n] &= -\frac{1}{5} \left(\frac{1}{4}\right)^n \sum_{k=0}^n (2)^k + \frac{6}{5} \left(\frac{1}{4}\right)^n \sum_{k=0}^n (12)^k \\
 &= -\frac{1}{5} \left(\frac{1}{4}\right)^n \frac{1-2^{n+1}}{1-2} + \frac{6}{5} \left(\frac{1}{4}\right)^n \frac{1-12^{n+1}}{1-12} \\
 &= \frac{1}{5} \left(\frac{1}{4}\right)^n (1-2^{n+1}) + -\frac{6}{55} \left(\frac{1}{4}\right)^n (1-12^{n+1}) \\
 &= \frac{1}{5} \left(\frac{1}{4}\right)^n - \frac{2}{5} \left(\frac{1}{2}\right)^n + -\frac{6}{55} \left(\frac{1}{4}\right)^n - \frac{72}{55} (3)^n \\
 &= \frac{1}{11} \left(\frac{1}{4}\right)^n - \frac{2}{5} \left(\frac{1}{2}\right)^n + \frac{72}{55} (3)^n, n \geq 0.
 \end{aligned}$$

While it took quite a bit of work to find $h[n]$, once $h[n]$ was known, the output due to any input could be found via the convolution formula. This is one of the key properties of linear, shift invariant systems that make them attractive for analysis and implementation. We can always implement an LSI system by directly implementing the convolution sum. This may not be the most efficient implementation, for example, if the system is described by a low-order difference equation, but it will always work. We will later develop an easier way to find $h[n]$ using the z-transform.

3.8.1 Convolution and the unit pulse response (impulse response)

We continue by considering another example system, as shown in Figure 3.15.

The output of this system is given by the relation

$$y[n] = -y[n-1] + x[n] + 3x[n-1].$$

When the input to the system is a discrete-time impulse, $x[n] = \delta[n]$, when the system has zero initial conditions, we have

$$h[n] = -h[n-1] + \delta[n] + 3\delta[n-1], \quad n \geq 0, h[-1] = 0.$$

We can use the initial rest condition, i.e. $h[-1] = 0$, to shift the equation two samples forward to obtain,

$$h[n] + h[n-1] = 0, \quad n \geq 2.$$

From the initial condition, we have

$$h[0] = -h[-1] + \delta[0] + 3\delta[-1] = 1,$$

and we also have

$$h[1] = -h[0] + \delta[1] + 3\delta[0] = 2.$$

Then for $n \geq 2$, we have to solve a simpler, homogeneous difference equation of the form

$$h[n] + h[n-1] = 0, \quad n \geq 2, \quad h[1] = 2.$$

We saw previously, that the natural form of a solution to a linear constant-coefficient homogeneous difference equation takes the form cz^n for (possibly complex) constants c and z . Substituting this form into the difference equation and factoring out the common terms, yields the characteristic equation,

$$z + 1 = 0,$$

which has the solution,

$$z = -1.$$

Therefore, the solution to the homogeneous difference equation is

$$h[n] = c(-1)^n, \quad n \geq 2,$$

where we can select the term c based on the condition that $h[1] = 2$, this yields

$$h[1] = c(-1) = 2 \implies c = -2.$$

Finally we have that

$$h[n] = -2(-1)^n, \quad n \geq 1, \quad h[0] = 1.$$

We have that $h[n] = 0, n < 0$, since we assumed the system started with zero initial state prior to the input. The net result for the discrete-time impulse response is

$$h[n] = \begin{cases} 0, & n < 0, \\ 1, & n = 0, \\ -2(-1)^n & n \geq 1. \end{cases}$$

The approach to discrete-time convolution is similar to that of continuous-time convolution, with the exception that summations are used, rather than integration. We will illustrate the basic mechanics of discrete-time convolution through several examples.

Example Consider a system with impulse response $h[n] = (1/4)^n u[n]$ and input $x[n] = u[n-7]$. Let us determine the output of this system that would be obtained through the convolution sum

$$y[n] = \sum_{k=-\infty}^{\infty} h[k]x[n-k],$$

which we recall involves flipping the time axis of the input to produce $x[-k]$, then sliding this flipped version along to line up with a particular time sample in the impulse response $h[k]$, such that we have $x[n-k]$, and then taking the pointwise product $h[k]x[n-k]$, and summing the result, to provide the single output $y[n]$. If you are wondering why this process involves flipping the time axis of the input, let us consider the difference between how signals are plotted (for example, in a text like this one) and how they appear in time. When we plot a signal in a text, we typically place the first samples of the signal to the left and let the time axis increase to the right. However, with $x[n]$ plotted in this manner it appears as if we would have the largest values of the time axis (and hence the last values of the input) appearing first at the input to the system. Since for a signal that has its first non-zero value at $n = 0$, this is precisely why we need to flip the time axis of $x[n]$ as a first step in performing convolution graphically.

Returning to the example, we have for the output

$$y[n] = \sum_{k=-\infty}^{\infty} h[k]x[n-k],$$

that we can interpret graphically, by plotting, for each value of n , the sequence $h[k]$ and the sequence $x[n-k]$. It is important to note that we seek a particular value of the output, $y[n]$, that is, we seek the output at time

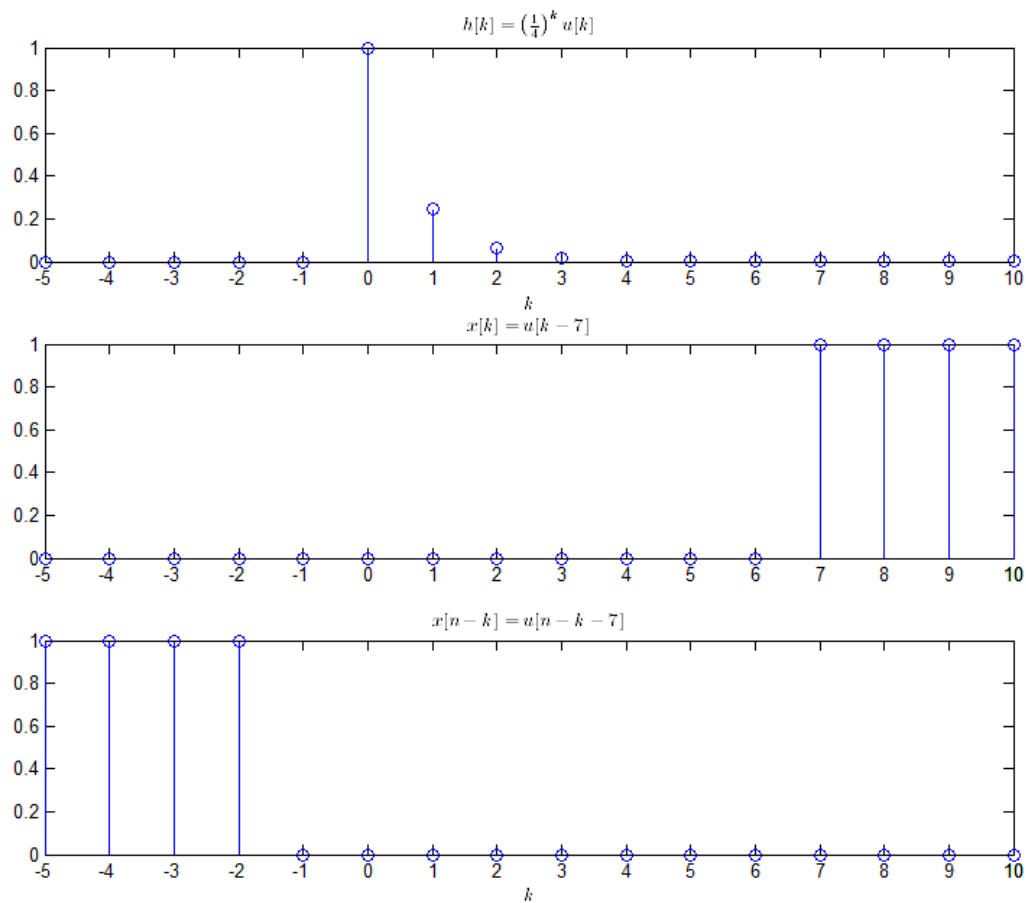


Figure 3.16: The sequences $h[k] = (1/4)^k u[k]$, $x[k] = u[k - 7]$, and $x[n - k]$, for $n = -2$, as they participate in the convolution $y[n] = \sum_{k=-\infty}^{\infty} h[k]x[n - k]$.

n . As a result, and to match the notation of the summation, we will graphically depict the sequences $h[k]$ and $x[n-k]$ as a function of the independent variable k . In this context, $x[n-k]$ corresponds to $x[-(k-n)]$, that is, the sequence $x[k]$ is flipped in time so that the sequence values are reversed with respect to the k axis, and then it is shifted so that the value of $x[0]$ sits on top of the time index $k = n$. Graphically, for the example above, we have the sequences as shown in Figure 3.16.

First we proceed with the convolution using the information provided by inspecting the signals graphically. We can observe from the plots of $h[k]$ and $x[n-k]$ that there will be no overlap of non-zero terms whenever the entire sequence $x[n-k]$ lies entirely to the left of $h[k]$. This will occur whenever we have $n-7 < 0$ or equivalently, whenever $n < 7$. Hence, we have

$$y[n] = 0, \quad n < 7.$$

For $n \geq 7$, we have at least one non-zero term of overlap and we can readily compute the output as

$$\begin{aligned} y[n] &= \sum_{k=0}^{n-7} \left(\frac{1}{4}\right)^k = \frac{1 - \left(\frac{1}{4}\right)^{n-7+1}}{1 - \frac{1}{4}} \\ &= \frac{4}{3} - \frac{4}{3} \left(\frac{1}{4}\right)^{n-6}, \quad n \geq 7. \end{aligned}$$

This process can also be observed from a purely mathematical (algebraic) perspective. Beginning with the expression for the output from the convolution sum, we have

$$\begin{aligned} y[n] &= \sum_{k=-\infty}^{\infty} h[k]x[n-k] \\ &= \sum_{k=-\infty}^{\infty} \left(\frac{1}{4}\right)^k u[k]u[(n-k)-7] \\ &= \sum_{k=0}^{\infty} \left(\frac{1}{4}\right)^k u[(n-k)-7] \\ &= \sum_{k=0}^{n-7} \left(\frac{1}{4}\right)^k \\ &= \begin{cases} 0, & n < 7 \\ \frac{4}{3} - \frac{4}{3} \left(\frac{1}{4}\right)^{n-6}, & n \geq 7. \end{cases} \end{aligned}$$

Taking a purely mathematical viewpoint, we began above with the definition of the output in terms of the convolution sum. The second line follows by expressing $h[k]$ and $x[n-k]$ in functional form. The third line follows from noting that $u[k] = 0$, for $k < 0$, and therefore the infinite sum will have no contribution for $k < 0$. The fourth line follows from a similar argument by noting that $u[n-k-7] = 0$ when $n-k-7 < 0$ which holds when $n-7 < k$; therefore, there will be no contribution to the infinite sum for values of $k > n-7$. Having established the limits to the summation first, we now have precisely the same form for the summation that we had in the graphical approach. Now we have one more issue to contend with. From the way that we arranged the limits of the summation, it is clear that whenever the term $u[k]u[n-k-7]$ is zero, there will be no contribution to the sum. Therefore, when the lower limit of the sum is greater than the upper limit of the sum, i.e. when $0 > n-7$ or $n < 7$, the output will be zero. This is the first term in the last line above, and the last term arises from summation of the finite-length geometric series. These simple steps will go a long way in either graphically, or algebraically computing convolutions with geometric terms containing unit step sequences.

Example We consider another, slightly more complicated example next. We consider the output $y[n]$ when the input is given by $x[n] = \left(\frac{1}{2}\right)^n u[n]$ and the impulse response is given by $h[n] = \left(\frac{1}{4}\right)^n u[n]$. Setting up the convolution sum, we have

$$y[n] = \sum_{k=-\infty}^{\infty} \left(\frac{1}{4}\right)^k u[k] \left(\frac{1}{2}\right)^{n-k} u[n-k].$$

This time we will proceed algebraically first, then graphically. Following the steps outlined in the previous example, we first use the unit step inside the infinite summation to determine the limits of the sum.

$$\begin{aligned} y[n] &= \sum_{k=-\infty}^{\infty} \left(\frac{1}{4}\right)^k u[k] \left(\frac{1}{2}\right)^{n-k} u[n-k] \\ &= \sum_{k=0}^n \left(\frac{1}{4}\right)^k \left(\frac{1}{2}\right)^{n-k}, \end{aligned}$$

where we again used that $u[k] = 0$ for negative k and that $u[n-k]$ is zero for $k > n$. Combining terms, and factoring out terms that do not depend on k , we obtain

$$\begin{aligned} y[n] &= \left(\frac{1}{2}\right)^n \sum_{k=0}^n \left(\frac{1}{4}\right)^k \left(\frac{1}{2}\right)^{-k} \\ &= \left(\frac{1}{2}\right)^n \sum_{k=0}^n \left(\frac{1}{2}\right)^k \\ &= \begin{cases} 0, & n < 0 \\ \left(\frac{1}{2}\right)^n \frac{1 - \left(\frac{1}{2}\right)^{n+1}}{1 - \frac{1}{2}}, & n \geq 0 \end{cases} \\ &= \begin{cases} 0, & n < 0 \\ \left(\frac{1}{2}\right)^{n-1} - \left(\frac{1}{4}\right)^n, & n \geq 0. \end{cases} \end{aligned}$$

This algebraic approach proceeded simply using the rules outlined above for determining limits of the convolution sum using the non-zero overlap regions of the unit step functions. These can also be determined graphically, by observing the sequence $h[k]$ and $x[n-k]$ graphically on similar axes as shown in Figure 3.17. It is clear from the figure, that for $n < 0$, there will be no overlap in the two sequences, while for $n \geq 0$, the result will be a finite-length sum (growing with n) that arises from the product of two geometric terms. The result is the algebraic sum we have just solved.

Example We now consider a finite-length input to an LSI system with an infinite-length impulse response. We want to determine the output $y[n]$ when the input is $x[n] = u[n] - u[n-N]$, for some $N > 0$, and the impulse response is given by $h[n] = a^n u[n]$. We will solve for the result in terms of N and a in general form. We begin again with the convolution sum,

$$\begin{aligned} y[n] &= \sum_{k=-\infty}^{\infty} h[k] x[n-k] \\ &= \sum_{k=-\infty}^{\infty} a^k u[k] (u[n-k] - u[n-k-N]) \\ &= \sum_{k=0}^{\infty} a^k (u[n-k] - u[n-k-N]). \end{aligned}$$

At this point, there are a few ways to proceed. We could either break this sum into two sums, which would provide

$$\begin{aligned} y[n] &= \sum_{k=0}^{\infty} a^k u[n-k] - \sum_{k=0}^{\infty} a^k u[n-k-N] \\ &= \sum_{k=0}^n a^k u[n-k] - \sum_{k=0}^{n-N} a^k u[n-k-N] \\ &= \frac{1 - a^{n+1}}{1 - a} u[n] - \frac{1 - a^{n-N+1}}{1 - a} u[n-N], \end{aligned}$$

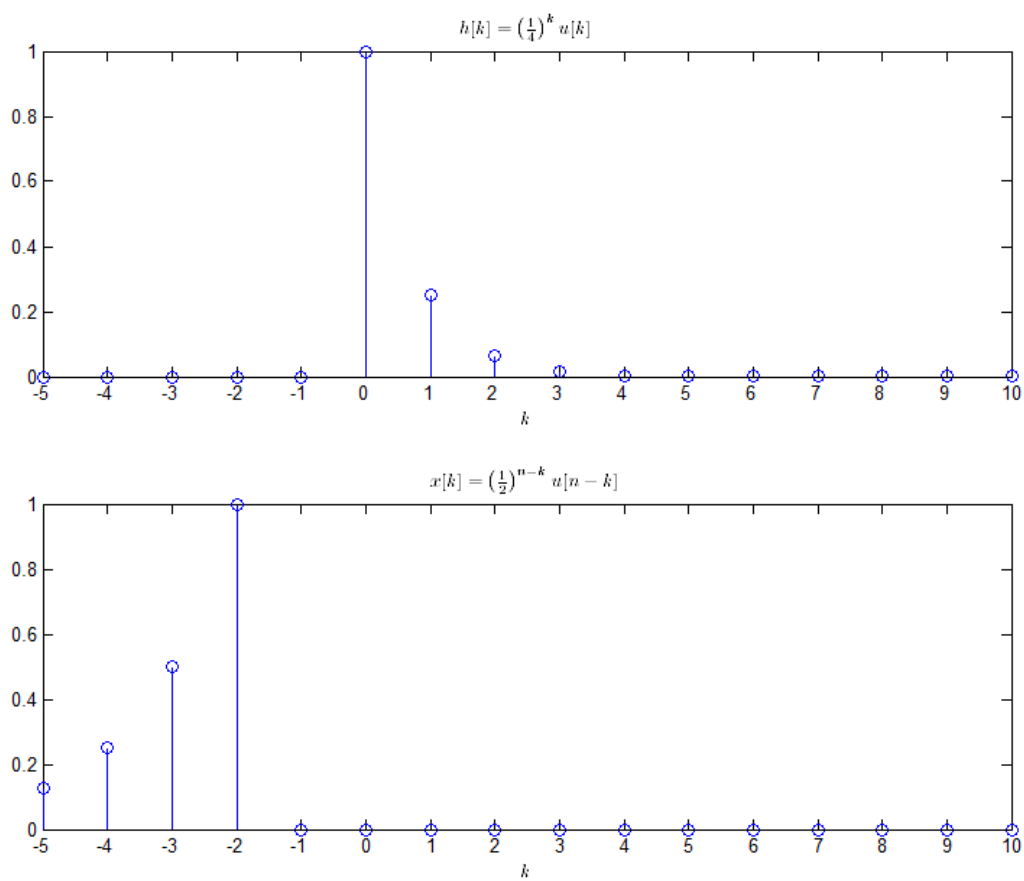


Figure 3.17: Sequences $h[k]$ and $x[n - k]$ shown for $n = -2$.

or we could have recognized that there will be three regions of interest: $n < 0$, $0 \leq n < N$, and $n \geq N$. This would have led us to evaluate on the the first term in the sum above for values of $0 \leq n < N$, and then introduced the second sum for $n \geq N$ which would enable use to combine the two algebraic expressions in each of these two regions. Sometimes this is a simpler approach, sometimes the purely algebraic approach is simpler. The results will always be the same in the end, if the calculations are carried out carefully.

Example We now consider a more complicated example with a two-sided convolution. Let the input signal $x[n]$ be given by $x[n] = (\frac{1}{3})^n u[n] + 4^n u[-n-1]$, which is a two-sided sequence, and let the impulse response be $h[n] = u[n-1]$. We will tackle this example using the mathematical approach described above. First, we write the output $y[n]$ in terms if of the two signals, i.e.

$$\begin{aligned}
 y[n] &= \sum_{k=-\infty}^{\infty} \left[\left(\frac{1}{3} \right)^k u[k] + 4^k u[-k-1] \right] u[n-k-1] \\
 &= \sum_{k=-\infty}^{\infty} \left[\left(\frac{1}{3} \right)^k u[k] + 4^k u[-k-1] \right] u[n-k-1] \\
 &= \sum_{k=-\infty}^{n-1} \left(\frac{1}{3} \right)^k u[k] + \sum_{k=-\infty}^{\infty} 4^k u[-k-1] u[n-k-1] \\
 &= \sum_{k=0}^{n-1} \left(\frac{1}{3} \right)^k + \sum_{k=-\infty}^{\infty} 4^k u[-k-1] u[n-k-1] \\
 &= \frac{1 - (\frac{1}{3})^n}{1 - \frac{1}{3}} u[n-1] + \sum_{m=-\infty}^{\infty} 4^{-m} u[m-1] u[m+n-1]
 \end{aligned}$$

where we have taken care of the first term through methods just like the previous example. We used the term $u[k]$ in the summation to eliminate values of k from the summation for $k < 0$ and we used the term $u[n-k-1]$ to eliminate terms from the summation for values of $k > n-1$. In the second summation above, in the last line, we have made the substitution $m = -k$ to help us handle the product $u[m-1]u[m+n-1]$, which will take some care to work through. Since each of these terms is of the form $u[n-N]$ for some N , then each is a right-sided unit step sequence, i.e., each is zero for $m < N$, for some N and then one for all $m \geq N$. Therefore, when you multiply them you obtain $u[m-N_1]u[m-N_2] = u[m - \max(N_1, N_2)]$. We next note that $u[m-1]$ is equal to zero for values of $m < 1$, i.e. $N_1 = 1$. Next, we note that $u[m+n-1] = u[m-(1-n)]$ is equal to zero for values of $m < 1-n$, i.e. $N_2 = 1-n$. So, since the summation will start at either $m = 0$ or at $m = 1-n$, we need to determine which of these terms wins out, i.e. we need to find $N = \max(1, 1-n)$. We see that when $n \geq 1$, we have $u[m-1]u[m+n-1] = u[m-1]$ (the sum starts at $m = 1$) and when $n < 1$, we have that $u[m-1]u[m+n-1] = u[m+n-1]$, i.e. the sum starts at $m = 1-n$. We can now

proceed, setting

$$\begin{aligned}
&= y[n] = \frac{1 - (\frac{1}{3})^n}{\frac{2}{3}} u[n-1] + \sum_{m=-\infty}^{\max(1, 1-n)} 4^{-m} u[m-1] u[m+n-1] \\
&= \frac{3 - (\frac{1}{3})^{n-1}}{2} u[n-1] + \begin{cases} \sum_{m=1}^{\infty} 4^{-m}, & n \geq 1 \\ \sum_{m=1-n}^{\infty} 4^{-m} & n < 1 \end{cases} \\
&= \frac{3 - (\frac{1}{3})^{n-1}}{2} u[n-1] + \begin{cases} \frac{\frac{1}{4}}{1 - \frac{1}{4}}, & n \geq 1 \\ \frac{4^{-(1-n)}}{1 - \frac{1}{4}} & n < 1 \end{cases} \\
&= \frac{3 - (\frac{1}{3})^{n-1}}{2} u[n-1] + \begin{cases} \frac{1}{3}, & n \geq 1 \\ \frac{4^n}{3} & n < 1 \end{cases} \\
&= \left(\frac{3}{2} + \frac{1}{3} - \frac{1}{2} \left(\frac{1}{3} \right)^{n-1} \right) u[n-1] + \frac{1}{3} 4^n u[1-n] \\
&= \left(\frac{11}{6} - \frac{1}{2} \left(\frac{1}{3} \right)^{n-1} \right) u[n-1] + \frac{1}{3} 4^n u[1-n].
\end{aligned}$$

3.9 Difference equations

Recall from (3.4) that a linear constant-coefficient difference equation (LCCDE) is given by the following input-output relation

$$y[n] + a_1 y[n-1] + \dots a_N y[n-N] = b_0 x[n] + \dots b_M x[n-M],$$

which can be more compactly written

$$y[n] + \sum_{k=1}^N a_k y[n-k] = \sum_{k=0}^M b_k x[n-k].$$

This is an input-output relationship between the input $x[n]$ and the output $y[n]$ that is both linear and shift-invariant. We note that the difference equation alone does not uniquely characterize the output $y[n]$ for a given $x[n]$, since the LCCDE depends on values of the output that occur either prior to the input, or after the input has terminated. If we consider a causal system described by an LCCDE, then we know that the output $y[n]$ for $n \geq m$ cannot depend on values of the input $x[n]$ for $n > m$. Therefore, if the input $x[n]$ is zero for $n < 0$, in order to determine the output $y[n]$, we need some auxilliary conditions, i.e. initial conditions $y[-k]$, $k = 1, \dots, N$. Since the system is LSI, we know that we can always decompose the output into the sum of two components, $y[n] = y_x[n] + y_s[n]$, i.e. that contribution to the outout from the input when the initial conditions are set to zero, $y_x[n]$, and the contribution to the output due only to the initial conditions (or the initial state of the system), when the input is set to zero, $y_s[n]$. We will see later in this text how to readily handle such situations using the one-sided (unilateral) z-transform. We note that it is also possible to directly find the solution for the output of an LCCDE given the input and initial conditions by solving the homogenous equation, as was done in a previous example, where we obtained the characteristic equation by setting the input to zero, and then adding in a particular solution that is matched to the form of the input. Then, since the homogenous equation leaves the right hand side of the LCCDE equal to zero, we can then use undetermined constants from the homogeneous solution to match the initial conditions.

When the initial conditions are set to zero, another method for finding the output of an LCCDE for a given input would be to solve for the homogeneous solution using the characteristic equation as before, but then use the implied initial conditions that result from application of a discrete-time impulse as input. We can then use the undetermined coefficients from the homogenous solution to find the response of the system to a discrete-time impulse, or, the impulse response of the system. Then, for any given input, we can find the output using convolution methods, as described earlier in this chapter.

Chapter 4

z-transform

4.1 The z-transform of sequences

Laplace transforms are used extensively to analyze continuous-time (analog) signals as well as systems that process continuous-time signals. As you may recall, the role of the Laplace transform was to represent a large class of continuous-time signals as a superposition of many simpler signals, sometimes called “basis functions” or “kernels”. For the Laplace transform, the kernels were complex exponential signals of the form, e^{st} , and we represented signals for which the Laplace transform existed according to the formula

$$x(t) = \frac{1}{2\pi j} \oint_C X(s) e^{st} ds,$$

where the integral is taken as a line integral along a suitable closed contour C in the complex plane. While the integral form of the inverse Laplace transform can be a powerful tool in the analysis of continuous-time signals and systems, we can often avoid its direct evaluation by algebraically manipulating the expression for $X(s)$ such that it can be represented as a sum of terms, each of which can be immediately recognized as the Laplace transform of a known signal $x(t)$. Then, using linearity of the Laplace transform, we can construct the inverse transform, term by term. We can view the inverse Laplace transform as a way of constructing $x(t)$, piece by piece, from many (an uncountably infinite number, actually) simpler signals of the form e^{st} , where the amount of each such signal contained in the signal $x(t)$ is given by $X(s)ds$. To determine how much of each complex exponential signal e^{st} is contained in $x(t)$, we have the Laplace transform formula given by

$$X(s) = \int_{-\infty}^{\infty} x(t) e^{-st} dt.$$

For signals that are zero, for negative time, this integral can be taken over positive time, giving the one-sided, or unilateral Laplace transform,

$$X(s) = \int_0^{\infty} x(t) e^{-st} dt.$$

For many linear time-invariant (LTI) continuous-time systems, the relationship between the input and output signals can be expressed in terms of linear constant coefficient differential equations. The one-sided Laplace transform can be a useful tool for solving these differential equations. For such systems, the Laplace transform of the input signal and that of the output signal can be expressed in terms of a “transfer function” or “system function.” In fact, many of the properties, such as causality or stability, of LTI systems can be conveniently explored by considering the system function of the continuous-time system. Another helpful property of the Laplace transform is that it maps the convolution relationship between the input and output signals in the time domain to a conceptually simpler multiplicative relationship. In this form, LTI systems can be thought of in terms of how they change the magnitude and phase of each of the kernel signals e^{st} individually, and then the output of the system is given by a superposition of each of these scaled kernel signals.

For discrete-time signals, we will see that an analogous relationship can be developed between signals and systems using the z-transform. The discrete-time complex exponential signal, z^n , where z is a complex number, plays a similar role to the continuous-time complex exponential signal e^{st} . We have already seen that discrete-time signals of this form play an important role in the analysis of linear, constant coefficient difference equations (LCCDEs), through their aid in developing the characteristic equation and finding solutions to homogenous LCCDEs. There is great elegance in the mathematics linking discrete-time signals and systems through the z-transform and we could delve deeply into this theory, devoting much more time than we will be able to here. While our treatment of the z-transform will be limited in scope, we will see that it is an equally valuable tool for the analysis of discrete-time signals and systems. We will use the z-transform to solve linear constant-coefficient difference equations, as well as develop the notion of discrete-time transfer functions. We can then use it to readily compute convolution and to analyze properties of discrete-time linear shift-invariant systems.

We note that as with the Laplace transform, the z-transform is a function of a complex variable. The transform itself can also take on complex values. As a result, it is a complex function of a complex variable.

4.2 Unilateral (one-sided) z-transform

Now, we will begin our study of the z-transform by first considering the one-sided, or unilateral, version of the transform. The unilateral z-transform of a sequence $\{x[n]\}_{n=-\infty}^{\infty}$ is given by the sum

$$X(z) = \sum_{n=0}^{\infty} x[n]z^{-n} \quad (4.1)$$

for all z such that (4.1) converges. Here, z is a complex variable and the set of values of z for which the sum (4.1) converges is called the region of convergence (ROC) of the z-transform. The z-transform maps sequences to functions and their associated region of convergence, such that $X(z)$ is the z-transform of the sequence $\{x[n]\}_{n=0}^{\infty}$. When it is clear that we are discussing sequences defined for non-negative values of the independent “time” axis, or n -axis, we will write $x[n]$ simply, and omit the brace notation $\{ \}_{n=0}^{\infty}$ indicating the positive n axis. The sequences for which the z-transform is defined can be real-valued, or complex valued. Note that the summation (4.1) multiplies $x[n]$ by a complex geometric sequence of the form z^{-n} , such that the series will converge whenever $|x[n]|$ grows no faster than exponentially. The region of convergence will be all z such that the geometrically-weighted series (4.1) converges. This region will be all values of z outside of some circle in the complex z -plane of radius R , the “radius of convergence” for the series (4.1) as depicted in Figure (4.1).

When we call $X(z)$ the transform of the sequence $\{x[n]\}_{n=0}^{\infty}$, we imply a form of uniqueness for the z-transform. Namely, we imply that for a given sequence $\{x[n]\}_{n=0}^{\infty}$, there exists one and only one z-transform $X(z)$ and its associated region of convergence. Similarly, for a given z-transform $X(z)$, there exists one and only one sequence $\{x[n]\}_{n=0}^{\infty}$ for which the series in (4.1) converges for $|z| > R$. The uniqueness for the z-transform derives from properties of power series expansions of complex functions of complex variables.

Example Consider the sequence $x[n] = 2^n$, defined for non-negative n as shown in Figure .

This discrete-time sequence has a z-transform given by

$$X(z) = \sum_{n=0}^{\infty} 2^n z^{-n},$$

which can be re-written as

$$X(z) = \sum_{n=0}^{\infty} \left(\frac{2}{z}\right)^n.$$

To determine the region of convergence of this z-transform, we simply need to consider the values of z for which the power series converges. This can be accomplished by recalling the method for summing an infinite geometric series. Recall that for a series of the form

$$S = \sum_{n=0}^{\infty} a^n$$

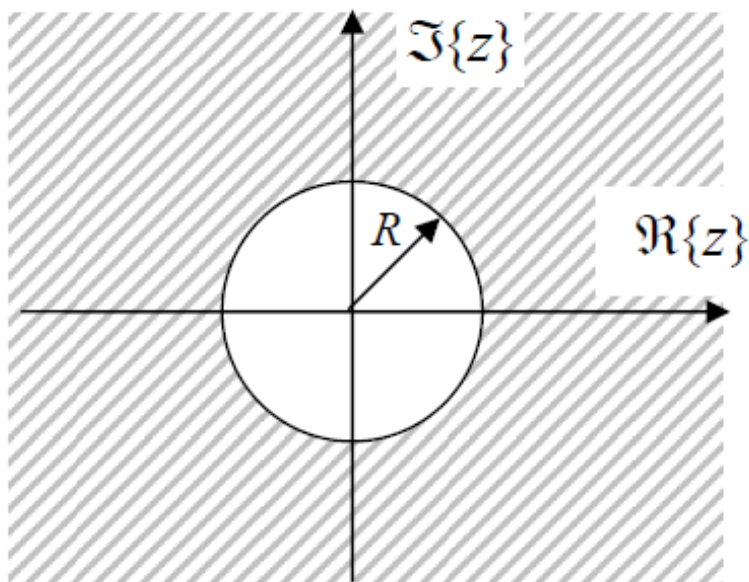


Figure 4.1: A typical region of convergence (ROC) for a unilateral z-transform. The radius of convergence, R , is shown and the ROC is all values of z such that $|z| > R$.

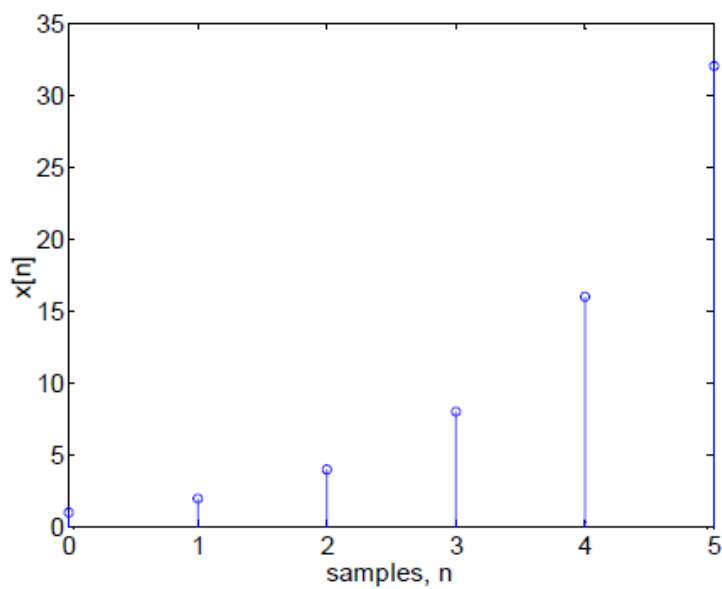


Figure 4.2: Discrete time sequence $x[n] = 2^n$ for $n \geq 0$.

where a is a complex number, we note that this is really shorthand notation for the limit

$$S = \lim_{N \rightarrow \infty} S_N = \lim_{N \rightarrow \infty} \sum_{n=0}^N a^n.$$

For the finite geometric series defining S_N , we write

$$S_N = (1 + a + a^2 + \dots + a^N).$$

Since this is a finite series, we can multiply both sides by a to obtain

$$aS_N = (a + a^2 + \dots + a^N + a^{N+1}).$$

Subtracting, we obtain

$$\begin{aligned} S_N - aS_N &= (1 - a^{N+1}) \\ S_N(1 - a) &= (1 - a^{N+1}). \end{aligned}$$

Now, if $a = 1$, we know that $S_N = N + 1$. When $a \neq 1$, can divide both sides by $(1 - a)$ to obtain

$$S_N = \frac{1 - a^{N+1}}{1 - a}$$

which is valid for all $a \neq 1$. Returning to the definition of S , we have that

$$S = \lim_{N \rightarrow \infty} S_N = \lim_{N \rightarrow \infty} \frac{1 - a^{N+1}}{1 - a},$$

which will only be finite when $|a| < 1$, for which we have

$$S = \frac{1}{1 - a}.$$

This is a special case of the series

$$\begin{aligned} S &= \sum_{n=N_1}^{N_2} a^n = (a^{N_1} + a^{N_1+1} + \dots + a^{N_2}) \\ aS &= (a^{N_1+1} + a^{N_1+2} + \dots + a^{N_2} + a^{N_2+1}), \end{aligned}$$

leading to

$$S(1 - a) = (a^{N_1} - a^{N_2+1})$$

or

$$S = \frac{a^{N_1} - a^{N_2+1}}{1 - a}$$

so long as $a \neq 1$. Note that this holds even for values of a that have magnitude greater than one. When $N_2 = \infty$, we may consider

$$\lim_{N_2 \rightarrow \infty} S = \lim_{N_2 \rightarrow \infty} \frac{a^{N_1} - a^{N_2+1}}{1 - a} = \frac{a^{N_1}}{1 - a},$$

so long as $|a| < 1$. When $N_1 = 0$, this takes the form $S = \frac{1}{1-a}$ seen above. To summarize, we have seen that

$$\boxed{\sum_{n=N_1}^{N_2} a^n = \frac{a^{N_1} - a^{N_2+1}}{1 - a}, \quad \text{for } a \neq 1} \quad (4.2)$$

and

$$\boxed{\sum_{n=N_1}^{\infty} a^n = \frac{a^{N_1}}{1 - a}, \quad \text{for } |a| < 1.} \quad (4.3)$$

Now returning to our example, for $x[n] = 2^n$, $n \geq 0$, let us find the ROC for $X(z)$, the z-transform of $x[n]$. Is $z = 1$ in the ROC of $X(z)$? Is $z = 3$ in the ROC? First consider $z = 1$.

$$\begin{aligned} X(1) &= \sum_{n=0}^{\infty} 2^n 1^{-n} \\ &= \sum_{n=0}^{\infty} 2^n, \end{aligned}$$

which clearly diverges. Therefore, $z = 1$ is not in the ROC. Now consider $z = 3$.

$$\begin{aligned} Z(3) &= \sum_{n=0}^{\infty} 2^n 3^{-n} \\ &= \sum_{n=0}^{\infty} \left(\frac{2}{3}\right)^n \\ &= \frac{1}{1 - \frac{2}{3}} \\ &= 3. \end{aligned}$$

Thus, $X(z)$ is well-defined at $z = 3$ and therefore $z = 3$ is a point in the ROC of $X(z)$.

In this example, we saw that a larger value of z was in the ROC, whereas a smaller value was not. It should not be a surprise that larger values of z are more likely to be in the ROC. Why so? Because, in the definition of the z-transform, z is raised to a negative power and multiplied by the sequence $x[n]$. Therefore, the z-transform is essentially a sum of the signal $x[n]$ multiplied by either a damped or a growing complex exponential signal z^{-n} . Thus, larger values of z offer greater likelihood for convergence of the z-transform sum, since these correspond to more rapidly decaying exponential signals. In general, $X(z)$ converges for all z that are large enough, that is, when z is sufficiently large, that the signal $x[n]z^{-n}$ becomes summable. Specifically, $X(z)$ converges for all z such that $|z| > R$ (for some R). Thus, the ROC of $X(z)$ includes all points z lying outside a circle of radius R , as illustrated in Figure 4.1. To discover the value of R for a given sequence, we need only consider the convergence test that we need to apply when we try to compute the z-transform sum.

For our example, we have

$$\sum_{n=0}^{\infty} \left(\frac{2}{z}\right)^n,$$

which, when applying the formula (4.3) for a geometric series, yields

$$\begin{aligned} X(z) &= \sum_{n=0}^{\infty} \left(\frac{2}{z}\right)^n \\ &= \frac{1}{1 - \left(\frac{2}{z}\right)}, \quad \left|\frac{2}{z}\right| < 1 \\ &= \frac{z}{z - 2}, \quad |z| > 2, \end{aligned}$$

that is the ROC of $X(z)$ is $|z| > 2$. We can look at a more general example, such as that considered next.

Example

Consider the sequence $x[n] = a^n$, for $n \geq 0$, where a is a possibly complex constant. To determine $X(z)$, we consider the sum

$$\begin{aligned} X(z) &= \sum_{n=0}^{\infty} a^n z^{-n} \\ &= \sum_{n=0}^{\infty} \left(\frac{a}{z}\right)^n, \end{aligned}$$

which for $|z| > |a|$ converges to

$$X(z) = \frac{z}{z-a}.$$

Note that

$$\left| \frac{a}{z} \right| < 1 \Leftrightarrow \left| \frac{a}{|z|} \right| < 1 \Leftrightarrow |a| < |z| \Leftrightarrow |z| > |a|.$$

This, we have

$$X(z) = \frac{z}{z-a}, |z| > |a|.$$

What happens for $|z| < |a|$? Although the algebraic expression $z/(z-a)$ can be evaluated for any value of $z \neq a$, this is most certainly not the z-transform, since we know that the infinite sum defining $X(z)$ does not converge for such values of z . Therefore, $X(z)$ is defined only on its ROC and is not defined elsewhere. Hence, when we mention the z-transform of a sequence, we need to not only provide an expression for $X(z)$, but to also define the values of z for which this expression holds, i.e. the ROC.

Linearity

We can also use some elementary calculus to extend some of the relationships developed thus far. First, let us show that the z-transform is linear, that is if $X_1(z)$ is the z-transform for the sequence $x_1[n]$ and $X_2(z)$ is the z-transform for the signal $x_2[n]$, then the signal $x_3[n] = ax_1[n] + bx_2[n]$ is given by $X_3(z) = aX_1(z) + bX_2(z)$. This superposition property can be shown directly from the definition of the z-transform,

$$\begin{aligned} X_3(z) &= \sum_{n=0}^{\infty} (ax_1[n] + bx_2[n])z^{-n} \\ &= \sum_{n=0}^{\infty} ax_1[n]z^{-n} + \sum_{n=0}^{\infty} bx_2[n]z^{-n} \\ &= a \sum_{n=0}^{\infty} x_1[n]z^{-n} + b \sum_{n=0}^{\infty} x_2[n]z^{-n} \\ &= aX_1(z) + bX_2(z). \end{aligned}$$

Example

Now, to determine the z-transform of a sequence of the form $x[n] = na^n$, we can use linearity of the transform to obtain the desired result. We know that for the sequence $x[n] = a^n$ we have

$$X(z) = \sum_{n=0}^{\infty} a^n z^{-n} = \frac{z}{z-a}, |z| > |a|$$

and that if we differentiate this expression with respect to z we have

$$\begin{aligned} \frac{d}{dz} X(z) &= \frac{d}{dz} \left(\sum_{n=0}^{\infty} a^n z^{-n} \right) = \frac{d}{dz} \left(\frac{z}{z-a} \right), |z| > |a| \\ &= - \sum_{n=0}^{\infty} na^n z^{-n-1} = \frac{-a}{(z-a)^2}, |z| > |a|. \end{aligned}$$

From this expression, we can multiply by $-z$ and obtain

$$-z \frac{d}{dz} X(z) = \sum_{n=0}^{\infty} na^n z^{-n} = \frac{az}{(z-a)^2}, |z| > |a|.$$

That is, we have the relation

$$\sum_{n=0}^{\infty} na^n z^{-n} = \frac{az}{(z-a)^2}, |z| > |a|.$$

In a similar manner, we can obtain the more general result

$$nx[n] \Leftrightarrow -z \left(\frac{d}{dz} X(z) \right),$$

for $X(z)$ the z-transform of $x[n]$. We can continue to differentiate to obtain the relation

$$\frac{1}{2}n(n-1)x[n] \Leftrightarrow \frac{a^2 z}{(z-a)^3}, |z| > |a|,$$

and m -fold differentiation leads to the relation

$$\frac{1}{m!}n(n-1)\cdots(n-m+1)a^n \Leftrightarrow \frac{a^m z}{(z-a)^{m+1}}, |z| > |a|.$$

Example

We can use linearity of the z-transform to compute the z-transform of trigonometric functions, such as $x[n] = \cos(\omega n)$, for $n \geq 0$. Note that rather than using $x[n] = \cos(\omega n)u[n]$, we instead use the notation $n \geq 0$, since the unilateral z-transform for both sequences would be the same. From Euler's relation, we have

$$\begin{aligned} X(z) &= \sum_{n=0}^{\infty} \cos(\omega n) z^{-n} \\ &= \sum_{n=0}^{\infty} \frac{1}{2} (e^{j\omega n} + e^{-j\omega n}) z^{-n} \\ &= \frac{1}{2} \sum_{n=0}^{\infty} (e^{j\omega} z^{-1})^n + \frac{1}{2} \sum_{n=0}^{\infty} (e^{-j\omega} z^{-1})^n \\ &= \frac{1}{2} \frac{1}{1 - e^{j\omega} z^{-1}} + \frac{1}{2} \frac{1}{1 - e^{-j\omega} z^{-1}}, \quad |z| > |e^{j\omega}| = 1 \\ &= \frac{1}{2} \frac{z}{z - e^{j\omega}} + \frac{1}{2} \frac{z}{z - e^{-j\omega}}, \quad |z| > 1 \\ &= \frac{1}{2} \left(\frac{z(z - e^{-j\omega})}{z^2 - z(e^{j\omega} + e^{-j\omega}) + 1} + \frac{z(z - e^{j\omega})}{z^2 - z(e^{j\omega} + e^{-j\omega}) + 1} \right), \quad |z| > 1 \\ &= \frac{z^2 - z \cos(\omega)}{z^2 - 2z \cos(\omega) + 1}, \quad |z| > 1. \end{aligned}$$

We could have shortened the derivation by using our knowledge that $\cos(\omega n)$ is a sum of two complex exponentials of the form a^n where $a = e^{\pm j\omega}$ and then use linearity together with our knowledge of the z-transform for a^n . Let us now use this approach to find the z-transform for $x[n] = \sin(\omega n)$. We have that

$$\begin{aligned} x[n] &= \frac{1}{2j} (e^{j\omega n} - e^{-j\omega n}) \\ &= \frac{1}{2j} (e^{j\omega})^n - \frac{1}{2j} (e^{-j\omega})^n \end{aligned}$$

to which we can apply transform pairs we already know. From the z-transform of a single complex exponential, we have

$$\begin{aligned} X(z) &= \frac{1}{2j} \frac{z}{z - e^{j\omega}} - \frac{1}{2j} \frac{z}{z - e^{-j\omega}}, \quad |z| > 1 \\ &= \frac{1}{2j} \frac{z(z - e^{-j\omega}) - z(z - e^{j\omega})}{z^2 - 2z \cos(\omega) + 1}, \quad |z| > 1 \\ &= \frac{z \sin(\omega)}{z^2 - 2z \cos(\omega) + 1}, \quad |z| > 1. \end{aligned}$$

Example

From the definition of the z-transform, it should be clear that the unit sample function, i.e. the discrete-time impulse, has a z-transform

$$\delta[n] \Leftrightarrow 1.$$

Similarly, directly from the definition of the z-transform, a discrete-time impulse at $n = k$, i.e. $\delta[n - k]$ has the z-transform

$$\delta[n - k] \Leftrightarrow z^{-k},$$

so long as $k \geq 0$. Note that if $k < 0$, then the summation for the unilateral z-transform will never “see” the only non-zero term, and hence the z-transform will be zero for $\delta[n + k]$ for $k > 0$.

Another sequence for which we can apply knowledge of an existing transform is the unit step, $u[n]$. Note that for $n \geq 0$, the unit step is a complex exponential sequence of the form a^n for the specific case $a = 1$. As a result, we know that the z-transform for $u[n]$ is given by

$$u[n] \Leftrightarrow \frac{z}{z - 1}, \quad |z| > 1.$$

4.3 Properties of the unilateral z-transform

We will discuss a few properties of the unilateral z-transform. To facilitate this discussion, we will use the following operator notation for the z-transform, $Z(y[n]) \triangleq Y(z)$. The first property has already been shown, and is that of linearity.

4.3.1 Linearity

The unilateral z-transform is a linear operation, i.e. it satisfies superposition. This has been shown previously, and we have that

$$Z(ay_1[n] + by_2[n]) = aY_1(z) + bY_2(z).$$

This is readily shown from the definition of the z-transform, i.e.

$$\begin{aligned} \sum_{n=0}^{\infty} (ay_1[n] + by_2[n])z^{-n} &= a \sum_{n=0}^{\infty} y_1[n]z^{-n} + b \sum_{n=0}^{\infty} y_2[n]z^{-n} \\ &= aY_1(z) + bY_2(z). \end{aligned}$$

4.3.2 Delay Property #1

The next property is the first delay property, that is, when a sequence is delayed by a positive amount. If a sequence is delayed by k samples, then we have that

$$Z(y[n - k]u[n - k]) = z^{-k}Y(z).$$

In words, this property states that truncating a sequence at the origin, and then shifting to the right by a positive integer k , is equivalent to multiplying the z-transform of the un-shifted sequence by z^{-k} . This can be proven from the definition of the z-transform. We have that

$$\begin{aligned} Z(y[n - k]u[n - k]) &= \sum_{n=0}^{\infty} y[n - k]u[n - k]z^{-n} \\ &= \sum_{n=k}^{\infty} y[n - k]z^{-n} \\ &= \sum_{m=0}^{\infty} y[m]z^{-(m+k)} \\ &= z^{-k}Y(z), \end{aligned}$$

where the second line follows from $u[n - k]$ being zero for $n < k$ and the third line follows from making the substitution $m = n - k$.

4.3.3 Delay Property #2

For cases where $y[-1], y[-2], \dots, y[-k]$ are known or defined ($k > 0$), we have the following property. Here, the sequence $y[n]$ is not truncated at the origin, prior to shifting.

$$Z(y[n-k]) = z^{-k} \left[Y(z) + \sum_{m=1}^k y[-m]z^m \right].$$

This can be shown from linearity and delay property #1. Specifically, we note that for $n \geq 0$, we have that

$$y[n-k] = y[n-k]u[n-k] + \sum_{m=1}^k y[-m]\delta[n-k+m]$$

by simply adding back into the sequence the “new” values that shift into the region $n \geq 0$ from the left. We now can use linearity together with delay property #1 and the z-transform for a shifted discrete-time impulse to obtain

$$\begin{aligned} Z(y[n-k]) &= z^{-k}Y(z) + \sum_{m=1}^k y[-m]z^{-(k-m)} \\ &= z^{-k} \left[Y(z) + \sum_{m=1}^k y[-m]z^m \right]. \end{aligned}$$

4.3.4 Advance Property

The following advance property can also be used in the solution of difference equations with initial conditions. We have that

$$Z(y[n+k]u[n]) = z^k \left[Y(z) - \sum_{m=0}^{k-1} y[m]z^{-m} \right].$$

This property is also readily shown by noting that

$$\begin{aligned} Z(y[n+k]u[n]) &= \sum_{n=0}^{\infty} y[n+k]z^{-n} \\ &= z^k \sum_{n=0}^{\infty} y[n+k]z^{-(n+k)} \\ &= z^k \sum_{m=k}^{\infty} y[m]z^{-m} \\ &= z^k \left(\sum_{m=0}^{\infty} y[m]z^{-m} - \sum_{m=0}^{k-1} y[m]z^{-m} \right) \\ &= z^k \left(Y(z) - \sum_{m=0}^{k-1} y[m]z^{-m} \right). \end{aligned}$$

4.3.5 Convolution

One of the useful properties of the z-transform is that it maps convolution in the time domain into multiplication in the z-transform domain. We will show this here for the unilateral z-transform and sequences that are only nonzero for $n \geq 0$ and revisit the more general case when we explore the two-sided z-transform. Specifically, we assume that $x[n] = h[n] = 0, n < 0$ and consider the convolution

$$y[n] = \sum_{m=-\infty}^{\infty} h[m]x[n-m].$$

Taking the z-transform of both sides, we have

$$\begin{aligned}
 Y(z) &= \sum_{n=0}^{\infty} y[n]z^{-n} \\
 &= \sum_{n=0}^{\infty} \sum_{m=-\infty}^{\infty} h[m]x[n-m]z^{-n} \\
 &= \sum_{m=-\infty}^{\infty} h[m] \sum_{n=0}^{\infty} x[n-m]z^{-n} \\
 &= \sum_{m=-\infty}^{\infty} h[m]X(z)z^{-m} \\
 &= X(z) \sum_{m=-\infty}^{\infty} h[m]z^{-m} \\
 &= X(z)H(z),
 \end{aligned}$$

where in the third line we used the delay property and that both sequences were zero for $n < 0$. When the sequences $x[n]$ and $h[n]$ are not both zero for $n < 0$, then multiplication of one-sided z-transforms can be shown to be equivalent to convolution of the sequences $x[n]u[n]$ and $h[n]u[n]$, i.e.

$$\sum_{k=-\infty}^{\infty} x[n-k]y[n-k]h[k]u[k] = \sum_{k=0}^n x[n-k]h[k] \longleftrightarrow X(z)H(z),$$

where $X(z)$ and $H(z)$ are the one-sided z-transforms of the sequences $x[n]$ and $h[n]$.

4.3.6 Inverse unilateral z-transform

One method that can be used to solve difference equations, is to take the z-transform of both sides of the difference equation, and solve the resulting algebraic equation for $Y(z)$, and then find the inverse transform to obtain $y[n]$. A formula for the inverse unilateral z-transform can be written

$$y[n] = \frac{1}{2\pi j} \oint Y(z)z^{n-1}dz$$

which is an integral taken over a closed contour in a counter clockwise direction in the region of converge of $Y(z)$, as shown in Figure . Other inversion methods exist if $Y(z)$ is a rational function (i.e., a ratio of polynomials), e.g.,

$$Y(z) = \frac{b_0 + b_1z + \dots + b_Mz^M}{a_0 + a_1z + \dots + a_Nz^N}.$$

Direct long division

A straightforward, but not entirely practical method, since it does not produce a closed-form expression for $y[n]$, is to employ long-division of the polynomials directly. This is a simple method for obtaining a power-series expansion for $Y(z)$ from the rational expression, and then from the definition of the z-transform, the terms of the sequence can be identified one at a time.

Example

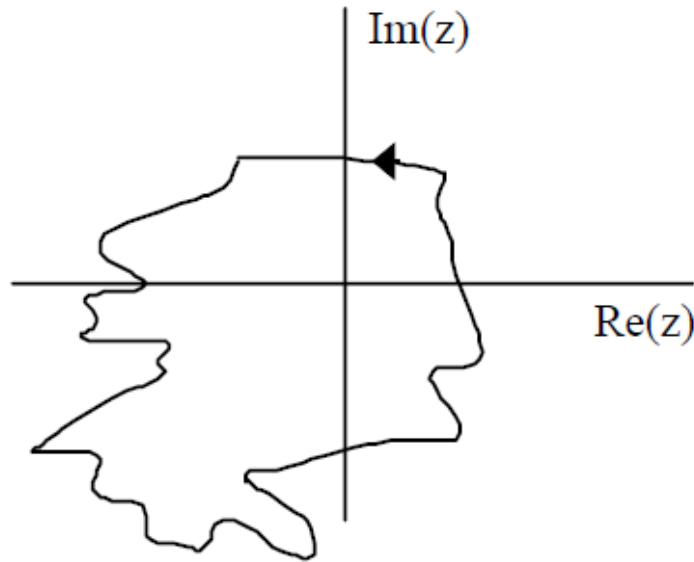


Figure 4.3: Contour integral for taking an inverse z-transform.

For the expression $Y(z) = z/(z - a)$, we have that

$$\begin{aligned}
 Y(z) &= \frac{z}{z - a} \\
 &= \frac{1 + \frac{a}{z} + \frac{a^2}{z^2}}{z - a} \\
 \frac{z}{z - a} &= \frac{\frac{z - a}{0 + a + 0}}{0 + a - \frac{a^2}{z}} \\
 &= \frac{0 + 0 + \frac{a^2}{z}}{0 + 0 + \frac{a^2}{z} - \frac{a^3}{z^2}}
 \end{aligned}$$

Note that from the above series expansion, together with the definition of the unilateral z-transform, i.e. $Y(z) = y[0] + y[1]z^{-1} + y[2]z^{-2} + \dots$, we can immediately identify all of the terms of the sequence $y[n]$. That is we have that

$$\begin{aligned}
 Y(z) &= 1 + az^{-1} + a^2z^{-2} + a^3z^{-3} + \dots \\
 &= y[0] + y[1]z^{-1} + y[2]z^{-2} + y[3]z^{-3} + \dots,
 \end{aligned}$$

from which we may infer that $y[n] = a^n, n \geq 0$.

4.3.7 z-transform properties

A short table of z-transform properties is given in Table (4.1). These can be proven either directly from the definition of the z-transform, or through application of other known properties.

4.3.8 Table of unilateral z-transform pairs

A short table of unilateral z-transforms is given in Table (4.2) below. These can also be derived directly from the definition of the unilateral z-transform, or through application of the theorems listed in Table (4.1).

Superposition	$ax_1[n] + bx_2[n]$	\Leftrightarrow	$aX_1(z) + bX_2(z)$
Advance	$x[n+1]u[n]$	\Leftrightarrow	$z(X(z) - x[0])$
Modulation	$a^n x[n]$	\Leftrightarrow	$X(a^{-1}z)$
Multiplication by n	$nx[n]$	\Leftrightarrow	$-z \left(\frac{dX(z)}{dz} \right)$
Convolution	$\sum_{k=0}^n x[k]y[n-k]$	\Leftrightarrow	$X(z)Y(z)$
Convolution when $x[n] = y[n] = 0, n < 0$	$\sum_{k=-\infty}^{\infty} x[k]y[n-k]$	\Leftrightarrow	$X(z)Y(z)$
Advance by k	$y[n+k]u[n]$	\Leftrightarrow	$z^k \left[Y(z) - \sum_{m=0}^{k-1} y[m]z^{-m} \right]$
Delay property #1	$y[n-k]u[n-k]$	\Leftrightarrow	$z^{-k} Y(z)$
Delay property #2	$y[n-k]$	\Leftrightarrow	$z^{-k} \left[Y(z) + \sum_{m=1}^k y[-m]z^m \right]$

Table 4.1: Table of unilateral z-transform properties.

$x[n]$	\Leftrightarrow	$X(z) = \sum_{n=0}^{\infty} x[n]z^{-n}$	ROC_X
$\delta[n] = \begin{cases} 1, & n = 0 \\ 0, & n \neq 0 \end{cases}$	\Leftrightarrow	1	all z
$\delta[n-k]$	\Leftrightarrow	$\begin{cases} z^{-k}, & k \geq 0 \\ 0, & k < 0 \end{cases}$	$z \neq 0$
a^n	\Leftrightarrow	$\frac{z}{z - a}$	$ z > a $
na^n	\Leftrightarrow	$\frac{z}{(z - a)^2}$	$ z > a $
$a^n \sin(\omega n)$	\Leftrightarrow	$\frac{az \sin(\omega)}{z^2 - 2az \cos(\omega) + a^2}$	$ z > a $
$a^n \cos(\omega n)$	\Leftrightarrow	$\frac{z^2 - az \cos(\omega)}{z^2 - 2az \cos(\omega) + a^2}$	$ z > a $
$u[n] = \begin{cases} 1, & n \geq 0 \\ 0, & n < 0 \end{cases}$	\Leftrightarrow	$\frac{z}{z - 1}$	$ z > 1$
1	\Leftrightarrow	$\frac{z}{z - 1}$	$ z > 1$

Table 4.2: Table of unilateral z-transform pairs.

4.4 Inverse z-transform by partial fraction expansion

One method for finding the inverse of a unilateral (one-sided) z-transform is to recognize the transform of interest as the transform of a signal whose z-transform you already know, or have access to via a lookup table, such as that found at the end of the last chapter. For example, if you know that the transform of the unit-sample (or discrete-time impulse) is $X(z) = 1$, then given a transform of the form $1/X_2(z) = 2 + z^{-1}$, you might use the linearity property of the z-transform together with the delay property to identify $x[n] = 2\delta[n] + \delta[n-1]$. This method is sometimes referred to as the “table lookup method”. We can generalize this idea to find the inverse transform of more elaborate functions by learning how to decompose complex expressions into a linear combination of terms, each of which we might be able to identify their inverse by inspection. This simply amounts to using linearity to break a complex transform into a sum of simpler terms, and then using a lookup table to find the inverse of each of the terms independently. The overall inverse transform would then be the sum of the inverses of each of the simpler terms, exploiting the linearity of the transform.

The inverse transform method we will describe will work well in the case when $X(z)$ is a rational function, that is, when it can be expressed as a ratio of finite order polynomials in z . The method is based on the notion that every rational function can be expanded in terms of partial fractions. If the rational function $X(z)$ is proper, that is, the degree of the numerator polynomial is less than the degree of the denominator polynomial, and if the roots of the denominator polynomial are distinct, then we can factor $X(z)$ in the form

$$X(z) = \frac{b_0 + b_1z + \cdots + b_Mz^M}{a_0 + a_1z + \cdots + a_Nz^N} = \frac{b_0 + b_1z + \cdots + b_Mz^M}{(z - r_1)(z - r_2) \cdots (z - r_N)},$$

where, here, $X(z)$ is proper if $M < N$, and the roots of denominator polynomial are $r_{k=1}^N$. When the r_k are distinct (or “simple”), then, we can write

$$X(z) = \sum_{k=1}^N \frac{A_k}{z - r_k},$$

where the constants A_k are called the residues of $X(z)$. In this form, we can use a simple method to find the residues when all of the roots are distinct. We see that they can be obtained by the formula

$$A_k = (z - r_k)X(z) \big|_{z=r_k},$$

since the term $(z - r_k)$ makes each term in the sum become zero when evaluated at $z = r_k$, except for the one term in the sum that had $(z - r_k)$ in the denominator. This term is has A_k in the numerator, and hence yields the formula above.

Once we have expanded $X(z)$ in this form, we can then read off the inverse transform as

$$X(z) = \sum_{k=1}^N \frac{A_k}{z - r_k} = \sum_{k=1}^N z^{-1} \frac{A_k z}{z - r_k} \Leftrightarrow x[n] = \sum_{k=1}^N A_k r_k^{n-1} u[n-1],$$

once again using a combination of the linearity property of the unilateral z-transform and the delay property. We can see how this works in practice by looking at an example.

Example

We can use this approach to find the inverse transform for the following unilateral z-transform:

$$Y(z) = \frac{z - 1}{(z - 2)(z - 3)}.$$

Now, we wish to find the sequence $y[n]$, for $n \geq 0$. We have that

$$Y(z) = \frac{z - 1}{(z - 2)(z - 3)} = \frac{A_1}{z - 2} + \frac{A_2}{z - 3},$$

so that when we multiply $Y(z)$ by $z - 2$ we obtain

$$(z - 2)Y(z) = A_1 + \frac{(z - 2)A_2}{z - 3}.$$

Now, setting $z = 2$, we have

$$(z - 2)Y(z)|_{z=2} = A_1,$$

since the second term on the right hand side becomes zero. We then find that

$$A_1 = \left. \frac{z-1}{z-3} \right|_{z=2} = \frac{1}{-1} = -1.$$

Similarly we find that

$$A_2 = \left. \frac{z-1}{z-2} \right|_{z=3} = \frac{2}{1} = 2.$$

Putting these together yields that

$$\begin{aligned} Y(z) &= \frac{-1}{z-2} + \frac{2}{z-3} \\ &= -z^{-1} \left[\frac{z}{z-2} \right] + 2z^{-1} \left[\frac{z}{z-3} \right]. \end{aligned}$$

From the table of unilateral z-transform pairs, we have that

$$a^n \Leftrightarrow \frac{z}{z-a},$$

and applying Delay Property #1, we have that

$$a^{n-1}u[n-1] \Leftrightarrow z^{-1} \frac{z}{z-a}.$$

From the linearity of the z-transform, we can now invert each of the terms individually, and then put them together to obtain

$$y[n] = -(2)^{n-1}u[n-1] + 2(3)^{n-1}u[n-1].$$

If we prefer, we can re-write this as

$$y[n] = \begin{cases} -\frac{1}{2}(2)^n + \frac{2}{3}3^n, & n \geq 1 \\ 0, & n=0. \end{cases}$$

We do not evaluate $y[n]$ for values of $n < 0$, since the unilateral z-transform does not tell us anything about this region. In this example, we needed to apply both linearity and Delay Property #1. We can avoid the need to apply the delay property to each term, by expanding $z^{-1}Y(z)$ in a PFE as

$$\frac{Y(z)}{z} = \frac{A_1}{z} + \frac{A_2}{z-2} + \frac{A_3}{z-3}.$$

Then we can obtain

$$Y(z) = A_1 + \frac{A_2 z}{z-2} + \frac{A_3 z}{z-3},$$

and each of the terms in this expansion can be inverted directly, without the need for the delay property. Working out the details for this example, we have

$$\begin{aligned} \frac{Y(z)}{z} &= \frac{z-1}{z(z-2)(z-3)} \\ &= \frac{A_1}{z} + \frac{A_2}{z-2} + \frac{A_3}{z-3}, \end{aligned}$$

and that

$$\begin{aligned} A_1 &= \left. \frac{z-1}{(z-2)(z-3)} \right|_{z=0} = \frac{-1}{(-2)(-3)} = -\frac{1}{6}, \\ A_2 &= \left. \frac{z-1}{z(z-3)} \right|_{z=2} = \frac{1}{(2)(-1)} = -\frac{1}{2}, \\ A_3 &= \left. \frac{z-1}{z(z-2)} \right|_{z=3} = \frac{2}{(3)(1)} = \frac{2}{3}. \end{aligned}$$

Putting these together, yields

$$\begin{aligned}\frac{Y(z)}{z} &= \frac{-\frac{1}{6}}{z} + \frac{-\frac{1}{2}}{z-2} + \frac{\frac{2}{3}}{z-3} \\ Y(z) &= \frac{-\frac{1}{6}z}{z} + \frac{-\frac{1}{2}z}{z-2} + \frac{\frac{2}{3}z}{z-3}.\end{aligned}$$

We can again invert each term, term by term, to obtain

$$y[n] = -\frac{1}{6}\delta[n] - \frac{1}{2}(2)^n u[n] + \frac{2}{3}(3)^n u[n].$$

Here we have identified that the inverse transform of a constant is a discrete-time impulse. This can be obtained either from the table of transforms, or by noting that if a z-transform is constant, say $X(z) = C$, then we have that

$$X(z) = x[0] + x[1]z^{-1} + x[2]z^{-2} + x[3]z^{-3} + \dots$$

and we see that the only way that $X(z)$ can be a constant (i.e. the only power of z in the expression is z^0) is for $x[0] = C$, i.e. we have that

$$X(z) = -\frac{1}{6} \Leftrightarrow x[n] = -\frac{1}{6}\delta[n].$$

Putting all of the terms together yields,

$$\begin{aligned}y[n] &= \begin{cases} -\frac{1}{2}(2)^n + \frac{2}{3}(3)^n, & n \geq 1 \\ -\frac{1}{6} - \frac{1}{2} + \frac{2}{3}, & n = 0 \end{cases} \\ &= \begin{cases} -\frac{1}{2}(2)^n + \frac{2}{3}(3)^n, & n \geq 1 \\ 0, & n = 0, \end{cases}\end{aligned}$$

as we had before. In this example, the PFE for $z^{-1}Y(z)$ was more complicated (involved one more term) than the PFE for $Y(z)$. In many cases this extra complication does not arise. If the numerator of $Y(z)$ contains a power of z (say z or z^2), then the z in the denominator of $z^{-1}Y(z)$ is cancelled, in which case the PFE for $z^{-1}Y(z)$ has exactly the same form as the PFE of $Y(z)$.

If the r_i are not distinct, we will need to modify the partial fraction expansion slightly. Suppose r_j is a root that is repeated q times. We then must replace the single term corresponding to r_j with a set of q terms, one for each occurrence of the root, where the denominator is raised to each power, starting from the first power up to the q th power, i.e. we replace

$$\frac{A_k}{(z - r_k)} \Rightarrow \sum_{\ell=1}^q \frac{B_\ell}{(z - r_k)^\ell}$$

in the partial fraction expansion, where the new constants satisfy

$$B_\ell = \frac{1}{(q - \ell)!} \left[\frac{d^{q-\ell}}{dz^{q-\ell}} (z - r_k)^q Y(z) \right] \Big|_{z=r_k}.$$

While it is important to know that this formula exists, in practice, the form of the expansion is more important than the explicit formula for determination of the constants. For example, you can determine the constants by simply matching terms in the expansion as shown in the next example.

Example

Determine the partial fraction expansion of the z-transform

$$Y(z) = \frac{z}{(z-1)(z-3)^2}.$$

To accomplish this, we need only know the form of the expansion, and not dwell on the formula for the constants of the repeated roots. First, we obtain

$$\frac{Y(z)}{z} = \frac{1}{(z-1)(z-3)^2} = \frac{A_1}{(z-1)} + \frac{A_2}{(z-3)} + \frac{A_3}{(z-3)^2}$$

as the form of the partial fraction expansion. We can now obtain the first term directly, using the non-repeated roots formula

$$A_1 = \frac{1}{(z-3)^2} \Big|_{z=1} = \frac{1}{4},$$

to get started. Now, we find A_3 before we find A_2 . In general, if we find the coefficient over the highest power denominator first, the resulting algebra will be simplified. By multiplying both sides of the PFE by $(z-3)^2$ we obtain

$$\frac{(z-3)^2 Y(z)}{z} = \frac{1}{(z-1)} = \frac{A_1(z-3)^2}{(z-1)} + A_2(z-3) + A_3.$$

Setting $z = 3$, we have

$$A_3 = \frac{1}{z-1} \Big|_{z=3} = \frac{1}{2}.$$

There are a few ways to determine A_2 . One is to first differentiate the expression $(z-3)^2 Y(z)/z$ with respect to z , which yields

$$\frac{-1}{(z-1)^2} = \frac{2A_1(z-3)(z-1) - A_1(z-3)^2}{(z-1)^2} + A_2,$$

which upon setting $z = 3$, yields

$$-\frac{1}{4} = A_2.$$

Another way to find A_2 would be to simply fill in the known constants, yielding

$$\begin{aligned} \frac{1}{(z-1)(z-3)^2} &= \frac{\frac{1}{4}}{(z-1)} + \frac{A_2}{(z-3)} + \frac{\frac{1}{2}}{(z-3)^2} \\ &= \frac{\frac{1}{4}(z-3)^2 + \frac{1}{2}(z-1) + A_2(z-1)(z-3)}{(z-1)(z-3)^2}. \end{aligned}$$

Now, the numerators must match, so we must have

$$1 = \frac{1}{4}(z-3)^2 + \frac{1}{2}(z-1) + A_2(z-1)(z-3),$$

which can be easily solved for A_2 . For example, both sides must have the same coefficient to the term z^2 , which, on the left hand side is zero, and on the right hand side is

$$0 = \frac{1}{4} + A_2,$$

which yields that

$$A_2 = -\frac{1}{4}$$

as before. Substituting these values into the original PFE yields

$$Y(z) = \frac{\frac{1}{4}z}{(z-1)} - \frac{\frac{1}{4}z}{(z-3)} + \frac{\frac{1}{2}z}{(z-3)^2}.$$

The first two terms are easy to invert from our table of known transforms. For the third term, we recall that

$$na^n \Leftrightarrow \frac{az}{(z-a)^2}.$$

Therefore we have that

$$\begin{aligned} y[n] &= \frac{1}{4}(1)^n - \frac{1}{4}(3)^n + \frac{1}{2} \left(\frac{1}{3} \right) n(3)^n, \quad n \geq 0 \\ &= \frac{1}{4} - \frac{1}{4}(3)^n + \frac{1}{6}n(3)^n, \quad n \geq 0. \end{aligned}$$

Let us consider another example.

Example

Given the unilateral z-transform of the sequence $y[n]$ is given by

$$Y(z) = \frac{2z^3 + z^2 - z + 4}{(z - 2)^3},$$

find $y[n]$. Recall that for a “strictly proper” rational function, we require that the degree of the numerator polynomial be strictly less than the degree of the denominator polynomial. This condition is necessary for us to use the form of the partial fraction expansion we have considered thus far. We can use the PFE form if we choose to expand $Y(z)/z$ in PFE, since this will be a strictly proper rational function. We begin with

$$\begin{aligned} \frac{Y(z)}{z} &= \frac{2z^3 + z^2 - z + 4}{z(z - 2)^3} \\ &= \frac{A_1}{z} + \frac{A_2}{(z - 2)} + \frac{A_3}{(z - 2)^2} + \frac{A_4}{(z - 2)^3} \end{aligned}$$

and immediately note that

$$A_1 = \left. \frac{2z^3 + z^2 - z + 4}{(z - 2)^3} \right|_{z=0} = \frac{4}{-8} = -\frac{1}{2}.$$

Now, we again find the coefficient of repeated-root term with highest power denominator first. Multiplying $Y(z)/z$ by $(z-2)^3$, we obtain

$$\frac{2z^3 + z^2 - z + 4}{z} = -\frac{(z - 2)^3}{2z} + A_2(z - 2)^2 + A_3(z - 2) + A_4,$$

which when evaluated for $z = 2$, yields

$$\begin{aligned} \frac{16 + 4 - 2 + 4}{2} &= A_4 \\ 11 &= A_4. \end{aligned}$$

Now putting the PFE into a common denominator and setting the numerators equal yields,

$$2z^3 + z^2 - z + 4 = -\frac{1}{2}(z - 2)^3 + A_2z(z - 2)^2 + A_3z(z - 2) + 11z.$$

We can now match terms with corresponding powers of z to obtain

$$\begin{aligned} 2z^3 &= -\frac{1}{2}z^3 + A_2z^3 \\ \frac{5}{2} &= A_2, \end{aligned}$$

and

$$\begin{aligned} z^2 &= \frac{1}{2}6z^2 + \frac{5}{2}(-4)z^2 + A_3z^2 \\ 8 &= A_3. \end{aligned}$$

Putting all of the terms together, yields,

$$Y(z) = -\frac{1}{2} + \frac{\frac{5}{2}z}{z - 2} + \frac{8z}{(z - 2)^2} + \frac{11z}{(z - 2)^3}.$$

Now we can invert each of the terms, one at a time, to yield,

$$y[n] = -\frac{1}{2}\delta[n] + \frac{5}{2}(2)^n + 4n(2)^n + \frac{11}{2}(n - 1)n(2)^{n-2}, \quad n \geq 0,$$

where for the last term, we used the transform pair

$$\frac{1}{2}n(n-1)a^n \Leftrightarrow \frac{a^2 z}{(z-a)^3}.$$

We could combine all of the results to obtain

$$y[n] = \begin{cases} 2, & n = 0 \\ \frac{1}{8}(11n^2 + 21n + 20)(2)^n, & n \geq 1. \end{cases}$$

4.5 Difference equations and the z-transform

Just as the Laplace transform was used to aid in the solution of linear differential equations, the z-transform can be used to aid in the solution of linear difference equations. Recall that linear, constant coefficient differential equations could be converted into algebraic equations by transforming the signals in the equation using the Laplace transform. Derivatives could be mapped into functions of the Laplace transform variable s , through the derivative law for Laplace transforms. Similarly, delayed versions of a sequence can be mapped into algebraic functions of z , using one of the delay rules for z-transforms.

In the case of continuous-time linear systems described by differential equations, in order to find the response of such a linear system to an particular input, the differential equations needed to be solved, using either time-domain or Laplace transform methods. For an N th-order differential equation, in general N conditions on the output were needed in order to specify the output in response to a given input. Similarly, for linear difference equations of N th-order, N pieces of information are needed to find the output for a given input. Unlike the continuous-time case, difference equations can often be simply iterated forward in time if these N conditions are consecutive. That is, given $y[-N+1], \dots, y[-1]$, then re-writing

$$\sum_{k=0}^N a_k y[n-k] = \sum_{k=0}^M b_k x[n-k]$$

in the form

$$a_0 y[0] = - \sum_{k=1}^N a_k y[n-k] = \sum_{k=0}^M b_k x[n-k],$$

from which $y[0]$ could be found. Iterating this process forward could find each value of the output without ever explicitly obtaining a general expression for $y[n]$.

In this chapter we will explore the z-transform for the explicit solution of linear constant coefficient difference equations. The properties of the z-transform that we have developed can be used to map the difference equations describing the relationship between the input and the output, into a simple set of linear algebraic equations involving the z-transforms of the input and output sequences. By solving the resulting algebraic equations for the z-transform of the output, we can then use the methods we've developed for inverting the transform to obtain an explicit expression for the output. We begin with an example.

Example

We revisit this simple linear, homogeneous difference equation, now using the unilateral ztransform. Again consider the difference equation

$$y[n] - 3y[n-1] = 0, \quad n \geq 0, \quad y[-1] = 2$$

Taking unilateral z-transform of both sides, and using the delay property, we obtain

$$\begin{aligned} Y(z) - 3z^{-1}[Y(z) + zy[-1]] &= 0 \\ Y(z)[1 - 3z^{-1}] &= 6, \end{aligned}$$

which can be solved for $Y(z)$ directly, yielding

$$\begin{aligned} Y(z) &= \frac{6z}{z-3}, \\ y[n] &= 6(3)^n u[n]. \end{aligned}$$

Another, slightly more involved example, repeats another example as well.

Example

Consider the following homogenous, linear constant coefficient difference equation, defined for nonnegative n and with initial conditions shown

$$y[n] + 4y[n-1] + 4y[n-2] = 0, \quad n \geq 0, \quad y[-1] = y[-2] = 1.$$

Taking the z-transform of both sides, again using the delay property and including the initial conditions, we obtain

$$\begin{aligned} Y(z) + 4z^{-1} [Y(z) + zy[-1]] + 4z^{-2} [Y(z) + zy[-1] + z^2y[-2]] &= 0 \\ Y(z) [1 + 4z^{-1} + 4z^{-2}] &= -4y[-1] - 4z^{-1}y[-1] - 4y[-2] \\ Y(z) &= \frac{-8 - 4z^{-1}}{1 + 4z^{-1} + 4z^{-2}} \\ &= \frac{-8z^2 - 4z}{z^2 + 4z + 4}. \end{aligned}$$

This is not in strictly proper rational form, i.e. the degree of the numerator is not strictly less than that of the denominator, however when we expand $z^{-1}Y(z)$, we have

$$\begin{aligned} \frac{Y(z)}{z} &= \frac{-8z - 4}{z^2 + 4z + 4} = \frac{-8z - 4}{(z + 2)^2} \\ &= \frac{A_1}{(z + 2)} + \frac{A_2}{(z + 2)^2}. \end{aligned}$$

Since we have repeated roots, we first seek the coefficient of the highest order root, A_2 . By cross multiplying, we obtain

$$-8z - 4 = A_1(z + 2) + A_2.$$

Setting $z = -2$ on both sides, we have that

$$16 - 4 = 12 = A_2.$$

We can also immediately see from the cross multiplication that

$$A_1 = -8,$$

by matching the terms on both sides that each multiply z . Putting these terms together, we have the full partial fraction expansion for $Y(z)$,

$$Y(z) = \frac{-8z}{(z + 2)} + \frac{12z}{(z + 2)^2}.$$

Using linearity to invert each term of the z-transform independently, we obtain

$$y[n] = -8(-2)^n u[n] - 6n(-2)^n u[n].$$

We now consider a case where the difference equation contains an input, or drive term, such that we no longer have a homogenous difference equation.

Example

Consider the following linear constant coefficient difference equation.

$$y[n + 2] - \frac{3}{2}y[n + 1] + \frac{1}{2}y[n] = \left(\frac{1}{3}\right)^n u[n], \quad y[0] = 4, \quad y[1] = 0.$$

Taking the unilateral z-transform of both sides and using the advance property, we obtain

$$\begin{aligned} z^2 [Y(z) - y[0] - z^{-1}y[1]] - \frac{3}{2}z [Y(z) - y[0]] + \frac{1}{2}Y(z) &= \frac{z}{z - \frac{1}{3}} \\ z^2 [Y(z) - 4] - \frac{3}{2}z [Y(z) - 4] + \frac{1}{2}Y(z) &= \frac{z}{z - \frac{1}{3}} \\ Y(z) \left[z^2 - \frac{3}{2}z + \frac{1}{2} \right] &= \frac{z}{z - \frac{1}{3}} + 4z^2 - 6z. \end{aligned}$$

We can now solve for $Y(z)$ and keep the terms on the right hand side separated into two distinct groups, namely,

$$Y(z) = \frac{1}{(z^2 - \frac{3}{2}z + \frac{1}{2})} \left(\underbrace{\frac{z}{z - \frac{1}{3}}}_{\text{term due to input}} + \underbrace{\frac{4z^2 - 6z}{(z - \frac{1}{2})(z - 1)}}_{\text{term due to initial conditions}} \right).$$

We can now write the z-transform as a sum of two terms, one due to the input, and one due to the initial conditions. Recall from our analysis of linear constant coefficient difference equations that these correspond to the zero-state response and the zero-input response of the system. Taking these two terms separately, again through linearity of the transform, we have that

$$Y(z) = T_z(z) + T_2(z)$$

where

$$\begin{aligned} T_1(z) &= \frac{z}{(z^2 - \frac{3}{2}z + \frac{1}{2})(z - \frac{1}{3})}, \\ T_2(z) &= \frac{4z^2 - 6z}{(z^2 - \frac{3}{2}z + \frac{1}{2})}. \end{aligned}$$

Here, $T_1(z)$ is the z-transform of the zero-state response, and $T_2(z)$ is the z-transform of the zero-input response. We can then take a partial fraction expansion of each of the terms independently. For the first term, we find it convenient to express the partial fraction expansion as

$$\frac{T_1(z)}{z} = \frac{1}{(z - \frac{1}{2})(z - 1)(z - \frac{1}{3})} = \frac{A_1}{(z - \frac{1}{2})} + \frac{A_2}{(z - 1)} + \frac{A_3}{(z - \frac{1}{3})}.$$

This leads to

$$\begin{aligned} A_1 &= -12, \quad A_2 = 3, \quad A_3 = 9, \\ T_1(z) &= \frac{-12z}{(z - \frac{1}{2})} + \frac{3z}{(z - 1)} + \frac{9z}{(z - \frac{1}{3})}, \end{aligned}$$

and the resulting zero state response is given by

$$y_x[n] = -12 \left(\frac{1}{2}\right)^n + 3 + 9 \left(\frac{1}{3}\right)^n, \quad n \geq 0.$$

For the zero-input response term, we have that

$$\frac{T_2(z)}{z} = \frac{4z - 6}{(z - \frac{1}{2})(z - 1)} = \frac{B_1}{(z - \frac{1}{2})} + \frac{B_2}{(z - 1)},$$

from which we can quickly solve for the constants, yielding

$$B_1 = 8, \quad B_2 = -4,$$

which gives the partial fraction expansion for the zero-input response as

$$T_2 = \frac{8z}{(z - \frac{1}{2})} - \frac{4z}{(z - 1)}.$$

The resulting zero-input response is then given by

$$y_s[n] = 8 \left(\frac{1}{2}\right)^n - 4, \quad n \geq 0.$$

Putting the zero-state response and the zero-input response together, we obtain the total response

$$y[n] = y_x[n] + y_s[n] = -4 \left(\frac{1}{2}\right)^n - 1 + 9 \left(\frac{1}{3}\right)^n, \quad n \geq 0.$$

In general, this method of solution can be applied to linear constant coefficient difference equations of arbitrary order. Note that while in this particular case, we applied the time advance property of the unilateral z-transform, when solving difference equations of the form

$$y[n] + a_1 y[n-1] + \cdots + a_N y[n-N] = x[n], \quad n \geq 0,$$

which initial conditions $y[-k], k = 1, \dots, N$, we can use the Delay Property #2.

4.5.1 General form of solution of linear constant coefficient difference equations (LCCDE)s

In this section, we will derive the general form of a solution to a linear constant coefficient difference equation. We will prove that the zero-state response (response to the input, when state is initially zero) is given by a convolution. Consider the following difference equation

$$y[n+K] + a_1 y[n+K-1] + \cdots + a_K y[n] = x[n], \quad n \geq 0$$

together with initial conditions $y[k], k = 0, 1, \dots, K-1$. Taking the one-sided z-transform of both sides, and using the Advance Property, we obtain

$$z^K \left[Y(z) - \sum_{m=0}^{K-1} y[m] z^{-m} \right] + a_1 z^{K-1} \left[Y(z) - \sum_{m=0}^{K-2} y[m] z^{-m} \right] + \cdots + a_{K-1} z [Y(z) - y[0]] + a_K Y(z) = X(z).$$

By defining

$$S(z) = z^K \left[\sum_{m=0}^{K-1} y[m] z^{-m} \right] + a_1 z^{K-1} \left[\sum_{m=0}^{K-2} y[m] z^{-m} \right] + \cdots + a_{K-1} z y[0],$$

we have that

$$Y(z)[z^K + a_1 z^{K-1} + \cdots + a_K] = X(z) + S(z),$$

where the *characteristic polynomial* is given by

$$z^K + a_1 z^{K-1} + \cdots + a_K.$$

We now define the *transfer function* $H(z)$ of the system described by the LCCDE as

$$H(z) = \frac{1}{z^K + a_1 z^{K-1} + \cdots + a_K}.$$

We then obtain that

$$Y(z) = H(z) \left[\underbrace{X(z)}_{\text{term do to the input}} + \underbrace{S(z)}_{\text{term due to initial conditions}} \right].$$

Notice that the decomposition property holds with

$$\begin{aligned} y_s[n] &= Z^{-1} \{H(z)S(z)\} \\ y_x[n] &= Z^{-1} \{H(z)X(z)\}. \end{aligned}$$

Both homogeneity and superposition hold with respect to $y_s[n]$ and $y_x[n]$ because the z-transform is linear. Linear constant coefficient difference equations (LCCDE)s describe linear systems, which have already explored the time-domain (sequence-domain). It is worthwhile to consider the form of the solution that $y_s[n]$ will take.

Consider first the case when the roots of the characteristic polynomial are distinct. In this case, we have

$$\frac{S(z)H(z)}{z} = \frac{B_1}{(z - r_1)} + \frac{B_2}{(z - r_2)} + \cdots + \frac{B_K}{(z - r_K)}.$$

From the definition of $S(z)$, z is a factor in $S(z)$, so there is no need for a $z^{-1}B_0$ term in the partial fraction expansion. Multiplying by z , we have

$$S(z)H(z) = \frac{B_1 z}{(z - r_1)} + \frac{B_2 z}{(z - r_2)} + \cdots + \frac{B_K z}{(z - r_K)},$$

from which we can easily recover the sequence

$$y_s[n] = \sum_{i=1}^K B_i (r_i)^n, \quad n \geq 0,$$

which is in the same form as the homogeneous solution that would be obtained from a time-domain solution of the LCCDE.

We can now observe the form of $y_x[n]$. Since we have that

$$y_x[n] = Z^{-1} \{H(z)X(z)\},$$

the partial fraction expansion shows that $y_x[n]$ will involve terms in both $y[n]$ and $x[n]$. We can also rewrite $y_x[n]$ using the convolution property:

$$y_x[n] = \sum_{m=0}^n h[m]x[n-m],$$

where

$$\begin{aligned} h[m] &= Z^{-1} \{H(z)\} = Z^{-1} \left\{ z \frac{H(z)}{z} \right\} \\ &= Z^{-1} \left\{ z \left(\frac{D_0}{z} + \frac{D_1}{z - r_1} + \cdots + \frac{D_K}{z - r_K} \right) \right\} \\ &= \begin{cases} D_0 + \sum_{i=1}^K D_i (r_i)^n, & n = 0 \\ \sum_{i=1}^K D_i (r_i)^n, & n \geq 1. \end{cases} \end{aligned}$$

So, we see that $y_x[n]$ is given by a convolution of the input with $h[n] = Z^{-1}\{H(z)\}$. Note that the sequence $h[n], n \geq 0$, can be interpreted as the system unit pulse response (u.p.r), or impulse response, assuming zero initial conditions.

Definition

The unit-pulse sequence, or the discrete-time impulse, is given by

$$\delta[n] = \begin{cases} 1, & n = 0 \\ 0, & n \neq 0. \end{cases}$$

The system response to a unit pulse, or discrete-time impulse, is given by

$$y[n] = y_x[n] \big|_{\text{assuming zero initial conditions}} = \sum_{m=0}^n h[m]\delta[n-m] = h[n].$$

We can explore the use of the impulse response to derive the response to more general signals through another example.

Example

Consider the following linear system with input $x[n]$ and output $y[n]$ as shown in Figure 4.4 .

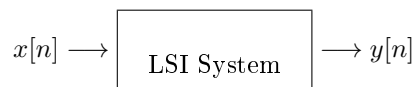


Figure 4.4: A linear shift-invariant system.

Suppose that when the input $x[n] = \delta[n]$ with zero initial conditions, then the output satisfies $y[n] = a^n$ for $n \geq 0$. Again, assuming zero initial conditions (i.e. that the system is *initially at rest*), determine $y[n]$ due to the input $x[n] = b^n, n \geq 0$.

Solution

Given $h[n] = a^n, n \geq 0$, we know that the output satisfies $y[n] = y_x[n]$, since the initial conditions are all zero, i.e. the system is initially at rest. We know from the convolution property that

$$\begin{aligned} y[n] &= \sum_{m=0}^n a^m b^{n-m} = b^n \sum_{m=0}^n \left(\frac{a}{b}\right)^m \\ &= \frac{b^{n+1}}{b} \frac{1 - \left(\frac{a}{b}\right)^{n+1}}{1 - \frac{a}{b}}, \quad a \neq b \\ &= \frac{b^{n+1} - a^{n+1}}{b - a}, \quad a \neq b. \end{aligned}$$

Comments

This discussion and these examples lead us to a number of conclusions about the solutions to linear constant coefficient difference equations. First, we can show (and we will see in the next sections) that the solution to a linear constant coefficient difference equation will have a essentially the same form when the input is merely shifted in time. Also, we will see that a similar form is maintained for inputs that are linear combinations of shifted versions of the input. For example, the response to an input of the form $x[n]$ will be similar in form to the response to the input $x[n] - 2x[n-1]$. We will also see that the solution methods developed here, as well as the unilateral z-transform, can be modified to accommodate situations when the input is applied earlier or later than for $n = 0$. While we discussed situations here that included both the zero-input response and the zero-state response, in practice we are generally interested in the zero-state response, or equivalently, we are interested in the response to an input when the system of interest is initially at rest. The reason for this is that we either have a system where the initial conditions are all zero, or for a stable system, such that the roots of the characteristic polynomial are all of modulus less than unity, $|r_i| < 1$, and that after some time, $y_s[n]$ has sufficiently decayed, such that for time scales of interest for a given application, $y[n] \approx y_x[n]$. As a result, from this point forward, we will assume that systems under discussion are initially at rest, and that all initial conditions are set to zero. As a result, the output of a linear system will be taken as the zero-state response, and we will be interested in the convolution relationship between the input and the output.

4.6 Two-sided z-transform

When the input to a discrete-time LSI system is of the form z^n for all n , i.e. the two-sided sequence that has non-zero terms for arbitrarily large positive and negative n , the output of the system is simply a scaled version of the input. This is the *eigenfunction* property of LSI systems in discrete-time. The eigenfunction property of continuous-time systems tells us that when the input to a continuous-time LTI system is of the form e^{st} for all t , then the output will be a scaled version of the input. This is easily shown as a consequence of the convolution integral for LTI systems

$$y(t) = \int_{-\infty}^{\infty} h(\tau) x(t - \tau) d\tau,$$

where $h(\tau)$ is the impulse response of the continuous-time LTI system. Letting the input take the form of a complex exponential, we have

$$\begin{aligned} y(t) &= \int_{-\infty}^{\infty} h(\tau) e^{s(t-\tau)} d\tau \\ &= e^{st} \int_{-\infty}^{\infty} h(\tau) e^{-s\tau} d\tau \\ &= e^{st} H(s), \end{aligned}$$

where $H(s)$ is the Laplace transform of the impulse response, when the integral exists. We call the signals of the form e^{st} eigenfunctions of continuous-time LTI systems, since they satisfy the property that, when taken as input to an LTI system, they produce an output that is identical except for a (possibly complex) scale factor. The scale factor $H(s)$ is called the eigenvalue associated with the eigenfunction. Note that eigenvalue for a given s is the same as the Laplace transform of the impulse response, evaluated at that value of s . The only signals that have this property, i.e. the only eigenfunctions for LTI systems, are signals of the form e^{st} , for different possible values of the complex parameter s . Note that sinusoids are not eigenfunctions for LTI systems! That means that if a sinusoid is input to an LTI system, the output will not be a simple scaled version of the input. However, since a sinusoid can be simply constructed as a sum of two such eigenfunctions, we can easily see what the output will be:

$$\begin{aligned} y(t) &= \int_{-\infty}^{\infty} h(\tau) \cos(\omega(t-\tau)) d\tau \\ &= \int_{-\infty}^{\infty} h(\tau) \frac{1}{2} \left(e^{j\omega(t-\tau)} + e^{-j\omega(t-\tau)} \right) d\tau \\ &= \int_{-\infty}^{\infty} h(\tau) \frac{1}{2} \left(e^{j\omega(t-\tau)} \right) d\tau + \int_{-\infty}^{\infty} h(\tau) \frac{1}{2} \left(e^{-j\omega(t-\tau)} \right) d\tau \\ &= \frac{1}{2} \left(e^{j\omega t} H(j\omega) + e^{-j\omega t} H(-j\omega) \right). \end{aligned}$$

Now, if the impulse response is a purely real-valued function, then its Fourier transform will have complex conjugate symmetry, such that

$$\begin{aligned} y(t) &= \frac{1}{2} \left(e^{j\omega t} H(j\omega) + e^{-j\omega t} H^*(j\omega) \right) \\ &= \frac{1}{2} \left(e^{j\omega t} |H(j\omega)| e^{j\angle H(j\omega)} + e^{-j\omega t} |H(j\omega)| e^{-j\angle H(j\omega)} \right) \\ &= \frac{1}{2} |H(j\omega)| \left(e^{j\omega t} e^{j\angle H(j\omega)} + e^{-j\omega t} e^{-j\angle H(j\omega)} \right) \\ &= |H(j\omega)| \cos(\omega t + \angle H(j\omega)). \end{aligned}$$

While the output is not simply a scaled version of the input, when we decompose the sinusoid into a sum of two eigenfunctions, we can use linearity of the LTI system to construct the output as a sum of the two eigenfunction outputs.

Returning to discrete-time LSI systems, when the input to an LSI system is of the form z^n for all n , the

convolution sum yields that

$$\begin{aligned} y[n] &= \sum_{m=-\infty}^{\infty} h[m]z^{(n-m)} \\ &= z^n \sum_{m=-\infty}^{\infty} h[m]z^{-m} \\ &= z^n H(z), \end{aligned}$$

when the sum converges. Once again, we call signals of the form z^n eigenfunctions of discrete time LSI systems, and the associated eigenvalues, $H(z)$, correspond to the two-sided z-transform of the impulse response, evaluated at the particular value of z .

We define the two-sided z-transform of a sequence $y[n]$ as follows

$$Y(z) = \sum_{n=-\infty}^{\infty} y[n]z^{-n},$$

for values of z for which the sum converges. We call the values of z for which the sum converges the region of convergence of $Y(z)$, or simply the ROC_Y . Note that as with the unilateral z-transform, the two-sided (or bilateral) z-transform is again a complex function of a complex variable, meaning that it can take on complex values and that its argument is itself a complex variable.

For the two-sided transform, we can consider again a few example sequences for which the sequence values are non-zero for both positive and negative index values.

Example

Consider the following sequence,

$$y[n] = a^n u[n] + b^n u[-n-1] = \begin{cases} a^n, & n \geq 0 \\ b^n, & n < 0. \end{cases}$$

Now, using the definition of the z-transform, we have for this sequence,

$$\begin{aligned} Y(z) &= \sum_{n=-\infty}^{\infty} (a^n u[n] + b^n u[-n-1]) z^{-n} \\ &= \sum_{n=-\infty}^{\infty} (a^n u[n]) z^{-n} + \sum_{n=-\infty}^{\infty} (b^n u[-n-1]) z^{-n} \\ &= \sum_{n=0}^{\infty} a^n z^{-n} + \sum_{n=-\infty}^{-1} b^n z^{-n} \\ &= \sum_{n=0}^{\infty} \left(\frac{a}{z}\right)^n + \sum_{n=-\infty}^{-1} \left(\frac{b}{z}\right)^n \\ &= \frac{z}{z-a}, |z| > |a| + \sum_{n=-\infty}^{-1} \left(\frac{b}{z}\right)^n \\ &= \frac{z}{z-a}, |z| > |a| + \sum_{m=1}^{\infty} \left(\frac{z}{b}\right)^m \\ &= \frac{z}{z-a}, |z| > |a| + \frac{z}{b-z}, |z| < |b|, \end{aligned}$$

where we must combine the two conditions on $|z|$, to ensure convergence of both of the summations in the expression. Otherwise, one of the terms in the expression will be invalid, and the resulting algebraic expression will not be meaningful. Hence, we have

$$Y(z) = \frac{z}{z-a} + \frac{z}{b-z}, |a| < |z| < |b|.$$

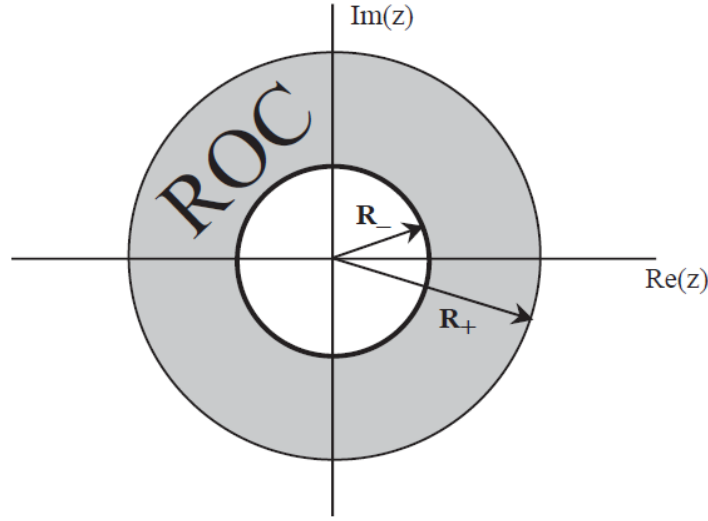


Figure 4.5: Region of convergence of the two-sided z-transform for a two-sided sequence.

Note that the region of convergence, ROC_Y , in this case is a ring, or annulus, in the complex plane as shown in Figure 4.5.

In this example,

$$R_- = |a|, \quad R_+ = |b|.$$

If $|a| \geq |b|$ then ROC_Y would be the empty set and z-transform would be undefined (i.e. is infinite) for all z . The reason that the region of convergence turns out to be a ring in the complex plane comes from properties of the summations that were assumed to converge in deriving the algebraic expression for the resulting z-transform. Specifically, looking at the definition of the z-transform, we obtain

$$Y(z) = \underbrace{\sum_{n=-\infty}^{-1} y[n]z^{-1}}_{\text{converges for } z \text{ small enough, i.e. } |z| < R_+} + \underbrace{\sum_{n=0}^{\infty} y[n]z^{-1}}_{\text{converges for } z \text{ large enough, i.e. } |z| > R_-}.$$

Note that R_- is determined by $y[n], n \geq 0$ and R_+ is determined by $y[n], n < 0$. If $y[n] = 0$ for $n < 0$, then we have

$$Y(z) = \sum_{n=0}^{\infty} y[n]z^{-n}$$

and $R_+ = \infty$, which is essentially a one-sided (unilateral) z-transform. As a result, the region of convergence corresponds to $|z| > R_-$, as in Figure 4.6.

If $y[n] = 0$ for $n > 0$, then we have that

$$Y(z) = \sum_{n=-\infty}^0 y[n]z^{-n}$$

and $R_- = 0$, which implies that the region of convergence corresponds to a solid disk in the complex plain, i.e. we have $|z| < R_+$ as in Figure 4.7. Note that in contrast to the one-sided z-transform, the two-sided z-transform can accommodate a wider range of signal behaviors, since they can be left-sided, right-sided, or two-sided and still have a bilateral z-transform. As such, we must state the ROC for $Y(z)$ to uniquely identify $y[n]$.

A *right-sided sequence* is one that is zero for all n before some time index, i.e. $y[n] = 0, n < n_0$, for some n_0 . A *left-sided sequence* is one that is zero for all n after some index, i.e. $y[n] = 0, n > n_0$, for some n_0 , and

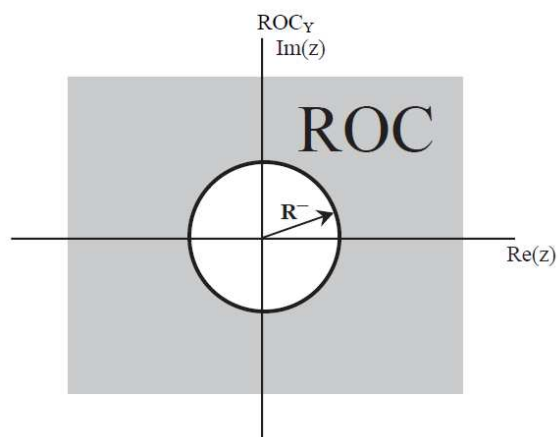


Figure 4.6: Region of convergence for a right sided sequence.

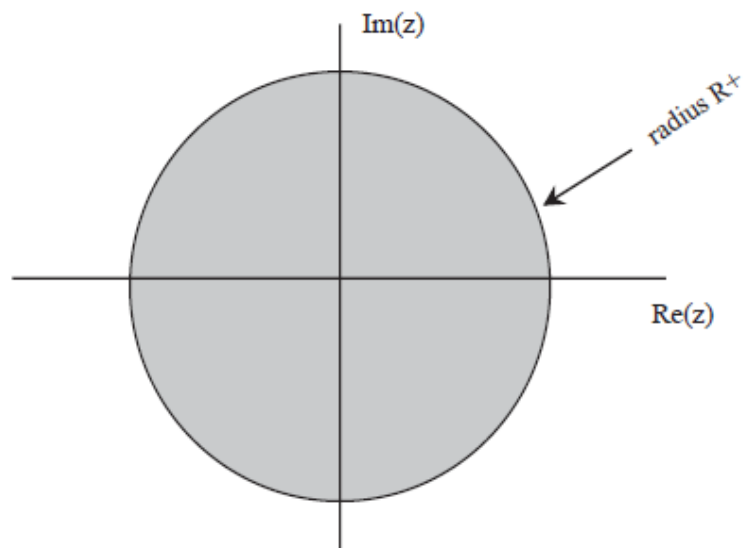


Figure 4.7: Region of convergence for a left-sided sequence.

a *two-sided sequence* is one that is neither left-sided nor right sided, i.e. it has non-zero terms for arbitrarily large positive and negative indices. Examples of a right-sided sequence, include the unit step sequence, $u[n]$, and the complex exponential sequence $a^n u[n]$. An example left-sided sequence could be $u[-n]$ or $a^n u[-n-1]$. A two-sided sequence is one such as $a^{-|n|}$, where, for $|a| < 1$ is a decaying geometric sequence for positive and negative n . Since the two-sided z-transform multiplies the sequence $y[n]$ by z^{-n} and then sums the resulting modulated sequence for each value of z , in $Y(z)$, then whether a sequence is left-sided, rightsided or two-sided play an important role in the convergence (and the ROC) of the z-transform. Specifically, a right-sided sequence will have an infinite number of terms for large positive n , and, hence, the z-transform can converge when the magnitude of z is sufficiently large that z^{-n} dominates, making the sequence convergent. Therefore, right-sided sequences will have a ROC that is the entire z-plane outside of a circle of some radius (with the possible exception of infinity). Similarly, a left-sided sequence can converge when the magnitude of z is sufficiently small, such that z^{-n} , for large negative n decays sufficiently rapidly to dominate, making the series convergent. Therefore, a left-sided sequence will have a ROC for a disc-shaped region in the complex plane (with the possible exception of zero). A two-sided sequence, having both left-sided and right-sided elements must balance the effects such that the ROC will result in an annulus (ring) in the complex plane.

Example

Consider the following two sequences,

$$\begin{aligned} x[n] &= -(a^n)u[-n-1] = \begin{cases} -(a^n), & n < 0 \\ 0, & n \geq 0 \end{cases} \\ y[n] &= a^n u[n] = \begin{cases} a^n, & n \geq 0 \\ 0, & n < 0. \end{cases} \end{aligned}$$

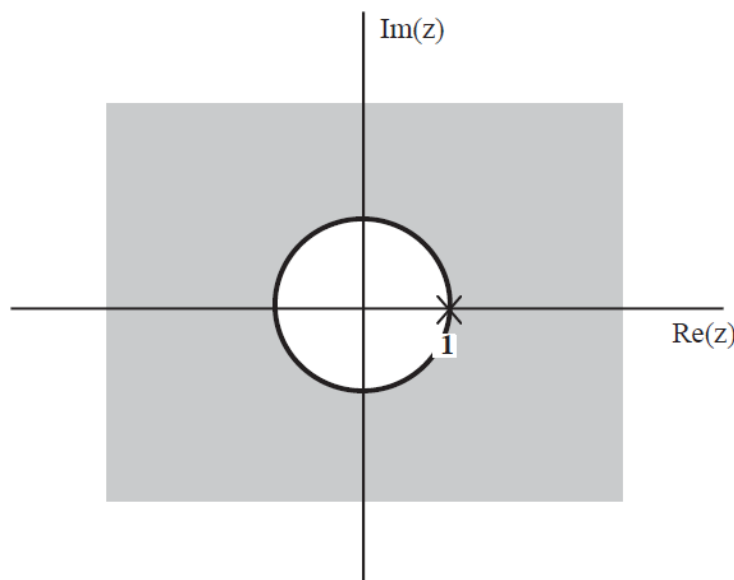
For $x[n]$, we have

$$\begin{aligned} X(z) &= \sum_{n=-\infty}^{\infty} x[n]z^{-n} \\ &= - \sum_{n=-\infty}^{-1} a^n z^{-n} \\ &= - \sum_{n=-\infty}^{-1} \left(\frac{a}{z}\right)^n \\ &= - \sum_{k=1}^{\infty} \left(\frac{z}{a}\right)^k \\ &= \frac{\frac{z}{a}}{\frac{z}{a} - 1}, \left|\frac{z}{a}\right| < 1 \\ &= \frac{z}{z - a}, |z| < |a|. \end{aligned}$$

Similarly, we have already seen that

$$Y(z) = \frac{z}{z - a}, |z| > |a|.$$

So, we see that the *algebraic form* of $X(z)$ and $Y(z)$ are identical, but they are not the same functions, since they are defined on completely different regions of the complex plane. The z-transform of a sequence is not simply defined by the algebraic expression alone, but rather, the combination of the algebraic expression together with the region of convergence. In order to uniquely specify a sequence from its z-transform, we must include both the algebraic form as well as the region of the complex plane over which the form is valid. This leads to the following set of relations.

Figure 4.8: Region of convergence of the two-sided z-transform of $u[n]$.

uniquely defined sequence	\iff	z-transform and region of convergence
$a^n u[n]$	\iff	$\frac{z}{z-a}, z > a $
$-(a^n)u[-n-1]$	\iff	$\frac{z}{z-a}, z < a $

Poles and Zeros

When sequences correspond to z-transforms that are rational functions (ratios of finite-order polynomials in z), we can explore some of the properties of the sequences and their z-transforms by examining the roots of the numerator and denominator polynomials. These are referred to as the zeros and the poles, respectively, of a rational z-transform. Specifically, for a z-transform given by

$$X(z) = \frac{B(z)}{A(z)}, z \in ROC_X,$$

we refer to the values of z such that $B(z) = 0$, as the zeros of $X(z)$, and the values of z for which $A(z) = 0$, as the poles of $X(z)$. That is,

$$\begin{aligned} \text{zeros:} &= \{z : B(z) = 0\} \\ \text{poles:} &= \{z : A(z) = 0\}, \end{aligned}$$

for rational $X(z)$. Rational z-transforms always have ROCs that are bounded by poles. This means that the ROC is either a disc, an annulus, or the entire plane minus a disc, with the possible exclusion of zero and infinity.

Example

Consider the rational transform

$$Y(z) = \frac{z}{z-1}, |z| > 1,$$

which has a pole at $z = 1$. This corresponds to the sequence $x[n] = u[n]$. The region of convergence for the z-transform is given by $|z| > 1$ as shown in Figure 4.8.

Example

Consider the sequence with rational transform

$$Y(z) = \frac{z}{z-2}, |z| < 2,$$

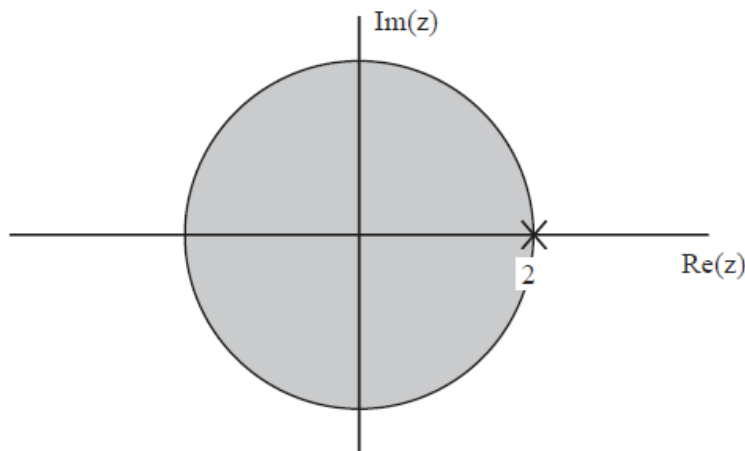


Figure 4.9: Region of convergence of the sequence $-(2^n)u[-n-1]$.

which has a pole at $z = 2$. This corresponds to the sequence $y[n] = -(2^n)u[-n-1]$. The region of convergence is now the disk shown in Figure 4.9.

Example

Now consider the sequence with rational transform

$$Y(z) = \frac{z}{(z-2)^2}, \quad |z| < 2,$$

which has a second-order pole at $z = 2$. For multiple poles and a left-sided sequence, we use the same methods we did for the right-sided case. We can easily show that

$$na^n u[-n-1] \iff \frac{-az}{(z-a)^2}, \quad |z| < |a|.$$

Thus, we have that

$$y[n] = -\frac{1}{2}n(2^n)u[-n-1].$$

Example

Now consider the sequence with rational transform given by

$$Y(z) = \frac{z}{z-1} + \frac{z}{z-2}, \quad 1 < |z| < 2,$$

which has poles at $z = 1$ and $z = 2$. The region of convergence is therefore an annulus in the complex plane, and the sequence will turn out to be two sided,

$$\begin{aligned} y[n] &= \begin{cases} 1, & n \geq 0 \\ -(2^n), & n < 0 \end{cases} \\ &= u[n] - (2^n)u[-n-1]. \end{aligned}$$

The region of convergence is depicted in Figure 4.10.

Example

Consider the sequence given by

$$x[n] = \left(\frac{1}{3}\right)^n, \quad -\infty < n < \infty.$$

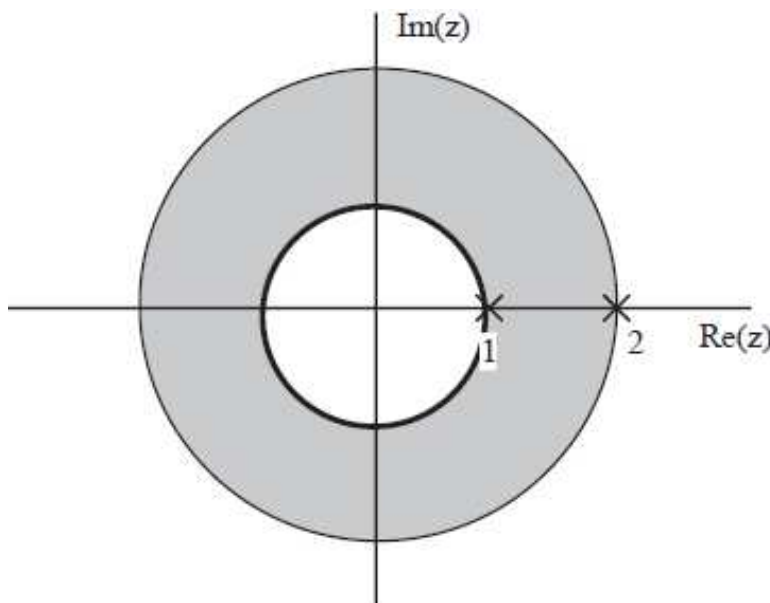


Figure 4.10: Region of convergence for the sequence $y[n] = u[n] - (2^n)u[-n-1]$.

For such a two-sided sequence, does the two-sided z-transform, $X(z)$ exist? Let us examine the z-transform of the sequence from the definition, from which we have

$$\begin{aligned} X(z) &= \sum_{n=-\infty}^{\infty} \left(\frac{1}{3}\right)^n z^{-n} \\ &= \sum_{n=-\infty}^{-1} \left(\frac{1}{3}\right)^n z^{-n} + \sum_{n=0}^{\infty} \left(\frac{1}{3}\right)^n z^{-n}. \end{aligned}$$

From here, we can see that the first sum will converge for $|z| < \frac{1}{3}$, but the second sum will only converge for $|z| > \frac{1}{3}$. As such, there is no value of z for which both sums will converge. Thus, $X(z)$ does not exist for any z . The z-transform of this sequence cannot be defined, since the sums do not converge.

Example

Now let us consider a slightly different variation on the two-sided above, let

$$x[n] = \left(\frac{1}{3}\right)^{|n|}, \quad -\infty < n < \infty.$$

For this sequence, we might have some hope of finding a range of values of z for which the z-transform will converge, since the sequence remains bounded for all n . In this case we write

$$x[n] = \left(\frac{1}{3}\right)^n u[n] + 3^n u[-n-1].$$

We can transform the right-sided and left-sided pieces individually, and add the results, by linearity of the transform, taking into account the regions in the complex plane for which the series will converge. Since each series has a different region of convergence, we need to consider, for the total sequence, only that portion of the complex plane that is common to both the ROC for the right-sided part and the left-sided part. That is, we need to know for which values of the complex plain will the total z-transform converge. This leads us to the following transform for the sequence:

$$X(z) = \frac{z}{z - \frac{1}{3}} - \frac{z}{z - 3}, \quad \frac{1}{3} < |z| < 3.$$

This transform brings to bear an important property of the region of convergence for a two-sided z-transform, i.e. the two-sided transform of a two-sided sequence. If the algebraic form for a z-transform is $A(z)$, e.g. $X(z) = A(z)$, $z \in ROC_X$, where

$$A(z) = \frac{N(z)}{(z - p_1)(z - p_2) \cdots (z - p_N)},$$

then ROC_X is generally smaller than the set of z where $A(z)$ alone is well defined. Indeed, $A(z)$ is well defined at all z except the pole locations $z = p_i$, $1 \leq i \leq N$, whereas ROC_X must be a ring in the complex plane. It is important to remember that the z-transform of a sequence is not defined solely by an algebraic expression, but rather by the combination of an algebraic expression and the region of the complex plane over which the expression is correct. Outside of this region, the algebraic expression is not the z-transform of the sequence of interest. Some points to remember are that

1. Poles cannot lie in ROC_X (because even $A(z)$ is undefined at the pole locations).
2. ROC_X is generally smaller than the set of z where $A(z)$ is defined.
3. The z-transform, $X(z)$, is given by the pair of $A(z)$ and ROC_X .

Another example that will illustrate this point follows.

Example

Let the sequence $x[n]$ be defined as $x[n] = \left(\frac{1}{2}\right)^n u[n]$. The z-transform of the sequence can readily be found to be

$$X(z) = \frac{z}{z - \frac{1}{2}}, \quad |z| > \frac{1}{2}.$$

The algebraic form for $X(z)$ is defined everywhere except at $z = \frac{1}{2}$, and yet, the z-transform is not defined for $|z| < \frac{1}{2}$. For example, consider when $z = \frac{1}{4}$, for which we can evaluate the algebraic expression to be

$$\left. \frac{z}{z - \frac{1}{2}} \right|_{z=\frac{1}{4}} = -1.$$

However, this does not imply that $X(\frac{1}{4}) = -1$. Indeed, at $z = \frac{1}{4}$, $X(z)$ is not defined, since this is not in the region of convergence of the z-transform, i.e.,

$$X\left(\frac{1}{4}\right) = \sum_{n=-\infty}^{\infty} \left(\frac{1}{2}\right)^n u[n] z^{-n} \bigg|_{z=\frac{1}{4}} = \sum_{n=0}^{\infty} 2^n,$$

which clearly fails to converge.

4.7 Properties of the two-sided z-transform

4.7.1 Linearity

When two sequences $x[n]$ and $y[n]$ have a two-sided z-transforms, $X(z)$ and $Y(z)$, respectively, then the superposition of these sequences will also have a two-sided z-transform, so long as $X(z)$ and $Y(z)$ are jointly defined on a non-null subset of the z-plane. Specifically, we have

$$w[n] = ax[n] + by[n] \iff W(z) = aX(z) + bY(z), \quad ROC_W \supseteq ROC_X \cap ROC_Y,$$

that is, the region of convergence is at least as large as the intersection $ROC_X \cap ROC_Y$.

Example

Let us consider $w[n] = x[n] + y[n]$ with

$$\begin{aligned} X(z) &= \frac{z}{(z+2)(z+3)}, \quad |z| < 2, \\ Y(z) &= \frac{2}{z+2}, \quad |z| < 2, \end{aligned}$$

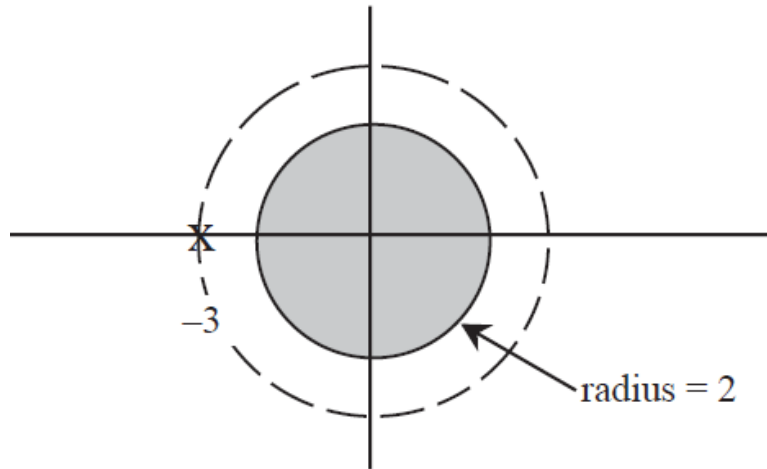


Figure 4.11: Region of convergence for the sum of two sequences.

from which we have that

$$\begin{aligned}
 W(z) &= X(z) + Y(z) \\
 &= \frac{z + 2(z + 3)}{(z + 2)(z + 3)} \\
 &= \frac{3(z + 2)}{(z + 2)(z + 3)} \\
 &= \frac{3}{z + 3}.
 \end{aligned}$$

Now, the region of convergence of this expression must be determined. We know two things,

1. The ROC is bounded by poles
2. The ROC contains $ROC_X \cap ROC_Y$.

For this example, there is a pole at $z = -3$. We also have that $ROC_X \cap ROC_Y = \{z : |z| < 2\}$ as shown in Figure 4.11.

We now can see that the proper region of convergence must be $ROC_W = \{z : |z| < 3\}$. So, the ROC can be larger than the intersection if we have pole-zero cancellation on the boundary of intersection, in which case, the ROC expands outward or inward to be bounded by another pole.

4.7.2 Shifting property

For the two-sided z-transform, the shifting properties are much simpler than their counterparts in the unilateral z-transform, since we do not need to worry about terms shifting in-to or out-of the summation defining the z-transform. We simply have

$$x[n] \longleftrightarrow X(z) \iff x[n - k] \longleftrightarrow z^{-k} X(z)$$

and the region of convergence of the shifted sequence remains unchanged, except for the possible addition or deletion of $z = 0$ or $|z| = \infty$.

Example

Consider the sequence $x[n] = \delta[n - 2]$ for which we have $Y(z) = z^{-2}$, $|z| > 0$. now, if we let $y[n] = x[n + 3] = \delta[n + 1]$, then we have $Y(z) = z$, $|z| < \infty$. In this case, we see that $z = 0$ was added to the region

of convergence and $|z| = \infty$ was removed from the region of convergence. The proof of the shifting property follows that for the unilateral z-transform, only simpler. We have

$$\begin{aligned}
 X(z) &= \sum_{n=-\infty}^{\infty} x[n]z^{-n} \\
 Y(z) &= \sum_{n=-\infty}^{\infty} y[n]z^{-n} \\
 &= \sum_{n=-\infty}^{\infty} x[n-k]z^{-n} \\
 &= \sum_{m=-\infty}^{\infty} x[m]z^{-(m+k)} \\
 &= z^{-k} \sum_{m=-\infty}^{\infty} x[m]z^{-m} \\
 &= z^{-k} X(z),
 \end{aligned}$$

where in the fourth line, the change of variable $m = n - k$ was made.

4.7.3 Convolution

The convolution property for the two-sided z-transform follows similarly from the unilateral case, for which we have

$$y[n] = \sum_{m=-\infty}^{\infty} h[m]x[n-m] \iff Y(z) = H(z)X(z), \text{ } ROC_Y \supseteq ROC_X \cap ROC_H,$$

so long as there exists a non-null intersection $ROC_X \cap ROC_H$. Just as with linearity, if there is pole-zero cancellation on a boundary of the intersection, then ROC_Y expands to the next pole.

Example

Consider the sequences $x[n]$ and $h[n]$ for which we have z-transforms $X(z)$ and $H(z)$ and define $Y(z)$ as follows

$$Y(z) = H(z)X(z),$$

where

$$\begin{aligned}
 H(z) &= \frac{1}{(z+1)(z+2)}, \quad 1 < |z| < 2, \\
 X(z) &= \frac{z+1}{z+2}, \quad |z| < 2.
 \end{aligned}$$

Note that $ROC_H \cap ROC_X = \{z : 1 < |z| < 2\}$, however we have that $ROC_Y = \{z : |z| < 2\}$.

The convolution formula can be readily shown by taking the z-transform of both sides of the convolution sum. Since each of the steps in this derivation is reversible, this shows the if and only if nature of the

convolution property. Specifically, we have

$$\begin{aligned}
 y[n] &= \sum_{m=-\infty}^{\infty} h[m]x[n-m] \\
 Y(z) &= \sum_{n=-\infty}^{\infty} \left(\sum_{m=-\infty}^{\infty} h[m]x[n-m] \right) z^{-n} \\
 &= \sum_{m=-\infty}^{\infty} h[m] \left(\sum_{n=-\infty}^{\infty} x[n-m]z^{-n} \right) \\
 &= \left(\sum_{m=-\infty}^{\infty} h[m]z^{-m} \right) X(z) \\
 &= H(z)X(z).
 \end{aligned}$$

4.8 The system function and poles and zeros of an LSI system

The transfer function of an LSI system with input $x[n]$ and output $y[n]$ is defined for two-sided z-transforms using

$$H(z) = \frac{Y(z)}{X(z)} \Big|_{\text{zero initial conditions.}}$$

Indeed, we have seen that $H(z)$ is independent of $X(z)$, and therefore independent of $x[n]$. For an LSI system, we can find $H(z)$ by a number of means. For example, we can

1. Directly compute the z-transform of $h[n]$ using the two-sided z-transform.
2. Compute the quantity $H(z) = Y(z)/X(z)$, for a given pair of input and output sequences $x[n]$ and $y[n]$.
3. Determine $H(z)$ directly from a block diagram description of the LSI system.

To further examine the last option, we will consider in more detail the methods used for analysis of LSI systems using a block diagram comprising delay, adder, and gain elements in Section 4.10.

4.9 Inverse two-sided z-transform

When taking an inverse two-sided z-transform, we can, once again, consider the complex contour-integral that defines its direct inversion, or, more simply, use methods such as partial fraction expansion to reduce a rational z-transform into a superposition of simpler terms, each of which can be inverted one at a time. Unlike the unilateral z-transform, for each term in the partial fraction expansion, we now must consider the region of convergence of the overall transform and select the appropriate inverse transform sequence whose ROC would intersect with that of the overall transform to be inverted. To capture this notion graphically, consider Figure 4.12.

The poles that lie outside the ROC, i.e. those poles located such that $|p_i| > R_+$ correspond to terms in the partial fraction expansion for which a left-sided inverse must be selected. The poles that lie inside the ROC, that is those poles located such that $|p_k| < R_-$ correspond to terms in the partial fraction expansion for which a right-sided inverse must be selected. These facts can be readily deduced as follows. The poles that lie inside the inner ring, i.e. those for which $|p_i| < R_-$ must have a term in the partial fraction expansion for which the ROC for each pole intersects that of the overall z-transform. Since the poles are inside the ROC, the only possibility (out of the two choices, $|z| < |p_i|$ and $|z| > |p_i|$) that could possibly overlap with that of the overall ROC, $R_- < |z| < R_+$ is $|z| > |p_i|$, which implies that each of these poles, labeled p_i^{RHS} correspond to right-sided inverse transforms, of the form $p_i^n u[n]$, assuming that the poles are not repeated roots. Similarly, the poles that lie outside the outer ring, i.e. those for which $|p_k| > R_+$ must have a term in the partial fraction expansion for which the ROC for each pole intersects that of the overall z-transform.

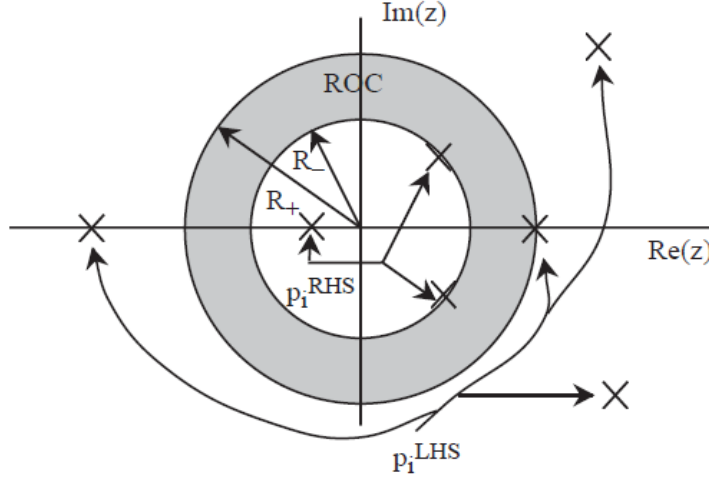


Figure 4.12: A graphical representation of the ROC for a two-sided rational z-transform that includes the locations of the poles.

Since the poles are outside the ROC, the only possibility (out of the two choices, $|z| < |p_k|$ and $|z| > |p_k|$) that could possibly overlap with that of the overall ROC, $R_- < |z| < R_+$ is $|z| < |p_k|$, which implies that each of these poles, labeled p_k^{LHS} correspond to right-sided inverse transforms, of the form $-(p_k^n)u[-n-1]$, assuming again that the poles are not repeated roots.

Example

Let us consider a two-sided z-transform to invert as an example. Let $Y(z)$ be given such that the algebraic form is as follows

$$Y(z) = \frac{z}{(z-1)(z-2)}.$$

From this information alone, we are unable to compute $y[n]$, since there are three different regions of convergence that could be possible for this algebraic expression, and each would lead to a distinct, and different, $y[n]$. The three possibilities are $ROC_1 = \{z : |z| < 1\}$, $ROC_2 = \{z : 1 < |z| < 2\}$, and $ROC_3 = \{z : |z| > 2\}$, depicted in Figure 4.13.

These three possible ROCs lead to three different sequences, since we know that ROC_1 yields a left-sided sequence, $y_1[n]$, ROC_2 yields a two-sided sequence, $y_2[n]$, and ROC_3 yields a right sided sequence, $y_3[n]$. From the partial fraction expansion, we have

$$\begin{aligned} \frac{Y(z)}{z} &= \frac{A}{z-1} + \frac{B}{z-2} \\ Y(z) &= \frac{-z}{z-1} + \frac{z}{z-2}. \end{aligned}$$

The corresponding three inverse transforms would yield,

$$\begin{aligned} y_1[n] &= u[-n-1] - (2^n)u[-n-1], \\ y_2[n] &= -u[n] - (2^n)u[-n-1], \\ y_3[n] &= -u[n] + (2^n)u[n]. \end{aligned}$$

Example

Let us consider another example, this time with the ROC given. Let

$$Y(z) = \frac{z}{(z-2)(z-3)(z-4)}, \quad 2 < |z| < 3.$$

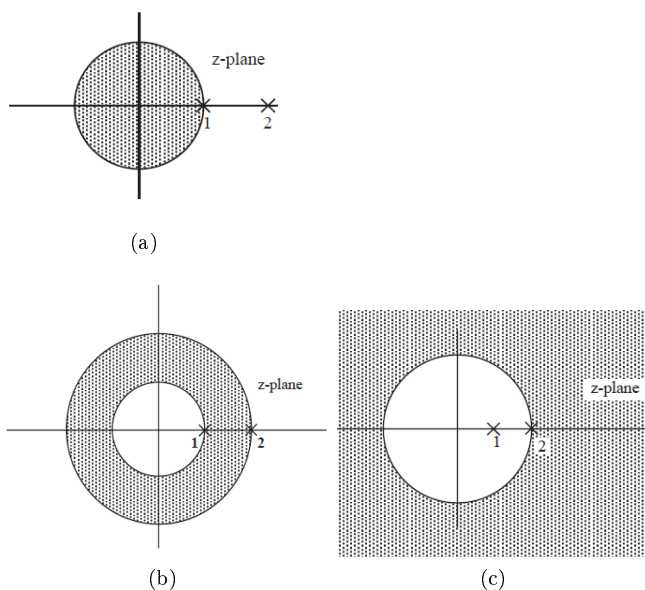


Figure 4.13: Three possible regions of convergence for the algebraic expression for $Y(z)$. Shown in (a) is ROC_1 corresponding to $y_1[n]$, in (b) is ROC_2 for $y_2[n]$ and in (c) is ROC_3 for $y_3[n]$.

From the partial fraction expansion, we have

$$Y(z) = \underbrace{\frac{\frac{1}{2}z}{z-2}}_{\text{right sided}} - \underbrace{\frac{z}{z-3}}_{\text{left sided}} + \underbrace{\frac{\frac{1}{2}z}{z-4}}_{\text{left sided}},$$

which yields,

$$y[n] = \frac{1}{2}(2^n)u[n] + 3^n u[-n-1] - \frac{1}{2}(4^n)u[-n-1].$$

Example

For another example, we consider a sequence with complex poles, i.e.

$$\begin{aligned} X(z) &= \frac{1}{(z+1)^2}, \quad |z| < 1. \\ &= \frac{1}{(z+j)(z-j)}, \end{aligned}$$

for which we have

$$\begin{aligned} \frac{1}{z(z+j)(z-j)} &= \frac{A}{z} + \frac{B}{(z+j)} + \frac{C}{(z-j)} \\ &= \frac{1}{z} + \frac{-\frac{1}{2}}{(z+j)} + \frac{-\frac{1}{2}}{(z-j)}. \end{aligned}$$

This yields,

$$X(z) = 1 - \underbrace{\frac{\frac{1}{2}z}{z+j} - \frac{\frac{1}{2}z}{z-j}}_{\text{left sided}},$$

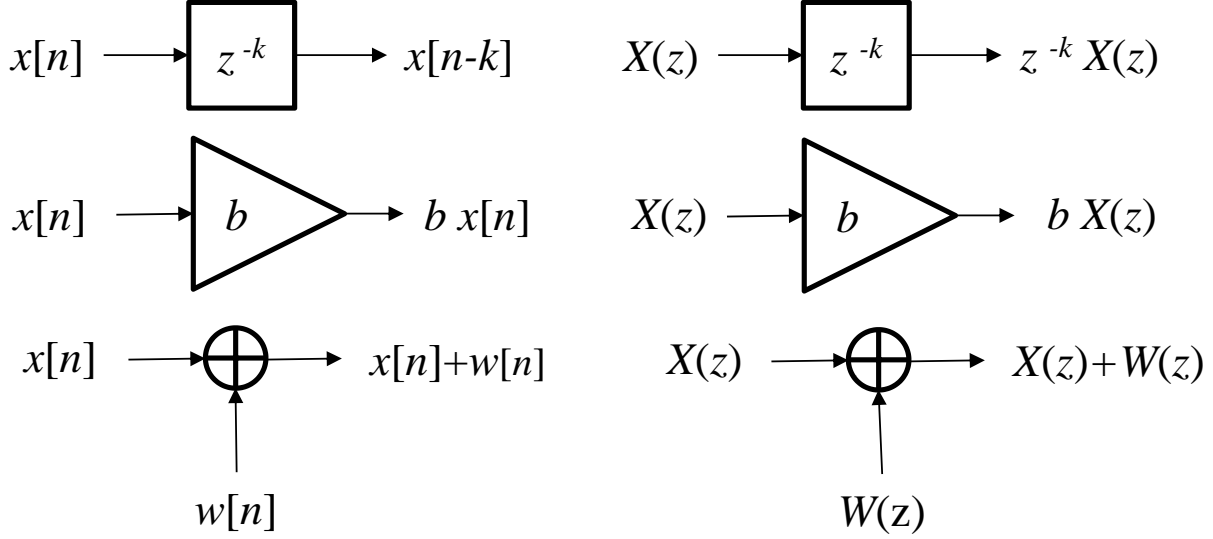


Figure 4.14: Basic elements of a delay-adder-gain flowgraph. To the left, the delay, gain, and adder elements are shown with their corresponding time-domain representation. To the right, the delay, gain and adder blocks are indicated with their corresponding z-transform representation.

from which we can obtain

$$\begin{aligned}
 x[n] &= \delta[n] + \frac{1}{2}(-j)^n u[-n-1] + \frac{1}{2}(j)^n u[-n-1] \\
 &= \delta[n] + \frac{1}{2} \left(e^{-j(\pi/2)n} + e^{j(\pi/2)n} \right) u[-n-1] \\
 &= \delta[n] + \cos\left(\frac{\pi}{2}n\right) u[-n-1] \\
 &= \cos\left(\frac{\pi}{2}n\right) u[-n].
 \end{aligned}$$

4.10 System Block Diagrams

To explore some of the methods for analyzing LSI system properties together with their implementation in hardware, we often use a delay-adder-gain model or flowgraph model for discrete-time LSI structures, with elements shown in Figure 4.14.

Shown in Figure 4.15 is a common delay-adder-gain block diagram for a second-order LSI system. In the figure, the notation for a delay element is that of a box labeled with z^{-1} inside. This is to denote that the operation of a delay element in the z-transform domain (through the delay property of z-transforms) is to multiply the input by z^{-1} . For example, the first delay element in the flowgraph, to the left, takes as input $x[n]$, which we depict in the z-transform domain as $X(z)$. The output of the delay element is the signal $x[n-1]$, i.e. the signal $x[n]$ delayed by one time unit. In the z-transform domain we write $x[n-1]$ as $z^{-1}X(z)$.

The transfer function of the LSI system shown in Figure 4.15 can be shown to be

$$H(z) = \frac{Y(z)}{X(z)} = \frac{b_0 + b_1 z^{-1} + b_2 z^{-2}}{1 - a_1 z^{-1} - a_2 z^{-2}}.$$

This can be shown as follows. First, we note that the flowgraph structure has only one adder node. If we write an equation for the output of the adder node as a function of its inputs, and do so using z-transform

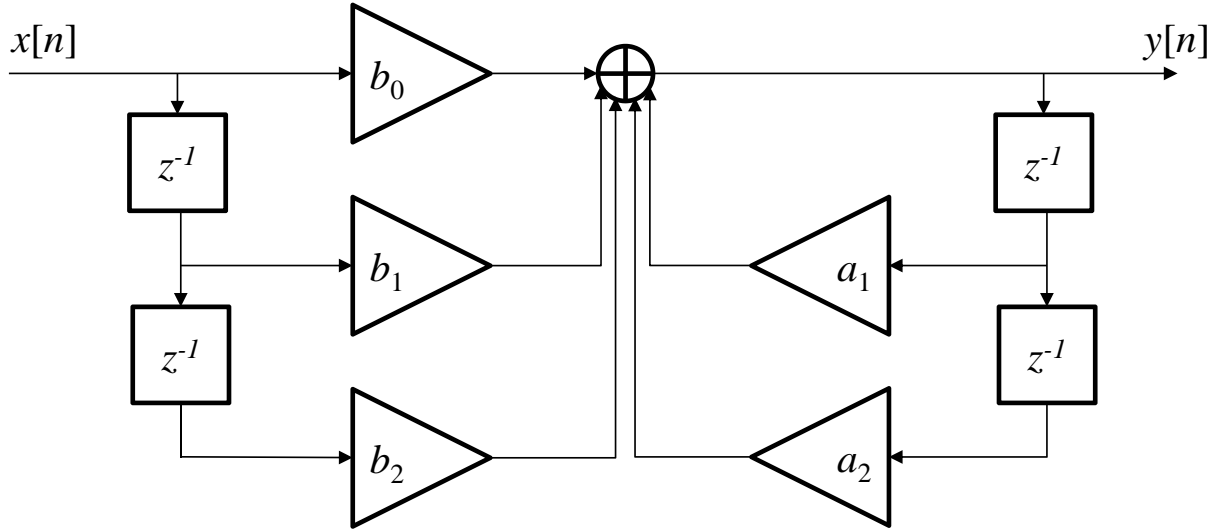


Figure 4.15: A direct-form I structure is a common delay-adder-gain model. Shown is a second-order DFI structure.

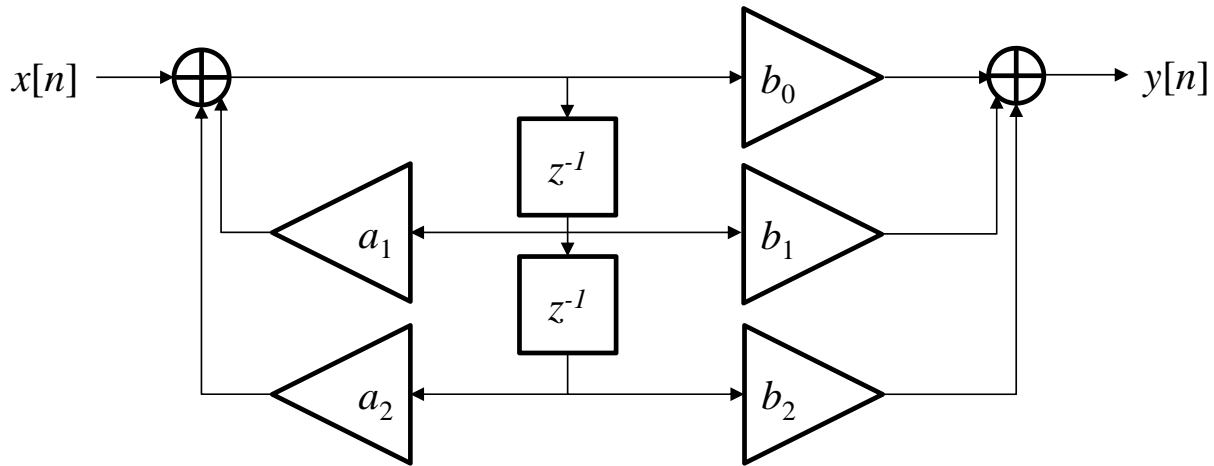


Figure 4.16: A delay-adder-gain model for a second order direct form II structure.

domain representation, using linearity and the delay property, we obtain

$$\begin{aligned}
 Y(z) &= b_0 X(z) + b_1 z^{-1} X(z) + b_2 z^{-2} X(z) + a_1 z^{-1} Y(z) + a_2 z^{-2} Y(z). \\
 Y(z) [1 - a_1 z^{-1} - a_2 z^{-2}] &= X(z) [b_0 + b_1 z^{-1} + b_2 z^{-2}] \\
 H(z) = \frac{Y(z)}{X(z)} &= \frac{b_0 + b_1 z^{-1} + b_2 z^{-2}}{1 - a_1 z^{-1} - a_2 z^{-2}}.
 \end{aligned}$$

A second structure, called a direct form II structure is shown in Figure 4.16.

This structure can also be shown to have the same transfer function given by

$$H(z) = \frac{b_0 + b_1 z^{-1} + b_2 z^{-2}}{1 - a_1 z^{-1} - a_2 z^{-2}}$$

through a method similar to that employed for the direct form I structure. Here we introduce a three-step method that is systematic and guaranteed to determine $H(z)$ for any cycle-free delay adder gain flowgraph. A cycle-free delay adder gain flowgraph is one in which all closed cycles contain at least one delay element. The three steps are as follows.

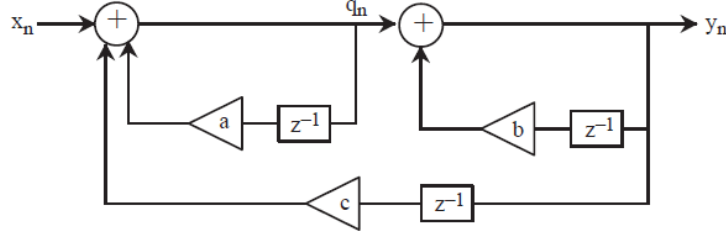


Figure 4.17: Flowgraph of a causal LSI system.

1. Label the output of each adder node in the flowgraph with a unique z-transform domain label.
2. Write an equation setting the output of each adder node in the flowgraph to the sum of the inputs to the adder node.
3. Use the resulting equations to remove all labels except for $X(z)$ and $Y(z)$, to obtain a single input-output relation from which $H(z)$ can be obtained by setting $H(z) = Y(z)/X(z)$.

The three steps are illustrated here for the direct form II structure. First, we note that there are two adder nodes in the flowgraph. The adder node to the left does not have a label, so we introduce a new sequence $q[n]$ as its output and label this $Q(z)$ in the z-transform domain. For this node, we obtain

$$Q(z) = X(z) + a_1 z^{-1} Q(z) + a_2 z^{-2} Q(z).$$

The output of the adder node to the right has already been labeled $y[n]$, so that in the z-transform domain we obtain

$$Y(z) = b_0 Q(z) + b_1 z^{-1} Q(z) + b_2 z^{-2} Q(z).$$

Finally, from these two equations, we can eliminate $Q(z)$ as follows

$$\begin{aligned} Q(z) [1 - a_1 z^{-1} - a_2 z^{-2}] &= X(z) \\ Q(z) &= \frac{X(z)}{1 - a_1 z^{-1} - a_2 z^{-2}} \end{aligned}$$

which can then be substituted into the expression for $Y(z)$ to yield

$$\begin{aligned} Y(z) &= [b_0 + b_1 z^{-1} + b_2 z^{-2}] Q(z) \\ Y(z) &= [b_0 + b_1 z^{-1} + b_2 z^{-2}] \frac{X(z)}{1 - a_1 z^{-1} - a_2 z^{-2}} \\ \frac{Y(z)}{X(z)} &= \frac{b_0 + b_1 z^{-1} + b_2 z^{-2}}{1 - a_1 z^{-1} - a_2 z^{-2}}, \end{aligned}$$

as before. To further illustrate this method, we consider another example.

Example

Consider the LSI system shown in Figure 4.17.

The first step in our three step method is to label the outputs of each of the adder nodes. The first adder node to the left has $q[n]$ as its output and the second adder node has $y[n]$ as its output. For the first adder node, we have

$$Q(z) = X(z) + a z^{-1} Q(z) + c z^{-1} Y(z)$$

and for the second adder node, we have

$$Y(z) = Q(z) + b z^{-1} Y(z).$$

Solving for $Q(z)$, we have

$$Q(z) = Y(z) (1 - b z^{-1}).$$

Plugging this into the other expression, we have

$$\begin{aligned} Y(z)(1 - bz^{-1})(1 - az^{-1}) &= X(z) + cz^{-1}Y(z) \\ Y(z)(1 - (a + b + c)z^{-1} + abz^{-2}) &= X(z) \\ H(z) = \frac{Y(z)}{X(z)} &= \frac{1}{1 - (a + b + c)z^{-1} + abz^{-2}}. \end{aligned}$$

Note that the impulse response $h[n]$ and the system transfer function $H(z)$ are input-output descriptions of discrete-time LSI systems. These are also called “digital filters.” Given an input $x[n]$ we can use either the impulse response to determine the output $y[n]$ through the convolution sum or we can use the system transfer function to compute the output through the z -transform. In this sense, both $h[n]$ and $H(z)$ summarize the behavior of the LSI system. However neither tells us what the internal structure of the digital filter is. Indeed, for any given system transfer function $H(z)$, there are an unlimited number of possible filter structures that have this same transfer function. For a second-order transfer function of the form

$$H(z) = \frac{b_0 + b_1z^{-1} + b_2z^{-2}}{1 - a_1z^{-1} - a_2z^{-2}}$$

just two of the possible realizations are the direct form I and direct form II structures we have just visited. At this point, you may wonder how the filter structure or delay-adder-gain flowgraph relates to the actual filter implementation. The answer to this is multifaceted. For example, let us consider the direct form I structure of Figure 4.15.

If the direct form I structure is implemented in a digital signal processing microprocessor, then we note that there is a system clock that guides the operation of the filter. While the clock is not shown in the flowgraph, we know that the operation of the system depends on shifting values of the input into the system and computing values of the output that are then shifted out. It may take several clock cycles (microprocessor instructions) to compute each single value of the output sequence $y[n]$. For example, if the DSP has a single multiplier/accumulator (MAC), then the clock might trigger the following sequence of instructions

1. multiply $x[n]$ by b_0
2. multiply $x[n - 1]$ by b_1 and add the result to 1)
3. multiply $x[n - 2]$ by b_2 and add the result to 2)
4. multiply $y[n - 1]$ by b_1 and add the result to 3)
5. multiply $y[n - 2]$ by b_2 and add the result to 4) to give $y[n]$.

The values of $x[n], x[n - 1], x[n - 2], y[n - 1], y[n - 2]$ are each stored in memory locations. You might expect that after $y[n]$ is computed, then in preparation for computing $y[n + 1]$ we would use a sequence of instructions to move $x[n + 1]$ into the old location for $x[n]$, move $x[n]$ into the old location for $x[n - 1]$, move $x[n - 1]$ into the old location for $x[n - 2]$, move $y[n]$ into the old location for $y[n - 1]$, and move $y[n - 1]$ into the old location for $y[n - 2]$. However, especially in higher order filters, this would be a huge waste of clock cycles. Instead, a pointer is used to address the proper memory location at each clock cycle. Therefore, it is not necessary to move data from memory location to memory location after computing each $y[n]$.

Just as there are a large number of filter structures that implement the same transfer, there are many algorithms (for a specific DSP) that can implement a given filter structure. Two important factors that you might consider in selecting a particular algorithm are the speed (number of clock cycles required to compute each output value) and the errors introduced through finite-precision effects, due to finite length registers used to represent the real-valued coefficients of the filter as well as the sequence values. We have not yet discussed finite register length effects, i.e. that the DSP has finite length registers for both memory locations as well as for the computations in the arithmetic units. This means that the digital filtering algorithm is not implemented in an exact manner. There will be error at the filter output due to coefficient quantization, and arithmetic roundoff. Of course, longer register lengths will reduce the error at the filter output. Generally, there is a tradeoff between algorithm speed and numerical precision. For a fixed register length, error usually can be reduced by using a more complicated (than Direct Form I or II) filter structure, requiring

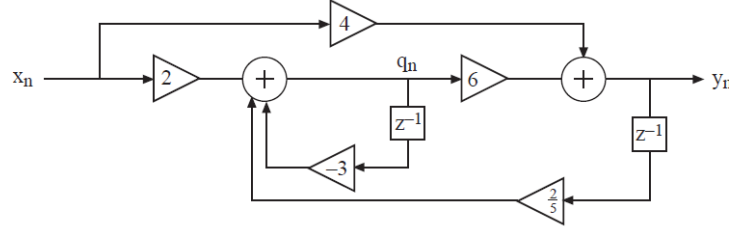


Figure 4.18: System flowgraph example.

more multiplications, additions, and memory locations. This in turn reduces the speed of the filter. The filter structure used in practice depends on $H(z)$ (some transfer functions are more difficult to implement with low error), on the available register length, and on the number of clock cycles available per output.

Example

Find the transfer function of the system in Figure 4.18 and construct a Direct Form II filter structure that implements the same transfer function.

We immediately label the output of the two adder nodes with the labels $y[n]$ and $q[n]$. From these we can then write

$$\begin{aligned} Y(z) &= 6Q(z) + 4X(z) \\ Q(z) &= 2X(z) - 3z^{-1}Q(z) + \frac{2}{5}z^{-1}Y(z). \end{aligned}$$

We can reduce these equations using

$$\begin{aligned} Q(z)(1 + 3z^{-1}) &= 2X(z) + \frac{2}{5}z^{-1}Y(z) \\ Q(z) &= \frac{2X(z) + \frac{2}{5}z^{-1}Y(z)}{(1 + 3z^{-1})} \end{aligned}$$

which yields

$$\begin{aligned} Y(z) &= 6 \frac{2X(z) + \frac{2}{5}z^{-1}Y(z)}{(1 + 3z^{-1})} + 4X(z) \\ Y(z) \left(1 - \frac{\frac{12}{5}z^{-1}}{1 + 3z^{-1}} \right) &= \left(\frac{12}{(1 + 3z^{-1})} + 4 \right) X(z) \\ H(z) = \frac{Y(z)}{X(z)} &= \frac{\left(\frac{12}{(1 + 3z^{-1})} + 4 \right)}{\left(1 - \frac{\frac{12}{5}z^{-1}}{1 + 3z^{-1}} \right)} \\ H(z) &= \frac{(16 + 12z^{-1})}{(1 + \frac{3}{5}z^{-1})}. \end{aligned}$$

The Direct Form II structure having this transfer function is now given in Figure 4.19 .

This structure is far simpler than the previous one and it computes exactly the same output $y[n]$. It is important to note that digital filter structures cannot have delay-free loops.

Example

Consider the filter structure shown in Figure 4.20.

This flowgraph depicts a system that is unrealizable. If we attempt to determine the input-output relation, we find

$$y[n] = x[n] + 3y[n] + 2y[n-1],$$

however the adder node has a delay-free loop which implies that the output at time n requires the addition of terms that include the output at time n . It is impossible therefore to compute $y[n]$ at any n .

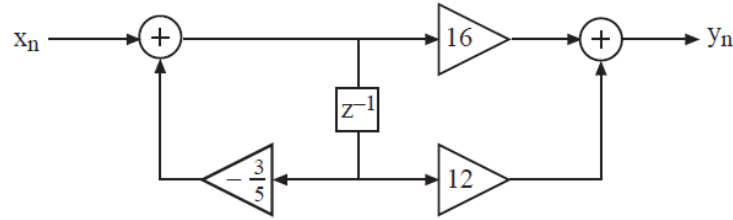


Figure 4.19: Direct Form II structure for this example.

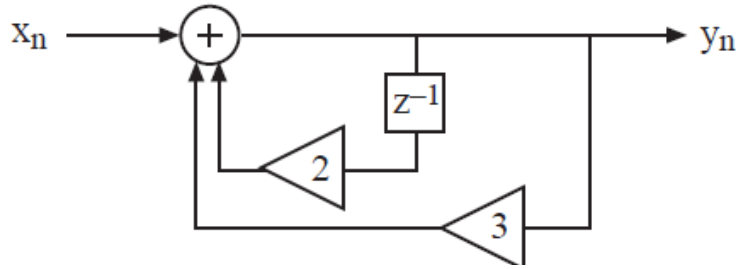


Figure 4.20: An unrealizable digital filter structure.

Consider the system shown in Figure 4.21 below.

We can immediately write that

$$W(z) = H_1(z)X(z)$$

and that

$$Y(z) = H_2(z)W(z)$$

which leads to

$$\begin{aligned} Y(z) &= H_2(z)H_1(z)X(z) \\ \frac{Y(z)}{X(z)} &= H(z) = H_2(z)H_1(z) = H_1(z)H_2(z), \end{aligned}$$

where the last line follows from commutativity of multiplication of z-transforms. This is known as a cascade combination of two LSI systems.

Consider the system shown in Figure 4.22 below.

We can immediately write that

$$\begin{aligned} Y(z) &= H_1(z)X(z) + H_2(z)X(z) \\ &= (H_1(z) + H_2(z))X(z) \end{aligned}$$

which yields that

$$H(z) = \frac{Y(z)}{X(z)} = (H_1(z) + H_2(z))X(z).$$

This is known as a parallel combination of two LSI systems.

A feedback connection of two LSI systems is depicted in Figure 4.23.

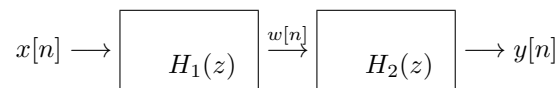


Figure 4.21: A cascade of two LSI systems.

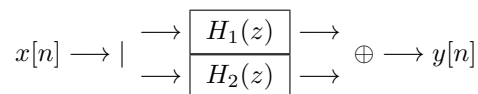


Figure 4.22: A parallel combination of two LSI systems.

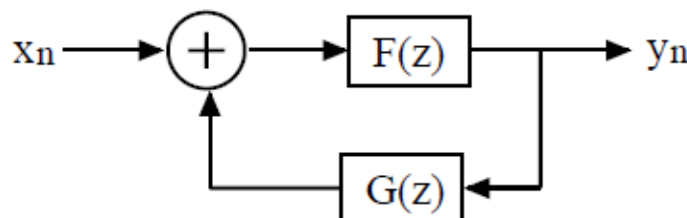


Figure 4.23: A feedback connection of two LSI systems.

The transfer function for a feedback connection of LSI systems can readily be obtained by again labeling the output of the adder node and writing an equation for its output. In this case, we have

$$W(z) = X(z) + G(z)Y(z)$$

and we have that

$$Y(z) = F(z)W(z)$$

which leads to

$$\begin{aligned} Y(z) &= F(z)(X(z) + G(z)Y(z)) \\ Y(z)(1 - F(z)G(z)) &= F(z)X(z) \\ Y(z) &= \frac{F(z)}{1 - F(z)G(z)}X(z) \end{aligned}$$

and finally,

$$H(z) = \frac{F(z)}{1 - F(z)G(z)}.$$

We see that for a feedback connection, the overall transfer function is given by the so-called “open loop gain” $F(z)$ divided by one minus the “closed loop gain”, i.e. $1 - F(z)G(z)$.

4.11 Flowgraph representations of complex-valued systems

4.12 System analysis

As we have seen, the input-output relationship of a linear-shift invariant (LSI) system is captured through its response to a single input, that due to a discrete-time impulse, or the impulse response of the system. There are a number of important properties of LSI systems that we can study by observing properties of its impulse response directly. Perhaps one of the more important properties of such systems is whether or not they are stable, that is, whether or not the output of the system will remain bounded for all time when the input to the system is bounded for all time. While for continuous-time systems and circuits stability may be required for ensuring that components do not become damaged as voltages or currents grow unbounded in a system, for discrete-time systems, stability can be equally important. For example, practical implementations of many discrete-time systems involve digital representations of the signals. To ensure proper implementation of the operations involved, the numerical values of the signal levels must remain within the limits of the

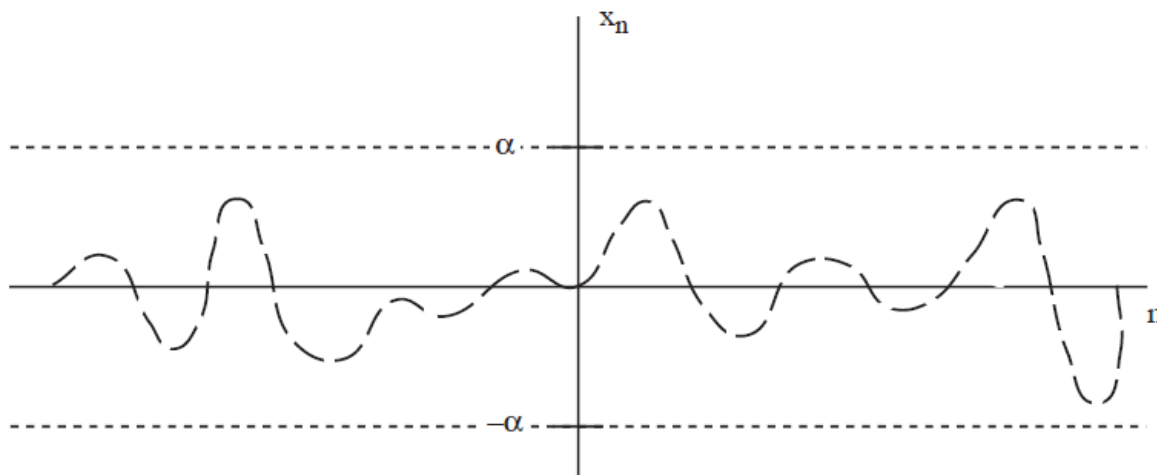


Figure 4.24: Bounded input $x[n]$, such that $|x[n]| < \alpha$.

number system used to represent the signals. If the signals are represented using fixed-point arithmetic, there may be strict bounds on the dynamic range of the signals involved. For example, any real number $-1 \leq x[n] \leq 1$ can be represented as an infinite binary string in two's complement notation as

$$x = -b_0 + \sum_{k=1}^N b_k 2^{-k}.$$

In a practical implementation, only finite-precision representations are available, such that all values might be represented and computed using fixed-point two's complement arithmetic where any signal at a given point in time would be represented as a $B + 1$ -bit binary string $-1 \leq x[n] < 1$,

$$x = -b_0 + \sum_{k=1}^B b_k 2^{-k}.$$

Now, if the input signal such a system was carefully conditioned such that it was less than 1 in magnitude, it is important that not only does the output remain less than 1 in magnitude, but also all intermediate calculations must also. If not, then the numbers would overflow, and produce incorrect results, i.e. they would not represent the true output of the LSI system to the given input. If the discrete-time system were used to control a mechanical system such as an aircraft, such miscalculations due to instability of the discrete-time system could produce erratic or even catastrophic results.

4.13 BIBO stability

A system is bounded-input, bounded-output (BIBO) stable if for every bounded input, $x[n]$, the resulting output, $y[n]$, is bounded. That is, if there exists a fixed positive constant α , such that

$$|x[n]| < \alpha < \infty, \text{ for all } n,$$

then there exists a fixed positive constant β , such that

$$|y[n]| < \beta < \infty, \text{ for all } n,$$

where the constants α and β are fixed, meaning that they do not depend on n . Graphically, if every bounded input $x[n]$ as shown in Figure 4.24

causes a bounded output $y[n]$ as shown in Figure 4.25

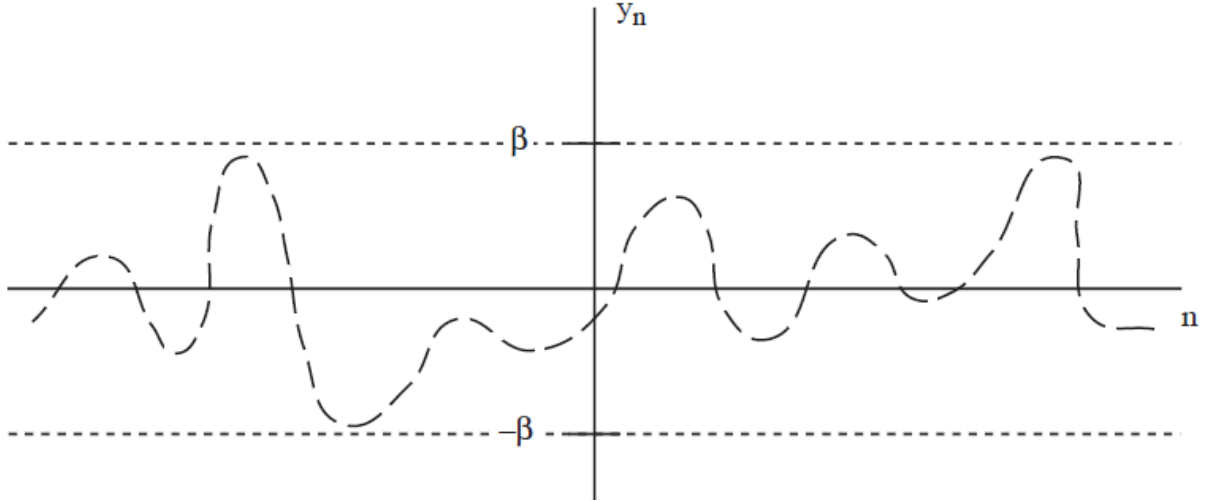


Figure 4.25: Bounded output $y[n]$, such that $|y[n]| < \beta$.

then the system is BIBO stable. Note that BIBO stability is a property of the system and not the inputs or outputs. While it may be possible to find specific bounded inputs such that the outputs remain bounded, a system is only BIBO stable if the output remains stable for all possible inputs. If there exists even one input for which the output grows unbounded, then the system is not stable in the BIBO sense.

How do we check if a system is BIBO stable? We cannot possibly try every bounded input and check that the resulting outputs are bounded. Rather, the input-output relationship must be used to prove that BIBO stability holds. Similarly, the following theorems can be used to provide simple tests for BIBO stability. It turns out that we can show that BIBO stability can be determined directly from the impulse response of an LSI system. Specifically, an LSI system with impulse response $h[n]$ is BIBO stable if and only if the impulse response is absolutely summable. That is,

$$\text{LSI system is BIBO stable} \iff \sum_{n=-\infty}^{\infty} |h[n]| < \infty.$$

To show both sides of the if and only if relationship, we start with assuming that $h[n]$ is absolutely summable, and seek to show that the output is bounded (sufficiency). This can be shown directly from the definition of an LSI system, i.e. from the convolution sum. We can write

$$y[n] = \sum_{m=-\infty}^{\infty} x[n-m]h[m].$$

Now, we take the absolute value of both sides and obtain

$$|y[n]| = \left| \sum_{m=-\infty}^{\infty} x[n-m]h[m] \right|,$$

which can be upper bounded by

$$|y[n]| \leq \sum_{m=-\infty}^{\infty} |x[n-m]||h[m]|.$$

Now we want to see that if $|x[n]| < \alpha$ that we can find a suitable β such that $|y[n]| < \beta$. We have that

$$|y[n]| \leq \alpha \sum_{m=-\infty}^{\infty} |h[m]|,$$

and since we assumed that

$$\sum_{n=-\infty}^{\infty} |h[n]| = \gamma < \infty,$$

we have

$$|y[n]| \leq \alpha\gamma = \beta < \infty.$$

To show the other direction of the if and only if relation (necessity), we need to show that when the impulse response is not absolutely summable, then there exists a sequence $x[n]$ that is bounded, but for which the output of the system is not bounded. That is, given that the sum $\sum_{m=-\infty}^{\infty} |h[m]|$ diverges, we need to show that there exists a bounded sequence $x[n]$ that produces an output $y[n]$ such that for some fixed n_0 the convolution sum diverges, i.e., $y[n_0]$ is not bounded. From the convolution sum, we have

$$y[n_0] = \sum_{m=-\infty}^{\infty} x[m]h[n_0 - m].$$

By selecting the sequence $x[n]$ to be such that $x[m] = h^*[n_0 - m]/|h[n_0 - m]|$, (for real-valued $h[n]$, this amounts to $x[m] = \text{sgn}(h[n_0 - m]) = \pm 1$), then we have that

$$\begin{aligned} y[n_0] &= \sum_{m=-\infty}^{\infty} \frac{h^*[n_0 - m]h[n_0 - m]}{|h[n_0 - m]|} \\ &= \sum_{m=-\infty}^{\infty} \frac{|h[n_0 - m]|^2}{|h[n_0 - m]|} \\ &= \sum_{m=-\infty}^{\infty} |h[n_0 - m]| \end{aligned}$$

and letting $k = n_0 - m$, we obtain that

$$y[n_0] = \sum_{k=-\infty}^{\infty} |h[k]|,$$

which diverges, completing the proof.

BIBO stability of a system can also be directly determined from the transfer function $H(z)$, relating the z-transform of the input to the z-transform of the output. Specifically, we have that for an LSI system with a rational transfer function, the system is BIBO stable if and only if the region of convergence includes the unit circle. For causal systems, this means that all of the poles of the system are inside the unit circle. Specifically, we have that

$$\text{An LSI system with transfer function } H(z) \text{ is BIBO stable} \iff \text{ROC}_H \supset |z| = 1.$$

We will show this result specifically for causal systems, noting that generalizing the result to left-sided and two-sided sequences is straightforward. First, to prove sufficiency, assume the region of convergence ROC_H includes the unit circle. Next, to illustrate that this implies absolute summability, i.e. $\sum_{n=-\infty}^{\infty} |h[n]| < \infty$, we consider the poles of the system function. First, the poles (roots of the denominator polynomial) must lie inside the unit circle since we have assumed that the region of convergence includes the unit circle, and for causal systems, i.e. systems for which $h[n] = 0$ for $n < 0$, we know ROC_H is given by $|z| > R$ for some $R > 0$. Since this must include the unit circle, then we have that $R < 1$ and all of the poles lie inside the unit circle.

The inverse z-transform, as determined by the partial fraction expansion of the system function $H(z)$ takes the form

$$h[n] = \sum_{k=0}^N b_k (p_k)^n, \quad n \geq 0,$$

assuming there are no repeated roots in the denominator polynomial. Since we have that $|p_k| < 1$ for all of the poles, we know that

$$\begin{aligned} \sum_{n=-\infty}^{\infty} |h[n]| &= \sum_{n=-\infty}^{\infty} \sum_{k=0}^N |b_k| |p_k|^n u[n] \\ &= \sum_{k=0}^N |b_k| \sum_{n=-\infty}^{\infty} |p_k|^n u[n] \\ &= \sum_{k=0}^N \frac{|b_k|}{1 - |p_k|} < \infty. \end{aligned}$$

For the case of repeated roots, we would simply have to show that series of the form

$$\sum_{k=0}^{\infty} n^L (p_k)^n$$

are convergent. This is readily shown by the ratio test, where we compare the $(n+1)$ th term to the n th term in the series. Here we have

$$\lim_{n \rightarrow \infty} \frac{(n+1)^L |p_k|^{n+1}}{n^L |p_k|^n} = \lim_{n \rightarrow \infty} \frac{(n+1)^L}{n^L} |p_k| = |p_k| < 1,$$

which implies that these series also all converge, indicating that even for repeated roots, we have that a causal LSI system whose ROC includes the unit circle will have an absolutely summable impulse response, and therefore will be BIBO stable.

To show necessity, we assume BIBO stability, and hence absolute summability of the impulse response, and then, for any point z on the unit circle, we have that

$$\begin{aligned} |H(z)|_{|z|=1} &= \left| \sum_{n=0}^{\infty} h[n] z^{-n} \right|_{|z|=1} \\ &\leq \sum_{n=0}^{\infty} |h[n]| |z|^{-n} \Big|_{|z|=1} \\ &\leq \sum_{n=0}^{\infty} |h[n]| |1|^{-n} \\ &\leq \sum_{n=0}^{\infty} |h[n]| < \infty, \end{aligned}$$

which implies that the region of convergence includes the unit circle and completes the proof. This indeed implies that for a causal LSI system with a rational transfer function (in minimal form), the system is BIBO stable if and only if all of its poles are inside the unit circle.

4.14 System properties from the system function

Some of the properties we have developed are explored in several examples.

Example

Consider the following LSI system with impulse response $h[n]$

$$h[n] = \cos(\theta n) u[n].$$

We have that

$$\sum_{n=-\infty}^{\infty} |h[n]| = \sum_{n=0}^{\infty} |\cos(\theta n)|,$$

which diverges. Therefore, the system is not BIBO stable.

Example

Consider the following transfer function for a causal LSI system,

$$H(z) = \frac{z^2 - 3z + 2}{z^3 - 2z^2 + \frac{1}{2}z - 1},$$

which after factoring the demoninator, yields,

$$H(z) = \frac{(z-1)(z-2)}{(z^2 + \frac{1}{2})(z-2)} = \frac{(z-1)}{z^2 + \frac{1}{2}}.$$

We see that $H(z)$ has poles at $z = \pm \frac{j}{\sqrt{2}}$. The system is causal and has all of its poles inside the unit circle. Therefore the system is BIBO stable. Note that as done in this example, factors that are common to the numerator and denominator must be cancelled before applying the stability test.

Example (Requires the use of the bilateral z-transform)

Consider the following system function of an LSI system,

$$H(z) = \frac{z}{z + 100}, \quad |z| < 100.$$

Note that this is a non-causal system, with a left-sided impulse response. The ROC in this case includes the unit circle, and therefore the system is BIBO stable.

Example

Consider the following impulse response of an LSI system,

$$h[n] = \begin{cases} 4^n, & 0 \leq n \leq 10^6, \\ n \left(\frac{1}{2}\right)^n, & n > 10^6 \\ 0, & n < 0. \end{cases}$$

Testing for absolute summability of the impulse response, we see that

$$\sum_{n=0}^{\infty} |h[n]| = \sum_{n=0}^{10^6} 4^n + \sum_{n=10^6+1}^{\infty} n \left(\frac{1}{2}\right)^n < \infty,$$

and therefore the system is BIBO stable.

We continue exploring the properties of LSI systems through observation of their system functions (that is, the z-transform of the impulse response), with a focus on the relationship between the region of convergence of the z-transform and the stability and causality of the system.

Example

Consider the following system function of a stable LSI system,

$$H(z) = \frac{z}{(z - \frac{1}{4})(z - 2)},$$

can it be causal?

Answer: No, it cannot be causal. First, note that although the region of convergence is not explicitly stated, it is implicitly determined. Noting that the system is stable, we know that the region of convergence must include the unit circle. Given the pole locations, we know that the region of convergence must be $z : \frac{1}{4} < |z| < 2$ implying that the impulse response will have leftsided and right-sided components and that $h[n]$ must be two-sided, i.e. that $H(z)$ is a two-sided z-transform. Since the impulse response is two-sided, this implies that the system cannot be causal, i.e. $h[n]$ is non-zero for $n < 0$ and from the convolution sum,

$$y[n] = \sum_{k=-\infty}^{\infty} h[k]x[n-k],$$

we see that this implies that $y[n]$ depends on values of $x[m]$ for $m > n$.

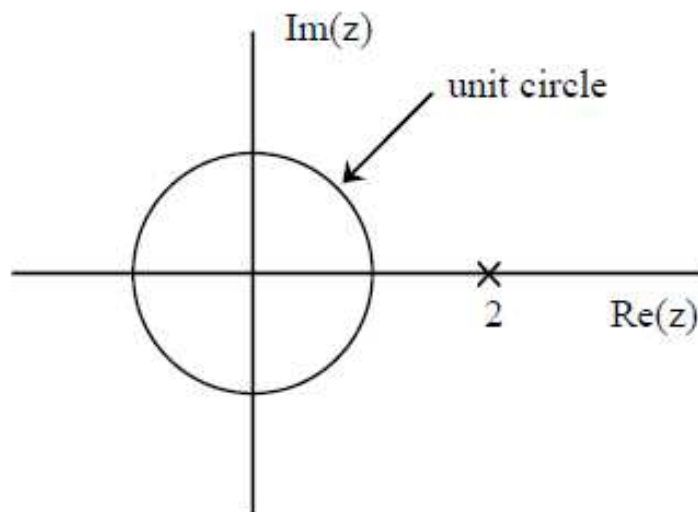


Figure 4.26:
tem.

Pole-zero plot for an LSI sys-

Example

Consider the following discrete time system,

$$y[n] = (x[n])^2.$$

Is this system stable?

Answer: This system is not linear. Therefore, we cannot apply a stability test involving either the impulse response or transfer function, since the tests discussed so far apply only to LSI systems. Since this system is not LSI, the convolution sum does not hold, so that the input output relationship does not satisfy $y[n] = x[n] * h[n]$ or $Y(z) = H(z)X(z)$. Instead, we appeal to the definition of BIBO stability. Since $|x[n]| < \alpha$ for all n , then we have that $|y[n]| < \alpha^2 < \infty$ for all n . Therefore, the system is indeed stable, albeit nonlinear.

Unbounded Outputs

Given an unstable LSI system, how do we find a bounded input that will cause an unbounded output? This will be illustrated by example for some causal systems in the following examples.

Example

Consider the following causal LSI system with pole-zero plot shown in Figure 4.26 and with system function $H(z)$ given by

$$H(z) = \frac{z}{z-2}, |z| > 2.$$

The impulse response is therefore given by $h[n] = 2^n u[n]$ and is itself unbounded. Since $h[n]$ grows without bound, almost any bounded input will cause the output to be unbounded. For example, taking $x[n] = \delta[n]$ would yield $y[n] = h[n]$.

Example

Now consider the following LSI system with system function

$$H(z) = \frac{z}{z-1}, |z| > 1.$$

Although the system is not stable, the impulse response remains bounded, as $h[n] = u[n]$, in this case. Here we could choose $x[n] = u[n]$ (which is bounded) so that $y[n]$ will be a linear ramp in time. Looking at the z-transform of the output, this corresponds to forcing $Y(z)$ to have a double pole at $z = 1$, i.e.

$$Y(z) = H(z)X(z) = \frac{z^2}{(z-1)^2},$$

which for the region of convergence of this output corresponds to a sequence that grows linearly in time.

Example

Here we consider an LSI system with a complex-conjugate pole pair on the unit circle. Let

$$H(z) = \frac{z^2 - z \cos(\alpha)}{(z - e^{j\alpha})(z - e^{-j\alpha})}, |z| > 1.$$

The complex conjugate pair of poles on the unit circle corresponds to a sinusoidal oscillating impulse response,

$$h[n] = \cos(\alpha n)u[n].$$

Thinking of the z-transform of the output, note that choosing $x[n] = h[n]$ will cause $Y(z)$ to have double poles at $z = e^{\pm j\alpha}$, which will in turn cause $y[n]$ to have the form of n times $\cos(\alpha n)$, which grows unbounded. From these examples with causal systems, we see that for systems with poles outside the unit circle, since the impulse response itself grows unbounded, substantial effort would be required to find a bounded input that will not cause an unbounded output. For poles on the unit circle, it is more difficult to find bounded inputs that ultimately cause the output to be unbounded. In some fields, such as dynamic systems or control, LSI systems with poles on the unit circle are called “marginally stable” systems. In our terminology, they are simply unstable systems.

Chapter 5

Frequency domain representations of systems

In Chapter 2 we considered a number of representations for discrete-time signals, including the Fourier representation introduced through the discrete-time Fourier transform, or DTFT. In Chapter 4 we extended the class of signal representations to include z-transforms. In both chapters, we emphasized properties of these representations and their ability to capture a broad class of signals of interest. While we touched on some of the aspects of input-output system behavior in Chapter 2, comparatively more time was spent in Chapter 4 on the use of the z-transform to describe linear, shift-invariant (LSI) systems through the development of the system function $H(z)$. In this chapter our focus will be on the use of the Fourier representation of discrete-time signals through the DTFT as we explore properties of LSI systems through the frequency response, which is the discrete-time Fourier transform of the impulse response of an LSI system.

5.1 The frequency response of a DT LSI system

We have seen that discrete-time systems that are both linear and shift invariant have an input-output relationship that can be characterized through the convolution sum. That is, an LSI system with input $x[n]$ and output $y[n]$ must satisfy

$$y[n] = \sum_{m=-\infty}^{\infty} h[m]x[n-m],$$

for all n and for every input $x[n]$, where $h[n]$ is the impulse response of the LSI system. By taking the discrete-time Fourier transform of both sides of the convolution sum, we obtain

$$\begin{aligned} Y_d(\omega) &= \sum_{n=-\infty}^{\infty} \left(\sum_{m=-\infty}^{\infty} h[m]x[n-m] \right) e^{-j\omega n} \\ &= \sum_{m=-\infty}^{\infty} h[m] \left(\sum_{n=-\infty}^{\infty} x[n-m] e^{-j\omega n} \right) \\ &= \left(\sum_{m=-\infty}^{\infty} h[m] e^{-j\omega m} \right) X_d(\omega) \\ &= H_d(\omega) X_d(\omega), \end{aligned}$$

where, $H_d(\omega)$ is the DTFT of the impulse response $h[n]$ and is referred to as the frequency response of the LSI system. This leads us to the relationship in the frequency domain, between the DTFT of the input sequence $x[n]$ and that of the output sequence $y[n]$,

$$Y_d(\omega) = H_d(\omega) X_d(\omega).$$

We refer to $H_d(\omega)$ as the frequency response of an LSI system owing to its role in the following mathematical experiment. Suppose the input to an LSI system is given by the infinite-length complex exponential signal $x[n] = e^{j\omega_0 n}$. Then we know from the convolution sum, that

$$\begin{aligned} y[n] &= \sum_{m=-\infty}^{\infty} h[m] e^{j\omega_0(n-m)} \\ &= e^{j\omega_0 n} \sum_{m=-\infty}^{\infty} h[m] e^{-j\omega_0 m} \\ &= e^{j\omega_0 n} H_d(\omega_0), \end{aligned}$$

when the summation in the second line is convergent. In this case, the output is the same as the input, except that it is scaled by the constant $H_d(\omega_0)$. This constant depends on the input frequency ω_0 , and is called the “eigenvalue” associated with the “eigensequence” $e^{j\omega_0 n}$.

There are a number of conceptual difficulties with the preceding thought-experiment. First, the sequence $e^{j\omega_0 n}$ is not the same as $e^{j\omega_0 n} u[n]$, i.e. the complex exponential sequence that starts at $n = 0$, but which is zero for $n < 0$. Note that $e^{j\omega_0 n} u[n]$ is not an eigensequence, since it does not satisfy the eigensequence property. Specifically, we have that

$$\begin{aligned} y[n] &= \sum_{m=-\infty}^{\infty} h[m] e^{j\omega_0(n-m)} u[n-m] \\ &= \sum_{m=-\infty}^n h[m] e^{j\omega_0(n-m)} \\ &= e^{j\omega_0 n} \sum_{m=-\infty}^n h[m] e^{-j\omega_0 m}, \end{aligned}$$

for which the output is not simply given as the input sequence, $e^{j\omega_0 n} u[n]$ times a possibly complex constant. Instead, assuming that $H_d(\omega_0)$ exists (that is, the sum defining it converges) we can only say that as $n \rightarrow \infty$

$$y[n]/e^{j\omega_0 n} \rightarrow H_d(\omega_0),$$

but for any finite n , the output is not as simply related to the input as would be the case for the eigensequence $e^{j\omega_0 n}$ for all n . This highlights one of the conceptual difficulties with our eigensequence notion, since it would be impossible to create a sequence that started at $n = -\infty$ and continued for all time through $n = \infty$. However, while we could never construct such a sequence, we can certainly imagine one, as we do fairly often in science and engineering when we envision sinusoidal signals that exist unperturbed for all time. A second conceptual difficulty is that the sequence $e^{j\omega_0 n}$ is a complex-valued sequence, which can be seen directly through Euler’s relation, whereby $e^{j\omega_0 n} = \cos(\omega_0 n) + j \sin(\omega_0 n)$. What is the meaning of having a complex input? If the impulse response, $h[n]$ is real-valued, then we simply have that

$$\begin{aligned} y[n] &= \sum_{m=-\infty}^{\infty} h[m] (\cos(\omega_0(n-m)) + j \sin(\omega_0(n-m))) \\ &= \sum_{m=-\infty}^{\infty} h[m] \cos(\omega_0(n-m)) + j \sum_{m=-\infty}^{\infty} h[m] \sin(\omega_0(n-m)), \end{aligned}$$

which corresponds to a pair of systems, each having real-valued inputs and outputs, i.e.

$$\begin{aligned} y[n] &= y_R[n] + j y_I[n] \\ y_R[n] &= \sum_{m=-\infty}^{\infty} h[m] \cos(\omega_0(n-m)) \\ y_I[n] &= \sum_{m=-\infty}^{\infty} h[m] \sin(\omega_0(n-m)). \end{aligned}$$

If $h[n]$ is complex-valued, then we can still represent the output using real-valued operations, by writing $h[n] = h_R[n] + jh_I[n]$ and then noting that

$$(h_R[n] + jh_I[n]) * (\cos(\omega_0 n) + j \sin(\omega_0 n)) = (h_R[n] * \cos(\omega_0 n) - h_I[n] * \sin(\omega_0 n)) + j(h_I[n] * \cos(\omega_0 n) + h_R[n] * \sin(\omega_0 n)).$$

Noting that $\cos(\omega_0 n) = \frac{1}{2}(e^{j\omega_0 n} + e^{-j\omega_0 n})$, we see that the response to $\cos(\omega_0 n)$ would be

$$y[n] = \frac{1}{2}H_d(\omega_0)e^{j\omega_0 n} + \frac{1}{2}H_d(-\omega_0)e^{-j\omega_0 n}.$$

We recall from the properties of the discrete-time Fourier transform, that when $h_d[n]$ is real-valued, we have that $H_d(\omega_0) = H_d(-\omega_0)^*$, which allows us to write

$$H_d(-\omega_0) = |H_d(\omega_0)|e^{-j\angle H_d(\omega_0)}.$$

This leads to the relation, for $h[n]$ real-valued, that

$$\begin{aligned} y[n] &= \frac{1}{2}|H_d(\omega_0)|e^{j\angle H_d(\omega_0)}e^{j\omega_0 n} + \frac{1}{2}|H_d(\omega_0)|e^{-j\angle H_d(\omega_0)}e^{-j\omega_0 n} \\ &= \frac{1}{2}|H_d(\omega_0)|\left(e^{j\angle H_d(\omega_0)}e^{j\omega_0 n} + e^{-j\angle H_d(\omega_0)}e^{-j\omega_0 n}\right) \\ &= |H_d(\omega_0)|\cos(\omega_0 n + \angle H_d(\omega_0)). \end{aligned}$$

That is, we have that the response of an LSI system with a real-valued impulse response $h[n]$ to an input $x[n] = \cos(\omega_0 n)$ is $y[n] = |H_d(\omega_0)|\cos(\omega_0 n + \angle H_d(\omega_0))$, i.e. a cosine of the same frequency with the magnitude and phase given by that of the frequency response. Note that this does not imply that $\cos(\omega_0 n)$ is an eigensequence, since the output is not the same as the input multiplied by a complex constant. However, $\cos(\omega_0 n)$ is the sum of two eigensequences, such that it is relatively easy to formulate the output given the frequency response. Note that this analysis assumes that the LSI system is stable, since $H_d(\omega)$ only exists if the region of convergence of the z-transform of $h[n]$ includes the unit circle.

Example

Let us consider an example of an LSI system given by the following input-output relation,

$$y[n] = x[n] + 2x[n-1],$$

for which we would like to find the output, when the input is given by $x[n] = \cos(\frac{\pi}{2}n)$, for all n . To find the output, it will be easy to use the eigensequence property of LSI systems, however we will require $H_d(\omega)$ in order to do this. Taking the DTFT of both sides, we have

$$\begin{aligned} Y_d(\omega) &= X_d(\omega) + 2e^{-j\omega}X_d(\omega) \\ Y_d(\omega) &= X_d(\omega)(1 + 2e^{-j\omega}) \\ H_d(\omega) = \frac{Y_d(\omega)}{X_d(\omega)} &= 1 + 2e^{-j\omega}. \end{aligned}$$

Now that we have $H_d(\omega)$, if $h[n]$ is real-valued, we can immediately write

$$y[n] = \left|H_d\left(\frac{\pi}{2}\right)\right| \cos\left(\frac{\pi}{2}n + \angle H_d\left(\frac{\pi}{2}\right)\right).$$

How can we determine whether $h[n]$ is real-valued? We know from the system definition, i.e. $y[n] = x[n] + 2x[n-1]$, that whenever $x[n]$ is real-valued, then the output $y[n]$ will also remain real-valued. Therefore, we must have that $h[n]$ is purely real-valued, otherwise we could find an input $x[n]$ that would produce complex outputs. In fact, $h[n] = \delta[n] + \delta[n-1]$, which we can obtain by taking the inverse DTFT of $H_d(\omega)$. Now, since

$$H_d\left(\frac{\pi}{2}\right) = 1 + 2e^{-j\frac{\pi}{2}} = 1 - j2 = \sqrt{5}e^{-j63.43^\circ},$$

we can write,

$$y[n] = \sqrt{5} \cos\left(\frac{\pi}{2}n - \frac{63.48}{180}\pi\right).$$

Example

As a second example, let us consider a stable LSI system with the system function given by

$$H(z) = \frac{z}{z - \frac{1}{2}},$$

for which we would like to determine the output when the input is $x[n] = \cos(\frac{\pi}{4}n)$ for all n . In order to determine the output, we first note that since the system is stable, we can determine the frequency response by evaluating $H(z)$ along the unit circle, i.e.

$$\begin{aligned} H_d(\omega) &= H(z)|_{z=e^{j\omega}} \\ &= \frac{1}{1 - \frac{1}{2}e^{-j\omega}}. \end{aligned}$$

Since the system is stable, the ROC of $H(z)$ includes the unit circle, and hence the DTFT is well defined. Also, since there is only one pole, and it is located at $z = \frac{1}{2}$, we know that this ROC corresponds to a causal system, so that $H(z)$ is the same, regardless of whether a unilateral or bilateral z-transform was used. Here, and for the remainder of this text, we will generally assume that when a z-transform is given without reference to whether it is a unilateral or bilateral transform, we will assume that it is the bilateral z-transform. For this example, we have that

$$\begin{aligned} H_d\left(\frac{\pi}{4}\right) &= \frac{1}{1 - \frac{1}{2}e^{-j\frac{\pi}{4}}} = \frac{1}{1 - \frac{1}{2}\left(\frac{\sqrt{2}}{2} - j\frac{\sqrt{2}}{2}\right)} \\ &= 1.36e^{-j28.68^\circ}, \end{aligned}$$

therefore, we have

$$y[n] = 1.36 \cos\left(\frac{\pi}{4}n - \frac{28.68}{180}\pi\right).$$

It is again useful to recall why we refer to the variable ω in the frequency response $H_d(\omega)$ as an angular frequency. Indeed, the lowest discrete-time frequency is given by $\omega_0 = 0$, for which $x[n] = \cos(0n) = 1$, i.e. $x[n]$ is a constant, unchanging value. The highest discrete-time frequency is given by $\omega_0 = \pi$ for which $x[n] = \cos(\pi n) = (-1)^n$, alternating sign with every sample. This is a fundamental difference between the concept of frequency discrete-time and that in continuous-time. Specifically, we have seen previously that discrete-time frequencies are only unique over an interval of length 2π , and outside of this range, the frequencies repeat. As a consequence, for example, since $\omega_0 = \frac{5\pi}{4} = 2\pi - \frac{3\pi}{4}$, then the signals $x[n] = \cos(\frac{5\pi}{4}n)$ and $x[n] = \cos(-\frac{3\pi}{4}n)$ must be identical.

This once again reminds us that discrete-time Fourier transforms are indeed periodic with period 2π , i.e. $H_d(\omega) = H_d(\omega + 2\pi)$. The notion of a frequency response, i.e. a response of a system to a signal of a given frequency (or to the component of an input signal at a given frequency) must clearly be periodic with period 2π , because the input signals themselves are exactly the same, so the outputs must be the same, i.e.

$$\begin{aligned} x[n] &= \cos(\omega_0 n) \longrightarrow \boxed{H_d(\omega)} \longrightarrow |H_d(\omega_0)| \cos(\omega_0 n + \angle H_d(\omega_0)) \\ &\Updownarrow \\ x[n] &= \cos((\omega_0 + 2\pi)n) \longrightarrow \boxed{H_d(\omega)} \longrightarrow |H_d(\omega_0 + 2\pi)| \cos((\omega_0 + 2\pi)n + \angle H_d(\omega_0 + 2\pi)). \end{aligned}$$

Since these two input signals with different frequencies, ω_0 and $\omega_0 + 2\pi$ are in fact identical frequencies, so the outputs must also be identical, i.e. we must have that

$$\begin{aligned} |H_d(\omega_0)| &= |H_d(\omega_0 + 2\pi)| \\ \angle H_d(\omega_0) &= \angle H_d(\omega_0 + 2\pi), \end{aligned}$$

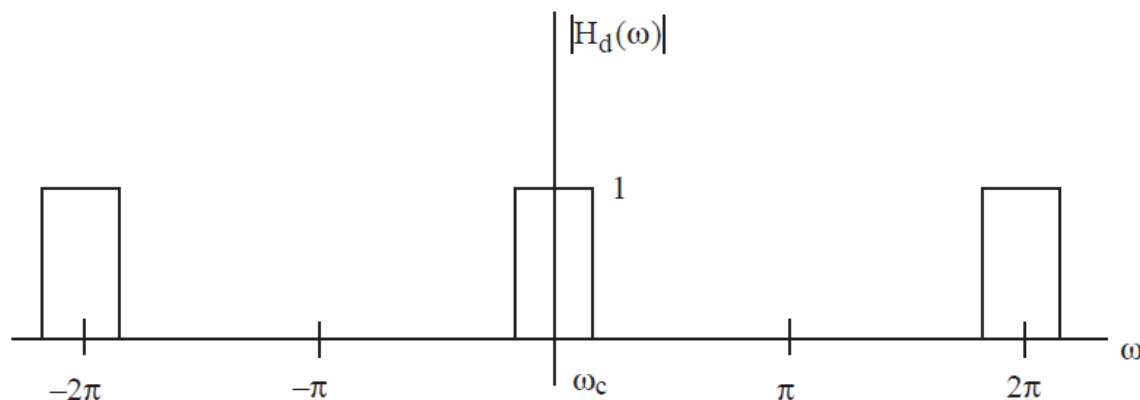


Figure 5.1: Magnitude of the frequency response $|H_d(\omega)|$ response of an ideal lowpass filter.

which means that

$$H_d(\omega_0) = H_d(\omega_0 + 2\pi).$$

Returning to the input-output relationship for stable LSI systems, we have that the DTFT of the input and output signals are related by

$$Y_d(\omega) = H_d(\omega)X_d(\omega),$$

where $X_d(\omega)$ and $Y_d(\omega)$ are the discrete-time Fourier transforms of the input and the output, respectively. Recalling our development of the discrete-time Fourier transform in Section 2.4 as a decomposition of a sequence into a linear combination of complex exponential signals, we can use a polar form representation of the frequency response to obtain

$$\begin{aligned} |Y_d(\omega)| &= |H_d(\omega)| |X_d(\omega)|, \\ \angle Y_d(\omega) &= \angle H_d(\omega) + \angle X_d(\omega), \end{aligned}$$

where $|H_d(\omega)|$ is the magnitude of the frequency response and is sometimes referred to as the magnitude response of the LSI system and $\angle H_d(\omega)$ is the phase of the frequency response and is also referred to as the phase response or phase shift of the system. Both the magnitude and phase of the frequency response have the effect of altering the contributions of the complex exponential signals that were originally in the input as they contribute to the output. These effects may be desirable, if the input signal is altered in a manner that was helpful, such as removal of unwanted frequency components, or a rebalancing of the contribution of various frequency elements that were present in the input. However they may also be unwanted effects that have altered the input signal in a manner that was deleterious, such as overemphasizing undesirable signal components while attenuating components of interest. In this case, the magnitude and phase response of the system might be called magnitude distortion and phase distortion.

In some cases, it is desirable to construct LSI systems whose frequency response serves the purpose of removing unwanted frequency components, while leaving others unchanged. This process of passing through some frequencies and stopping others from passing through the system is called frequency selective filtering. As an example, the frequency response magnitude depicted in Figure 5.1, shows that of an ideal low-pass filter that passes all frequencies less than ω_c and rejects all others.

Such an ideal lowpass filter has a magnitude response $|H_d(\omega)|$ satisfying

$$|H_d(\omega)| = \begin{cases} 1, & |\omega| < \omega_c \\ 0, & \omega_c < |\omega| < \pi \end{cases}$$

which, for an ideal lowpass filter, also has zero phase, such that,

$$H_d(\omega) = \begin{cases} 1, & |\omega| < \omega_c \\ 0, & \omega_c < |\omega| < \pi. \end{cases}$$

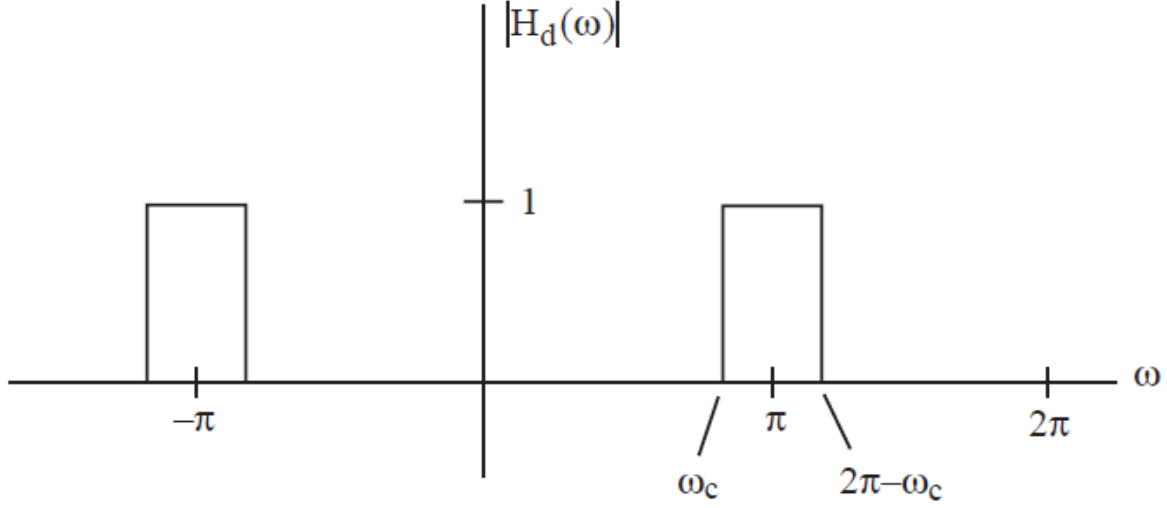


Figure 5.2: Magnitude of the frequency response of an ideal highpass filter.

By taking the inverse-DTFT, we can obtain the corresponding impulse response of an ideal lowpass filter,

$$\begin{aligned}
 h_{lp}[n] &= \int_{-\omega_c}^{\omega_c} e^{j\omega n} d\omega \\
 &= \begin{cases} \frac{\sin(\omega_c n)}{\pi n}, & n \neq 0 \\ \frac{\omega_c}{\pi}, & n = 0, \end{cases} \\
 &= \frac{\omega_c}{\pi} \text{sinc}(\omega_c n).
 \end{aligned}$$

An ideal highpass filter is depicted in Figure 5.2, in which all frequencies above ω_c are passed through the system, however all frequencies below ω_c are rejected. Note that this corresponds to a non-causal filter, since $h_{lp}[n]$ is non-zero for $n < 0$. We will discuss methods for making causal approximations to the ideal lowpass filter in Chapter 6.

The ideal high-pass filter has frequency response given by

$$H_d(\omega) = \begin{cases} 1, & \omega_c < |\omega| < \pi, \\ 0, & |\omega| < \omega_c, \end{cases}$$

which would have impulse response given by

$$\begin{aligned}
 h_{hp}[n] &= \int_{-\pi}^{-\omega_c} e^{j\omega n} d\omega + \int_{\omega_c}^{\pi} e^{j\omega n} d\omega \\
 &= \frac{e^{-j\omega_c n} - e^{-j\pi n}}{j\omega} + \frac{e^{j\pi n} - e^{j\omega_c n}}{j\omega} \\
 &= \text{sinc}(\pi n) - \frac{\omega_c}{\pi} \text{sinc}(\omega_c n) \\
 &= \delta[n] - h_{lp}[n].
 \end{aligned}$$

An ideal bandpass filter has a frequency response magnitude shown in Figure 5.3.

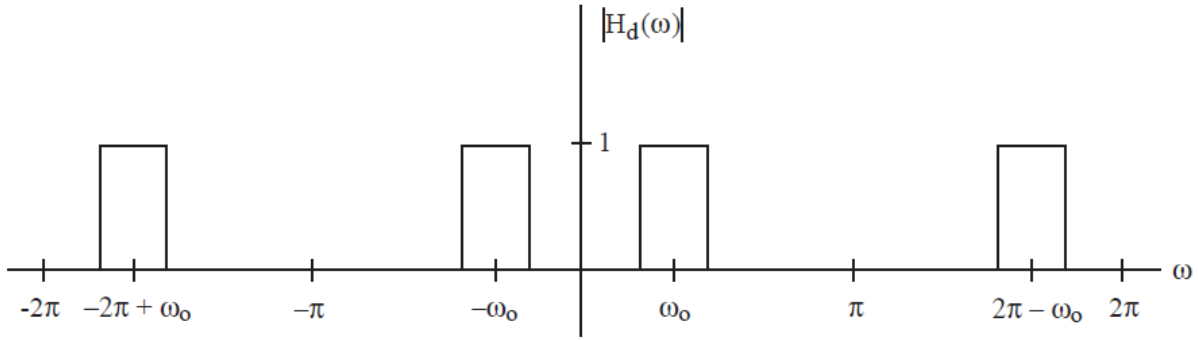


Figure 5.3: Frequency response magnitude for an ideal bandpass filter.

An ideal bandpass filter has frequency response given by

$$H_d(\omega) = \begin{cases} 0, & 0 < |\omega| < \omega_0 - \omega_c, \\ 1, & \omega_0 - \omega_c < |\omega| < \omega_0 + \omega_c \\ 0 & \omega_0 + \omega_c < |\omega| < \pi, \end{cases}$$

which has an impulse response given by

$$\begin{aligned} h_{bp}[n] &= \cos(\omega_0 n) h_{lp}[n] \\ &= \cos(\omega_0 n) \frac{\omega_c}{\pi} \text{sinc}(\omega_c n), \end{aligned}$$

so long as $\omega_0 - \omega_c > 0$, or, equivalently, $\omega_0 > \omega_c$. We can also define an ideal bandstop filter to have a frequency response magnitude satisfying,

$$H_d(\omega) = \begin{cases} 1, & 0 < |\omega| < \omega_0 - \omega_c, \\ 0, & \omega_0 - \omega_c < |\omega| < \omega_0 + \omega_c \\ 1 & \omega_0 + \omega_c < |\omega| < \pi, \end{cases}$$

whose impulse response would be given by

$$\begin{aligned} h_{bs}[n] &= \delta[n] - h_{bp}[n], \\ &= \delta[n] - \cos(\omega_0 n) \frac{\omega_c}{\pi} \text{sinc}(\omega_c n), \end{aligned}$$

again, assuming that $\omega_0 > \omega_c$.

Since the ideal lowpass filter, ideal highpass filter, ideal bandpass filter, and ideal bandstop filter each are defined in terms of the non-causal, infinite duration sinc sequence, we see that such ideal responses are unrealizable using finite-order systems, i.e. using any practical implementation that has a finite number of delay elements. A practical (finite-order) system can approximate such an ideal response, where the approximation can improve as the complexity of the approximating system increases. Considering a simple example, a two-sample moving average filter has the input-output relationship

$$y[n] = \frac{1}{2} (x[n] + x[n-1]),$$

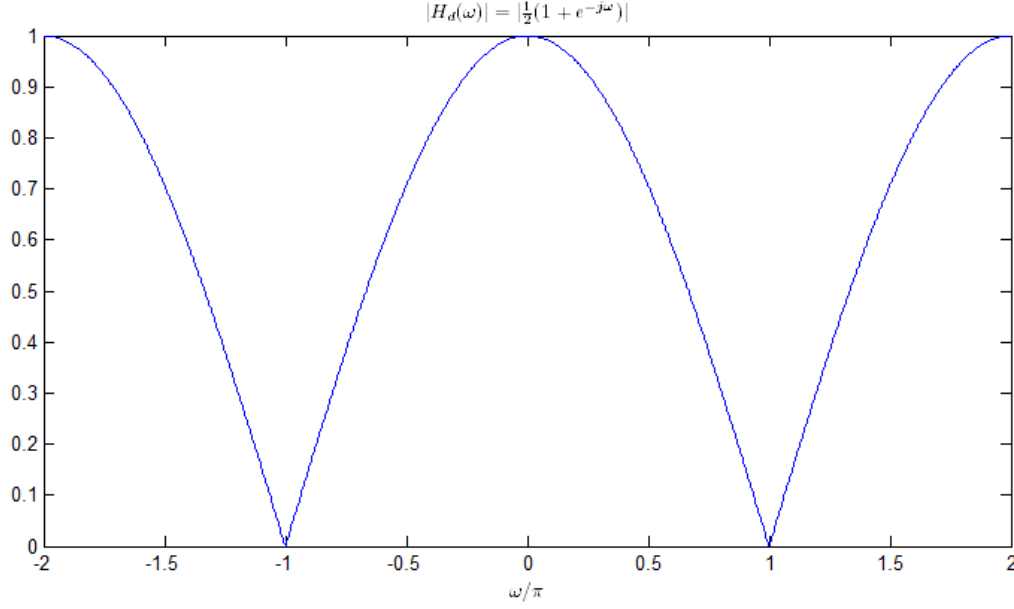


Figure 5.4: Frequency response magnitude for the simple system with impulse response $h[n] = \frac{1}{2}(\delta[n] + \delta[n - 1])$.

for which we can determine the frequency response,

$$\begin{aligned} Y_d(\omega) &= \frac{1}{2} (X_d(\omega) + e^{-j\omega} X_d(\omega)), \\ H_d(\omega) &= \frac{1}{2} (1 + e^{-j\omega}) \\ &= \frac{1}{2} e^{-j\omega/2} (e^{j\omega/2} + e^{-j\omega/2}) \\ &= e^{-j\omega/2} \cos(\omega/2). \end{aligned}$$

The frequency response for this filter is shown in Figure and can be seen to be a simple approximation to a lowpass filter.

We can similarly consider the simple LSI system whose input-output relationship is given by

$$y[n] = \frac{1}{2} (x[n] - x[n - 1]),$$

for which the frequency response is given by

$$\begin{aligned} H_d(\omega) &= \frac{1}{2} (1 - e^{-j\omega}) \\ &= \frac{1}{2} e^{-j\omega/2} (e^{j\omega/2} - e^{-j\omega/2}) \\ &= e^{-j(\pi-\omega)/2} \sin(\omega/2). \end{aligned}$$

The magnitude of the frequency response for this crude highpass filter is shown in Figure 5.5.

As an additional example, consider the input-output relation

$$y[n] = \frac{1}{2} (x[n] + x[n - 2]),$$

for which the frequency response is given by

$$\begin{aligned} H_d(\omega) &= \frac{1}{2} (1 + e^{-j2\omega}) \\ &= e^{-j\omega} \cos(\omega), \quad < |\omega| < \pi, \end{aligned}$$

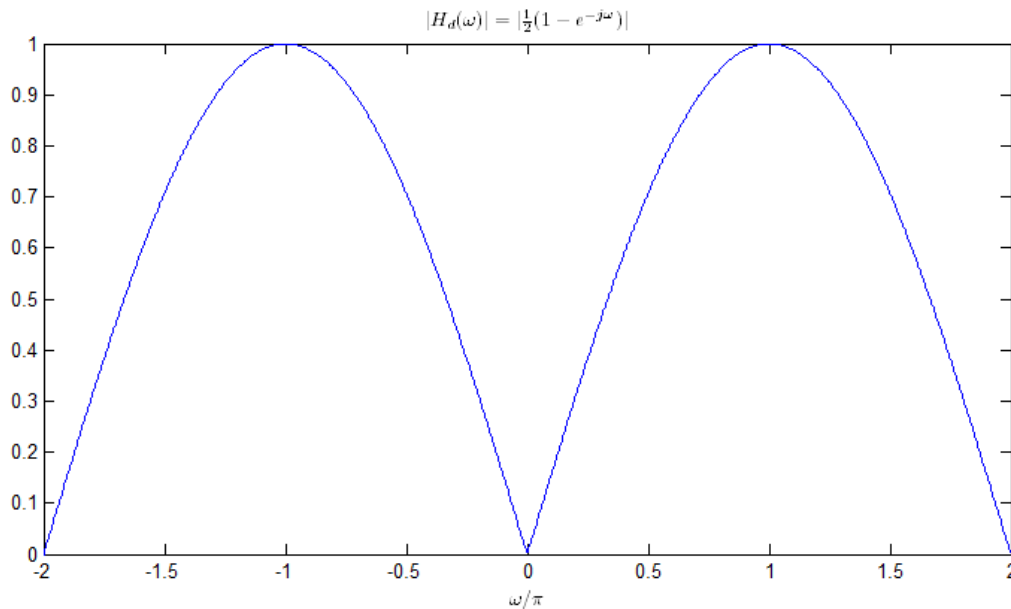


Figure 5.5: Magnitude of the frequency response of the system with impulse response $h[n] = \frac{1}{2}(x[n] - x[n-1])$.

as shown in Figure 5.6.

This is a crude band stop filter with center frequency $\omega_0 = \frac{\pi}{2}$. In these last few examples, we have looked at frequency responses of simple nonrecursive filters. We can achieve responses that are much closer to ideal (as close as we would like) by considering nonrecursive filters with more coefficients and through use of recursive filters. The design of such filters will be an important topic later in the text.

5.2 The phase of the frequency response

Frequency selective filters help us to visualize and understand the effects of attenuation or frequency-selectivity of the magnitude of the frequency response. To better understand the effects of the phase of the frequency response, consider frequency selective filter that has an ideal magnitude response, such that

$$|H_d(\omega)| = \begin{cases} 1, & |\omega| < \omega_c \\ 0, & \omega_c < |\omega| < \pi. \end{cases}$$

Now suppose that the input to this filter is given by

$$x[n] = \cos(\omega_1 n) + \cos(\omega_2 n) + \cos(\omega_3 n),$$

where it is known that $\omega_1 < \omega_2 < \omega_c < \omega_3 < \pi$, however the values of ω_1 , ω_2 and ω_3 are unknown. If $\cos(\omega_3 n)$ were a contaminating sinusoid and you wanted to precisely recover the desired components of $x[n]$, i.e., we want

$$\hat{x}[n] = \cos(\omega_1 n) + \cos(\omega_2 n),$$

how does the phase $\angle H_d(\omega)$ affect the output $y[n]$? If the filter has a real-valued impulse response, then we know that

$$y[n] = \cos(\omega_1 n + \angle H_d(\omega_1)) + \cos(\omega_2 n + \angle H_d(\omega_2)).$$

If we want to obtain $y[n] = \hat{x}[n]$, then we require that

$$\angle H_d(\omega) = 0, \quad 0 \leq |\omega| \leq \omega_c,$$

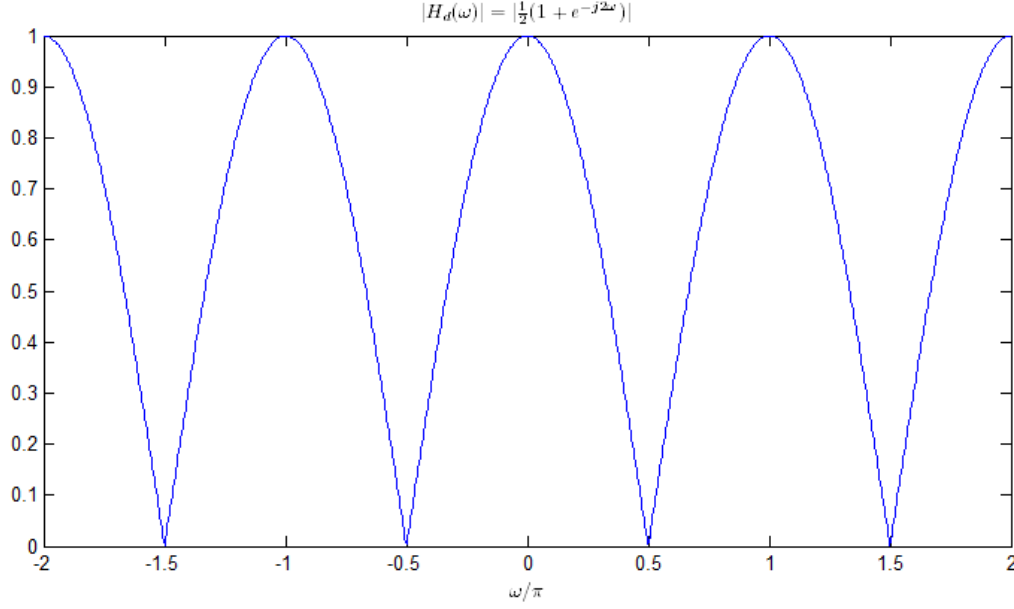


Figure 5.6: Frequency response magnitude for the system with impulse response $h[n] = \frac{1}{2}(\delta[n] + \delta[n-2])$.

i.e., the phase of the frequency response must be zero for all frequencies in the pass band. Therefore, we have that

$$H_d(\omega) = |H_d(\omega)|e^{j0} = |H_d(\omega)| = 1,$$

in the passband. From the inverse discrete-time Fourier transform, we know that the impulse response $h[n]$ must satisfy

$$\begin{aligned} h[n] &= \frac{1}{2\pi} \int_{-\omega_c}^{\omega_c} 1e^{j\omega n} d\omega \\ &= \frac{\omega_c}{\pi} \text{sinc}(\omega_c n), \end{aligned}$$

for all n . Note that this corresponds to a noncausal system, since $h[n]$ is nonzero for negative values of n . If we desire a causal filter, this type of impulse response cannot be well-approximated. If we were willing to accept a delayed version of the two lower frequency signals, i.e. if we would accept

$$y[n] = \hat{x}[n - M] = \cos(\omega_1(n - M)) + \cos(\omega_2(n - M))$$

for some $M > 0$, then we might be able to exploit the phase of $H_d(\omega)$ to achieve this output. Specifically, we would require that

$$\begin{aligned} -\omega_1 M &= \angle H_d(\omega_1) \\ -\omega_2 M &= \angle H_d(\omega_2) \end{aligned}$$

which can actually be achieved, even though we do not know the values of ω_1 or ω_2 by setting

$$\angle H_d(\omega) = -\omega M,$$

for all ω in the passband. This is referred to as “linear phase,” since the phase of the frequency response is linear with frequency. This makes sense intuitively, since a sinusoid of a lower frequency ω_1 changes slowly in time and would need a smaller amount of phase added to its argument in order to delay the sinusoid as much as a sinusoid of a higher frequency ω_2 . Specifically, consider for the moment that $\omega_1 = 2\pi/M$.

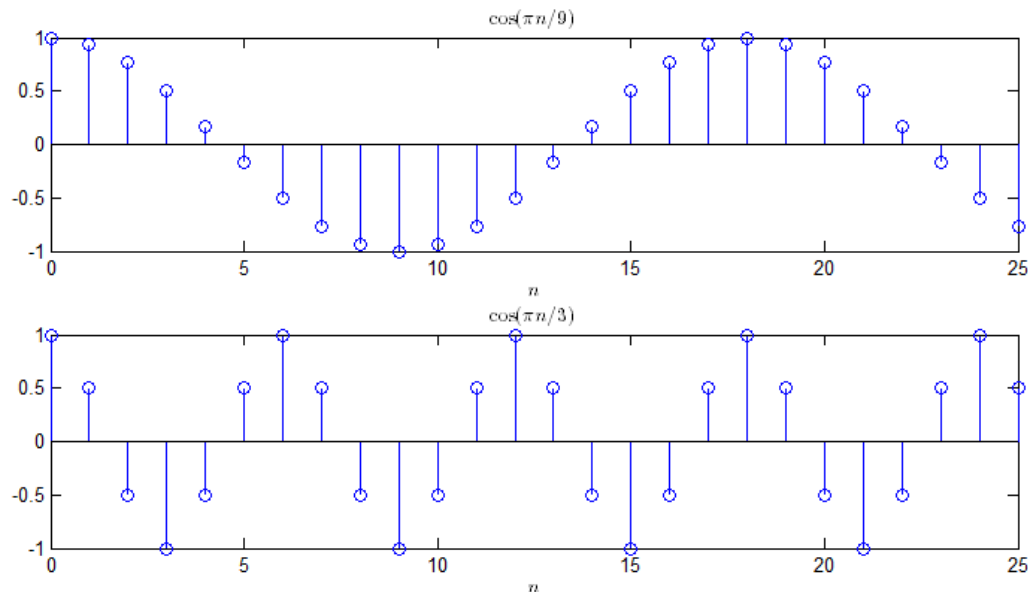


Figure 5.7: Note that the sequence $x[n] = \cos(\pi n/9)$ would require one third as much phase to be subtracted from the argument of the cosine in order to delay it the same amount as the sequence $x[n] = \cos(\pi n/3)$.

Then, delaying the sinusoid M samples in time would be equivalent to subtracting 2π from the phase of the sinusoid. On the other hand, if $\omega_2 = 2\pi k/M$, then in order to delay the sinusoid M samples in time, it would require changing the phase of the sinusoid by $2\pi k$, that is k times as much phase is required to delay the high frequency sinusoid the same number of samples in time, as shown in Figure 5.7. This is because the period of the higher frequency sinusoid is k times smaller than that of the lower frequency sinusoid.

For the case where we permit the phase in the passband to be linear phase, we find that the impulse response must satisfy,

$$\begin{aligned}
 h[n] &= \frac{1}{2\pi} \int_{-\pi}^{\pi} H_d(\omega) e^{j\omega n} d\omega \\
 &= \frac{1}{2\pi} \int_{-\omega_c}^{\omega_c} 1 e^{-j\omega M} e^{j\omega n} d\omega \\
 &= \frac{\omega_c}{\pi} \text{sinc}(\omega_c(n - M)),
 \end{aligned}$$

which is nearly causal, as seen in Figure 5.8.

By truncating the linear phase version of the lowpass filter to the left of $n = 0$, we can obtain a causal $h[n]$ whose discrete-time Fourier transform magnitude will only be slightly affected. In general, the process of adding linear phase to a system introduces a delay to the overall processing of the system, which is often acceptable, e.g.,

$$\begin{aligned}
 x[n] &\longrightarrow \boxed{H_d(\omega)} \longrightarrow y[n], \\
 x[n] &\longrightarrow \boxed{H_d(\omega)e^{-j\omega M}} \longrightarrow y[n - M],
 \end{aligned}$$

when M is an integer. This can be readily shown using the delay property of the DTFT. While linear phase (with an integer-valued slope) introduces a processing delay and zero phase introduces no distortion at all, in general, nonlinear phase is undesirable. Nonlinear phase can cause substantial distortion to a signal of interest, especially if the phase has a slope that changes dramatically over values of frequency in which the input signal has appreciable energy.

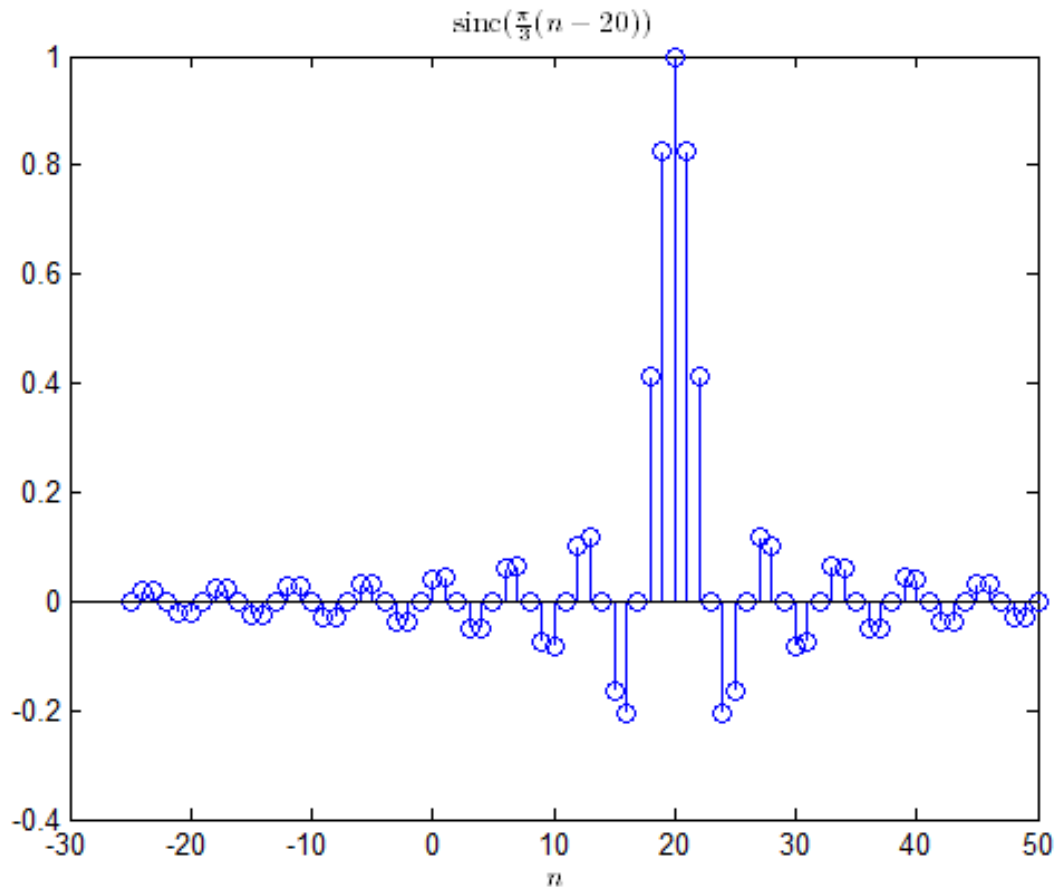


Figure 5.8: When the linear phase term is assumed, the resulting impulse response $h[n] = \text{sinc}\left(\frac{\pi}{3}(n - 20)\right)$ is nearly causal, and can be suitably approximated through windowing or truncation.

To be precise, we make a distinction between linear phase and what we call “generalized linear phase.” Specifically, for a given frequency response $H_d(\omega)$, we can write

$$H_d(\omega) = \underbrace{|H_d(\omega)|}_{\text{non-negative}} e^{j\angle H_d(\omega)}.$$

When written in this form, if

$$\angle H_d(\omega) = \alpha\omega,$$

where α is a real number, then we say that $H_d(\omega)$ has linear phase, which is sometimes called “strictly linear phase.” More generally, if we rewrite $H_d(\omega)$ in the following form

$$H_d(\omega) = \underbrace{R(\omega)}_{\text{real-valued function}} e^{j\angle H_d(\omega)},$$

where we permit $R(\omega)$ to be a real-valued (i.e., positive and negative) function of ω . In this case, when the function

$$\angle H_d(\omega) = \beta + \alpha\omega,$$

we call $H_d(\omega)$ a “generalized linear phase” response. This is a topic to which we will return in subsequent chapters when we discuss FIR filter design methods.

5.3 DT processing of CT signals, Analog frequency response of a digital system

As discussed early in this book, a common manner in which discrete-time signal processing is employed, is through the processing of sampled-continuous-time signals, where the output of the discrete-time processing is then converted back to continuous-time for interaction with the analog world around us, i.e.

$$x_c(t) \longrightarrow \boxed{\text{A/D}} \xrightarrow{\uparrow T} x[n] \longrightarrow \square \longrightarrow y[n] \longrightarrow \boxed{\text{D/A}} \xrightarrow{\uparrow T} y_c(t),$$

where the overall processing from $x(t)$ to $y(t)$ can be viewed as “discrete-time processing of a continuous-time signal.” Since the overall system has a continuous-time input and continuous-time output, we would like to understand if an overall transfer function

$$H_c(\Omega) = \frac{Y_c(\Omega)}{X_c(\Omega)}$$

can be defined, and if so, how it may depend on the frequency response $H_d(\omega)$. We will see that the formula for $Y_c(\Omega)$ in terms of $X_c(\Omega)$ is complicated, and that in general we cannot determine this ratio in closed form (more importantly, this ratio is often not meaningful when the operation from $x_c(t)$ to $y_c(t)$ is not linear and time-invariant). However, it is possible to find this ratio if we assume that $x_c(t)$ is sufficiently bandlimited and that we sample above the Nyquist rate. To find $Y_c(\Omega)$ in terms of $X_c(\Omega)$, we consider the components in the overall system, one at a time, in the frequency domain.

5.3.1 Analog to digital converter (A/D)

We explored ideal analog to digital conversion in Section 3.2 for which the relationship between $x[n] = x_a(nT)$ is depicted as follows

$$x_a(t) \longrightarrow \boxed{\text{A/D}} \xrightarrow{\uparrow T} x[n] = x_a(nT).$$

We have shown the important relationship between the discrete-time Fourier transform of $x[n]$, $X_d(\omega)$, and the continuous-time Fourier transform of the signal $x_a(t)$, to be

$$X_d(\omega) = \frac{1}{T} \sum_{n=-\infty}^{\infty} X_a\left(\frac{\omega + 2\pi n}{T}\right).$$

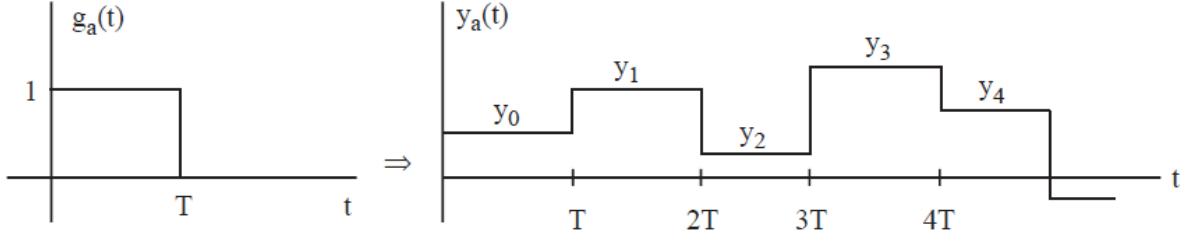


Figure 5.9: Output waveform for a zero-order-hold D/A converter, i.e. when $g_a(t) = u(t) - u(t - T)$.

5.3.2 Discrete-time linear shift invariant system

Once the discrete-time signal $x[n]$ is obtained through sampling the continuous-time signal $x(t)$, subsequent processing with a discrete-time LSI system with frequency response $H_d(\omega)$ yields an output, $y[n]$ satisfying

$$Y_d(\omega) = H_d(\omega)X_d(\omega).$$

The relationship between $Y_d(\omega)$ and the continuous-time Fourier transform of the signal $x(t)$ is then readily given by

$$Y_d(\omega) = \frac{1}{T}H_d(\omega) \sum_{n=-\infty}^{\infty} X_a\left(\frac{\omega + 2\pi n}{T}\right).$$

5.3.3 Digital to analog (D/A) conversion

Our model developed in Section 3.2 for a D/A converter was that the output signal $y(t)$ is given by

$$y_a(t) = \sum_{n=-\infty}^{\infty} y[n]g_a(t - nT),$$

so that $y_a(t)$ is modeled as a weighted pulse train. For example, if $g_a(t)$ is a rectangular pulse, of duration T , then $y_a(t)$ is a staircase waveform, as shown in Figure 5.9.

For this model, we have shown that the continuous-time Fourier transform, $Y_a(\Omega)$ satisfies

$$Y_a(\Omega) = G_a(\Omega)Y_d(\Omega T).$$

Taking each of the models in succession, we obtain the end-to-end relationship from $X_a(\Omega)$ to $Y_a(\Omega)$,

$$Y_a(\Omega) = \frac{1}{T}G_a(\Omega)H_d(\Omega T) \sum_{n=-\infty}^{\infty} X_a\left(\Omega + \frac{2\pi n}{T}\right). \quad (5.1)$$

Note that this equation is cumbersome, and, in general, we cannot directly solve for an effective continuous-time frequency response $H_{eff}(\Omega) = \frac{Y_a(\Omega)}{X_a(\Omega)}$. In fact, we cannot even suitably define what is meant by $H_{eff}(\Omega)$, since, while the overall system from $x(t)$ to $y(t)$ is linear, in general it is not time-invariant. As such, the system functionality is not captured by a single end-to-end frequency response. Fortunately, 5.1 simplifies tremendously when the input signal $x_a(t)$ is sufficiently bandlimited, such that $|X_a(\Omega)| = 0$, for $|\Omega| > \frac{\pi}{T}$ (i.e. that the system employed sampling at or above the Nyquist rate), and ideal A/D and D/A converters. Under these conditions, the overall system behaves as if it were time-invariant and it can be described by an overall equivalent frequency response. Exploring 5.1 under this assumption, we see that in the range within the range $|\Omega| < \frac{\pi}{T}$, we have that

$$Y_a(\Omega) = \frac{1}{T}G_a(\Omega)H_d(\Omega T)X_a(\Omega), \quad |\Omega| < \frac{\pi}{T},$$

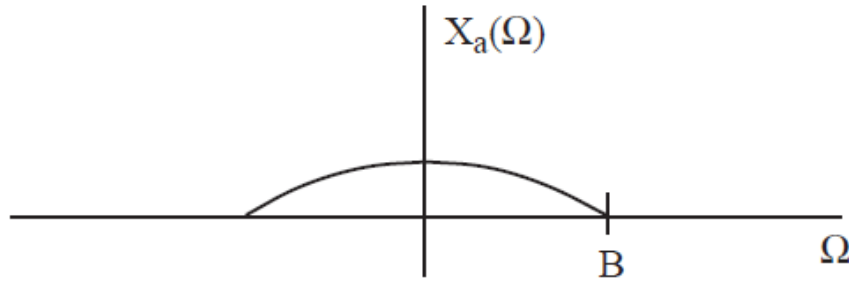


Figure 5.10: Input signal $x_a(t)$ is bandlimited such that $|X_a(\Omega)| = 0$, for $|\Omega| > B$.

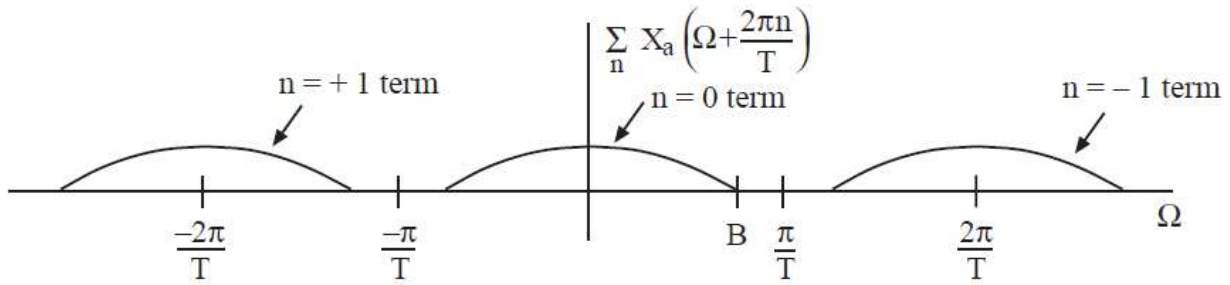


Figure 5.11: Three terms in the summation of (5.1).

since the summation that included multiple shifted copies of $X_a(\Omega + \frac{2\pi n}{T})$ only has contribution from the $n = 0$ term over the range of frequencies $|\Omega| < \frac{\pi}{T}$. Outside of this range, of $G_a(\Omega)$ is similarly bandlimited, i.e. $|G_a(\Omega)| = 0$, for $|\Omega| < \frac{\pi}{T}$, then the Fourier transform of the output is given by

$$Y_a(\Omega) = \begin{cases} \frac{1}{T} G_a(\Omega) H_d(\Omega T) X_a(\Omega), & |\Omega| \leq \frac{\pi}{T} \\ 0, & |\Omega| > \frac{\pi}{T}. \end{cases}$$

As an example, assuming that the input signal $x_a(t)$ is bandlimited such that $|X_a(\Omega)| = 0$, for $|\Omega| > B$ where $B < \frac{\pi}{T}$, we might graphically depict this as in Figure 5.10.

When $B < \frac{\pi}{T}$, the summation in (5.1) can be depicted graphically as shown in Figure 5.11.

Since there is no aliasing due to the bandlimited assumption, we have in the range $|\Omega| < \frac{\pi}{T}$ that

$$\sum_{n=-\infty}^{\infty} X_a\left(\Omega + \frac{2\pi n}{T}\right) = X_a(\Omega), \quad |\Omega| < \frac{\pi}{T}.$$

Assuming that an ideal digital to analog converter is used, then we have

$$G_a(\Omega) = \begin{cases} T, & |\Omega| < \frac{\pi}{T} \\ 0 & |\Omega| > \frac{\pi}{T}, \end{cases}$$

which corresponds to the pulse shape

$$g_a(t) = \text{sinc}\left(\frac{\pi}{T}t\right).$$

The output of the D/A converter, after filtering with the ideal sinc reconstruction filter, can be graphically depicted as shown in Figure 5.12.

From our earlier relationship between the CTFT of the input to the A/D converter and the CTFT of the output of the D/A converter, we had,

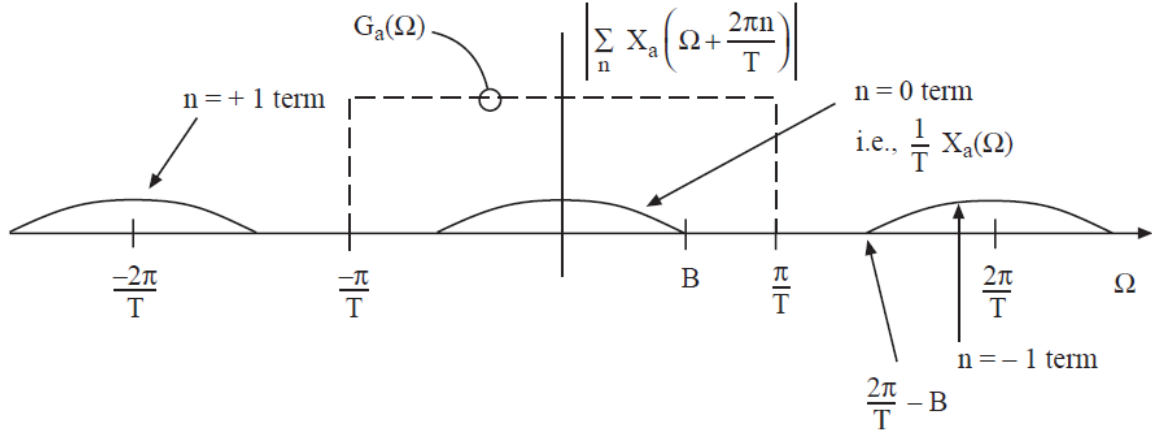


Figure 5.12: A graphical depiction of the use of an ideal sinc reconstruction filter in the D/A converter.

$$Y_a(\Omega) = \begin{cases} \frac{1}{T} G_a(\Omega) H_d(\Omega T) X_a(\Omega), & |\Omega| \leq \frac{\pi}{T} \\ 0, & |\Omega| > \frac{\pi}{T}, \end{cases}$$

which, for an ideal sinc reconstruction filter yields,

$$Y_a(\Omega) = \begin{cases} H_d(\Omega T) X_a(\Omega), & |\Omega| \leq \frac{\pi}{T} \\ 0, & |\Omega| > \frac{\pi}{T}. \end{cases}$$

This implies that we can consider the entire system, from input to the A/D converter to the output of the D/A converter as a linear time invariant system, with effective frequency response

$$H_{\text{eff}}(\Omega) = \frac{Y_a(\Omega)}{X_a(\Omega)},$$

which can be written

$$H_{\text{eff}}(\Omega) = \begin{cases} H_d(\Omega T), & |\Omega| \leq \frac{\pi}{T}, \\ 0 & |\Omega| > \frac{\pi}{T}. \end{cases}$$

The connection between the discrete-time frequency response $H_d(\omega)$ and the effective continuous-time frequency response $H_{\text{eff}}(\Omega)$ is an important one, and worth investigating in a bit more detail. For example, if there is a specific desired overall effective frequency response, $H_a(\Omega)$ to be implemented in discrete-time, we can make the change of variable, $\omega = \Omega T$, to explore precisely which discrete-time filter $H_d(\omega)$ would be needed such that in the end $H_{\text{eff}}(\Omega) = H_a(\Omega)$. To this end, if we design $H_d(\omega)$ such that

$$H_d(\omega) = H_a\left(\frac{\omega}{T}\right), \quad |\omega| < \pi,$$

then we would precisely realize $H_{\text{eff}}(\Omega) = H_a(\Omega)$. As such, given a desired $H_a(\Omega)$, we see that $H_d(\omega)$ has the same shape, however the region $|\Omega| < \frac{\pi}{T}$ is mapped into the range $|\omega| < \pi$, as shown in the example in Figure 5.13 .

Note that for an ideal frequency-selective filter, we have that to achieve a desired continuous-time cutoff frequency Ω_c , we require a discrete-time filter with cutoff frequency $\omega_c = \Omega_c T$. This relationship is particularly useful and can be used in both directions, both to design a given discrete-time filter to achieve a desired CT response, as well as to determine the CT response as a function of discrete-time system parameters, such as ω_c and T .

Example

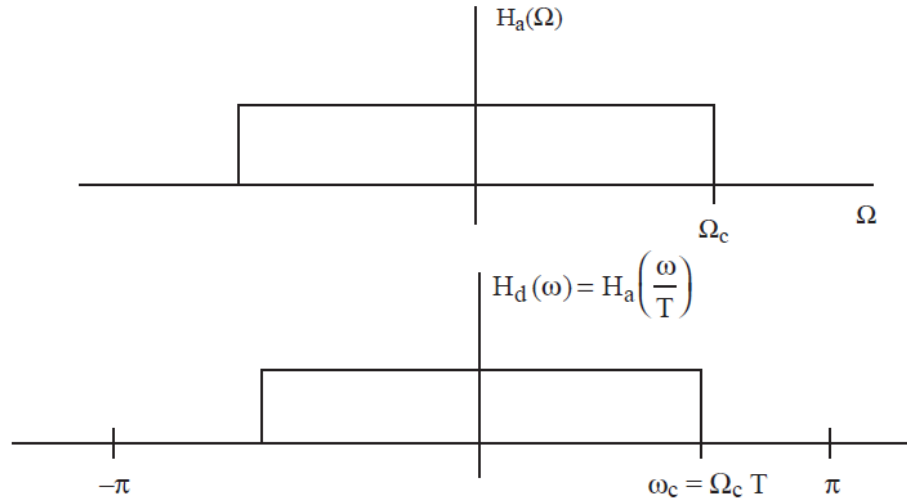


Figure 5.13: Mapping of a desired continuous-time frequency response $H_a(\Omega)$ to the needed discrete-time frequency response $H_d(\omega)$.

Consider a continuous-time signal $x_a(t)$ that is bandlimited to 50kHz , for which we wish to implement an analog lowpass filter with cutoff frequency $\Omega_c = 2\pi \times 25,000$ rad/sec. To accomplish this, we select the sampling rate according to the Nyquist criterion, such that $\frac{1}{T} > 100\text{ kHz}$, or $T < 10^{-5}\text{sec}$. Our desired cutoff frequency would map to the discrete-time frequency $\omega_c = \Omega_c T = 2\pi(25,000)10^{-5} = \frac{\pi}{2}$. In this example, the ratio of the desired analog cutoff to the analog bandwidth was $1/2$. Likewise, the passband of $H_d(\omega)$ filled half of the digital frequency band $|\omega| \leq \pi$. This proportional relationship will always hold if we sample at the Nyquist rate. A question that might naturally arise is, why did we sample at the Nyquist rate instead of above it? Or, for example, why did we not sample at a rate much greater than 100,000 samples per second? The answer is straightforward. Sampling faster than needed would increase the overall hardware costs since it would require a faster analog-to-digital converter and a digital filter operating at a faster data rate, which would not only be more expensive to purchase (or build), but would also require more power to operate.

Example

As a second example, consider a continuous-time signal that is bandlimited to $2\pi \times 10^6$ rad/sec for which we would like to implement a continuous-time highpass filter with cutoff frequency $f_c = 250,000$ Hz. To accomplish this, we select $\frac{1}{T} = 2\left(\frac{2\pi \times 10^6}{2\pi}\right) = 2 \times 10^6$ samples/sec. This implies a discrete-time filter with cutoff frequency of $\omega_c = 2\pi\left(\frac{250,000}{2 \times 10^6}\right) = \frac{\pi}{4}$. Hence, to realize such a high-pass filter, we need to design a discrete-time high-pass filter with cutoff frequency $\omega_c = \frac{\pi}{4}$. Note that the overall frequency response of this continuous-time system would be

$$H_{eff}(\Omega) = \begin{cases} 0, & |\Omega| < 2\pi(250,000) \\ 1, & 2\pi(250,000) \leq |\Omega| \leq 2\pi \times 10^6, \end{cases}$$

and for frequencies above $2\pi \times 10^6$, the system would not behave as an LTI system. However, since the input signal is bandlimited to $2\pi \times 10^6$, then we know that for all of the input signals of interest (and all input signals for which the system behaves as an LTI system), the effective frequency response is that of a high-pass filter.

Example

Suppose that we wanted to build a digital version of an echo generator, as in Figure 5.14.

As such, we desire an overall effective input-output relationship that implements

$$y_a(t) = x_a(t) + \alpha x_a(t - \tau_d),$$

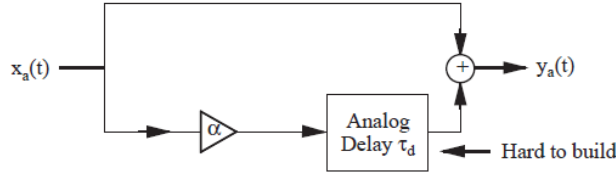


Figure 5.14: An echo generator.

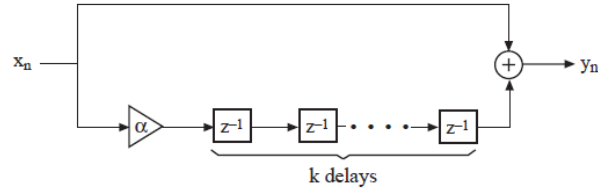


Figure 5.15: A discrete-time echo generator.

where we will assume that $x_a(t)$ is bandlimited to 20kHz. The approach we will take is to first select the sampling rate T for a digital implementation. Then we will determine the desired continuous-time response $H_a(\Omega)$. We will then determine the needed discrete-time response $H_d(\omega)$ and assuming that $\tau_d = kT$, we will sketch an implementation of the discrete-time system.

Since the signal is bandlimited to 20kHz, we will use Nyquist sampling and set $T = \frac{1}{40,000}$. The needed continuous-time frequency response can be readily seen to be $H_a(\Omega) = 1 + \alpha e^{-j\Omega\tau_d}$. Letting $H_d(\omega) = H_a\left(\frac{\omega}{T}\right)$, and setting $\tau_d = kT$, we have

$$\begin{aligned} H_d(\omega) &= 1 + \alpha e^{-j\omega kT/T} \\ &= 1 + \alpha e^{-j\omega k}. \end{aligned}$$

This can be readily implemented using the discrete-time system shown in Figure (5.15).

Note that using this digital filter between an A/D and D/A implements the desired $H_a(\Omega)$. If we had $\tau_d \neq kT$, then $H(z)$ would not be a rational function in the variable z^{-1} , and we would only be able to approximate the desired frequency response. Filter design (and approximation) will be a major topic later in the text.

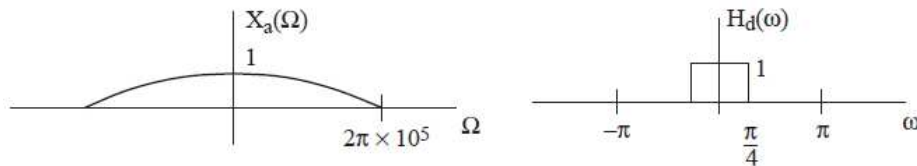
Example

Consider the following continuous-time processor with input $x_a(t)$ and output $y_a(t)$,

$$x_a(t) \longrightarrow \boxed{\text{A/D}} \xrightarrow{\uparrow T} x[n] \longrightarrow \boxed{H_d(\omega)} \longrightarrow y[n] \longrightarrow \boxed{\text{ideal D/A}} \xrightarrow{\uparrow T} y_a(t),$$

with $\frac{1}{T} = 3 \times 10^5$ samples/sec and $X_a(\Omega)$ and $H_d(\omega)$ as shown in Figure 5.16.

Let us now sketch $X_d(\omega)$, $Y_d(\omega)$ and $Y_a(\Omega)$. We can readily map the CT Fourier transform to the DTFT using the relation $X_d(\omega) = \frac{1}{T} X_a\left(\frac{\omega}{T}\right)$, for $|\omega| < \pi$, since the signal is bandlimited to $2\pi \times 10^5$ and we see that $2\pi \times 10^5 < \frac{\pi}{T} = 3\pi \times 10^5$. We simply need to scale the amplitude of $X_d(\Omega)$ by the factor $\frac{1}{T} = 3 \times 10^5$ and scale

Figure 5.16: Fourier transform of the input signal $x_a(t)$ and discrete-time frequency response $H_d(\omega)$.

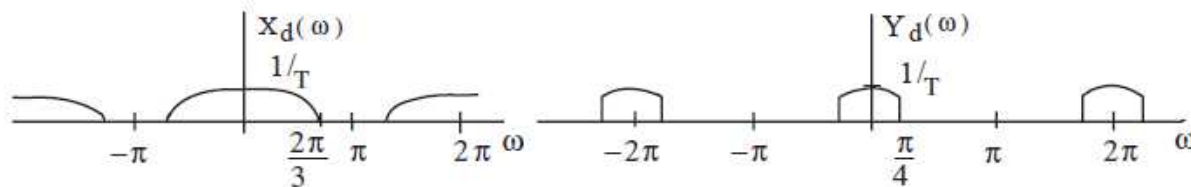


Figure 5.17: Discrete-time Fourier transforms for the discrete-time input and output signals, $x[n]$ and $y[n]$.

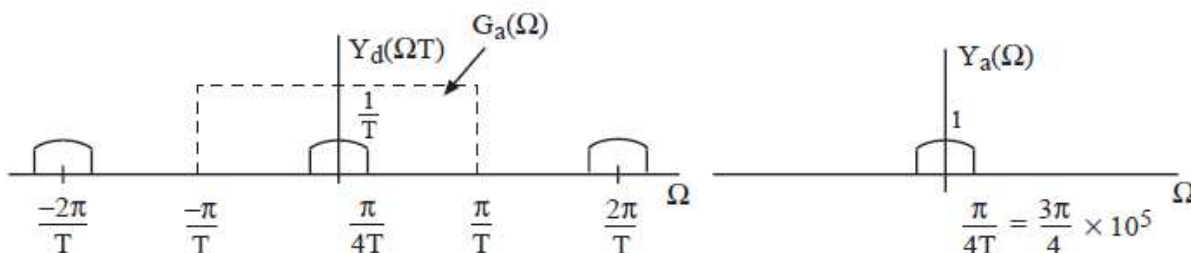


Figure 5.18: The mapping of $Y_d(\Omega T)$ and subsequent filtering with the reconstruction filter $G_a(\Omega)$ are shown yielding the overall output spectrum $Y_a(\Omega)$.

the frequency axis such that the frequency $2\pi \times 10^5$ maps to the discrete-time frequency $2\pi \times 10^5 T = \frac{2\pi}{3}$. The output of the discrete-time filter can then be readily obtained such that $X_d(\omega)$ and $Y_d(\omega)$ are as shown in Figure 5.17.

For an ideal D/A converter, we have that $Y_a(\Omega) = Y_d(\Omega T)G_a(\Omega)$, with

$$G_a(\Omega) = \begin{cases} T, & |\Omega| \leq \frac{\pi}{T} \\ 0, & |\Omega| > \frac{\pi}{T}. \end{cases}$$

Therefore, the output CTFT, $Y_a(\Omega)$ is as shown in Figure 5.18.

Notice that if the D/A were not ideal, and $G_a(\Omega)$ did not completely remove the signal components in $Y_d(\Omega T)$ for $|\Omega| > \frac{\pi}{T}$, but instead had a nonzero response in this region, then $Y_a(\Omega)$ would have undesired high-frequency components due to the periodic nature of $Y_d(\Omega T)$. Thus, a critical job of the D/A is to suppress these high-frequency replicas.

5.4 Applications of DSP systems

Chapter 6

Discrete time Filters and Filter Design

6.1 Discrete-time frequency-selective filters, filter properties, frequency response magnitude, phase, group delay

6.2 Implementations of discrete-time filters: digital filter structures (flowgraphs) and algorithmic representation (programs)

6.3 FIR and IIR filters

In discrete-time, linear shift invariant systems can either have an impulse response that is finite in length or that is infinite in length. When the impulse response is of finite length, we call such a system an “FIR” filter, where “FIR” stands for “finite-length impulse response.” A causal FIR filter of length N will satisfy

$$h[n] = 0, \quad n < 0, \text{ and } n \geq N,$$

for integer $N > 0$. When the impulse response is not FIR, i.e. the impulse response is infinite in length, then we call such a system an “IIR” filter, where “IIR” stands for “infinite-length impulse response.”

- An FIR filter has an impulse response $h[n]$ that is finite in length.
- An IIR filter has an impulse response $h[n]$ that is infinite in length.

Recalling the discussion from Section 4.10, we can represent a causal, linear shift invariant system using an interconnection of delays, adders, and gains, in what is known as a “flow-graph.”

An FIR filter with impulse response

$$h[n] = a_0\delta[n] + a_1\delta[n-1] + \dots + a_{N-1}\delta[n-N+1],$$

has a transfer function

$$H(z) = a_0 + a_1z^{-1} + \dots + a_{N-1}z^{-(N-1)},$$

which is a polynomial in z^{-1} . Such an FIR filter can be implemented using a direct form structure as shown in Figure 6.1.

The implementation of a transfer function is not unique. The transfer function describes only the input-output properties of the system. For any transfer function, there are an infinite number of possible realizations of that transfer function. For example, consider the transpose-form structure (obtained by reversing all arrows and swapping the input and the output), shown in Figure 6.2.

This structure has the same transfer function as the Direct Form structure and is commonly used. An advantage of the transposed form is that it is easier to fully parallelize. Note that there is no adder tree needed at the output as in Direct Form. FIR filters are nearly always implemented *nonrecursively* as in the above diagrams. Theoretically, though, FIR filters can be recursive, as shown in the following example.

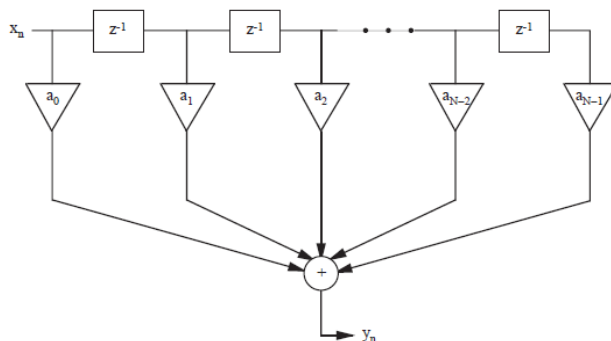


Figure 6.1: Due to the arrangement of the delays, this direct-form structure is also called a “transversal filter” or “tapped delay-line” filter.

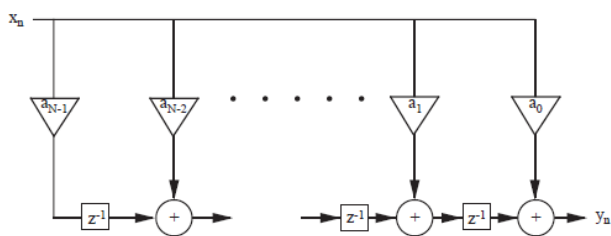


Figure 6.2: Transposed direct form I flowgraph for an FIR filter.

Example

We can disguise the FIR transfer function as a rational transfer function with non-unity denominator. Here’s one of many ways to do it:

$$\begin{aligned}
 H(z) &= a_0 + a_1 z^{-1} + a_2 z^{-2} \\
 &= \frac{1 + z^{-1}}{1 + z^{-1}} (a_0 + a_1 z^{-1} + a_2 z^{-2}) \\
 &= \frac{a_0 + z^{-1}(a_0 + a_1) + z^{-2}(a_1 + a_2) + a_2 z^{-3}}{1 + z^{-1}}
 \end{aligned}$$

Now we can obtain a difference equation for this system that is recursive, even though the system is FIR.

$$\begin{aligned}
 Y(z)(1 + z^{-1}) &= [a_0 + z^{-1}(a_0 + a_1) + z^{-2}(a_1 + a_2) + a_2 z^{-3}]X(z) \\
 &= -z^{-1}Y(z) + [a_0 + z^{-1}(a_0 + a_1) + z^{-2}(a_1 + a_2) + a_2 z^{-3}]X(z),
 \end{aligned}$$

which has the following flowgraph representation:

Transfer functions for IIR filters are not polynomials in z^{-1} . We consider *rational* transfer functions here. An IIR filter must have a recursive implementation, otherwise it would require an infinite number of delays, adders, and gains. Let’s consider a second-order example.

$$H(z) = \frac{a_0 + a_1 z^{-1} + a_2 z^{-2}}{1 + b_1 z^{-1} + b_2 z^{-2}}.$$

This can be implemented using a direct-form 1 structure:

We can also implement $H(z)$ using a direct-form 2 structure:

We have shown previously that this structure has the same transfer function $H(z)$ as the direct form 1 structure.

- IIR filters are always recursive.
- FIR filters are usually implemented in non-recursive form.

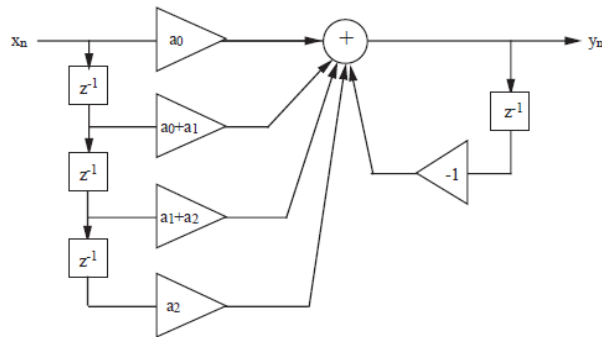


Figure 6.3: This is a recursive structure, since $y[n]$ depends on $y[n-1]$. However, this recursive structure realizes the transfer function $H(z)$ corresponding to an FIR system.

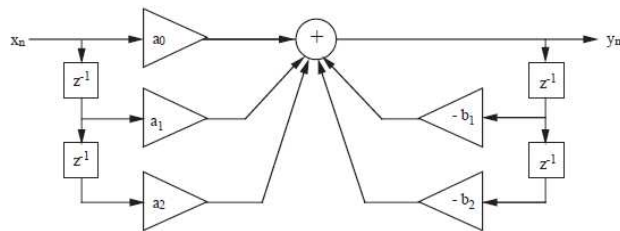


Figure 6.4: Direct form 1 structure implementing $H(z)$.

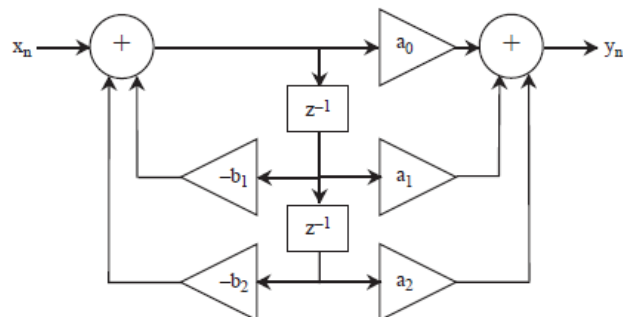


Figure 6.5: Direct form 2 structure implementing $H(z)$.

When implementing higher-order systems, there are many design choices available. We refer to the order of a filter as the larger of the degree of the numerator and denominator polynomials. This is also the number of delay elements required to implement the filter using a direct form 2 structure. Higher order direct-form filters can have large errors at their outputs due to multiplication roundoff. They also suffer greatly from errors due to coefficient quantization. That is, the resulting frequency response $H_d(\omega)$ may differ considerably from that which was desired, if the coefficients were rounded-off (i.e. represented using finite precision). These detrimental effects can be avoided by breaking the higher-degree system into a number of lower-degree subsections. Specifically, using a cascaded or parallel combination of second-order subsections can result in considerably smaller error than a direct-form implementation. Also, breaking the transfer function into lower-order subsections can make the filter easier to parallelize.

Recall that to obtain a **cascade form** representation, we begin with the transfer function

$$\begin{aligned} H(z) &= \frac{a_0 + a_1 z^{-1} + \dots + a_N z^{-N}}{1 + b_1 z^{-1} + b_2 z^{-2} + \dots + b_N z^{-N}} \\ &= \frac{a_0 z^N + a_1 z^{N-1} + \dots + a_N}{z^N + b_1 z^{N-1} + b_2 z^{N-2} + \dots + b_N}, \end{aligned}$$

which we can write in factored form, as

$$H(z) = a_0 \prod_{i=0}^N \frac{z - z_i}{z - p_i},$$

where z_i and p_i are the poles and zeros of $H(z)$. Since the coefficients a_k and b_k are real-valued, the poles and zeros must come in complex-conjugate pairs, or be real-valued. If we pair-up the complex-conjugate poles and zeros and any remaining real-valued poles and zeros (assuming that N is even), we can obtain:

$$H(z) = a_0 \prod_{i=0}^{N/2} H_i(z),$$

where

$$H_i(z) = \frac{(z - z_k)(z - z_\ell)}{(z - p_m)(z - p_n)},$$

is a second-order subsection satisfying $z_k = z_\ell^*$ (or they are real-valued) and $p_n = p_m^*$ (or they are real-valued). Pairing them in this way, ensures that all multiplier coefficients in the second-order subsections are also real-valued. This way we can use real arithmetic. If any pole is real-valued, then we can pair it with any other real-valued pole, similarly for real-valued zeros.

As an example, suppose we factor $H(z)$ and obtain two poles $p_m = 1 + j$ and $p_n = 1 - j$, then these can be paired such that

$$\begin{aligned} H_i(z) &= \frac{(z - z_k)(z - z_\ell)}{(z - (1 + j))(z - (1 - j))} \\ &= \frac{(z - z_k)(z - z_\ell)}{z^2 - z - jz - z + jz + (1 + j)(1 - j)} \\ &= \frac{(z - z_k)(z - z_\ell)}{\underbrace{z^2 - 2z + 2}_{\text{real filter coefficients}}} \end{aligned}$$

Implemented as a cascade of second-order subsections, $H(z)$ would look as follows: where each $H_i(z)$ is a second-order subsection. If N were odd, then one of the above sections would be a first-order filter, with a single pole and zero.

To implement a higher order filter in parallel form, we can expand $H(z)$ in a partial fraction expansion as follows:

$$\begin{aligned} \frac{H(z)}{z} &= \frac{A}{z} + \frac{B_1}{z - p_1} + \dots + \frac{B_N}{z - p_N} \\ H(z) &= A + \frac{B_1 z}{z - p_1} + \dots + \frac{B_N z}{z - p_N}. \end{aligned}$$

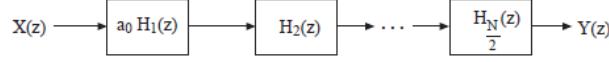


Figure 6.6: Cascade of second-order subsections.

We once again pair the complex conjugate poles, such that $p_k = p_\ell^*$, which implies that $B_k = B_\ell^*$ so that

$$\begin{aligned}
 \frac{B_k z}{z - p_k} + \frac{B_\ell z}{z - p_\ell} &= \frac{B_\ell^* z}{z - p_\ell^*} + \frac{B_\ell z}{z - p_\ell} \\
 &= \frac{B_\ell^* z(z - p_\ell) + B_\ell z(z - p_\ell^*)}{(z - p_\ell^*)(z - p_\ell)} \\
 &= \underbrace{\frac{z^2(B_\ell^* + B_\ell) - z(B_\ell^* p_\ell + B_\ell p_\ell^*)}{z^2 - z(p_\ell^* + p_\ell) + p_\ell p_\ell^*}}_{\text{coefficients are all real}}.
 \end{aligned}$$

This leads to the following parallelization, assuming that N is even,

$$H(z) = A + \sum_{i=1}^{N/2} H_i(z),$$

where

$$\begin{aligned}
 H_i(z) &= \frac{a_{1i} z^2 + a_{2i} z}{z^2 + b_{1i} z + b_{2i}} \\
 &= \frac{a_{1i} + a_{2i} z^{-1}}{1 + b_{1i} z^{-1} + b_{2i} z^{-2}}
 \end{aligned}$$

are second-order subsections. Note that, due to the form of the numerator, each of these second-order subsections requires one fewer multiplication than was needed for cascade form. This implementation takes the following form: If N is odd, then one of the subsections would be first-order.

Example

Suppose we have a fourth-order system with transfer function

$$H(z) = \frac{z^4 + 1}{z^4 - \frac{1}{16}}.$$

To draw a cascade structure of two second-order subsections implementing $H(z)$, we factor $H(z)$ as follows

$$\begin{aligned}
 H(z) &= \frac{(z - e^{j\frac{\pi}{4}})(z - e^{-j\frac{\pi}{4}})(z + e^{j\frac{\pi}{4}})(z + e^{-j\frac{\pi}{4}})}{(z - \frac{1}{2})(z + \frac{1}{2})(z - \frac{j}{2})(z + \frac{j}{2})} \\
 &= \frac{z^2 - (2 \cos(\frac{\pi}{4}))z + 1}{z^2 - \frac{1}{4}} \frac{z^2 + (2 \cos(\frac{\pi}{4}))z + 1}{z^2 + \frac{1}{4}} \\
 &= \frac{z^2 - \sqrt{2}z + 1}{z^2 - \frac{1}{4}} \frac{z^2 + \sqrt{2}z + 1}{z^2 + \frac{1}{4}} \\
 &= \frac{1 - \sqrt{2}z^{-1} + z^{-2}}{1 - \frac{1}{4}z^{-2}} \frac{1 + \sqrt{2}z^{-1} + z^{-2}}{1 + \frac{1}{4}z^{-2}}.
 \end{aligned}$$

Using direct form 2 second-order subsections, the cascade structure would be To implement $H(z)$ using a

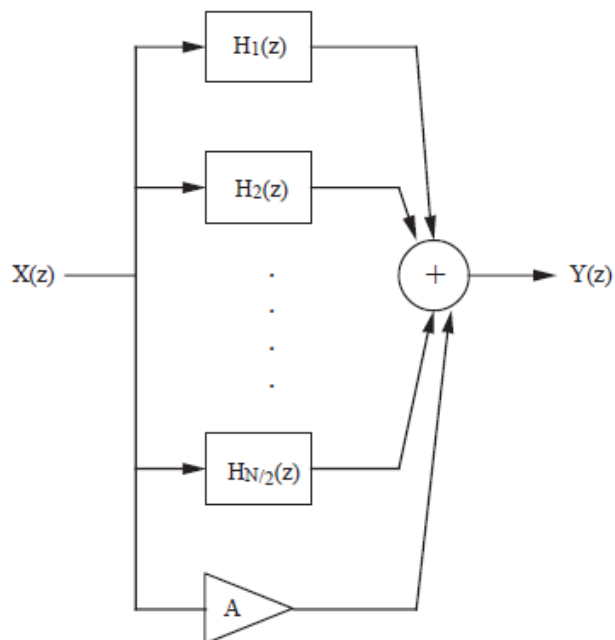


Figure 6.7: Parallel form using second-order subsections.

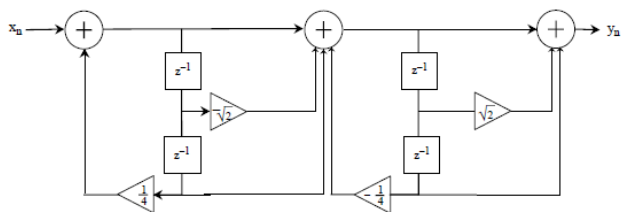


Figure 6.8: $H(z)$ implemented as a cascade of two second-order subsections.

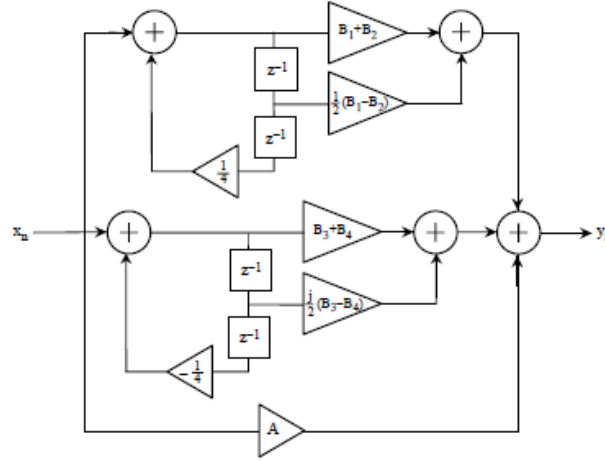


Figure 6.9: A parallel implementation of $H(z)$ using second-order direct form 2 subsections.

parallel structure, we write the transfer function as

$$\begin{aligned}
 \frac{H(z)}{z} &= \frac{z^4 + 1}{z(z - \frac{1}{2})(z + \frac{1}{2})(z - \frac{j}{2})(z + \frac{j}{2})} \\
 &= \frac{A}{z} + \frac{B_1}{z - \frac{1}{2}} + \frac{B_2}{z + \frac{1}{2}} + \frac{B_3}{z - \frac{j}{2}} + \frac{B_4}{z + \frac{j}{2}} \\
 H(z) &= A + \frac{B_1 z}{z - \frac{1}{2}} + \frac{B_2 z}{z + \frac{1}{2}} + \frac{B_3 z}{z - \frac{j}{2}} + \frac{B_4 z}{z + \frac{j}{2}} \\
 &= A + \frac{(B_1 + B_2)z^2 + \frac{1}{2}(B_1 - B_2)z}{(z - \frac{1}{2})(z + \frac{1}{2})} + \frac{(B_3 + B_4)z^2 + \frac{j}{2}(B_3 - B_4)z}{(z - \frac{j}{2})(z + \frac{j}{2})} \\
 &= A + \frac{(B_1 + B_2) + \frac{1}{2}(B_1 - B_2)z^{-2}}{1 - \frac{1}{4}z^{-2}} + \frac{(B_3 + B_4) + \frac{j}{2}(B_3 - B_4)z^{-1}}{1 + \frac{1}{4}z^{-2}}
 \end{aligned}$$

Using direct form 2 second-order subsections, the parallel structure for implementing $H(z)$ would be as follows. Note that in the parallel implementation, A and B_i are the coefficients of the partial fraction expansion. Since B_4 is the complex conjugate of B_3 , and B_1 and B_2 are real, so all of the multiplier values are real. Both the cascade and parallel structures will implement the original transfer function $H(z)$ and will generally do so with less error due to finite register length than a fourth-order direct form implementation.

6.4 Generalized linear phase filters

In designing frequency selective filters, the frequency response magnitude of the filter should remain roughly constant over the portion of the frequency band that is desired to be passed. The frequency response magnitude should be as small as possible over the frequency band that is desired to be rejected. Ideally, the phase response of the filter should be zero over the band of frequencies to be passed. However, for causal systems, it is not possible to have zero phase in the pass band. As a result, some phase distortion is necessary. From the properties of the discrete-time Fourier transform, we know that a simple delay of a sequence corresponds to an addition of a linear phase component with a negative slope equal to the amount of the delay, i.e.

$$x[n - d] \longleftrightarrow X_d(\omega)e^{-j\omega d}.$$

This type of distortion is likely acceptable, as it merely corresponds to a delay of an otherwise undistorted signal. As long as the delay is not excessively long, such an effect on the signal components in the pass band are reasonable. However, nonlinear phase can have the effect of delaying different portions of the desired

frequency band by different amounts and lead to massive signal distortion in the time domain. As a result, it is desirable in many applications to achieve linear or approximately linear phase. In this section, we will describe a class of approximately linear phase systems by considering the class of systems that have *generalized linear phase*.

The phase of the frequency response $H_d(\omega)$ is defined in terms of the polar form representation of the complex value, that is, we write

$$H_d(\omega) = |H_d(\omega)|e^{j\angle H_d(\omega)},$$

where the frequency response magnitude is $|H_d(\omega)|$, which by definition is nonnegative, and the phase of the frequency response is $\angle H_d(\omega)$. For a system to have exactly linear phase, we would require the frequency response to satisfy

$$H_d(\omega) = |H_d(\omega)|e^{-j\omega M},$$

for some real number M . However, it is generally not the case that a discrete-time system has exactly linear phase, due to the strict non-negativity of the magnitude function when the frequency response is written in polar form. However, it is not difficult to design FIR filters having *generalized linear phase*.

Generalized linear phase filters satisfy

$$H_d(\omega) = R(\omega)e^{j(\alpha - \omega M)},$$

where $R(\omega)$ is a real-valued function, but may not be nonnegative. It turns out that the important aspects of linear phase (that the effect of the phase-response on the input be merely a delay) is captured by this more general notion. In fact, generalized linear phase is related to the *group delay* of a filter, which is given by the following expression

$$\tau(\omega) = -\frac{d}{d\omega} \arg H_d(\omega),$$

where $\arg H_d(\omega)$ is the unwrapped phase of $H_d(\omega)$, i.e. it is the phase response with jumps of π and 2π removed. A generalized linear phase filter would have a group delay given by

$$\tau(\omega) = -\frac{d}{d\omega}(\alpha - \omega M) = M,$$

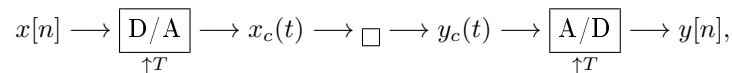
so that a generalized linear phase filter is also a *constant group delay* filter. We will see that it is in general easy to construct FIR filters that have generalized linear phase. It turns out that it is impossible to create IIR filters with rational transfer functions that have generalized linear phase. An example of an IIR filter (with a non-rational transfer function) that has generalized linear phase is given by

$$h[n] = \frac{\sin(\omega_c(n - \beta))}{\pi(n - \beta)},$$

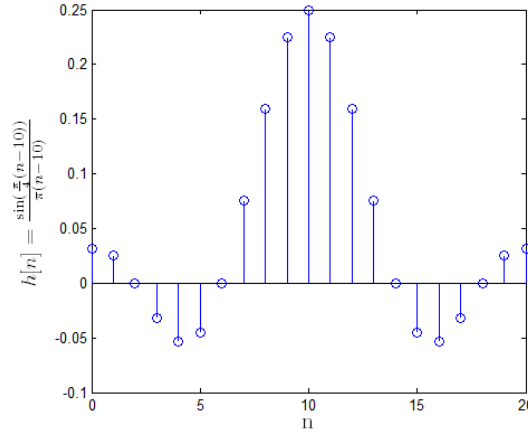
for β a real constant. Note that this impulse response corresponds to a frequency response of

$$H_d(\omega) = \begin{cases} e^{-j\omega\beta}, & |\omega| < \omega_c \\ 0, & \text{otherwise,} \end{cases}$$

which can be viewed as a cascade of an ideal low pass filter with cutoff frequency ω_c followed by a filter with frequency response $H_d(\omega) = e^{-j\omega\beta}$. If β is an integer, then this corresponds to a simple delay of β samples. If β is not an integer, then this corresponds to something more subtle. Specifically, this “fractional sample delay” filter is best considered as “samples of a delayed version of the bandlimited interpolation of the input,” as expressed by the following block diagram.



While IIR filters with rational transfer functions (and therefore finite order difference equation representations) cannot obtain generalized linear phase, an IIR filter can generally achieve frequency response magnitude specifications with a much lower order filter than an FIR filter.

Figure 6.10: FIR filter with generalized linear phase of length $N = 21$.

6.4.1 Causal Generalized Linear Phase Filters

For FIR filters, there are four ways in which to achieve generalized linear phase. For simplicity, these are called type I, type II, type III and type IV generalized linear phase filters. Each of these exploits symmetries in the FIR filter impulse response in order to guarantee generalized linear phase.

Type I Generalized Linear Phase

A causal FIR filter with real-valued impulse response, $h[n]$ of length N , i.e. $h[n]_{n=0}^{N-1}$, has Type I generalized linear phase with $H_d(\omega) = R(\omega)e^{-j\omega M}$, if and only if $h[n]$ satisfies

$$h[n] = h[N - 1 - n], \quad 0 \leq n \leq N - 1,$$

where $M = (N - 1)/2$ is an integer and N an odd integer. An example with $M = 10$, and $N = 21$, is as shown below. To show that Type I FIR filters have generalized linear phase, we write

$$\begin{aligned} H_d(\omega) &= \sum_{n=0}^{N-1} h[n]e^{-j\omega n} \\ &= \sum_{n=0}^{M-1} h[n]e^{-j\omega n} + h[M]e^{-j\omega M} + \sum_{n=M+1}^{N-1} h[n]e^{-j\omega n} \\ &= e^{-j\omega M} \left[h[M] + \sum_{n=0}^{M-1} h[n]e^{-j\omega(n-M)} + \sum_{n=M+1}^{N-1} h[n]e^{-j\omega(n-M)} \right] \end{aligned}$$

Making the change of variable $n = N - 1 - k$ and using $M = (N - 1)/2$ the second sum above can be rewritten

$$\begin{aligned} H_d(\omega) &= e^{-j\omega M} \left[h[M] + \sum_{n=0}^{M-1} h[n]e^{-j\omega(n-M)} + \sum_{k=M-1}^0 h[N - 1 - k]e^{-j\omega(M-k)} \right] \\ &= e^{-j\omega M} \left[h[M] + \sum_{n=0}^{M-1} \left(h[n]e^{-j\omega(n-M)} + h[N - 1 - n]e^{-j\omega(M-n)} \right) \right], \end{aligned}$$

and using that $h[n] = h[N - 1 - n]$, we have

$$\begin{aligned} H_d(\omega) &= e^{-j\omega M} \left[h[M] + 2 \sum_{n=0}^{M-1} h[n] \cos(\omega(n - M)) \right] \\ &= e^{-j\omega M} R(\omega), \end{aligned}$$

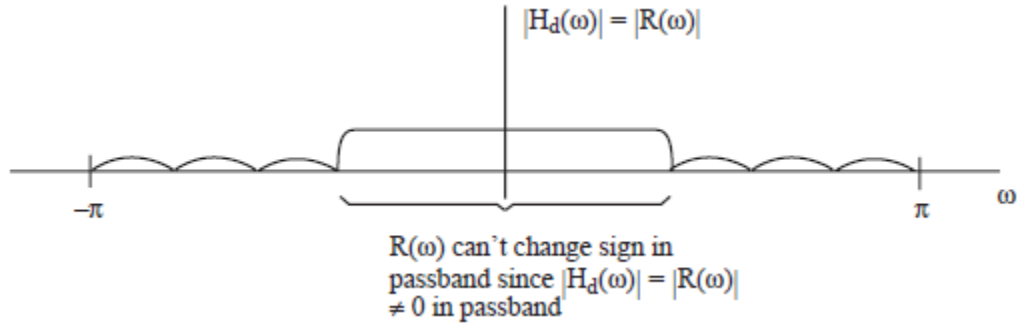


Figure 6.11: Frequency-selective generalized linear phase filter.

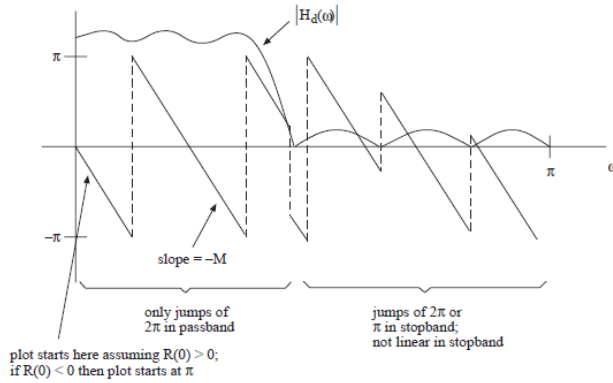


Figure 6.12: Phase characteristic of a generalized linear phase FIR filter.

where $R(\omega)$ is a real-valued function of ω . Note that

$$|H_d(\omega)| = |R(\omega)|$$

and that

$$\angle H_d(\omega) = \begin{cases} -\omega M, & \{\omega : R(\omega) > 0\} \\ -\omega M \pm \pi, & \{\omega : R(\omega) < 0\}, \end{cases}$$

where the sign change of $R(\omega)$ is taken into account using that $-1 = e^{\pm j\pi}$. Note that the phase is actually linear except where $R(\omega)$ changes sign, in which case the phase jumps by π . This implies that a generalized linear phase frequency-selective filter has linear phase over the passband, since To show that a generalized linear phase filter with frequency response given by

$$H_d(\omega) = R(\omega)e^{-j\omega M},$$

for $M = (N - 1)/2$, an integer satisfies

$$h[n] = h[N - 1 - n],$$

we can simply shift the sequence to the right by M samples, yielding $h[n + M]$, which now has a purely real-valued DTFT. From properties of the DTFT, we know that symmetric real-valued sequences have a real-valued DTFT, which yields the desired symmetry property for the unshifted sequence.

A generalized linear phase FIR filter has a phase characteristic exemplified in the following figure, assuming a frequency-selective FIR filter.

Type II Generalized Linear Phase Filters

If the FIR filter has a symmetric impulse response, satisfying

$$h[n] = h[N - 1 - n], \quad 0 \leq n \leq N - 1,$$

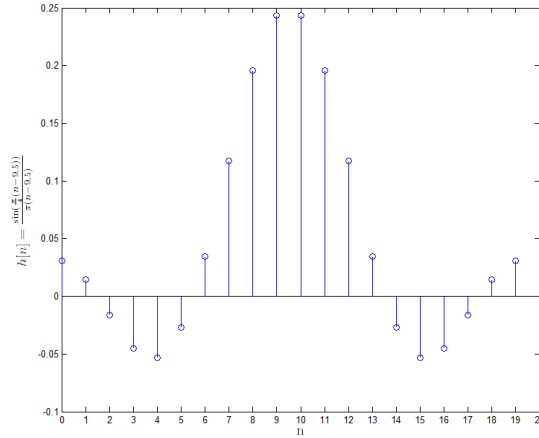


Figure 6.13: FIR filter with generalized linear phase of length $N = 20$.

for N an even integer (filter is even-length), and $M = (N - 1)/2$ a half-integer, then by reasoning similar to the steps for a Type I FIR generalized linear phase filter, we can show that

$$H_d(\omega) = e^{-j\omega M} \left[\sum_{k=1}^{N/2} 2h[(N/2) - k] \cos \left[\omega \left(k - \frac{1}{2} \right) \right] \right], \quad 1 \leq k \leq N/2.$$

Once again, this leads to $H_d(\omega) = R(\omega)e^{-j\omega M}$. The point of symmetry in the impulse response $h[n]$ is now a half-integer, rather than an integer as in the following example.

Type III Generalized Linear Phase Filters

Type III and IV generalized linear phase filters satisfy

$$H_d(\omega) = R(\omega)e^{j(\alpha - \omega M)},$$

where $\alpha \neq 0$, and where $R(\omega)$ is a real-valued, odd function of ω . In this case, for a filter $\{h[n]\}_{n=0}^{N-1}$ and $\alpha \neq 0$, we can show that $\alpha = \frac{\pi}{2}$ and that the impulse response must have odd symmetry, i.e.

$$h[n] = -h[N - 1 - n],$$

and

$$\angle H_d(\omega) = \begin{cases} \frac{\pi}{2} - \omega M, & \{\omega : R(\omega) > 0\} \\ -\frac{\pi}{2} - \omega M, & \{\omega : R(\omega) < 0\}, \end{cases}$$

with $M = (N - 1)/2$ for N even and odd. Specifically for Type III generalized linear phase FIR filters, the impulse response satisfies

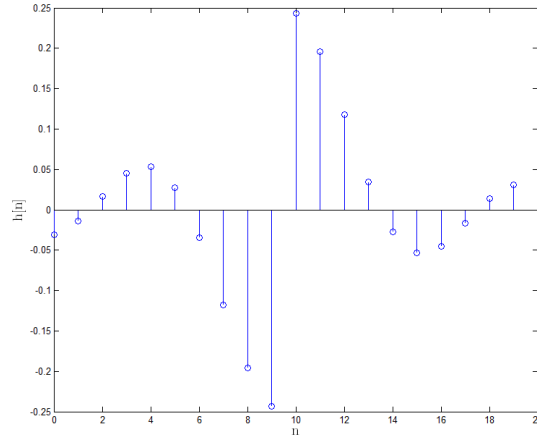
$$h[n] = -h[N - 1 - n], \quad 0 \leq n \leq N - 1,$$

where N is an odd integer (odd-length filter) and $M = (N - 1)/2$ is an integer. In this case, it can be shown using an approach similar to that for Type I FIR filters that $H_d(\omega)$ satisfies

$$H_d(\omega) = je^{-j\omega M} \left[\sum_{k=1}^M 2h[M - k] \sin(\omega k) \right].$$

In this case, $H_d(\omega)$ satisfies

$$H_d(\omega) = R(\omega)e^{j(\alpha - \omega M)},$$

Figure 6.14: Type III generalized linear phase filter with $N = 21$.Figure 6.15: Type IV generalized linear phase FIR filter with $N = 20$.

where $\alpha = \pm\pi/2$, and $R(\omega)$ is a real-valued, odd function of ω . The odd symmetry of the impulse response gives rise to a frequency response that is a linear combination of sines, rather than cosines, leading to $R(\omega)$ being a real-valued, odd function, and the offset of $\pm\pi/2$ in the phase. To show that this type of antisymmetry is necessary for a filter satisfying $H_d(\omega) = R(\omega)e^{j(\alpha-\omega M)}$, we can again appeal to properties of the DTFT. Shifting this sequence to be centered about $n = 0$, would give rise to a DTFT that was purely-imaginary and odd. DTFT properties reveal that this would correspond to an odd function of n , which, when delayed by M samples yields the necessary antisymmetry condition. An example of such a Type III generalized linear phase filter is given in the following figure.

Type IV Generalized Linear Phase Filters

If the impulse response is antisymmetric and satisfies

$$h[n] = -h[N-1-n], \quad 0 \leq n \leq N-1,$$

for N and even integer and $M = (N-1)/2$ a half integer, then the frequency response satisfies

$$H_d(\omega) = R(\omega)e^{j(\frac{\pi}{2}-\omega M)},$$

where $R(\omega)$ is a real-valued odd function of ω . Again, using a similar derivation as for Type III FIR generalized linear phase, we can show that the frequency response can be written

$$H_d(\omega) = je^{-j\omega M} \left[\sum_{k=1}^{N/2} 2h \left[\frac{N}{2} - k \right] \sin \left(\omega \left(k - \frac{1}{2} \right) \right) \right],$$

which has the desired generalized linear phase form. An example Type IV generalized linear phase filter is shown in the following figure.

Example

Determine whether or not a filter with an impulse response given by

$$h[n] = \delta[n] - \delta[n-1] + \delta[n-2]$$

has generalized linear phase, and if so, whether or not it has linear phase. Note that linear phase implies generalized linear phase, but not vice versa.

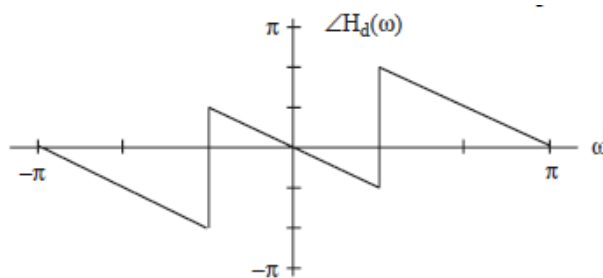


Figure 6.16: Example with generalized linearphase, but not linear phase.

Solution

The impulse response $h[n]$ is symmetric about its midpoint, so it has Type I generalized linear phase. to check whether or not it has linear phase, we compute the frequency response.

$$\begin{aligned} H_d(\omega) &= 1 - e^{-j\omega} + e^{-j2\omega} \\ &= e^{-j\omega} [e^{j\omega} - 1 + e^{j2\omega}] \\ &= e^{-j\omega} [2\cos(\omega) - 1] \end{aligned}$$

so that $R(\omega) = 2\cos(\omega) - 1$, which changes sign in the range $-\pi < \omega < \pi$, so this filter does not have linear phase, but it does have Type I generalized linear phase. The phase of this filter satisfies

$$\angle H_d(\omega) = \begin{cases} -\omega, & \{\omega : 2\cos(\omega) - 1 > 0\} \\ \pi - \omega & \{\omega : 2\cos(\omega) - 1 < 0\} \end{cases}$$

which is clearly not linear, since there are jumps of π at $\omega = \pm\frac{\pi}{3}$ as shown below.

Example

Change the impulse response in the previous example to be

$$h[n] = \frac{1}{4}\delta[n] - \delta[n-1] + \frac{1}{4}\delta[n-2].$$

In this case, the filter is not only of generalized linear phase, but also has linear phase. Work this example out as an exercise.

Example

Determine whether $H_d(\omega)$ for the impulse response

$$h[n] = -\delta[n] + 3\delta[n-1] + \delta[n-2]$$

has generalized linear phase.

Solution

At first it may appear that this filter is of Type III generalized linear phase, however this is not the case, since the middle coefficient is nonzero, which violates the antisymmetry condition. Note that in order for $h[1] = -h[1]$, we must have that $h[1] = 0$. Examining the DTFT, we obtain

$$\begin{aligned} H_d(\omega) &= -1 + 3e^{-j\omega} + e^{-j2\omega} \\ &= e^{-j\omega} (-e^{j\omega} + 3 + e^{j2\omega}) \\ &= e^{-j\omega} (3 - j2\sin(\omega)). \end{aligned}$$

Note that this cannot be put in the form

$$H_d(\omega) = e^{j(\frac{\pi}{2} - \omega M)} R(\omega),$$

for real-valued $R(\omega)$. In this case, it is the non-zero middle coefficient that is preventing this.

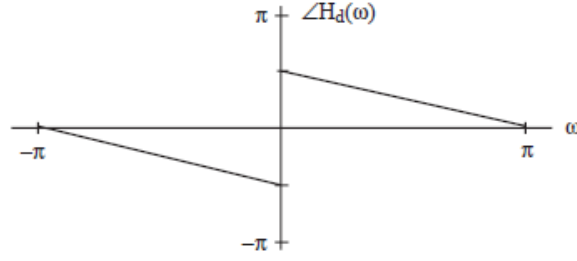


Figure 6.17: Example generalized linear phase filter with nonlinear phase.

Example

Determine whether or not $H_d(\omega)$ corresponding to

$$h[n] = \delta[n] - \delta[n - 1]$$

has generalized linear phase and linear phase or not.

Solution

The frequency response $H_d(\omega)$ has Type IV generalized linear phase, since $h[n]$ is antisymmetric about a half integer. To verify, we have

$$\begin{aligned} H_d(\omega) &= 1 - e^{-j\omega} \\ &= e^{-j\omega/2} (e^{j\omega/2} - e^{-j\omega/2}) \\ &= e^{-j\omega/2} (2j \sin(\omega/2)) \\ &= e^{j(\frac{\pi}{2} - \frac{\omega}{2})} (2 \sin(\omega/2)). \end{aligned}$$

Here, $R(\omega)$ is odd, and therefore must change sign at $\omega = 0$. This implies that we do not have linear phase. Indeed, the phase is given by

$$\begin{aligned} \angle H_d(\omega) &= \begin{cases} \frac{\pi}{2} - \frac{\omega}{2}, & \{\omega : \sin(\omega/2) > 0\} \\ -\frac{\pi}{2} - \frac{\omega}{2}, & \{\omega : \sin(\omega/2) < 0\} \end{cases} \\ &= \begin{cases} \frac{\pi}{2} - \frac{\omega}{2}, & 0 < \omega < \pi \\ -\frac{\pi}{2} - \frac{\omega}{2}, & -\pi < \omega < 0. \end{cases} \end{aligned}$$

This is clearly not linear, as shown below. Since $R(\omega)$ will be odd for any antisymmetric filter, we conclude that antisymmetric impulse responses cannot have linear phase, though they will have generalized linear phase.

Example

Given the impulse response

$$h[n] = \delta[n] + \delta[n - 1],$$

does the filter have generalized linear phase or linear phase?

Solution

Because of coefficient symmetry, we know that this filter has Type II generalized linear phase. To check whether or not the filter has linear phase, we check

$$\begin{aligned} H_d(\omega) &= 1 + e^{-j\omega} \\ &= e^{-j\omega/2} (e^{j\omega/2} + e^{-j\omega/2}) \\ &= e^{-j\omega/2} 2 \cos(\omega/2), \end{aligned}$$

which satisfies $R(\omega) > 0$ on the interval $|\omega| < \pi$, and the phase is given by

$$\angle H_d(\omega) = -\omega/2, \quad |\omega| < \pi.$$

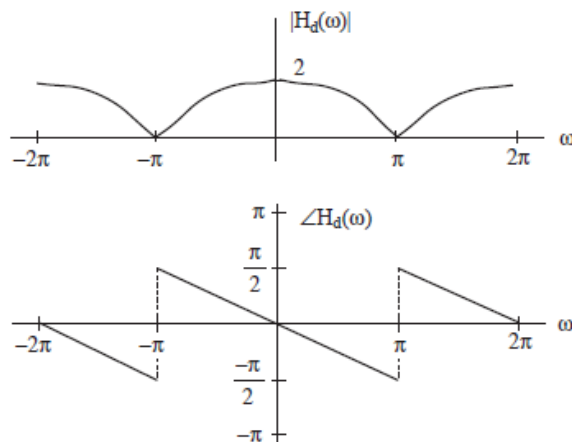


Figure 6.18: Here we do have jumps of π at multiples of π , however we only consider whether or not there is linear phase in the range $-\pi < \omega < \pi$.

Therefore, this filter has linear phase. Of course, since $H_d(\omega)$ is periodic with period 2π , we have

$$\begin{aligned} |H_d(\omega)| &= 2 \cos(\omega/2), \quad |\omega| < \pi, \\ \angle H_d(\omega) &= -\omega/2, \quad |\omega| < \pi, \end{aligned}$$

so we have the following Impact of Coefficient Symmetry on Realizable Frequency Responses

Depending on whether or not $h[n]$ is a symmetric or antisymmetric FIR filter, and whether or not N is even or odd, there can be restrictions on the types of filters that can be realized.

Example

If N is even, and the impulse response is symmetric, then a high-pass filter cannot be realized. This can be seen from properties of the DTFT. Note that $H_d(\pi) = 0$ for an even-length, symmetric impulse response, so $\omega = \pi$ cannot be in the passband. To verify this, we see that

$$\begin{aligned} H_d(\pi) &= \sum_{n=0}^{N-1} h[n] e^{-j\pi n} \\ &= \sum_{n=0}^{N-1} h[n] (-1)^n, \end{aligned}$$

but for a symmetric, even-length impulse response, we have

$$H_d(\pi) = h[0] - h[1] + h[2] - h[3] + \cdots + h[3] - h[2] + h[1] - h[0] = 0.$$

In practice, it is important to be aware of these and other constraints. Note that for a high-pass filter, we could simply take N to be odd and avoid this problem. Let us consider a few FIR filters with small N and evaluate restrictions on $H_d(0)$ and $H_d(\pi)$ as a function of coefficient symmetry and the value of N . Consider the following examples:

$$h[n] = a_0 \delta[n] + a_1 \delta[n-1] + a_1 \delta[n-2] + a_0 \delta[n-3], \quad (\text{even symmetry, } N \text{ even})$$

$$\begin{aligned} H_d(\omega) &= a_0 + a_1 e^{-j\omega} + a_1 e^{-j2\omega} + a_0 e^{-j3\omega} \\ H_d(0) &= 2a_0 + 2a_1 \\ H_d(\pi) &= 0 \end{aligned}$$

$$h[n] = a_0 \delta[n] + a_1 \delta[n-1] + a_2 \delta[n-2] + a_1 \delta[n-3] + a_0 \delta[n-4], \quad (\text{even symmetry, } N \text{ odd})$$

$$\begin{aligned}
H_d(\omega) &= a_0 + a_1 e^{-j\omega} + a_2 e^{-j2\omega} + a_1 e^{-j3\omega} + a_0 e^{-j4\omega} \\
H_d(0) &= 2a_0 + 2a_1 + a_2 \\
H_d(\pi) &= 2a_0 - 2a_1 + a_2
\end{aligned}$$

$$h[n] = a_0 \delta[n] + a_1 \delta[n-1] - a_1 \delta[n-2] - a_0 \delta[n-3], \quad (\text{odd symmetry, } N \text{ even})$$

$$\begin{aligned}
H_d(\omega) &= a_0 + a_1 e^{-j\omega} - a_1 e^{-j2\omega} - a_0 e^{-j3\omega} \\
H_d(0) &= 0 \\
H_d(\pi) &= 2a_0 - 2a_1
\end{aligned}$$

$$h[n] = a_0 \delta[n] + a_1 \delta[n-1] + 0 \delta[n-2] - a_1 \delta[n-3] - a_0 \delta[n-4], \quad (\text{odd symmetry, } N \text{ odd})$$

$$\begin{aligned}
H_d(\omega) &= a_0 + a_1 e^{-j\omega} + 0 e^{-j2\omega} - a_1 e^{-j3\omega} - a_0 e^{-j4\omega} \\
H_d(0) &= 0 \\
H_d(\pi) &= 0
\end{aligned}$$

Looking at these examples, we can conclude that in general, we have:

FIR GLP Type	Symmetry	N	Unrealizable Filters
I	even	odd	no restrictions
II	even	even	high-pass, bandstop
III	odd	odd	low-pass, high-pass, bandstop
IV	odd	even	low-pass, bandstop

Notice that a bandstop filter has its stopband located between 0 and π , and therefore has passbands that include both $\omega = 0$ and $\omega = \pi$. Thus, if either a lowpass or a highpass filter cannot be realized, then a bandstop filter similarly cannot be realized.

6.5 FIR filter design: truncation, windows, least-squares, frequency sampling, min-max and other computer optimizations

6.6 IIR filter design; design via bilinear transformation; design via least-squares methods (can be skipped)

6.7 Applications of digital filtering

Implementation of Ideal D/A

Consider



Recall that any D/A we encounter in this course can be modeled by

$$y_a(t) = \sum_{n=-\infty}^{\infty} y_n g_a(t - nT) \quad (1)$$

and that the Fourier-domain relation is

$$Y_a(\Omega) = G_a(\Omega) Y_d(\Omega T) \quad (2)$$

For the ideal D/A, we have $g_a(t) = \text{sinc}\left(\frac{\pi}{T}t\right)$, giving

$$y_a(t) = \sum_{n=-\infty}^{\infty} y_n \text{sinc}\left[\frac{\pi}{T}(t - nT)\right] \quad (3)$$

and

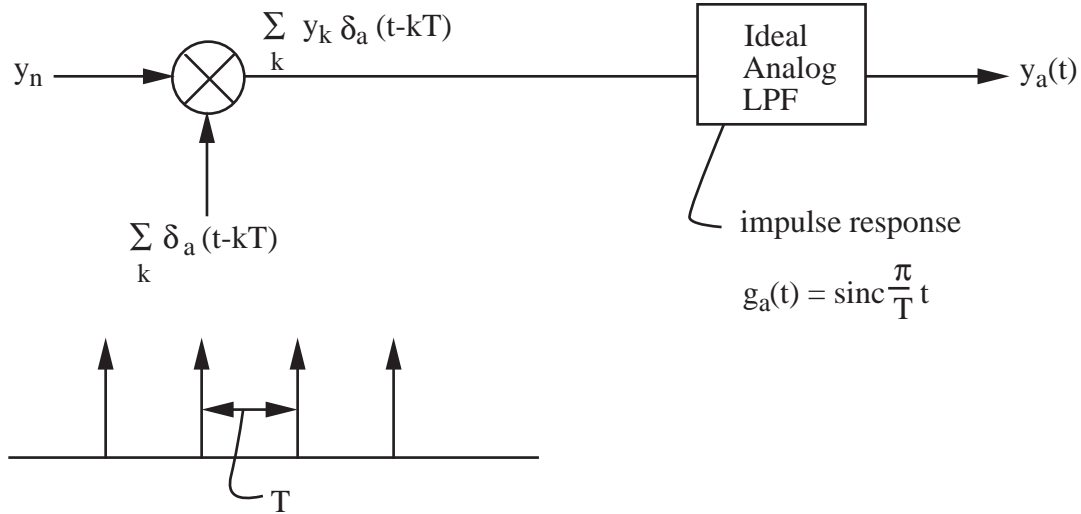
$$G_a(\Omega) = \begin{cases} T & |\Omega| \leq \frac{\pi}{T} \\ 0 & \text{else} \end{cases}$$

so that (2) gives

$$Y_a(\Omega) = \begin{cases} T Y_d(\Omega T) & |\Omega| \leq \frac{\pi}{T} \\ 0 & \text{else} \end{cases} \quad (4)$$

How might we implement the ideal D/A, described by (3)?

Conceptually, we might think along the lines of:

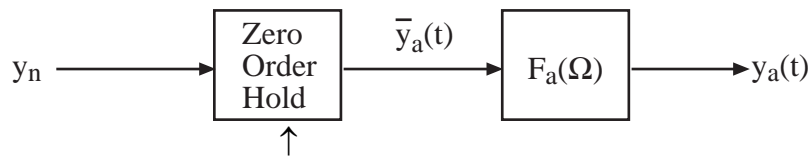


Then:

$$y_a(t) = g_a(t) * \sum_n y_n \delta_a(t-nT) = \sum_n y_n g_a(t-nT) \text{ as desired.}$$

For an actual implementation, we might consider approximating the impulse train by a periodic sequence of very tall, narrow pulses. **However, this would be difficult in practice. As a result, D/A's are not implemented as suggested above!**

In practice, the ideal D/A is approximated with the following two-stage system:

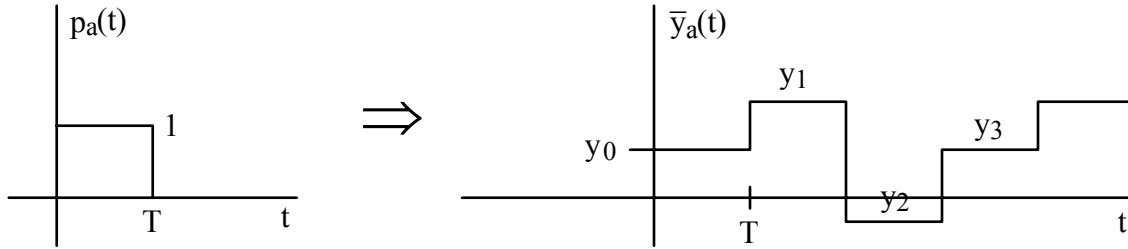


↑
in manufacturer's catalog just the ZOH may be called a D/A

What is a zero-order hold (ZOH)? It is a D/A that uses rectangular pulses, i.e.,

$$\bar{y}_a(t) = \sum_n y_n p_a(t - nT) \tag{5}$$

where



Thus, the ZOH output is a staircase approximation to the desired $y_a(t)$. This staircase must be smoothed by $F_a(\Omega)$ to produce the proper $y_a(t)$.

The Fourier-domain relation for the ZOH has the form given by (2), but now

$$\begin{aligned}
 G_a(\Omega) &= \int_0^T 1 \cdot e^{-j\Omega t} dt \\
 &= \frac{e^{-j\Omega t}}{-j\Omega} \Big|_0^T = \frac{e^{-j\Omega T} - 1}{-j\Omega} \\
 &= \frac{e^{-j\Omega \frac{T}{2}} \left(e^{-j\Omega \frac{T}{2}} - e^{j\Omega \frac{T}{2}} \right)}{-j\Omega} = e^{-j\Omega \frac{T}{2}} \frac{2 \sin \frac{\Omega T}{2}}{\Omega} \\
 &= T e^{-j\Omega \frac{T}{2}} \text{sinc} \frac{\Omega T}{2}
 \end{aligned}$$

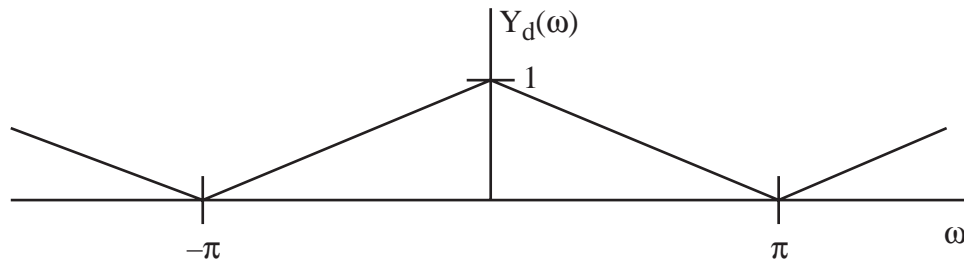
Thus,

$$\bar{Y}_a(\Omega) = T e^{-j\Omega \frac{T}{2}} \text{sinc} \left(\frac{\Omega T}{2} \right) Y_d(\Omega T) \quad (6)$$

Before deciding how to choose $F_a(\Omega)$, which follows the ZOH, let's see how the effect of the ZOH differs from the ideal D/A, in the Fourier domain.

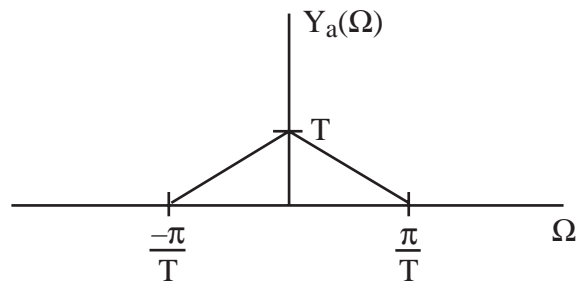
Example

Suppose have

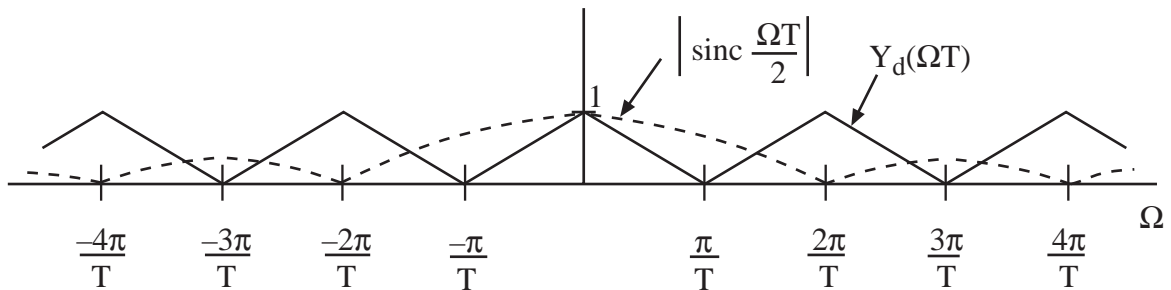


Sketch $Y_a(\Omega)$, the Fourier transform of the output of an ideal D/A, and $\bar{Y}_a(\Omega)$, the Fourier transform of the output of a ZOH.

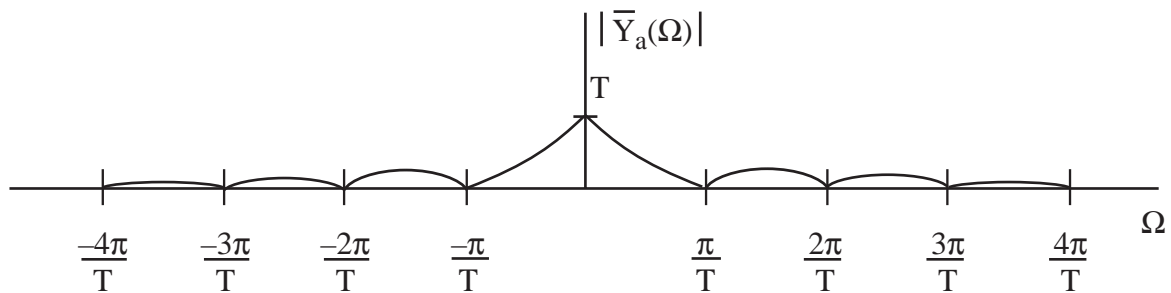
Using (4), we have for the ideal D/A:



For the ZOH, let's plot $|\bar{Y}_a(\Omega)|$. The terms in (6) look like:



$|\bar{Y}_a(\Omega)|$ is T times the product of the above two curves:



Notice that unlike $Y_a(\Omega)$ for the ideal D/A, $[\bar{Y}_a(\Omega)]$ for the ZOH has frequency content that extends all the way to $\Omega = \pm \infty$. This is not surprising, since $\bar{y}_a(t)$, for the ZOH, is a staircase function with discontinuities. Sharp edges (discontinuities) always correspond to a frequency content extending to $\pm \infty$.

Now, if we have $\bar{Y}_a(\Omega)$ from the ZOH, how do we choose $F_a(\Omega)$ to produce $Y_a(\Omega)$? The above sketches suggest that we need $F_a(\Omega)$ to be a LPF with cutoff at $\Omega_c = \pm \frac{\pi}{T}$. To investigate this thoroughly, note that for the ZOH system we have

$$\begin{aligned} Y_a(\Omega) &= F_a(\Omega) \bar{Y}_a(\Omega) \\ &= F_a(\Omega) T e^{-j\frac{\Omega T}{2}} \text{sinc}\left(\frac{\Omega T}{2}\right) Y_d(\Omega T) \end{aligned} \quad (7)$$

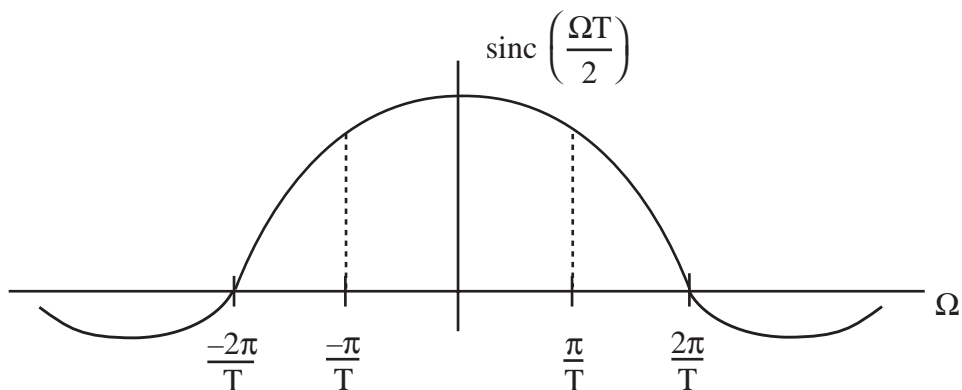
For the ideal D/A, the relation is given by (4). To have (7) correspond to (4) we must have

$$F_a(\Omega) T e^{-j\frac{\Omega T}{2}} \text{sinc}\left(\frac{\Omega T}{2}\right) Y_d(\Omega T) = \begin{cases} T Y_d(\Omega T) & |\Omega| \leq \frac{\pi}{T} \\ 0 & \text{else} \end{cases}$$

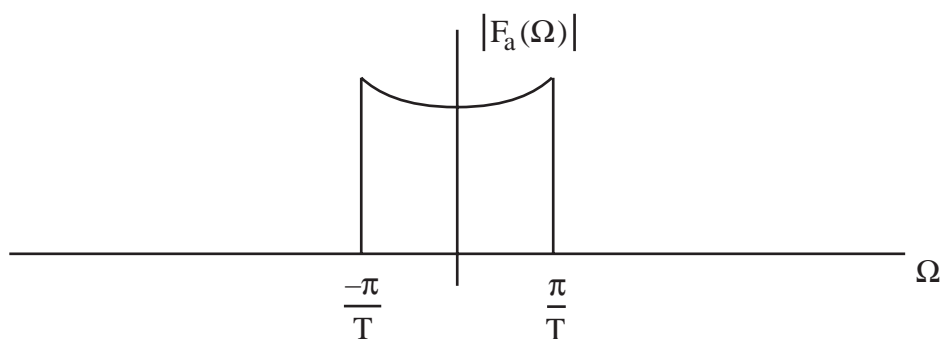
or

$$F_a(\Omega) = \begin{cases} \frac{e^{j\frac{\Omega T}{2}}}{\text{sinc}\left(\frac{\Omega T}{2}\right)} & |\Omega| \leq \frac{\pi}{T} \\ 0 & |\Omega| > \frac{\pi}{T} \end{cases}$$

The first zero-crossing of $\text{sinc} \frac{\Omega T}{2}$ occurs when $\frac{\Omega T}{2} = \pi \Rightarrow \Omega = \frac{2\pi}{T}$.

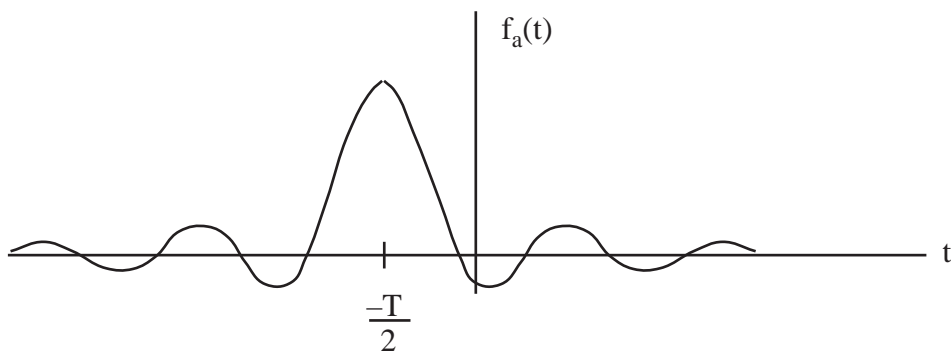


So, $|F_a(\Omega)|$ looks like:

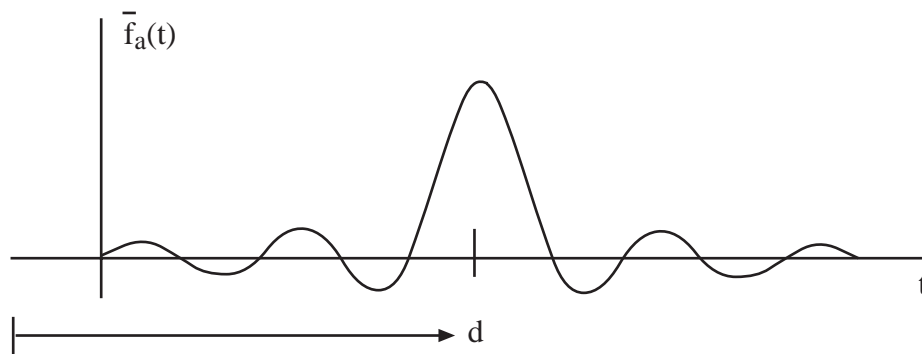


Thus, the ideal $F_a(\Omega)$ is a LPF that emphasizes the higher frequencies in its passband. (Surprising!)

$F_a(\Omega)$ has finite support $\Rightarrow f_a(t)$ has infinite support. $f_a(t)$ might look something like:



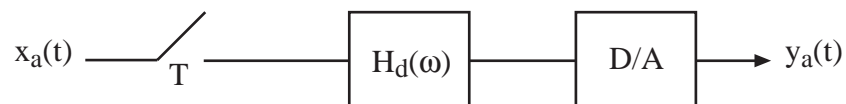
In practice, we would use a filter with a causal impulse response $\bar{f}_a(t)$ with $\bar{f}_a(t) \approx f_a(t-d) u_a(t)$ (delayed and truncated version of $f_a(t)$).



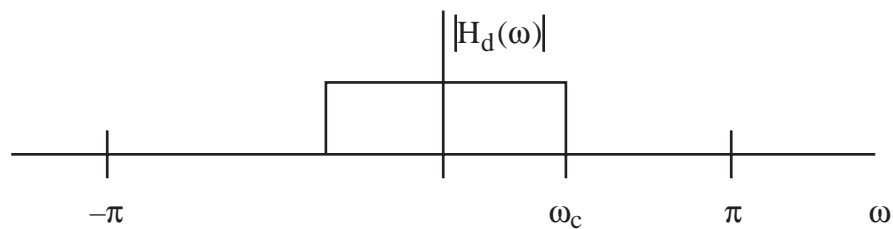
Using $\bar{f}_a(t)$ will delay the desired output by d seconds, but this is no problem in most applications if d is small.

Notes:

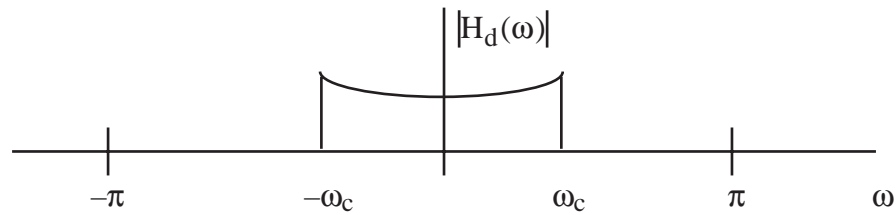
1. In cheaper D/As, we may use a very simple R-C network to crudely approximate the desired $F_a(\Omega)$.
2. The high-frequency emphasis within the passband of $F_a(\Omega)$ can be performed digitally as part of the digital filter function. For example, if wish to realize an analog LPF using



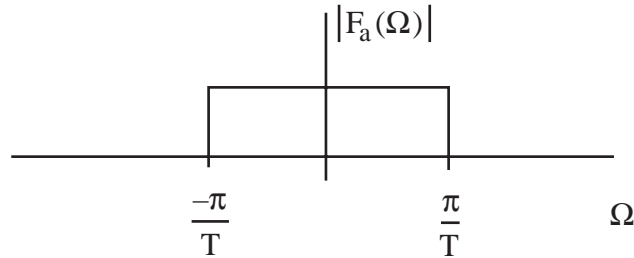
then instead of using



could use



In this case, we still need an $F_a(\Omega)$ after the ZOH, but now $F_a(\Omega)$ can be a regular LPF with a flat response in the passband:

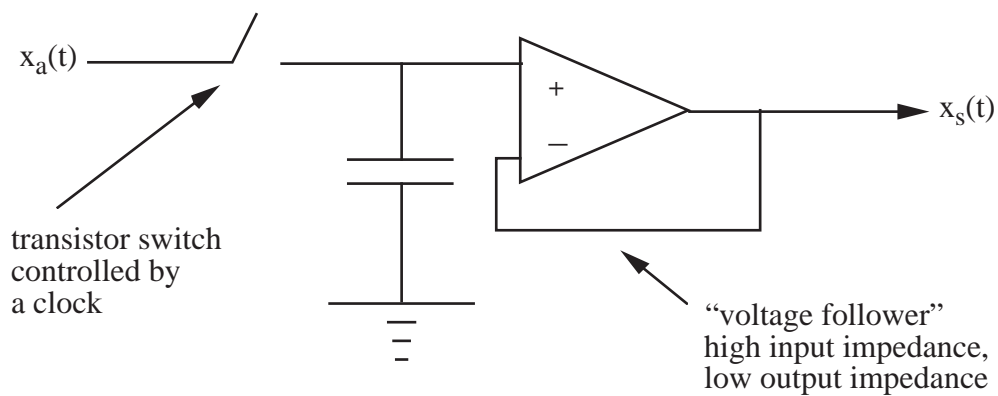


A/D and D/A Circuits

A/D consists of sample and hold followed by a quantizer.

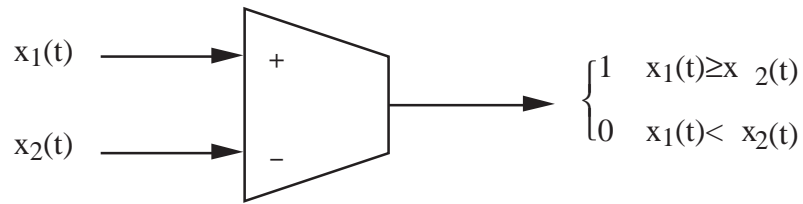
In catalogs, just the quantizer is called an A/D (unless A/D is referred to as a “sampling A/D”). As we shall see, the sample and hold is very simple, whereas the quantizer is much more complicated.

Sample and Hold:



A/D (Quantizer)

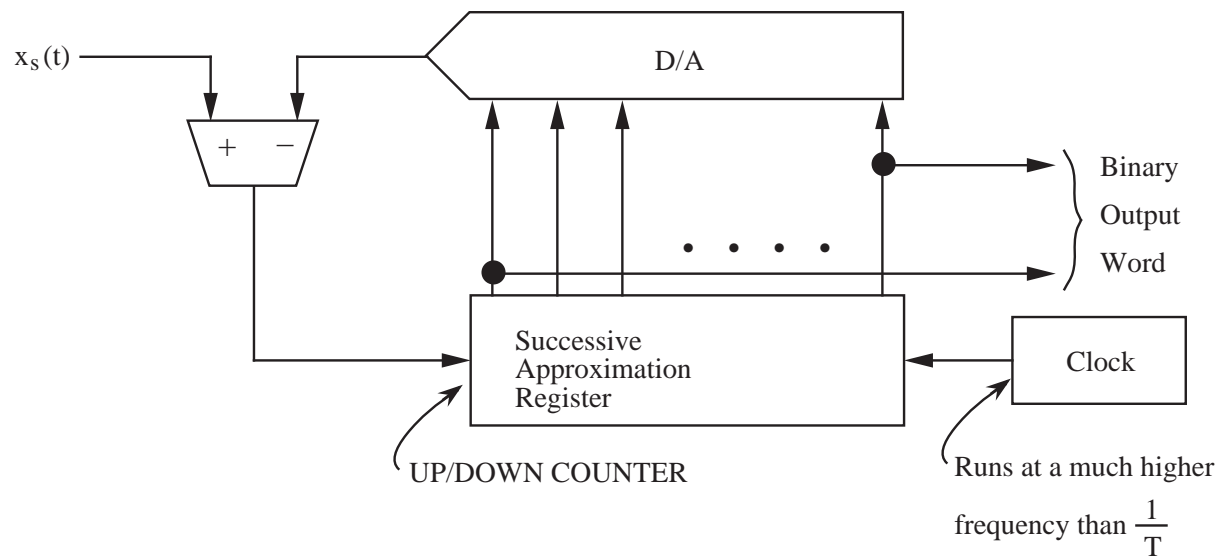
Uses comparators:



Two popular types of A/D's:

a) Successive Approximation

~ for low and medium sampling rates; uses a D/A!



Here, $x_s(t)$ is the input from the sample and hold. The above system quantizes $x_s(t)$ to fit into a computer register. The comparator output signal causes the up-down counter to either increment or decrement, at a high rate, until it contains a binary approximation of $x_s(t)$. When the counter has settled around the correct digital representation of $x_s(t)$, it simply toggles back and forth in its least significant bit until the value of $x_s(t)$ changes.

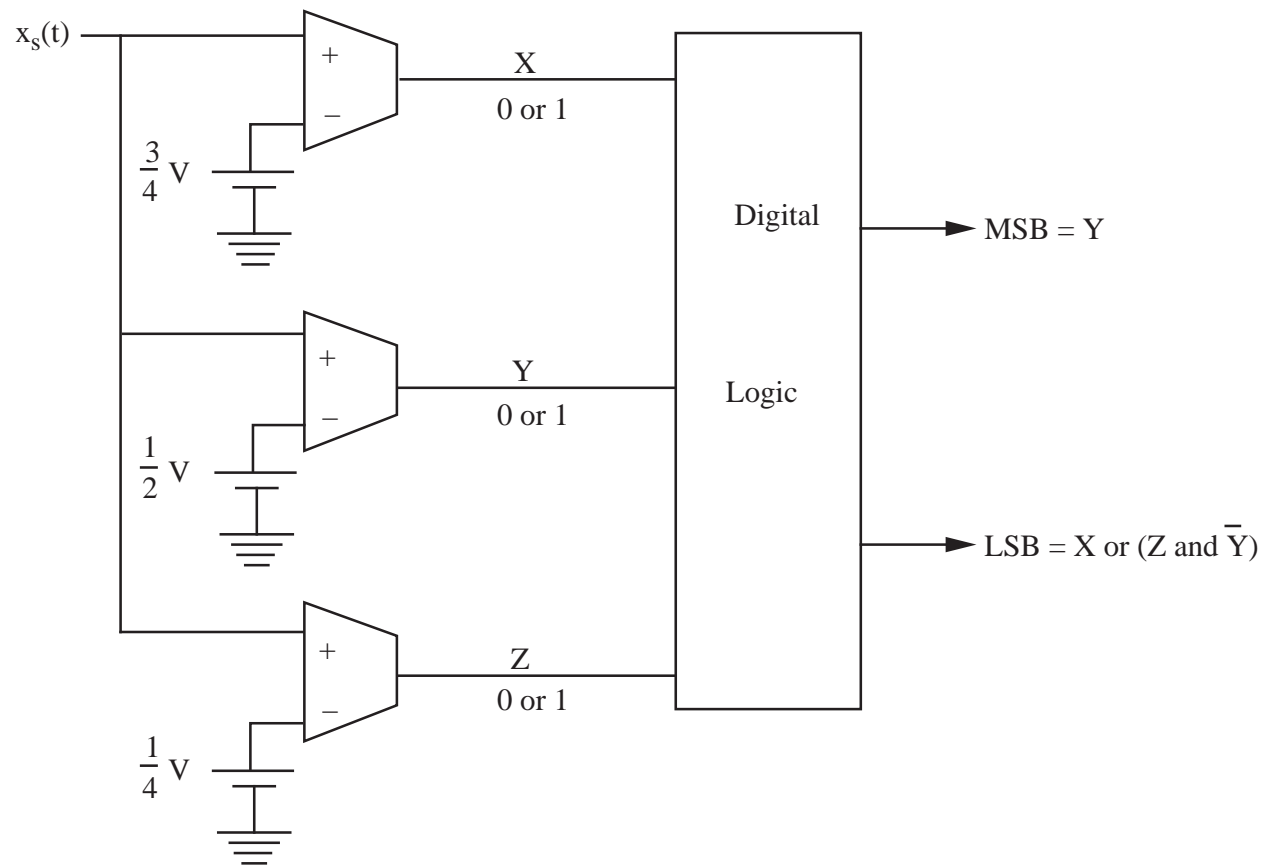
Successive approximation A/D's are fairly slow (and thus used for low and medium bandwidth applications) because it may take several clock cycles for the counter to settle on a new value of $x_s(t)$.

b) Parallel or Flash A/D

For high speed (8 bits/sample at 500 MHz is currently possible).

Uses $2^N - 1$ comparators for N-bit output word.

Example 2 bit quantizer:

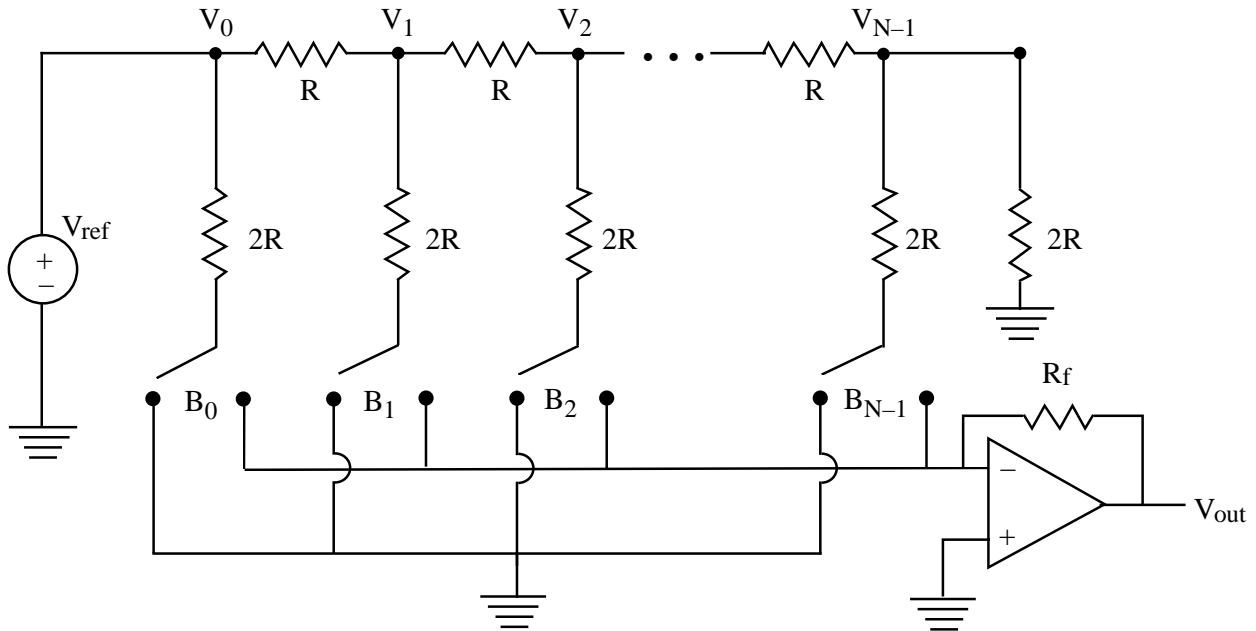


Here, $0 \leq x_s(t) < \frac{1}{4}$ is mapped to (0, 0), $\frac{1}{4} \leq x_s(t) < \frac{1}{2}$ is mapped to (0, 1), $\frac{1}{2} \leq x_s(t) < \frac{3}{4}$ is mapped to (1, 0), and $x_s(t) \geq \frac{3}{4}$ is mapped to (1, 1).

D/A Converters ~ Zero Order Hold (ZOH)

The contents of a binary register containing y_n are the input to a D/A. Let $[B_0, B_1, B_2, \dots, B_{N-1}]$ be the binary representation of y_n . The B_i change with period T as y_{n+1} replaces y_n in the D/A input register.

One popular type of D/A uses a resistor ladder (can also use a capacitor ladder):



The switches are transistors, where the B_i control whether the transistors conduct to ground (left position, $B_i = 0$) or to the op amp (right position, $B_i = 1$). The op amp then adds all signals input to its minus terminal, with a weighting determined by the resistor values. To find the exact relationship between V_{out} and the B_i , first apply KCL at Node $N-1$ at the upper right, to give:

$$\frac{V_{N-1}}{2R} + \frac{V_{N-1}}{2R} + \frac{V_{N-1} - V_{N-2}}{R} = 0$$

$$\Rightarrow V_{N-1} + V_{N-1} - V_{N-2} = 0 \Rightarrow V_{N-2} = 2 V_{N-1}$$

Similarly: $V_{n-1} = 2V_n$ $n = 1, 2, \dots, N-2$

$$\Rightarrow V_n = V_{N-1} 2^{N-1-n}$$

Using KCL at the minus terminal of the op amp gives:

$$\frac{1}{2R} \sum_{i=0}^{N-1} B_i V_i = \frac{0 - V_{out}}{R_f}$$

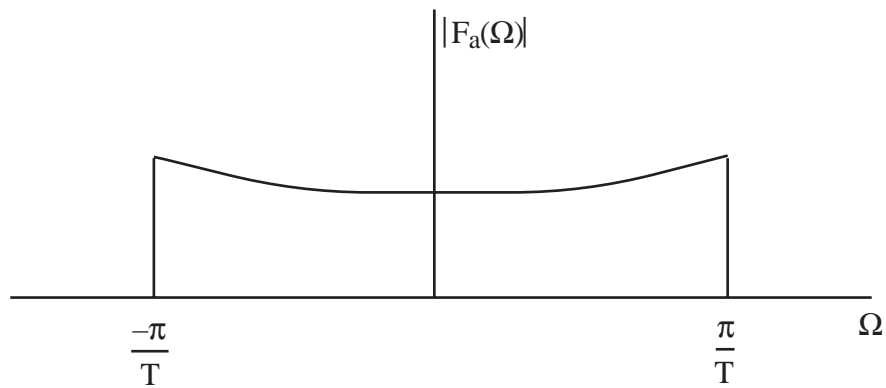
where each B_i is 0 or 1.

9.12

$$\begin{aligned}\Rightarrow V_{\text{out}} &= \frac{-R_f}{2R} \sum_{i=0}^{N-1} B_i V_{N-1} 2^{N-1-i} \\ &= \frac{-R_f}{2R} V_{N-1} [2^{N-1} B_0 + 2^{N-2} B_1 + \dots + 2 B_{N-2} + B_{N-1}]\end{aligned}$$

So, V_{out} is proportional to the number stored in the binary register representing y_n . This number changes according to a clock ($y_n \rightarrow y_{n+1}$), so $V_{\text{out}}(t)$ is a staircase function (edges won't be perfectly square, though — op amp has a nonzero rise time).

The ZOH is followed with the analog LPF, below, as discussed previously.



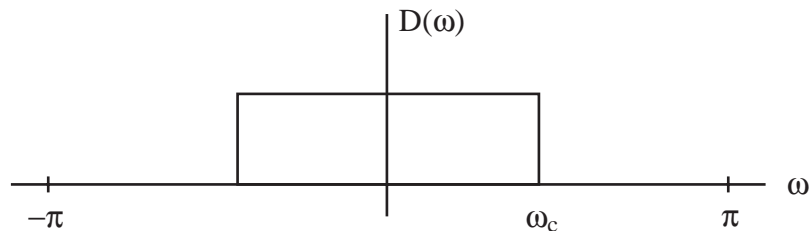
DIGITAL FILTER DESIGN**FIR Design Methods**

- 1) Windowing
 - a) Truncation
 - b) General windowing
- 2) Frequency Sampling ~ will cover later in connection with the DFT
- 3) Computer-Aided Optimization
 - a) Parks - McClellan (✓) ~ widely used
 - b) Linear Programming

1a) Truncation

Illustrate by example.

Suppose we want a LPF with frequency response:

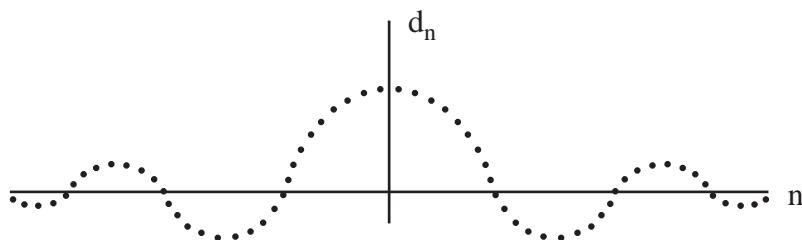


We might choose the filter coefficients $\{h_n\}$ to be

$$d_n = \frac{1}{2\pi} \int_{-\pi}^{\pi} D(\omega) e^{j\omega n} d\omega = \frac{1}{2\pi} \int_{-\omega_c}^{\omega_c} 1 e^{j\omega n} d\omega = \frac{\omega_c}{\pi} \text{sinc } \omega_c n$$

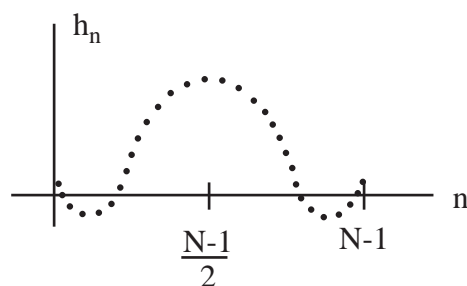
(Then frequency response $H_d(\omega) = \text{DTFT} [\{d_n\}] = D(\omega)$ exactly.)

Look at the d_n :



This sequence is infinite in length and noncausal. So, let's choose (assume N odd, for now):

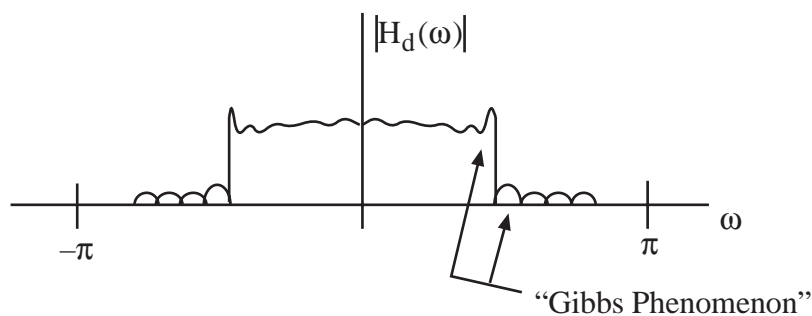
$$h_n = \begin{cases} d_{n - \frac{N-1}{2}} & 0 \leq n \leq N-1 \\ 0 & \text{else} \end{cases}$$



If N is large, then h_n consists of all the larger values of d_n and

$$H_d(\omega) \approx D(\omega) e^{-j\omega \frac{N-1}{2}}.$$

But this approximation is poor in the following sense. The frequency response will look like:



The ripples are due to the Gibbs' phenomenon. Get tall ripples at sharp transitions. As N increases, ripples become narrower and more numerous, but the heights of the ripples nearest the discontinuity remain large. We will soon develop our own explanation for why this occurs. For now, it is worth noting that the DTFT

$$\sum_{n=-\infty}^{\infty} d_n e^{-j\omega n}$$

is actually a Fourier series expansion of $D(\omega)$. We had not thought of the DTFT in this way before, because there was no advantage in doing so. Here, though, we note that $H_d(\omega)$ is obtained by truncating this Fourier series (i.e., choosing $h_n = d_{n-\frac{N-1}{2}}$ for $0 \leq n \leq N-1$.)

Gibbs and other mathematicians studied truncation of Fourier series and showed that ripples will occur around locations where the periodic function is discontinuous. These ripples can be made narrower and to bunch up around the points of discontinuity by taking N larger. However, a larger N does not reduce the heights of the ripples!

How can we reduce the ripple heights?

1b) General Windowing

Given $D(\omega)$ and the corresponding infinite-length $\{d_n\}$, choose the coefficients $\{h_n\}_{n=0}^{N-1}$ to be (again, assume N odd for now):

$$h_n = w_n d_{n-\frac{N-1}{2}} \quad 0 \leq n \leq N-1$$

where $w_n = 0$, $n \notin [0, N-1]$, is a window sequence that gently tapers to zero.

For truncation we used

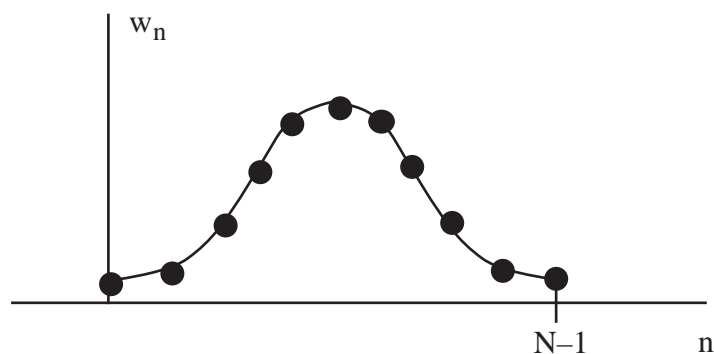
$$w_n = \begin{cases} 1 & 0 \leq n \leq N-1 \\ 0 & \text{else} \end{cases}$$

which does *not* taper gently to zero. Smoother windows can lead to much lower ripple.

An example of a good window is the Hamming window:

$$w_n = .54 - .46 \cos\left(\frac{2\pi n}{N-1}\right), \quad 0 \leq n \leq N-1.$$

This is plotted below



How does the window choice affect the frequency response of the designed filter $\{h_n\}_{n=0}^{N-1}$?

Let

$$g_n = d_{n - \frac{N-1}{2}}.$$

Then:

$$h_n = w_n g_n$$

\uparrow \uparrow \uparrow
 coeffs. of designed FIR filter window desired u.p.r. after shifting

In the frequency domain this corresponds to:

$$\begin{aligned}
 H_d(\omega) &= \sum_n w_n g_n e^{-j\omega n} \\
 &= \sum_n w_n \frac{1}{2\pi} \int_{-\pi}^{\pi} G_d(\theta) e^{j\theta n} d\theta e^{-j\omega n} \\
 &= \frac{1}{2\pi} \int_{-\pi}^{\pi} G_d(\theta) \sum_n w_n e^{-jn(\omega-\theta)} d\theta \\
 &= \frac{1}{2\pi} \int_{-\pi}^{\pi} G_d(\theta) W_d(\omega-\theta) d\theta \quad (*)
 \end{aligned}$$

Notice that this has the form of a convolution. Since the integrand is periodic and we integrate over only a single period, this is called a periodic convolution.

Since our goal is to have $H_d(\omega) \approx G_d(\omega)$, we see from (*) that we would like

$$W_d(\omega) = 2\pi \delta(\omega)$$

But, $W_d(\omega) = 2\pi \delta(\omega) \Rightarrow$

$$w_n = \frac{1}{2\pi} \int_{-\pi}^{\pi} 2\pi \delta(\omega) e^{j\omega n} d\omega = 1 \quad \text{for all } n$$

$\Rightarrow w_n$ is not a window sequence!

w_n nonzero only on $n \in [0, N-1]$ results in (at best) either:

i) $W_d(\omega)$ is a narrow pulse around $\omega = 0$, but has high sidelobes.

or

ii) $W_d(\omega)$ is wider around the origin but the sidelobes are lower.

So, we have a tradeoff.

From (*) we see that the ripple in $H_d(\omega)$ is caused by integrating the product of G_d and W_d as the ripples in W_d are shifted across the discontinuity of G_d . Likewise, the width of the transition band for H_d will depend on the width of the mainlobe (center lobe) of W_d . We conclude:

High sidelobes of $W_d \Rightarrow$ Large ripple in H_d .

Wide center lobe of $W_d \Rightarrow$ Wide transition band in H_d .

Our goal is to achieve moderately low sidelobes and a moderately narrow transition width in W_d simultaneously.

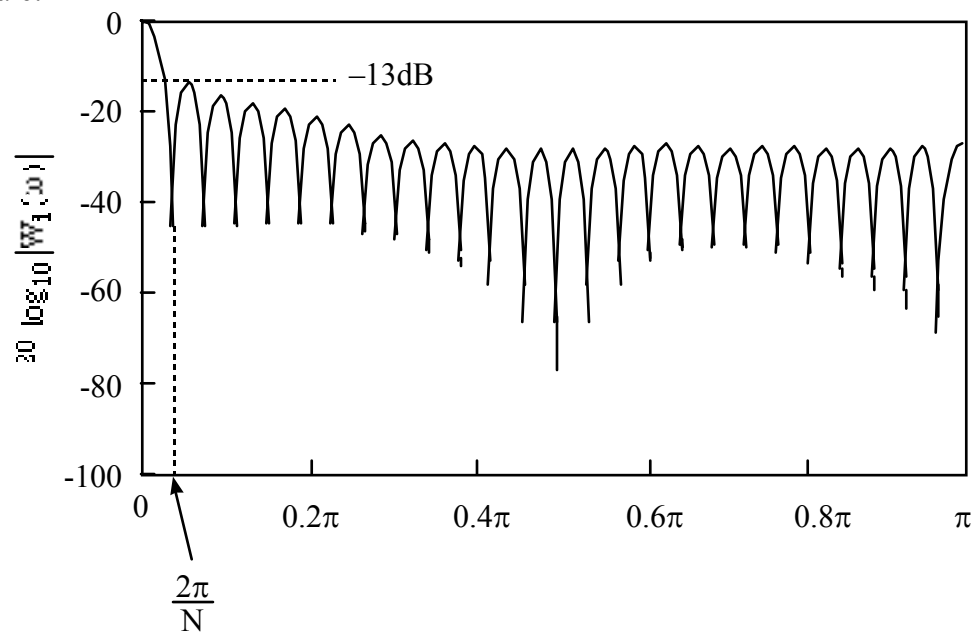
What does $W_d(\omega)$ look like for some common windows?

Truncation

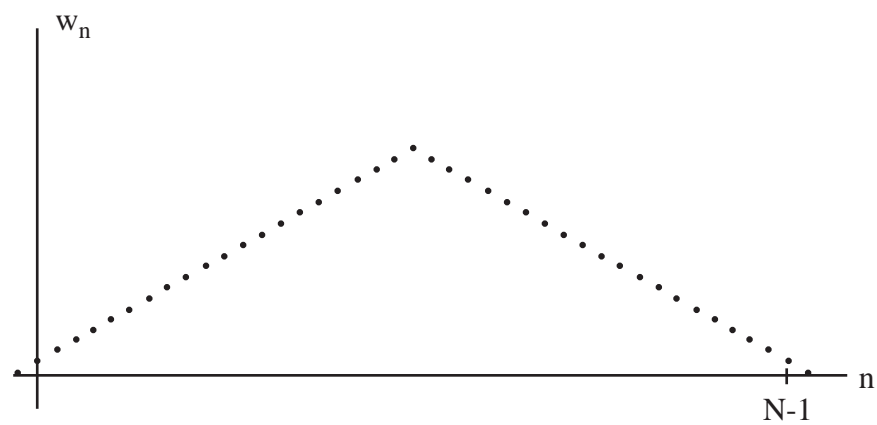
$$|W_d(\omega)| = \left| \sum_{n=0}^{N-1} 1 e^{-j\omega n} \right| = \left| \frac{\sin \frac{N}{2} \omega}{\sin \frac{1}{2} \omega} \right|$$

11.6

Plot on log scale:

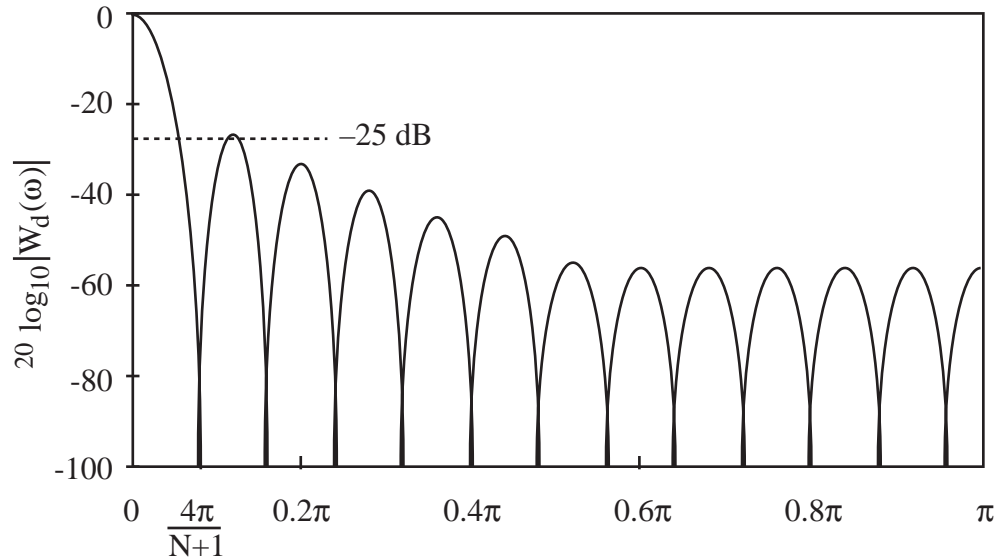


Triangular (Bartlett):



$$|W_d(\omega)| = \left| \frac{\sin \frac{N+1}{4} \omega}{\sin \frac{1}{2} \omega} \right|^2$$

Plot on log scale:

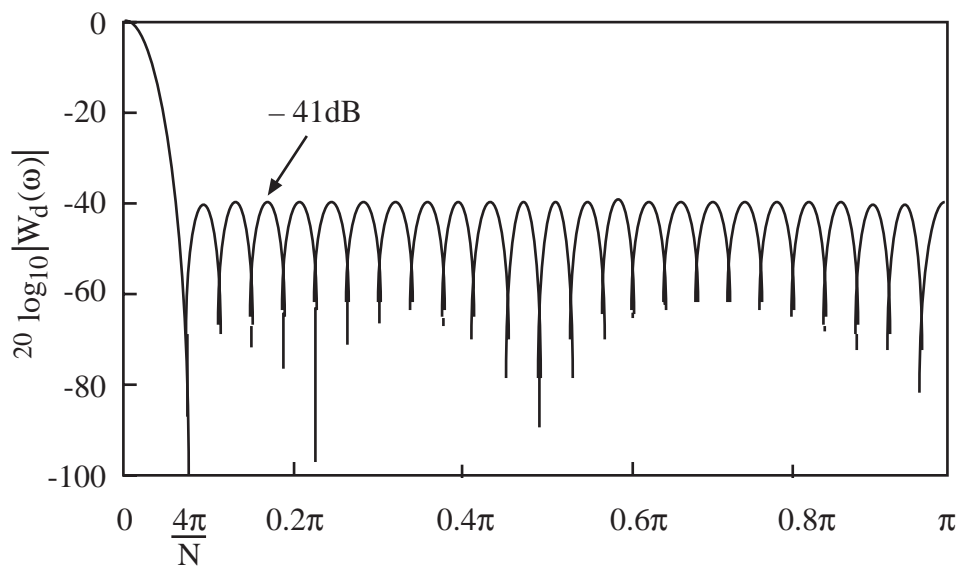


From this plot, we see that the triangular window has a mainlobe that is twice as wide as that of the rectangular window, but the highest sidelobe is reduced by 12 db.

Hamming:

$$w_n = .54 - .46 \cos\left(\frac{2\pi n}{N-1}\right) \quad 0 \leq n \leq N-1$$

Plot of $|W_d(\omega)|$ on a log scale:



From this plot, we see that the Hamming window has essentially the same mainlobe width as the triangular window, and sidelobes that are reduced an additional 16 dB to -41 dB. Thus, the

Hamming window is preferred over the triangular window. Comparing the Hamming window to the truncation window, we see that the highest sidelobe is reduced by 28 dB (more than a factor of 10) at the expense of increasing the mainlobe width by a factor of 2.

Best window: Kaiser

$$w_n = I_0 \left[\beta \left(1 - \left[\left(n - \frac{N-1}{2} \right) / \frac{N-1}{2} \right]^2 \right)^{1/2} \right] \quad 0 \leq n \leq N-1$$

I_0 is the zeroth-order modified Bessel function of the first kind:

$$I_0(x) = \frac{1}{\pi} \int_0^\pi e^{\pm x \cos \theta} d\theta = \frac{1}{\pi} \int_0^\pi \cosh(x \cos \theta) d\theta$$

The choice of β affects the tradeoff between the mainlobe width and sidelobe heights. β is user specified.

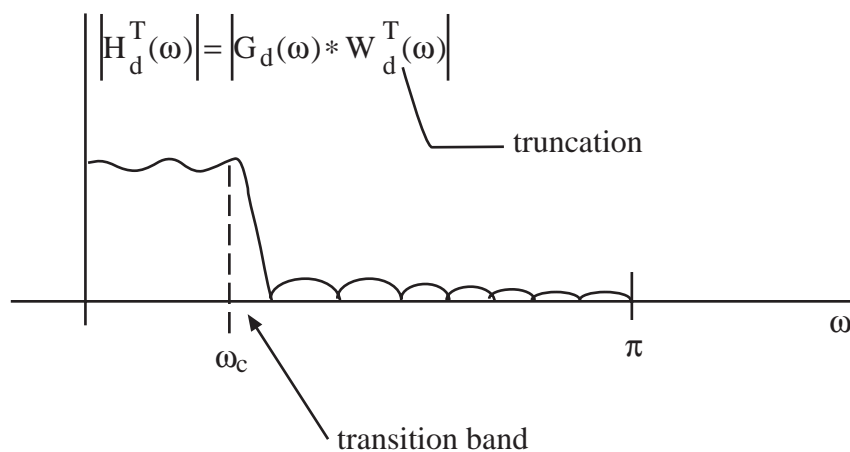
The Kaiser window can achieve slightly narrower mainlobe with the same sidelobe height as Hamming window.

Typical Frequency Responses Using Window Design

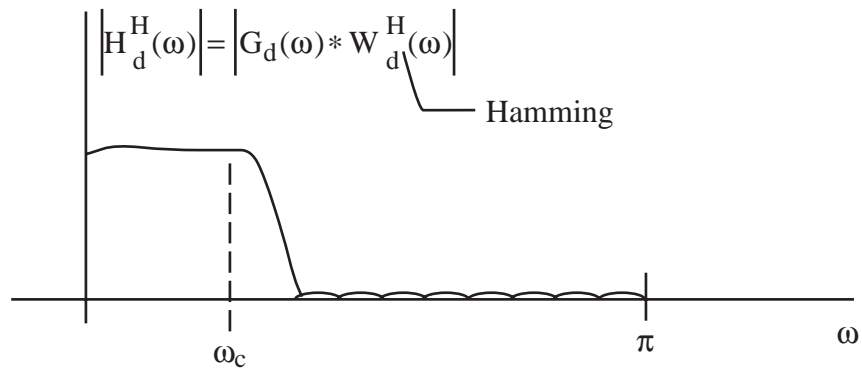
If the desired magnitude response is



then the frequency response of a truncation design may look like:



and the frequency response of a Hamming design will look like:



So, Hamming widens the transition band by a factor of two, but greatly reduces ripple.

Note: The actual filter design procedure is

$$h_n = w_n g_n \quad 0 \leq n \leq N-1.$$

The above Fourier-domain concepts are to help us visualize the resulting $H_d(\omega)$.

Now, so far we have considered only the case with N odd, where we defined

$$g_n = d_{n-\frac{N-1}{2}}$$

where $D(\omega)$ is the desired $H_d(\omega)$.

How do we find g_n if N is even? Answer: Select g_n as shown in the following procedure, which works for both N odd and N even.

General Window Design Procedure

To design a generalized linear phase $\{h_n\}_{n=0}^{N-1}$ with $|H_d(\omega)| \approx D(\omega)$ do this:

$$1) \text{ Let } G_d(\omega) = D(\omega) e^{-j\frac{N-1}{2}\omega}$$

$$2) \text{ Find } g_n = \text{DTFT}^{-1} [G_d(\omega)]$$

$$3) \text{ Let } h_n = w_n g_n.$$

Notes:

- 1) For N odd this procedure gives $g_n = d_{n-\frac{N-1}{2}}$ as before. For N even, steps 1) and 2) give $\{g_n\}$ as an interpolated set of values lying between $\left\{d_{n-\frac{N}{2}}\right\}$ and $\left\{d_{n-\frac{N-2}{2}}\right\}$.

2) We wish to know whether $H_d(\omega)$, designed via the window method, will have generalized linear phase. The answer is ordinarily yes, since $\{h_n\}$ will be symmetric or antisymmetric if $\{w_n\}$ is symmetric and $\{g_n\}$ is either symmetric or antisymmetric.

FIR Window Design Examples

Example

Design generalized linear-phase, low-pass FIR filters having coefficients $\{h_n\}_{n=0}^{29}$ and cutoff

$\omega_c = \frac{\pi}{4}$ using the window design procedure with both truncation and Hamming windows.

Solution

$$G_d(\omega) = D(\omega)e^{-j\frac{N-1}{2}\omega}$$

$$= \begin{cases} e^{-j\frac{29}{2}\omega} & |\omega| \leq \frac{\pi}{4} \\ 0 & \frac{\pi}{4} < |\omega| \leq \pi \end{cases}$$

$$\Rightarrow g_n = \frac{1}{2\pi} \int_{-\frac{\pi}{4}}^{\frac{\pi}{4}} e^{-j\frac{29}{2}\omega} e^{j\omega n} d\omega$$

$$= \frac{1}{2\pi} \left. \frac{e^{j\omega(n-\frac{29}{2})}}{j(n-\frac{29}{2})} \right|_{-\frac{\pi}{4}}^{\frac{\pi}{4}}$$

$$= \frac{\sin \frac{\pi}{4} \left(n - \frac{29}{2} \right)}{\pi \left(n - \frac{29}{2} \right)}$$

$$= \frac{1}{4} \operatorname{sinc} \left[\frac{\pi}{4} \left(n - \frac{29}{2} \right) \right]$$

Now, for truncation $h_n = w_n g_n$ with $w_n = \begin{cases} 1 & 0 \leq n \leq 29 \\ 0 & \text{else} \end{cases}$.

So:

$$\boxed{h_n = \frac{1}{4} \operatorname{sinc} \frac{\pi}{4} \left(n - \frac{29}{2} \right) \quad 0 \leq n \leq 29}$$

For the Hamming window design we have

$$h_n = \left[.54 - .46 \cos \frac{2\pi n}{29} \right] \frac{1}{4} \text{sinc} \frac{\pi}{4} \left(n - \frac{29}{2} \right) \quad 0 \leq n \leq 29$$

Example

Design generalized linear phase high-pass FIR filters having coefficients $\{h_n\}_{n=0}^{60}$ and cutoff $\omega_c = \frac{2\pi}{3}$ using the window design procedure with both truncation and Hamming windows.

Solution

$$G_d(\omega) = \begin{cases} e^{-j30\omega} & \frac{2\pi}{3} \leq |\omega| \leq \pi \\ 0 & |\omega| < \frac{2\pi}{3} \end{cases}$$

$$\Rightarrow g_n = \frac{1}{2\pi} \int_{-\pi}^{\pi} G_d(\omega) e^{j\omega n} d\omega$$

⏟

periodic with period = 2π

$$= \frac{1}{2\pi} \int_0^{2\pi} G_d(\omega) e^{j\omega n} d\omega \quad (*)$$

$$= \frac{1}{2\pi} \int_{\frac{2\pi}{3}}^{\frac{4\pi}{3}} e^{-j30\omega} e^{j\omega n} d\omega \quad (\square)$$

$$= \frac{e^{j\omega(n-30)}}{2\pi j(n-30)} \bigg|_{\frac{2\pi}{3}}^{\frac{4\pi}{3}} \quad (\Delta)$$

$$\begin{aligned}
&= \frac{1}{2\pi j(n-30)} \left[e^{j\frac{4\pi}{3}(n-30)} - e^{j\frac{2\pi}{3}(n-30)} \right] \\
&= \frac{1}{2\pi j(n-30)} e^{j\pi(n-30)} \left[e^{j\frac{\pi}{3}(n-30)} - e^{-j\frac{\pi}{3}(n-30)} \right] \\
&= \frac{1}{2\pi j(n-30)} (-1)^n 2j \sin \frac{\pi}{3} (n-30) \\
&= (-1)^n \frac{1}{3} \operatorname{sinc} \frac{\pi}{3} (n-30)
\end{aligned}$$

So, using a truncation window gives:

$$h_n = (-1)^n \frac{1}{3} \operatorname{sinc} \frac{\pi}{3} (n-30) \quad 0 \leq n \leq 60$$

and applying a Hamming window gives:

$$h_n = \left[.54 - .46 \cos \frac{2\pi n}{60} \right] (-1)^n \frac{1}{3} \operatorname{sinc} \frac{\pi}{3} (n-30) \quad 0 \leq n \leq 60$$

Notes:

1) Since $G_d(\omega)$ is nonzero on two subintervals of $-\pi \leq \omega < \pi$ for the high-pass case, it can save algebra if we use periodicity to rewrite the inverse DTFT as in (*) across the interval $0 \leq \omega \leq 2\pi$. This trick is straightforward if N is odd. For N even, however, there are two extra things to think about. First, in view of the table on p. 35.8, we should use an odd-symmetric design with Type 2 generalized linear phase. Second, for N even, the slope of the phase, $-\frac{N-1}{2}$, is noninteger and the phase will take a jump of π at $\omega = \pi$. Thus, $G_d(\omega)$

seemingly will have two different forms on the interval $0 \leq \omega \leq 2\pi$. See the next example for details.

2) Since the denominator of (Δ) is zero at $n = 30$, we cannot presume that (Δ) follows from (\square) at $n = 30$. Thus, we must be careful to check that our expressions for $\{h_n\}$ hold at $n =$

30. Our final expression for g_n , which follows from (Δ) , gives:

$$g_{30} = (-1)^{30} \cdot \frac{1}{3} \cdot 1 = \frac{1}{3}$$

Evaluating (\square) at $n = 30$ gives

$$g_{30} = \frac{1}{2\pi} \left[\frac{4\pi}{3} - \frac{2\pi}{3} \right] \cdot 1 = \frac{1}{3}$$

which agrees with (Δ) . Thus, our expressions for h_n are valid for $0 \leq n \leq 60$.

Now, let's change N in the previous example from $N = 61$ to $N = 62$ and see how the algebra associated with the design changes for N even.

Example

Design a generalized linear phase high-pass FIR filter having coefficients $\{h_n\}_{n=0}^{61}$ and cutoff $\omega_c = \frac{2\pi}{3}$ using the window design procedure with a Hamming window.

Solution

A filter with real-valued unit-pulse response satisfies $G_d(\omega) = G_d^*(-\omega)$. Thus, for an antisymmetric design with Type 2 generalized linear phase, we have

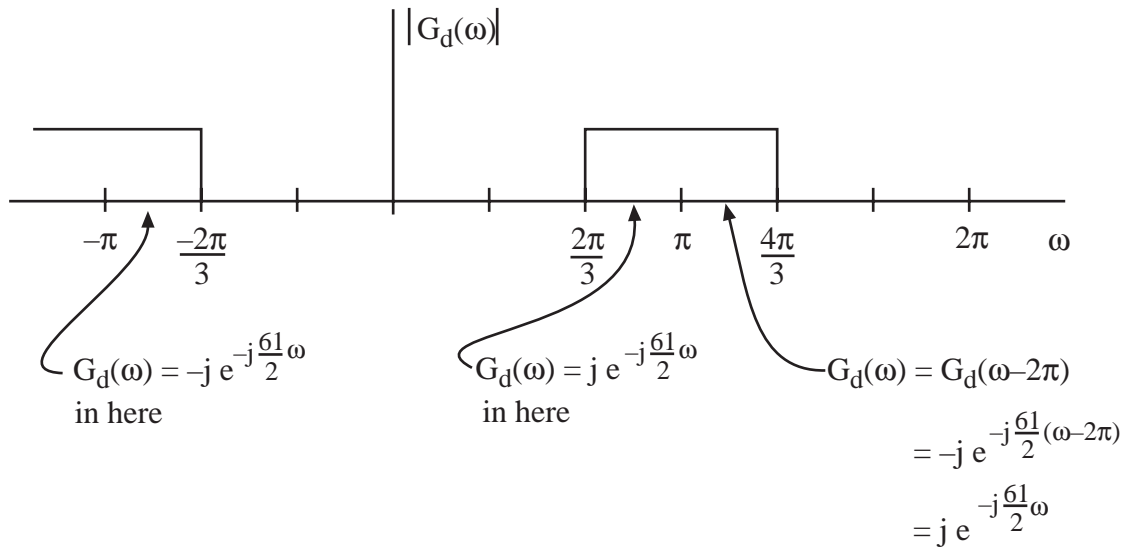
$$G_d(\omega) = \begin{cases} e^{j\left(\frac{\pi}{2} - \frac{61}{2}\omega\right)} & \frac{2\pi}{3} \leq \omega < \pi \\ 0 & |\omega| < \frac{2\pi}{3} \\ e^{j\left(-\frac{\pi}{2} - \frac{61}{2}\omega\right)} & -\pi < \omega \leq -\frac{2\pi}{3} \end{cases}$$

$$= \begin{cases} j e^{-j\frac{61}{2}\omega} & \frac{2\pi}{3} \leq \omega < \pi \\ 0 & |\omega| < \frac{2\pi}{3} \\ -j e^{-j\frac{61}{2}\omega} & -\pi < \omega \leq -\frac{2\pi}{3} \end{cases} \quad (*)$$

As in the last example we can write

$$g_n = \frac{1}{2\pi} \int_{\frac{2\pi}{3}}^{\frac{4\pi}{3}} G_d(\omega) e^{j\omega n} d\omega \quad (**)$$

Equation (*) specifies $G_d(\omega)$ on $|\omega| < \pi$. To find $G_d(\omega)$ for $\pi < \omega < \frac{4\pi}{3}$ consider



So, $G_d(\omega)$ in (**) maintains the same form across the full range of integration in (**) and we have

$$\begin{aligned}
 g_n &= \frac{1}{2\pi} \int_{\frac{2\pi}{3}}^{\frac{4\pi}{3}} j e^{-j\frac{61}{2}\omega} e^{j\omega n} d\omega \\
 &= \frac{e^{j\omega\left(n-\frac{61}{2}\right)} \Big|_{\frac{2\pi}{3}}^{\frac{4\pi}{3}}}{2\pi\left(n-\frac{61}{2}\right)} \\
 &= \frac{1}{2\pi\left(n-\frac{61}{2}\right)} \left[e^{j\frac{4\pi}{3}\left(n-\frac{61}{2}\right)} - e^{j\frac{2\pi}{3}\left(n-\frac{61}{2}\right)} \right]
 \end{aligned}$$

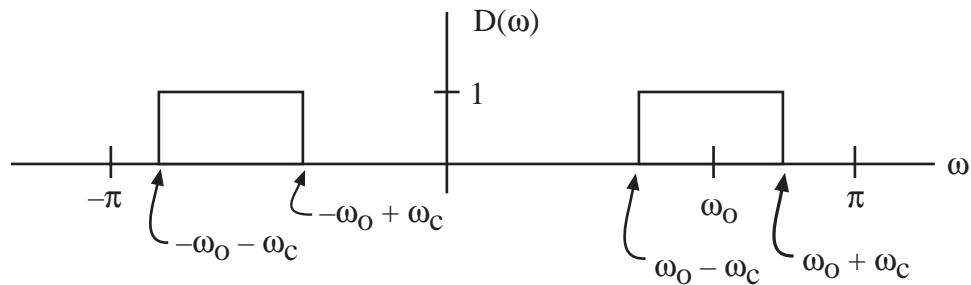
$$\begin{aligned}
&= \frac{1}{2\pi\left(n - \frac{61}{2}\right)} e^{j\pi\left(n - \frac{61}{2}\right)} \left[e^{j\frac{\pi}{3}\left(n - \frac{61}{2}\right)} - e^{-j\frac{\pi}{3}\left(n - \frac{61}{2}\right)} \right] \\
&= \frac{1}{2\pi\left(n - \frac{61}{2}\right)} (-1)^n 2 \sin\left[\frac{\pi}{3}\left(n - \frac{61}{2}\right)\right] \\
&= (-1)^n \frac{1}{3} \operatorname{sinc} \frac{\pi}{3} \left(n - \frac{61}{2}\right)
\end{aligned}$$

Applying the Hamming window gives

$$h_n = \left[.54 - .46 \cos \frac{2\pi n}{61} \right] (-1)^n \frac{1}{3} \operatorname{sinc} \frac{\pi}{3} \left(n - \frac{61}{2}\right) \quad 0 \leq n \leq 61$$

Example

Window design of bandpass filter. Find $\{h_n\}_{n=0}^{N-1}$ so that $|H_d(\omega)|$ approximates



For lowpass filter had $d_n = \frac{\omega_c}{\pi} \operatorname{sinc} \omega_c n$. By modulation property, here for BP case we expect $d_n \approx (\cos \omega_o n) \frac{\omega_c}{\pi} \operatorname{sinc} [\omega_c n]$. Let's see:

$$\begin{aligned}
d_n &= \frac{1}{2\pi} \int_{-\omega_o - \omega_c}^{-\omega_o + \omega_c} 1 e^{j\omega n} d\omega + \frac{1}{2\pi} \int_{\omega_o - \omega_c}^{\omega_o + \omega_c} 1 e^{j\omega n} d\omega \\
&= \frac{e^{j\omega n}}{2\pi j n} \Big|_{-\omega_o - \omega_c}^{-\omega_o + \omega_c} + \frac{e^{j\omega n}}{2\pi j n} \Big|_{\omega_o - \omega_c}^{\omega_o + \omega_c}
\end{aligned}$$

$$\begin{aligned}
&= \frac{e^{jn(-\omega_0 + \omega_c)} - e^{jn(-\omega_0 - \omega_c)} + e^{jn(\omega_0 + \omega_c)} - e^{jn(\omega_0 - \omega_c)}}{2\pi jn} \\
&= \frac{1}{2\pi jn} \left[e^{-jn\omega_0} (e^{jn\omega_c} - e^{-jn\omega_c}) + e^{jn\omega_0} (e^{jn\omega_c} - e^{-jn\omega_c}) \right] \\
&= \frac{1}{\pi n} \left[e^{-jn\omega_0} \sin \omega_c n + e^{jn\omega_0} \sin \omega_c n \right] = \frac{\sin \omega_c n}{\pi n} 2 \cos \omega_0 n \\
&= 2(\cos \omega_0 n) \frac{\omega_c}{\pi} \text{sinc } \omega_c n \quad \leftarrow \text{what we expected.}
\end{aligned}$$

Now, to design $\{h_n\}_{n=0}^{N-1}$ with linear phase, need to incorporate shift to give:

$$g_n = 2 \cos \omega_0 \left(n - \frac{N-1}{2} \right) \frac{\omega_c}{\pi} \text{sinc } \omega_c \left(n - \frac{N-1}{2} \right) \quad 0 \leq n \leq N-1$$

Windowed coefficients are then

$h_n = w_n g_n \quad 0 \leq n \leq N-1$ ~ coefficients for FIR filter where w_n is a Hamming or other window.

In MATLAB, the command to design FIR filters using the window method is called `fir1`.

Parks-McClellan

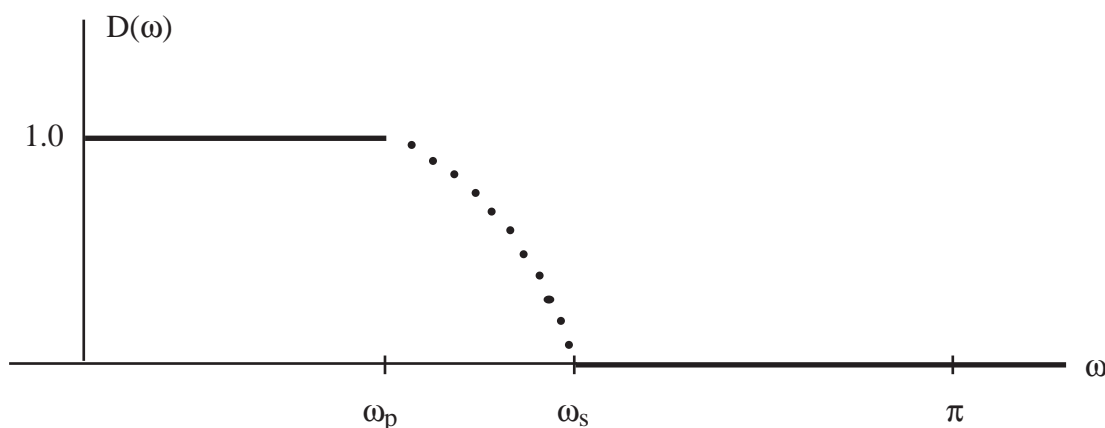
Parks and McClellan developed a computer program for solving the following problem:

Define the error

$$E(\omega) = W(\omega)[D(\omega) - R(\omega)]$$

\nwarrow arbitrary weighting \nwarrow desired response \nwarrow from
 $H_d(\omega) = R(\omega)e^{j\left(\alpha - \frac{N-1}{2}\omega\right)}$
 \uparrow
 $0 \text{ or } \frac{\pi}{2}$

Let ω_p , ω_s be the passband and stopband cutoff frequencies so that $D(\omega)$ might look like:



Ordinarily $D(\omega)$ is unspecified on $\omega_p < \omega < \omega_s$ because we are not concerned with the precise shape of $H_d(\omega)$ or $R(\omega)$ in this transition band.

The Parks-McClellan algorithm finds $\{h_n\}_{n=0}^{N-1}$ that minimizes

$$\begin{aligned} &\max |E(\omega)| \\ &0 \leq \omega \leq \omega_p \\ &\omega_s \leq \omega \leq \pi \end{aligned}$$

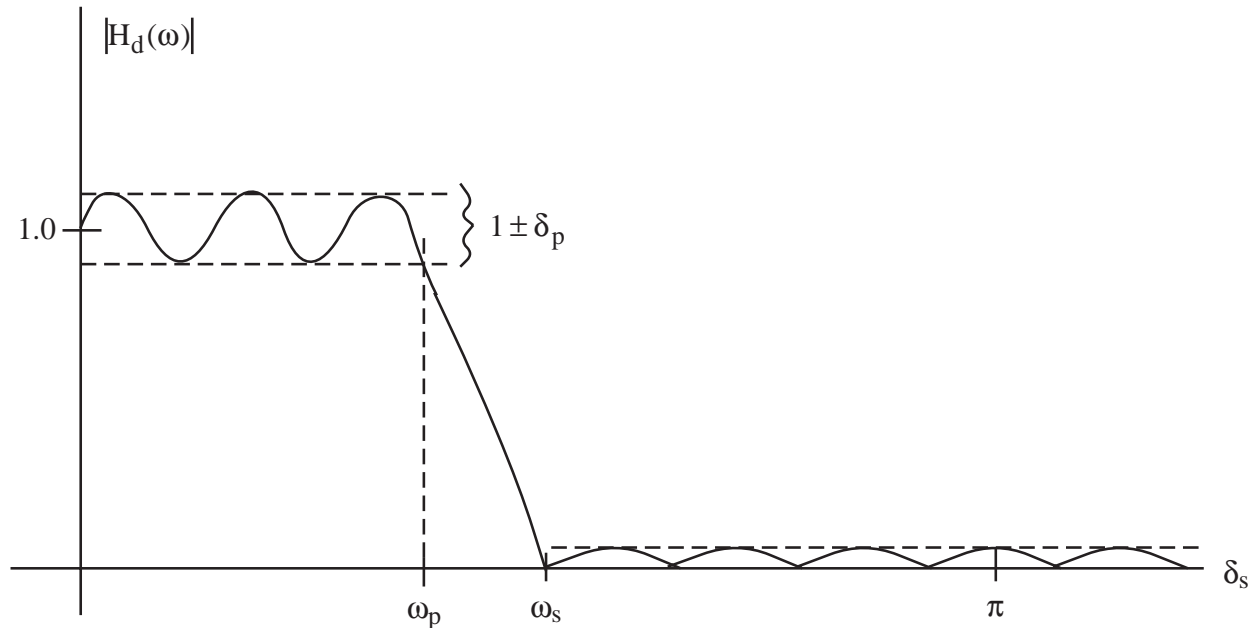
This error measure is called the minimax or Chebyshev error norm.

In the standard P-M algorithm, $W(\omega)$ can be selected to have one value, W_p , on the passband and another, W_s , on the stopband. Frequently, W_s is chosen larger than W_p so that the designed filter will have a smaller stopband error than passband error.

The program user specifies:

N , ω_p , ω_s , W_p , and W_s

The designed filter has equiripple behavior:



How are the ripple heights related to W_p and W_s ?

Answer: They satisfy $\delta_p W_p = \delta_s W_s$.

Thus, $\frac{\delta_p}{\delta_s} = \frac{W_s}{W_p}$.

What filter order is required to meet given specifications?

Answer: It has been found empirically that

$$N \approx \frac{-10 \log_{10}(\delta_p \delta_s) - 13}{2.324(\omega_s - \omega_p)}$$

Note: The filter order is not too sensitive to δ_p , and δ_s . But, N is inversely proportional to the transition bandwidth! Halving the transition bandwidth doubles the required filter length!

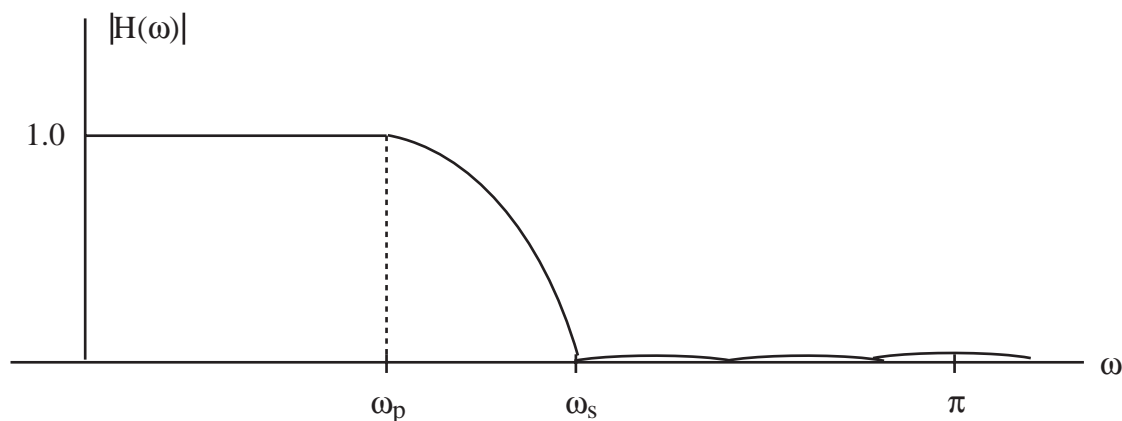
All students will get experience with the Parks-McClellan algorithm in a Matlab assignment.

Linear Programming

Linear programming is a fairly general optimization algorithm that can solve the Parks-McClellan problem and many others. LP is slower, but its generality can be exploited to incorporate time-domain or additional frequency-domain constraints.

For example, it is possible to eliminate ripple in the passband by constraining the derivative of $R(\omega)$ to be ≤ 0 in the passband.

The result is a monotone decreasing response in the passband, with ripple remaining in the stopband:



Incorporating the monotone passband constraint increases the required filter order slightly.

In MATLAB, the command to design FIR filters using the P-M method is called `remez`.

Frequency Sampling FIR Filter Design

Given $G_d(\omega) \sim$ desired frequency response with linear phase

Idea: Choose $H_d(\omega)$ to agree with $G_d(\omega)$ at $\omega = \frac{2\pi}{N} m$, $0 \leq m \leq N-1$.

Take $\{h_n\}_{n=0}^{N-1}$ to be $\text{DFT}^{-1} \left[\left\{ G_d \left(\frac{2\pi m}{N} \right) \right\}_{m=0}^{N-1} \right]$, i.e.,

$$h_n = \frac{1}{N} \sum_{m=0}^{N-1} G_d \left(\frac{2\pi}{N} m \right) e^{j \frac{2\pi}{N} nm} \quad 0 \leq n \leq N-1 \quad (\text{FS})$$

Using $\{h_n\}_{n=0}^{N-1}$ as our FIR filter coefficients will give a frequency response $H_d(\omega)$ satisfying

$$H_d(\omega) = G_d(\omega) \text{ at } \omega = \frac{2\pi m}{N} \quad 0 \leq m \leq N-1$$

\uparrow \uparrow
 actual desired

Why?

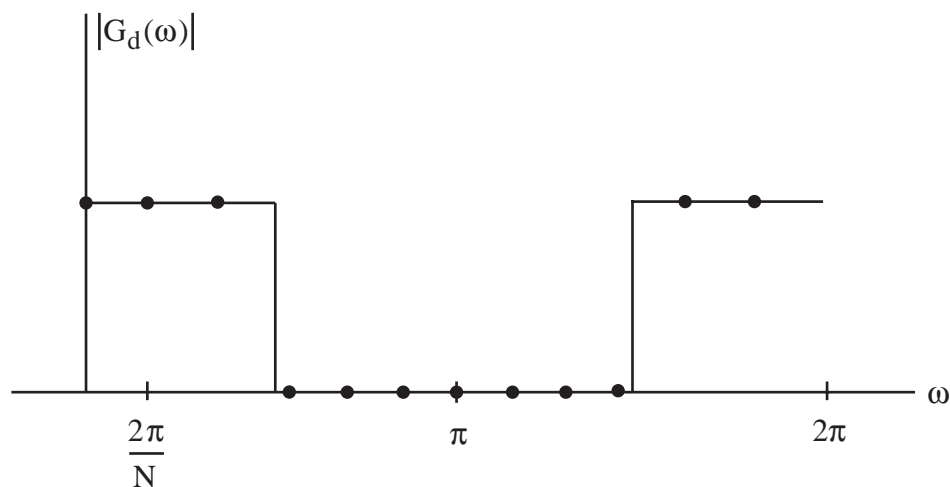
$$\begin{aligned}
 H_d(\omega) \Big|_{\omega = \frac{2\pi}{N} m} &= \text{DFT} [\{h_n\}] \\
 &\stackrel{\substack{\uparrow \\ \text{by (FS)}}}{=} \text{DFT} \left[\text{DFT}^{-1} \left[\left\{ G_d \left(\frac{2\pi}{N} m \right) \right\} \right] \right] \\
 &= G_d \left(\frac{2\pi}{N} m \right) \quad \checkmark
 \end{aligned}$$

But in general $H_d(\omega) \neq G_d(\omega)$ for $\omega \neq \frac{2\pi}{N} m$.

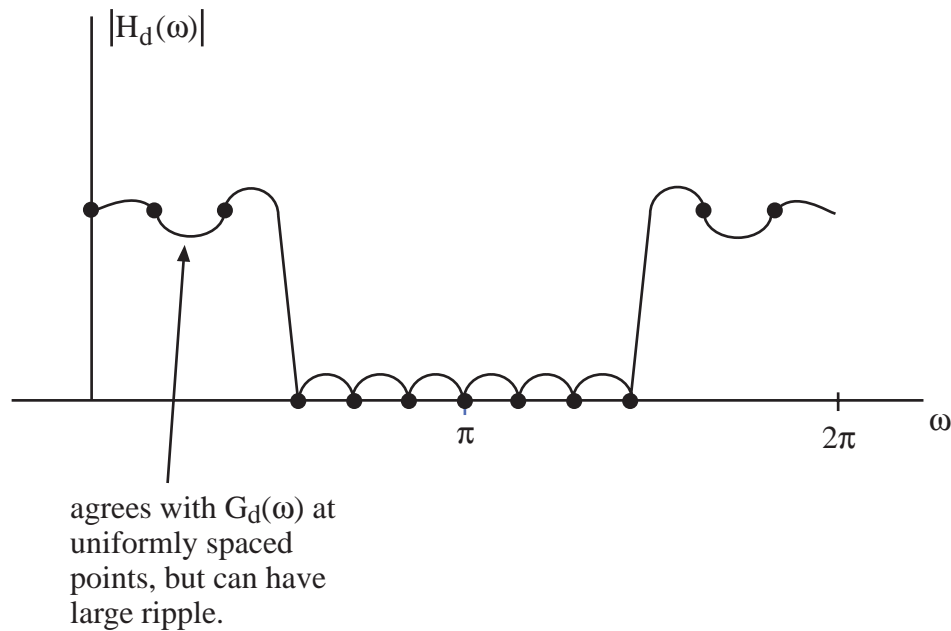
This approach can be too simplistic.

Example

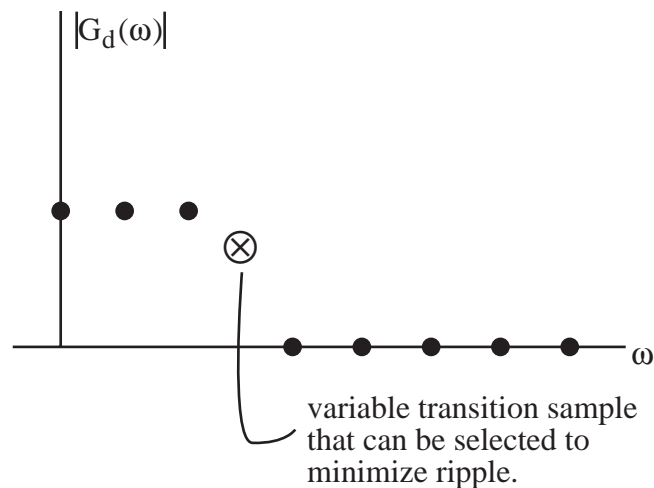
Let $G_d(\omega)$ be an ideal LPF with linear phase and delay $\frac{N-1}{2}$.

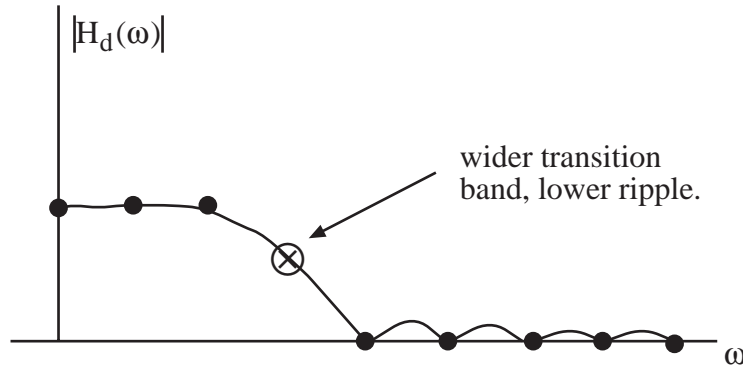


Using (FS), will produce an $H_d(\omega)$ that agrees with $G_d(\omega)$ at the points shown above. The resulting $H_d(\omega)$ might look like:



There is a modified frequency sampling design procedure that works better. In the modified procedure, one or more frequency samples in the filter's transition band are left unconstrained as free variables. The values of these free variables are then selected via linear programming to minimize some measure of ripple. This results in a wider transition band, but lower ripple, as suggested in the figures below.





Note: If you take $G_d(\omega)$ to have zero phase, the designed H_d will still pass through the correct samples of G_d , but the response will be terrible off the grid $\omega = \frac{2\pi m}{N}$. Hoping for zero phase (no delay) in a causal filter is a pipe dream!

Example

Use the frequency sampling method to design a linear-phase HPF $\{h_n\}_{n=0}^{60}$, with cutoff $\omega_c = .6\pi$.

Solution

$$N = 61 \Rightarrow \text{phase} = -\frac{N-1}{2} \omega = -30 \omega$$

$$\Rightarrow G_d(\omega) = \begin{cases} 0 & 0 \leq \omega < .6\pi \\ e^{-j30\omega} & .6\pi \leq \omega \leq 1.4\pi \\ 0 & 1.4\pi < \omega \leq 2\pi \end{cases}$$

$$\Rightarrow G_d\left(\frac{2\pi m}{61}\right) = \begin{cases} 0 & 0 \leq m \leq 18 \\ e^{-j30\frac{2\pi}{61}m} & 19 \leq m \leq 42 \\ 0 & 43 \leq m \leq 60 \end{cases}$$

Now, $\{h_n\}$ is the inverse DFT of $\left\{G_d\left(\frac{2\pi m}{61}\right)\right\}$ as given by

$$h_n = \frac{1}{61} \sum_{m=0}^{60} G_d\left(\frac{2\pi m}{61}\right) e^{j\frac{2\pi}{61}nm}$$

$$= \frac{1}{61} \sum_{m=19}^{42} e^{-j30\frac{2\pi}{61}m} e^{j\frac{2\pi}{61}nm}$$

$$= \frac{1}{61} \sum_{m=19}^{42} e^{j\frac{2\pi}{61}(n-30)m}$$

↑
effect of linear phase is to circularly shift the $\{h_n\}$ since replacing $n-30$ with $\langle n-30 \rangle_{61}$ does not change this equation

$$= \frac{1}{61} \sum_{k=0}^{23} e^{j\frac{2\pi}{N}(n-30)(k+19)}$$

↑
 $k = m - 19$

$$= \frac{1}{61} e^{j\frac{2\pi}{61}(n-30)19} \frac{1 - e^{j\frac{2\pi}{61}(n-30)24}}{1 - e^{j\frac{2\pi}{61}(n-30)}}$$

$$= \frac{\frac{1}{61} e^{j\frac{2\pi}{61}(n-30)31}}{e^{j\frac{2\pi}{61}(n-30)}} \bullet \frac{e^{-j\frac{2\pi}{61}(n-30)12} - e^{j\frac{2\pi}{61}(n-30)12}}{e^{-j\frac{\pi}{61}(n-30)} - e^{j\frac{\pi}{61}(n-30)}}$$

$$= \frac{1}{61} e^{j\pi(n-30)} \frac{-2j \sin\left(\frac{2\pi}{61}(n-30)12\right)}{-2j \sin\left(\frac{\pi}{61}(n-30)\right)}$$

$$= \frac{1}{61} (-1)^n \frac{\sin\left(24 \frac{\pi}{61}(n-30)\right)}{\sin\left(\frac{\pi}{61}(n-30)\right)} \quad 0 \leq n \leq 60$$

sampled periodic sinc

Here, the factor $(-1)^n$ makes this a high-pass filter rather than a low-pass filter. Since this term multiplies a periodic sinc, which is similar to a sinc, we expect that the resulting frequency

response will not be too different from that obtained using the window design procedure with a truncation window.

Let's next consider the design of a low-pass filter $\{h_n\}_{n=0}^{N-1}$ where N is even. This example will be more complicated than the previous one in two respects. First, since N is even, the formula for $G_d(\omega)$ will take two different forms on $0 \leq \omega < 2\pi$. Second, since this is a low-pass filter, there will be two separate bands where $G_d(\omega)$ is nonzero on $0 \leq \omega < 2\pi$.

Example

Frequency sampling design of $\{h_n\}_{n=0}^{21}$, linear-phase LPF with $\omega_c = \frac{\pi}{2}$.

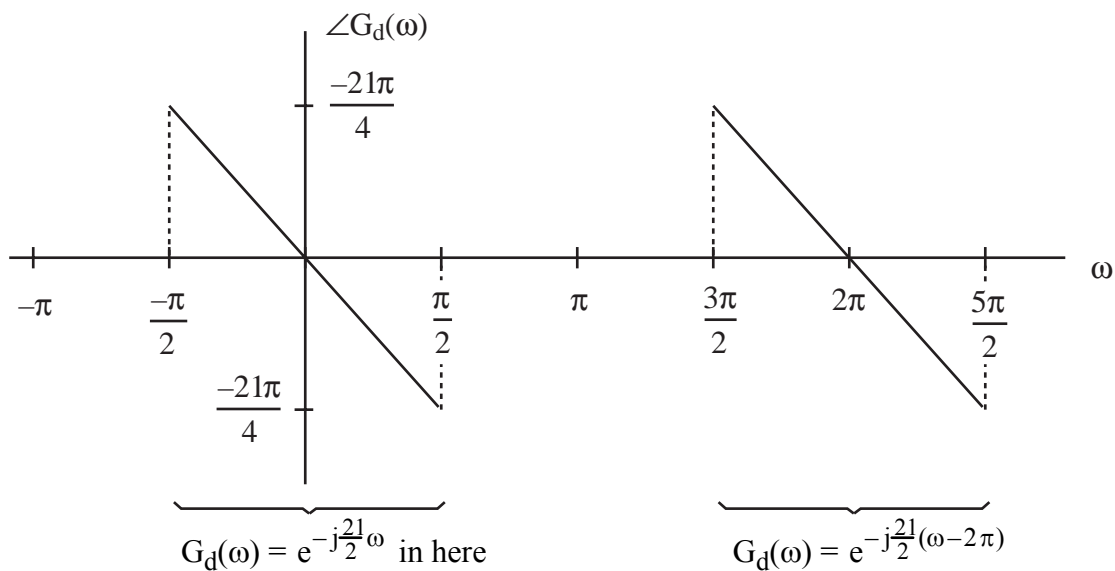
Solution

$$N = 22 \Rightarrow \text{phase} = -\frac{N-1}{2} \omega = \frac{-21}{2} \omega$$

$$\Rightarrow G_d(\omega) = \begin{cases} e^{-j\frac{21}{2}\omega} & |\omega| \leq \frac{\pi}{2} \\ 0 & \frac{\pi}{2} < |\omega| \leq \pi \end{cases}$$

But, for a frequency sampling design, we need samples of $G_d(\omega)$ on $\omega \in [0, 2\pi)$. For N even, with $\frac{N-1}{2}$ noninteger, we must be careful! Consider the phase of $G_d(\omega)$. Here for clarity, we will not wrap the phase inside the interval $(-\pi, \pi)$ and will instead show its linear extension.

11.26



$$= e^{j\pi} e^{-j\frac{21}{2}\omega}$$

$$= -e^{-j\frac{21}{2}\omega}$$

in here

Note: Minus sign doesn't occur if N is odd.

So:

$$G_d(\omega) = \begin{cases} e^{-j\frac{21}{2}\omega} & 0 \leq \omega \leq \frac{\pi}{2} \\ 0 & \frac{\pi}{2} < \omega < \frac{3\pi}{2} \\ -e^{-j\frac{21}{2}\omega} & \frac{3\pi}{2} \leq \omega \leq 2\pi \end{cases}$$

$$\Rightarrow G_d\left(\frac{2\pi m}{22}\right) = \begin{cases} e^{-j\frac{21}{2}\left(\frac{2\pi m}{22}\right)} & 0 \leq m \leq 5 \\ 0 & 6 \leq m \leq 16 \\ -e^{-j\frac{21}{2}\left(\frac{2\pi m}{22}\right)} & 17 \leq m \leq 21 \end{cases}$$

Thus,

$$\begin{aligned}
 h_n &= \frac{1}{22} \sum_{m=0}^5 e^{-j\frac{21}{2}\left(\frac{2\pi m}{22}\right)} e^{j\frac{2\pi}{22}mn} + \frac{1}{22} \sum_{m=17}^{21} -e^{-j\frac{21}{2}\left(\frac{2\pi m}{22}\right)} e^{j\frac{2\pi}{22}mn} \\
 &= \frac{1}{22} \sum_{m=0}^5 e^{j\frac{2\pi}{22}\left(n-\frac{21}{2}\right)m} - \frac{1}{22} \sum_{m=17}^{21} e^{j\frac{2\pi}{22}\left(n-\frac{21}{2}\right)m}
 \end{aligned}$$

Making the change of variable $\ell = m - 22$, the second sum can be rewritten as

$$\sum_{\ell=-5}^{-1} e^{j\frac{2\pi}{22}\left(n-\frac{21}{2}\right)(\ell+22)} = \sum_{\ell=-5}^{-1} e^{j\frac{2\pi}{22}\left(n-\frac{21}{2}\right)\ell} \underbrace{e^{-j21\pi}}_{=-1}$$

Thus,

$$\begin{aligned}
 h_n &= \frac{1}{22} \sum_{m=-5}^5 e^{j\frac{2\pi}{22}\left(n-\frac{21}{2}\right)m} \\
 &= \frac{1}{22} \sum_{k=0}^{10} e^{j\frac{2\pi}{22}\left(n-\frac{21}{2}\right)(k-5)} \\
 &\quad \uparrow \\
 &\quad k = m + 5 \\
 &= \frac{1}{22} e^{j\frac{2\pi}{22}\left(n-\frac{21}{2}\right)(-5)} \frac{1 - e^{j\frac{2\pi}{22}\left(n-\frac{21}{2}\right)11}}{1 - e^{j\frac{2\pi}{22}\left(n-\frac{21}{2}\right)}} \\
 &= \frac{1}{22} e^{-j\frac{10\pi}{22}\left(n-\frac{21}{2}\right)} \frac{e^{j\frac{2\pi}{22}\left(n-\frac{21}{2}\right)\frac{11}{2}}}{e^{j\frac{2\pi}{22}\left(n-\frac{21}{2}\right)\frac{1}{2}}} \cdot \frac{-j2 \sin \frac{11\pi}{22}\left(n-\frac{21}{2}\right)}{-j2 \sin \frac{\pi}{22}\left(n-\frac{21}{2}\right)} \\
 &= \boxed{\frac{1}{22} \frac{\sin \frac{\pi}{2}\left(n-\frac{21}{2}\right)}{\sin \frac{\pi}{22}\left(n-\frac{21}{2}\right)} \quad 0 \leq n \leq 21}
 \end{aligned}$$

Thus, h_n is a sampled, periodic sinc, which is similar to the sinc-type design that would have resulted from a window design using a truncation window.

In general, the formula for the coefficients of either an FIR LPF or HPF, designed using the frequency sampling technique, are given by

$$\text{LPF: } h_n = \frac{1}{N} \frac{\sin\left(\gamma \frac{\pi}{N} \left(n - \frac{N-1}{2}\right)\right)}{\sin\left(\frac{\pi}{N} \left(n - \frac{N-1}{2}\right)\right)}$$

$$\text{HPF: } h_n = (-1)^n \frac{1}{N} \frac{\sin\left(\gamma \frac{\pi}{N} \left(n - \frac{N-1}{2}\right)\right)}{\sin\left(\frac{\pi}{N} \left(n - \frac{N-1}{2}\right)\right)}$$

where γ is the number of samples $G_d\left(\frac{2\pi m}{N}\right)$, $0 \leq m \leq N-1$, that are nonzero (number of samples in the passband).

IIR Filter Design

- 1) Based on Analog Prototype
 - a) Impulse invariant design
 - b) Bilinear transformation (✓) ~ widely used
- 2) Computer-Aided Optimization

Designs in category 1) proceed by first designing an analog filter having a frequency response with the desired shape, and then “transforming” it to a digital filter. To use these design methods, we must first learn just a bit about analog filter design.

Elements of Analog Filter Design

Notation:

$$H_L(s) = \int_{-\infty}^{\infty} h_a(t) e^{-st} dt \quad (\text{Laplace transform})$$

$$\Rightarrow H_a(\Omega) = H_L(j\Omega) \quad (\text{Fourier transform})$$

Consider only lowpass Butterworth, Chebyshev, and elliptic (Cauer) filters.

For each of these types of filters, $H_L(s)$ is found indirectly from a specified $|H_a(\Omega)|^2$.

We need $H_L(s)$ because, later, this is what will be transformed into $H(z)$.

For Butterworth, Chebyshev, and elliptic filters, $|H_a(\Omega)|^2$ has the form:

$$|H_a(\Omega)|^2 = M(\Omega^2) = \frac{1}{1 + F(\Omega^2)}$$

\uparrow
 rational with
 real coeffs.

How do we get $H_L(s)$ from $|H_a(\Omega)|^2$? That is, how do we find $H_L(s)$ satisfying

$$|H_L(j\Omega)|^2 = |H_a(\Omega)|^2 = M(\Omega^2) \quad (*)$$

Answer:

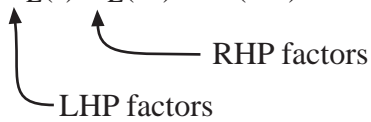
- 1) First find poles and zeros of $M(-s^2)$ where s is a complex variable. Since M has real coefficients and is a function of s^2 , the poles and zeros will have symmetry around both the real and imaginary axis.
- 2) Take $H_L(s)$ to be the left-half-plane pole factors (for stability) and left-half-plane zero factors (for smallest delay, called “minimum phase”).

But, does this work?

Need to show

$$|H_L(j\Omega)|^2 = M(\Omega^2) \quad (1)$$

Have:

$$H_L(s) H_L(-s) = M(-s^2)$$


which implies

$$H_L(j\Omega) H_L(-j\Omega) = M(\Omega^2)$$

So, (1) will be true if

$$H_L(-j\Omega) = H_L^*(j\Omega) \quad (2)$$

This follows, though, because the poles and zeros of $H_L(s)$ are symmetric around the real axis, and therefore occur in complex-conjugate pairs. For any pole pair or zero pair $(s-p)$ $(s-p^*)$ in $H_L(s)$, we have

$$(s-p)(s-p^*) \Big|_{s=-j\Omega} = (-j\Omega-p)(-j\Omega-p^*) = [(j\Omega-p^*)(j\Omega-p)]^* = \left[(s-p)(s-p^*) \Big|_{s=j\Omega} \right]^*$$

which proves (2), and therefore (1).

Example

$$|H_a(\Omega)|^2 = M(\Omega^2) = \frac{1}{1 + \Omega^2}$$

Find $H_L(s)$.

We have

$$\begin{aligned} M(-s^2) &= \frac{1}{1-s^2} \\ &= \frac{1}{(1-s)(1+s)} \\ &\quad \underbrace{\hspace{1.5cm}}_{\text{LHP factor}} \end{aligned}$$

$$\Rightarrow \left[H_L(s) = \frac{1}{s+1} \right]$$

Let's check to see if $|H_a(\Omega)|^2 =$ above $M(\Omega^2)$:

$$\begin{aligned} |H_a(\Omega)|^2 &= |H_L(j\Omega)|^2 \\ &= \left| \frac{1}{j\Omega + 1} \right|^2 = \frac{1}{|j\Omega + 1|^2} \\ &= \frac{1}{\Omega^2 + 1} = M(\Omega^2) \quad \checkmark \end{aligned}$$

Example

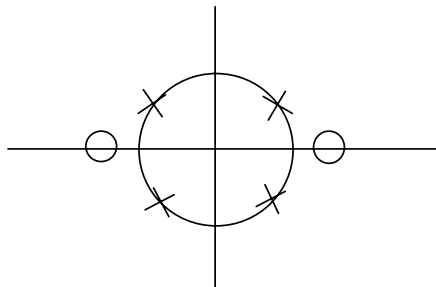
Suppose $M(\Omega^2) = \frac{2 + \Omega^2}{1 + \Omega^4}$ (not for a B, C, or E filter!)

Then

$$\begin{aligned} M(-s^2) &= \frac{2-s^2}{1+s^4} \\ &= \frac{(\sqrt{2}-s)(\sqrt{2}+s)}{\underset{\uparrow}{(s+\gamma)}(s+\gamma^*)(s-\gamma)(s-\gamma^*)} \end{aligned}$$

$$\gamma = e^{j\frac{\pi}{4}} = \frac{1+j}{\sqrt{2}}$$

Pole-zero diagram:



$$\Rightarrow \text{Take } H_L(s) = \frac{\sqrt{2} + s}{(s + \gamma)(s + \gamma^*)} \quad (\text{LHP factors})$$

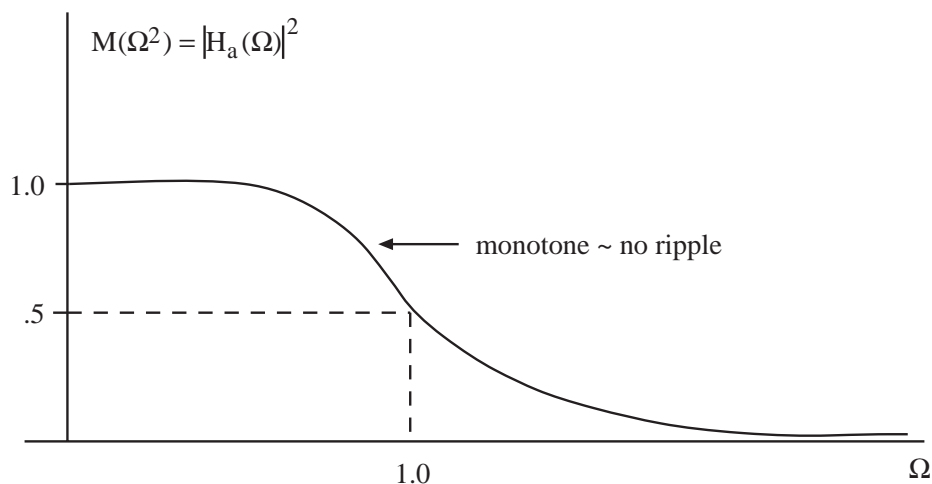
Can check that $|H_L(j\Omega)|^2 = M(\Omega^2)$.

$M(\Omega^2)$ for B, C, and E Filters

Butterworth

$$M(\Omega^2) = \frac{1}{1 + F(\Omega^2)} \text{ with } F(\Omega^2) = \Omega^{2n} \text{ for } n\text{-th-order filter}$$

Result:



$$M(\Omega^2) = .5 \text{ at } \Omega = \Omega_c = 1.0. \text{ For a general cutoff frequency } \Omega_c, \text{ use } F(\Omega^2) = \left(\frac{\Omega}{\Omega_c}\right)^{2n} .$$

Here, we are defining the cutoff frequency to be the value of Ω where $|H_a(\Omega)|^2$ is reduced to one-half its maximum height, or correspondingly, $|H_a(\Omega)|$ reaches $1/\sqrt{2}$ times its maximum value. This definition of cutoff frequency is common, particularly for smooth frequency responses that contain little or no ripple.

Optimality: This $M(\Omega^2)$ has maximum # of derivatives = 0 at the origin for its order. Thus, the response is very flat across lower frequencies.

Can show poles of $M(-s^2) = H_L(s) H_L(-s)$ are equally spaced on the unit circle. This fact helps in factoring $M(-s^2)$.

Chebyshev

$$F(\Omega^2) = \varepsilon^2 C_n^2(\Omega)$$

where ε is a real constant chosen by the designer and $C_n(\bullet)$ is the n th-order Chebyshev polynomial:

$$C_n(\Omega) = \begin{cases} \cos(n \cos^{-1}(\Omega)) & |\Omega| \leq 1 \\ \cosh(n \cosh^{-1}(\Omega)) & |\Omega| > 1 \end{cases}$$

with

$$\cosh t = \frac{e^t + e^{-t}}{2}$$

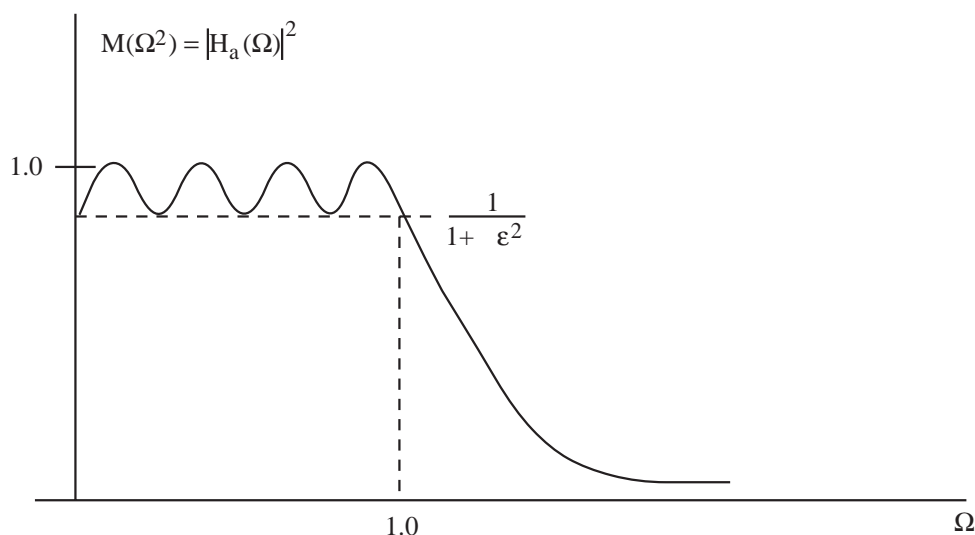
Can show:

$$C_0(\Omega) = 1, C_1(\Omega) = \Omega, C_2(\Omega) = 2\Omega^2 - 1,$$

and that there is a recursion relation:

$$C_{n+1}(\Omega) = 2\Omega C_n(\Omega) - C_{n-1}(\Omega)$$

Result:



For this type of filter, the cutoff frequency is defined to be the value of Ω where $|H_a(\Omega)|^2$ first drops below $1/(1 + \epsilon^2)$ or, correspondingly, $|H_a(\Omega)|$ first drops below $1/\sqrt{1 + \epsilon^2}$.

This is a “Type 1” Chebyshev filter. Its response is equiripple in the passband and monotone decreasing in the stopband. It has a narrower transition band than a Butterworth filter.

Tradeoff: Smaller ϵ gives smaller passband ripple but a wider transition band.

Poles of $M(-s^2) = H_L(s) H_L(-s)$ lie on an ellipse.

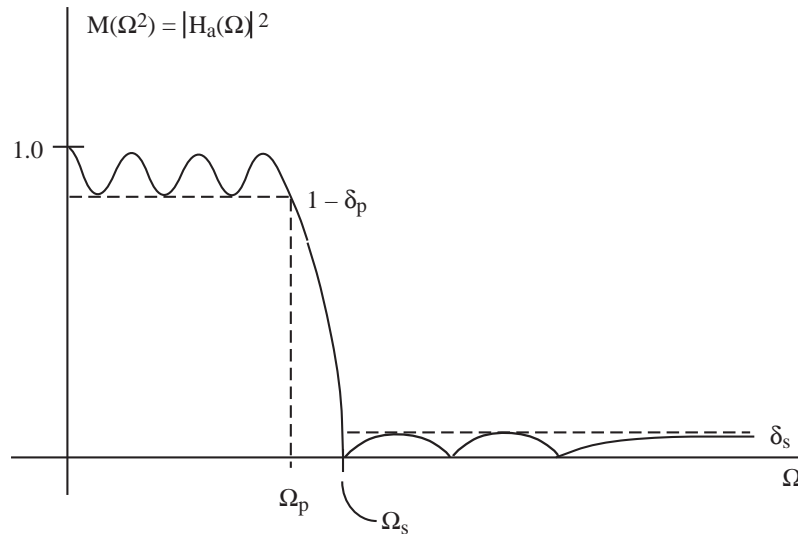
There is also a “Type 2” Chebyshev filter that has a monotone response in its passband and equiripple behavior in its stopband.

Elliptic

$F(\Omega^2) = \epsilon^2 J_n^2(\Omega)$ where J_n is the Jacobi elliptic function.

The defining formulas for J_n are so cumbersome that they are not presented here.

Result:



The response is equiripple in both the passband and stopband.

Elliptic filters are optimal in the sense that for a given n , δ_p , δ_s , Ω_p , the transition bandwidth $\Omega_s - \Omega_p$ is the smallest possible.

$\angle H_a(\Omega)$ for B, C, and E filters is reasonably linear till you get near the edge of the passband, where it can be quite nonlinear.

The phase response is closest to linear for B, then C. Elliptic is worst.

All-pass filters are sometimes cascaded onto elliptic filters to compensate for the nonlinear phase of elliptic filters.

All-pass filters have $|H_a(\Omega)| = \text{constant}$ and the coefficients are chosen to shape $\angle H_a(\Omega)$ in a desired way.

Bilinear Transformation

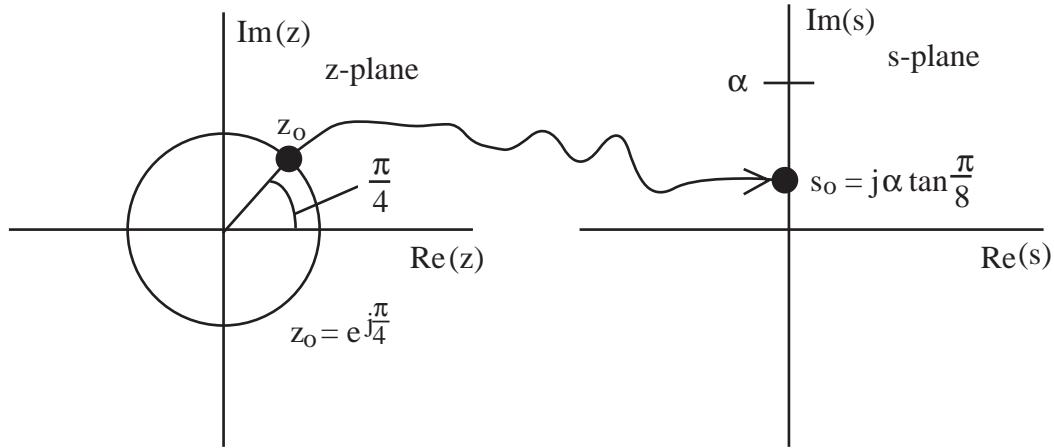
Start with analog prototype $H_L(s)$.

Take

$$H(z) = H_L(s) \bigg|_{s=\alpha \frac{1-z^{-1}}{1+z^{-1}}}$$

α is a real positive constant that we will be able to choose to control the cutoff frequency of the digital filter.

$s = \alpha \frac{1 - z^{-1}}{1 + z^{-1}}$ is a bilinear transformation (BLT) of the z-plane to the s-plane. For example, the point z_0 maps to the point s_0 as shown below.



To see this, note:

$$\begin{aligned}
 s_0 &= \alpha \frac{1 - z_0^{-1}}{1 + z_0^{-1}} = \alpha \frac{1 - e^{-j\frac{\pi}{4}}}{1 + e^{-j\frac{\pi}{4}}} = \alpha \frac{e^{-j\frac{\pi}{8}}}{e^{-j\frac{\pi}{8}}} \frac{e^{j\frac{\pi}{8}} - e^{-j\frac{\pi}{8}}}{e^{j\frac{\pi}{8}} + e^{-j\frac{\pi}{8}}} \\
 &= \alpha \frac{2j \sin \frac{\pi}{8}}{2 \cos \frac{\pi}{8}} = j \alpha \tan \frac{\pi}{8}
 \end{aligned}$$

So, if we design a digital filter using the BLT, then $H(z_0) = H_d\left(\frac{\pi}{4}\right)$ will have the same value as $H_L(s_0) = H_a\left(\alpha \tan \frac{\pi}{8}\right)$.

We must have a much broader understanding than this, however. Questions:

- i) Stable $H_L(s) \Rightarrow$ stable $H(z)$?
- ii) How is $H_d(\omega) = H(e^{j\omega})$ related to $H_L(s)$?

Answer i) by considering a point $s = s_0$ and determining what z it gets mapped to.

$$\text{BLT mapping is } s = \alpha \frac{1 - z^{-1}}{1 + z^{-1}}$$

$$\Rightarrow s(1 + z^{-1}) = \alpha(1 - z^{-1})$$

$$\Rightarrow z^{-1}(s + \alpha) = \alpha - s$$

$$\Rightarrow z = \frac{\alpha + s}{\alpha - s}$$

So, a point $s_0 = \sigma_0 + j \Omega_0$.

gets mapped to:

$$z_0 = \frac{\alpha + \sigma_0 + j\Omega_0}{\alpha - \sigma_0 - j\Omega_0} \quad (*)$$

i.e., $H(z_0) = H_L(s_0)$.

From (*)

$$|z_0| = \left[\frac{(\alpha + \sigma_0)^2 + \Omega_0^2}{(\alpha - \sigma_0)^2 + \Omega_0^2} \right]^{1/2}$$

So:

$$|z_0| \begin{cases} < 1 & \sigma_0 < 0 \\ = 1 & \sigma_0 = 0 \\ > 1 & \sigma_0 > 0 \end{cases}$$

giving:

- a) Left-half s-plane is mapped inside the unit circle in the z-plane.
- b) Right-half s-plane is mapped outside the unit circle in the z-plane.
- c) Imaginary axis in s-plane is mapped onto the unit circle in the z-plane.

Note:

$$[a] \Rightarrow \text{stable } H_L(s) \text{ results in stable } H(z)]$$

$$[c] \Rightarrow H_d(\omega) = H(e^{j\omega}) \text{ depends only on } H_L(j\Omega) = H_a(\Omega)]$$

What is the relationship between $H_d(\omega)$ and $H_a(\Omega)$? $H_d(\omega)$ is given by

12.10

$$H_d(\omega) = H(e^{j\omega}) = H_L(s) \bigg|_{s=\alpha \frac{1-e^{-j\omega}}{1+e^{-j\omega}}}$$

Note:

$$\begin{aligned} \alpha \frac{1-e^{-j\omega}}{1+e^{-j\omega}} &= \alpha \frac{e^{-j\omega/2}}{e^{-j\omega/2}} \frac{e^{j\omega/2} - e^{-j\omega/2}}{e^{j\omega/2} + e^{-j\omega/2}} \\ &= \alpha \frac{2j \sin \frac{\omega}{2}}{2 \cos \frac{\omega}{2}} = j \alpha \tan \frac{\omega}{2} \end{aligned}$$

So,

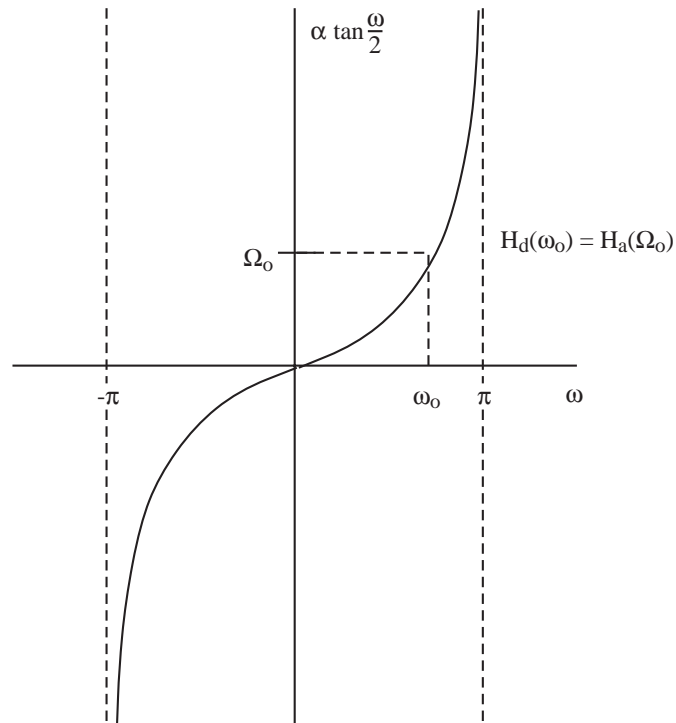
$$H_d(\omega) = H_L(s) \bigg|_{s=j\alpha \tan \frac{\omega}{2}}$$

Since $H_a(\Omega) = H_L(j\Omega)$ we have

$$\boxed{H_d(\omega) = H_a\left(\alpha \tan \frac{\omega}{2}\right)} \quad (\square)$$

This equation tells us exactly how, when using the bilinear transformation design method, the frequency response of the designed digital filter will depend on the frequency response of the analog prototype.

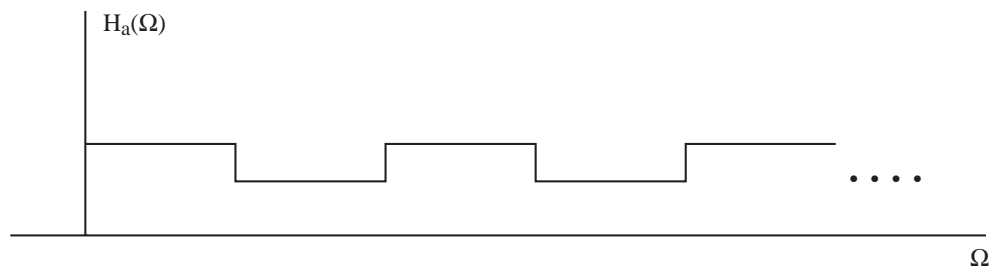
Pictorial interpretation of (□):



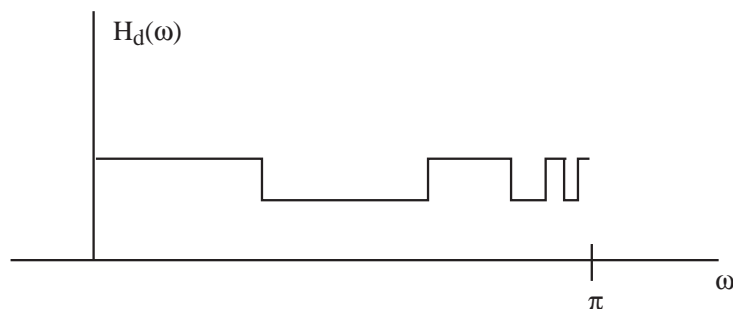
So, $H_d(\omega)$ takes on exactly the same set of values as $H_a(\Omega)$, but there is a squashing of the analog frequency axis, according to the above curve. This mapping is nonlinear, and it has to be, since the infinite-length analog frequency axis $-\infty < \Omega < \infty$ is mapped onto the finite-length interval $-\pi < \omega < \pi$. Because of this, $H_d(\omega)$ won't look like $H_a(\Omega)$ in general. It will be a warped version. This effect is sometimes called “frequency warping.”

Example

Applying the BLT to an analog prototype having frequency response:



results in:



In general, to design $H_d(\omega)$ having a desired shape, we would need to design $H_a(\Omega)$ so that after application of the BLT, the frequency warping produces the desired $H_d(\omega)$. Thus, we would need to “prewarp.”

Let the desired $H_d(\omega)$ be $D(\omega)$.

$$(\square) \Rightarrow \text{want } H_a\left(\alpha \tan \frac{\omega}{2}\right) = D(\omega)$$

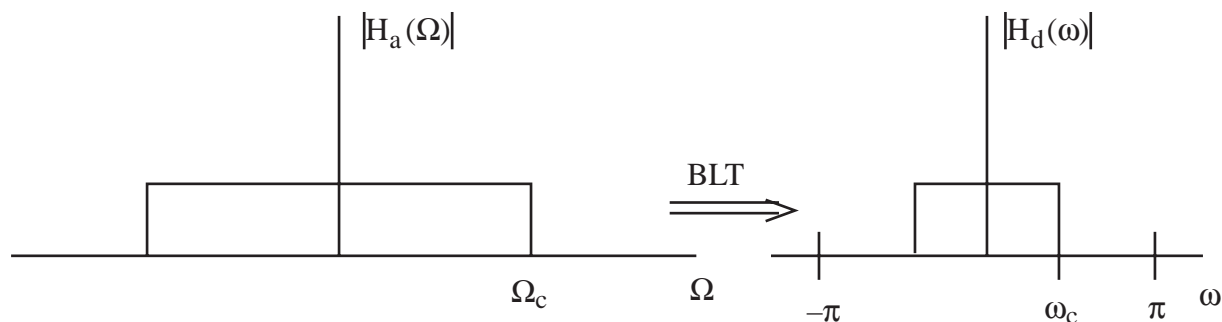
$$\Rightarrow H_a(\Omega) = D\left(2 \tan^{-1} \frac{\Omega}{\alpha}\right) \quad (\Delta)$$

If we *could* design $H_L(s)$ to satisfy (Δ) , the BLT, would then give

$$H_d(\omega) = D(\omega) .$$

This is problematic, however. The design of H_L with a general shape will require computer optimization. Thus, we may as well design H_d directly, using computer optimization.

Fortunately, for LPF's, BPF's and HPF's, there is no such problem. For these kinds of filters, frequency warping just affects the cutoff frequencies, e.g.,



From (\square) :

$$\Omega_c = \alpha \tan \frac{\omega_c}{2} \quad (\square\square)$$

So, we can simply pick Ω_c to give the desired ω_c . Equivalently, if $H_a(\Omega)$ is normalized to $\Omega_c = 1$, we can choose α in the BLT to give the desired ω_c .

This suggests two alternative, but equivalent, design procedures:

1. a) Choose α arbitrarily, say $\alpha = 1$.
 b) Then design the analog prototype to have cutoff Ω_c given by (□□).
 c) Apply the BLT.
2. a) Use an analog prototype with Ω_c .
 b) Choose α to give the desired ω_c .

From (□□),

$$\alpha = \Omega_c \cot\left(\frac{\omega_c}{2}\right)$$

so that the BLT method becomes

$$H(z) = H_L(s) \bigg|_{s = \Omega_c \cot \frac{\omega_c}{2} \frac{1-z^{-1}}{1+z^{-1}}}$$

Analog prototype filters are usually designed with normalized cutoff frequencies $\Omega_c = 1.0$. In this case, the bilinear transformation method of design reduces to

$$H(z) = H_L(s) \bigg|_{s = \cot \frac{\omega_c}{2} \frac{1-z^{-1}}{1+z^{-1}}}$$

(BLT)

In this course, we will use the second option, with Eq. (BLT), to perform the bilinear transformation method of design.

Example

Design a first-order Butterworth digital filter with $\omega_c = \frac{\pi}{4}$, using the BLT method

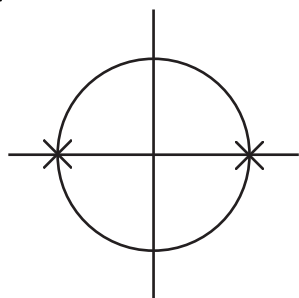
Solution:

First, find the analog prototype:

$$|H_a(\Omega)|^2 = B(\Omega^2) = \frac{1}{1 + \Omega^2}$$

$$B(-s^2) = \frac{1}{1 - s^2} = \frac{1}{1 - s} \cdot \frac{1}{1 + s}$$

Pole locations:



Take LHP factor for $H_L(s)$:

$$H_L(s) = \frac{1}{s + 1}$$

Apply (BLT):

$$H(z) = \frac{1}{s + 1} \bigg|_{s = \cot \frac{\pi}{8} \frac{1 - z^{-1}}{1 + z^{-1}}}$$

\uparrow
 2.4142

$$\begin{aligned} \Rightarrow H(z) &= \frac{1}{2.4142 \frac{1 - z^{-1}}{1 + z^{-1}} + 1} \\ &= \frac{1 + z^{-1}}{2.4142 (1 - z^{-1}) + 1 + z^{-1}} \\ &= \frac{1 + z^{-1}}{3.4142 - 1.4142 z^{-1}} \end{aligned}$$

$$= \boxed{\frac{.2929 + .2929 z^{-1}}{1 - .4142 z^{-1}}}$$

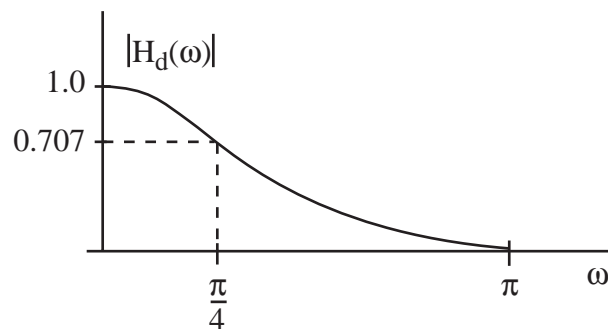
Now, since $H(z)$ resulted from a BLT design using an analog prototype filter with $|H_a(0)| = 1$ and $|H_d(\infty)| = 0$, we know

$$|H_d(0)| = |H_a(0)| = 1 \quad \text{and} \quad |H_d(\pi)| = |H_a(\infty)| = 0$$

Furthermore, since the digital cutoff is $\frac{\pi}{4}$, we should have

$$\left| H_d\left(\frac{\pi}{4}\right) \right| = \frac{1}{\sqrt{2}}$$

Thus, $|H_d(\omega)|$ should look like



The correctness of the values of $|H_d(\omega)|$ at $\omega = 0, \pi$ can be easily verified from the transfer function $H(z)$. Note that

$$H_d(0) = H(e^{j0}) = H(1) = \frac{.2929 + .2929}{1 - .4142} = 1.0$$

$$H_d(\pi) = H(e^{j\pi}) = H(-1) = \frac{.2929 - .2929}{1 - .4142} = 0$$

For $\omega \neq 0$ or π we can always evaluate the magnitude response via the lengthier calculation

$$\begin{aligned} |H_d(\omega)| &= \frac{|.2929 + .2929 e^{-j\omega}|}{|1 - .4142 e^{-j\omega}|} \\ &= \frac{\sqrt{(.2929 + .2929 \cos \omega)^2 + (.2929 \sin \omega)^2}}{\sqrt{(1 - .4142 \cos \omega)^2 + (.4142 \sin \omega)^2}} \end{aligned}$$

Finally, a plot of $\angle H_d(\omega)$ would show that the phase is nearly linear for $|\omega| < \frac{\pi}{4}$ and becomes more nonlinear for $|\omega| \approx \frac{\pi}{4}$ and larger.

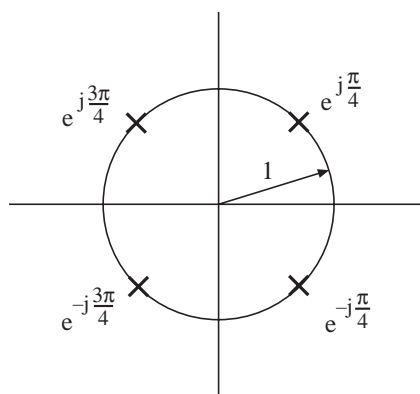
Example

Similar to previous example, but now design a second-order Butterworth digital filter with $\omega_c = \frac{\pi}{4}$.

To find analog prototype, note

$$|H_a(\Omega)|^2 = M(\Omega^2) = \frac{1}{1 + \Omega^4}$$

$$\Rightarrow B(-s^2) = \frac{1}{1 + s^4}$$



Left-half-plane poles are used for $H_L(s)$:

$$H_L(s) = \frac{1}{\left(s - e^{j\frac{3\pi}{4}}\right)\left(s - e^{-j\frac{3\pi}{4}}\right)} = \frac{1}{s^2 + \sqrt{2}s + 1}$$

$$H(z) = H_L(s) \Big|_{s = \cot \frac{\pi}{8} \frac{1-z^{-1}}{1+z^{-1}}}$$

$$= \frac{1}{(2.4142)^2 \frac{(1-z^{-1})^2}{(1+z^{-1})^2} + 2.4142 \sqrt{2} \frac{1-z^{-1}}{1+z^{-1}} + 1}$$

$$= \frac{(1+z^{-1})^2}{(2.4142)^2 (1-2z^{-1}+z^{-2}) + 2.4142\sqrt{2}(1-z^{-2}) + (1+2z^{-1}+z^{-2})}$$

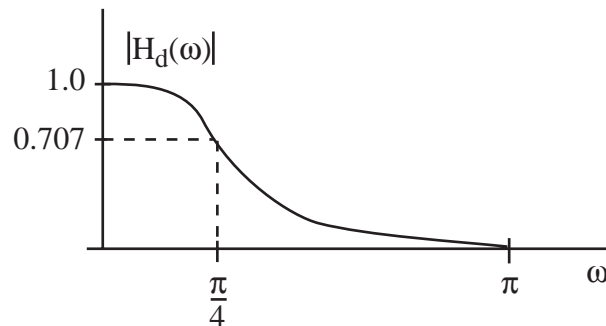
$$= \frac{1 + 2z^{-1} + z^{-2}}{10.23 - 9.66z^{-1} + 3.41z^{-2}}$$

$$= \frac{0.098 + 0.196z^{-1} + 0.098z^{-2}}{1 - 0.944z^{-1} + 0.333z^{-2}}$$

Now, once again, from the shape of the analog prototype $H_a(\Omega)$ we know

$$H_d(0) = 1, \quad \left| H_d\left(\frac{\pi}{4}\right) \right| = \frac{1}{\sqrt{2}}, \quad |H_d(\pi)| = 0$$

However, for the second-order filter, the frequency response makes a sharper transition around $\omega_c = \frac{\pi}{4}$ and looks like

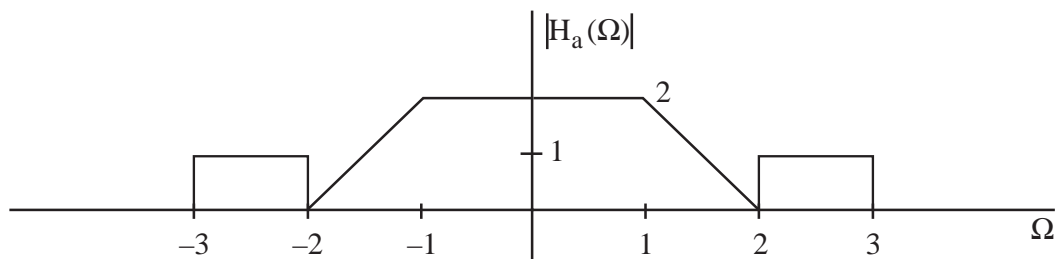


The phase $\angle H_d(\omega)$ will again be quite linear across the passband and more nonlinear across the stopband.

Let's try to get a better feel for the BLT mapping by considering one further example.

Example

Suppose that an analog prototype filter $H_L(s)$ has the frequency response



and that the bilinear transformation is used to produce a digital filter with $H(z) = H_L(s) \Big|_{s=\frac{1-z^{-1}}{1+z^{-1}}}$.

Sketch $|H_d(\omega)|$. Label all critical frequencies and amplitudes.

Solution

$H_d(\omega)$ is a squashed version of $H_a(\Omega)$, described by

$$H_d(\omega) = H_a\left(\alpha \tan \frac{\omega}{2}\right) = H_a\left(\tan \frac{\omega}{2}\right)$$

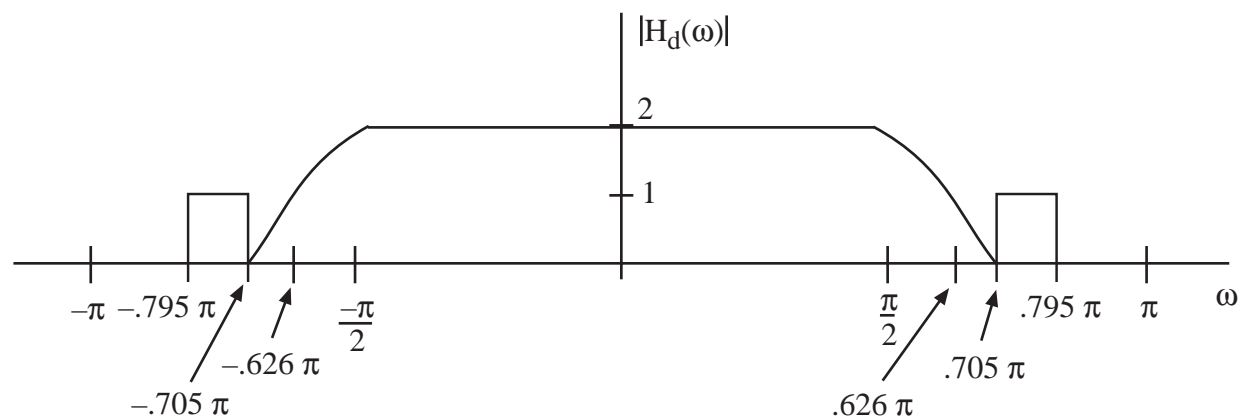
Thus, the value of $H_d(\omega)$ equals the value of $H_a(\Omega)$ at $\Omega = \tan \frac{\omega}{2}$. So a feature (e.g., jump) in $H_a(\Omega)$ that occurs at $\Omega = \Omega_0$ will occur in $H_d(\omega)$ at

$$\omega_0 = 2 \tan^{-1} \Omega_0$$

The interesting features in $H_a(\Omega)$ occur at $\Omega_0 = 1, 2$, and 3 . In addition let's also consider $\Omega_0 = 1.5$. The corresponding ω_0 are given in the table below.

Ω_0	1	1.5	2	3
ω_0	0.5π	0.626π	0.705π	0.795π

Thus, $|H_d(\omega)|$ looks like



Notice that $H_d(\omega)$ takes on exactly the same set of values taken on by $H_a(\Omega)$. It just does so at different frequencies, which causes a change in shape.

2. Computer-Aided Optimization

Used for IIR designs with general magnitude and/or phase specifications (i.e., $H_d(\omega)$ not LPF, HPF, or BPF).

Digital Frequency Transformation

By making a “change of variable” in $H_L(s)$ or $H(z)$, we can transform an analog or digital LPF to a LPF having a different cutoff frequency, or to a HPF or BPF.

We will consider only digital transformations (transformations of $H(z)$).

Procedure:

Let $H(z)$ be the transfer function of a low-pass digital filter. Then simply substitute for z^{-1} in $H(z)$, using the expressions below, to produce filters having the described characteristics.

Lowpass \rightarrow Lowpass

$$z^{-1} \rightarrow \frac{z^{-1} - \beta}{1 - \beta z^{-1}}$$

where

ω'_c = cutoff of new filter

$$\beta = \frac{\sin [(\omega_c - \omega'_c)/2]}{\sin [(\omega_c + \omega'_c)/2]}$$

Lowpass \rightarrow Highpass

$$z^{-1} \rightarrow -\frac{z^{-1} - \beta}{1 - \beta z^{-1}}$$

ω'_c = cutoff of new filter

$$\beta = \frac{\cos [(\omega_c + \omega'_c)/2]}{\cos [(\omega_c - \omega'_c)/2]}$$

Lowpass \rightarrow Bandpass

$$z^{-1} \rightarrow -\frac{z^{-2} - \beta_1 z^{-1} + \beta_2}{\beta_2 z^{-2} - \beta_1 z^{-1} + 1}$$

ω_ℓ = lower cutoff of BPF

ω_u = upper cutoff of BPF

$$\beta_1 = 2\gamma K/(K+1)$$

$$\beta_2 = (K-1)/(K+1)$$

$$\gamma = \frac{\cos [(\omega_u + \omega_\ell)/2]}{\cos [(\omega_u - \omega_\ell)/2]}$$

$$K = \cot \frac{\omega_u - \omega_\ell}{2} \tan \frac{\omega_c}{2}$$

Relationship Between Pole and Zero Locations and Frequency Response

In digital filter design we choose the coefficients of

$$H(z) = \frac{a_0 + a_1 z^{-1} + \dots + a_N z^{-N}}{1 + b_1 z^{-1} + \dots + b_N z^{-N}}$$

to shape the frequency response $H_d(\omega) = H(e^{j\omega})$ in a desired way. Since $H(z)$ can also be written in terms of its poles and zeros as

$$H(z) = a_0 \prod_{i=1}^N \frac{z - z_i}{z - p_i}$$

this provides an alternative parameterization of $H(z)$. Choosing the pole and zero locations of the filter is basically equivalent to choosing the $\{a_i\}$ and $\{b_i\}$. In this connection, it is worth exploring how the pole and zero locations affect the shape of $H_d(\omega)$.

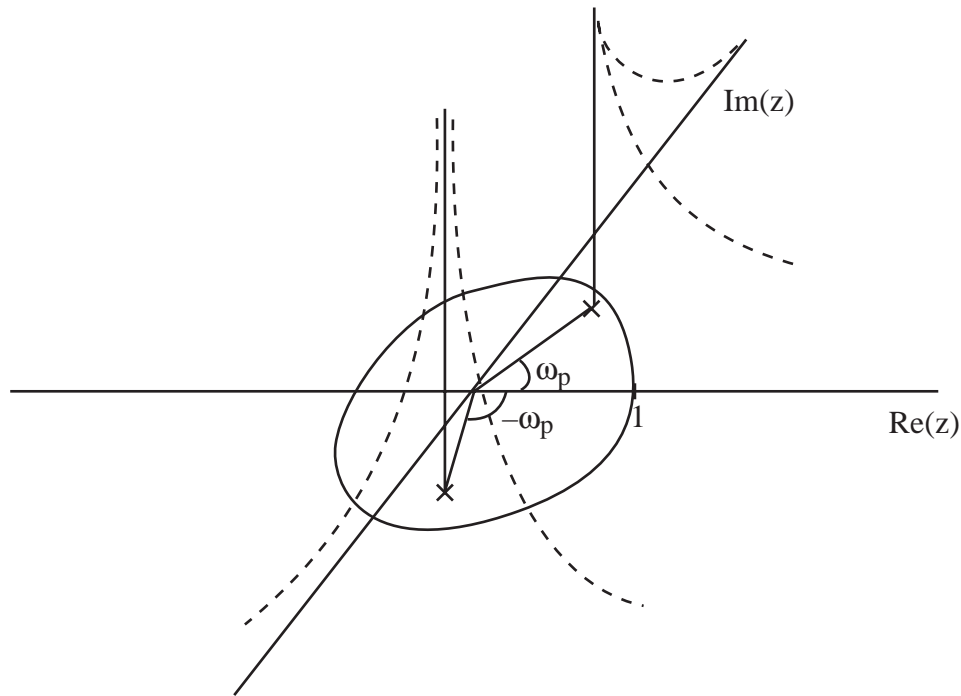
The general shape of $|H_d(\omega)|$ often can be visualized from knowledge of the pole and zero locations of $H(z)$. This is especially true for situations where poles are near the unit circle and zeros are either on or near the unit circle.

Example

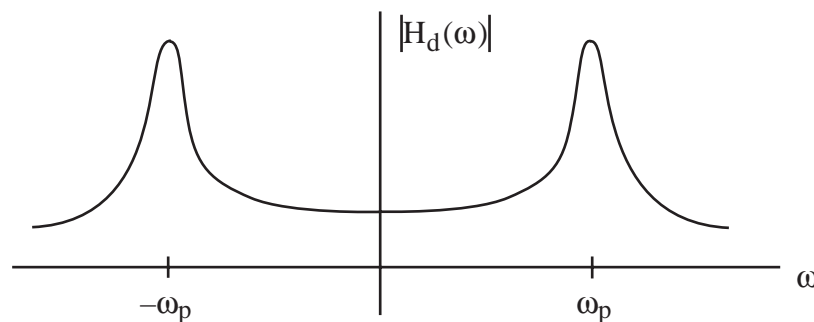
Consider a causal, stable all-pole filter with

$$H(z) = \frac{1}{z^2 - (2\alpha \cos \omega_p)z + \alpha^2} = \frac{1}{(z - \alpha e^{j\omega_p})(z - \alpha e^{-j\omega_p})}$$

and $0 < \alpha < 1$. $H(z)$ approaches ∞ at the pole locations and approaches zero for $|z|$ large. Thus, we expect $|H(z)|$ to look somewhat like a two-pole circus tent:



Here, the pole locations are marked by \times and are at a distance α from the origin. Since $H(z)$ is causal, its ROC is $\{z : |z| > \alpha\}$ and the above tent covers only this set of z . (The tent is undefined elsewhere.) Since $\alpha < 1$, ROC_H includes the unit circle. Thus, the frequency response $H_d(\omega) = H(e^{j\omega})$ is well defined and is a circular slice of the circus tent, around the unit circle. Now, since $H(z)$ is infinite at $z = \alpha e^{\pm j\omega_p}$, we expect that $H(z)$ will be large for z near the poles. If α is nearly one then the poles are close to the unit circle and $H_d(\omega)$ will be large for ω such that $e^{j\omega}$ is close to the poles. This suggests that $|H_d(\omega)|$ will look like

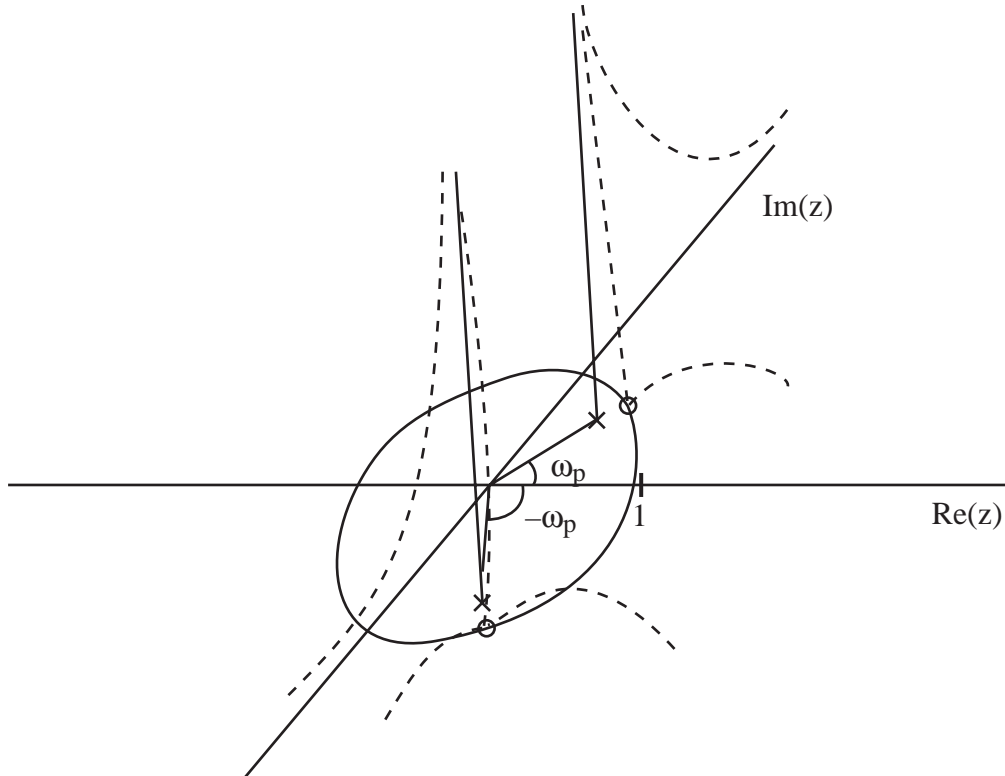


where the peaks occur near $\omega = \omega_p$.

Example

$$H(z) = \frac{z^2 - (2 \cos \omega_p)z + 1}{z^2 - (2\alpha \cos \omega_p)z + \alpha^2} = \frac{(z - e^{j\omega_p})(z - e^{-j\omega_p})}{(z - \alpha e^{j\omega_p})(z - \alpha e^{-j\omega_p})}$$

As before, $H(z)$ approaches ∞ at the pole locations $z = \alpha e^{\pm j\omega_p}$. $H(z) = 0$ at the zero locations $z = e^{\pm j\omega_p}$. Thus, $|H(z)|$ is similar to the previous two-pole circus tent except it “touches the ground” at the zero locations $z = e^{\pm j\omega_p}$ as shown below, where poles are indicated by \times and zeros are represented by \circ .



Since the pole and zero locations are close together, it may seem difficult to determine what $H_d(\omega) = \{H(z) \text{ for } z \text{ on the unit circle}\}$ will look like. A simple observation helps greatly, though. Suppose

$$H(z) = \frac{(z - z_1)(z - z_2)}{(z - p_1)(z - p_2)} \quad (\square)$$

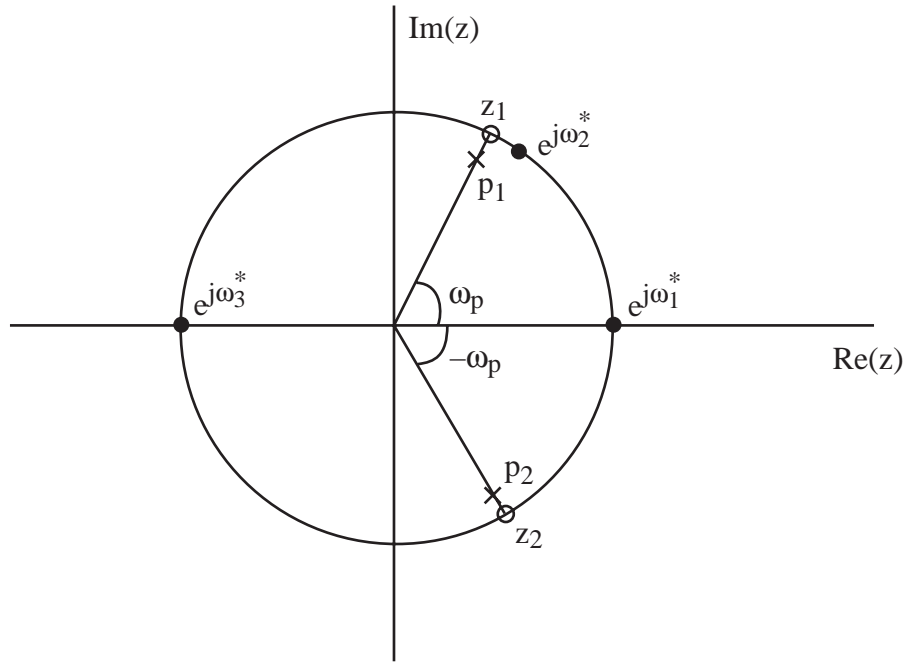
so that

$$|H_d(\omega)| = |H(e^{j\omega})| = \frac{|e^{j\omega} - z_1| |e^{j\omega} - z_2|}{|e^{j\omega} - p_1| |e^{j\omega} - p_2|}$$

Then, the value of $|H_d(\omega)|$ at some specific frequency ω^* is

$$\frac{|e^{j\omega^*} - z_1| |e^{j\omega^*} - z_2|}{|e^{j\omega^*} - p_1| |e^{j\omega^*} - p_2|}.$$

The factor $|e^{j\omega^*} - z_i|$ is the distance in the complex plane between $e^{j\omega^*}$ and z_i . Likewise, the factor $|e^{j\omega^*} - p_i|$ is the distance in the complex plane between $e^{j\omega^*}$ and p_i . Thus, $|H_d(\omega^*)|$ is the product of the distances between $e^{j\omega^*}$ and z_1 , and between $e^{j\omega^*}$ and z_2 , divided by the product of the distances between $e^{j\omega^*}$ and p_1 , and between $e^{j\omega^*}$ and p_2 . In our example, these distances can be visualized for three different frequencies ω_1^* by examining the figure below.



We see that the distances from $e^{j\omega_1^*}$ to the zero z_1 at $e^{j\omega_p}$ and to the neighboring pole p_1 are nearly the same. Likewise, the distances from $e^{j\omega_1^*}$ to the zero z_2 at $e^{-j\omega_p}$ and its neighboring pole p_2 are nearly the same. Thus,

$$|H_d(\omega_1^*)| = \frac{|e^{j\omega_1^*} - z_1|}{|e^{j\omega_1^*} - p_1|} = \frac{|e^{j\omega_1^*} - z_2|}{|e^{j\omega_1^*} - p_2|} \approx (1)(1) = 1$$

The same result holds for any ω_1^* that is close to zero.

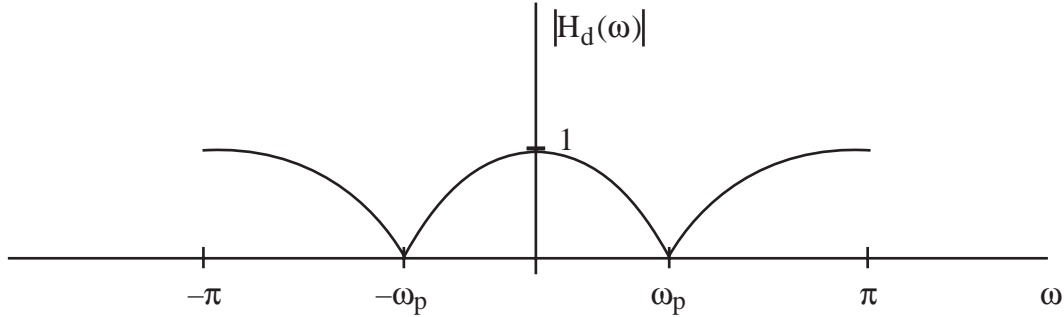
Similarly, in the case of $e^{j\omega_3^*}$ we see that distances to all poles and zeros are nearly equal. Thus,

$$|H_d(\omega_3^*)| \approx 1,$$

which holds for any ω_3^* roughly satisfying $\frac{\pi}{2} \leq |\omega_3^*| \leq \pi$. The distance between $e^{j\omega_2^*}$ and the zero at $e^{j\omega_p}$ approaches zero as $\omega_2^* \rightarrow \omega_p$. Thus

$$|H_d(\omega_2^*)| \approx 0$$

for ω_2^* close enough to ω_p . These considerations lead to the $|H_d(\omega)|$ sketched below.



Here, we can find the precise values of $|H_d(0)|$ and $|H_d(\pi)|$ by using

$$H_d(0) = H(1) = \frac{2 - 2\cos\omega_p}{1 + \alpha^2 - 2\alpha\cos\omega_p}$$

$$H_d(\pi) = H(-1) = \frac{2 + 2\cos\omega_p}{1 + \alpha^2 + 2\alpha\cos\omega_p}.$$

The above frequency response is that of a crude notch filter where signal components near $\omega = \omega_p$ are greatly attenuated and signal components at other frequencies are passed with nearly unit amplitude. The nulls (notches) in $H_d(\omega)$ at $\omega = \omega_p$ are caused by the zeros of $H(z)$ at $z = e^{\pm j\omega_p}$.

It is only slightly more difficult to gain a rough idea of what $\angle H_d(\omega)$ will look like. From (□) we have

$$\angle H_d(\omega) = \angle(e^{j\omega} - z_1) + \angle(e^{j\omega} - z_2) - \angle(e^{j\omega} - p_1) - \angle(e^{j\omega} - p_2)$$

Each term $(e^{j\omega} - z_i)$ or $(e^{j\omega} - p_i)$ is a vector in the complex plane. $\angle(e^{j\omega} - z_i)$ and $\angle(e^{j\omega} - p_i)$ are simply the angles of these vectors with respect to the positive real axis. This interpretation can be helpful when trying to visualize $\angle H_d(\omega)$ for low-order filters. In general, however, Matlab should be used to plot both $|H_d(\omega)|$ and $\angle H_d(\omega)$ for higher-order filters

Example

For an FIR lowpass filter, use Matlab to find the zero locations of $H(z)$. (All poles are at $z = 0$.) You will find that zeros in $|H_d(\omega)|$ within the stopband are caused by zeros of $H(z)$ on the unit circle. Other zeros of $H(z)$ are strategically placed off the unit circle to give a flat response in the passband.

Example

For a Butterworth lowpass filter you will find that some poles are located near the unit circle $e^{j\omega}$ for ω corresponding to the cutoff frequency.

Example

For an elliptic lowpass filter you will find poles near $e^{j\omega}$ for $\omega =$ cutoff frequency, and some zeros on the unit circle at locations corresponding to the stopband.

Digital Interpolation

Suppose have $y_n = y_a(nT_1)$ as pictured:



and want $\tilde{y}_n = y_a(nT_2)$ where $T_2 = \frac{T_1}{L}$, and L is integer :



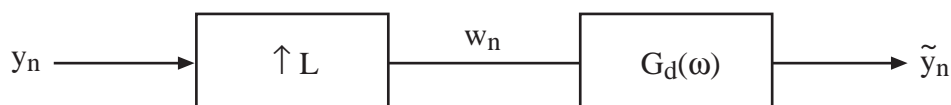
Thus, $\{\tilde{y}_n\}$ are denser samples of $y_a(t)$. How do we get $\{\tilde{y}_n\}$ from $\{y_n\}$? Could use

$$y_a(t) = \sum_{k=-\infty}^{\infty} y_k \operatorname{sinc} \left[\frac{\pi}{T_1} (t - kT_1) \right]$$

to get

$$\tilde{y}_n = y_a(nT_2) = \sum_{k=-\infty}^{\infty} y_k \operatorname{sinc} \left[\frac{\pi}{T_1} (nT_2 - kT_1) \right]$$

But, this involves an infinite sum (which must be truncated in practice) and evaluation of the sinc function. Alternatively, we might try something simpler, such as a piecewise linear or polynomial approximation to $y_a(t)$, but these methods are not particularly accurate.

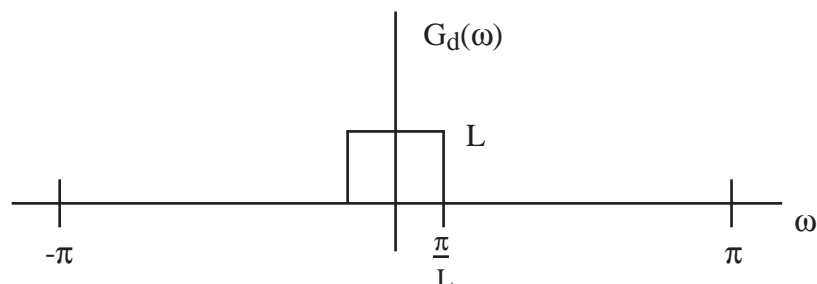
Alternative Digital Approach

where the first box is an up-sampler that inserts $L-1$ zeros between each pair of inputs:

13.2

$$w_n = \{0, 0, \dots, 0, y_{-1}, \underbrace{0, 0, \dots, 0}_{L-1 \text{ zeros}}, y_0, 0, 0, \dots, 0, y_1, 0, \dots\}$$

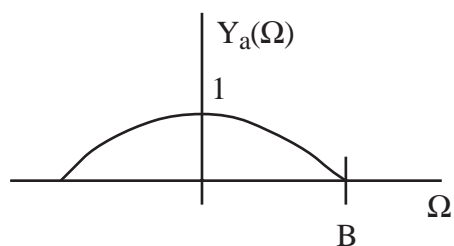
and $G_d(\omega)$ is an ideal LPF with cutoff π/L and passband gain L :



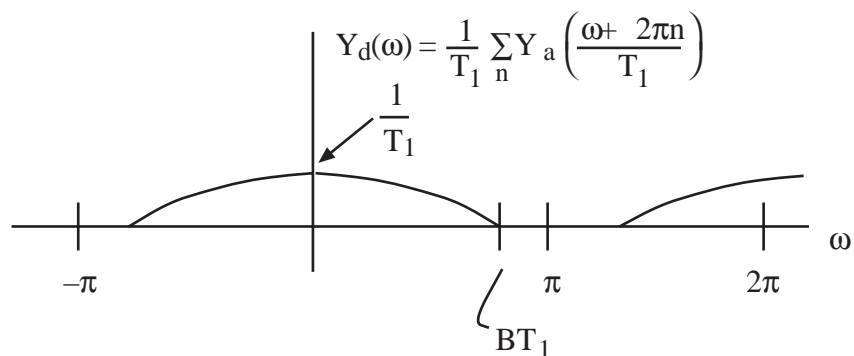
Why does this work??

Analyze the problem in the Fourier domain.

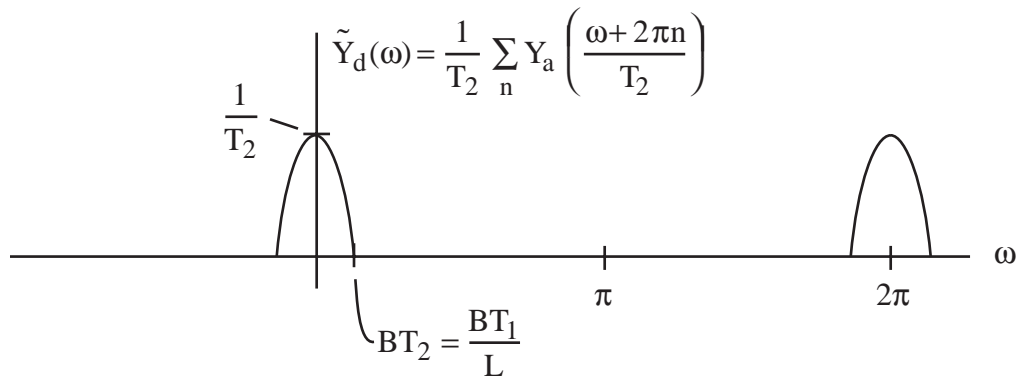
First, note that if



then sampling $y_a(t)$ at times nT_1 (with $T_1 < \frac{\pi}{B}$) would give $\{y_n\}$ with



Sampling $y_a(t)$ on the denser grid nT_2 would give $\{\tilde{y}_n\}$ with



(Sampling at a higher frequency shrinks the DTFT of the A/D output).

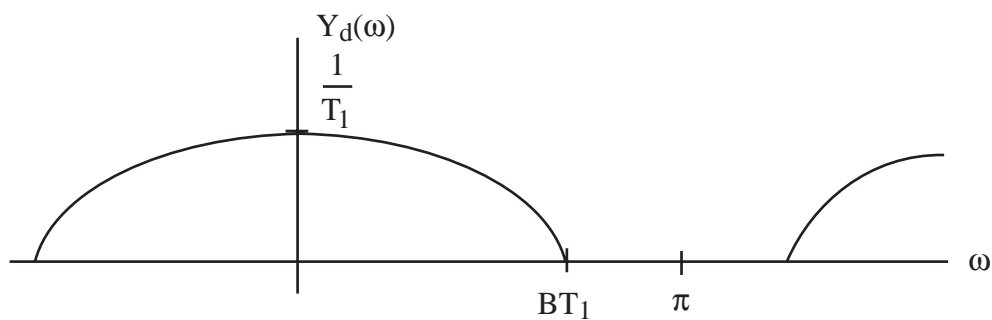
Now, show that the above digital interpolation approach gives \tilde{Y}_d from Y_d (and therefore \tilde{y}_n from y_n).

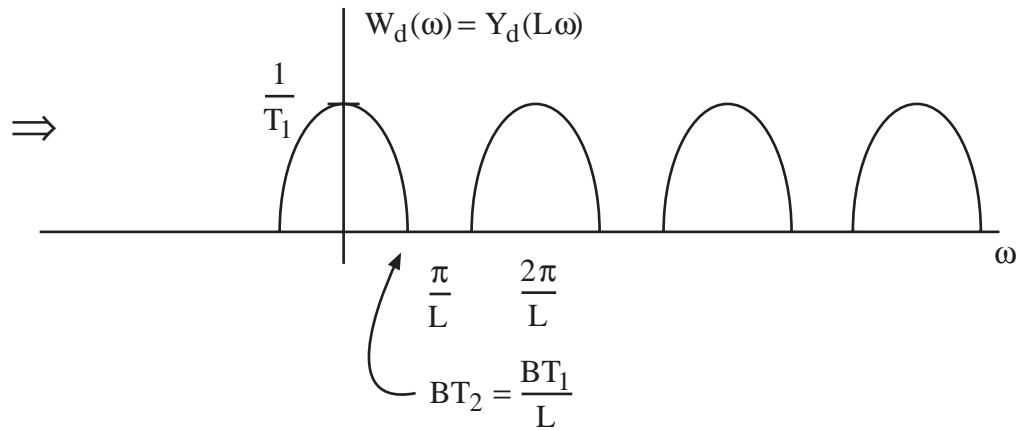
We have

$$W_d(\omega) = \sum_n w_n e^{-j\omega n} = \sum_n y_n e^{-j\omega L n}$$

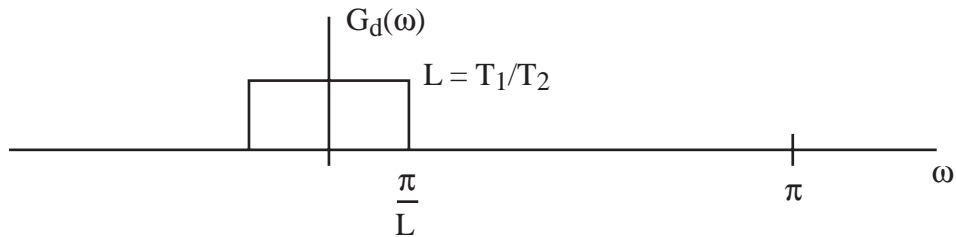
$$\Rightarrow \boxed{W_d(\omega) = Y_d(L\omega)}$$

So,



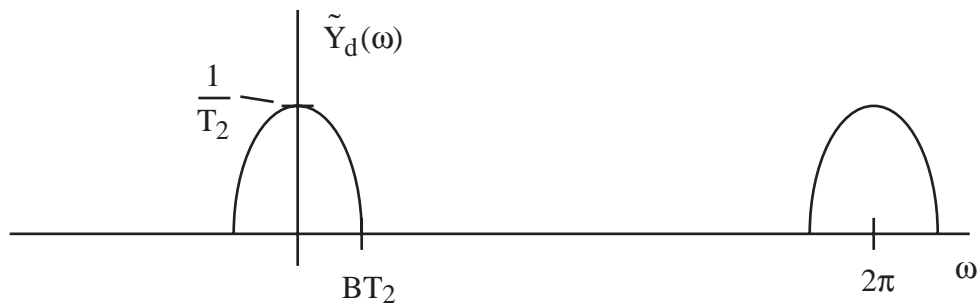


Now, since



we have

$\tilde{Y}_d(\omega) = G_d(\omega) W_d(\omega)$ given by



as desired. Thus, in principle, the digital interpolator will compute $\{\tilde{y}_n\}$ from $\{y_n\}$ exactly. In practice, the quality of the interpolator depends on the quality of $G_d(\omega)$, i.e., on how close $G_d(\omega)$ is to the ideal low-pass shape.

Comments:

- 1) $L-1$ out of every L inputs to $G_d(\omega)$ are zero. This saves many multiplications for L large! This is readily apparent for nonrecursive $G_d(\omega)$, but is also true for some recursive $G_d(\omega)$.
- 2) There exist efficient digital interpolation schemes for $T_2 = \alpha T_1$, where α is any real number (doesn't have to be $\frac{1}{L}$).

A Further Look at Up-Sampler

A digital interpolator uses an up-sampler as one of its components.



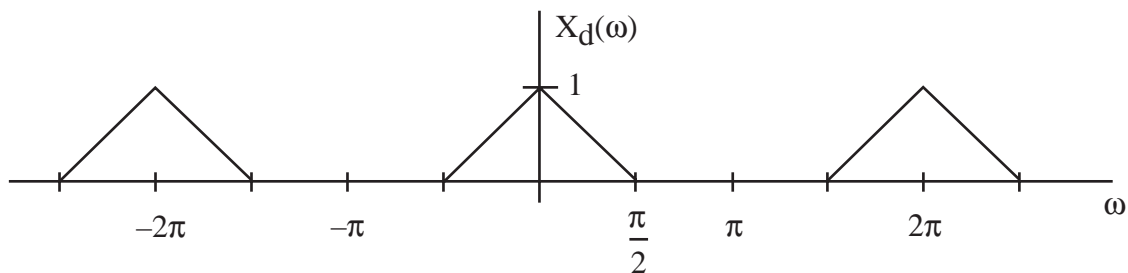
We have shown that $Y_d(\omega)$ is a squashed version of $X_d(\omega)$, namely

$$Y_d(\omega) = X_d(L\omega).$$

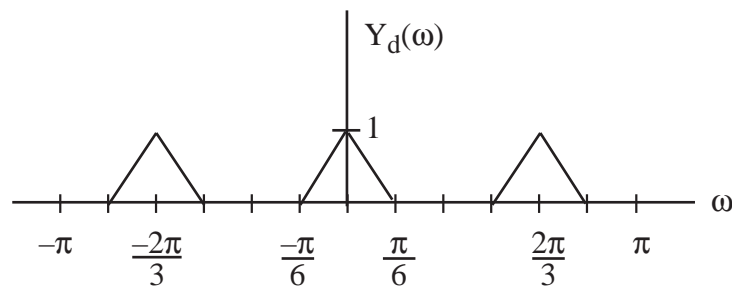
Notice that the amplitude of Y_d is the same as the amplitude of X_d . This makes intuitive sense since the energy in the y_n sequence is the same as that of the x_n sequence, because the up-sampler inserts just zeros between the x_n elements.

Example (Up-Sampler)

Suppose $L = 3$. Sketch $Y_d(\omega)$, assuming

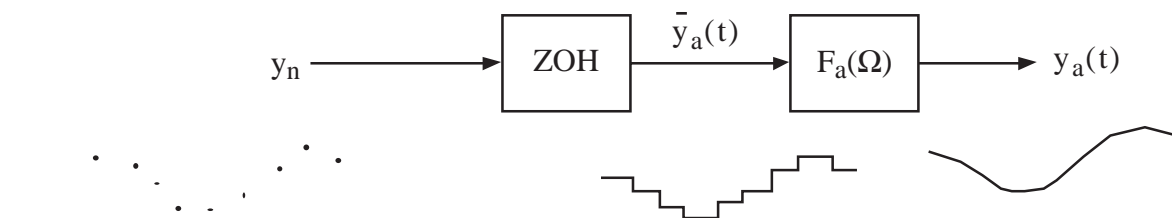


The entire ω axis is squashed by a factor of 3 to give

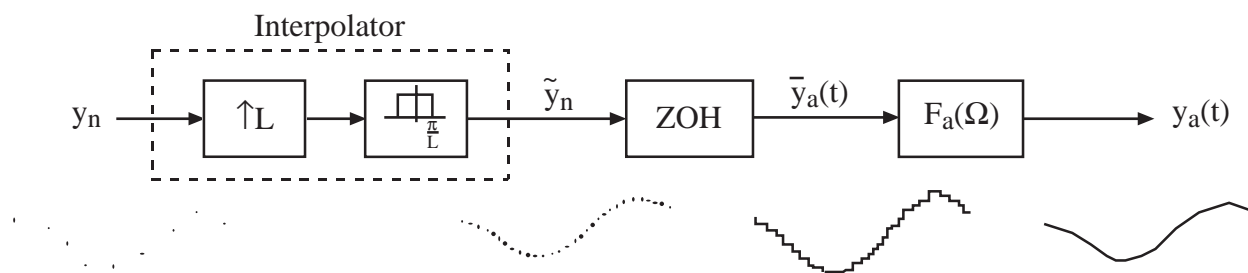


Oversampling D/A

Used in C-D players, for example. Idea is to simplify analog filter in D/A by using interpolation prior to the D/A. Interpolating $\{y_n\}$ prior to the D/A permits the use of a ZOH with a smaller step-size. This ZOH puts out a finer staircase approximation to $y_a(t)$, which relaxes the requirements on $F_a(\Omega)$. So, instead of this:

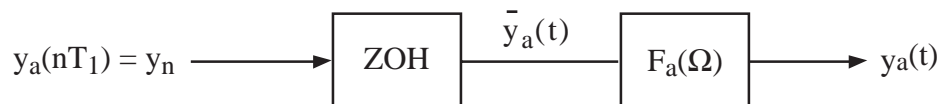


do this:



As you can imagine, a far simpler filter $F_a(\Omega)$ can be used in the second system to produce $y_a(t)$ from $\bar{y}_a(t)$, since $\bar{y}_a(t)$ is much smoother in the second system than in the first system. We gain considerable insight into this via the following analysis.

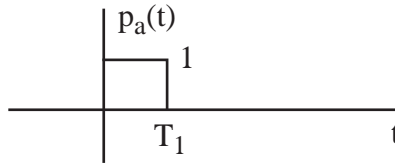
Our analysis of the oversampling D/A is facilitated by first, considering a usual D/A, assuming sampling period of T_1 . The standard way to reconstruct $y_a(t)$ from $y_n = y_a(nT_1)$ is:



where

$$\bar{y}_a(t) = \sum_n y_n p_a(t - nT_1)$$

with



and

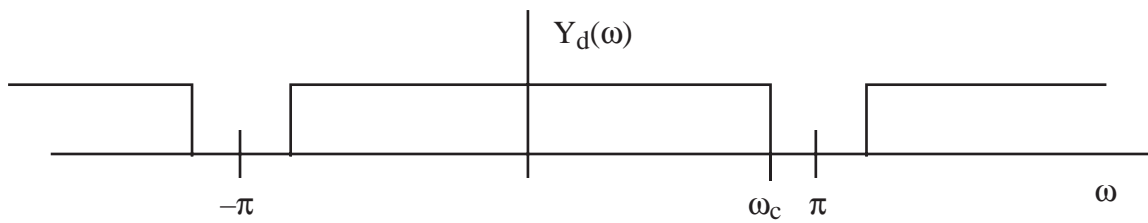
$$\bar{Y}_a(\Omega) = P_a(\Omega) Y_d(\Omega T_1)$$

\uparrow
 from analysis of general D/A

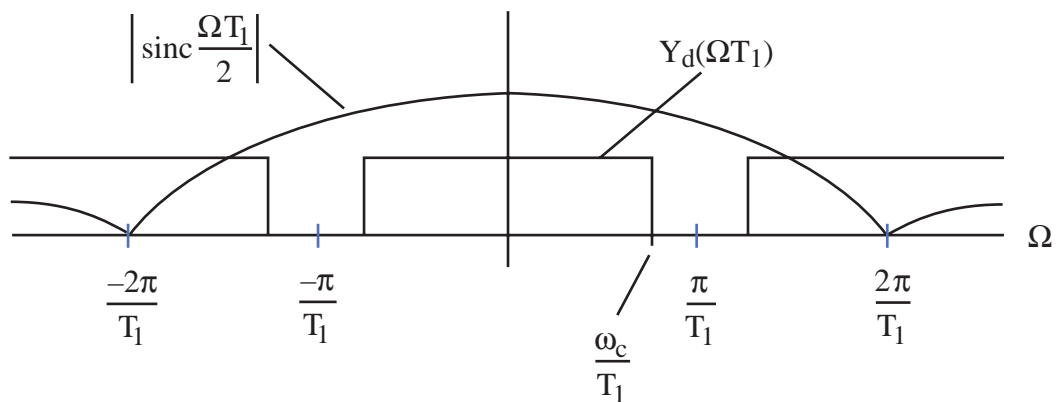
so that

$$\bar{Y}_a(\Omega) = T_1 \operatorname{sinc} \frac{\Omega T_1}{2} e^{-j\frac{\Omega T_1}{2}} Y_d(\Omega T_1) \quad (\square)$$

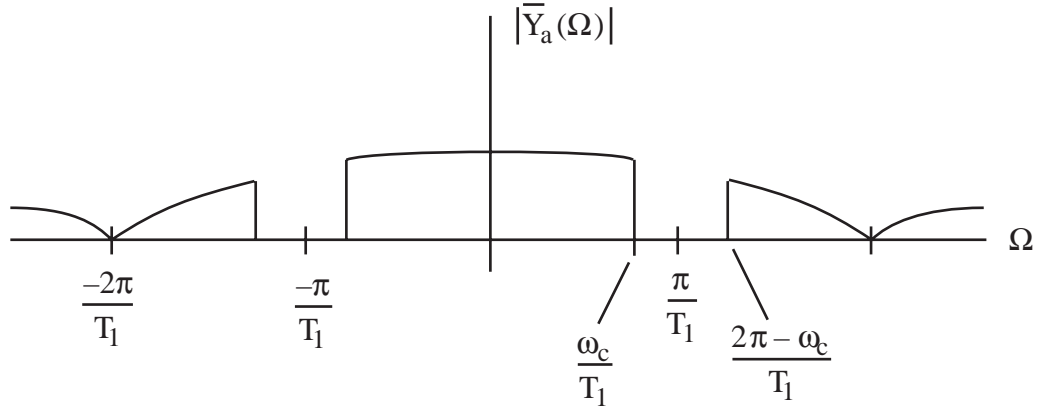
As a specific example, assume



Then $|\bar{Y}_a(\Omega)|$ is the product of the following two curves:



giving

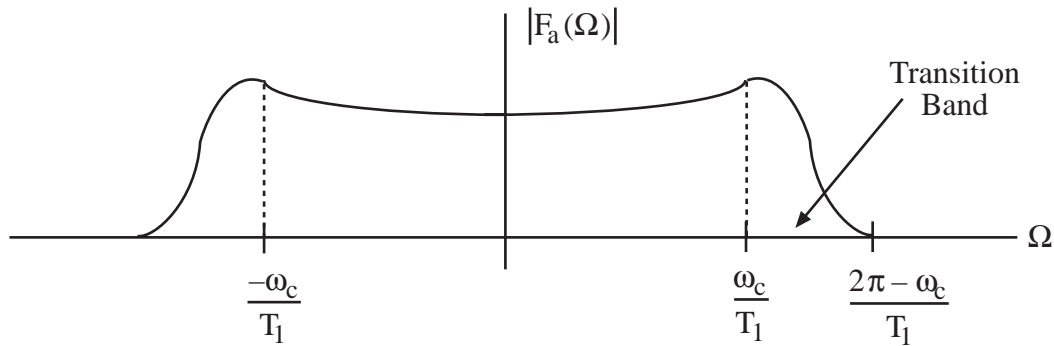


Now, as we know, $F_a(\Omega)$ should be a LPF with a

$$\frac{1}{\text{sinc} \frac{\Omega T_1}{2}}$$

shape in its passband. For the situation above, with $\omega_c < \pi$, there is room for a transition band of $F_a(\Omega)$ on the interval $\frac{\omega_c}{T_1} < |\Omega| < \frac{2\pi - \omega_c}{T_1}$. A finite-order (realizable) $F_a(\Omega)$ needs room for a transition band (transition cannot be infinitely sharp). A wider transition band permits a lower order (less complicated) $F_a(\Omega)$.

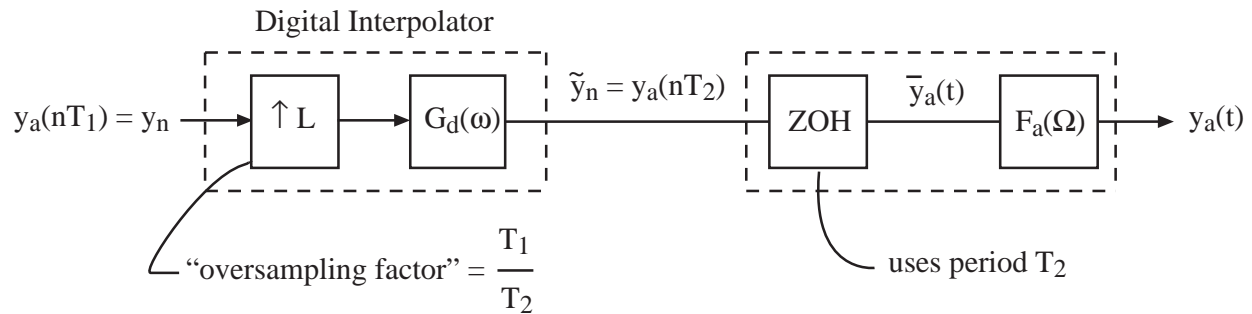
A realizable $F_a(\Omega)$ might look like:



This filter is permitted a transition bandwidth of

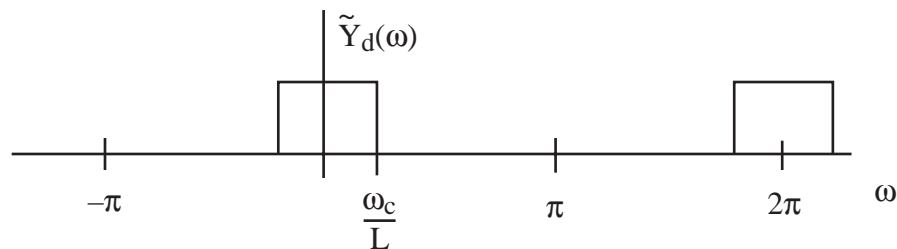
$$\frac{2\pi - \omega_c}{T_1} - \frac{\omega_c}{T_1} = \frac{2(\pi - \omega_c)}{T_1}$$

Now, consider oversampling D/A:

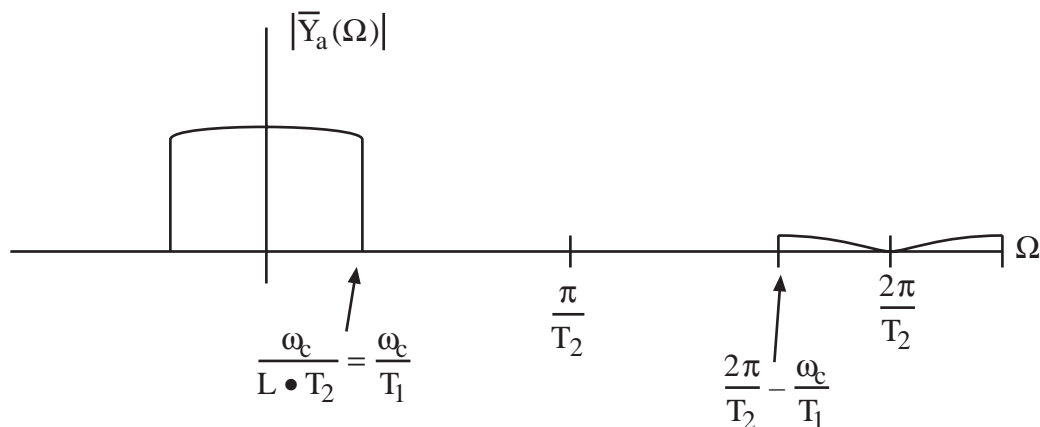


Due to the interpolation, the above ZOH puts out a finer staircase approximation with narrow steps (width T_2). Thus, we expect that $F_a(\Omega)$ can be simpler in this scheme. Let's analyze this in the frequency domain:

The interpolator squashes the DTFT of y_n :



So, $|\bar{Y}_a(\Omega)|$ now looks like the curve below (use eqn. (□) except with T_2 instead of T_1 and \tilde{Y}_d instead of Y_d):



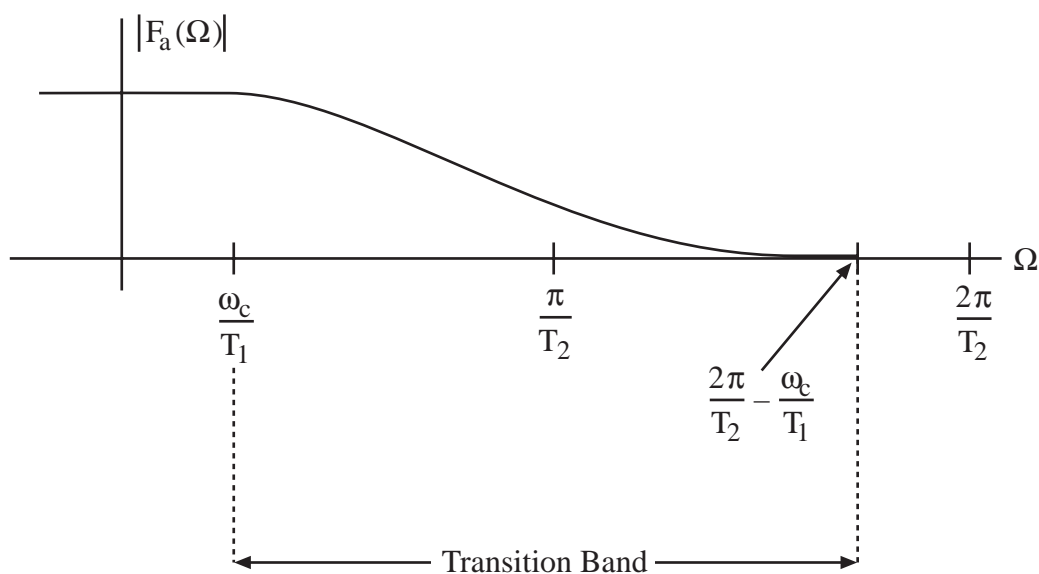
Thus, the transition band of $F_a(\Omega)$ can now be much wider.

$$\begin{aligned}
 \text{Transition BW} &= \frac{2\pi}{T_2} - \frac{\omega_c}{T_1} - \frac{\omega_c}{T_1} \\
 &= \frac{2(L\pi - \omega_c)}{T_1} \gg \frac{2(\pi - \omega_c)}{T_1} \\
 &\quad \uparrow \text{ from before for regular D/A}
 \end{aligned}$$

so that implementation of $F_a(\Omega)$ can be far simpler.

Also, from the picture above we see that the center pulse of $\bar{Y}_a(\Omega)$ is almost flat and that the artifact centered at $\frac{2\pi}{T_2}$ is nearly zero, so even a fairly crude $F_a(\Omega)$ will do a good job. $F_a(\Omega)$ should have a nearly flat response in its passband, can have a huge transition band, and needs only moderate attenuation in its stopband.

$F_a(\Omega)$ in an oversampling D/A can look like:

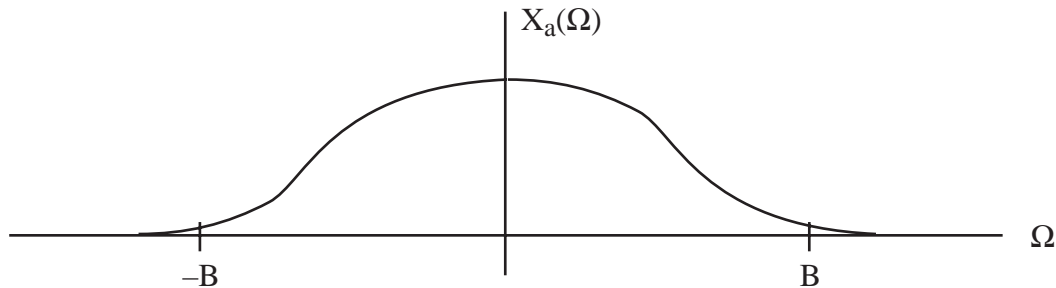


Oversampling A/D

A different type of oversampling is sometimes used to limit aliasing in the A/D. We will examine this as the second method, described below, for preventing aliasing at the A/D.

Prevention of Aliasing at A/D

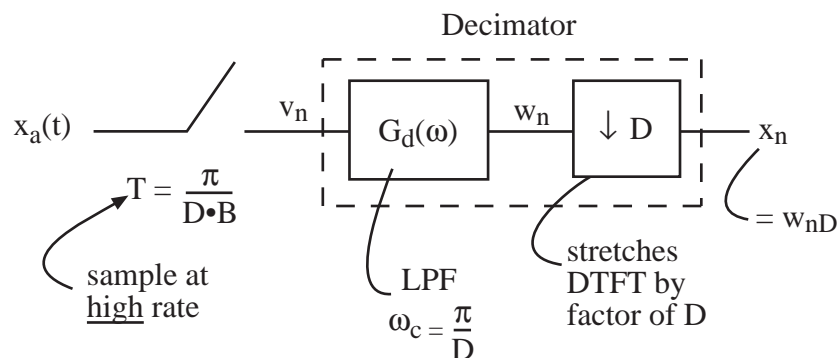
Suppose $x_a(t)$ is nearly (not exactly) BL to B rad/sec.



Here, B is an “effective band limit,” but sampling with $T = \frac{\pi}{B}$ will still cause measurable aliasing.

How do we prevent aliasing at the sampler? Two possibilities:

- 1) Precede the A/D with an analog “antialiasing” LPF with cutoff B rad/sec. Then sample using $T < \frac{\pi}{B}$. This approach is very common.
- 2) Alternatively, sample at a high rate with $T = \frac{\pi}{B \cdot D}$ where D is an integer and is large enough to virtually prevent aliasing (choose D so that $X_a(\Omega)$ is virtually limited to $D \cdot B$ rad/sec). Then digitally LPF with cutoff $\omega_c = \frac{\pi}{D}$. Then decimate by a factor of D (discard $D-1$ of every D samples). This is called an oversampling A/D:

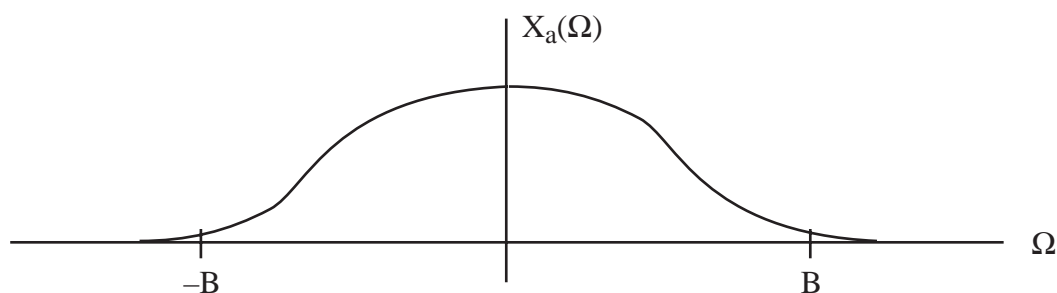


Ordinarily, sampling at such a high rate would be an expensive proposition, since this could create a very high data rate. The decimator, however, reduces the sampling rate back down by a factor of D . Note that implementation of $G_d(\omega)$ is not nearly so complicated as you might expect. Since $D-1$ of every D outputs of $G_d(\omega)$ will be discarded, only every D th output need be computed!

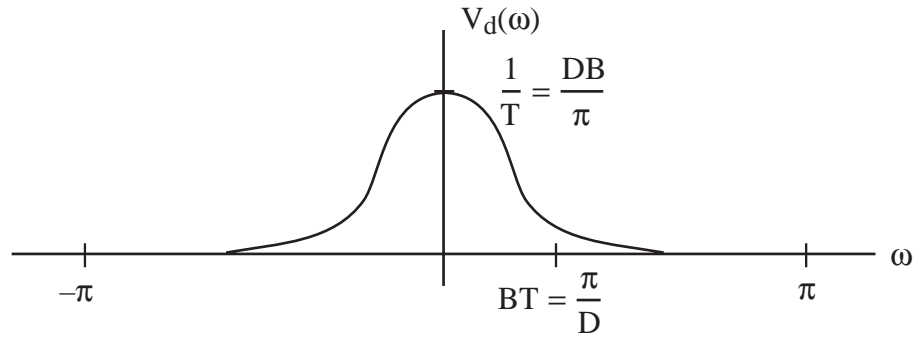
Choosing between 1) and 2) is simply an issue of whether you put the complexity in the analog or digital part of your system.

Analysis of Oversampling A/D

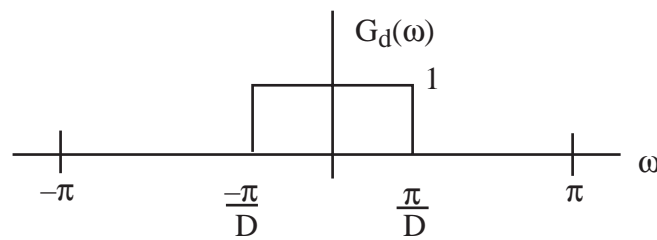
We will show that Option 2 (oversampling approach) produces exactly the same output $\{x_n\}$ as does Option 1. Suppose:



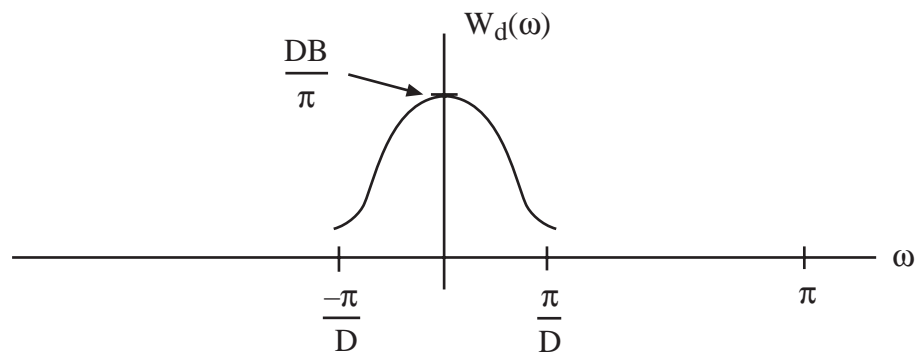
If $T = \frac{\pi}{D \cdot B}$ then



We have



So:



Now, what is the relationship between $X_d(\omega)$ and $W_d(\omega)$?

Digression

Note

$$\frac{1}{D} \sum_{k=0}^{D-1} e^{j\frac{2\pi}{D}kn} = \begin{cases} 1 & n = mD \\ \frac{1}{D} \frac{1 - e^{j\frac{2\pi}{D}nD}}{1 - e^{j\frac{2\pi}{D}n}} & n \neq mD \end{cases}$$

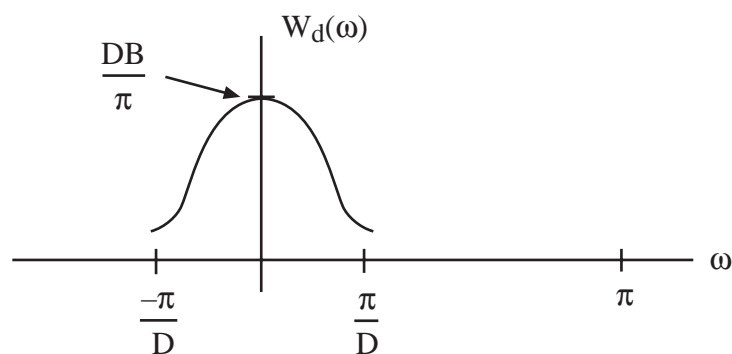
$$= \begin{cases} 1 & n = mD \\ 0 & n \neq mD \end{cases}$$

13.14

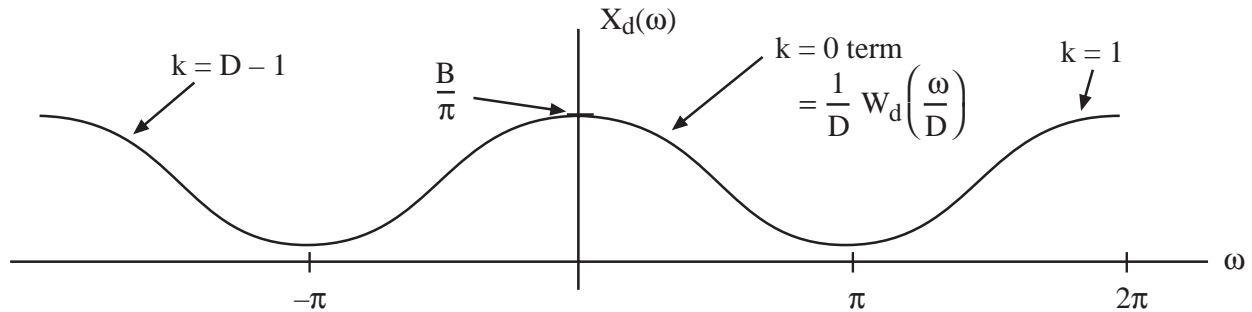
Now,

$$\begin{aligned}
 X_d(\omega) &= \sum_{n=-\infty}^{\infty} x_n e^{-j\omega n} \\
 &= \sum_{n=-\infty}^{\infty} w_{nD} e^{-j\omega n} = \sum_{\substack{n=mD \\ m=-\infty}}^{\infty} w_n e^{-j\omega \frac{n}{D}} \\
 &\stackrel{\substack{= \\ \uparrow \\ \text{trick from} \\ \text{digression}}}{=} \sum_{n=-\infty}^{\infty} w_n \underbrace{\frac{1}{D} \sum_{k=0}^{D-1} e^{j\frac{2\pi}{D} kn}}_{= 0 \text{ unless } n = mD} e^{-j\omega \frac{n}{D}} \\
 &= \frac{1}{D} \sum_{k=0}^{D-1} \sum_{n=-\infty}^{\infty} w_n e^{-jn(\frac{\omega - 2\pi k}{D})} \\
 \Rightarrow \quad &\boxed{X_d(\omega) = \frac{1}{D} \sum_{k=0}^{D-1} W_d\left(\frac{\omega - 2\pi k}{D}\right)} \quad (\Delta)
 \end{aligned}$$

Now, had



Using this $W_d(\omega)$ in (Δ) gives



Note: This X_d is just what we would have obtained if we had analog low-pass filtered $x_a(t)$ to B rad/sec and then sampled with period $T = \frac{\pi}{B}$!

Thus, 2) does an equivalent job to 1).

Note:

How can (Δ) produce a periodic $X_d(\omega)$? (Δ) has only a finite number of terms in its sum.

Answer: Each term is a periodic DTFT, not a FT as in Eq. (\diamond) .

$k=0$ term in (Δ) has pulses centered at $0, \pm 2\pi D, \pm 4\pi D$, etc.

$k=1$ term has pulses centered at $2\pi, 2\pi \pm 2\pi D, 2\pi \pm 4\pi D$, etc.

\vdots

$k = D - 1$ term has pulses centered at $(D-1)2\pi, (D-1)2\pi \pm 2\pi D, (D-1)2\pi \pm 4\pi D$, etc.

A Further Look at Down-Sampler

A decimator uses a down-sampler as one of its components:



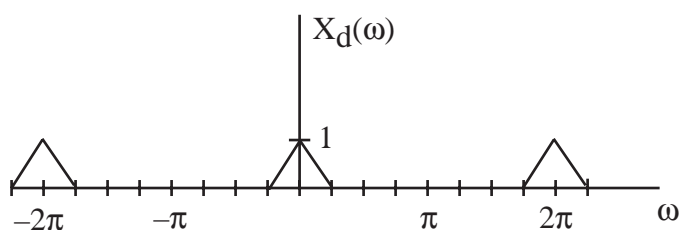
The down-sampler essentially stretches X_d . However, if $X_d(\omega)$ is not limited to $|\omega| < \frac{\pi}{D}$, then aliasing also occurs. Specifically,

$$Y_d(\omega) = \frac{1}{D} \sum_{k=0}^{D-1} X_d\left(\frac{\omega - 2\pi k}{D}\right). \quad (\Delta)$$

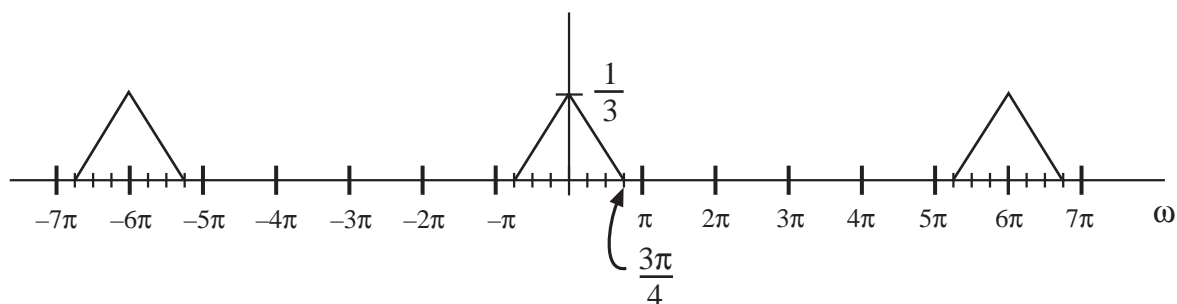
Notice the scaling in amplitude by $\frac{1}{D}$. This factor is not surprising, given that in the time domain, the down-sampler discards $D-1$ out of every D samples. By contrast, the up-sampler does not discard any samples, and inserts only zero-valued samples, so that there is no amplitude scaling in the Fourier domain for the up-sampler.

Example (Down-Sampler)

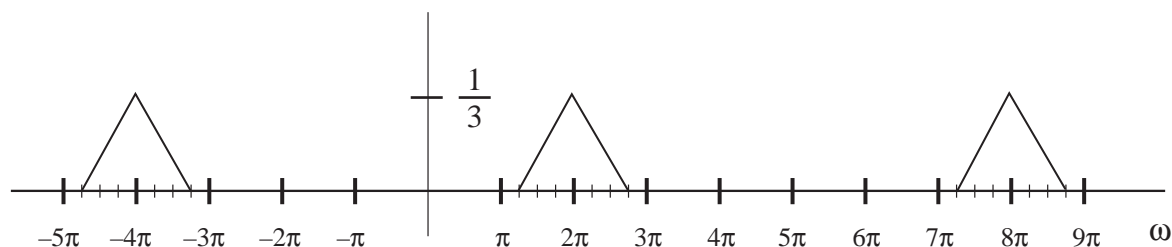
Suppose $D = 3$. Sketch $Y_d(\omega)$, assuming



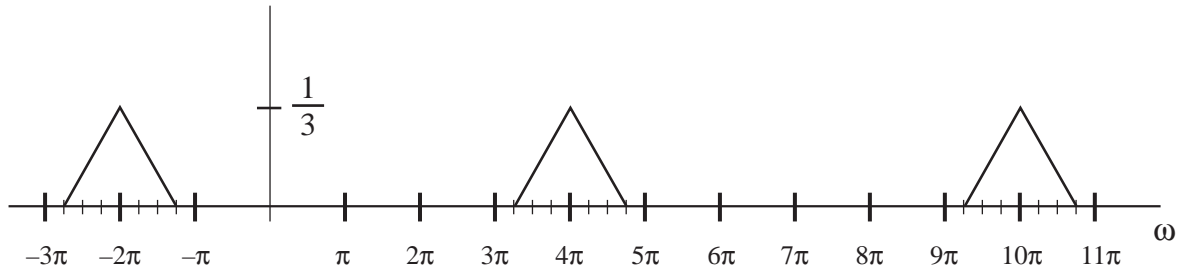
Then the $k = 0$ term in (Δ) is



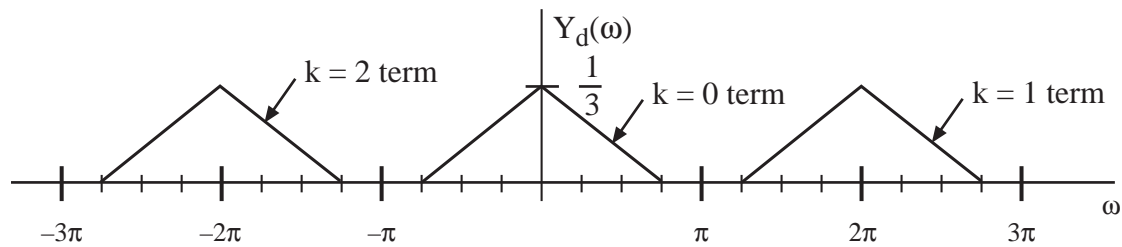
The $k = 1$ term in (Δ) is a 2π -shifted version of the above, namely



Likewise, the $D - 1 = 2$ term in (Δ) is a 4π -shifted version of the $k = 0$ term:



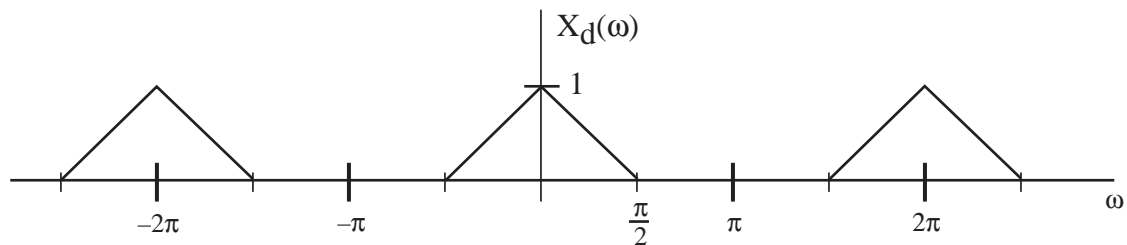
Adding the three previous plots together gives $Y_d(\omega)$:



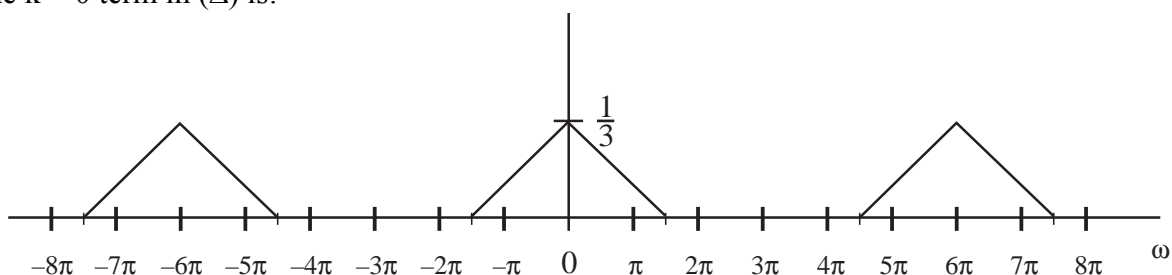
Note that the various terms in (Δ) interlace to produce a 2π -periodic $Y_d(\omega)$. In this example there was no need to plot the $k = 0, 1, 2$ terms, since the $k = 0$ term, alone, determines the shape of $Y_d(\omega)$ for $|\omega| < \pi$. In the next example, the downsampler causes aliasing, so that the terms in (Δ) overlap. This situation is more complicated than in the previous example.

Example (Down-Sampler)

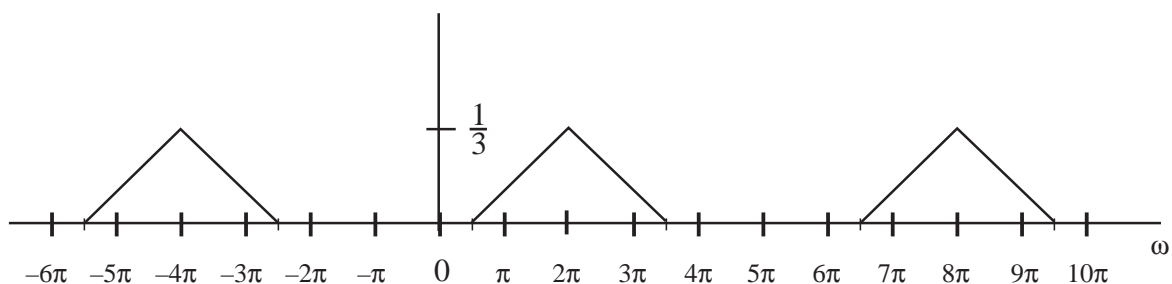
Suppose $D = 3$ as before, but now with



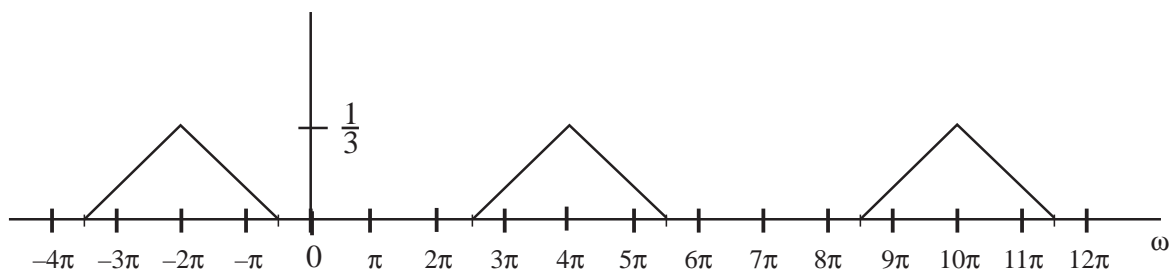
The $k = 0$ term in (Δ) is:



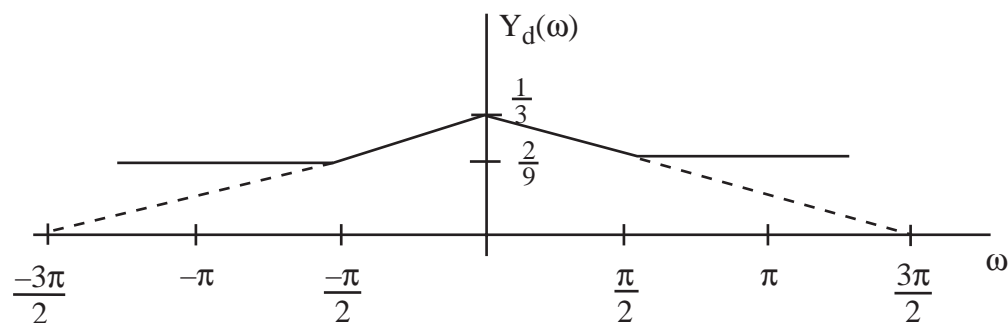
Notice that the center pulse extends beyond $\omega = \pm \pi$, which is an indication of aliasing. The $k = 1$ term in (Δ) is a 2π -shifted version of the above plot, namely:



The $k = 2$ term in (Δ) is a 4π -shifted version of the $k = 0$ term:



Adding the $k = 0, 1, 2$ terms gives $Y_d(\omega)$, which we plot only for $|\omega| \leq \pi$:



In this example, we have aliasing because $X_d(\omega)$ extends beyond $\omega = \pm \frac{\pi}{D} = \frac{\pi}{3}$. In a decimator, the job of the LPF that precedes the down-sampler is to cut off $X_d(\omega)$ at $\omega = \frac{\pi}{D}$ to prevent this aliasing.

Fast Fourier Transform (FFT)

FFTs comprise a class of algorithms for quickly computing the DFT.

DFT:

$$X_p = \sum_{n=0}^{N-1} x_n \bullet W_N^{np} \quad 0 \leq p \leq N-1$$

\uparrow
 $W_N \triangleq e^{-j\frac{2\pi}{N}}$

A straightforward computation requires:

$$N^2 \otimes, \quad N(N-1) \oplus$$

where these multiplications and additions are generally complex.

There are many different FFTs. We will consider only radix-2 decimation-in-time and decimation-in-frequency algorithms.

Radix-2 FFTs, where the sequence length N is restricted to be a power of two, require only $O(N \log_2 N)$ computations.

Decimation-in-Time Radix-2 FFT

Suppose $N = 2^M$

Idea: Divide input sequence into two groups, those elements of $\{x_n\}$ with n even and those with n odd. Then combine the size $N/2$ DFTs of these two subsequences to calculate the first half of $\{X_m\}_{m=0}^{N-1}$ and the second half of $\{X_m\}_{m=0}^{N-1}$.

$$\text{Let } \left. \begin{array}{l} y_n = x_{2n} \\ z_n = x_{2n+1} \end{array} \right\} \quad 0 \leq n \leq \frac{N}{2} - 1$$

Show $\{X_p\}_{p=0}^{N-1}$ can be obtained from the $\frac{N}{2}$ point DFTs $\{Y_p\}_{p=0}^{\frac{N}{2}-1}$ and $\{Z_p\}_{p=0}^{\frac{N}{2}-1}$.

Splitting a size N problem into two size $\frac{N}{2}$ problems will reduce computation because

$$\left(\frac{N}{2}\right)^2 + \left(\frac{N}{2}\right)^2 = \frac{N^2}{2} < N^2$$

Our strategy will then be to divide each size $\frac{N}{2}$ problem into two size $\frac{N}{4}$ problems, etc.

Derivation Relating X_p to Y_p and Z_p :

$$\begin{aligned}
 X_p &= \sum_{k=0}^{\frac{N}{2}-1} \left(x_{2k} W_N^{2kp} + x_{2k+1} W_N^{(2k+1)p} \right) \\
 &= \sum_{k=0}^{\frac{N}{2}-1} y_k W_{N/2}^{kp} + W_N^p \sum_{k=0}^{\frac{N}{2}-1} z_k W_{N/2}^{kp} \quad (1)
 \end{aligned}$$

since $W_N^{2kp} = e^{-j\frac{2\pi}{N}2kp} = e^{-j\frac{2\pi}{N/2}kp} = W_{N/2}^{kp}$

For $p = 0, 1, \dots, \frac{N}{2} - 1$, the first sum in (1) is Y_p , and the second sum is $W_N^p Z_p$.

$$\Rightarrow \left[X_p = Y_p + W_N^p Z_p \quad 0 \leq p \leq \frac{N}{2} - 1 \right] \quad (2)$$

What about X_p for $p > \frac{N}{2} - 1$? We can get these by using (1) to write:

$$X_{p+\frac{N}{2}} = \sum_{k=0}^{\frac{N}{2}-1} y_k W_{N/2}^{k(p+\frac{N}{2})} + W_N^{p+\frac{N}{2}} \sum_{k=0}^{\frac{N}{2}-1} z_k W_{N/2}^{k(p+\frac{N}{2})}$$

Note that:

$$W_{N/2}^{k(p+\frac{N}{2})} = W_{N/2}^{kp} W_{N/2}^{k\frac{N}{2}} = W_{N/2}^{kp} \bullet 1$$

and

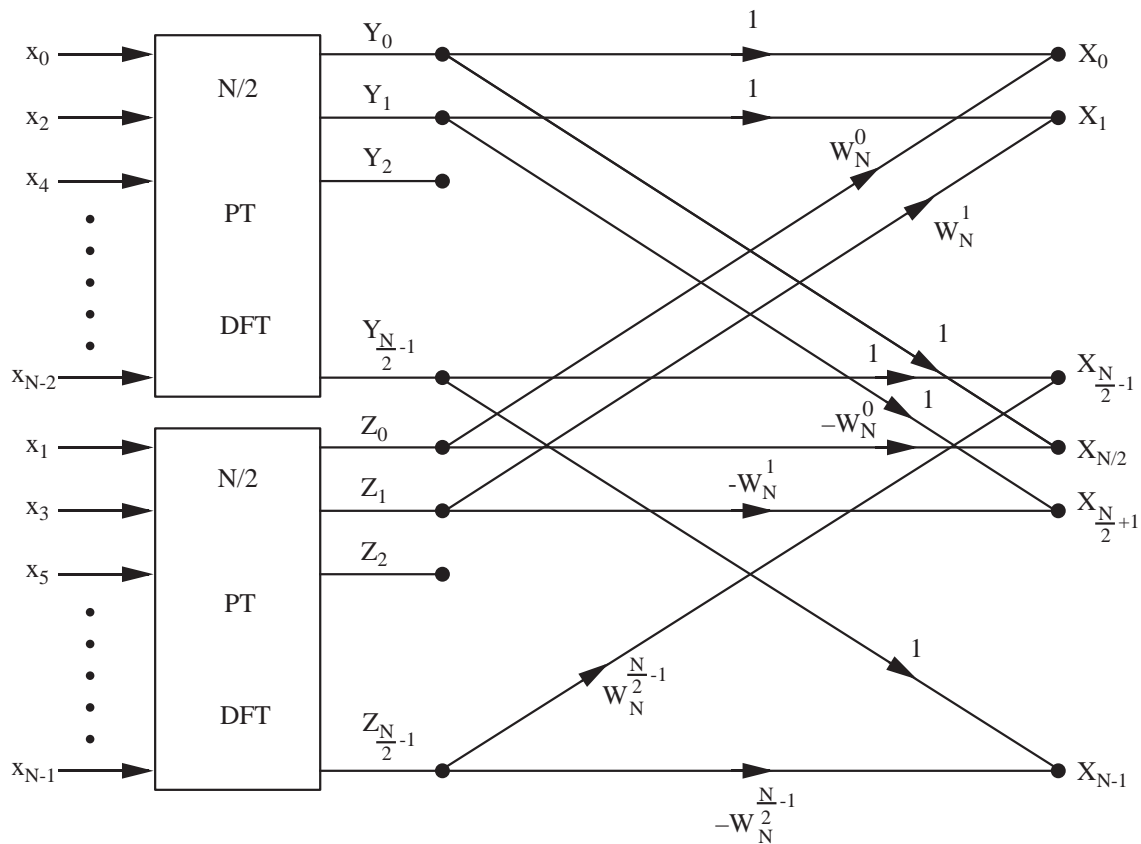
$$W_N^{p+\frac{N}{2}} = W_N^p e^{-j\frac{2\pi}{N}\frac{N}{2}} = -W_N^p$$

So:

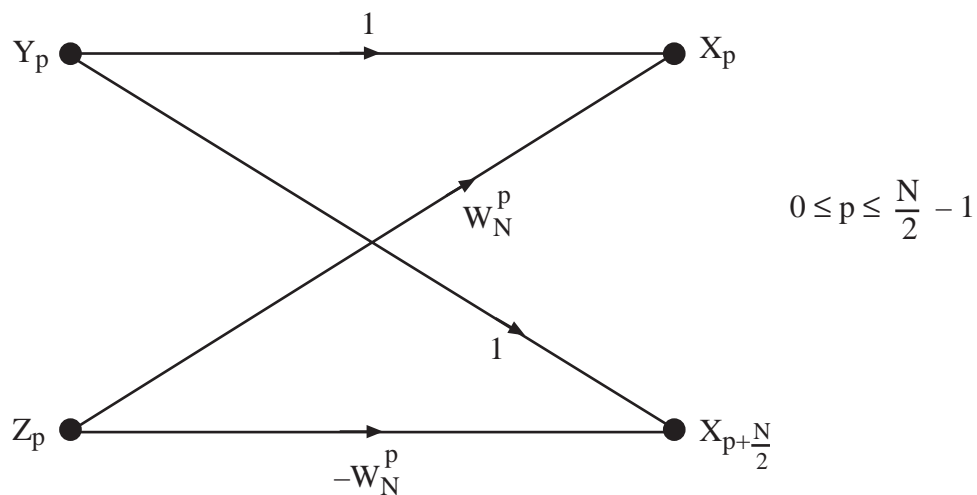
$$W_{p+\frac{N}{2}} = \sum_{k=0}^{\frac{N}{2}-1} y_k W_{N/2}^{kp} - W_N^p \sum_{k=0}^{\frac{N}{2}-1} z_k W_{N/2}^{kp}$$

$$\Rightarrow \left[X_{p+\frac{N}{2}} = Y_p - W_N^p Z_p \quad 0 \leq p \leq \frac{N}{2} - 1 \right] \quad (3)$$

(2) and (3) show how to compute an N point DFT using two $\frac{N}{2}$ point DFTs. These two equations are the essence of the FFT and describe the following flow graph:



The operation to combine the $\frac{N}{2}$ point DFT outputs Y_p and Z_p is called a butterfly:



This butterfly diagram summarizes (2) and (3).

Our overall strategy will be to:

Replace the N -point DFT by $\frac{N}{2}$ butterflies preceded by the $\frac{N}{2}$ -point DFTs.

Replace each $\frac{N}{2}$ -point DFT by $\frac{N}{4}$ butterflies preceded by two $\frac{N}{4}$ -point DFTs.

⋮

Replace each 4-point DFT by two butterflies preceded by two 2-point DFTs.

Replace each 2-point DFT by a single butterfly preceded by two one-point DFTs. But, a one-point DFT is the identity operation, so a two-point DFT is just a single butterfly.

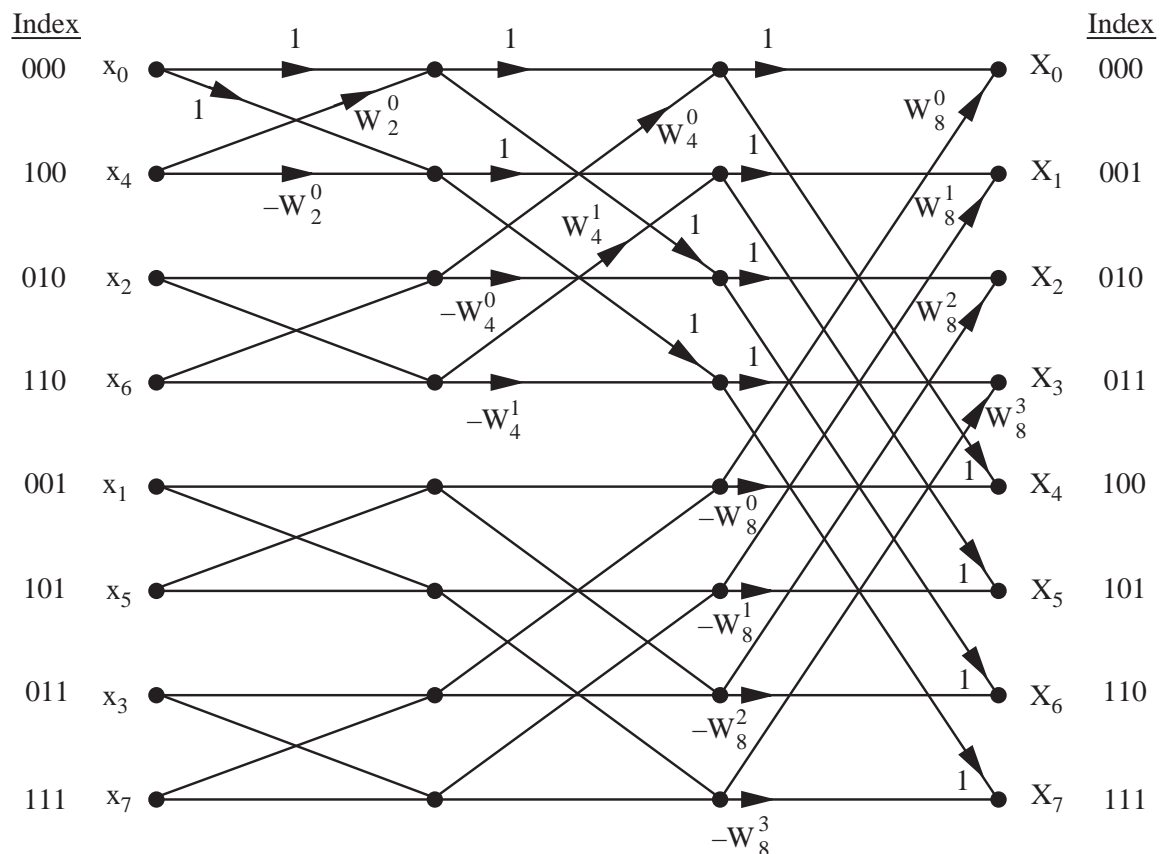
Since $N = 2^M$, this recursion leads to $M = \log_2 N$ stages of $\frac{N}{2}$ butterflies each.

Thus, for a DSP chip that can perform one multiplication and one addition (one multiply-accumulate) in each clock cycle, a radix-2 DIT FFT requires

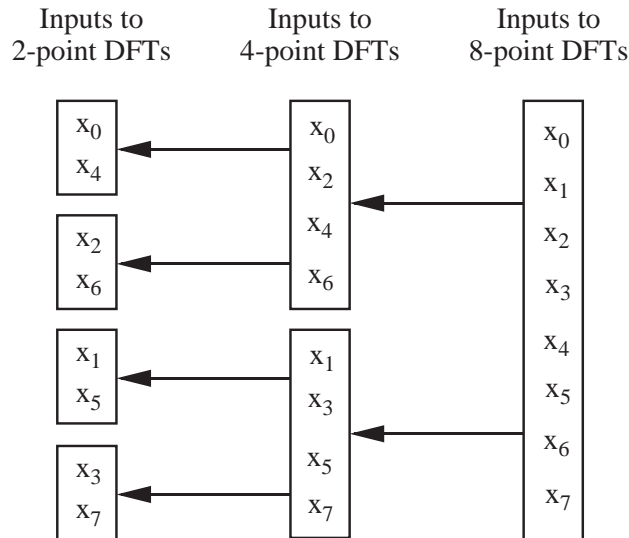
$$N \log_2 N \text{ multiply-accumulates}$$

which can be far less than the N^2 multiply-accumulates required by a straightforward DFT.

Example ($N = 8$, DIT FFT)



The input x_n is required in “bit-reversed” order. Why? This follows since to compute an N -point DFT using two $N/2$ point DFTs, we break up the input into even and odd points. We do this successively as we work backward in the flow diagram:



Note: FFT computation can be performed “in place.” We need only one length- N array in memory since the output of a butterfly can be written back into the input locations.

Example ~ computational comparison

Suppose $N = 2^{14} = 16,384$.

Compare the number of multiply-accumulates in straightforward and DIT FFT implementations of the DFT.

Straightforward: $N^2 = 268,435,456$ multiply-accumulates

FFT: $N \log_2 N = 2^{14} (14) = 229,376$ multiply-accumulates

$$\text{Savings factor} = \frac{268,435,456}{229,376} = 1170!$$

Suppose that in 1964 a state-of-the-art computer required 10 hours to compute a straightforward length 2^{14} DFT. Then, in 1965, after publication of the FFT, this same computation could be performed in about 30 seconds!

Decimation in Frequency Radix – 2 FFT

Idea: Essentially is backwards from DIT. Separate $\{x_n\}_{n=0}^{N-1}$ into first half and second half and then compute even and odd points in $\{X_p\}_{p=0}^{N-1}$ separately, using two $\frac{N}{2}$ -point DFTs.

Derivation of algorithm:

$$\begin{aligned}
 X_p &= \sum_{n=0}^{N-1} x_n W_N^{np} \\
 &= \sum_{m=0}^{\frac{N}{2}-1} x_m W_N^{mp} + \sum_{m=0}^{\frac{N}{2}-1} x_{m+N/2} W_N^{(m+N/2)p} \\
 &= \sum_{m=0}^{\frac{N}{2}-1} (x_m + x_{m+N/2} W_N^{(N/2)p}) W_N^{mp} \quad (10)
 \end{aligned}$$

Look at even and odd points in X_p separately.

Evens:

(10) \Rightarrow

$$\begin{aligned}
 X_{2q} &= \sum_{m=0}^{\frac{N}{2}-1} (x_m + x_{m+N/2} \bullet 1) W_{N/2}^{mq} \\
 &\Rightarrow \left[\begin{array}{c} \{X_{2q}\}_{q=0}^{N/2-1} \\ \uparrow \\ \text{even points in desired} \\ \text{length-N DFT} \end{array} \right] = \begin{array}{c} \text{DFT} \\ \uparrow \\ \text{N/2 point DFT} \end{array} \left[\{x_m + x_{m+N/2}\}_{m=0}^{N/2-1} \right] \quad (11)
 \end{aligned}$$

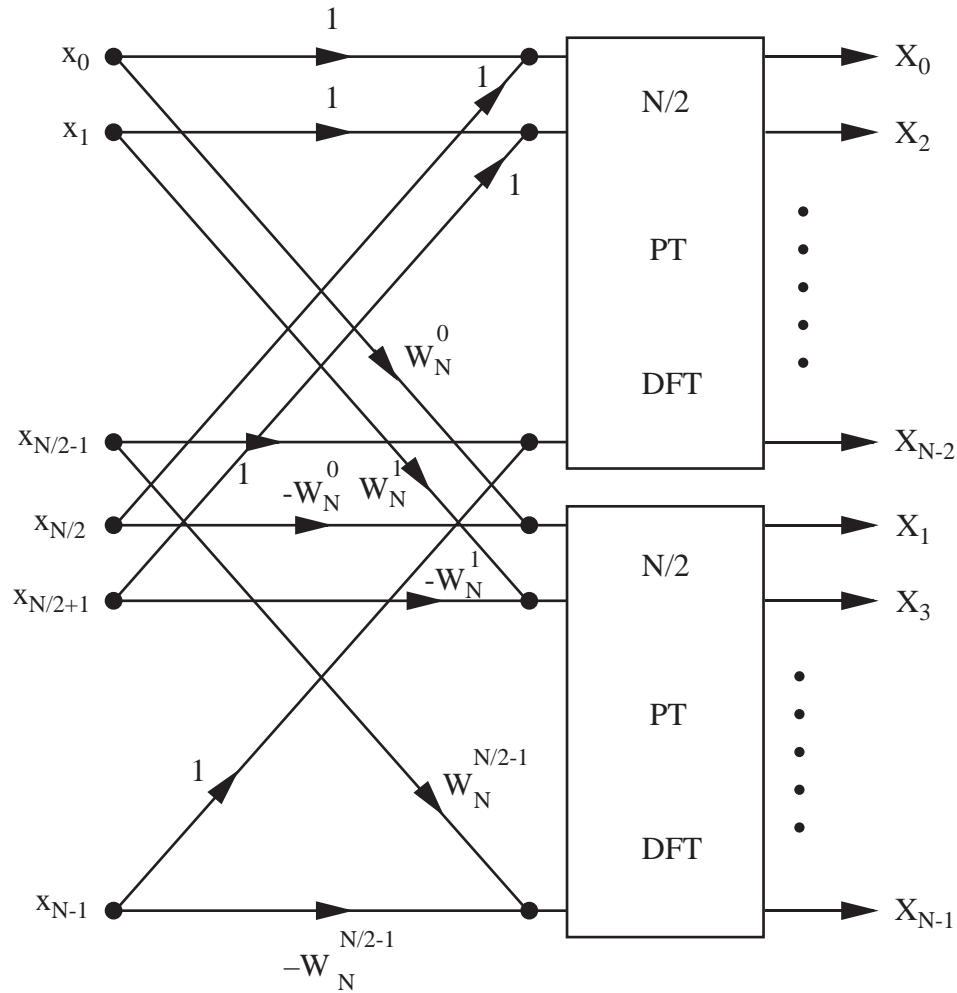
Odds:

(10) \Rightarrow

$$\begin{aligned}
 X_{2q+1} &= \sum_{m=0}^{\frac{N}{2}-1} (x_m + x_{m+N/2} W_N^{(N/2)(2q+1)}) W_{N/2}^{mq} W_N^m \\
 &= \sum_{m=0}^{\frac{N}{2}-1} [(x_m - x_{m+N/2}) W_N^m] W_{N/2}^{mq}
 \end{aligned}$$

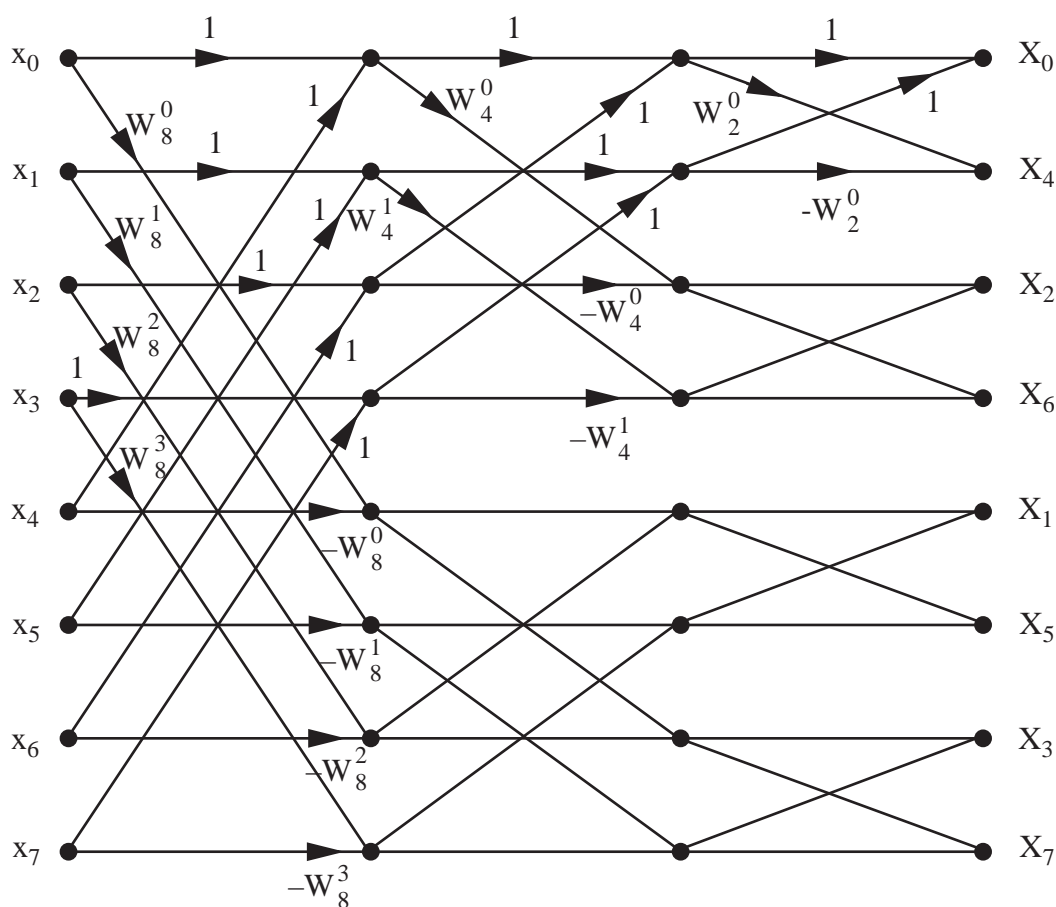
$$\Rightarrow \left[\begin{array}{c} \{X_{2q+1}\}_{q=0}^{N/2-1} \\ \uparrow \\ \text{odd points in desired} \\ \text{length-N DFT} \end{array} \right] = \text{DFT} \left[\{(x_m - x_{m+N/2})W_N^m\}_{m=0}^{N/2-1} \right] \quad (12)$$

(11) and (12) give:



The complete DIF algorithm computes each $\frac{N}{2}$ -point DFT using two $\frac{N}{4}$ -point DFTs, etc. As in the DIT algorithm, we get $\log_2 N$ stages of $\frac{N}{2}$ butterflies each, but now the output appears in bit-reversed order.

Example ($N = 8$, DIF FFT)



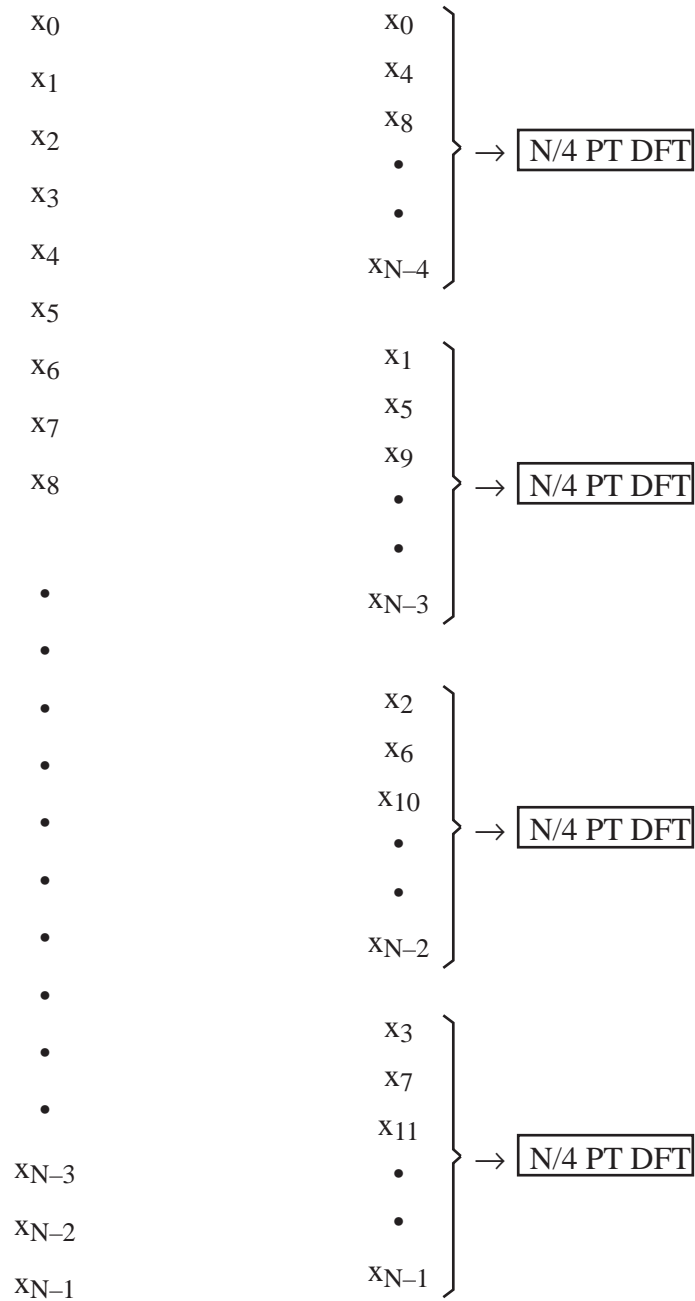
The branch weights are found by using (11) and (12).

Note: As mentioned above, the output appears in bit-reversed order.

Comment: The DIF flow diagram is simply the transpose of the DIT diagram (switch input and output, and reverse all flows).

Other Comments:

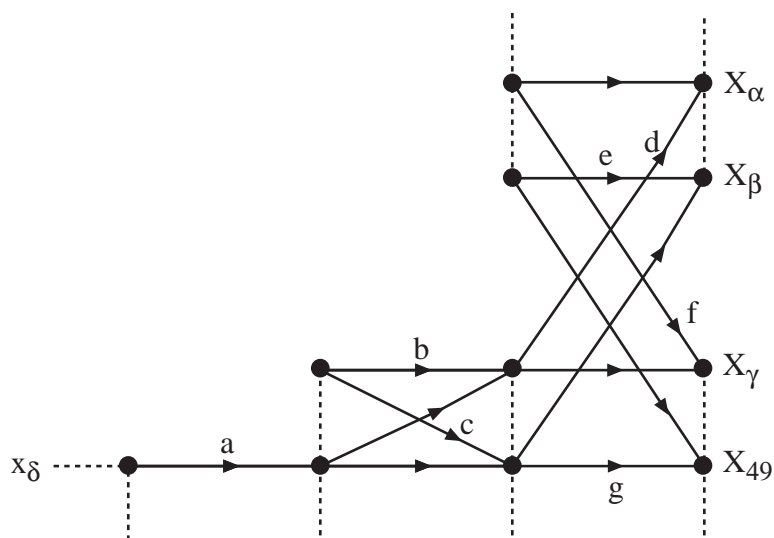
- 1) FFT computer algorithms incorporate the reordering (“bit reversal”) of input or output. You don’t have to do this yourself.
- 2) Can generalize Radix-2 approach to Radix-3, Radix-4, etc. with $N = 3^M$, $N = 4^M$, etc. For a Radix-4 DIT algorithm, break input up into four groups.



The outputs of the $N/4$ -point DFTs can then be combined, using modified butterflies with 4 inputs and 4 outputs each, to calculate $\{X_m\}_{m=0}^{N-1}$.

Example

Shown below is part of a radix-2, 64-point DIT FFT. Determine the indices α – δ and the coefficients a–g.



Solution: Use Eqs. (2) and (3) from p. 47.2 in course notes:

$$X_p = Y_p + W_N^p Z_p \quad 0 \leq p \leq \frac{N}{2} - 1$$

$$X_{p+\frac{N}{2}} = Y_p - W_N^p Z_p \quad 0 \leq p \leq \frac{N}{2} - 1$$

$$N = 64, \beta + \frac{N}{2} = 49 \Rightarrow \beta = \underline{17}$$

$$\gamma = 49 - \frac{N}{4} = \underline{33}$$

$$\alpha = 33 - \frac{N}{2} = \underline{1}$$

$$\delta \text{ is bit reversal of } 49 = (110001)_2 \Rightarrow \delta = (100011)_2 = \underline{35}$$

$$d = W_{64}^1 = e^{-j\frac{2\pi}{64}} \quad g = -W_{64}^{17} = -e^{-j\frac{34\pi}{64}}$$

$$e = 1 \quad b = 1$$

$$f = 1 \quad c = 1 \quad a = 1$$

← since this is a top
branch in butterfly
of 16 pt DFT

Fast Linear Convolution

Recall the cyclic convolution property of the DFT:

$$y_n = \sum_{m=0}^{N-1} h_m x_{\langle n-m \rangle_N} \quad \text{iff} \quad Y_m = H_m X_m \quad 0 \leq m \leq N-1$$

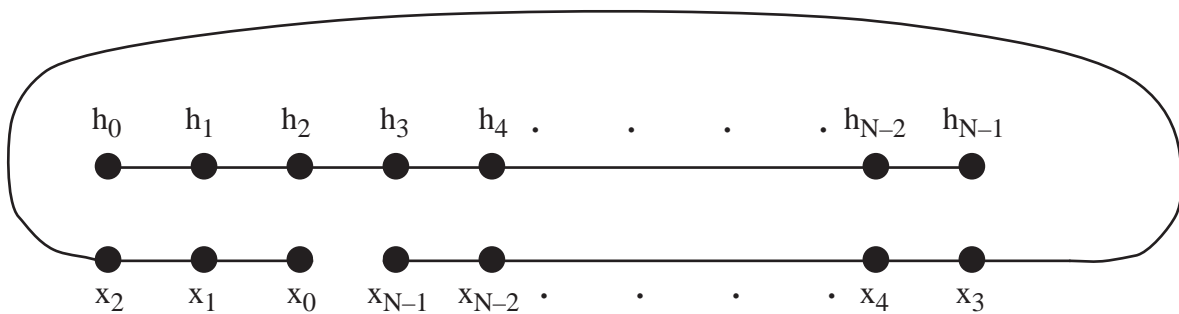
So, we can implement cyclic convolution via

$$\{y_n\} = \text{DFT}^{-1} \left[\text{DFT} [\{h_n\}] \bullet \text{DFT} [\{x_n\}] \right] \quad (\Delta\Delta)$$

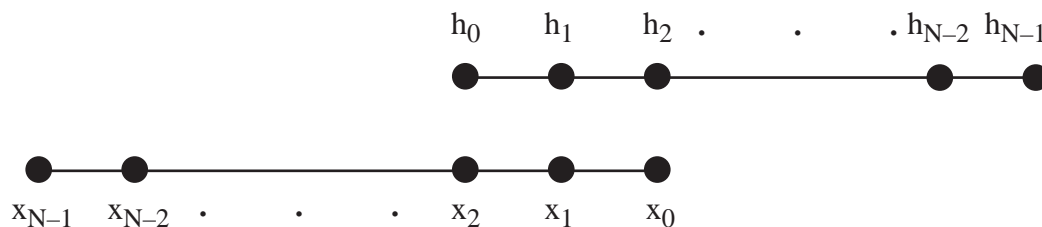
This can be done quickly for long sequence lengths using the FFT.

But, what is cyclic convolution?

To compute y_2 :



We would rather implement a linear (regular) convolution:



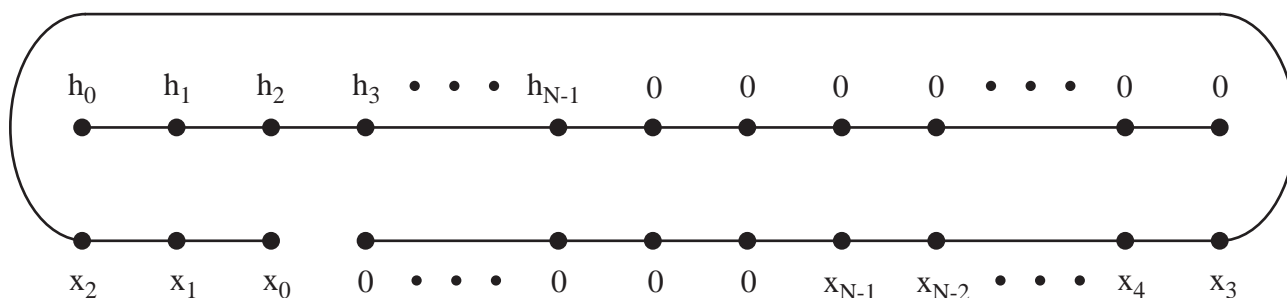
To compute a linear convolution via a cyclic convolution, we must eliminate the wrap-around of nonzero terms in the cyclic convolution. Use zero-padding with $N-1$ zeros, i.e., let:

$$\hat{h}_n = \begin{cases} h_n & 0 \leq n \leq N-1 \\ 0 & N \leq n \leq 2N-2 \end{cases}$$

$$\hat{x}_n = \begin{cases} x_n & 0 \leq n \leq N-1 \\ 0 & N \leq n \leq 2N-2 \end{cases}$$

Now, cyclically convolve the zero-padded sequences.

The result is that $\{\hat{y}_n\}_{n=0}^{2N-2}$ will be a linear convolution of $\{h_n\}_{n=0}^{N-1}$ with $\{x_n\}_{n=0}^{N-1}$. For example, in computing \hat{y}_2 , we will have:



Obviously, the zero-padding eliminates the wrap-around problem. Using an FFT with $(\Delta\Delta)$, and zero-padded sequences, provides a fast means of performing linear convolution.

What if $\{h_n\}$ and $\{x_n\}$ are not of the same length?

If $\{h_n\}$ is of length M and $\{x_n\}$ is of length N , then pad each sequence to length $N + M - 1$ (or nearest larger power of 2 if you are using a radix-2 FFT).

Let's check and see that $(\Delta\Delta)$, with zero padding, works for a specific example.

Example

$$h_n = \{1, 1, 1\}, x_n = \{1, -1, 1\}$$

$\uparrow \qquad \qquad \uparrow$

To produce a linear convolution via $(\Delta\Delta)$, first pad each sequence with $N - 1 = 2$ zeros:

$$\hat{h}_n = \{1, 1, 1, 0, 0\}$$

$$\hat{x}_n = \{1, -1, 1, 0, 0\}$$

Now,

$$\begin{aligned} \hat{H}_m &= \sum_{n=0}^4 \hat{h}_n e^{-j\frac{2\pi}{5}nm} \\ &= 1 + e^{-j\frac{2\pi}{5}m} + e^{-j\frac{4\pi}{5}m} \end{aligned}$$

Likewise,

$$\hat{X}_m = 1 - e^{-j\frac{2\pi}{5}m} + e^{-j\frac{4\pi}{5}m}$$

So,

$$\begin{aligned}\hat{Y}_m &= \hat{H}_m \hat{X}_m = 1 + \cancel{e^{-j\frac{2\pi}{5}m}} + \cancel{e^{-j\frac{4\pi}{5}m}} \\ &\quad - \cancel{e^{-j\frac{2\pi}{5}m}} - \cancel{e^{-j\frac{4\pi}{5}m}} - \cancel{e^{-j\frac{6\pi}{5}m}} \\ &\quad + e^{-j\frac{4\pi}{5}m} + \cancel{e^{-j\frac{6\pi}{5}m}} + e^{-j\frac{8\pi}{5}m} \\ &= 1 + e^{-j\frac{4\pi}{5}m} + e^{-j\frac{8\pi}{5}m} \\ &= 1 + e^{-j\frac{2\pi}{5}2m} + e^{-j\frac{2\pi}{5}4m}\end{aligned}$$

Since

$$\hat{Y}_m = \sum_{n=0}^4 \hat{y}_n e^{-j\frac{2\pi}{5}m}$$

we see that

$$\hat{y}_n = \{1, 0, 1, 0, 1\}$$

It is easy to see that this is the correct linear convolution:

$$\begin{array}{r} 1 \quad 1 \quad 1 \\ 1 \quad -1 \quad 1 \end{array}$$

Performing the usual shift and add operations gives the sequence $\{1, 0, 1, 0, 1\}$. ✓

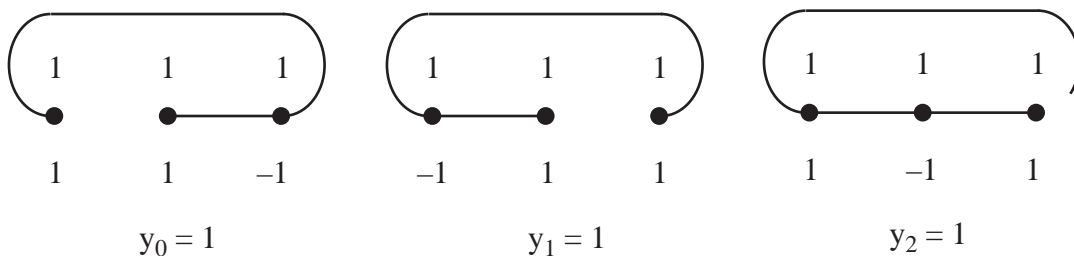
Now, what if we had not zero padded?

Then $(\Delta\Delta)$ would have produced a cyclic convolution.

The cyclic convolution formula is

$$y_n = \sum_{m=0}^2 h_m x_{\langle n-m \rangle_3}$$

which is computed pictorially as



Let's check that $(\Delta\Delta)$ without zero-padding gives this same result.

$$\begin{aligned}
 H_m &= \sum_{n=0}^2 h_n e^{-j\frac{2\pi}{3}nm} \\
 &= 1 + e^{-j\frac{2\pi}{3}m} + e^{-j\frac{4\pi}{3}m} \\
 X_m &= 1 - e^{-j\frac{2\pi}{3}m} + e^{-j\frac{4\pi}{3}m} \\
 Y_m &= H_m X_m \\
 &= 1 + \cancel{e^{-j\frac{2\pi}{3}m}} + \cancel{e^{-j\frac{4\pi}{3}m}} \\
 &\quad - \cancel{e^{-j\frac{2\pi}{3}m}} - \cancel{e^{-j\frac{4\pi}{3}m}} - \cancel{e^{-j\frac{6\pi}{3}m}} \\
 &\quad + e^{-j\frac{4\pi}{3}m} + \cancel{e^{-j\frac{6\pi}{3}m}} + e^{-j\frac{8\pi}{3}m}
 \end{aligned}$$

Interchanging the latter two terms and using 2π periodicity of the complex exponential gives

$$Y_m = 1 + e^{-j\frac{2\pi}{3}m} + e^{-j\frac{2\pi}{3}2m}$$

Matching up terms with

$$Y_m = \sum_{n=0}^2 y_n e^{-j\frac{2\pi}{3}nm} = y_0 + y_1 e^{-j\frac{2\pi}{3}m} + y_2 e^{-j\frac{2\pi}{3}2m}$$

gives

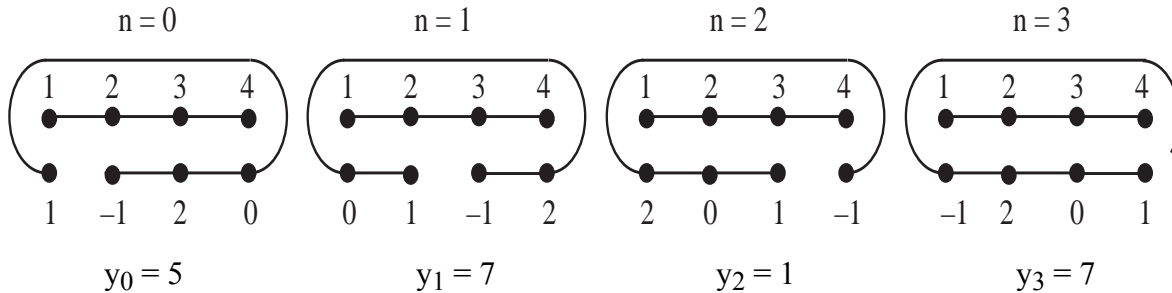
$$\begin{array}{ccc}
 \{y_n\} = \{1, 1, 1\} & \checkmark \\
 \uparrow &
 \end{array}$$

Note: We worked through this example to show that $(\Delta\Delta)$ can give a linear convolution or a cyclic convolution, depending on whether we first zero pad. In practice, if N is large the DFTs and inverse DFT would be computed using FFTs. If N is small, then it is faster to perform the convolution in the sequence domain.

For practice at computing cyclic convolution in the sequence domain, consider the following example.

Example

Find $y_n = h_n \circledast x_n$ where $\{h_n\}_{n=0}^3 = \{1, 2, 3, 4\}$ and $\{x_n\}_{n=0}^3 = \{1, 0, 2, -1\}$.



Example (Convolution via FFT)

Suppose that a sequence $\{x_n\}_{n=0}^{7000}$ is to be filtered with an FIR filter having coefficients $\{h_n\}_{n=0}^{1100}$.

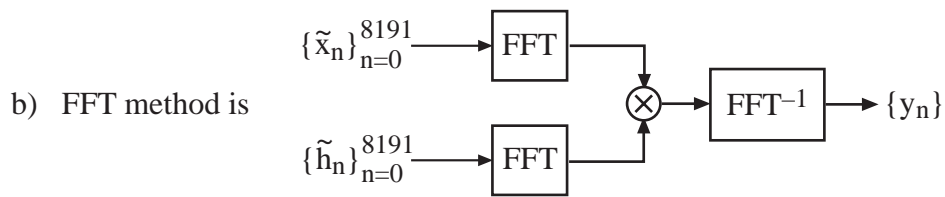
- Ignoring possible savings from coefficient symmetry, what is the total number of multiplications required to compute the output $\{y_n\}_{n=0}^{8100}$ by implementing the usual convolution formula with a direct-form filter structure?
- Using the FFT method (with a radix-2 FFT and zero-padding to length 8192), how many complex multiply-accumulates (MAs) are required to compute $\{y_n\}_{n=0}^{8100}$? How many real MAs are required? (For simplicity, count all “multiplications” in an FFT, even those by ± 1 , $\pm j$, as complex multiplications.)

Solution

- Output of regular convolution is composed of 3 parts:

	$\begin{aligned} \# \text{ of MAs is } & 1 + 2 + 3 + \dots + 1100 \\ & = \frac{(1100)(1101)}{2} \end{aligned}$
	$\# \text{ of MAs is } 1101 \text{ (} 7001 - 1100 \text{)}$
	$\begin{aligned} \# \text{ of MAs is } & 1100 + 1099 + \dots + 1 \\ & = \frac{(1100)(1101)}{2} \end{aligned}$

$$\text{Total \# MAs} = 1100(1101) + 1101(5901) = \boxed{7,708,101}$$



where $\{\tilde{x}_n\}$ and $\{\tilde{h}_n\}$ are zero-padded versions of $\{x_n\}$ and $\{h_n\}$.

$$\# \text{ complex MAs} = 3 (N \log_2 N) + N = 3 (8192 \bullet 13) + 8192 = \boxed{327,680}$$

The number of real MAs required to implement a complex MA is generally 4. To see this, write out the detailed calculation (a) (b) + c where a, b, and c are all complex. Assuming this factor of 4 overhead, we have

$$\# \text{ real MAs} = 4 (327,680) = \boxed{1,310,720}$$

Thus, in this example the FFT approach requires fewer than 20% of the MAs required by a straightforward convolution.

Block Convolution

Given $\{x_n\}_{n=0}^{N-1}$ and $\{h_n\}_{n=0}^{M-1}$, we have developed an approach for efficiently computing $y_n = h_n * x_n$ using zero-padding and FFTs. But, what if $N \gg M$? If N , the length of the input, is really large, we are faced with two problems:

- 1) Very long FFTs will be required, which will lead to computational inefficiency.
- 2) There will be a very long delay in computing $\{y_n\}$ since our scheme requires that all of $\{x_n\}$ be acquired before any element in the output sequence can be computed.

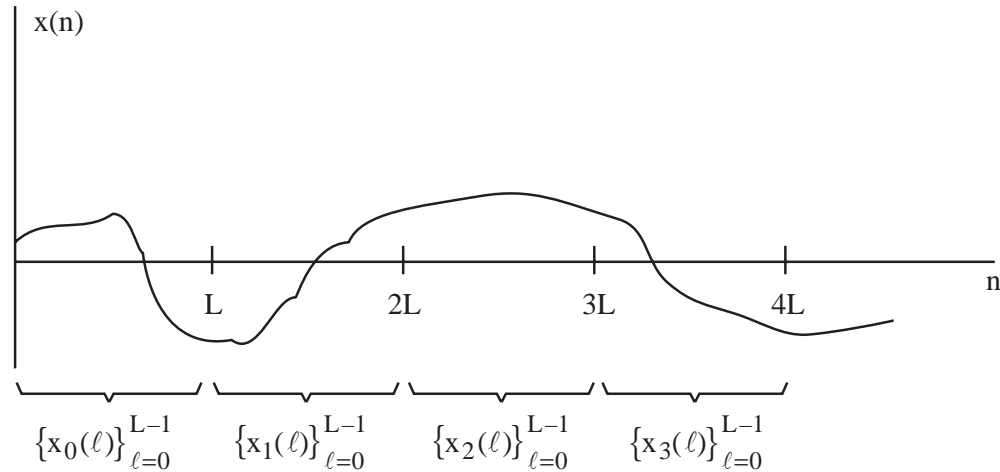
What to do? Answer: Segment the long input $\{x_n\}_{n=0}^{N-1}$ into shorter pieces, convolve the individual pieces with $\{h_n\}_{n=0}^{M-1}$ and then stitch together the results of the shorter convolutions to form $\{y_n\}$. There are two popular ways of doing this.

Method 1: Overlap and Add

Here, we divide up the input into nonoverlapping sections of length L . Let

$$x_k(\ell) = x(kL + \ell) \quad 0 \leq \ell \leq L - 1, \quad k = 0, 1, 2, \dots$$

Picture:



We have

$$x(n) = \sum_k x_k(n - kL) \quad 0 \leq n \leq N - 1.$$

Now, convolution is a linear operation, so

$$y(n) = h(n) * x(n) = h(n) * \left[\sum_k x_k(n - kL) \right] = \sum_k h(n) * x_k(n - kL)$$

Let $y_k(n) = h(n) * x_k(n)$. Then by shift-invariance,

$$y(n) = \sum_k y_k(n - kL) . \quad (1)$$

We compute each $\{y_k(n)\}$ via the FFT as in the previous lecture. For simplicity, assume $M + L - 1$ is a sequence length for which we have an FFT algorithm. Then

1) Pad $\{x_k(n)\}_{n=0}^{L-1}$ with $M-1$ zeros to give $\{\tilde{x}_k(n)\}_{n=0}^{L+M-2}$.

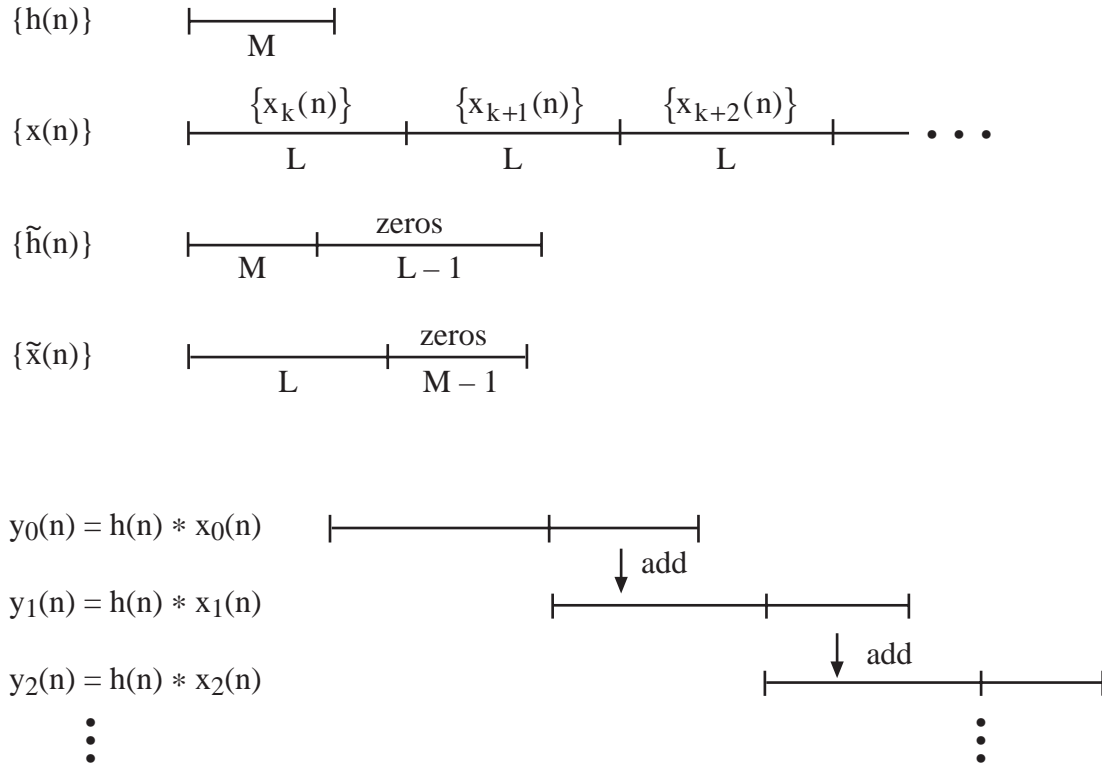
Pad $\{h(n)\}_{n=0}^{M-1}$ with $L-1$ zeros to give $\{\tilde{h}(n)\}_{n=0}^{L+M-2}$.

2) Calculate the FFTs of $\{\tilde{x}_k(n)\}_{n=0}^{L+M-2}$ and $\{\tilde{h}(n)\}_{n=0}^{L+M-2}$.

3) Multiply FFTs together and take FFT⁻¹ to give $\{y_k(n)\}_{n=0}^{L+M-2}$.

Finally, calculate $\{y(n)\}$ via (1) by adding together the appropriately shifted $\{y_k(n)\}$.

Pictorially:



Sum of the shifted (by kL) $y_k(n)$ gives $\{y(n)\}$.

Example

Given $\{h(n)\}_{n=0}^{249}$ and $\{x(n)\}_{n=0}^{\infty}$ we wish to compute $\{y(n)\} = \{h(n)\} * \{x(n)\}$ using the FFT method. What is the best block length L , using the Overlap and Save method with radix-2 FFTs?

We have $M = 250$. Let $K = \text{FFT length}$. Then since $K = L + M - 1$, the block length will be $L = K - 249$. Each length- K FFT and inverse FFT requires $K \log_2 K$ MAs. Multiplication of FFTs requires K MAs. We shall assume that the FFT of $\{\tilde{h}(n)\}$ is precomputed once and stored. Thus, the amount of computation for each input block will be

$$2 K \log_2 K + K = K (2 \log_2 (K) + 1) \quad \text{MAs.}$$

This amount of computation is needed to compute each $\{y_k(n)\}$ $k = 0, 1, 2, \dots$ from each input block $\{x_k(n)\}$ of length $L = K - 249$. Thus, the computation per input sample (or per output sample), ignoring the few additions needed to sum the overlapping $\{y_k(n)\}$ blocks, is

$$\frac{K \lceil 2 \log_2 K + 1 \rceil}{K - 249} \quad (2)$$

Trying some different values for the FFT length K , we find:

K	L	Complex MAs Per output	
256	7	621.7	$K = \text{FFT length}$
512	263	37.0	$L = \text{input block length}$
1024	775	27.7	# MAs given by (2)
2048	1799	26.2	
4096	3847	26.6	

For larger K , (2) approaches $(2 \log_2 K) + 1$, which grows with K .

Even allowing for the required complex arithmetic (4 real MAs per complex MA), the FFT approach offers considerable savings over a direct filter implementation, which would require 250 MAs per output.

Notes:

1)Based on the above table, and if we are at all concerned about delay, we would select an FFT block length of either 512 or 1024.

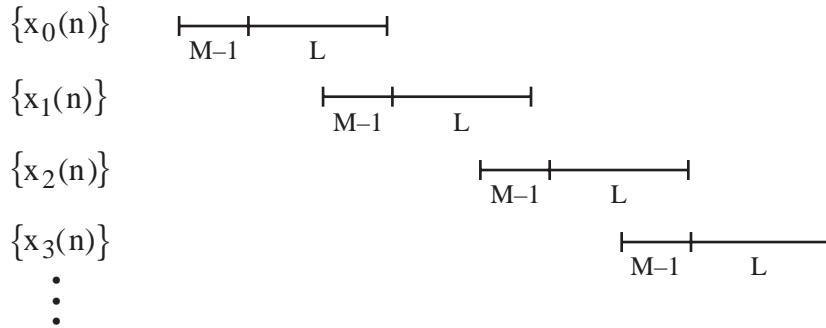
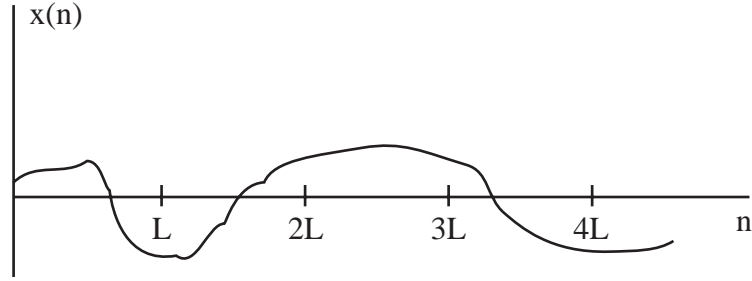
2)If $\{x_n\}$ and $\{h_n\}$ were complex-valued, then the direct filter implementation would require roughly 1000 MAs per filter output.

3)If a sequence is real, there are tricks that can be used to speed up computation (by a factor of approximately two) of its DFT. If both $\{x(n)\}$ and $\{h(n)\}$ are real, in which case $\{y(n)\}$ is real, these tricks can be used to reduce the number of MAs in the FFT approach by nearly a factor of two over the entries shown in the above table.

Method 2: Overlap and Save

Could just as easily be called Overlap and Discard.

Here, we define the $\{x_k(n)\}$ to be overlapping as shown below.



The first $M-1$ entries of $\{x_0(n)\}$ are filled with zeros. All other entries of $\{x_0(n)\}$ and all entries of all other subsequences $\{x_k(n)\}$ are filled with the values of $\{x(n)\}$ directly above. In general, each subsequence overlaps with its two neighboring subsequences. The algorithm to calculate $\{y(n)\}$ is then:

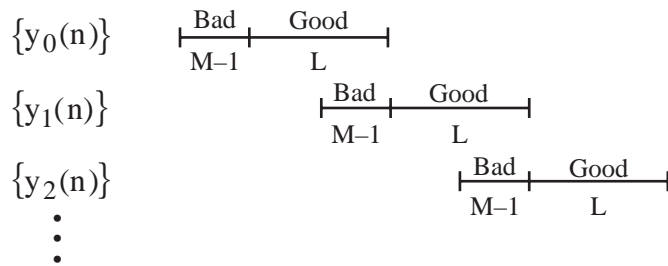
1) Zero-pad $\{h(n)\}_{n=0}^{M-1}$ with $L-1$ zeros to produce $\{\tilde{h}(n)\}_{n=0}^{M+L-2}$.

2) Cyclically convolve (via FFT) $\{\tilde{h}(n)\}_{n=0}^{M+L-2}$ with each $\{x_k(n)\}_{n=0}^{M+L-2}$ to give

$$y_k(n) = \tilde{h}(n) \circledast x_k(n), \quad 0 \leq n \leq M + L - 2$$

The result is that the first $M-1$ samples of each $\{y_k(n)\}$ will be useless, but the last L samples will be samples of $\{y(n)\}$.

3) Assemble $\{y(n)\}$ as shown:

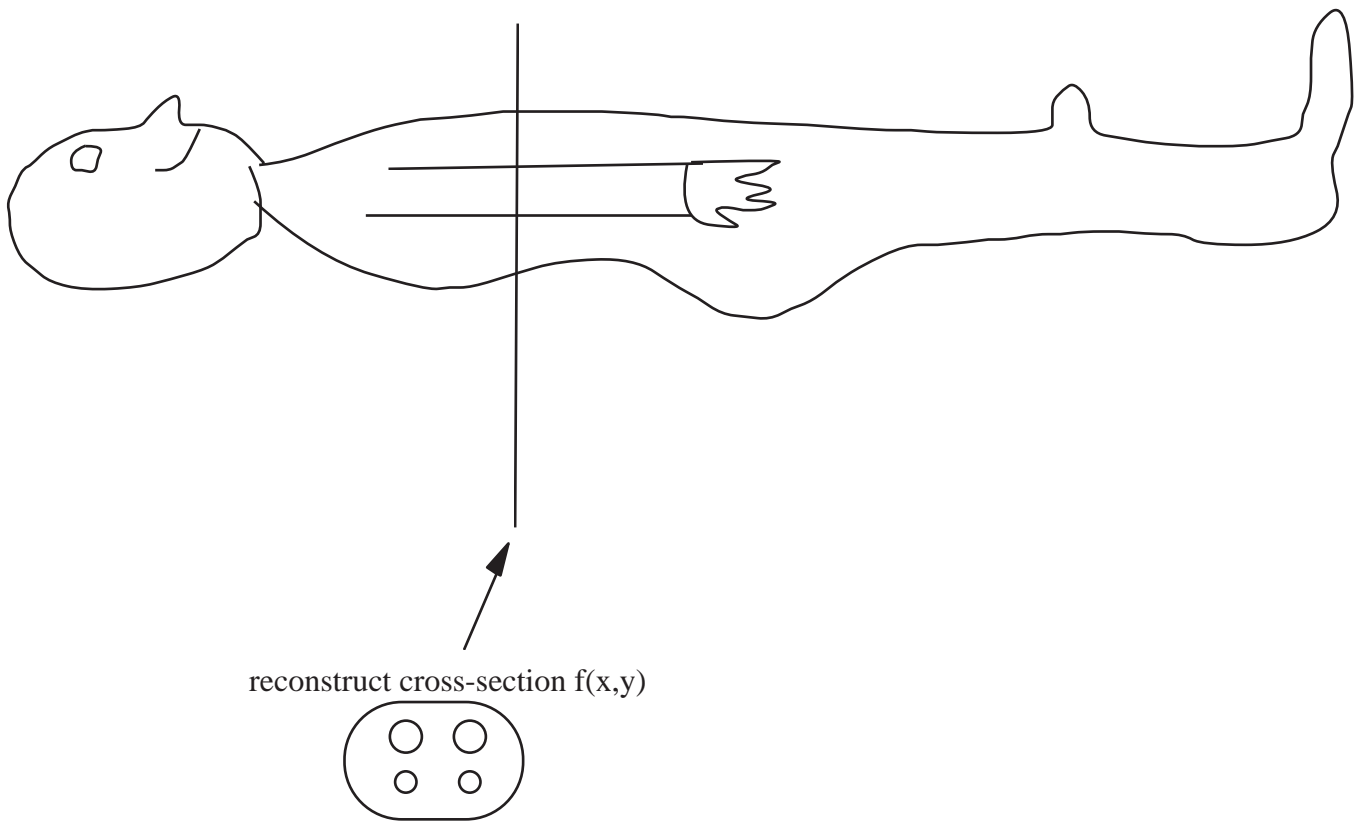


The “bad” samples are discarded and the “good” samples are concatenated to form $\{y(n)\}$.

Application 1: Computer Tomography (CT)

Used extensively for medical imaging, nondestructive testing.

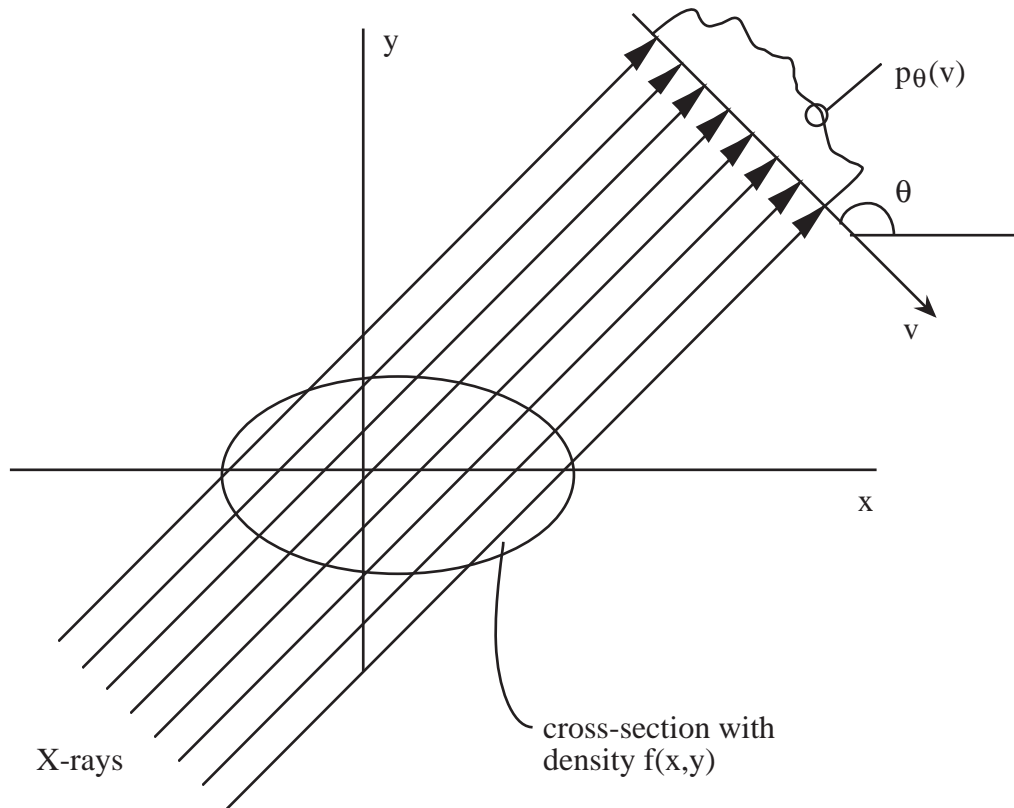
Objective is to reconstruct a cross-sectional view of a 3-D object:



Accomplish this by shining x-rays sideways through the object and collecting “projections” at various angles. The projection data is then processed digitally to produce the image of $f(x,y)$.

The oldest CT machines used narrow, parallel x-ray beams. Modern-day machines use a fan-beam geometry. Since the digital processing in both systems is similar, we will consider the parallel-beam case, which is a bit simpler mathematically.

Parallel beam geometry



$p_\theta(v)$ is a set of line integrals called a **projection**.

$p_\theta(v_0)$ is the integral of $f(x,y)$ along the path of the x-ray at angle θ impinging at $v = v_0$.

Typically, projections $p_\theta(v)$ are collected through a full 360° by rotating the x-ray source(s) and detectors around the object being imaged.

How do we recover $f(x,y)$ from the projections $p_\theta(v)$?

Define the 2-D Fourier transform of $f(x,y)$ as

$$F(\Omega_1, \Omega_2) = \int_{-\infty}^{\infty} \int_{-\infty}^{\infty} f(x,y) e^{-j(\Omega_1 x + \Omega_2 y)} dx dy$$

The inverse 2-D Fourier transform is

$$f(x,y) = \frac{1}{(2\pi)^2} \int_{-\infty}^{\infty} \int_{-\infty}^{\infty} F(\Omega_1, \Omega_2) e^{j(\Omega_1 x + \Omega_2 y)} d\Omega_1 d\Omega_2$$

Notation:

Let $F(\Omega_1, \Omega_2)$ in polar coordinates be written as

$$F_{\text{pol}}(r, \phi) = F(r \cos \phi, r \sin \phi)$$

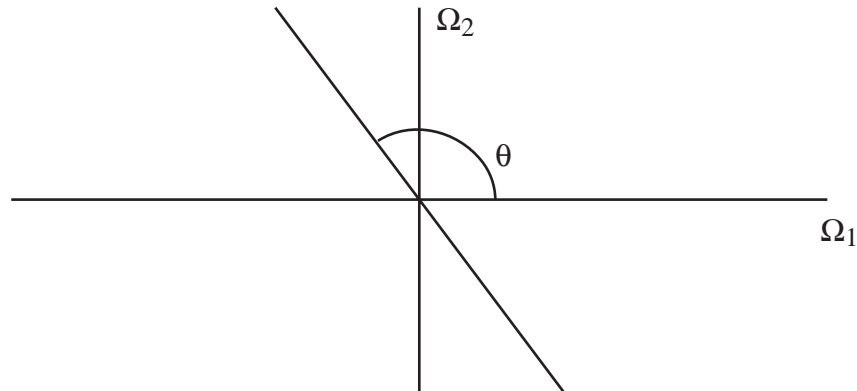
Then the following famous theorem forms the basis for reconstructing $f(x, y)$ from its projections.

Projection-Slice Theorem

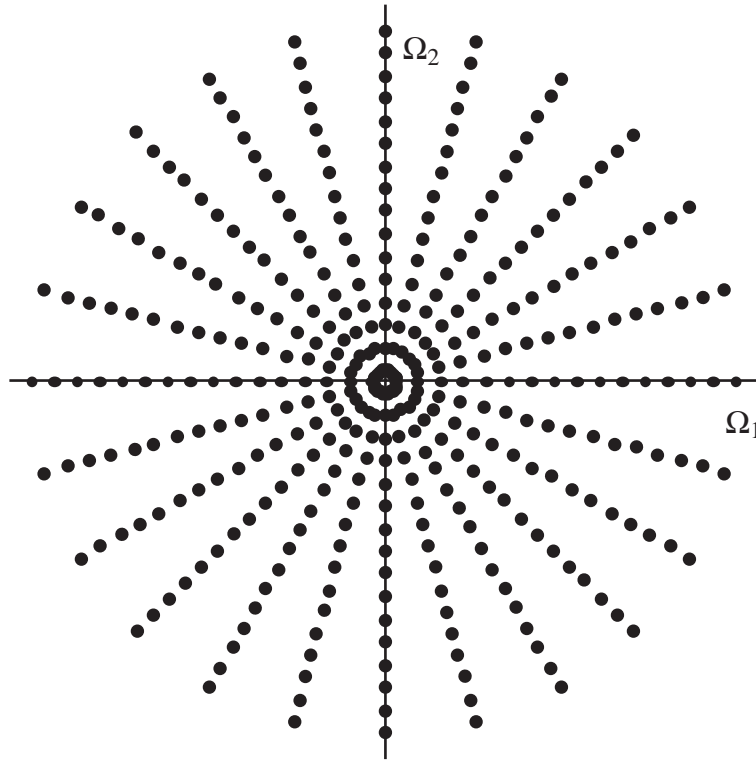
Let $P_\theta(\Omega)$ be the 1-D Fourier transform of $p_\theta(v)$. Then

$$[P_\theta(\Omega) = F_{\text{pol}}(\Omega, \theta)]$$

So, the Fourier transform of a projection is a radial slice of the 2-D Fourier transform of $f(x, y)$ at angle θ :



Collecting sampled projections at many (usually hundreds) of angles and taking the DFT (via FFT) of each projection gives samples of $F(\Omega_1, \Omega_2)$ on a polar grid:



To reconstruct samples of $f(x,y)$ we might try discretization of the inverse 2-D Fourier transform.

We had:

$$f(x,y) = \frac{1}{(2\pi)^2} \int_{-\infty}^{\infty} \int_{-\infty}^{\infty} F(\Omega_1, \Omega_2) e^{j(\Omega_1 x + \Omega_2 y)} d\Omega_1 d\Omega_2$$

Writing this integral in polar coordinates, and then discretizing, would give an approximate formula for $f(nT, mT)$ in terms of the available polar samples of $F(\Omega_1, \Omega_2)$. Computing N^2 samples of $f(x,y)$ from N^2 samples of F would require

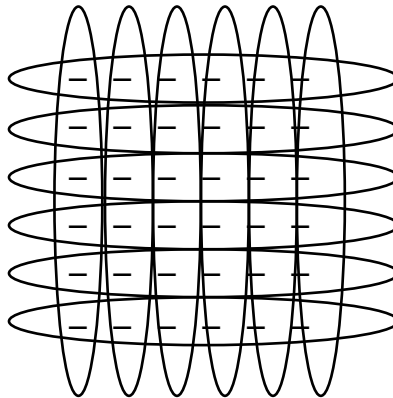
$$N^2 \times N^2 = N^4 \otimes$$

which is excessive. For example, if $N = 512$, this approach would require about 64×10^9 MAs.

A faster alternative would be to

- 1) Interpolate the polar Fourier data to a Cartesian grid.
- 2) Compute a 2-D FFT⁻¹ (requires $\sim 2N^2 \log_2 N$ MAs)

A 2-D DFT is implemented by a series of row FFTs, followed by a series of column FFTs:



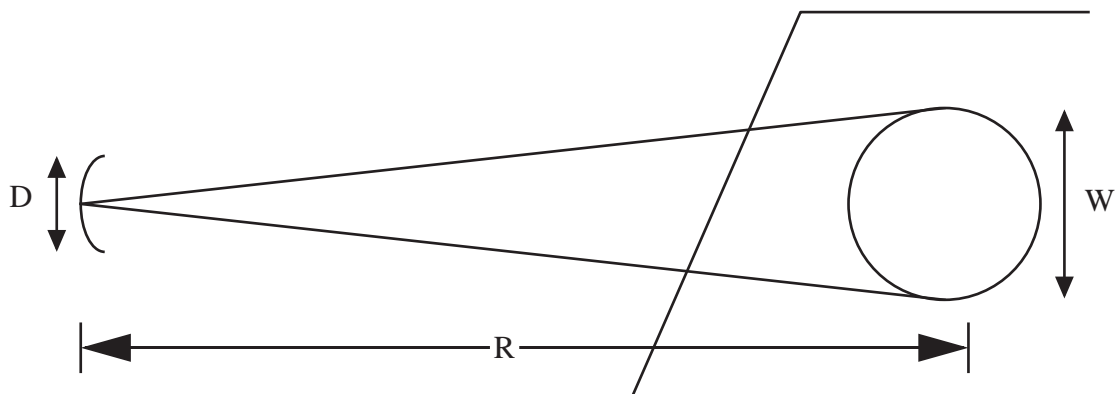
In practice, an accurate implementation of Step 1) requires more computation than the 2-D FFT¹. The most popular image reconstruction algorithm for computer tomography is “convolution-back-projection” (also called filtered back-projection) which is essentially an accurate and efficient way to accomplish 1) and 2) in $O(N^3)$ MAs. Researchers are now working on convolution-back-projection algorithms that require only $O(N^2 \log_2 N)$ MAs.

Application 2: Synthetic Aperture Radar (SAR)

SAR is a high-resolution microwave imaging system. It is used widely in applications such as earth resources monitoring, military reconnaissance, planetary imaging, etc.

Same advantages of microwave imaging over optical: can penetrate fog, cloud cover, atmosphere of Venus, etc., and does not rely on illumination by the sun.

Disadvantage: It is hard to achieve optical resolution. Why? Because, although we can get high resolution in range via delay measurements, the cross-range resolution is seemingly limited by the antenna beamwidth, which can be very wide at microwave frequencies:



If D is the antenna diameter, R is the range to the scene, and λ is the wavelength of radiation, then the width of the antenna-footprint is

$$W = \frac{R \lambda}{D}$$

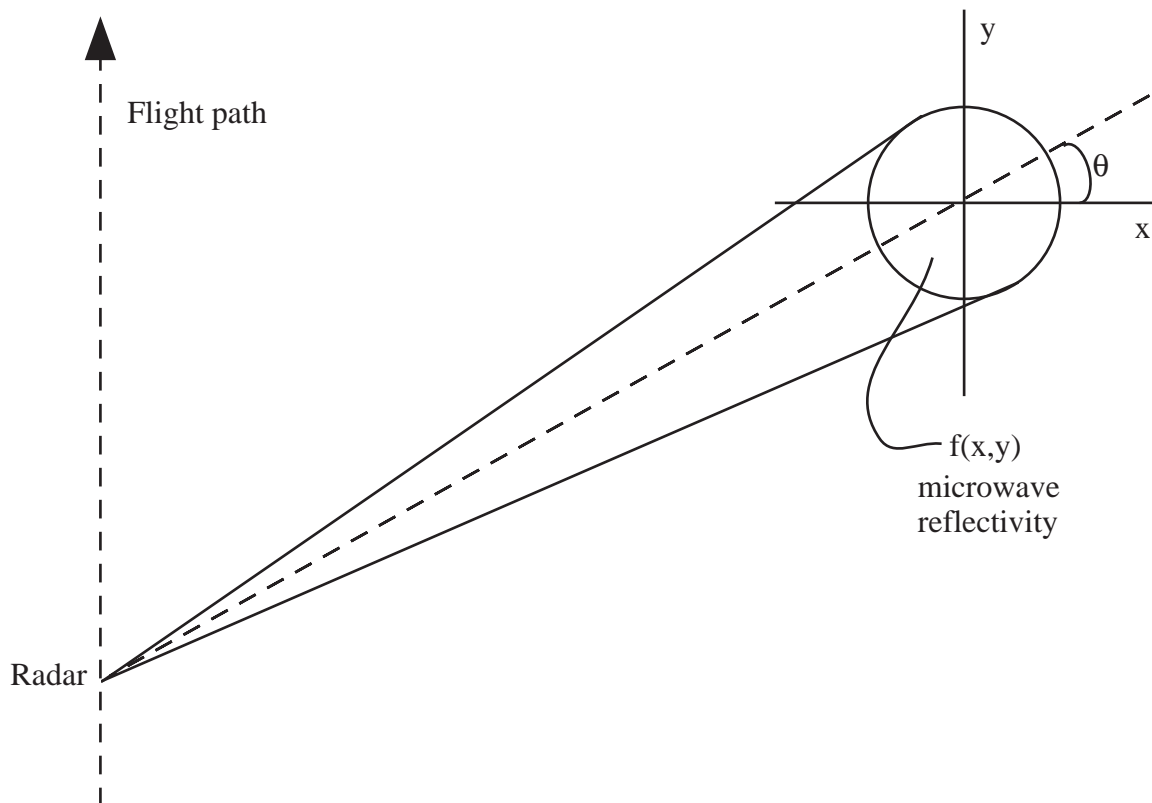
For high cross-range resolution, we want W to be small, but this is hard to get. R may be large and dictated by the imaging scenario, and you hope to use an antenna of practical size (D small).

For microwaves, λ is much larger than for visible light. So, with microwaves, D may need to be impractically-large to achieve a desired cross-range resolution.

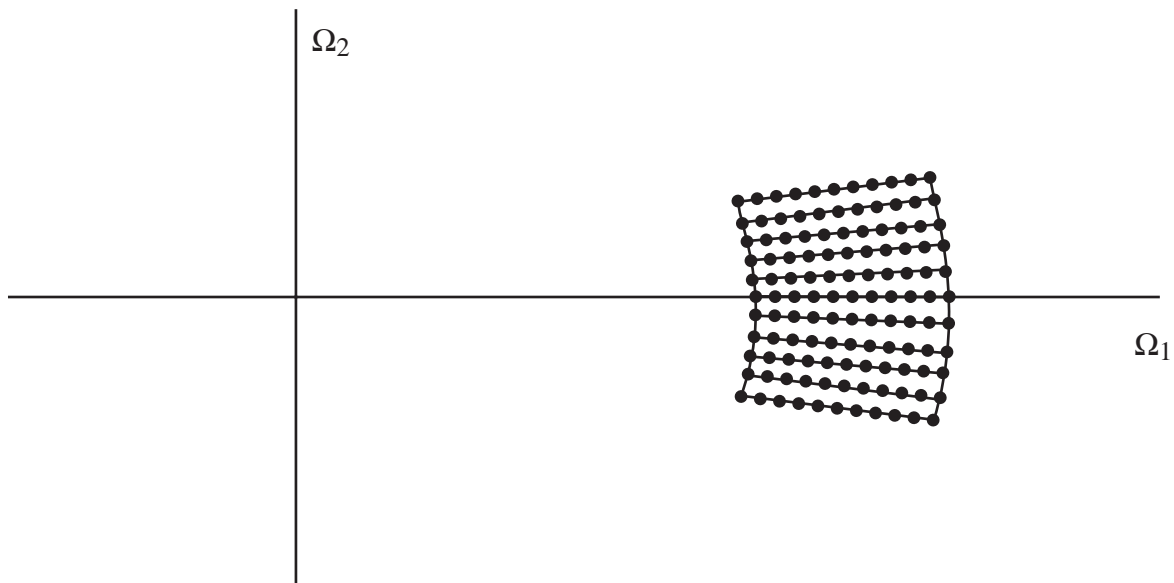
Solution:

Use small D with large W , but collect and process data from many angles. This is called spotlight-mode SAR.

Imaging geometry



If a linear FM waveform $\cos(\Omega_0 t + \alpha t^2)$ is transmitted, it can be shown that demodulated, sampled returns provide Fourier data on a polar grid:



The return collected at angle θ in the spatial domain gives Fourier data on the radial trace at the same angle θ in the Fourier domain. (Proof of this fact uses the projection-slice theorem.) The inner and outer radii of the Fourier data region are proportional to the lowest and highest frequencies, respectively, of the transmitted linear FM signal.

Reconstruction algorithm:

- 1) Polar-to-Cartesian interpolation
- 2) 2-D FFT⁻¹
- 3) Display magnitude of the result.

Typical resolution:

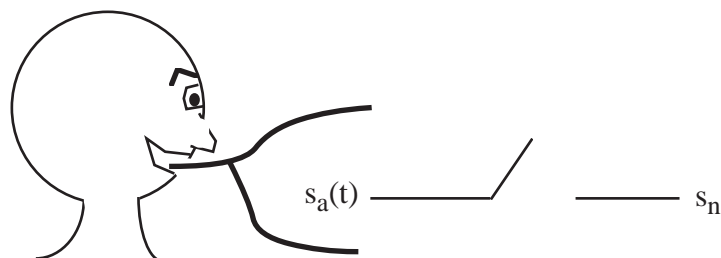
1 ft., or less, to 20 m, depending on the application

These resolutions are achievable at exceedingly long ranges (e.g., space-based monitoring of the earth).

Application 3: Speech Analysis/Synthesis

Consider an approach to speech coding called LPC – Linear Predictive Coding.

This scheme is used in many speech communication systems, automated answering systems and electronic games.



Speech samples are highly correlated, so that s_n can often be fairly-well predicted from its past values.

Suppose we wish to predict s_N from $s_{N-1}, s_{N-2}, \dots, s_{N-K}$. Try linear prediction.

Estimate s_N by:

$$\hat{s}_N = \sum_{k=1}^K a_k s_{N-k}$$

The $\{a_k\}$ are called LPC coefficients.

Choose the $\{a_k\}$ to minimize $E \{s_N - \hat{s}_N\}^2$.

So, do this

$$\begin{aligned} \min_{\{a_i\}_{i=1}^K} E \left\{ \left(s_N - \sum_{k=1}^K a_k s_{N-k} \right)^2 \right\} \\ \Rightarrow \frac{\partial}{\partial a_i} E \left\{ \left(s_N - \sum_{k=1}^K a_k s_{N-k} \right)^2 \right\} = 0 \quad i = 1, \dots, K \\ \Rightarrow E \left\{ 2 \left(s_N - \sum_{k=1}^K a_k s_{N-k} \right) (-s_{N-i}) \right\} = 0 \quad i = 1, \dots, K \end{aligned}$$

$$\Rightarrow \sum_{k=1}^K a_k E \{s_{N-k} s_{N-i}\} = E \{s_N s_{N-i}\} \quad i = 1, 2, \dots, K \quad (1)$$

Suppose $\{s_n\}$ is short-term “wide-sense stationary.” Then $E \{s_m s_n\}$ depends only on the separation between m and n , i.e., on $|m-n|$, not on m and n individually.

In this case we can write $E \{s_n s_m\}$ as some function $R_s(n-m) = R_s(m-n)$ where R_s is called the autocorrelation.

Substituting R_s into (1) gives

$$\sum_{k=1}^K a_k R_s(i-k) = R_s(i) \quad i = 1, 2, \dots, K$$

This set of K equations can be expressed in matrix form as

$$\begin{bmatrix} R_s(0) & R_s(1) & \dots & R_s(K-1) \\ R_s(1) & R_s(0) & \dots & \vdots \\ \vdots & \vdots & \ddots & \vdots \\ \vdots & \vdots & \vdots & R_s(1) \\ R_s(K-1) & R_s(1) & \dots & R_s(0) \end{bmatrix} \begin{bmatrix} a_1 \\ a_2 \\ \vdots \\ a_K \end{bmatrix} = \begin{bmatrix} R_s(1) \\ R_s(2) \\ \vdots \\ R_s(K) \end{bmatrix} \quad (2)$$

Given the $R_s(i)$, this set of equations can be solved for the optimal $\{a_k\}_{k=1}^K$

We might approximate $R_s(i)$ as:

$$R_s(i) = \frac{1}{L_i} \sum_n s_n s_{n+i}$$

\uparrow
 # terms in sum = L_i

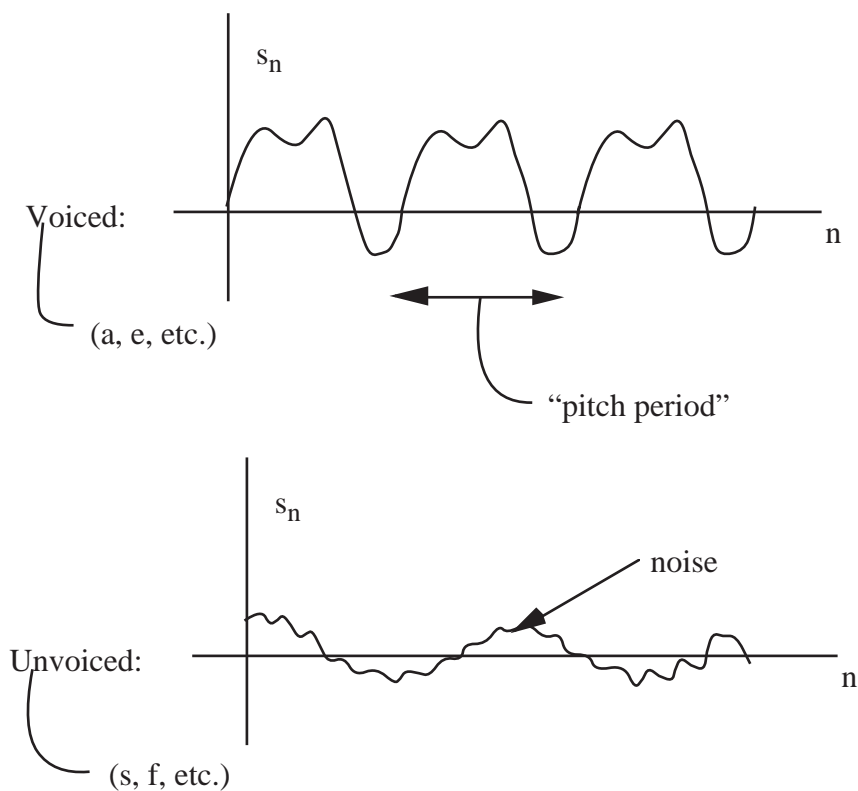
The solution of (2) would ordinarily require $O(K^3)$ operations.

But, the matrix has a special Toeplitz structure \Rightarrow faster algorithms exist.

The Levinson - Durbin algorithms require $O(K^2)$ operations.

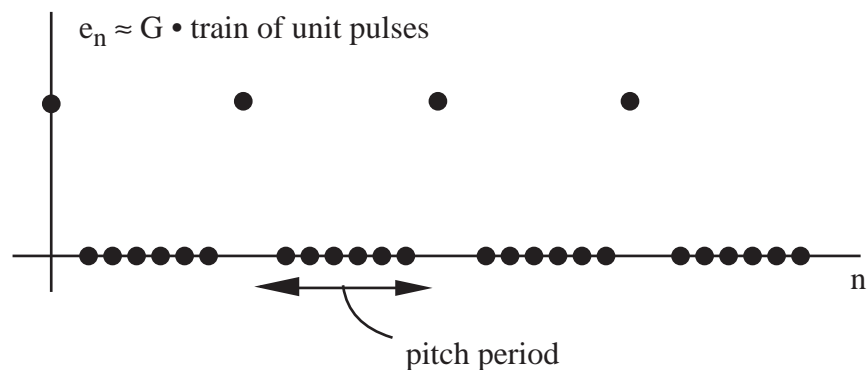
Now, look at speech!

Classification of speech segments:



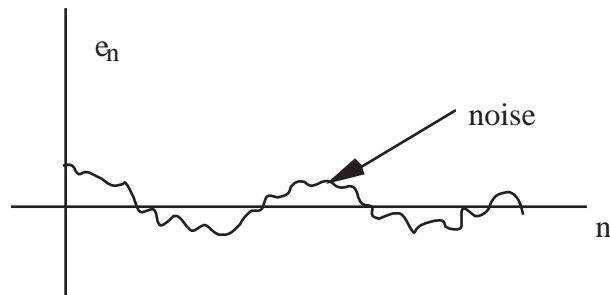
Now, suppose we have the optimal $\{a_k\}$ and we look at the prediction error $e_n = s_n - \hat{s}_n$.

It turns out that for voiced sounds e_n is well approximated by a pulse train:



where G is a slowly varying gain.

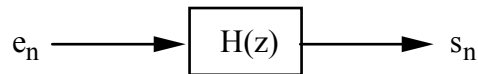
For unvoiced sounds, e_n looks like noise:



Using our definition of e_n and the LPC model, we have

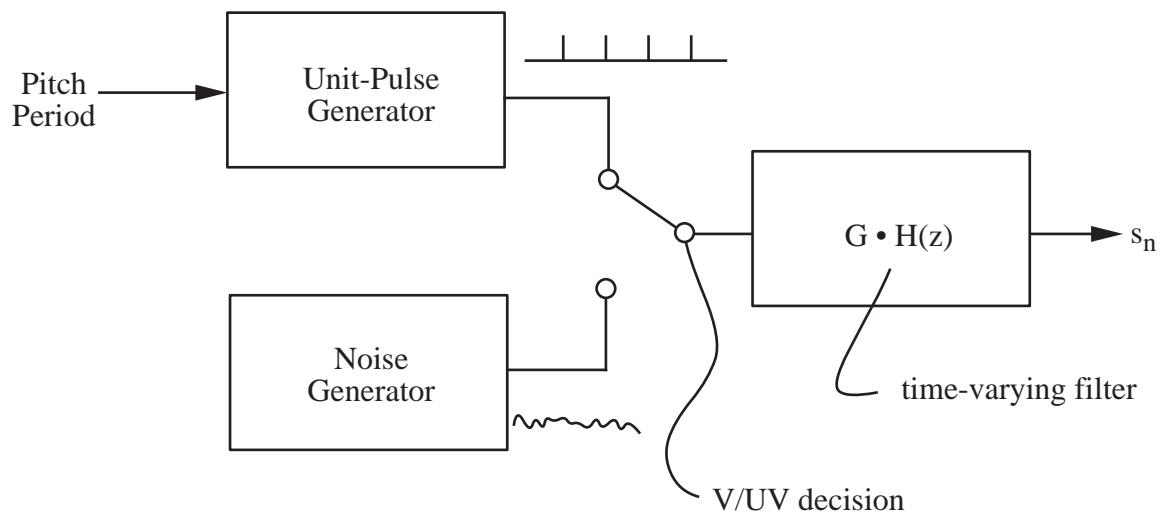
$$s_n = \hat{s}_n + e_n = \sum_{k=1}^K a_k s_{n-k} + e_n$$

Thus, we can obtain s_n from e_n via



where
$$H(z) = \frac{1}{1 - \sum_{k=1}^K a_k z^{-k}}$$

Standard Speech Model for Analysis/Synthesis:



This model provides the basis for a speech analysis/synthesis scheme:

- 1) Analyze each 20 msec segment of the speech waveform to get:
 - a) V/UV decision
 - b) Pitch period (if voiced)
 - c) $\{a_k\}_{k=1}^K \sim$ by solving equations in (2)
 - d) Gain $\sim G$

Transmit a) – d) every 20 msec. At the receiver, reconstruct an approximation to the original speech waveform by using the above model.

Comparison with PCM

PCM: Sample speech at ~ 8 kHz; use 7 bits/sample

$\Rightarrow 56$ K bits/sec.

Analysis/Synthesis:

(assuming a fancier version of LPC than we just covered)

8 K bits/sec: very close to regular telephone quality

2 K bits/sec: very understandable, somewhat machine-like

600 bits/sec: understandable, quite machine-like

Thus, we see that the LPC scheme can greatly reduce the bit rate for both transmission and storage of speech.

Appendix A

Appendix on complex numbers:

A.1 complex numbers

We begin with a review of several properties of complex numbers, their representation, and some of their basic properties. The use of complex numbers, complex-valued functions, and functions of a complex variable will prove essential for an understanding of the material in this text, so it is important that before proceeding with the rest of this material, some basic notions are well understood. Without the ability to manipulate complex numbers and functions, our treatment of discrete-time system theory would be much more cumbersome.

There are many ways in which complex numbers may be represented. Two representations that will be used extensively in this text are the “rectangular” form and the “polar” form. The rectangular form, also called the “Cartesian” form, represents a complex number z as an ordered pair of real numbers, usually written

$$z = x + jy$$

where x and y are real numbers, with x referred to as the “real part” of z and y referred to as the “imaginary part” of z and $j = \sqrt{-1}$. We can write

$$x = \Re z \text{ and } y = \Im z$$

to illustrate taking the “real part” and the “imaginary part” of the complex number z . In polar form, we can write

$$z = re^{j\theta},$$

where $r > 0$ is referred to as the magnitude of the complex number z and θ is the phase or angle of z . We can then express these relationships as

$$r = |z|, \text{ and } \theta = \angle z,$$

and use Euler’s relation

$$e^{j\theta} = \cos(\theta) + j \sin(\theta),$$

to relate the complex cartesian and polar representations as

$$r = \sqrt{x^2 + y^2}, \text{ and } \theta = \arctan(y/x).$$

These relationships can be obtained by considering the real and imaginary parts of a complex number as points in the complex (x, y) plane. Then the complex number can be thought of as a vector in the plane from the origin to the point (x, y) , with the magnitude of the vector being r and the angle formed from the real line to the vector yielding θ , as in figure A.1.

We see that by Euler’s relation, we have

$$z = re^{j\theta} = (r \cos(\theta)) + j(r \sin(\theta))$$

and then we obtain

$$x = r \cos(\theta) \text{ and } y = r \sin(\theta).$$

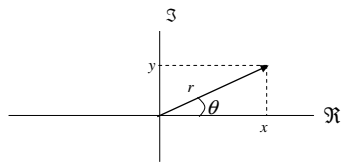


Figure A.1: Vector representation of a complex number, relating the polar and Cartesian forms. Euler's relation can be used to relate the real part and imaginary parts with the magnitude and phase.

We can similarly write

$$\sqrt{x^2 + y^2} = \sqrt{r^2(\cos(\theta)^2 + \sin(\theta)^2)} = r,$$

and

$$\frac{y}{x} = \frac{r \sin(\theta)}{r \cos(\theta)} = \tan(\theta),$$

such that

$$\theta = \arctan(y/x).$$

Complex numbers are simply a useful tool that enables us to describe a wider class of equations than do the real numbers alone. For example, if we consider the equation

$$x^2 + 1 = 0,$$

and ask for what values of x does this equation have a solution? We find that when x takes on values from the real numbers, then there are no solutions. However we can learn more about this equation, and about equations involving higher order polynomials in x if we can introduce a solution to this equation. In order to do so, we must now think of the function

$$f(x) = x^2 + 1$$

not as a function over the reals, but rather as a function over a new number system - one for which a solution to this equation exists. By creating this solution, and giving it the name j , we “create” a number that did not exist in the reals, namely the square root of -1 . By constructing a field of numbers over which our algebraic structures behave as we have come to expect, based on the real numbers, we need to introduce a way to add, subtract, and multiply complex numbers. In Cartesian form, we have that the sum of two complex numbers can be written

$$(x_1 + jy_1) + (x_2 + jy_2) = (x_1 + x_2) + j(y_1 + y_2)$$

that is, to add two complex numbers, we simply can use real addition of the real parts and real addition of the imaginary parts, separately to construct the real part and the imaginary part of the sum.

Multiplication of two complex numbers in Cartesian form can be written

$$(x_1 + jy_1)(x_2 + jy_2) = (x_1x_2 - y_1y_2) + j(x_1y_2 + x_2y_1),$$

where we can apply the distributive law of multiplication over addition, and use our newly formed relation that $j^2 = -1$. By using this relation, we can think of j as a variable, and apply the same algebraic manipulations to complex numbers as we would to polynomials in the variable j , so long as once the algebraic manipulations are completed, we agree to replace j^2 with the number -1 , and repeat this process until we have exhausted all powers of j . We can then write the resulting complex number in Cartesian form by collecting the remaining terms without this variable, and call them the real part and those that contain the variable become the imaginary part.

Suppose we use a different notation for a complex number, such that

$$c = a + \odot b$$

Using this notation, the real number sitting next to the smiling face is the imaginary part of c and the real number not sitting next to the smiling face is the real part of c . Now, pretend that c is a polynomial in the “variable” \odot . Then write:

$$c_1 \cdot c_2 = (a_1 + \odot b_1)(a_2 + \odot b_2) = a_1 a_2 + a_1 b_2 \odot + a_2 b_1 \odot + b_1 b_2 \odot^2.$$

If we agree to replace \odot^2 by -1 , we have

$$c_1 \cdot c_2 = (a_1 a_2 - b_1 b_2) + \odot(a_1 b_2 + a_2 b_1)$$

which is the right answer! We agree to use j instead of \odot , and everywhere j^2 appears we replace it with -1 . So, in this sense “ $j^2 = -1$ ” but j is just a notational aid.

A.2 Complex-valued functions

Now that we have introduced complex numbers to our field of operation, we can now extend the notion of a function to include the possibility of a function that takes on values from this complex field. Specifically, we considered a function to be a mapping from an independent variable, say t to the real numbers, such that $f(t) = c$, where $c \in \mathbb{R}$. By simply extending this notion to include the possibility that the function $f(t) = z$, where $z \in \mathcal{C}$, where \mathcal{C} denotes the field of complex numbers, such that $z = x + jy$, and $x, y \in \mathbb{R}$

A.3 Complex variables

To this point, we have considered the independent variable in our functions to be taken from either the integers or the reals. However, now that we have extended our field of operation to include the field of complex numbers, it is only natural to consider extending the notion of a function from one that operates not on just real-valued independent variables, but also, possibly, complex-valued variables. A complex variable is simply a variable that can take on values from the field of complex numbers. So the variable $z = x + jy$ is a complex variable and any function of z must be considered carefully, as it is now a function of a complex variable and as such is considerably more complex than a function of a real variable.

A.4 Functions of a complex variable

We can now consider algebraic functions of complex variables by considering the functions as taking algebraic operations on the complex numbers, again treating them as polynomials in j , and then reducing the resulting expression into a single complex number after the algebraic operations are complete. For example, for the function

$$f(z) = z^2 + 1$$

we can simply write

$$f(x + jy) = (x + jy)^2 + (1 + j0) = (x^2 - y^2 + 1) + j(2xy)$$

and see that the resulting value has both a real part and an imaginary part, each of which can be expressed in terms of the real parts and imaginary parts of z . It is often useful to consider the function $f(z)$ in terms of its real part and imaginary part separately, so that each might more simply be written as a real-valued function of two real-valued variables. Specifically, we have

$$f(z) = f(x + jy) = u(x, y) + jv(x, y),$$

where x and y are real-valued variables, and u and v are real-valued functions of two real-valued variables. In this example, we have

$$\begin{aligned} f(z) &= u(x, y) + jv(x, y) = (x^2 - y^2 + 1) + j(2xy), \\ u(x, y) &= x^2 - y^2 + 1, \\ v(x, y) &= 2xy. \end{aligned}$$

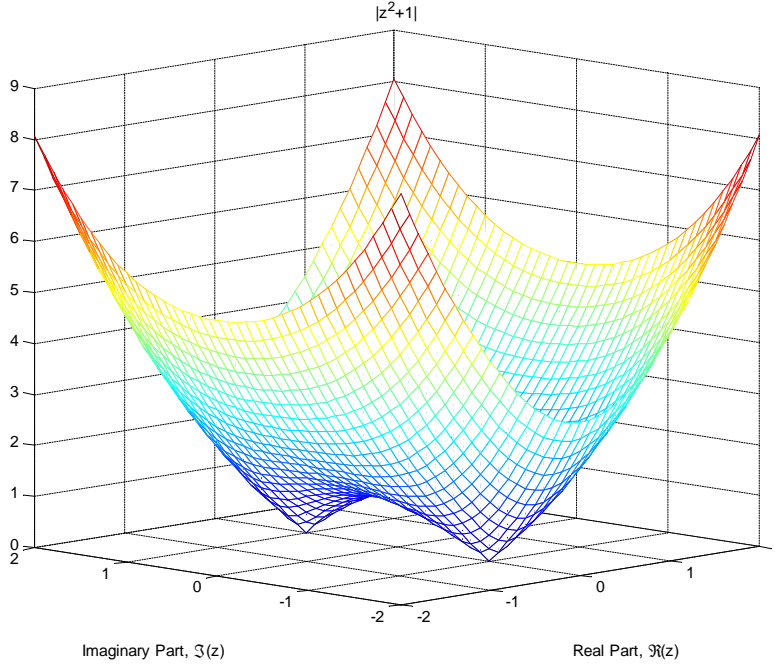


Figure A.2: Magnitude of the function $f(z) = z^2 + 1$, i.e. $|z^2 + 1|$.

Now the function f itself is complex valued, and notions of graphically displaying such functions is no longer as simple as it was for real-valued functions. However we can simply plot the real part, u or the imaginary part v of $f(z)$, to graphically depict its behavior. Similarly, we could consider other representations of the resulting complex number, such as its polar form, and plot the magnitude, $|f|$, and the phase, $\angle f$ over the complex (x, y) plane. As a result, we can then ask whether there is any $(x + jy)$ at which

$$f(x + jy) = (0 + j0) = 0,$$

which is true if and only if $\Re[f] = \Im[f] = 0$, or if and only if $|f| = 0$.

We can check this:

$$\begin{aligned} f(x + jy) &= (x + jy)^2 + (1 + j0) \\ &= \underbrace{(x^2 - y^2 + 1)}_{\Re\{z\}} + j \underbrace{(2xy)}_{\Im z} \end{aligned}$$

which equals $(0 + j0)$ if and only if $x = 0$ and $y = \pm 1$, i.e. if z is a complex variable, then

$$f(z) = 0 \text{ at } z = (0 \pm 1j) \triangleq \pm j.$$

If $z = x + jy$ is a complex variable, then we can plot $|f(z)|$ as a surface over the $x - y$ plane. It hits zero at the points shown in figure A.2.

We can similarly plot the phase of the function, i.e. we can plot $\angle f(z)$, over the (x, y) plane as shown in figure A.3.

To simplify notation, and to accommodate a broad class of operations using complex numbers, we call the “complex conjugate”, denoted z^* , of a complex number z to represent the complex number that has the same real part but an imaginary part with the opposite sign, i.e. for $z = x + jy$, we have $z^* = x - jy$, and $z^* = re^{-j\theta}$. As a result, we can compactly represent the relationship between the magnitude of a complex number and the number itself, i.e. we have $r^2 = z^*z$. We can also obtain $(z + z^*) = 2x$, and $(z - z^*) = j2y$. Complex conjugation distributes over addition and multiplication (and division) of complex numbers, i.e. $(z_1 + z_2)^* = z_1^* + z_2^*$, and $(z_1 z_2)^* = z_1^* z_2^*$.

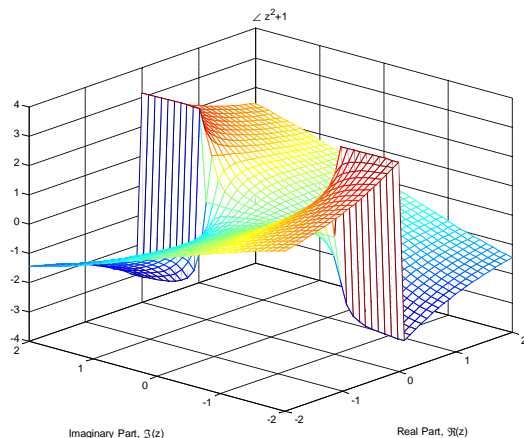
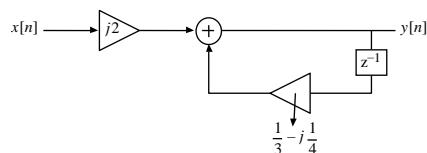
Figure A.3: Phase of the function $f(z) = z^2 + 1$, i.e. $\angle f(z)$.

Figure A.4: Representation of a complex-valued linear shift invariant system.

A.5 Complex Systems

Complex numbers are often used in real systems, even when only real-valued quantities exist in the constituent components of the system itself. Applications such as digital communications (modems), radar, sonar, and computed imaging systems are just a few applications where complex operations are computed using real-valued constituent components.

Consider the linear shift-invariant system described by the flowgraph in figure A.4.

where $x[n] = x_R[n] + jx_I[n]$ and $y[n] = y_R[n] + jy_I[n]$ are complex-valued sequences. We can draw a block diagram that can implement the above system using real signals and real multipliers, adders and delays.

The first step is to realize that $x[n] = x_R[n] + jx_I[n]$ and $y[n] = y_R[n] + jy_I[n]$ are pairs of real-valued sequences, i.e., the system above has two inputs $x_R[n]$ and $x_I[n]$ and two outputs $y_R[n]$ and $y_I[n]$. The second step is to recall that complex multiplication and complex addition are defined in terms of real multiplication and real addition, as described previously. We call the output of first multiplication, by $0 + j2$, $v[n] = v_R[n] + jv_I[n]$. This multiplication is accomplished as

$$v[n] = j2(x_R[n] + jx_I[n]) = -2x_I[n] + j2x_R[n]$$

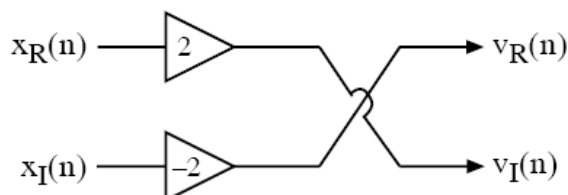
Thus,

$$v_R[n] = -2x_I[n]$$

and

$$v_I[n] = 2x_R[n],$$

which is implemented as



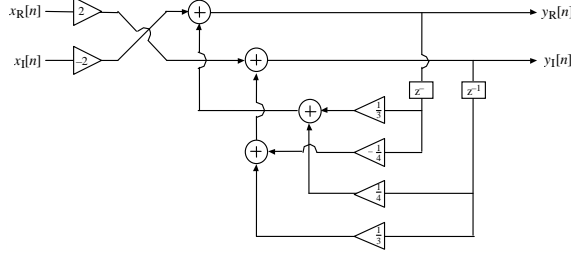


Figure A.5: Flowgraph implementing the system of Figure A.4 using real-valued signals.

Now, let $w[n]$ be the output of the multiplication by $0 - j$. We see that $w[n]$ can be computed as

$$\begin{aligned} w[n] &= \left(\frac{1}{3} - j\frac{1}{4} \right) (y_R[n-1] + jy_I[n-1]) \\ &= \frac{1}{3}y_R[n-1] + \frac{1}{4}y_I[n-1] + j\left(-\frac{1}{4}y_R[n-1] + \frac{1}{3}y_I[n-1] \right). \end{aligned}$$

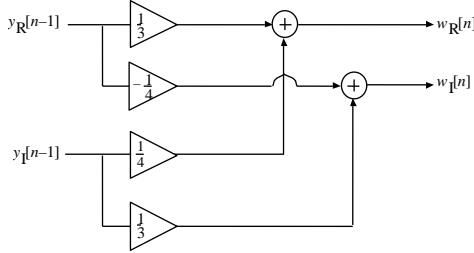
Thus we have,

$$w_R[n] = \frac{1}{3}y_R[n-1] + \frac{1}{4}y_I[n-1]$$

and

$$w_I[n] = -\frac{1}{4}y_R[n-1] + \frac{1}{3}y_I[n-1],$$

which can be implemented using the following flowgraph



Now using that $y[n] = v[n] + w[n]$, so that $y_R[n] = v_R[n] + w_R[n]$ and $y_I[n] = v_I[n] + w_I[n]$, we have the complete block diagram implementation using only real-valued signals as shown in figure A.5 below.

The original block diagram is simply a concise way of representing this complicated system.

A.6 Complex Functions of Complex Variables

Recall that $X(s)$, the Laplace transform as given by $X(s) = \int_{-\infty}^{\infty} x(t)e^{-st}dt$, is a complex function of a complex variable. This has a number of important mathematical implications and can be developed in great detail. In this text, however, we will keep our treatment of such functions brief and limited in scope. To aid with the development of the z -transform for sequences, we will briefly review some of the properties of such complex functions. When we say that the function is a “complex function,” we simply mean that the function takes on values in the complex numbers. That is has both real and imaginary parts, as well as a magnitude and phase. Similarly, when we say that a function is a function of a complex variable, then the argument of the function takes on values in the complex numbers. For example, consider the complex function of the complex variable

$$\underset{\substack{\uparrow \\ \text{complex variable}}}{f(z)} = z$$

which takes on values exactly equal to its argument. Now, since the function is complex, it has both real and imaginary parts, and since its argument is complex, it also has both real and imaginary parts. As a

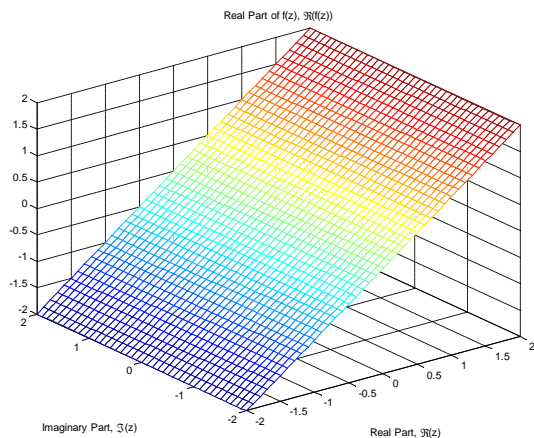


Figure A.6: The surface defined by the real-part of the function $f(z) = z = x + jy$ is shown as a plane over the complex plane, intersecting complex plane along the y -axis, and linearly increasing as a function of x .

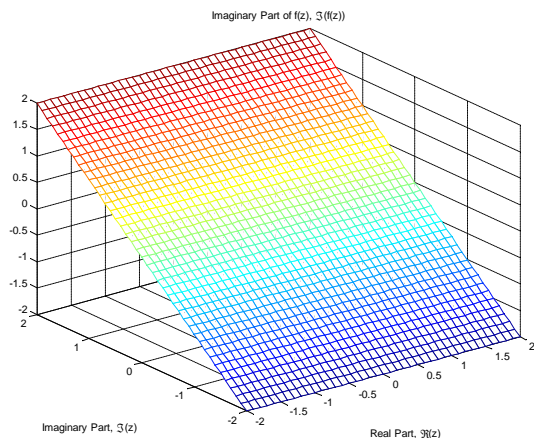


Figure A.7: 2 The surface defined by the imaginary-part of the function $f(z) = z = x + jy$ is shown as a plane over the complex plane, intersecting the complex plane along the x -axis, and linearly increasing as a function of y .

result, it is difficult to conceptualize, or to plot, the whole function all at once. This is why we often look at one real-valued property of $f(z)$ at a given time, and since the variable is complex, then a single real-valued property can be thought of as a surface over the complex plane. As the variable z takes on all possible values, for which $f(z)$ is defined, we can imagine a surface defined by, say, the real-part of $f(z)$. We can now describe the surfaces $\Re f(z)$, $\Im f(z)$, $|f(z)|$, and $\angle f(z)$ as surfaces over the 2-D complex z -plane.

Recall that

$$f(z) = z = x + jy$$

so we have that the real-part satisfies,

$$\Re f(z) = x$$

which defines a plane through y -axis of the complex z -plane with unit slope. This is shown in figure A.6.

For the imaginary part, we have that

$$\Im f(z) = y$$

which defines a plane through x -axis with unit slope as shown in Figure A.7.

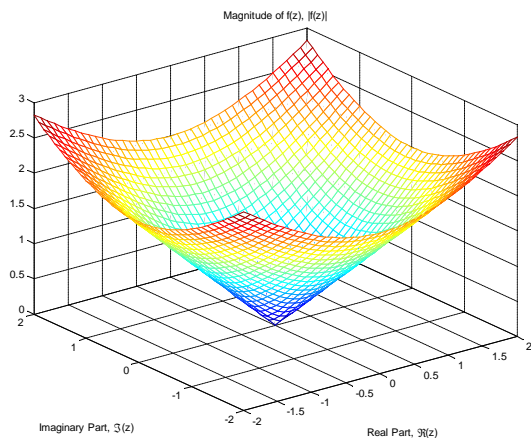


Figure A.8: The surface defined by the magnitude of the function $f(z) = z = x + jy$ is shown as a cone of slope one over the complex plane, centered at the origin.

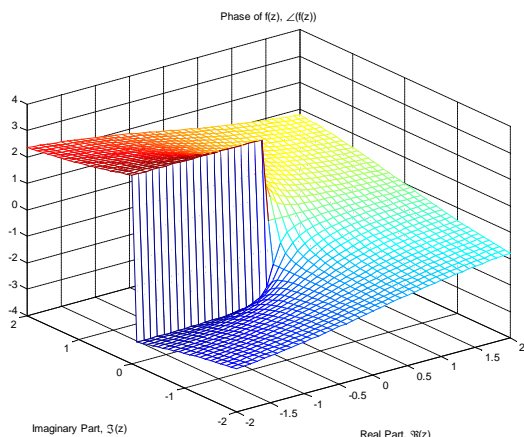


Figure A.9: The surface defined by the phase of the function $f(z) = z = x + jy$ is shown as a spiral ramp through the complex plane.

We can also consider the magnitude of the function, $|f(z)|$, which is non-negative and will always lie on or above the complex plane as shown in Figure A.8. Note that for a given value of z , the magnitude is given by

$$|f(z)| = \sqrt{x^2 + y^2}.$$

All values of z that take on the same magnitude would trace out a circle in the complex plane. As the magnitude increases, the radius of the circle also increases. As a result, the surface defined by the magnitude, $|f(z)|$, is an inverted cone, of slope one, centered at the origin.

Finally, the phase of the function is given by

$$\angle f(z) = \arctan\left(\frac{y}{x}\right),$$

which defines a spiral ramp starting at $+x$ -axis (which $\angle z$ cuts through), and which ramps up in a counter clockwise direction to the height π along the $-x$ -axis. In the clockwise direction from the $+x$ -axis, the surface ramps down to the level $-\pi$ along the $-x$ -axis. This is shown in Figure A.9.

A real-valued function can be fully described by a plot of the values of the function along an axis describing its independent variable. A complex-valued function of a complex variable can be fully described by the

surfaces defined by its real and imaginary parts. Similarly, it can be fully described by the surfaces defined by its magnitude and phase.

Appendix B

Appendix on vectors and matrices:

- B.1 basic vector and matrix algebra,
- B.2 solutions of systems of difference equations instead of higher order equations
- B.3 Linear algebraic representations of signals and systems (could be a whole chapter)

Appendix C

appendix/chapter on image processing
or multidimensional signal processing, 2d
and projection slice theorem, etc.

Appendix D

Appendix: Impulses, samples, and delta's, Oh My!

D.1 The Dirac delta

The Dirac delta is best described as a distribution, rather than as a function, since, strictly speaking, it is not a function. A distribution is defined as follows

A *distribution* maps a function to a number.

With that out of the way, we can now define the Dirac delta, or impulse as follows

The *Dirac delta* is the distribution operating on the function $f(t)$, where $f(t)$ is assumed to be continuous near $t = 0$, is given by

$$\delta\{f(t)\} \triangleq f(0).$$

We refer to the Dirac delta interchangeably as an “impulse,” and colloquially as a “delta function,” even though it is not a function, but rather a distribution. Using this slight abuse of terminology, we also often will replace the form $\delta f(t)$ with the less convenient, but more natural form

$$\int_{-\infty}^{\infty} \delta(t)f(t)dt \triangleq f(0). \tag{D.1}$$

In this form, we can imagine the impulse as having a “sifting property” whereby when placed within an integral, it “sifts out” the value of the integrand at the precise value of $t = 0$. Note that this special form does not provide any additional properties to the impulse other than its definition within an integral. Outside of an integral, an impulse is meaningless, since it is not a function and is only defined by how it operates on a function when placed within an integral of the form above. For the special case of $f(t) = 1$, we have that

$$\int_{-\infty}^{\infty} \delta(t)dt = 1.$$

Unfortunately, now that you are comfortable as accepting an impulse as a distribution, and that it is only defined when placed in an integral of the form D.1, the integral in D.1 is not truly an integral. In fact, it is completely defined by D.1. However, we can manipulate D.1 and properties of continuous functions $f(t)$ to obtain forms such as

$$\int_{-\infty}^{\infty} \delta(at)f(t)dt = \frac{1}{|a|} \int_{-\infty}^{\infty} \delta(\tau)f(\tau/a)d\tau = \frac{1}{|a|}f(0),$$

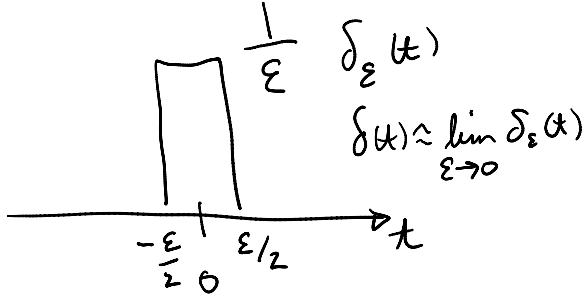


Figure D.1: A conceptual limiting process for the delta function, $\delta(t) \approx \lim_{\epsilon \rightarrow 0} \delta_\epsilon(t)$.

through the change of variables $\tau = at$, where the absolute value arises from a combination of replacing $adt = d\tau$. Note that if $a < 0$ then the sign of the integral would change by this substitution, however we would also need to swap the limits of integration also due to this change of variable, leaving the overall sign the same, which is why we can simply use an absolute value and leave the limits unchanged, regardless of the sign. From this we can equate

$$\delta(at) = \frac{1}{|a|} \delta(t).$$

We can also use the sifting property that arises when the Dirac delta is shifted by a fixed amount c ,

$$\int_{-\infty}^{\infty} \delta(t - c) f(t) dt = f(c),$$

through a change of variable $\tau = t - c$, which leaves scale and sign of the integral intact. Combining these two approaches yields

$$\int_{-\infty}^{\infty} \delta(at - c) f(t) dt \stackrel{(\tau=at)}{=} \frac{1}{|a|} \int_{-\infty}^{\infty} \delta(\tau - c) f(\tau/a) d\tau \stackrel{(\sigma=\tau-c)}{=} \frac{1}{|a|} \int_{-\infty}^{\infty} \delta(\sigma) f((\sigma + c)/a) d\sigma = \frac{1}{|a|} f(c/a),$$

which gives the relation

$$\delta(at - c) = \frac{1}{|a|} \delta(t - c/a).$$

The sifting property of the delta function makes one tempted to think of it as a limiting process for a short, tall pulse of the form, $\frac{1}{\epsilon} [u(t + \epsilon/2) - u(t - \epsilon/2)]$, although the limit shown in figure D.1 is not a function, though when the limit of such a function is placed in an integral, the limit of the integral, for certain well-behaved functions $f(t)$, will behave like the impulse distribution.

We can say the following

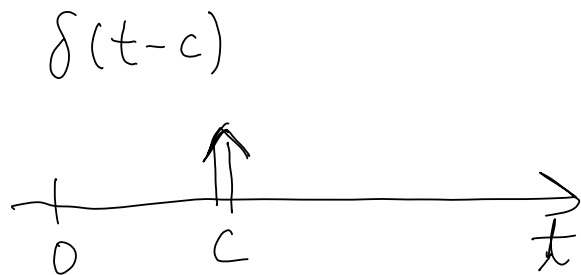
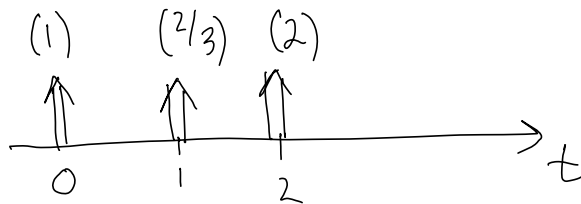
$$f(0) = \lim_{\epsilon \rightarrow 0} \int_{-\infty}^{\infty} \delta_\epsilon(t) f(t) dt = \int_{-\infty}^{\infty} \delta(t) f(t) dt,$$

however, saying that $\delta(t) = \lim_{\epsilon \rightarrow 0} \delta_\epsilon(t)$ would require bringing the limit inside the integral, which is mathematically incorrect, since the limit $\lim_{\epsilon \rightarrow 0} \delta_\epsilon(t)$ does not exist. An impulse is usually pictorially depicted as an arrow as shown in figure D.2.

where if the impulse is drawn without an “amplitude” it is assumed to have unit area. When multiple impulses arise, as in $\delta(t) + \frac{2}{3}\delta(t - 1) + 2\delta(t - 2)$, the “amplitude” of the impulse is used to denote the scale factor to be applied to the sifted value of the function at that location, as in figure D.3.

D.2 The Kronecker Delta

In discrete-time systems, we are often interested in forming a sequence that is zero at every sample value, except for a single value, for which the sequence takes on the value one. In mathematics, a function that has

Figure D.2: Graphical depiction of an impulse $\delta(t - c)$.Figure D.3: Graphical depiction of the function $\delta(t) + \frac{2}{3}\delta(t - 1) + 2\delta(t - 2)$.

a property similar to this one is known as the Kronecker delta function, or Kronecker delta. The Kronecker delta is a function of two variables, i and j and has the property that it is zero for all values of i and j except for the case when $i = j$, i.e., we have

$$\delta_{ij} = \begin{cases} 0, & i \neq j, \\ 1, & \text{otherwise.} \end{cases}$$

In some texts, a one-argument variant of the Kronecker delta is used that takes the form

$$\delta_k = \begin{cases} 0, & k \neq 0, \\ 1, & k = 0. \end{cases}$$

In discrete-time signal processing, we will make extensive use of the Kronecker delta function in a slightly different variation of the one-argument version given above. When doing so, we often refer to this as a sequence, and call it a “unit pulse” sequence, defined as

$$\delta[n] = \begin{cases} 0, & n \neq 0, \\ 1, & n = 0. \end{cases}$$

We note the similarity in notation, and definition of the “unit pulse” with the “impulse” or Dirac delta, $\delta(t)$, and as a result, we often use the term “unit pulse,” “discrete-time impulse,” and “impulse” interchangeably. A plot of the sequence corresponding to a discrete-time impulse is shown in figure D.4.

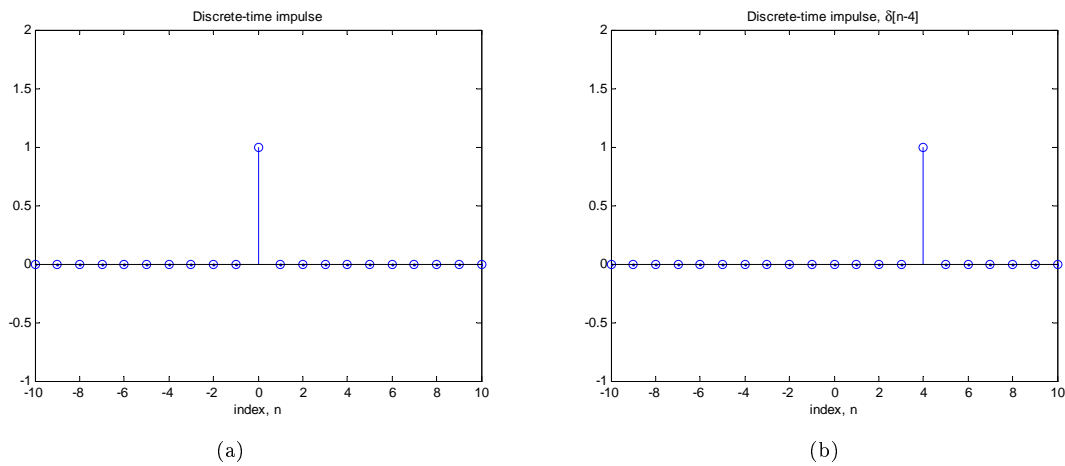


Figure D.4: A discrete-time impulse, which is also referred to as a unit pulse. In (a), $\delta[n]$ is shown as a single non-zero value, at $n = 0$. In (b), the sequence $\delta[n - 4]$ is shown as a single nonzero value at $n = 4$.